Homogénéisation des quasi-cristaux et analyse des modes dans des fibres optiques de type cristal photonique

Sébastien Guenneau

Homogénéisation des quasi-cristaux et analyse des modes dans des fibres optiques de type cristal photonique.

Sébastien Guenneau

2001

UNIVERSITE DE PROVENCE- AIX-MARSEILLE I
U.F.R SCIENCES

N^0 attribué par la bibliothèque :

THESE

pour obtenir le grade de

DOCTEUR DE L'UNIVERSITE DE PROVENCE

École doctorale : Sciences et Structures de la Matière

Discipline : Physique des particules, physique mathématique, et modélisation

présentée et soutenue publiquement

par

Sébastien GUENNEAU

le 2 Avril 2001

Titre :

Homogénéisation des quasi-cristaux et analyse des modes dans des fibres optiques de type cristal photonique.

JURY :

Pr.	B. TORRÉSANI,	Université de Provence,	Président du jury
Pr.	G. BOUCHITTÉ,	Université de Toulon et du Var,	Directeur de thèse
Dr.	F. ZOLLA,	Université de Provence,	Co-directeur de thèse
Pr.	A. NICOLET,	Université Aix-Marseille III,	Examinateur
Dr.	H. AMMARI,	École polytechnique,	Rapporteur
Pr.	A. B. MOVCHAN,	University of Liverpool,	Rapporteur
Pr.	R.Mc. PHEDRAN,	School of Physics, Sydney,	Invité

À Fanny, ma fille.

FIGURE 1 – Ce dessin reprend les différents thèmes abordés dans la thèse, savoir la diffraction par des cristaux et quasi-cristaux photoniques (motifs du papillon et pavage de Penrose) aux grandes longueurs d'ondes par des méthodes de type deux-échelles (symbolisées par l'effet "loupe") et la propagation de la lumière dans les fibres optiques.

Remerciements

Je remercie,

Guy BOUCHITTÉ et Frédéric ZOLLA qui ont co-dirigé cette thèse pour leurs enseignements et l'aide prcieuse et bienveillante qu'ils m'ont apportés tout au long de ces trois annes.

André NICOLET pour son accompagnement dans la partie numrique et sans qui l'tude sur les fibres optiques n'aurait pas vue le jour.

Bruno TORESANNI qui me fait l'honneur de présider le jury de la thèse et rend compte du caractère transdisciplinaire de cette thèse.

Habbib AMMARI pour l'intérêt qu'il a porté à ce travail et pour avoir accepté de rapporter sur cette thèse.

Alexander MOVCHAN qui me fait l'honneur de m'accueillir au sein du département de mathématiques appliquées de l'Université de Liverpool, pour m'avoir permis d'achever la thèse dans les meilleures conditions entre Liverpool et Marseille, et pour rapporter sur cette thèse.

Ross Mac PHEDRAN qui me fait l'honneur de rapporter sur cette thèse, pour ses remarques constructives et ses discussions enrichissantes sur l'homogénéisation et les fibres optiques.

Daniel MAYSTRE pour son écoute et son soutien sans faille, les deux équipes de l'ex-Laboratoire d'Optique Électromagnétique, ainsi que tous les membres du nouvel Institut Fresnel ; avec une mention spéciale pour Stéphane ÉNOCH, Boris GRALAK, Michel NEVIÈRE, Gilles RENVERSEZ, Brian STOUT, Gérard TAYEB, Patrick VINCENT pour l'équipe CLARTÉ et Kamal BELKEBIR, Charles Antoine GUERIN, Gilles MICOLAU, Marc SAILLARD, Gabriel SORIANO, Hervé TORTEL pour l'équipe TEM, ainsi qu'à l'informaticien des deux équipes, Frédéric FORESTIER.

Jean Jacques FERMÉ directeur de la Société Européenne de Systèmes Optiques, pour son engagement en tant que partenaire industriel du projet scientifique, et sa participation au co-financement avec la Région PACA.

Christophe GEUZAINE et Patrick DULAR de l'équipe du Service d'Électricité Appliquée de l'Université de Liège développeurs du code d'éléments finis GETDP, pour leur aide précieuse sur l'étude des fibres optiques.

Philippe TCHAMITCHIAN pour sa collaboration essentielle sur la partie théorie des nombres.

Mireille FRIZZI pour sa gentillesse et son efficacité, Anne SENTENAC pour sa bonne humeur permanente et Sophie LASQUELLEC avec qui j'ai eu beaucoup de plaisir à travailler.

L'équipe pédagogique de la licence de Physique de l'Université d'Aix Marseille III, pour la qualité de la formation qu'elle dispense.

Et enfin ma famille et mes amis pour leur soutien affectif constant et leurs encouragements.

Résumé

Discipline : Physique Mathématique

L'objet de cette thèse est d'une part l'étude théorique et numérique de la diffraction des ondes électromagnétiques en régime harmonique par des structures finies constituées de matériaux hétérogènes périodiques ou quasi-périodiques, à la limite des grandes longueurs d'ondes, et d'autre part l'analyse des modes propagatifs dans des guides périodiques dans le domaine de résonance.

Dans la première partie, nous cherchons à remplacer des structures ferro-magnétiques de type "cristal photonique" par un matériau effectif défini par des matrices de permittivité et de perméabilité anisotropes déduites de la résolution de problèmes annexes de type électrostatique sur un tore. Nous nous interessons ensuite à l'homogénéisation des structures quasi-cristallines et introduisons pour cela une notion de convergence deux-échelles coupe-projection. Enfin, nous estimons le comportement asymptotique de l'erreur entre la solution homogénéisée et la solution quasi-périodique d'un problème d'électrostatique 1D.

Dans la seconde partie, nous utilisons des méthodes numériques de type "éléments finis" pour l'analyse des modes dans des fibres optiques de type "cristal photonique", qui permettent de propager la lumière dans un défaut d'indice faible (par exemple, de l'air) grâce à l'existence de bandes interdites. On s'intéresse aussi à la propagation des ondes centimétriques dans des structures constituées de matériaux diélectriques et métalliques.

Dans la troisième partie, nous appliquons des méthodes asymptotiques à l'analyse spectrale des guides de type "cristal photonique" pour les basses fréquences (homogénéisation) et pour les hautes fréquences (domaine de résonnance). Nous donnons des résultats numériques pour les modes de tels guides aux basses fréquences (méthode des éléments finis) et pour des modes hautes fréquences dans des cavités multicouches 1D (matrices de transfert).

Mots-clés : homogénéisation, électromagnétisme, cristaux-photoniques, quasi-cristaux, convergence deux-échelles, fibres optiques, guides métalliques, cavités, théorie spectrale, éléments finis d'arête.

Summary

Subject : Mathematical Physics

This thesis treats diffraction of time harmonic electromagnetic fields by finite size crystals and quasi-crystals for large wavelengths and propagation of modes in photonic crystal fibers near resonance.

In the first part, we attempted to replace ferro-magnetic photonic crystals by homogeneous structures with anisotropic matrices of permittivity and permeability, deduced from the resolution of annex problems of electrostatic type on a periodic cell. Then, we give effective permittivity for quasi-crystalline phasis, thanks to the so-called "cut-projection convergence". Finally, we estimate the asymptotic behaviour of the error in the one-dimensional case.

In the second part, we make use of "finite element methods" to study the propagation of leaky modes in low index structural defects of photonic crystal fibers (the existence of which depends upon the photonic band gap effects). Furthermore, we outline a numerical approach for complex waveguides mixing dielectric and metallic materials.

In the third part, we make an asymptotic analysis of photonic crystal waveguides for both the quasi-static limit (homogenization) and the high frequency limit (resonance). We give some numerical results for low-frequency modes of such waveguides, thanks to finite elements. In the high frequency limit, we use the transfer matrices to compute the surface modes of a 1D cavity.

Key-words : homogenization, electromagnetism, photonic crystals, quasi-crystals, two-scale convergence, optical fibers, metallic waveguides, cavities, spectral theory, edge-elements.

Table des matières

Préambule

> From a long view of the history of mankind -seen from, say, ten thousand years from now- there can be little doubt that the most significant event of the 19 th century will be judged as Maxwell's discovery of the laws of electrodynamics. The American Civil War will pale into provincial insignifiance in comparison with this important scientific event of the same decade.
>
> R. P. Feynman

Cette thèse se veut transdisciplinaire en ce qu'elle aborde des problèmes qui intéressent les physiciens avec des outils mathématiques récemment développés. Les thèmes abordés dans cette thèse se trouvent en effet à l'interface de plusieurs champs de la physique et des mathématiques : il y est question d'électromagnétisme, de cristallographie, de méthodes asymptotiques en homogénéisation, de théorie spectrale, de théorie des nombres (un soupçon) et de méthodes numériques. La partie mathématique de la thèse a été rédigée au laboratoire d'Analyse Non Linéaire Appliquée et Modélisation de l'Université de Toulon et du Var de Guy Bouchitté. La partie théorie des nombres fait l'objet d'une collaboration avec Philippe Tchamitchian. Les parties physique et numérique ont été mises en œuvre, sous la direction de Frédéric Zolla, dans l'équipe CLARTÉ (ex. Laboratoire d'Optique Électromagnétique de Roger Petit et Daniel Maystre) de l'Institut Fresnel de Claude Amra à Marseille : ces parties sont le fruit d'une collaboration avec d'une part André Nicolet et Sophie Lasquellec de l'institut Fresnel, et d'autre part Christophe Geuzaine et Patrick Dular du Service d'Électricité Appliquée de Willy Legros de l'Université de Liège.

La thèse est bilingue : il nous est en effet apparu nécessaire que les les résultats figurant dans la thèse soient rédigés en anglais, ou pour le moins accessibles à un anglophone. Nous avons fondu dans la thèse les articles acceptés [105][100], soumis [101] ou à soumettre [106][97][104][128][103] dans des revues scientifiques ainsi que les actes de conférences donnés [214][99][98] [96], acceptés [102] ou soumis [95] dans les parties physiques et numériques de la thèse, qui sont donc rédigées dans la langue de Shakespeare (en moins plaisant). Les développements mathématiques sont rédigés en langue française après avoir été introduits dans un chapitre précédent en anglais ou sous forme d'addenda en début de chapitre. Les chapitres 4, 5 et 10 font l'objet d'articles en préparation [34][36][35].

La thèse est divisée en chapitres et sections qui ont une nature philosophique différente et que l'on peut sommairement diviser en quatre catégories : Mathématiques (M), Physique (P), Numérique (N) et Histoire des Sciences (H). Voila le découpage que nous proposons :
Introduction. (H)
1) Homogenization of finite photonic crystals. (P)

2) Justification by two-scale convergence. (M)
3) Some concepts related to quasi-crystalline phasis. (H+M+P)
4) A two-scale approach to quasi-periodic homogenization. (M)
5) Asymptotic behaviour of the error. (M)
6) Propagating modes in dielectric waveguides. (N)
8) Propagating modes in waveguides mixing metallic and dielectric media. (N)
9) Homogenization of dielectric PCF with metallic boundary. (P)
10) Spectral aymptotic analysis of cavities. (M)
Conclusion.
A) The geometry of electromagnetism. (H+P)
B) Quasi-periodic structures. (M+P)
La frontière entre ces catégories étant perméables, nous espérons que les mathématiciens trouveront quelque intéret à la lecture des chapitres normalement dévolus aux physiciens (P) et que la lecture des chapitres estampillés (H) leur soit ludique. Réciproquement, nous avons mis l'accent sur les rappels des notions mathématiques nécessaires à la lecture des chapitres estampillés (M), pour les lecteurs physiciens.

A remarkable stroke of insight

Numerous mathematicians and physicists had proposed systems of equations for the effects of moving electric charges which had seemed to be satisfactory within the general Newtonian framework. In the Newtonian scheme, the forces of electricity and magnetism (the existence of both having been known since the antiquity, and studied in some detail by William Gilbert in 1600 and Benjamin Franklin in 1752) act in a way similar to gravitational forces in that they also fall off as the inverse square of the distance, though sometimes repulsively rather than attractively, as shown by Coulomb's law. Here, the electric charge (and the magnetic pole stength), rather than the mass, measures the strength of the force. The first scientist to have made a serious challenge to the Newtonian picture seems to have been the English experimentalist and theorician Michel Faraday (1791-1867). Faraday's profound experimental findings (with moving coils, magnet and the like) led him to believe that electric and magnetic fields have physical reality and, moreover, that varying electric and magnetic fields might sometimes be able to push each other along through otherwise empty space to produce a kind of disembodied wave. He conjectured that light itself might consist of such waves. Such a vision would have been at variance with the prevailing Newtonian wisdom, whereby such fields were not thought as real in any sense, but merely convenient mathematical auxiliaries to the true Newtonian point particle action, picture of actual reality. Confronted with Faraday's experimental findings, together with earlier ones by the French physicist André Marie Ampère (1775-1836) and others, and inspired by Faraday's vision, the Scottish physicist and mathematician James Clerk Maxwell (1831-1879) puzzled about the mathematical form of the equations for the electric and magnetic fields that arose from those findings. With a remarkable stroke of insight he proposed a change in the equations, seemingly perhaps rather slight, but fundamental in its implications. This change was not at all suggested by (although it was consistent with) the known experimental facts. It was a result of Maxwell's own theoretical requirements, partly physical, partly mathematical, and partly aesthetic. One implication of Maxwell's equations was

that electric and magnetic fields would indeed push each other along through empty space. An oscillating magnetic field would give rise to an oscillating electric field (this was implied by Faraday's experimental findings), and this oscillating electric field would, in turn, give rise to an oscillating magnetic field (by Maxwell's theoretical inference), and this again would give rise to an electric field and so on. Maxwell was able to calculate the speed that this effect would propagate through space and he found that this would be the speed of light ! Moreover these so-called **electromagnetic waves** would exhibit the interference and the puzzling polarization properties of light that had long been known (see Young and Fresnel). In addition to accounting for the properties of visible light, for which the waves would have a particular range of wavelengths (4 to 7.10^{-7}m), electromagnetic waves of other wavelengths were predicted to occur and to be produced by electric currents in wires. The existence of such waves was established experimentally by the German physicist Heinrich Hertz in 1888. Faraday's inspired hope had indeed found a firm basis in the equations of Maxwell. One of the main differences of the Maxwell's equations compared to the Newtonian framework is that there are field equations rather than particle equations, which means that one needs an infinite number of parameters to describe the state of the system (the field vectors at every single point in space), rather than just the finite number that is needed for a particle theory (three coordinates of position and three momenta for each particle). The so-called Newtonian field was studied in details by Laplace in its famous electrostatic equation $\Delta V = \rho$, where V is the electrostatic potential in a dielectric body and ρ its volumic density of charges. More precisely, denoting respectively by the vector fields $\mathbf{E}$, $\mathbf{B}$, $\mathbf{J}$ and ρ the electric field, the magnetic field, the electric current, and the density of electric charge, Maxwell stated that in *vaccuo* :

$$\begin{cases} \operatorname{rot} \mathbf{B} & = \mu_0 \varepsilon_0 \dfrac{\partial \mathbf{E}}{\partial t} + \mu_0 J \\ \operatorname{rot} \mathbf{E} & = -\dfrac{\partial \mathbf{B}}{\partial t} \\ \operatorname{div} \mathbf{E} & = \dfrac{\rho}{\varepsilon_0} \\ \operatorname{div} \mathbf{H} & = 0 \end{cases} \tag{1}$$

where $\mu_0 \varepsilon_0$ is a constant equal to the inverse of the square of the speed of light usually denoted by c ; This so-called Maxwell's system still holds in material. Because the optical wavelength are very large compared to the atomic scale, we are rather interested in the mean value ($< \mathbf{E} >, < \mathbf{B} >$) : we call this first homogenization process (from the microscopic scale to the mesoscopic one), **natural homogenization**. It is well known that if we assume that the material is constituted of neutral molecules with dipole momenta p_i and charges q_i located at points r_i, we can define a field $\mathbf{D}$ such that :

$$\mathbf{D} = \varepsilon_0 < \mathbf{E} > + \mathbf{P}$$

$$\operatorname{div} \mathbf{D} = \rho_c$$

where $\mathbf{P} = \sum_i p_i \delta(r - r_i)$ is the electric polarization vector and ρ_c is the density of charges of conduction.

Similarly, we define the current of conduction :

$$\mathbf{J}_c = \sum_i < q_i \Big(\frac{\partial r_i(t)}{\partial t} \Big) \delta(r - r_i) >$$

and the magnetic polarization vector :

$$\mathbf{M} = \sum_i < \frac{\mu_0}{2} \Big(\int_{\mathbb{R}^3} (r' - r_i) \times \mathbf{J}(r', t) dr' \Big) \delta(r - r_i) >$$

We therefore have :

$$\mathrm{rot}\, \mathbf{H} = \mathbf{J}_c + \frac{\partial \mathbf{D}}{\partial t}$$

where $\mathbf{H}$ is defined by :

$$\mathbf{H} = \frac{1}{\mu_0} (< \mathbf{B} > - \mathbf{M})$$

In the following, we will always assume that (perfect media) :

$$\mathbf{P} = \varepsilon_0 \chi_e < \mathbf{E} >$$

where χ_e is a positive real called electric susceptibility. We thus have :

$$\mathbf{D} = \varepsilon_0 (1 + \chi_e) < \mathbf{E} > := \varepsilon_0 \varepsilon_r < \mathbf{E} >$$

Analogously, we assume that :

$$\mathbf{M} = \frac{\chi_m}{1 + \chi_m} < \mathbf{B} >$$

where χ_m is a positive real called magnetic susceptibility. We thus have :

$$\mathbf{B} = \mu_0 (1 + \chi_m) < \mathbf{B} > := \mu_0 \mu_r < \mathbf{B} >$$

μ_r and ε_r are functions which can either depend upon the space variable x and the time variable t, respectively called relative permeability and relative permittivity (note that they have no physical dimensions). From now on, we will denote the mesoscopic electromagnetic field $(< \mathbf{E} >, < \mathbf{H} >)$ by $(\mathbf{E}, \mathbf{H})$, because we will consider another homogenization process from the mesoscopic scale to the macroscopic one (artificial homogenization) i.e. we will consider some large optical wavelengths in conjunction with the size of mesoscopic heterogeneities in some specific materials called photonic crystals.

In this thesis, we will assume that μ_r is equal to 1 and ε_r only depends upon the space variable x, except in the first chapter for the homogenization of ferro-magnetic media. In that case, we will assume that μ_r depends upon the space variable i.e. we place our study in the linear approximation for ferro-magnetic materials. It should be noted that fields cannot be regarded as mere mathematical appendages, because Maxwell showed that when the fields propagate as electromagnetic waves they actually carry definite amounts of energy with them. The fact that energy can indeed be transported from place to place by these electromagnetic waves was experimentally confirmed by Hertz's detection of such waves (radio waves). It should also be noted that the presence of $\dfrac{\partial \mathbf{E}}{\partial t}$ in the system (1) was

Maxwell's master stroke of theoretical inference. All the remaining terms in (1) were, in effect known from direct experimental evidence. The constant $\mu_0\varepsilon_0 = \frac{1}{c^2}$ is very tiny, which is why that term had not been experimentally observed [1] : in the nineteenth century, the physicists had access to the electric conductivity σ ($\mathbf{J} = \sigma\mathbf{E}$ for conducting materials for centimeter wavelengths) which is very large, compared to the rate of the electric field pulsation ω over c.

1. It is worth noting that Römer deduced a time delay for light travelling from Jupiter to Earth in 1676 by observing Jupiter's satellites, and Christian Huyghens used Römer's result together with the results of French measurements which established the size of the Solar System, to give the first estimate $3.610^8 m.s^{-1}$ for c. From that time, Fizeau found $c \sim 310^8 m.s^{-1}$ in 1849 and Michelson and Morlay obtained the Nobel Price for proving the isotropy of space together with getting the constant c precisely in 1907.

Introduction

"The remarkable formula, arrived at almost simultaneously by L. Lorenz and H. A. Lorentz, and expressing the relation between refractive index and density, is well known ; but the demonstrations are rather difficult to follow and the limits of application are far from obvious. Indeed, in some discussions the necessity for any limitation at all is ignored. I have thought that it might be worth while to consider the problem in the more definite form which it assumes when the obstacles are supposed to be arranged in rectangular or square order, and to show how the approximation may be pursued when the dimensions of the obstacles are no longer very small in comparison with the distances between them."

Lord Rayleigh (1892) [194].

0.1 Some issues of homogenization theory in electromagnetism

0.1.1 Homogenization of static problems

The philosophy of the necessity for rigour expressed by Lord Rayleigh in 1892 [194] concerning the Lorentz-Lorenz equations acts as the fundation of homogenization. In his paper of 1892, John William Strutt, the third Lord Rayleigh, was able to solve Lapace's equation in two dimensions for rectangular arrays of cylinders, and in three-dimensions for cubic lattices of spheres. As far as we know, the first theoretical works related to homogenization in electromagnetism began with the static effective medium models of Mossotti (1836) and Faraday (1837), which proceeded in a similar way to analyse the distribution of electric charge on several metallic bodies embedded in a dielectric medium. Mossotti's analysis was based on earlier closely related work by Poisson on magnetic media. He analyzed the interaction between the polarizable entities, invoking the first of many cavity considerations in the derivation of the effective field for a dielectric. The english version of the original paper of Mossotti (1896) [158] "Analytical discussion of the influence which the action of a dielectric medium exerts on the distribution of the electricity on the surfaces of several bodies dispersed in it" is explicit. Since Ottavanio Fabrizio Mossotti was made prisoner by the Austrians during the first war for Italian independence (1848-49), his paper which had been submitted in 1846 was only published in 1850. A subsequent step was taken by Lorenz, whose 1869 and 1875 papers in Danish were succeeded by one

in German, in 1880 [132]. In this paper, Lorenz assigns a refractive index to the interior of the molecules which differs from that of the surroundings and then proceeds in a akin to the Coherent Potential Approximation and other modern wave propagation theories in stochastic media. In the presence of the irregularly distributed molecules Lorenz asks for the value of the propagation constant of light such that the deviations from this well behaved *sine* wave average out to zero, and do not build up [131]. Clausius, in his 1879 book [52], assumes, as did Mossotti and Faraday, that the molecules are conducting spheres. He then takes each molecule as contained in a small sphere, cut out of the continuous surrounding medium, which is characterized by the final dielectric constant of the material. In contrast to some of the other derivations, Clausius' sphere fits tightly around the molecule under consideration. In 1870, Lorentz invoked a well-known large sphere cut out of the dielectric, centered about the molecule in consideration, to derive the effective field. The large sphere separates the far away molecules, which can be treated as a continuum, from the close molecules which have to be taken into account more explicitly. The expression for the "macroscopic" electric field in a inhomogeneous media which was derived simultaneously by Lorenz and Lorentz takes the following form :

$$\mathbf{E}_{eff} = \mathbf{E}_{applied} + \frac{1}{\varepsilon_0}\mathbf{P} \tag{2}$$

where ε_0 is the permittivity of free space, and $\mathbf{P}$ is the dipole moment per unit volume. The effective field $\mathbf{E}_{eff}$ is known as the Lorentz field. Lorentz's proof used essentially the spherical shape of the inclusions to replace them by point dipoles. Such a derivation does not hold for a high density of inclusions and there exists more rigorous derivations of the same expressions (Landauer,1972 [126]). Cohen *et al.* even derived an expression of the effective field for ellipsoidal inclusions from that of Lorentz in 1952.

Furthermore, Lorentz derived the following effective dielectric constant ε_{eff} of two-dimensional composite, from (2) :

$$\frac{\varepsilon_{eff} - \varepsilon_m}{\varepsilon_{eff} + \varepsilon_m} = f_i \frac{\varepsilon_i - \varepsilon_m}{\varepsilon_i + \varepsilon_m}$$

where ε_i and ε_m are the dielectric constants of the inclusions and the background material, respectively, and f_i is the volume fraction of the inclusions. The expression is known as Clausius-Mossotti approximation in electrostatics and Lorenz-Lorentz equation in dynamics. In optics, it is referred to as Maxwell-Garnett equation, since J. C. Maxwell-Garnett used Maxwell's equations for propagating waves to derive it in 1904 [136] (note that Maxweel himself derived the formula (2) when the volume fraction of inclusions is small, in his "Treatise on Electricity and Magnetism" [135], whose first edition appeared in 1873). J. C. Maxwell-Garnett derived the expression for the Lorentz field and also arrived at a correction term for the Lorentz-Lorenz equation which depended on the density, or filling fraction, of the inclusions. However, the original proof of Rayleigh suffers a conditionally convergent sum in order to calculate the dipolar field within the array. Many authors proposed extensions of Rayleigh's method to avoid this drawback, amongst them Batchelor (1972). Another limit of Rayleigh's method is that it does not hold when the volume fraction of the inclusions increases : there is a point where there exists a connected path

through the material, along which a current may flow. This phenomenon is known as a percolation threshold. Bruggeman developped two effective medium theories for dielectric materials in 1935-1936 [45]. The first one made a distinction (like previous theories), between the inclusions and the background matrix, whereas the second one exhibited a percolation threshold. His two theories agreed well with the Lorenz-Lorentz equation for the small volume fractions.

An important act in homogenization theory takes place in the ETOPIM congress of 1977, where R. Mc. Phedran and Mc. Kenzie proposed to extend Rayleigh's fundamental work of 1892 [145][141]. At this occasion further developments were discussed with Ping Sheng, Bergman and Milton in relation with new mathematical techniques which appeared one year after in a fundamental book by Bensoussan, Lions and Papanicolaou [18]. The first mathematical results obtained in homogenization were in fact that of Spagnolo (1968). Spagnolo studied elliptic and parabolic problems of diffusion, when the operators were symmetric, and he chose the term of G-convergence to refer to convergence of Green functions [192]. The term of homogenization was first introduced in mathematics by Babuska [15][16]. In the early seventies, Tartar and Murat developed the mathematical tools for homogenization theory. In 1974, Tartar described the notion of weak convergence to link microscopic and macroscopic scales [195] in relation to effective properties in homogenization which were derived heuristically by Sanchez-Palencia [188], thanks to asymptotic expansions for periodic structures. In 1974, Murat refered to the method of H-convergence (H for homogenization) in a seminar he gave in Alger. The H-convergence inspired probabilistic models, such that ones of Papanicolaou and Varadhan [170][171]. Afterwards, Oleinik extended the method to the almost-periodic case and then to the general case.

From this time a great number of papers appeared on homogenization theory in electromagnetism, among them a series of three papers (Mc. Phedran and Mc. Kenzie, 1978 [145][141], Mc. Kenzie *et al* [142], 1978, Perrin *et al* [175], 1979) which extended Rayleigh's technique to arbitrary multiple orders and gave formulae for the conductivity to an arbitrary accuracy. Later, Mc. Phedran, Milton and Poladian provided an effective medium model for arrays of circular inclusions which were both close to touching and highly conducting (1986 [143] [179], 1987 [146] and 1988 [148]) ; Bouchitté and Petit introduced at this time asymptotic methods for the homogenization of gratings ([37], 1985 and [177], 1987).

0.1.2 Homogenization of dynamic problems

In the case of a dynamic problem in a periodic medium, say a periodic arrangement of rods (photonic crystal fiber), the solutions are in general not unique and exist in modes, or energy bands, which are functions of the spatial frequency of the solution. Using the so-called plane wave expansion method allows to satisfy exactly the periodicity conditions, but the boundary conditions on the surface of each cylinder are satisfied only approximatively. It works well in case of low index contrast (weak-coupling assumptions). On the contrary, the so-called Generalized Rayleigh Method, which is inspired of Rayleigh technique for static problems (1892) [194] expands the solution in terms of a set of functions which can be made to satisfy the boundary conditions exactly. The periodicity conditions are then satisfied approximatively, by the appropriate choice of expansion coefficients (Mc. Phedran

and Dawes, 1992 [144], Chin *et al.* 1994 [53], Nicorovicci *et al.*, 1995 [168]). This multiple method has been applied to linear elasticity by Mc. Phedran and Movchan (1994, [147]) who also gave the lattice sum for elastodynamics (Movchan *et al.*, 1997 [159]).

The quoted authors use a dynamic theory to solve Maxwell's equations in a heterogeneous periodic media and then take the long wavelength limit in order to determine the effective properties of the structures. It is noticed by Poulton (Poulton, 1999 [180]), that in doing so, one encounters a problem of definition, in that there is more than one characteristic of the dynamic solution which can be used to define the corresponding effective property. Indeed, there is an ambiguity when one uses the change of phase accross the unit cell to define a phase refractive index, or the reflection coefficient from the exterior surface of the heterogeneous structure, in order to define an amplitude index. Another possibility is also to use the dispersion relation of a particular mode to find a group velocity which defines the group index for waves in the material.

0.1.3 Exact formulae and the theory of bounds

Some mathematical works devoted to the theory of composites go back to Wiener (1912, [207]) by interchanging the roles of background and matrix in the Lorentz-Lorenz formula. A classical theorem is that of Keller (1964) [117] which found a relation between the transverse effective conductivity of an array of cylinders and the conductivity when the phases are interchanged. The essence of Keller's theorem is that if in a 2 dimensional potential problem for Laplace's equation, u is a solution for a problem with one type of inclusion, then its Cauchy-Riemann partner v is the solution for the problem with dielectric constant inverted and the electric field rotated by 90 degrees. In 1970, Dykhne [68], using the fact that a divergence-free field when rotated locally at each point by 90 degrees produces a curl-free field and vice versa, could generalize Keller's result to isotropic multiphase and polycrystalline media. He noted that the duality relations implied exact formulae for the conductivity of phase interchange invariant two-phase media (such as checkerboards) and for polycrystals constructed from a single crystal. In the chapter 2 of the thesis, we get a similar result to that of Keller and Dykhne which expresses the homogenenized permittivity of a two dimensional electrostatic problem in terms of the homogenized inverse permittivity up to a rotation of 90 degrees. In the particular case of a checkerboard i.e. a planar body of square symmetry characterized by a piecewise constant permittivity which takes the values ε_1 and ε_2, it can be then deduced the well known formula [68] :

$$\varepsilon_{eff} = \sqrt{\varepsilon_1 \varepsilon_2}\ .$$

This formula has been generalized by Kozlov in the random case and also the asymptotic behavior of ε_{eff} when ε_1 is small in term of percolation thresholds ([123], 1983). This formula was independently derived by Golden and Papanicolaou ([91], 1983).

The pioneering works of Keller and Dykhne stimulated a large body of research : Berdichevski (1983) [20] derived an exact formula for the effective shear modulus of a checkerboard of two incompressible phases. The duality and phase interchange relations of Berdichevski were extended to anisotropic composite materials by Hesling, Milton and Movchan (1995) [112] together with numerical results of high accuracy. Ni and Nemat-Nasser (1995)

[163] obtained duality transformations for three-dimensional anisotropic bodies with stress and strain fields indepndent of the x_3 coordinate. Milton and Movchan (1995) [155] found an equivalence between planar elasticity problems and antiplane elasticity problems in inhomogeneous bodies. These results and additional duality relations were then discussed in detailed by Hesling, Milton and Movchan (1997[112]). A plethora of three-dimensional exact relations from pyroelectricity to thermopiezoelectric composites has recently been given by Grabovsky, Milton and Sage (2000 [92]).

Besides, when no explicit formulae are available, it is an important matter to have *a priori* estimates on the effective matrix in term of the statistical properties of each component of the composite. This is the so-called theory of bounds which motivated a lot of contributions in several fields of physics, mechanics an mathematics. The pioneering work was done by Hashin and Shtrikman in (1962) [111] where a complete description of all possible effective tensors was derived. This result was proved later by Tartar [196] who extended the result to the anisotropic case. Then a lot of papers appeared in the literature among them we may quote Benveniste (1995) [19] who obtained bound results in piezoelectricity, Francfort (1992) [82] who made a correspondence between the equ ations of incompressible elasticity and the duality relations for conductivity.

The rigorous mathematical theory of the homogenization of elliptic operators with random coefficients proposed by Jikov, Kozlov and Oleinik ([115],1995) is closely related to the Bergman-Milton theory of bounds ([156],1982 and [22], 1992) who obtained some maximal and minimal bounds for the effective properties of fractal structures.

0.2 Synopsis of the thesis

This thesis is divided in three parts. In the first part, we are interested in the asymptotic behaviour of the harmonic Maxwell system when the size of inclusions tends to zero for a fixed given wavelength (in other words, the wavelength is large compared to the distance between dielectric inclusions). In the second part, we consider optical fibers obtained by mixing dielectric and metallic materials, and we implement numerical methods in order to analyze propagating modes in all the range of frequencies. The last part (part III) is devoted to the homogenization of optical fibers and in particular to the asymptotic analysis of spectral properties.

0.2.1 Part I : Homogenization of the Maxwell system

In chapter 1, we consider the homogenization of finite photonic crystals in the periodic case by using multiple-scale expansions. These results are justified mathematically in chapter 2 by using the two-scale convergence method. In chapter 3, we introduce different approaches of quasi-crystalline structures for which we develop in chapter 4 a variant of the two-scale convergence adapted to quasi-periodic structures obtained by the so-called cut-projection method. This enables us to give explicitely the effective limit behaviour of the crystal in term of a unit cell periodic problem which is detailed in the one and two-dimensional cases. A last chapter (chapter 5) is devoted to the estimate of the order of convergence as the size parameter η tends to 0. We expect that, in dimension 1, this order

of convergence lies between that of the periodic case (η) and that of the purely random case ($\sqrt{\eta}$) depending on the irrational character of the slope used in the cut-projection method.

0.2.2 Part II : Discrete models for spectral problems in electromagnetism

Let us now describe the plan of the second part of the thesis. In this part, we use numerical methods (the Finite Element Method) to compute propagating modes in waveguides. Dealing with 2D geometries (problems are described by their cross section), we will focus on waveguides made of regular patterns of rods. This allow us to show homogenization and to determine photonic band gap modes. In the first chapter, we numerically investigate the case of dielectric waveguides i.e. we deal with spectral problems having a continuous spectrum. We give a theoretical criterion to discriminate the bound modes, which is of the foremost importance for the practical use of a numerical algorithm such as the Lanczos algorithm. The model involves no approximation such as the weak coupling and is therefore a three-components vector model. We propose a finite element scheme with edge elements (Nédelec, 1980 [160]) for the transverse component and node elements for the longitudinal component to eliminate the well-known spurious modes (Bossavit, 1990 [30]). Furthermore, we make use of a geometric transformation (Nicolet, 1994 [166]) to deal with the unboundness of the domain (infinite elements). In the second chapter, we focus on metallic waveguides that is bounded problems (and therefore without a continuous spectrum). We choose an electric field formulation to deal with the boundary conditions (the tangential part of the electric field is null, unlike that of the magnetic field on the metallic boundaries). We place our study in the framework of weighted Sobolev spaces to keep self-adjointness properties of the operator. To find the so-called leaky modes in photonic crystal fibers (guided in a central air region), it is necessary to embed the structure in a metallic guide (also called jacket). We give some numerical examples of PCF with metallic exterior boundary, and we take into account the symmetries to study only one quater of the guide. In the third chapter, we study the case of complex structures mixing metallic and dielectric media in open domains. For this, we use both the electric field formulation and the geometric transformation for unbounded domains. It is to be noticed that we can calculate the magnetic current on the metallic boundaries of the structure, because we use a vector model (it would not be the case if we did not take into account the longitudinal part of the electric field). We achieve a numerical treatment of grooved metallic waveguides.

0.2.3 Part III : Asymptotic methods in high frequencies

In the third part of the thesis, we make an asymptotic analysis of spectral problems in both low and high frequency limits. We first investigate the case of the homogenization of Photonic Crystal Fibers (see chapter 9) with a metallic boundary (bounded domain, hence discrete spectrum) thanks to the multi-scale expansion method. We then exhibit birefringence phenomena in an anisotropic homogenized circular waveguide (using the GetDP software), whose tensor of permittivity is derived from the resolution of two annex problems of electrostatic types (solved by the Method of Fictitious Sources). Secondly, we

use a notion of "Bloch wave homogenization" introduced by Allaire and Conca in [5] to perform the asymptotic analysis of Photonic Crystal Cavities in the resonance domain (surface modes coming from photonic band gap effects). We introduce a notion of "two-scale convergence for operators" which allows us to deduce a result of convergence for spectral families of operators, and in particular of the sequence of renormalized spectra (eigenvalues of the order of the square of the medium period) towards the Bloch part of the limit spectrum. We then analyse the so-called boundary layer part of the limit spectrum in the one-dimensional case, by the use of monodromy matrices. Following Allaire and Conca [7][8], we assume that the cavity is filled with an entire number of cells, and we also characterize the boundary layer spectrum thanks to a limit problem settled in the half plane (but with Neumann conditions instead of Dirichlet ones). The originality is that we explicit the discrete part of the boundary spectrum thanks to a new spectral problem settled in $]0;1[$: we show that each eigenvalue of this spectral problem belongs to a different gap and we give the expression of its decrease. Finally, we illustrate this theoretical study by numerical results deduced from this spectral problem.

Première partie

Homogénéisation des structures cristallines et quasi-cristallines finies.

Chapitre 1

Homogenization of finite photonic crystals.

"In the application of our results to the electric theory of light we contemplate a medium interrupted by spherical, or cylindrical, obstacles, whose inductive capacity is different from that of the undisturbed medium. On the other hand, the magnetic constant is supposed to retain its value unbroken. This being so, the kinetic energy of the electric currents for the same total flux is the same as if there were no obstacles, at least if we regard the wave-length as infinitely great."

Lord Rayleigh (1892) [194].

1.1 Concept of homogenization of diffraction

In the last decade, some advances have been made towards a deeper understanding of the optical properties of photonic crystals. Such remarkable structures prohibit the propagation of light, or allow it only in certain directions at certain frequencies, or localize light in specified areas. These materials, which affords us complete control on light propagation, result when a small block of dielectric material is repeated in space. The optical properties of such **photonic crystals** depend on the geometry of the crystal lattice [116, 61, 137, 75, 138, 213, 74, 73]. PC are periodic devices which induce the so-called photonic band gaps just as electronic band gaps exist in semiconductors : light propagation is forbidden for certain frequencies in certain directions. This effect is well known and forms the basis of many devices, including Bragg mirror, dielectric Fabry -Perot filters, and distributed feedback lasers. All of these devices employ low-loss dielectrics that are periodic in one dimension, and are therefore called one-dimensional photonic crystals. However, while such mirrors are tremendously useful, their reflecting properties depend greatly upon the frequency of the incident wave in conjunction with its incidence. In practice, one wishes to reflect light of any polarization at any angle (complete photonic band gap) for some frequency range. This could be achieved with certain structures with periodicity in three dimensions. Such a three dimensional photonic crystal has been engineered by Yablonovitch in 1987 [209]. The recent thrust in this area is partly fueled by advances in theoretical

techniques, based on Fourier expansions in the vector electromagnetic Maxwell equations [57], [108], which allow non prohibiting computations. This plane wave expansion method is by far the most popular theoretical tool employed for studying the photonic band gap problem. In this thesis, we adopt another point of view, based on asymptotic analysis techniques which have been used for a long time as applied to many problems of mechanic or electrostatic types [18]. Following the works of G.Bouchitté, R.Petit and D.Felbacq [37], [177], [72] , we adapt these classical methods to electromagnetism for "three-dimensional finite periodic" structures.

At an atomic scale, matter behaves as if it were highly heterogeneous, but experience shows that it can frequently be treated as being homogeneous. Indeed, microscopic inhomogeneities can smooth at a macroscopic scale (fluid aspect of fine sand...). At first glance, one can say that there are two kinds of inhomogeneities : the first ones of a periodic type (such as photonic crystals) and the others of a random type (such as amorphous glass).

In this thesis, we will deal with photonic structures, but it seems possible to adapt the results to the stochastic case : roughly speaking, the period is changed in the mean distance between the scatterers. The incoming wave "averages" the microscopic asperities (microscopic in regard with its wavelength) whenever they are randomly or periodically arranged, provided that one makes the assumption that the obstacle is densely filled. Indeed the incident wave "sees" the average of the asperities.

Hence, we consider a structure of constant permeability μ_0 (permeability in vaccum) illuminated by a monochromatic wave, whose wavelength λ is large in comparison with typical heterogeneity sizes. Consequently **the wavelength is large compared to the period η of the medium**. Using these hypotheses, our goal is to replace the photonic crystal by an equivalent homogeneous structure having analogous electromagnetic properties.

Thanks to our formalism, **we can treat three-dimensional structures of arbitrary shape Ω_f having a piecewise continuous complex valued permittivity. Such hypotheses cover the physical domains of application**. In the sequel, we will pay special attention to the case where the permittivity is a piecewise constant function. Such a function describes the inclusions in the scattering object we are studying. These inclusions are usually called scatterers. It is worth noting that a scatterer can possibly touch the sides of the basic cells ; for instance, this allows us to study compact cubic structures such as face-centered cubic and simple cubic ones (fig. 1.1) or the well-known "Yablonovite" [209], [116], [61]. Moreover, when the number of scatterers is great, and when they are very small with regard to the wavelength, one can expect the structure to become homogeneous : that is to say that the scattering object behaves as if it were made of a homogeneous material with a permittivity usually called effective permittivity by physicists.

From a theoretical point of view, one can only hope to obtain relevant results when the number of scatterers is infinite. Therefore, there are two ways of tackling this problem : the old one used by most of people, consists in assuming that the size of the scatterers is fixed, while the obstacle filled up by these scatterers is increasing until it covers the overall space $\mathbb{R}^3$, and the wavelength goes to infinity. It is a useful method in solid state physics, since it enables physicists to use the powerful tools of Bloch Wave Decomposition. The main

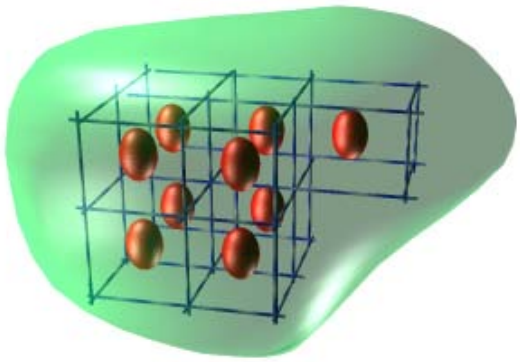

FIGURE 1.1 – Homogenization of a photonic crystal made of ellipsoidal scatterers. The grid of dotted lines defines a virtual "scaffolding" Ω_η of the whole obstacle Ω_f. For the sake of simplicity, we give an example with η near to 1, i.e. with a small number of rather big scatterers (here 9). The reader has to imagine the same body (Ω_f) filled with a great number of scatterers (on the order of 1000) of small size (η near to 0).

drawback of this method, when applied to electromagnetism, is that the diffraction problem does not make sense anymore at the limit. In fact, the incident field is then confined to the complement of the overall space, and it is of null pulsatance ! Nevertheless, as was discussed in the introduction of the thesis, the advantage of this method is that it gives information for every size of wavelength : one can therefore "homogenize" the PC even in the resonance domain (Gralak *et al.*, 2000 [94]). On the contrary, if one considers that the obstacle and the wavelength remain fixed, while the size of scatterers goes to zero and their number to infinity, the boundary of the obstacle still has an influence in this limit, and one can still speak of incident wave. This process is much more complicated to perform than the first one, but the results it provides are closer to physical reality.

Homogenization techniques used in this thesis, namely homogenization of diffraction, allow us to study structures of practical interest, for wavelengths large compared to the size of the scatterers of the obstacle. We achieve proofs by using the so-called two-scale convergence method [2] and, to be more precise, find what is generally called the effective permittivity of the homogeneous object. This depends upon a local problem arising in the crystal lattice unlike that one of solid state physics which takes place in the first Brillouin zone. Contrary to the effective permittivity given by the method of Bloch waves decomposition, our permittivity also depends upon a global problem which takes into account the boundary conditions. This work is actually an extension of those performed in the 2D scalar cases (TE and TM) by D.Felbacq and G.Bouchitté ([72], 1997), who were among the pioneers in the homogenization of diffraction.

In the context of interferometric experiments, one will be concerned with the phase change of an electromagnetic wave as it crosses the composite material. In this latter context, **homogenization using the Bloch Theorem in the long wavelength**

limit is perfectly reasonnable physically and can be carried out in a rigorous mathematical fashion ([151], 1996).

1.2 Set up of the problem

From now on, assuming a time dependance in $e^{-i\omega t}$, we will deal with time harmonic Maxwell equations.

For this study, we have to consider objects of opposite natures : the first ones are purely geometrical and the others physical.

The first approach is a geometrical description of the obstacle, which lies in a fixed domain Ω_f not necessarily simply connected. Furthermore, although our study only deals with the bounded case, it remains relevant for Ω_f infinite in one (fig. 1.2) or two directions (fig. 1.3). In such cases, one just has to adapt the study with "ad hoc" outgoing wave conditions (as for gratings, the reader may refer to [152]).

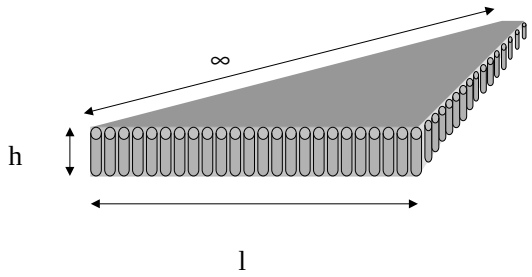

FIGURE 1.2 – Band of finite parallel rods seen as a three-dimensional photonic crystal infinite in one dire

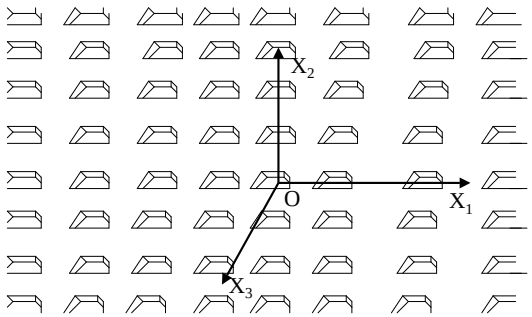

FIGURE 1.3 – Bi-grating seen as a three-dimensional photonic crystal bounded in the x_3 axis.

The second approach (a physical one) describes the optical characteristics of the material illuminated by the electromagnetic wave.

Let us begin by the geometrical description of the objects involved in our study.

Let (O, x_1, x_2, x_3) be a Cartesian coordinates system of axes of origin O, $\mathbf{i} = (i_1, i_2, i_3)$ a multi-integer of $\mathbb{Z}^3$ and η a small positive real. Let $Y =]0;1[^3$ be a basic cell, and $\tau_i\, Y$ be the translation of Y by the vector $\mathbf{i}$:

$$\tau_i(Y) =]i_1, i_1+1[\times]i_2, i_2+1[\times]i_3, i_3+1[= Y + \mathbf{i}$$

Let us design by η $(\tau_i Y)$ the homothety on $\tau_i Y$ of ratio η : thus we form a box of size η and center $\eta\mathbf{i}$ (fig. 1.4).

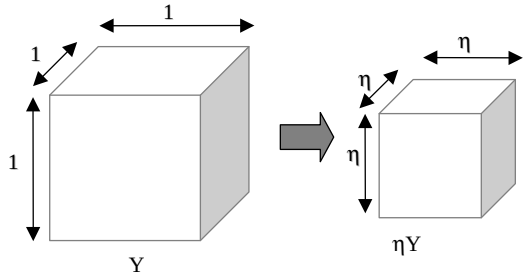

FIGURE 1.4 – The elementary cell of the photonic crystal is the homothety on a unit cell of ratio η.

Under such considerations, one can now define a "scaffolding" Ω_η of Ω_f in the following manner : Ω_η is defined as the greatest union of boxes of size η which is entirely enclosed in Ω_f and whose fineness is controlled by η. More precisely, the finer the scaffolding (the smaller the η), the better the imitation (fig. 1.5). Obviously, as we wish to "build up" Ω_f, the number N_η of cells depends upon η, since it corresponds the following equivalence :

$$N_\eta = \frac{meas(\Omega_\eta)}{\eta^3} \simeq \frac{meas(\Omega_f)}{\eta^3}$$

where $meas(\Omega_\eta)$ and $meas(\Omega_f)$ respectively denotes the measure (volume) of Ω_η and Ω_f.

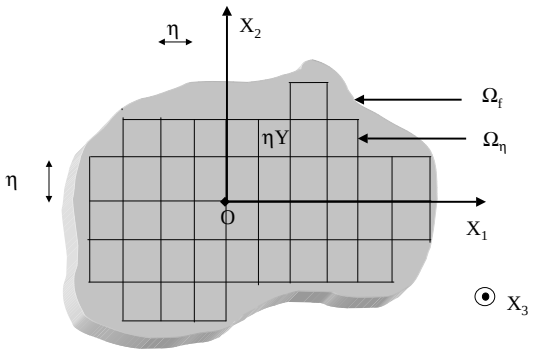

FIGURE 1.5 – The process of homogenization consists in a periodic arrangement of rescaled unit cells, forming a succession of "scaffoldings" Ω_η entirely enclosed in the diffracting object Ω_f.

We can now start the description of the physical problem we are interested in.

Let us define what we will call up to the end a Scattering-Box (SB) : we note B an obstacle merely defined by its relative permittivity $\varepsilon_r^B(\mathbf{x})$:

$$\forall \mathbf{x} \in \mathbb{R}^3,\ \varepsilon_{\mathbf{r}}^{\mathbf{B}}(\mathbf{x}) = \mathbf{1} - \chi_{\mathbf{Y}} + \chi_{\mathbf{Y}}\ \tilde{\varepsilon}_{\mathbf{r}}(\mathbf{x})\ ,$$

with χ_Y the characteristic function of Y (i.e. $\chi_Y = 1$ when $x \in Y$ and $\chi_Y = 0$ elsewhere) and where $\tilde{\varepsilon}_r(\mathbf{x})$ is a given piecewise continuous complex valued function, which denotes the relative permittivity in the overall physical space. By analogy with the geometrical study developed above, we define $\tau_i B$, η $(\tau_i B)$ and B_η. Thus, as η goes to 0, we build up a sequence of three-dimensional bounded structures B_η made of a periodic arrangement of an increasing number N_η of identical SB of decreasing size, whose global shape Ω_η tends to Ω_f.

For each obstacle B_η, we can define a total field $F_\eta = (E_\eta, H_\eta)$, corresponding to the field generated by the N_η SB when they are illuminated by a given incident monochromatic wave of wavelength λ. As explained above, our purpose is to make clear the behavior of F_η when η goes to zero. In other words, we try to understand the electromagnetic behavior of our set of SB when their size tends to zero and their number to infinity. It is obvious that for all $\mathbf{x}$ in Ω_η, $\varepsilon_r^{B_\eta}(\mathbf{x}) = \varepsilon_{\mathbf{r}}^{\mathbf{B}}(\frac{\mathbf{x}}{\eta})$, where ε_r^B is a Y-periodic complex valued function in Ω_f such that $0 \leq arg(\varepsilon) < \pi$ i.e. Re $(i\varepsilon) \leq 0$. **Hence, unlike most of the articles dealing with solid state physics, we do not assume periodicity of ε_r^B in the overall space $\mathbb{R}^3$.**

Moreover, let us note the relative permittivity at every point $\mathbf{x} \in \mathbb{R}^{\mathbf{3}}$ by $\varepsilon_\eta(\mathbf{x}) = \tilde{\varepsilon}(\mathbf{x}, \frac{\mathbf{x}}{\eta})$, with

$$\tilde{\varepsilon}(\mathbf{x}, \mathbf{y}) = \begin{cases} 1 & , \text{ if } \mathbf{x} \in \Omega_\eta^c \\ \varepsilon_r^{B_\eta}(\mathbf{y}) & , \text{ if } \mathbf{x} \in \Omega_\eta \end{cases}$$

where Ω_η^c denotes the complementary of the obstacle in the overall space $\mathbb{R}^3$ i.e. $\mathbb{R}^3 \backslash \bar{\Omega}_\eta$.

This is the crucial point of our discussion : unlike ε_r^B, this function can be seen as a Y-periodic function of the y variable (which continuously depends on its variable x). Therefore, we can introduce $(\mathbf{E}_\eta^d, \mathbf{H}_\eta^d)$ the diffracted field (which only makes sense outside the structure) deduced from the incident field $(\mathbf{E}^i, \mathbf{H}^i)$ illuminating the structure by $(\mathbf{E}_\eta^d, \mathbf{H}_\eta^d) = (\mathbf{E}_\eta, \mathbf{H}_\eta) - (\mathbf{E}^i, \mathbf{H}^i)$. It is worth noting that we can rigorously define the diffracted field, since the structure does not cover the overall space, which emphasizes the importance of its boundary. Thus by defining the complex wave number k_0 as $k_0 = \omega(\varepsilon_0 \mu_0)^{\frac{1}{2}}$, we obtain the following problem of electromagnetic scattering :

$$\mathcal{P}_\eta = \begin{cases} (1)\ \text{rot}\, \mathbf{E}_\eta + i\omega\mu_0 \mathbf{H}_\eta = 0 \\ (2)\ \text{rot}\, \mathbf{H}_\eta - i\omega\varepsilon_0\varepsilon_\eta \mathbf{E}_\eta = 0 \\ (SM1)\ \mathbf{H}_\eta^d = O(\frac{1}{|\mathbf{x}|}),\ \mathbf{E}_\eta^d = O(\frac{1}{|\mathbf{x}|}) \\ (SM2)\ k_0 \mathbf{E}_\eta^d + \omega\mu(\frac{\mathbf{x}}{|\mathbf{x}|} \wedge \mathbf{H}_\eta^d) = o(\frac{1}{|\mathbf{x}|}) \end{cases}$$

where $(SM1), (SM2)$ denote the outgoing wave conditions of Silver-Müller type, which play a fundamental role by insuring existence and uniqueness of the solution of $\mathcal{P}_\eta$ (see for example Cessenat [51]).

Of course, equations (1) and (2) of the above system make sense when assuming that $\mathbf{E}_\eta$ and $\mathbf{H}_\eta$ and all their derivatives are taken in the sense of distributions in the overall space $\mathbb{R}^3$. The radiation conditions are relevant in $C^\infty(\mathbb{R}^3 \setminus \bar{\Omega}_\eta)$. That is to say, $\mathbf{E}_\eta$ and $\mathbf{H}_\eta$ are continuous, as all their derivatives outside the obstacle (this is a consequence of the

Helmholtz equation arising outside the obstacle, which induces analiticity of the diffracted electromagnetic field). From now on, we will always assume these hypotheses.

If we take the curl of the former equations we then have two similar problems :

$$(\mathcal{P}_\eta^E)\begin{cases} (1^E)\ \operatorname{rot}\operatorname{rot}\mathbf{E}_\eta - k_0^2\varepsilon_\eta\mathbf{E}_\eta = 0 \\ (SM1^E)\ \mathbf{E}_\eta^d = O(\frac{1}{|\mathbf{x}|}) \\ (SM2^E)\ \frac{\mathbf{x}}{|\mathbf{x}|}\wedge\operatorname{rot}\mathbf{E}_\eta^d + ik\mathbf{E}_\eta^d = o(\frac{1}{|\mathbf{x}|}) \end{cases}$$

$$(\mathcal{P}_\eta^H)\begin{cases} (1^H)\ \operatorname{rot}\Big({\varepsilon_\eta}^{-1}\operatorname{rot}\mathbf{H}_\eta\Big) - k_0^2\mathbf{H}_\eta = 0 \\ (SM1^H)\ \mathbf{H}_\eta^d = O(\frac{1}{|\mathbf{x}|}) \\ (SM2^H)\ \frac{\mathbf{x}}{|\mathbf{x}|}\wedge\operatorname{rot}\mathbf{H}_\eta^d + ik\mathbf{H}_\eta^d = o(\frac{1}{|\mathbf{x}|}) \end{cases}$$

At this point, let us note that it appears much more difficult to perform the study of the problem $\mathcal{P}_\eta^E$ than the one of the problem $\mathcal{P}_\eta^H$: the magnetic field $\mathbf{H}_\eta$ is divergence free, in contrast with the Electric field for which $\operatorname{div}\mathbf{E}_\eta$ behaves like $\dfrac{1}{\eta}$. Indeed, taking the divergence in the second equation in $\mathcal{P}\eta$, we obtain $\operatorname{div}(\varepsilon_\eta\mathbf{E}_\eta) = 0$ which implies that $\operatorname{div}\mathbf{E}_\eta = -\dfrac{\bigtriangledown\varepsilon_\eta}{\varepsilon_\eta}\mathbf{E}_\eta \sim -\dfrac{\bigtriangledown y\varepsilon}{\eta\varepsilon}\mathbf{E}_\eta$. The behavior of the gradient of $\mathbf{E}_\eta$ being related to the ones of the divergence and the curl of $\mathbf{E}_\eta$, it implies strong oscillations for the gradient of the electric field $\mathbf{E}_\eta$.

Hence, in the rest of the study we will exclusively deal with $\mathcal{P}_\eta^H$. Taking into account that $\mathbf{E}_\eta = \dfrac{i}{\omega\varepsilon_0\varepsilon_\eta}\operatorname{rot}\mathbf{H}_\eta$ (from equation (2)), we will come back to the couple $(\mathbf{E}_\eta, \mathbf{H}_\eta)$, solution of the initial problem $\mathcal{P}_\eta$ by taking the curl of $\mathbf{H}_\eta$, solution of the problem $\mathcal{P}_\eta^H$.

To conclude this introduction, let us recall that in this thesis, we will only pass to the limit on the problem $(\mathcal{P}_\eta^H)$, for the reason explained above. Furthermore, we will show in which sense the field $\mathbf{H}_\eta$ tends to a field $\mathbf{H}_{hom}$, solution of the so-called homogenized diffraction problem $(\mathcal{P}_{hom}^H)$, whose resolution leads to an annex problem of electrostatic type which will be explained further.

It is worth noting that we then let the conductivity tend to infinity in the homogenized problem to modelize a problem of scattering by a finite size photonic crystal filled with small metallic inclusions : we consider a static problem on a basic cell with an highly conducting inclusion and we then take the limit when the refractive index of the inclusion tends to infinity. On the other hand, one can consider a body filled with perfectly conducting inclusions and then take the static limit when the incident wavelength tends to infinity. The answers in these two cases are different [181]. More precisely, if one consider a trajectory in the coordinates (frequency,inverse of conductivity), then the result will depend on this trajectory in the vicinity of the origin. Since there is a unique solution to the problem of diffraction by a photonic crystal with perfectly conducting inclusions, there is a physical subtlety which was addressed in [181]. in the two-dimensional case, one considers Dirichlet or Neumann boundary conditions depending upon the polarization [72]. In the 3D case, one just has the nullity of the tangential trace of the electric field (the tangential trace of the magnetic field gives the surface current) and it sounds reasonable to choose the electric field as unknown (even if it is not divergence free). We refer for that case to recent works by G. Bouchitté and D. Felbacq [33].

1.3 Asymptotic analysis

The main idea underlying our asymptotic analysis is to select two scales in the study : a microscopic one (the size of the basic cell) and a mesoscopic one (the size of the whole obstacle of shape Ω_f). From a physical point of view, one can say that the modulus of the incident field is forced to oscillate like the permittivity in the illuminated periodic structure. In fact, the smaller the size η of the SB, the faster the modulus of the field F_η oscillates. Hence, we suppose that $\mathbf{H}_\eta$, solution of the problem $\mathcal{P}_\eta^{\mathbf{H}}$ has a two-scale expansion of the form :

$$\forall \mathbf{x} \in \Omega_f, \;\; \mathbf{H}_\eta(\mathbf{x}) = \mathbf{H}_0(\mathbf{x}, \frac{\mathbf{x}}{\eta}) + \eta \mathbf{H}_1(\mathbf{x}, \frac{\mathbf{x}}{\eta}) + \eta^2 \mathbf{H}_2(\mathbf{x}, \frac{\mathbf{x}}{\eta}) + ...$$

where $\mathbf{H}_i : \Omega_f \times Y \longmapsto \mathbb{C}^3$ is a smooth function of 6 variables, independent of η, such that $\forall \mathbf{x} \in \Omega_f$, $\mathbf{H}_i(\mathbf{x}, \cdot)$ is Y-periodic.

Our goal is to characterize the electromagnetic field when η tends to 0. If the coefficients $\mathbf{H}_i$ do not increase "too much" when η tends to 0, the limit of $\mathbf{H}_\eta$ will be $\mathbf{H}_0$, a rougher approximation to $\mathbf{H}_\eta$. Hence, we make the assumption that for all $\mathbf{x} \in \mathbb{R}^3$, $\mathbf{H}_i(\mathbf{x}, \frac{\mathbf{x}}{\eta}) = o(\frac{\mathbf{x}}{\eta^i})$, so that the expansion (also denoted by the german word "ansatz") still makes sense in neighbourhood of 0. If the above expansion is relevant, we can state the following fundamental result :

Theorem 1 *When η tends to zero, $\mathbf{H}_\eta$ solution of the problem $(\mathcal{P}_\eta^H)$, converges (for the norm of energy on every compact subset of $\mathbb{R}^3$) to the unique solution $\mathbf{H}_{hom}$ of the following problem $(\mathcal{P}_{hom}^{\mathbf{H}})$:*

$$(\mathcal{P}_{hom}^{\mathbf{H}}) = \left\{ \begin{array}{l} \mathrm{rot}(\varepsilon_{hom}^{-1}(\mathbf{x}) \mathrm{rot}\, \mathbf{H}_{hom}(\mathbf{x})) - k_0^2 \mathbf{H}_{hom}(\mathbf{x}) = 0 \\ \mathbf{H}_{hom}^d(\mathbf{x}) = O(\frac{1}{|\mathbf{x}|}) \\ \frac{\mathbf{x}}{|\mathbf{x}|} \wedge \mathrm{rot}\, \mathbf{H}_{hom}^d(\mathbf{x}) + ik \mathbf{H}_{hom}^d(\mathbf{x}) = o(\frac{1}{|\mathbf{x}|}) \end{array} \right.$$

With

$$\left\{ \begin{array}{ll} \varepsilon_{hom}(\mathbf{x}) = < \tilde{\varepsilon}(\mathbf{x}, \mathbf{y})(I - \bigtriangledown_{\mathbf{y}} \mathbf{V}_Y(\mathbf{y})) >_Y & , in\ \Omega_f \\ \varepsilon_{hom}(\mathbf{x}) = 1 & , in\ \Omega_f^c \end{array} \right.$$

Where $< f >_Y$ and $\tilde{\varepsilon}(\mathbf{x}, \mathbf{y})$ respectively denote the average of f in Y (i.e. $\int_Y f(x, y)\, dy$) and

$$\tilde{\varepsilon}(\mathbf{x}, \mathbf{y}) = \left\{ \begin{array}{ll} 1 & , \; if\ \mathbf{x} \in \Omega_f^c \\ \varepsilon_r^B(\mathbf{y}) & , \; if\ \mathbf{x} \in \Omega_f \end{array} \right.$$

Besides, $\mathbf{V}_Y = (V_1, V_2, V_3)$, where V_j , $j \in \{1, 2, 3\}$ is the unique solution in $H_\sharp^1(Y)/\mathbb{R}$ (that is to say that V_j are defined up to an additive constant in the Hilbert space of Y-periodic functions $H_\sharp^1(Y)$) of one of the three following problems $(\mathcal{K}_j)$ of electrostatic type :

$$(\mathcal{K}_j) : -\mathrm{div}_{\mathbf{y}} \Big[\varepsilon_r^B(\mathbf{y})(\bigtriangledown_{\mathbf{y}}(V_j(\mathbf{y}) - y_j)) \Big] = 0 \;, j \in \{1, 2, 3\}$$

Roughly speaking, as η tends to zero, we can replace the isotropic heterogeneous diffracting obstacle of shape Ω_η, by an anisotropic homogeneous obstacle of shape Ω_f (fig. 1.6). In other terms, the effective permittivity is given as follows.

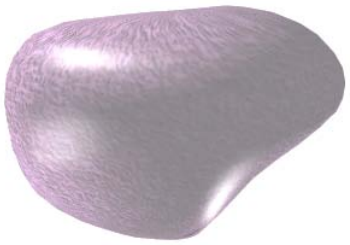

FIGURE 1.6 – The result of the process of homogenization is a finite homogeneous anisotropic object.

Developed form for the matrix of effective permittivity

The relative permittivity matrix of the homogenized problem is equal to :

$$\varepsilon_{hom} = \begin{pmatrix} < \varepsilon_r^B(\mathbf{y}) >_Y & 0 & 0 \\ 0 & < \varepsilon_r^B(\mathbf{y}) >_Y & 0 \\ 0 & 0 & < \varepsilon_r^B(\mathbf{y}) >_Y \end{pmatrix} - \begin{pmatrix} \varphi_{11} & \varphi_{12} & \varphi_{13} \\ \varphi_{21} & \varphi_{22} & \varphi_{23} \\ \varphi_{31} & \varphi_{32} & \varphi_{33} \end{pmatrix}$$

where φ_{ij} represent corrective terms defined by :

$\forall i,j \in \{1,2,3\}$, $\varphi_{ij} =< \varepsilon_r^B \frac{\partial V_j}{\partial y_i} >_Y =< \varepsilon_r^B \frac{\partial V_i}{\partial y_j} >_Y = - < \varepsilon_r^B \bigtriangledown V_i \cdot \bigtriangledown V_j >_Y$

the brackets denoting averaging over Y, and V_j being the unique solutions in $H^1_\sharp(Y)/\mathbb{R}$ of the three partial differential equations $\mathcal{K}_j$ (fig.1.7). Hence, thanks to the symmetry of the matrix on the right ($\varphi_{ij} = \varphi_{ji}$), the homogenized permittivity is given by the knowledge of six terms φ_{ij}, depending upon the resolution of three annex problems $\mathcal{K}_j$.

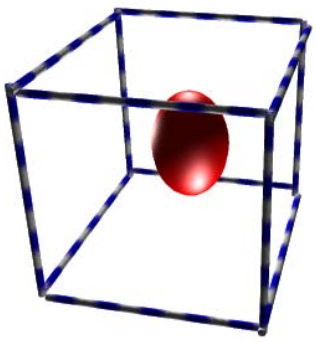

FIGURE 1.7 – Basis cell Y with an ellipsoidal scatterer.

Proof of the corollary

As for the homogenized permittivity, $\bigtriangledown_y \mathbf{V}_Y$ denoting the Jacobian matrix $\frac{\partial V_j}{\partial y_i}$ of $\mathbf{V}_Y$, ε_{hom} clearly derives from the equation of the theorem.

Multiplying $\mathrm{div}_y(\varepsilon \bigtriangledown_y (V_i - y_i))$ by V_j, $j \in \{1,2,3\}$, and integrating by parts over the basic cell Y leads to :

$$\left\langle \varepsilon_r^B(\mathbf{y})(\bigtriangledown_y(V_i - y_i)) \cdot \bigtriangledown V_j \right\rangle_Y = 0 \, .$$

Therefore, we get the equality :

$$\begin{aligned} \varphi_{ij} &= < \varepsilon_r^B \frac{\partial V_i}{\partial y_j} >_Y \\ &= - < \varepsilon_r^B \bigtriangledown V_i \cdot \bigtriangledown V_j >_Y \\ &= < \varepsilon_r^B \frac{\partial V_j}{\partial y_i} >_Y \quad ,i \text{ and } j \text{ playing a symmetrical rôle} \end{aligned}$$

Hence, we derive that $\varphi_{ij} = \varphi_{ji}$.

Comments on the theorem 1 :

Our purpose is to study the behavior of the electromagnetic field $\mathbf{F}_\eta = (\mathbf{E}_\eta, \mathbf{H}_\eta)$ in order to answer the following question : does this function converge, in some sense which remains to be cleared up, to some function $\mathbf{F}_0$? If so, is it possible to characterize $\mathbf{F}_0$ as solution of the problem of diffraction of incident wave $\mathbf{F}^i$ by a certain structure which we are able to give "clearly" ? This is done in the next chapter using a notion of two-scale convergence [2] for the convergence of the field in the photonic crystal together with considerations on the convergence of the diffracted field outside the photonic crystal, which have been successfully applied, among others, by G.Bouchitté and R.Petit in the electromagnetic theory of gratings [37][177] and by G.Bouchitté and D.Felbacq in the case of a two-dimensional finite photonic crystal [72]. Let us briefly outline this asymptotic approach.

Forgetting physics for a while, let us consider the Hilbert space

$$H(\mathrm{rot}, \Omega_f) = \left\{ v \in L^2(\Omega_f) \, , \, \mathrm{rot}\, v \in L^2(\Omega_f) \right\} ,$$

and its Hilbert subspace

$$H^1(\Omega_f) = \left\{ v \in L^2(\Omega_f) \, , \, \bigtriangledown v \in L^2(\Omega_f) \right\} .$$

It is well-known, in functional analysis [51], that the Hilbert space $H^1(\Omega_f)$ has got a behavior close to $H^1(\mathrm{rot}, \Omega_f)$'s provided one gets some control on the divergence in $L^2(\Omega_f)$ norm and on the trace on $\partial\Omega_f$. In fact, if we want to control the gradient of a function in $L^2(\Omega_f)$, we just have to keep controlling its curl and divergence in $L^2(\Omega_f)$. That is to say that the vectorial aspect of the diffraction by three dimensional photonic structures appears in the decomposition of the gradient on its tangential (curl) and normal (divergence) components. Our battle plan is then to get enough information on the curl and on the divergence of the field to realize a study similar to the one of the two-dimensional case [72]. It is for this reason that we will give preference to the study of the magnetic field $\mathbf{H}_\eta$, whose divergence vanishes in Ω_f, in contrast with $\mathbf{E}_\eta$.

Let us first assume that, for physical reasons, the electromagnetic field of each problem $\mathcal{P}_\eta$, namely $\mathbf{F}_\eta = (\mathbf{E}_\eta, \mathbf{H}_\eta)$ is locally of finite energy. In mathematical terms, it means that for all η, $\mathbf{F}_\eta$ is locally square integrable, that is to say that :

$\forall \eta > 0\ , \exists M_\eta > 0\ ,\ \int_{\Omega_f} |\ \mathbf{E}_\eta\ |^2\ dx + \int_{\Omega_f} |\ \mathbf{H}_\eta\ |^2\ dx \leq M_\eta$

The proof of the next chapter, based upon this hypothesis, is rather subtle and proceeds in two steps : in step 1, we assume $(\mathbf{H}_\eta)$ to be uniformly bounded in $L^2(\Omega_f)$, thanks to a notion of two-scale convergence, we deduce some important results allowing us notably to determine completely the limit function H_0, thanks to the two-scale convergence. In step 2, assuming $\mathbf{H}_\eta$'s boundedness in $L^2(\Omega_f)$ for a given η, using a *reductio ad absurdum* method and theoretical results obtained in step 1, we prove that $(\mathbf{H}_\eta)$ is actually uniformly bounded in $L^2(\Omega_f)$.

Remark on the convergence of the permittivity

It is worth noting that we cannot expect a nice convergence for the sequence of permittivities ε_η. Indeed, ε_η is proportional to the identity matrix, hence characterizes an isotropic medium, unlike its limit which characterizes an anisotropic medium. It is a typical difficulty encountered in many homogenization problems (ε_η is just bounded which implies bad convergence properties for $\varepsilon_\eta \operatorname{rot} H_\eta$). Hence, there is no hope to get control on the convergence of the diffracted field, by means of volume integral equations[204].

In fact, it is to be understood that in both mathematical and physical aspects in homogenization of diffraction, the good parameter is the diffracted field. Hence, our goal is to show in what sense does the electromagnetic field $\mathbf{F}_\eta = (\mathbf{E}_\eta, \mathbf{H}_\eta)$ converge towards the first term of its asymptotic expansion, and to be more precise to verify that the limit field $\mathbf{F}_{hom}$ is still solution of a diffraction problem. This can be done, thanks to the Stratton-Chu formula, which assures that we only have to control the restriction of the electromagnetic field on the boundary of the lit body to keep control on the field in the overall space. Here is the main difficulty of the homogenization of diffraction of three-dimensional finite structures : the divergence of the sequence of electric-fields goes to infinity, hence we cannot easily keep controlling $\mathbf{F}_{\eta|\partial\Omega_f}$. Therefore, we consider a ball strictly including the obstacle. By the knowledge of the convergence of the diffracted field on the boundary of the ball, we deduce the convergence of the diffracted field outside the obstacle, thanks to the Stratton-Chu formula. Let us recall that there is no alternative way to achieve the proof by means of volume integral equations[204].

To conclude this paragraph, we want to point out that the main problem of homogenization of diffraction comes from the strong oscillations of the electromagnetic field near the interior boundary of the obstacle. Mathematically speaking, unlike physicists of solid state physics who consider an obstacle whose boundary is going to infinity, we deal with global problems : the boundary of the obstacle remaining fixed, its influence is still sensible at the limit.

1.4 Practical application

In most applications, one has just to consider a two valued piecewise constant permittivity in the unit cell Y and more precisely, the relative permittivity yields ε_r in what we will

call, from now on, the scatterer S and 1 elsewhere. It is the case, for instance, of the structures studied by E. Yablonovitch [209]. Consequently, the problem we are dealing with is only defined by a complex number ε_{scat} and the shape of the scatterers $\Omega_S = Supp\{\varepsilon_r - 1\}$ (in other words, the scatterers lie in the volume area, support of the above function). It is worth noting that one can give many shapes to S, except the ones with very irregular boundaries : this covers most of the structures encountered in physics (cubic compact structures, Yablonovite...). Before going further, it is worth noting that the limit behavior of the complex permittivity ε_η of the set Ω_η is crucially related to the limit filling ratio of the elementary cells :

$$\theta = \lim_{\eta \to 0} \frac{meas(f(\eta)\Omega_S)}{\eta^3}$$

where $meas(f(\eta)\Omega_S)$ denotes the volume occupied by the homothety on Ω_S of ratio $f(\eta)$ i.e. $f(\eta)\Omega_S$ in Y_η (fig. 1.8). Indeed, when θ equals zero the scatterers "disappear" when η tends to 0, and the effective medium is completely transparent (e.g. $f(\eta) = \eta^2$).

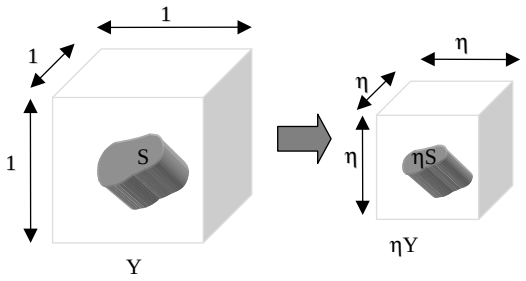

FIGURE 1.8 – The elementary cell of the three-dimensional photonic crystal's lattice results of a homothety of ratio η over a unit cell.

On the contrary, the structure becomes homogeneous (but not invisible) at the limit when $\theta \neq 0$ i.e. when $f(\eta) = \eta$ (if the reader wants to convince himself from this remark, he just has to make an expansion (ansatz) with functions $H_i(x, \frac{x}{\eta^\alpha})$, $\alpha > 1$).

This remark seems trivial at first glance, but one has to be careful with the behavior of the structure in the case where it is filled up by infinite conducting scatterers. Indeed, having regard to the theoretical results obtained by D.Felbacq and G.Bouchitté in [72], in the two-dimensional case, we can see that, even if θ equals zero, (the scatterers therefore vanish at the limit), their influence is still sensible on the effective medium. In [210][186][211], some numerical computations have been made to illustrate this phenomena in case of arrays of infinite conducting elliptical cylinders.

In daily experiments, scatterers are made of one isotropic material characterized by a permittivity ε_{scat} (fig. 1.9). Then, for every point $\mathbf{x} \in \mathbb{R}^3$, the permittivity is defined by :

$$\tilde{\varepsilon}_\eta(\mathbf{x}) = \varepsilon_{scat} \text{ ,if } \mathbf{x} \in \eta\Omega_S \text{ , } \tilde{\varepsilon}_\eta(\mathbf{x}) = 1 \text{ if } \mathbf{x} \notin \eta\Omega_S$$

where ε_{scat} is a bounded function, supposed to be $Y-$ periodic with :

$$\mathcal{R}e(\varepsilon_{scat}(y)) > 0 \text{ , } \mathcal{I}m(\varepsilon_{scat}(y)) \geq 0 \text{ .}$$

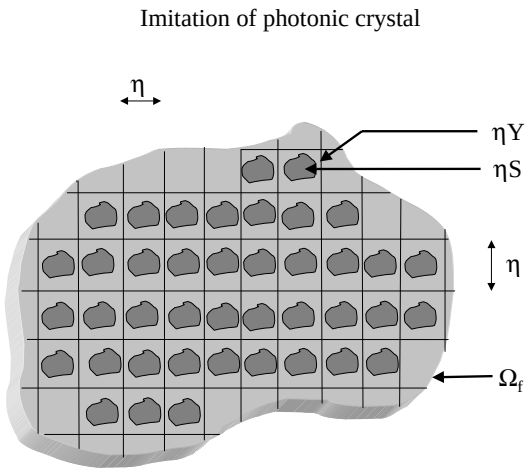

FIGURE 1.9 – The imitation of the photonic crystal results when a small scatterer ηS is periodically distributed in the whole diffracting object Ω_f.

Dielectric case

As η tends to zero, the collection of scatterers may be replaced by an anisotropic homogeneous obstacle of shape Ω_f. The relative permittivity is then given by the following lemma :

Lemma 1 *The resolution of the three annex problems $\mathcal{K}_i$ introduced in the fundamental theorem 1 amounts to looking for functions V_i solutions of the following system (fig. 1.10), where derivatives are taken in the usual sense :*

$$\begin{cases} \Delta V_i & = 0 \ , \ in \ Y \setminus \partial\Omega_S \\ [\varepsilon \ \frac{\partial V_i}{\partial n}]_{\partial\Omega_S} & = -[\varepsilon]_{\partial\Omega_S} \ n_i \\ [V_i]_{\partial\Omega_S} & = 0 \end{cases}$$

$$\text{with } \varepsilon = \begin{cases} \varepsilon_{scat} & , \ in \ \Omega_S \\ 1 & , \ in \ Y \setminus \bar{\Omega}_S \end{cases}$$

$[f]_{\partial\Omega_S}$ denotes the jump of f across the boundary $\partial\Omega_S$, and n_i, $i \in \{1,2,3\}$, denotes the projection on the axis e_i of a normal of $\partial\Omega_S$.

Proof :

Let us denote by e_i, $i \in \{1,2,3\}$ the three vectors of the orthonormal base of $\mathbb{R}^3$. As already seen, the problem verified by V_i can be written :

$\mathcal{K}_i$: $\text{div}_y\Big(\varepsilon(y)(\bigtriangledown_y V_i + e_i)\Big) = 0 \ , i \in \{1,2,3\}$

This expression must be taken in the sense of distributions. Applying the formula of derivatives in the sense of distributions and keeping in mind that all functions of $H^1_\sharp(Y)/\mathbb{R}$ are continuous leads to :

$$\varepsilon \bigtriangledown V_i = \varepsilon\{\bigtriangledown V_i\}$$

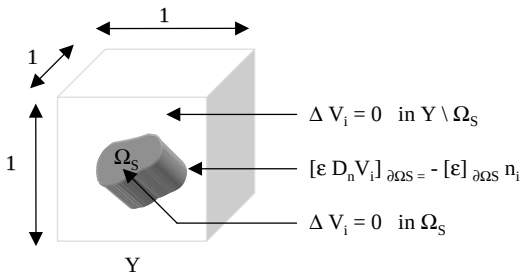

FIGURE 1.10 – Description of the annex problem in the dielectric case. The scatterer can possibly touch the boundary of the elementary cell, which allows us studying dielectric structures made for example of parallel rods (fig. 1.2)

Where the derivatives in the left member must be taken in distribution sense and the ones in the right member in usual sense (brackets).

Taking the divergence of this expression we get :

$$\mathrm{div}(\varepsilon \bigtriangledown V_i + \varepsilon e_i) \quad = \quad \varepsilon\{\Delta V_i\} + [\varepsilon]_{\partial\Omega_S} n \cdot e_i \delta_{\partial\Omega_S} + \underbrace{[\varepsilon \bigtriangledown V_i] n}_{[\varepsilon \frac{\partial V_i}{\partial n}]} \delta_{\partial\Omega_S}$$

Equating on the one hand the regular part and on the other hand the singular part of the above distribution we obtain the expected result.

These results call for further comments detailed in the two following remarks.

Remark about the physical sense of the annex problem

Coming back for a while to the general case, the annex problem can be rewritten as $\mathrm{div}_y(\varepsilon(y) \bigtriangledown_y V_i) = -\mathrm{div}_y(\varepsilon \bigtriangledown_y y_i)$ which can be seen as an electrostatic problem with a volumic distribution of charges $\rho_i = \mathrm{div}_y(\varepsilon \bigtriangledown_y y_i)$.

In a similar way, in the case were ε is a two valued piecewise constant function (the case encountered in most manufactured optical devices), we can write that :

$\mathrm{div}_y(\varepsilon(y) \bigtriangledown_y V_i) = -\sigma_i \delta_{\partial\Omega_S}$

where σ_i is a surfacic distribution of charges defined by $\sigma_i = [\varepsilon] n_i \delta_{\partial\Omega_S}$.

Solving the annex problem for a two valued piecewise constant permittivity, reduces then to looking for the potential induced by a surface density of charges on the edge of the scatterer. This result is not surprising, unlike the following remark which plays a fundamental role in numerical implementations.

Remark about the numerical calculus of the permittivity

In the fundamental theorem we have seen that the relative permittivity matrix of the homogenized problem is deduced from 6 numbers φ_{ij} ($\varphi_{ij} = \varphi_{ji}$) defined as follows :

$$\varphi_{ij} = \int_Y \varepsilon(y) \frac{\partial V_i}{\partial y_j} \, dy \, ,$$

ε being a two-valued piecewise permittivity, we then deduce that :

$$\varphi_{ij} = 1 \int_{Y - \bar{\Omega}_S} \frac{\partial V_i}{\partial y_j} \, d\mathbf{y} - \varepsilon_{scat} \int_{\Omega_S} \{\frac{\partial V_i}{\partial y_j}\} \, d\mathbf{y}$$

It then follows that :

$$\begin{aligned}\varphi_{ij} &= 1\int_{Y-\bar{\Omega}_S} \mathrm{div}(V_i e_j)\, d\mathbf{y} - \varepsilon_{scat}\int_{\Omega_S} \mathrm{div}(V_i e_j)\, d\mathbf{y} \\ &= \int_Y \mathrm{div}(V_i e_j)\, dy + (\varepsilon_{scat}-1)\int_{\Omega_s} \mathrm{div}(V_i e_j)\, dy\end{aligned}$$

Applying the Green formula, due to the antiperiodicity of the outer normal $\mathbf{n}$ to ∂Y the integral over Y vanishes, and we obtain that :

$$\varphi_{ij} = (\varepsilon_{scat}-1)\int_{\partial\Omega_S} V_i\, n_j\, ds \;=\; [\varepsilon]\int_{\partial\Omega_S} V_i\, n_j\, ds$$

Let us remark that V_i is well defined on $\partial\Omega_S$ because it doesn't suffer a jump accross the boundary of the scatterer. This last formula is very important for numerical implementations : it is not necessary to compute the gradient of V (which gives rise to numerical inaccuracy) to perform the calculus of the homogenized permittivity, which is far beyond our first thoughts on the matter. We can then hope for a faster convergence than was first expected.

The reader may be surprised at the last expression which seems to give a permittivity depending upon the choice of the potential V (V is defined up to an additive constant). In fact thanks to the nullity of $\int_{\partial\Omega_S} n_i\, ds$, the permittivity is well defined.

As concerns the numerical implementation, a method of fictitious sources is being adapted by F. Zolla to the resolution of the annex problem on the torus $\boldsymbol{T}_Y$ [215]. Roughly speaking, $\boldsymbol{T}_Y = Y/\mathbb{R}^3$ is a unit cell whose opposite sides are stuck together. This geometrical vision enables to take once more into account the boundedness of the whole obstacle. In the next paragraph, we propose another numerical approach based on a finite difference scheme coupled with Fast Fourier Transform. A third way to solve numerically the annex problem is to take the variational form of problem $\mathcal{J}_j$:

$$\left\langle \varepsilon_r^B(\mathbf{y})(\bigtriangledown_y(V_i - y_i)) \cdot \bigtriangledown V_j \right\rangle_Y = 0\ .$$

One can then make use of a Finite Element Scheme on the torus to solve the problem : this method takes advantage of the wide variety of geometries it can solves.

Infinite conducting case

Let us first notice that in this section, we do not pretend to achieve the study of homogenization of photonic crystals with metallic inclusions (the reader can refer to [38] for the mathematical model of an infinite conducting scattering obstacle in electromagnetism). Here, we just study a case consisting in letting the conductivity tend to infinity in the homogenized problem. Therefore, we do not face problems of the cohomology type when deriving the expression of $\mathbf{E}_0$ from $\mathrm{rot}_{\mathbf{y}}(\mathbf{E}_0(\mathbf{x},\mathbf{y})) = 0$ (see equations (9) and (10) of the next section).

This case has been treated in the case of conical incidence on a set of parallel metallic rods by D.Felbacq and G.Bouchitté [33]. Following the results obtained by these authors

in the two dimensional case [71][72], it can be seen that the limit problem rely on the manner in which the volume of the scatterers vanish in conjunction with the volume of the basic cells. Although different, our limit problem gives an idea of the behavior of metallic photonic crystals at large wavelengths when the basic cell and its scatterer vanish in the same way).

Lemma 2 *If we assume that* $\Theta \neq 0$*, we get the following expression for the effective permittivity (note that the average is taken on the complementary of the metallic scatterer) :*

$$\varepsilon_{hom} =< (I - \bigtriangledown_y \mathbf{V}_Y >_{Y \setminus \Omega_S}$$

with

$$\begin{cases} \Delta V_i &= 0 \ , \ in \ Y \setminus \Omega_S \\ \frac{\partial V_i}{\partial n} &= -n_i \ , \ on \ \partial\Omega_S \end{cases}$$

Denoting by Ψ_{ij} *the average* $< \frac{\partial V_i}{\partial y_j} >_{Y \setminus \Omega_S}$*, as for the dielectric case, we prove that :*
$\forall i,j \in \{1,2,3\}$, $\varphi_{ij} =< \frac{\partial V_j}{\partial y_i} >_{Y\setminus\Omega_S} =< \frac{\partial V_i}{\partial y_j} >_{Y\setminus\Omega_S} = - < \bigtriangledown V_i \cdot \bigtriangledown V_j >_{Y\setminus\Omega_S}$

A way to get this system (fig. 1.11) is to let the conductivity tend to infinity in the annex problem of the dielectric case : we first get the homogenized problem for an array of conducting scatterers and we then take the limit when the effective index of the scatterers tends to infinity. Another way to proceed is to assume that the inclusions are perfectly conducting, and then to take the long-wavelength limit [72][180][181]. The two answers are different : we face a mathematical problem of non-commuting limits. Due to the uniqueness of the electromagnetic field solution of the problem, there is a dicussion to avoid this paradox in [180][181][167], where Poulton *et al.* and Nicorovicci *et al.* explain that the mathematical dynamic problem associated with an array of highly conducting inclusions is a "singularly perturbed problem" for the case when the wavenumber is fixed and the refractive index of inclusions tends to infinity. These problems are characterized by highly oscillating fields which vary rapidly in the presence of a metallic boundary. They give numerical results which corroborate this theory. Finally, they note that in the case of cylinders with refractive index, the internal wavelength is zero, and is thus never larger than their cross-section, which emphasizes that one has to be very careful when dealing with infinite conducting inclusions : in the literature on homogenization, it is usual to state that an effective refractive index can always be attributed to a composite material, provided the wavelength of electromagnetic radiation is much larger than a characteristic size (period of the lattice, size of inclusions...), which is obviously no more the case.

The case of spherical scatterers

In that case, for both dielectric and metallic scatterers, the homogenized medium is isotropic, and the tensor of the effective permittivity reduces to a scalar which appears to be $\varepsilon_{hom} = < \varepsilon(y) >_Y - \varphi_{11}$, in the dielectric case and $\varepsilon_{hom} = (1 - \Theta) - \Psi_{11}$ in the metallic case, since $\varphi_{ii} = \varphi_{jj}$ (resp. $\Psi_{ii} = \Psi_{jj}$) and $\varphi_{ij} = 0$ (resp. $\Psi_{ij} = 0$) for $i \neq j$, $i,j \in \{1,2,3\}$.

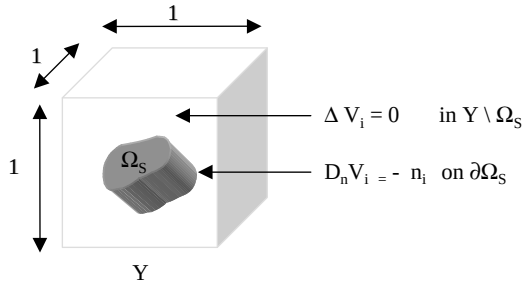

FIGURE 1.11 – Description of the annex problem in the metallic case. One has to be carefull if the scatterer touch the boundary of the unit cell : when some scatterers are stuck together to form a set of parallel rodes, there are numerical inaccuracies.

1.5 Numerical implementation

1.5.1 Resolution of the annex problem

In this section, we present a numerical approach based on a finite difference scheme coupled with a Fast Fourier Transform. This method has been applied for a long time to solve the Laplace equation

$$\Delta u(x,y,z) = \rho(x,y,z)$$

in a periodic media, which is closely related to our annex problem. Let us recall the underlying ideas. We first represent the function $u(x,y,z)$ by its values at the discrete set of points :

$$x_j = x_0 + jh \ , \ j = 0,\ 1,\ ...,\ J$$

$$y_l = x_0 + lh \ , \ l = 0,\ 1,\ ...,\ L$$

$$z_m = x_0 + mh \ , \ m = 0,\ 1,\ ...,\ M$$

where h is the grid spacing. From now on, we will write $u_{j,l,m}$ for $u(x_j, y_l, z_m)$, and $\rho_{j,l,m}$ for $\rho(x_j, y_l, z_m)$. The discrete form of the Laplace equation is thus given by :

$$\frac{u_{j+1,l,m} - 2u_{j,l,m} + u_{j-1,l,m}}{h^2} + \frac{u_{j,l+1,m} - 2u_{j,l,m} + u_{j,l-1,m}}{h^2} + \frac{u_{j,l,m+1} - 2u_{j,l,m} + u_{j,l,m-1}}{h^2} = \rho_{j,l,m}$$

We can rewrite this expression as follows :

$$u_{j+1,l,m} + u_{j-1,l,m} + u_{j,l+1,m} + u_{j,l-1,m} + u_{j,l,m+1} + u_{j,l,m-1} - 6u_{j,l,m} = h^2 \rho_{j,l,m}$$

To take into account the periodic boundary conditions, we make a discrete inverse Fourier transform in the variables x, y and z of u and ρ, and we get :

$$u_{jlm} = \frac{1}{JLM} \sum_{p=0}^{J-1} \sum_{q=0}^{L-1} \sum_{r=0}^{M-1} \hat{u}_{pqr} e^{\frac{-2i\pi jp}{J}} e^{\frac{-2i\pi lq}{L}} e^{\frac{-2i\pi mr}{M}}$$

$$\rho_{jlm} = \frac{1}{JLM} \sum_{p=0}^{J-1} \sum_{q=0}^{L-1} \sum_{r=0}^{M-1} \hat{\rho}_{pqr} e^{\frac{-2i\pi jp}{J}} e^{\frac{-2i\pi lq}{L}} e^{\frac{-2i\pi mr}{M}}$$

If we substitute these two expressions on the discrete form of Laplace equation, we get :

$$\hat{u}_{pqr}\Big(e^{\frac{2\pi ip}{J}}+e^{\frac{-2\pi ip}{J}}+e^{\frac{2\pi iq}{L}}+e^{\frac{-2\pi iq}{L}}+e^{\frac{2\pi ir}{M}}+e^{\frac{-2\pi ir}{M}}-6\Big)=\hat{\rho}_{pqr}h^2$$

We then deduce that

$$\hat{u}_{pqr}=\frac{\hat{\rho}_{pqr}h^2}{2\Big(\cos\frac{2\pi p}{J}+\cos\frac{2\pi q}{L}+\cos\frac{2\pi r}{M}-2\Big)}$$

Thus, the strategy for solving the discrete Laplace equation with periodic conditions is to compute the discrete Fourier transform

$$\hat{\rho}_{pqr}=\sum_{p=0}^{J-1}\sum_{q=0}^{L-1}\sum_{r=0}^{M-1}\rho_{pqr}e^{\frac{2i\pi jp}{J}}e^{\frac{2i\pi lq}{L}}e^{\frac{2i\pi mr}{M}}$$

We then compute $\hat{u}_{pqr}$ thanks to the above equation and get u_{pqr} by a discrete inverse Fourier transform. The algorithm is performant, since we can use Fast Fourier Transforms to compute the solution. We now want to adapt this classical algorithm to our case. For this, we note that :

$$\mathrm{div}\Big(\varepsilon\bigtriangledown u(x,y,z)\Big)=\varepsilon\Delta u+\bigtriangledown\varepsilon\cdot\bigtriangledown u$$

We can compute $\bigtriangledown\varepsilon\cdot\bigtriangledown u$ thanks to an iterative process. If ε takes two values ε_1 and ε_2, let us denote by χ the susceptibility of the media :

$$\chi=\frac{\varepsilon_1-\varepsilon_2}{\varepsilon_1}$$

If u^n_{pqr} denotes the value of u_{pqr} at the n-th iteration, we get :

$$\varepsilon_k\Big(u^{n+1}_{j+1,l,m}+u^{n+1}_{j-1,l,m}+u^{n+1}_{j,l+1,m}+u^{n+1}_{j,l-1,m}+u^{n+1}_{j,l,m+1}+u^{n+1}_{j,l,m-1}-6u^{n+1}_{j,l,m}\Big)$$

$$=h^2\rho_{j,l,m}+\chi\Big(u^n_{j+1,l,m}+u^n_{j,l+1,m}+u^{n+1}_{j,l,m+1}-3u^n_{j,l,m}\Big)$$

where ε_k is either equal to ε_1 or to ε_2, depending on which media is u^n_{pqr}.

This iterative method is being implemented for ellipsoidal scatterers. Although we are not yet capable to give the complete result (we have to avoid problems of convergence during the iterative process), we show in figure 1.12 the behaviour of the periodic potential for the first iterations. This scheme can be used for every scatterer with a parametric equation. For bodies with complicated shapes, work is in progress to solve the variational equation associated to the annex problem by the use of the GetDP software [64] : we want to implement a finite element scheme analogous to that of Laminie and Mefire [125] where we take periodic conditions (periodic cell) instead of boundary elements.

1.5.2 Connection between Bloch eigenvalues and homogenized coefficients

In this section, we show the connection between the homogenization via the Bloch method (slope of the dispersion curve at this origin), and that of the multiple scale method.

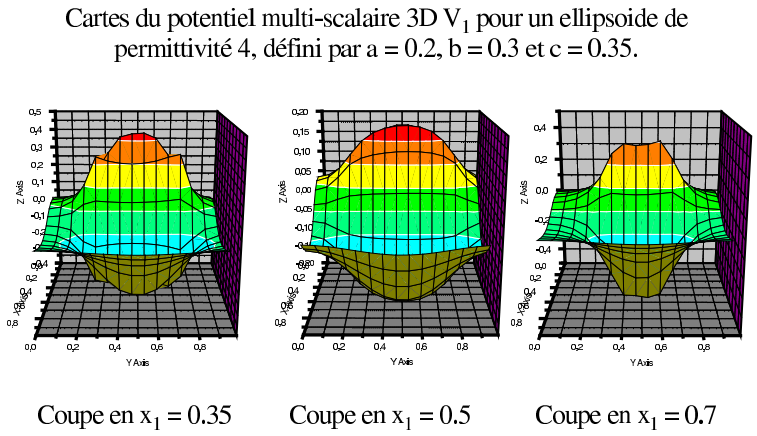

FIGURE 1.12 – Behavior of the 3D multi-scalar potential V_1 in the planes $x_1 = 0.35$, $x_1 = 0.5$ and $x_1 = 0.7$, for ellipsoidal inclusions characterized by $a = 0.2$, $b = 0.3$, $c = 0.35$ and $\varepsilon = 4$.

Let us consider the operator A defined by the coefficients $(a_{pq}(y))$ where $a_{pq} = a_{qp}$:

$$A = -\frac{\partial}{\partial y_p}(a_{pq}(y)\frac{\partial}{\partial y_p})$$

Associated with it are the Bloch eigenvalues $\{\lambda_k(\zeta)\}$ and the corresponding eigenfunctions $\{\Phi(\zeta,.)\}$.$A\psi = \lambda\psi$ dans $\mathbb{R}^N$ avec $\psi(x) = e^{i\zeta.x}\Phi(x)$ p.p. $x \in \mathbb{R}^N$. Donc

$$A(\zeta)\Phi(\zeta,.) = \lambda(\zeta)\Phi(\zeta,.)\ \forall\zeta \in Y$$

where $A(\zeta)$ is the shifted operator

$$A^(\zeta) = -(\frac{\partial}{\partial y_p} + i\zeta_p) + [a_{pq}(y)(\frac{\partial}{\partial y_q} + i\zeta_q)]$$

There is a remarkable relation between the second derivatives of the first eigenvalue $\lambda_1(\zeta)$ and the effective matrix ε^{-1}_{hom} of the homogenized problem for the $\mathbf{H} \parallel$ polarization :

$$\mathcal{P}^{H\parallel}_{hom}\begin{cases} -div\Big(\varepsilon^{-1}_{hom} \bigtriangledown \mathbf{H}_{hom}\Big) = k_0^2\mathbf{H}_{hom} \\ \mathbf{H}^d_{hom} = O\Big(\frac{1}{\sqrt{|\ \mathbf{x}\ |}}\Big)\ ,\ \mathbf{H}^d_{hom} - ik_0\frac{\partial\mathbf{H}^d_{hom}}{\partial\mathbf{x}} = o\Big(\frac{1}{\sqrt{|\ \mathbf{x}\ |}}\Big) \end{cases}$$

with

$$\varepsilon^{-1}_{homij} = (\int_Y \varepsilon^{-1}(\mathbf{y})(e_i + \bigtriangledown w_i(\mathbf{y}))(e_i + \bigtriangledown w_j(\mathbf{y}))\,d\mathbf{y} = \int_Y \varepsilon^{-1}(\mathbf{y})(e_j + \bigtriangledown w_j(\mathbf{y}))\,d\mathbf{y})e_i$$

where w_j is the unique solution in $H^1_\sharp(Y)\backslash\mathbb{R}$) of the annex problem

$$\mathcal{P}_j\ :\ -div[\varepsilon^{-1}(\mathbf{y})(e_j + \bigtriangledown_y w)] = 0$$

The link between these two matrices is given by the following classical lemma [18] :
Lemma

$$\varepsilon^{-1}_{hompq} = \frac{1}{2}\frac{\partial^2 \lambda_1}{\partial\zeta_p \partial\zeta_q}(0) \ \forall p,q = 1,...,N$$

Proof :

Here, we just give a sketch of the proof which can be found in the book of Bensoussan, Lions and Papanicolaou (pp. 633-638, [18]).

We first note that :

$$\begin{aligned}
\frac{\partial \lambda_1(\zeta)}{\partial\zeta_p} &= (\frac{\partial A(\zeta)}{\partial\zeta_p}\Phi_1(\zeta), \Phi_1(\zeta)) \\
\frac{1}{2}\frac{\partial^2 \lambda_1(\zeta)}{\partial\zeta_p \partial\zeta_q} &= (a_{pq}\Phi_1(\zeta), \Phi_1(\zeta)) + ((\frac{\partial A(\zeta)}{\partial\zeta_p} - \frac{\partial \lambda_1(\zeta)}{\partial\zeta_p})\frac{\partial\Phi_1(\zeta)}{\partial\zeta_q}, \Phi_1(\zeta)) \\
&\quad +((\frac{\partial A(\zeta)}{\partial\zeta_q} - \frac{\partial \lambda_1(\zeta)}{\partial\zeta_q})\frac{\partial\Phi_1(\zeta)}{\partial\zeta_p}, \Phi_1(\zeta))
\end{aligned}$$

Moreover, the first derivative of $\Phi_1(\zeta)$ satisfies :

$$(A^{hom}(\zeta) - \lambda_1(\zeta))\frac{\partial\Phi_1(\zeta)}{\partial\zeta_p} + (\frac{\partial A^{hom}(\zeta)}{\partial\zeta_p} - \frac{\partial\lambda_1(\zeta)}{\partial\zeta_p})\Phi_1(\zeta) = 0$$

We know that $\lambda_1(0) = 0$ and $\Phi_1(0) = 1$. If we use this information in the above formulae evaluated at $\zeta = 0$, we get :

$$\begin{aligned}
\frac{\partial \lambda_1(0)}{\partial\zeta_p} &= 0 \ \forall p = 1,...,N \\
\frac{\partial \Phi_1(0)}{\partial\zeta_p} &= iw_p \ \forall p = 1,...,N
\end{aligned}$$

Inserting these expressions into the above expression for the second derivative of λ_1, we arrive at the desired relation between ε^{-1}_{hom} and the second derivative of λ_1.

Remark :

There is a paradox between our annex problem in $\mathbf{H} \parallel$ polarization, derived from the annex problem of the three-dimensional case, and that of [72] : in their annex problem, ε is replaced by ε^{-1}. In the lemma 14 of chapter 2, we establish a variant of the classical theorems of Keller [117] and Dykhne [68] to explain these difference.

1.6 Homogenization of ferro-magnetic structures

In this section, we use a heuristic method to homogenize a three-dimensional structure filled with a periodic arrangement of ferro-magnetic inclusions. More precisely, using a multiscale expansion technique applied to a scattering problem, we prove that a three-dimensional finite crystal behaves as if it were homogeneous, when the period becomes very small in regard with a fixed wavelength. We show that the homogeneous medium is actually anisotropic, and we derive the expression of its tensors of permittivity and permeability from the calculus of six scalar periodic potentials, solutions of two partial differential equations of electrostatic type. The question of the convergence of the solution $\mathbf{H}_\eta$ of the problem $\mathcal{P}^H_\eta$ towards the solution $\mathbf{H}_{hom}$ of the problem $\mathcal{P}^H_{hom}$, will be addressed in [104].

1.6.1 The Multiple-Scale expansion of H_η

Let $\mathbf{H}_\eta$ be a sequence of locally square integrable functions on $\mathbb{R}^3$ solutions of

$$\mathcal{P}_\eta^H \left\{ \begin{array}{ll} \mathrm{rot}\, \tilde{\varepsilon}^{-1}(\mathbf{x}, \frac{\mathbf{x}}{\eta})\, \mathrm{rot}\, \mathbf{H}_\eta - k_0^2 \tilde{\mu}(\mathbf{x}, \frac{\mathbf{x}}{\eta}) \mathbf{H}_\eta = 0 & ,\text{in } \mathcal{D}'(\mathbb{R}^3) \\ \mathbf{H}_\eta^d = O(\frac{1}{|\mathbf{x}|}) & ,\text{in } C^\infty(\mathbb{R}^3 - \bar{\Omega}_\eta) \\ \frac{\mathbf{x}}{|\mathbf{x}|} \wedge \mathrm{rot}\, \mathbf{H}_\eta^d + ik\mathbf{H}_\eta^d = o(\frac{1}{|\mathbf{x}|}) & ,\text{in } C^\infty(\mathbb{R}^3 - \bar{\Omega}_\eta) \end{array} \right.$$

where $\tilde{\varepsilon}^{-1}(\mathbf{x}, \frac{\mathbf{x}}{\eta})$ and $\tilde{\mu}^{-1}(\mathbf{x}, \frac{\mathbf{x}}{\eta})$ respectively denote the relative permittivity and permeability of the media.

We suppose that $\mathbf{H}_\eta$, solution of the problem $\mathcal{P}_\eta^{\mathbf{H}}$ has a two-scale expansion of the form :

$$\forall \mathbf{x} \in \Omega_f, \;\; \mathbf{H}_\eta(\mathbf{x}) = \mathbf{H}_0(\mathbf{x}, \frac{\mathbf{x}}{\eta}) + \eta \mathbf{H}_1(\mathbf{x}, \frac{\mathbf{x}}{\eta}) + \eta^2 \mathbf{H}_2(\mathbf{x}, \frac{\mathbf{x}}{\eta}) + ...$$

where $\mathbf{H}_i : \Omega_f \times Y \longmapsto \mathbb{C}^3$ is a smooth function of 6 variables, independent of η, such that $\forall \mathbf{x} \in \Omega_f$, $\mathbf{H}_i(\mathbf{x}, \cdot)$ is Y-periodic.

Our goal is to characterize the electromagnetic field when η tends to 0. If the coefficients $\mathbf{H}_i$ do not increase "too much" when η tends to 0, the limit of $\mathbf{H}_\eta$ will be $\mathbf{H}_0$, a rougher approximation to $\mathbf{H}_\eta$. Hence, we make the assumption that for all $\mathbf{x} \in \mathbb{R}^3$, $\mathbf{H}_i(\mathbf{x}, \frac{\mathbf{x}}{\eta}) = o(\frac{\mathbf{x}}{\eta^i})$, so that the expansion (also denoted by the german word "ansatz") still makes sense in neighbourhood of 0. If the above expansion is relevant, we can state the following fundamental result :

Theorem 2

When η tends to zero, $\mathbf{H}_\eta$ solution of the problem $(\mathcal{P}_\eta^H)$, converges weakly in $L^2(\Omega)$ to the first term of its asymptotic expansion $H_0(\mathbf{x}, \mathbf{y})$. The average field $\mathbf{H}_{hom}(\mathbf{x})$ of $H_0(\mathbf{x}, \mathbf{y})$ on the basic cell Y ($\mathbf{H}_{hom}(\mathbf{x}) = \int_Y H_0(\mathbf{x}, \mathbf{y})\, d\mathbf{y}$) is the unique solution of the following problem $(\mathcal{P}_{hom}^{\mathbf{H}})$:

$$(\mathcal{P}_{hom}^{\mathbf{H}}) = \left\{ \begin{array}{l} \mathrm{rot}(\varepsilon_{hom}^{-1}(\mathbf{x}) \mathrm{rot}\, \mathbf{H}_{hom}(\mathbf{x})) - k_0^2 \mu_{hom} \mathbf{H}_{hom}(\mathbf{x}) = 0 \\ \mathbf{H}_{hom}^d(\mathbf{x}) = O(\frac{1}{|\mathbf{x}|}) \\ \frac{\mathbf{x}}{|\mathbf{x}|} \wedge \mathrm{rot}\, \mathbf{H}_{hom}^d(\mathbf{x}) + ik\mathbf{H}_{hom}^d(\mathbf{x}) = o(\frac{1}{|\mathbf{x}|}) \end{array} \right.$$

with

$$\left\{ \begin{array}{ll} \varepsilon_{hom}(\mathbf{x}) = < \tilde{\varepsilon}(\mathbf{x}, \mathbf{y})(I - \bigtriangledown_{\mathbf{y}} \mathbf{V}_Y(\mathbf{y})) >_Y & ,in\ \Omega_f \\ \varepsilon_{hom}(\mathbf{x}) = 1 & ,in\ \Omega_f^c \end{array} \right.$$

and

$$\left\{ \begin{array}{ll} \mu_{hom}(\mathbf{x}) = < \tilde{\mu}(\mathbf{x}, \mathbf{y})(I - \bigtriangledown_{\mathbf{y}} \mathbf{W}_Y(\mathbf{y})) >_Y & ,in\ \Omega_f \\ \mu_{hom}(\mathbf{x}) = 1 & ,in\ \Omega_f^c \end{array} \right.$$

Here, $< f >_Y$ is the average of f in Y (i.e. $\int_Y f(x, y)\, dy$). Furthermore, $\tilde{\varepsilon}(\mathbf{x}, \mathbf{y})$ and $\tilde{\mu}(\mathbf{x}, \mathbf{y})$ respectively denote

$$\tilde{\varepsilon}(\mathbf{x}, \mathbf{y}) = \left\{ \begin{array}{ll} 1 & ,\ if\ \mathbf{x} \in \Omega_f^c \\ \varepsilon_r^B(\mathbf{y}) & ,\ if\ \mathbf{x} \in \Omega_f \end{array} \right.$$

and

$$\tilde{\mu}(\mathbf{x},\mathbf{y}) = \begin{cases} 1 & , \text{ if } \mathbf{x} \in \Omega_f^c \\ \mu_r^B(\mathbf{y}) & , \text{ if } \mathbf{x} \in \Omega_f \end{cases}$$

Besides, $\mathbf{V}_Y = (V_1, V_2, V_3)$ *and* $\mathbf{W}_Y = (V_1, V_2, V_3)$*, where* V_j *,*$j \in \{1,2,3\}$ *and* W_j *,*$j \in \{1,2,3\}$*, are the unique solutions in* $H^1_\sharp(Y)/\mathbb{R}$ *of one of the six following problems* $(\mathcal{K}_j)$ *and* $(\mathcal{M}_j)$ *of electrostatic type :*

$$(\mathcal{K}_j) : -\mathrm{div}_{\mathbf{y}}\Big[\varepsilon_r^B(\mathbf{y})(\bigtriangledown_{\mathbf{y}}(V_j(\mathbf{y}) - y_j))\Big] = 0 \ , j \in \{1,2,3\}$$

$$(\mathcal{M}_j) : -\mathrm{div}_{\mathbf{y}}\Big[\mu_r^B(\mathbf{y})(\bigtriangledown_{\mathbf{y}}(W_j(\mathbf{y}) - y_j))\Big] = 0 \ , j \in \{1,2,3\}$$

As η tends to zero, we can replace the isotropic heterogeneous ferro-magnetic diffracting obstacle of shape Ω_η, by an homogeneous obstacle of shape Ω_f with both anisotropic permittivity and permeability which are given by what follows :

Developed form for the matrices of effective permittivity and permeability

It is clear from the corollary of theorem 1 that the relative permittivity and permeability matrices of the homogenized problem are equal to :

$$\varepsilon_{hom} = \begin{pmatrix} < \varepsilon_r^B(\mathbf{y}) >_Y & 0 & 0 \\ 0 & < \varepsilon_r^B(\mathbf{y}) >_Y & 0 \\ 0 & 0 & < \varepsilon_r^B(\mathbf{y}) >_Y \end{pmatrix} - \begin{pmatrix} \varphi_{11} & \varphi_{12} & \varphi_{13} \\ \varphi_{21} & \varphi_{22} & \varphi_{23} \\ \varphi_{31} & \varphi_{32} & \varphi_{33} \end{pmatrix}$$

and

$$\mu_{hom} = \begin{pmatrix} < \mu_r^B(\mathbf{y}) >_Y & 0 & 0 \\ 0 & < \mu_r^B(\mathbf{y}) >_Y & 0 \\ 0 & 0 & < \mu_r^B(\mathbf{y}) >_Y \end{pmatrix} - \begin{pmatrix} \psi_{11} & \psi_{12} & \psi_{13} \\ \psi_{21} & \psi_{22} & \psi_{23} \\ \psi_{31} & \psi_{32} & \psi_{33} \end{pmatrix}$$

where φ_{ij} *and* ψ_{ij} *represent corrective terms defined by :*

$$\forall i,j \in \{1,2,3\},\ \varphi_{ij} = < \varepsilon_r^B \frac{\partial V_j}{\partial y_i} >_Y = < \varepsilon_r^B \frac{\partial V_i}{\partial y_j} >_Y = - < \varepsilon_r^B \bigtriangledown V_i \cdot \bigtriangledown V_j >_Y$$

and

$$\forall i,j \in \{1,2,3\},\ \psi_{ij} = < \mu_r^B \frac{\partial W_j}{\partial y_i} >_Y = < \mu_r^B \frac{\partial W_i}{\partial y_j} >_Y = - < \mu_r^B \bigtriangledown W_i \cdot \bigtriangledown W_j >_Y$$

Here, the brackets denote averaging over Y*. Furthermore,* V_j *and* W_j *are the unique solutions in* $H^1_\sharp(Y)/\mathbb{R}$ *of the six partial differential equations* $\mathcal{K}_j$ *and* $\mathcal{M}_j$ *(fig.1.7). Hence, thanks to the symmetry of the matrices on the right (*$\varphi_{ij} = \varphi_{ji}$ *and* $\psi_{ij} = \psi_{ji}$*), the homogenized permittivity and permeability are given by the knowledge of twelve terms* φ_{ij} *and* ψ_{ij}*, depending upon the resolution of six annex problems* $\mathcal{K}_j$ *and* $\mathcal{M}_j$*.*

For η fixed, $\mathbf{H}_\eta$ is the unique solution of the above problem (the reader may refer to [51] for existence and uniqueness theorems). Let us now assume that $\mathbf{H}_\eta$ satisfies the following two-scale expansion :

$$\mathbf{H}_\eta = \mathbf{H}_0(\mathbf{x}, \frac{\mathbf{x}}{\eta}) + \eta \mathbf{H}_1(\mathbf{x}, \frac{\mathbf{x}}{\eta}) + \eta^2 \mathbf{H}_2(\mathbf{x}, \frac{\mathbf{x}}{\eta}) + ... + \eta^N \mathbf{H}_\eta(\mathbf{x}, \frac{\mathbf{x}}{\eta}) + o(\eta^N) \quad \text{(E1)}$$

where $\mathbf{H}_i : \Omega_f \times \mathbb{R}^3 \longmapsto \mathbb{C}^3$ are smooth complex valued functions of the variables $(\mathbf{x}, \mathbf{y})$, independent of η, periodic in $\mathbf{y}$ of period 1. The introduction of the variable $\mathbf{y} = \frac{\mathbf{x}}{\eta}$ takes into account the periodic dependance on $\mathbf{x}$ of the permittivity ε_η in the "bounded periodic" structure.

Assuming that the above expansion is relevant, we can state the following lemma :

Lemma 1 *The Maxwell operator $A_\eta = \mathrm{rot}\, \tilde{\varepsilon}_\eta^{-1} \mathrm{rot}$ associated to the problem $\mathcal{P}_\eta$ satisfies the following operator expansion $A_\eta = \eta^{-2} A_{\mathbf{yy}} + \eta^{-1} A_{\mathbf{xy}} + \eta^0 A_{\mathbf{xx}} + o(1)$, where $A_{\mu,\nu}$ denotes the operator $\mathrm{rot}_\mu\, \tilde{\varepsilon}^{-1}(\mathbf{x}, \mathbf{y})\, \mathrm{rot}_\nu$, the couple $(\mu,\ \nu)$ being in $\{\mathbf{x}, \mathbf{y}\} \times \{\mathbf{x}, \mathbf{y}\}$.*

Besides, the asymptotic terms of A_η are solutions of :

$$\mathcal{S}_0 = \begin{cases} A_{\mathbf{yy}} \mathbf{H}_0 = 0 & (1) \\ A_{\mathbf{yy}} \mathbf{H}_1 + A_{\mathbf{xy}} \mathbf{H}_0 + A\mathbf{yx} \mathbf{H}_0 = 0 & (2) \\ A\mathbf{yy} \mathbf{H}_2 + A_{\mathbf{xy}} \mathbf{H}_1 + A_{\mathbf{yx}} \mathbf{H}_1 + A_{\mathbf{xx}} \mathbf{H}_0 - k_0^2 \tilde{\mu}(\mathbf{x}, \mathbf{y}) \mathbf{H}_0 = 0 & (3) \end{cases}$$

Proof :

For convenience in the following calculations, we denote by R_η the operator of restriction onto the overplane $\{\mathbf{y} = \frac{\mathbf{x}}{\eta}\}$:

$$R_\eta : f(\mathbf{x}, \mathbf{y}) \longmapsto f(\mathbf{x}, \frac{\mathbf{x}}{\eta})$$

where $f(\mathbf{x}, \mathbf{y})$ and $f(\mathbf{x}, \frac{\mathbf{x}}{\eta})$ are respectively locally square integrable functions of $\Omega \times \mathbb{R}^3 \to \mathbb{C}^3$ and $\Omega \to \mathbb{C}^3$ of finite energy.

It is worth noting that R_η obeys the following rules of calculation :

properties of R_η 1 *R_η is a "distributive operator", that is to say that*

$$R_\eta(f)\ R_\eta(g) = R_\eta(fg)$$

Furthermore, we can define the action of the differential operator on the projector R_η by :

$$\frac{\partial}{\partial \mathbf{x}_i}(R_\eta f(\mathbf{x}, \mathbf{y})) = R_\eta(\frac{\partial}{\partial \mathbf{x}_i} f(\mathbf{x}, \mathbf{y})) + \frac{1}{\eta} R_\eta(\frac{\partial}{\partial \mathbf{y}_i} f(\mathbf{x}, \mathbf{y}))$$

that is to say that $[\frac{\partial}{\partial \mathbf{x}_i}, R_\eta] = \frac{1}{\eta} R_\eta \frac{\partial}{\partial \mathbf{y}_i}$.

With the help of the operator R_η, $(E1)$ can be rewritten in the form :

$$\begin{aligned}\mathbf{H}_\eta(\mathbf{x}) &= R_\eta\mathbf{H}_0(\mathbf{x},\mathbf{y}) + \eta R_\eta\mathbf{H}_1(\mathbf{x},\mathbf{y}) + ... + \eta^N R_\eta\mathbf{H}_N(\mathbf{x},\mathbf{y}) + o(\eta^N)\\ &= R_\eta\{\sum_{j=0}^{N}\eta^j\ \mathbf{H}_j(\mathbf{x},\mathbf{y})\} + o(\eta^N) \quad \text{(E2)}\end{aligned}$$

Thus, the partial differential operator $\dfrac{\partial}{\partial\mathbf{x}_i}$ acting on $\mathbf{H}_\eta(\mathbf{x})$ satisfies the following equality :

$$\begin{aligned}\frac{\partial}{\partial\mathbf{x}_i}\mathbf{H}_\eta(\mathbf{x}) &= \frac{\partial}{\partial\mathbf{x}_i}R_\eta\{\sum_{j=0}^{N}\eta^j\ \mathbf{H}_j(\mathbf{x},\mathbf{y})\} + o(\eta^N)\\ &= (R_\eta\frac{\partial}{\partial\mathbf{x}_i} + \frac{1}{\eta}R_\eta\frac{\partial}{\partial\mathbf{y}_i})\{\sum_{j=0}^{N}\eta^j\ \mathbf{H}_j(\mathbf{x},\mathbf{y})\} + o(\eta^{N-1})\end{aligned}$$

We now want to deduce the action of the second order differential operator $\mathrm{rot}(\tilde{\varepsilon}_\eta^{-1}\,\mathrm{rot})$ involved in the problem $\mathcal{P}_\eta^H$, on the field $\mathbf{H}_\eta$. Taking into account that $[\mathrm{rot}_\mathbf{x}, R_\eta] = \dfrac{1}{\eta}R_\eta\,\mathrm{rot}_\mathbf{y}$, we obtain that :

$$\begin{aligned}&\mathrm{rot}_\mathbf{x}\Big((R_\eta\tilde{\varepsilon}^{-1}(\mathbf{x},\mathbf{y}))(\mathrm{rot}_\mathbf{x}\,R_\eta\mathbf{H}_j)\Big)\\ =\ &\mathrm{rot}_\mathbf{x}\Big((R_\eta\tilde{\varepsilon}^{-1}(\mathbf{x},\mathbf{y}))(R_\eta\,\mathrm{rot}_\mathbf{x}\,\mathbf{H}_j + \frac{1}{\eta}R_\eta\,\mathrm{rot}_\mathbf{y}\,\mathbf{H}_j)\Big)\end{aligned}$$

We then use the distributivity of R_η to get :

$$\begin{aligned}&\mathrm{rot}_\mathbf{x}\Big((R_\eta\tilde{\varepsilon}^{-1}(\mathbf{x},\mathbf{y}))(\mathrm{rot}_\mathbf{x}\,R_\eta\mathbf{H}_j)\Big)\\ =\ &\mathrm{rot}_\mathbf{x}\,R_\eta(\tilde{\varepsilon}^{-1}\,\mathrm{rot}_\mathbf{x}\,\mathbf{H}_j) + \frac{1}{\eta}\,\mathrm{rot}_\mathbf{x}\,R_\eta(\tilde{\varepsilon}^{-1}\,\mathrm{rot}_\mathbf{y}\,\mathbf{H}_j)\end{aligned}$$

We iterate the process, by taking into account once more that $\mathrm{rot}_\mathbf{x}$ and R_η do not commute :

$$\begin{aligned}&\mathrm{rot}_\mathbf{x}\Big((R_\eta\tilde{\varepsilon}^{-1}(\mathbf{y}))(\mathrm{rot}_\mathbf{x}\,R_\eta\mathbf{H}_j)\Big)\\ =\ &R_\eta\Big[\mathrm{rot}_\mathbf{x}(\tilde{\varepsilon}^{-1}\,\mathrm{rot}_\mathbf{x}\,\mathbf{H}_j) + \frac{1}{\eta}\,\mathrm{rot}_\mathbf{y}(\tilde{\varepsilon}^{-1}\,\mathrm{rot}_\mathbf{x}\,\mathbf{H}_j\Big]\\ +\ &\frac{1}{\eta}R_\eta\Big[\mathrm{rot}_\mathbf{x}(\tilde{\varepsilon}^{-1}\,\mathrm{rot}_\mathbf{y}\,\mathbf{H}_j) + \frac{1}{\eta}\,\mathrm{rot}_\mathbf{y}(\tilde{\varepsilon}^{-1}\,\mathrm{rot}_\mathbf{y}\,\mathbf{H}_j)\Big]\end{aligned}$$

We then apply this two-scale second order operator in the expansion of the magnetic field $\mathbf{H}_\eta$. Assuming that the terms of the development of the powers higher than 2 are bounded, we can write :

$$
\begin{aligned}
& \operatorname{rot}_{\mathbf{x}}\Big(\tilde{\varepsilon}^{-1}\operatorname{rot}_{\mathbf{x}}(\mathbf{H}_0+\eta\mathbf{H}_1)\Big)+\frac{1}{\eta}\operatorname{rot}_{\mathbf{x}}\Big(\tilde{\varepsilon}^{-1}\operatorname{rot}_{\mathbf{y}}(\mathbf{H}_0+\eta\mathbf{H}_1)\Big)\\
+\ & \frac{1}{\eta}\Big(\operatorname{rot}_{\mathbf{y}}\tilde{\varepsilon}^{-1}\operatorname{rot}_{\mathbf{x}}(\mathbf{H}_0+\eta\mathbf{H}_1)\Big)\\
+\ & \frac{1}{\eta}\operatorname{rot}_{\mathbf{y}}\Big(\tilde{\varepsilon}^{-1}\operatorname{rot}_{\mathbf{y}}(\mathbf{H}_0+\eta\mathbf{H}_1+\eta^2\mathbf{H}_2)\Big)\\
-\ & k_0^2\tilde{\mu}(\mathbf{H}_0+\eta\mathbf{H}_1)+O(\eta)=0
\end{aligned}
$$

In a neighborhood of $\eta=0$, we express the vanishing of the coefficients of successive powers of $\frac{1}{\eta}$. Thus, we have to consider the following system :

$$
\mathcal{S}_0=\left\{\begin{array}{lll}
\eta^{-2} & & A_{\mathbf{yy}}\mathbf{H}_0 = 0 \quad (1)\\
\eta^{-1} & : & A_{\mathbf{yy}}\mathbf{H}_1+A_{\mathbf{xy}}\mathbf{H}_0+A\mathbf{yx}\mathbf{H}_0 = 0 \quad (2)\\
\eta^{0} & : A\mathbf{yy}\mathbf{H}_2+A_{\mathbf{xy}}\mathbf{H}_1+A_{\mathbf{yx}}\mathbf{H}_1+A_{\mathbf{xx}}\mathbf{H}_0-k_0^2\tilde{\mu}(\mathbf{x},\mathbf{y})\mathbf{H}_0 = 0 \quad (3)
\end{array}\right.
$$

where $A_{\mu,\nu}$ denotes the operator $\operatorname{rot}_\mu\tilde{\varepsilon}^{-1}(\mathbf{x},\mathbf{y})\operatorname{rot}_\nu$, the couple (μ,ν) being in $\{\mathbf{x},\mathbf{y}\}\times\{\mathbf{x},\mathbf{y}\}$.

Let us rewrite the equation (1) of the previous system $\mathcal{S}_0$:

$$
\operatorname{rot}_y\Big(\tilde{\varepsilon}^{-1}(\mathbf{x},\mathbf{y})\operatorname{rot}_y\mathbf{H}_0\Big)=0 \tag{1}
$$

The next step in the asymptotic expansion is to show the link between $\Big(\mathbf{E}_0\ ,\ \mathbf{H}_0\Big)(\mathbf{x},\mathbf{y})$ and the so-called homogenized electromagnetic field $\Big(\mathbf{E}_{hom}\ ,\ \mathbf{H}_{hom}\Big)(\mathbf{x})$.

Lemma 2 *Let for fixed* $\mathbf{x}\in\Omega_f$, $\mathbf{H}_0$ *be a* Y *periodic function in* $\mathbf{y}$, *such that* $\operatorname{rot}_{\mathbf{y}}\mathbf{H}_0(x,.)\in H(\operatorname{rot},Y)$, *solution of equation* (1). *Then*

$$
\operatorname{rot}_{\mathbf{y}}\mathbf{H}_0(\mathbf{x},.)=0\ ,\quad \textit{a.e. on } Y
$$

Proof :

Multiplying equation (1) in $\mathcal{S}_0$ by the conjugate of $\mathbf{H}_0^*$ of $\mathbf{H}_0$ and integrating over Y leads to :

$$
\int_Y \operatorname{rot}_{\mathbf{y}}\Big[\tilde{\varepsilon}^{-1}(\mathbf{x},\mathbf{y})(\operatorname{rot}_{\mathbf{y}}\mathbf{H}_0(\mathbf{x},\mathbf{y}))\Big]\cdot\mathbf{H}_0^*(\mathbf{x},\mathbf{y})\,d\mathbf{y}=0
$$

By applying the Poynting Identity ($\operatorname{div}(A\wedge B)=-A\cdot\operatorname{rot}B+B\cdot\operatorname{rot}A$) and summing on Y, we have :

$$
\begin{aligned}
& \int_Y\Big[\tilde{\varepsilon}^{-1}(\mathbf{x},\mathbf{y})(\operatorname{rot}_{\mathbf{y}}\mathbf{H}_0(\mathbf{x},\mathbf{y}))\Big]\cdot\operatorname{rot}_{\mathbf{y}}\mathbf{H}_0^*(\mathbf{x},\mathbf{y})\,d\mathbf{y}\\
-\ & \int_Y\operatorname{div}_{\mathbf{y}}\Big[\tilde{\varepsilon}^{-1}(\mathbf{x},\mathbf{y})(\operatorname{rot}_{\mathbf{y}}\mathbf{H}_0(\mathbf{x},\mathbf{y}))\wedge\mathbf{H}_0^*(\mathbf{x},\mathbf{y})\Big]\,d\mathbf{y}=0
\end{aligned}
$$

The Green-Ostrogradsky formula then gives us :

$$\int_Y \Big[\tilde{\varepsilon}^{-1}(\mathbf{x},\mathbf{y})(\mathrm{rot}_{\mathbf{y}}\mathbf{H}_0(\mathbf{x},\mathbf{y}))\Big]\cdot \mathrm{rot}_{\mathbf{y}}\,\mathbf{H}_0^*(\mathbf{x},\mathbf{y})\,d\mathbf{y}$$
$$- \int_{\partial Y}\Big[\tilde{\varepsilon}^{-1}(\mathbf{x},\mathbf{y})(\mathrm{rot}_{\mathbf{y}}\mathbf{H}_0(\mathbf{x},\mathbf{y}))\wedge \mathbf{H}_0^*(\mathbf{x},\mathbf{y})\Big]\cdot \mathbf{n}\,ds = 0$$

From the anti-periodicity of the unit outgoing normal $\mathbf{n}$ to ∂Y and the periodicity in the $\mathbf{y}$ variable of $\mathbf{H}_0$, we deduce that :

$$\int_Y \tilde{\varepsilon}^{-1}(\mathbf{x},\mathbf{y})\Big[\mathrm{rot}_{\mathbf{y}}\mathbf{H}_0(\mathbf{x},\mathbf{y})\Big]^2\,d\mathbf{y} = 0$$

Let us assume that the real or imaginary parts of ε^{-1} keep a constant sign. We deduce that :

$$a.e.\mathbf{y}\in Y,\ \ \mathrm{rot}_{\mathbf{y}}\,\mathbf{H}_0(\mathbf{x},\mathbf{y}) = 0 \tag{4}$$

(QED)

From lemma 2, we can derive the following result.

Lemma 3 *H_0, solution of the system $\mathcal{S}_0$, is such that*

$$\textit{For almost every } \mathbf{y} \textit{ in } Y,\ \mathrm{div}_y\Big(\tilde{\mu}(\mathbf{x},\mathbf{y})\mathbf{H}_0(\mathbf{x},\mathbf{y})\Big) = 0$$

Remark :

In [105][214], we studied the homogenization of a three dimensional diffracting problem using the same multi-scale expansion method in the magnetic field formulation. We also deduced that $\mathrm{rot}_y\,\mathbf{H_0}(\mathbf{x},\mathbf{y}) = 0$. Noting that $\mu = \mu_0$ (non magnetic medium) we knew that $\mathrm{div}_y\,\mathbf{H_0}(\mathbf{x},\mathbf{y}) = 0$, which is obviously no more the case. We therefore deduced that $\Delta_y\mathbf{H_0}(\mathbf{x},\mathbf{y}) = 0$, which ensured us that $\mathbf{H}_0$ did not depend on the microscopic variable $\mathbf{x}$. Consequently, $\mathbf{H}_0$ could be seen as a homogenized magnetic field $\mathbf{H_{hom}}(\mathbf{x})$ i.e. $\mathbf{H_0}(\mathbf{x},\mathbf{y}) = \mathbf{H_{hom}}(\mathbf{x})$. The main difference with [105][214] is thus that the first term $\mathbf{H_0}$ of the ansatz is here dependent of the $\mathbf{y}$ variable.

Proof :

From equations (2) and (4) we have :

$$\mathrm{rot}_{\mathbf{y}}\Big(\tilde{\varepsilon}^{-1}(\mathbf{x},\mathbf{y})\,\mathrm{rot}_{\mathbf{x}}\,\mathbf{H}_0(\mathbf{x},\mathbf{y})\Big) + \mathrm{rot}_{\mathbf{y}}\Big(\tilde{\varepsilon}^{-1}(\mathbf{x},\mathbf{y})\,\mathrm{rot}_{\mathbf{y}}\,\mathbf{H}_1(\mathbf{x},\mathbf{y})\Big) = 0 \tag{5}$$

By applying $\mathrm{div}_{\mathbf{y}}$ to (3) we derive :

$$\mathrm{div}_{\mathbf{y}}\Big(\mathrm{rot}_{\mathbf{x}}(\tilde{\varepsilon}^{-1}\,\mathrm{rot}_{\mathbf{x}}\,\mathbf{H}_0)\Big) + \mathrm{div}_{\mathbf{y}}\Big(\mathrm{rot}_{\mathbf{x}}(\tilde{\varepsilon}^{-1}\,\mathrm{rot}_{\mathbf{y}}\,\mathbf{H}_1)\Big)$$
$$+ \mathrm{div}_{\mathbf{y}}\Big(\mathrm{rot}_{\mathbf{y}}(\tilde{\varepsilon}^{-1}\,\mathrm{rot}_{\mathbf{x}}\,\mathbf{H}_1)\Big) + \mathrm{div}_{\mathbf{y}}\Big(\mathrm{rot}_{\mathbf{y}}(\tilde{\varepsilon}^{-1}\,\mathrm{rot}_{\mathbf{y}}\,\mathbf{H}_2)\Big) + k_0^2\,\mathrm{div}_{\mathbf{y}}\Big(\tilde{\mu}(\mathbf{x},\mathbf{y})\mathbf{H}_0\Big) = 0$$

Noticing that

$$\operatorname{div}_y \operatorname{rot}_x A(x,y) = \bigtriangledown_y \cdot \Big(\bigtriangledown_x \wedge A(x,y)\Big) = -\bigtriangledown_x \cdot \Big(\bigtriangledown_y \wedge A(x,y)\Big) = -\operatorname{div}_x \operatorname{rot}_y A(x,y)\ ,$$

this expression reduces to :

$$-\operatorname{div}_{\mathbf{x}}\Big(\underbrace{\operatorname{rot}_{\mathbf{y}}(\tilde{\varepsilon}^{-1}\operatorname{rot}_{\mathbf{x}}\mathbf{H}_0) + \operatorname{rot}_{\mathbf{y}}(\tilde{\varepsilon}^{-1}\operatorname{rot}_{\mathbf{y}}\mathbf{H}_1)}_{=0(5)}\Big) + k_0^2 \operatorname{div}_{\mathbf{y}}\Big(\tilde{\mu}(\mathbf{x},\mathbf{y})\mathbf{H}_0\Big) = 0$$

Finally, we get the following formulation :

$$\operatorname{div}_{\mathbf{y}}\Big(\tilde{\mu}(\mathbf{x},\mathbf{y})\mathbf{H}_0(\mathbf{x},\mathbf{y})\Big) = 0 \tag{6}$$

(QED)

We want to show some analogous properties for $\mathbf{E}_0$. Having a look at (5) :

$$\operatorname{rot}_{\mathbf{y}}\Big(\tilde{\varepsilon}^{-1}(\mathbf{x},\mathbf{y})(\operatorname{rot}_{\mathbf{y}}\mathbf{H}_1(\mathbf{x},\mathbf{y}) + \operatorname{rot}_{\mathbf{x}}\mathbf{H}_0(\mathbf{x},\mathbf{y}))\Big) = 0\ , \tag{5}$$

for reasons of coherence in the physical units, we can state that :

$$\mathbf{E}_0(\mathbf{x},\mathbf{y}) = \frac{i}{\omega\varepsilon_0}\tilde{\varepsilon}^{-1}(\mathbf{x},\mathbf{y})(\operatorname{rot}_{\mathbf{y}}\mathbf{H}_1(\mathbf{x},\mathbf{y}) + \operatorname{rot}_{\mathbf{x}}\mathbf{H}_0(\mathbf{x},\mathbf{y})) \tag{$\tilde{5}$}$$

This is just a definition, since it has not been proved that $\mathbf{E}_\eta$ were converging towards $\mathbf{E}_0$. Consequently, the equation (5) can be written as :

$$\operatorname{rot}_{\mathbf{y}}(-i\omega\varepsilon_0\ \mathbf{E}_0(\mathbf{x},\mathbf{y})) = 0 \tag{7}$$

$\tilde{\varepsilon}$ goes in the left side of the expression ($\tilde{5}$), and we take its divergence in the $\mathbf{y}$ variable. Noting once more that $\operatorname{div}_y \operatorname{rot}_x A(x,y) = -\operatorname{div}_x \operatorname{rot}_y A(x,y)$, thanks to the lemma 2 we get that :

$$\operatorname{div}_{\mathbf{y}}(\tilde{\varepsilon}\mathbf{E}_0(\mathbf{x},\mathbf{y})) = 0 \tag{8}$$

The results derived from the equations (7) and (8) are thus summed up in the following system :

$$\begin{cases} \operatorname{rot}_{\mathbf{y}}(\mathbf{E}_0(\mathbf{x},\mathbf{y})) = 0 \\ \operatorname{div}_{\mathbf{y}}(\tilde{\varepsilon}\mathbf{E}_0(\mathbf{x},\mathbf{y})) = 0 \end{cases}$$

Making the obvious remark that the average of $\mathbf{E}_0$ on Y gives us a field independant of the microscopic variable, we denote by $\mathbf{E}_{hom}$ the following quantity :

$$\mathbf{E}_{hom}(\mathbf{x}) = \langle \mathbf{E}_0 \rangle_Y = \frac{1}{meas(Y)} \int_Y \mathbf{E}_0(\mathbf{x},\mathbf{y})\, d\mathbf{y} \tag{9}$$

Where $meas(Y)$ denotes the volume area of the unit cell Y.

Hence, $\operatorname{rot}_{\mathbf{y}}(\mathbf{E}_0 - \mathbf{E}_{hom}) = 0$. In general, this merely implies that $\mathbf{E}_0 = \mathbf{E}_{hom}(\mathbf{x}) - \bigtriangledown_{\mathbf{y}} V(\mathbf{x},\mathbf{y}) + \mathbf{E}_{cohom}(\mathbf{x})$, where $\mathbf{E}_{cohom}$ belongs to the so called cohomology space whose dimension depends upon the number of cuts made in the complex plane to obtain a simply

connected open set $\tilde{Y}$. In our case, $< \mathbf{E}_0 >_Y = < \mathbf{E}_{hom} >_Y$ and $< \bigtriangledown_{\mathbf{y}} V >_Y = 0$ which implies that $\mathbf{E}_{cohom} = 0$. Then, $\mathbf{E}_0 - \mathbf{E}_{hom}$ derives from a scalar potential denoted by V. That is to say that there exists a Y-periodic function $V(\mathbf{x}, \mathbf{y})$ such as :

$$\mathbf{E}_0 = \mathbf{E}_{hom} - \bigtriangledown_{\mathbf{y}} V \tag{10}$$

It is worth noting that this deduction would not hold necessarily if there were currents in the Scattering-Box. This would be the case for a domain Ω_f filled up by diffracting objects of infinite conductivity.

Injecting (10) in (8), leads us to :

$$\mathrm{div}_{\mathbf{y}}\Big(\tilde{\varepsilon}(\mathbf{E}_{hom} - \bigtriangledown_{\mathbf{y}} V)\Big) = 0 \tag{11}$$

By linearity of the divergence, we can write that :

$$\begin{aligned} -\mathrm{div}_{\mathbf{y}}\Big(\tilde{\varepsilon}(\bigtriangledown_{\mathbf{y}} V)\Big) &= -\mathrm{div}_{\mathbf{y}}(\tilde{\varepsilon}\mathbf{E}_{hom}) \\ &= -\mathrm{div}_{\mathbf{y}}\Big(\tilde{\varepsilon}\sum_{j=1}^{3}\mathbf{E}_{hom,j}e_j\Big) \\ &= -\sum_{j=1}^{3}\mathrm{div}_{\mathbf{y}}\Big(\tilde{\varepsilon}(\mathbf{x},\mathbf{y})e_j\Big)\mathbf{E}_{hom,j}(\mathbf{x}) \end{aligned}$$

We are thus led to solve an annex problem of electrostatic type $\mathcal{K}_j$:

$$\mathcal{K}_j : \ -\mathrm{div}_{\mathbf{y}}\Big(\tilde{\varepsilon}(\mathbf{x},\mathbf{y})(\bigtriangledown_{\mathbf{y}} V_j - e_j)\Big) = 0 \ , j \in \{1,2,3\} \tag{12}$$

The variational form associated to this problem having the good properties (sesquilinear, continue and coercive) in the Hilbert space $H^1_\sharp(Y)/\mathbb{R}$, the Lax-Milgram lemma assures the existence and uniqueness of the solution of this problem in $H^1_\sharp(Y)/\mathbb{R}$, that is, up to an additive constant.

Let us remark that $\tilde{\varepsilon}(\mathbf{x},\mathbf{y})$ being a data of the problem $\mathcal{P}_\eta$, $\mathrm{div}_{\mathbf{y}}\Big(\tilde{\varepsilon}(\mathbf{x},\mathbf{y})e_j\Big)$ is a known function. Therefore, we have to solve an annex problem where the unknowns are the three components of the potential V_j. The solutions of (11) are given by the functions :

$$V(\mathbf{x},\mathbf{y}) = \sum_{j=1}^{3} V_j(\mathbf{y})E_{hom,j}(\mathbf{x}) = \mathbf{V}_Y \cdot \mathbf{E}_{hom} \tag{13}$$

where $\mathbf{V}_Y = (V_1, V_2, V_3)$ and V_j denote respectively the vectorial potential of the basic cell and one of the scalar potentials associated with the density of charges $\mathrm{div}_{\mathbf{y}}(\varepsilon(\mathbf{y})e_j)$.

Before going further, it is worth noting that the problem $\mathcal{K}_j$ is of interest by itself. In the previous section, we have proposed to solve it thanks to a finite difference scheme. We are also working on a finite element modelization with periodic conditions. It is worth noting that the annex problem has been solved in the scalar case thanks to a method of fictitious sources [47][215][178] that is used in the third part of the thesis for the homogenization of metallic waveguides filled with a periodic assembly of dielectric rods.

From (10) and (13) we get that :

$$\mathbf{E}_0 = (I - \bigtriangledown_{\mathbf{y}} \mathbf{V}_Y)\mathbf{E}_{hom} \tag{14}$$

where I denotes the identity matrix and $\bigtriangledown_{\mathbf{y}} \mathbf{V}_Y$ denotes the jacobian of $\mathbf{V}_Y$.
That is to say that :

$$\mathbf{E}_0 = \left(I - \begin{bmatrix} \frac{\partial V_1}{\partial y_1} & \frac{\partial V_2}{\partial y_1} & \frac{\partial V_3}{\partial y_1} \\ \frac{\partial V_1}{\partial y_2} & \frac{\partial V_2}{\partial y_2} & \frac{\partial V_3}{\partial y_2} \\ \frac{\partial V_1}{\partial y_3} & \frac{\partial V_2}{\partial y_3} & \frac{\partial V_3}{\partial y_3} \end{bmatrix} \right) \mathbf{E}_{hom}$$

We want now to precise the link between $\mathbf{E}_{hom}$ and the average $\mathbf{H}_{hom}$ of $\mathbf{H}_0(\mathbf{x}, \mathbf{y})$ over the basic cell Y :

$$\mathbf{H}_{hom}(\mathbf{x}) = \langle \mathbf{H}_0 \rangle_Y = \frac{1}{meas(Y)} \int_Y \mathbf{H}_0(\mathbf{x}, \mathbf{y})\, d\mathbf{y}$$

From ($\tilde{5}$) we know that :

$$\mathbf{E}_0 = \frac{i}{\omega \varepsilon_0} \tilde{\varepsilon}^{-1} (\mathrm{rot}_{\mathbf{y}} \mathbf{H}_1 + \mathrm{rot}_{\mathbf{x}} \mathbf{H}_0(\mathbf{x}, \mathbf{y}))$$

We then deduce from (14) that :

$$(I - \bigtriangledown_{\mathbf{y}} \mathbf{V}_Y)\mathbf{E}_{hom} = \frac{i}{\omega \varepsilon_0} \tilde{\varepsilon}^{-1} (\mathrm{rot}_{\mathbf{y}} \mathbf{H}_1 + \mathrm{rot}_{\mathbf{x}} \mathbf{H}_0(\mathbf{x}, \mathbf{y}))$$

Making the sum over Y of this expression leads us to :

$$\int_Y \mathrm{rot}_{\mathbf{y}} \mathbf{H}_1(\mathbf{x}, \mathbf{y})\, dy + \mathrm{rot}_{\mathbf{x}} \mathbf{H}_{hom}(\mathbf{x}) = -i\omega\varepsilon_0 < \tilde{\varepsilon}(I - \bigtriangledown_{\mathbf{y}} \mathbf{V}_Y) >_Y \mathbf{E}_{hom} \tag{15}$$

Thanks to the periodicity of $\mathbf{H}_1$ and due to the antiperiodicity of the outer normal $\mathbf{n}$ to ∂Y, by virtue of the Green formula, we have :

$$\int_Y \mathrm{rot}_y\, \mathbf{H}_1(\mathbf{x}, \mathbf{y})\, d\mathbf{y} = \int_{\partial Y} n \wedge \mathbf{H}_1\, ds = 0$$

Then, we are led to the following system :

$$\begin{cases} \mathrm{rot}_{\mathbf{x}} \mathbf{H}_{hom}(\mathbf{x}) = -i\omega\varepsilon_0 \varepsilon_{hom} \mathbf{E}_{hom} \\ \varepsilon_{hom} = < \tilde{\varepsilon}(I - \bigtriangledown_{\mathbf{y}} \mathbf{V}_Y) >_Y \end{cases} \tag{16}$$

It remains to give the equation verified by $\mathbf{H}_{hom}(\mathbf{x})$. Summing the equation (3) in the system $\mathcal{S}_0$ over Y, we derive that :

$$\begin{aligned} & \int_Y \mathrm{rot}_{\mathbf{y}} \Big(\tilde{\varepsilon}^{-1} (\mathrm{rot}_{\mathbf{y}}\, \mathbf{H}_2) \Big)\, d\mathbf{y} \\ = \; & k_0^2 \int_Y \tilde{\mu}(\mathbf{x}, \mathbf{y}) \mathbf{H}_0(\mathbf{x}, \mathbf{y})\, d\mathbf{y} - \int_Y \mathrm{rot}_{\mathbf{x}} \Big(\tilde{\varepsilon}^{-1} (\mathrm{rot}_{\mathbf{x}}\, \mathbf{H}_0(\mathbf{x}, \mathbf{y})) \Big)\, d\mathbf{y} \\ - \; & \int_Y \mathrm{rot}_{\mathbf{x}} \Big(\tilde{\varepsilon}^{-1} (\mathrm{rot}_{\mathbf{y}}\, \mathbf{H}_1) \Big)\, d\mathbf{y} - \int_Y \mathrm{rot}_{\mathbf{y}} \Big(\tilde{\varepsilon}^{-1} (\mathrm{rot}_{\mathbf{x}}\, \mathbf{H}_1) \Big)\, d\mathbf{y} \end{aligned} \tag{17}$$

Due to the periodicity of $\mathbf{H}_1$, $\mathbf{H}_2$ and $\tilde{\varepsilon}$, and due to the antiperiodicity of the outer normal $\mathbf{n}$ to ∂Y, by virtue of the Green formula ($\int_Y \mathrm{rot}\, A\, d\mathbf{y} = \int_{\partial Y} n \wedge A\, ds$), we get that :

$$\int_Y \mathrm{rot}_{\mathbf{y}}\Big(\tilde{\varepsilon}^{-1}(\mathrm{rot}_{\mathbf{x}}\,\mathbf{H}_1(\mathbf{x},\mathbf{y}))\Big) = \int_Y \mathrm{rot}_{\mathbf{y}}\Big(\tilde{\varepsilon}^{-1}(\mathrm{rot}_{\mathbf{y}}\,\mathbf{H}_2(\mathbf{x},\mathbf{y}))\Big) = 0$$

Therefore, the equation (17) reduces to :

$$\begin{aligned} - \quad & k_0^2 \int_Y \tilde{\mu}(\mathbf{x},\mathbf{y})\mathbf{H}_0(\mathbf{x},\mathbf{y})\,d\mathbf{y} + \int_Y \mathrm{rot}_{\mathbf{x}}\Big(\tilde{\varepsilon}^{-1}(\mathrm{rot}_{\mathbf{x}}\,\mathbf{H}_0(\mathbf{x},\mathbf{y}))\Big)\,d\mathbf{y} \\ + \quad & \int_Y \mathrm{rot}_{\mathbf{x}}\Big(\tilde{\varepsilon}^{-1}(\mathrm{rot}_{\mathbf{y}}\,\mathbf{H}_1)\Big)\,d\mathbf{y} = 0 \end{aligned}$$

Taking into account the equation ($\tilde{5}$), we get :

$$-k_0^2 \int_Y \tilde{\mu}(\mathbf{x},\mathbf{y})\mathbf{H}_0(\mathbf{x},\mathbf{y})\,d\mathbf{y} + i\omega\varepsilon_0 \int_Y \mathrm{rot}_{\mathbf{x}}\,\mathbf{E}_0 = 0$$

Thanks to the definition of $\mathbf{E}_{hom}$, if we commute the summation over Y and the rotational in the $\mathbf{x}$ variable in the second integrand, we obtain :

$$k_0^2 \int_Y \tilde{\mu}(\mathbf{x},\mathbf{y})\mathbf{H}_0(\mathbf{x},\mathbf{y})\,d\mathbf{y} + i\omega\varepsilon_0\,\mathrm{rot}\,\mathbf{E}_{hom} = 0 \tag{19}$$

To conclude the proof, we must express the first integrand in terms of μ_{hom} and $\mathbf{H}_{hom}$. From the lemmae 2 and 3, we know that :

$$\begin{cases} \mathrm{rot}_{\mathbf{y}}(\mathbf{H}_0(\mathbf{x},\mathbf{y})) = 0 \\ \mathrm{div}_{\mathbf{y}}(\tilde{\mu}(\mathbf{x},\mathbf{y})\mathbf{H}_0(\mathbf{x},\mathbf{y})) = 0 \end{cases} \tag{20}$$

From the first equation of the system (20), we deduce that $\mathbf{H}_0 - \mathbf{H}_{hom}$ derives from a scalar potential denoted by W. That is to say that there exists a Y-periodic function $W(\mathbf{x},\mathbf{y})$ such as :

$$\mathbf{H}_0 = \mathbf{H}_{hom} - \bigtriangledown_{\mathbf{y}} W \tag{21}$$

Injecting (21) in the second equation of the system (20), we get that :

$$\mathrm{div}_{\mathbf{y}}\Big(\tilde{\mu}(\mathbf{x},\mathbf{y})(\mathbf{H}_{hom} - \bigtriangledown_{\mathbf{y}} W)\Big) = 0 \tag{22}$$

By linearity of the divergence, we can write that :

$$\begin{aligned} -\,\mathrm{div}_{\mathbf{y}}\Big(\tilde{\mu}(\mathbf{x},\mathbf{y})(\bigtriangledown_{\mathbf{y}} W)\Big) &= -\,\mathrm{div}_{\mathbf{y}}(\tilde{\mu}(\mathbf{x},\mathbf{y})\mathbf{H}_{hom}) \\ &= -\,\mathrm{div}_{\mathbf{y}}\Big(\tilde{\mu}(\mathbf{x},\mathbf{y})\sum_{j=1}^{3}\mathbf{H}_{hom,j}e_j\Big) \\ &= -\sum_{j=1}^{3}\mathrm{div}_{\mathbf{y}}\Big(\tilde{\mu}(\mathbf{x},\mathbf{y})e_j\Big)\mathbf{H}_{hom,j}(\mathbf{x}) \end{aligned}$$

We are thus led to solve an annex problem of electrostatic type $\mathcal{M}_j$:

$$\mathcal{M}_j : \; -\mathrm{div}_{\mathbf{y}}\Big(\tilde{\mu}(\mathbf{x},\mathbf{y})(\bigtriangledown_{\mathbf{y}} W_j - e_j)\Big) = 0 \;, j \in \{1,2,3\} \tag{23}$$

The variational form associated to this problem having the good properties (sesquilinear, continue and coercive) in the Hilbert space $H^1_\sharp(Y)/\mathbb{R}$, the Lax-Milgram lemma assures the existence and uniqueness of the solution of this problem in $H^1_\sharp(Y)/\mathbb{R}$, that is, up to an additive constant.

Let us remark that $\tilde{\mu}(\mathbf{x},\mathbf{y})$ being a data of the problem $\mathcal{P}_\eta$, $\mathrm{div}_\mathbf{y}\Big(\tilde{\mu}(\mathbf{x},\mathbf{y})e_j\Big)$ is a known function. Therefore, we have to solve an annex problem where the unknowns are the three components of the potential W_j. The solutions of (22) are given by the functions :

$$W(\mathbf{x},\mathbf{y}) = \sum_{j=1}^{3} W_j(\mathbf{y}) H_{hom,j}(\mathbf{x}) = \mathbf{W}_Y \cdot \mathbf{H}_{hom} \tag{25}$$

where $\mathbf{W}_Y = (W_1, W_2, W_3)$ and W_j denote respectively the vectorial potential of the basic cell and one of the scalar potentials associated with the density of charges $\mathrm{div}_\mathbf{y}(\mu(\mathbf{y})e_j)$.

From (21) and (25) we get that :

$$\mathbf{H}_0 = (I - \bigtriangledown_\mathbf{y}\mathbf{W}_Y)\mathbf{H}_{hom} \tag{26}$$

where I denotes the identity matrix and $\bigtriangledown_\mathbf{y}\mathbf{W}_Y$ denotes the jacobian of $\mathbf{W}_Y$.
That is to say that :

$$\mathbf{H}_0 = \left(I - \begin{bmatrix} \frac{\partial W_1}{\partial y_1} & \frac{\partial W_2}{\partial y_1} & \frac{\partial W_3}{\partial y_1} \\ \frac{\partial W_1}{\partial y_2} & \frac{\partial W_2}{\partial y_2} & \frac{\partial W_3}{\partial y_2} \\ \frac{\partial W_1}{\partial y_3} & \frac{\partial W_2}{\partial y_3} & \frac{\partial W_3}{\partial y_3} \end{bmatrix} \right) \mathbf{H}_{hom}$$

From (19) and (26), we deduce that :

$$k_0^2\Big(\int_Y \mu(\mathbf{x},\mathbf{y})(I - \bigtriangledown_\mathbf{y}\mathbf{W}_Y)\,d\mathbf{y}\Big)\mathbf{H}_{hom} + i\omega\varepsilon_0\,\mathrm{rot}\,\mathbf{E}_{hom} = 0 \tag{27}$$

The homogenized equation then clearly follows from the system (16) :

$$\mathrm{rot}\Big(\varepsilon_{hom}^{-1}(\mathrm{rot}\,\mathbf{H}_{hom}(\mathbf{x}))\Big) - k_0^2\mu_{hom}\mathbf{H}_{hom}(\mathbf{x}) = 0 \tag{28}$$

with the effective permittivity defined by :

$$\varepsilon_{hom} = < \tilde{\varepsilon}(\mathbf{x},\mathbf{y})(I - \bigtriangledown_\mathbf{y}\mathbf{V}_Y) >_Y$$

and the effective permeability defined by :

$$\mu_{hom} = < \tilde{\mu}(\mathbf{x},\mathbf{y})(I - \bigtriangledown_\mathbf{y}\mathbf{W}_Y) >_Y$$

Comments :

The mutiple-scale method which relies on the boundedness of the asymptotic terms of the expansion $(E1)$, risks being mathematicaly unsound, and hence leading to untrue equations. Nevertheless, in our case, we believe that the multiple-scale method gives the good form of the homogenized equation : in case of dielectric media, this heuristic method has been successfully applied to various problems [18]. It remains to get the same results

using the two-scale convergence relying on the following theorem : Let $\mathbf{u}(\mathbf{x},\mathbf{y})$ be a function $\Omega_f \times \mathbb{R}^3 \longmapsto \mathbb{C}^3$ periodic and regular in $\mathbf{y}$ with period $Y =]0;1[^3$ and square integrable on Ω_f. Then, the sequence $(\mathbf{u}_\eta)$ defined by $\mathbf{u}_\eta(\mathbf{x}) = \mathbf{u}(\mathbf{x}, \frac{\mathbf{x}}{\eta})$, which of course fails to converge everywhere, tends weakly in $L^2(\Omega_f)$ to the "average function" $< \mathbf{u} > (\mathbf{x}) = \int_Y \mathbf{u}(\mathbf{x},\mathbf{y})\, d\mathbf{y}$ that is to say that *we can extract a subsequence of* u_η *still denoted by* u_η, such that :

$$\forall \varphi \in L^2(\Omega_f)\ ,\ \int_{\Omega_f} \mathbf{u}_\eta(\mathbf{x})\varphi(\mathbf{x})\, d\mathbf{x} \to \Big(\int_{\Omega_f} (\int_Y \mathbf{u}(\mathbf{x},\mathbf{y})\, d\mathbf{y})\varphi(\mathbf{x})\, d\mathbf{x}\Big)$$

Roughly speaking, this method is based on a variational approach of the problem and uses suitable test functions of the form :

$\varphi_\eta(\mathbf{x}) = \varphi_0(\mathbf{x}, \frac{\mathbf{x}}{\eta}) + \eta\varphi_1(\mathbf{x}, \frac{\mathbf{x}}{\eta})$,

which can be seen as an ansatz of the first order. This is the object of an article in preparation for mathematicians [104].

Coming back to the multiple scale method, the first order term $\mathbf{H}_1$ provides the likely form of a corrector $\mathbf{C}_1$ chosen in such a way that

$\|\mathbf{H}_\eta - (\mathbf{H}_{hom} + \eta\mathbf{C}_1)\|_{H^1(\Omega_f)} \to 0$. In other words, this expression converges to 0 for the Hilbert norm L^2 and for the L^2 norm of its gradient. Roughly speaking, the corrector $\mathbf{C}_1$ is given for correcting strong oscillations near the obstacle. It is very important in numerical computation since it gives a convergence criterion. At this time, we have not been able to prove this choice to be in agreement with the requirement $\|\mathbf{H}_\eta - (\mathbf{H}_{hom} + \eta\mathbf{H}_1)\|_{H^1(\Omega_f)} \to 0$, since $\mathbf{H}_\eta$ belongs to another Hilbert space (which is very close to H^1).

Let us repeat once more that the mutiple-scale method which rests upon the existence of the expansion $(E1)$ risks being mathematically unsound in homogenization process dealing with metallic inclusions. Hence, it remains to show that the heuristic calculus of the preceding section leads to the good homogenized problem, and in what sense. In other words, the diffraction problem $\mathcal{P}_\eta$ being well posed for a given η, in what sense does it converge to an homogenized problem, and is it still a diffraction problem at the limit ?

In conclusion, the multiple-scale method leads here to the right formula, which is probably the essential point for most physicists. In fact, it remains to relate the limit of the inner field in the finite obstacle (given by the multiple-expansion) to the one of the diffracted field.

1.6.2 Perspectives on diffractive properties of such structures

In the last section, we outlined an asymptotic approach of scattering by finite photonic crystals with heterogeneous permittivity and permeability in the quasi-static limit thanks to the so-called multi-scale expansion method. Let us briefly discuss the physics underlying counter-intuitive phenomena. We note that there exists some Ferro-magnetic media whose relative permeability is lower than 1 (contrary to the relative permeability which is always greater than 1). On the first hand, thanks to the homogenization process, one can adjust the effective permittivity and the effective permeability in such a way that $\varepsilon_{eff}\mu_{eff} = Id$. The effective media therefore transmits light without deviation and reflects light as an ordinary medium (note that both effective permeability and permittivity can

be anisotropic, although their product is the identity matrix, which certainly leads to astonishing phenomena !). On the second hand, one can adjust ε_{eff} and μ_{eff} such that their ratio is the impedance of the air : in the one-dimensional case, it can be seen that there is a Brewster incidence in both $E_{\|}$ and $H_{\|}$ polarizations. Furthermore, we note that bodies of various permittivity and permeability can verify $\varepsilon_{eff}\mu_{eff} = Id$, and one has thus to define a class of equivalence for such heterogeneous structures, which behaves in the same way for the long wavelength, although they are quite different structures. One cannot distinguish such bodies in transmission (even if their shapes are quite different), since the transmitted waves does not see them !

In the three-dimensional case, the physics of these effective structures sounds therefore far from obvious and one needs to improve his conjectures with numerical computations. We therefore propose a numerical approach based on a finite difference scheme coupled with Fast Fourier Transforms (this method works either for annex problem involving ε or μ). We are only capable to present partial numerical results (we just give the behavior of the multi-scalar potential on the basic cell and do not compute explicitely the effective matrices of anisotropy), but work is in progress to improve this method with a second approach based on a finite element scheme. The numerical implementations will certainly lead to astonishing results in case of metallic inclusions : the British physicist R. Pendry has recently numerically exhibited composite structures with previously inaccessible values of effective permittivity and permeability [172]. He proposed some micro-structures which can be designed to have positive or negative values of ε_{eff} and μ_{eff} for low frequencies. He exploited a combination of negative ε_{eff} with μ_{eff} to get "negative refractive index" : the structure can bend light in the opposite direction to normal materials. Such a material will be a perfect lens, able to focus the magnetic as well as the electric part of the evanescent field in the opposite way to other materials : this novel type of lens can make an image of the evanescent field that mirrors the original light source. As a result, one can produce images smaller than the wavelength of light : such a material could be used to form high-resolution images. Pendry although exploited *adequate* values of the effective permeability μ_{eff} of microstructures on a scale much less than the wavelength of radiation, which are not resolved by incident microwaves, and used a very low density of metal (dilute composite) so that these structures can be extremely lightweight [173]. Most of the structures are resonant due to internal capacitance and inductance, and resonant enhancement combined with compression of electrical energy into a very small volume greatly enhances the energy density at critical locations in the structures. Weakly nonlinear materials placed at these critical locations will show greatly enhanced effects.

To conclude with ferro-magnetic structures, we believe that they may exhibit complete gaps in high frequencies even in the one-dimensional case (no dependence of the gaps upon the incident field when the ferro-magnetic medium has the index of the vaccum), unlike the traditional Bragg mirrors.

1.7 Conclusion

In this chapter, we have introduced an alternative to the use of the plane-wave-expansion method as applied to the homogenization of three-dimensional finite photonic crystals. The so called multi-scale method (the heuristic analog of the two-scale convergence) allows us to consider, unlike the Fourier expansion method, taking into account the effects of the crystal's boundary on the diffracted field. Furthermore, we give explicitely the expression of the effective permittivity (and effective permeability in case of ferro-magnetic media) which characterizes a finite anisotropic medium and thus that may exhibit sizable birefringence. We have then proposed two numerical approaches to give the terms of the tensor of permittivity (note that all these developments hold for the tensor of permeability) : these approaches consist in deriving its terms from the resolution of three annex problems of electrostatic type by using a finite difference scheme combined with a Fourier transformation and a method of fictitious sources [47] on a torus (the annex problem obtained by D. Felbacq and G. Bouchitté in the $H \parallel$ case [72] has been recently solved by this way). It is to be noticed that our asymptotic analysis still holds when applied to the study of crystals bounded solely in one direction (bi-gratings) or two directions (rods). It is then straightforward to study the homogenization of bigratings : (the reader may refer to [62], [13] or [152] to find adapted radiation conditions), which is a natural extension of the works led in [149] and [151]. Work is also proceeding on the homogenization of finite photonic crystals, whose basic cell is not paralellepipedical, by the use of differential forms [9], [10],[11],[12].

Chapitre 2

Justification par la méthode deux-échelles

A ce discours, nos deux voyageurs se laissrent aller l'un contre l'autre en touffant de ce rire inextinguible qui, selon Homre, est le partage des dieux ; leurs paules et leurs ventres allaient et venaient, et, dans ces convulsions, le vaisseau que le Sirien avait sur son ongle tomba dans une poche de la culotte du Saturnien. Ces deux bonnes gens le recherchrent longtemps ; enfin ils retrouvrent l'quipage, et le rajustrent fort proprement. Le Sirien reprit les petites mites ; il leur parla encore avec beaucoup de bont, quoiqu'il ft fch dans le fond du cœur de voir que les infiniments petits eussent un orgueil presque infiniment grand."

"Micromgas" in "Les contes philosophiques" (1752) Voltaire

Addendum

This chapter is devoted to the asymptotic analysis of the vector Maxwell system for a 3D finite photonic crystal in the case where $\mu = \mu_0$ is constant. We prove the theorem 1 of chapter 1 and derive the annex problem for the two dimensional case in $H \parallel$ polarization with a variant of the classical results of Keller [117] and Dykhne [68] on the chess-board problem (in our case, the permittivity ε can be a continuous function). It is worth noting that Milton *et al* proved analogous duality relations for multiphase media in electromagnetics and acoustics [156][155][112][92].

2.1 Notion de convergence deux-échelles

La méthode utilisée repose sur la notion de convergence à deux échelles qui est liée à une classe de fonctions dites admissibles dont nous allons rappeler la définition.

Définition :

Soit Ω un ouvert de $\mathbb{R}^N$ et $Y =]0;1[^N$. $\varphi \in L^2(\Omega \times Y)$ est dite admissible si la suite $\varphi_\eta(x) = \varphi(x, \frac{x}{\eta})$ est bornée dans $L^2(\Omega)$ et vérifie :

$$\lim_{\eta \to 0} \int_\Omega \mid \varphi(x, \frac{x}{\eta}) \mid^2 dx = \iint_{\Omega \times Y} \mid \varphi \mid^2 (x, y)\, dxdy$$

Il est important de noter que les fonctions $\varphi(x,y) \in L^2(\Omega; L^2_\sharp(Y))$ ne satisfont pas cette définition puisque l'on ne peut pas assurer que $x \longmapsto \varphi(x, \frac{x}{\eta})$ soit mesurable sur Ω. Un résultat classique [69] assure que les éléments de $L^2(\Omega, C_\sharp(Y))$ satisfont cette dernière propriété (noter pour cela que ces fonctions sont mesurables en x, et continues en y pour presque tout x). De plus, on a l'inégalité :

$$\int_\Omega \mid \varphi(x, \frac{x}{\eta}) \mid^2 dx \leq \int_\Omega \sup_{y\in Y} \mid \varphi(x,y) \mid^2 dx = \|\varphi\|^2_{L^2(\Omega, C_\sharp(Y))} < +\infty$$

qui montre que $\varphi(x, \frac{x}{\eta}) \in L^2(\Omega)$. Partant de cette constatation, Nguetseng a établi dans [164] les deux résultats suivants :

Lemme 1
Les espaces fonctionnels $L^2(\Omega, C_\sharp(Y))$, $L^2{}_\sharp(Y, C(\Omega))$, et $C(\Omega; L^\infty_\sharp(Y))$ qui s'identifient à des sous-espaces denses de $L^2(\Omega \times Y)$ sont des espaces de fonctions admissibles.

Proposition 2
Soit (u_η) une suite bornée dans $L^2(\Omega)$. Alors $\exists \eta_k$ suite tendant vers 0 et $\exists u_0(x,y) \in L^2(\Omega \times Y)$ (Y-périodique en y) tels que $\forall \varphi$ admissible

$$\lim_{k\to+\infty} \int_\Omega u_{\eta_k}(x)\varphi(x, \frac{x}{\eta_k})\, dx = \iint_{\Omega\times Y} u_0(x,y)\varphi(x,y)\, dxdy$$

Ce type de convergence est baptisé "convergence faible à deux-échelles". Le passage à la limite dans des intégrales du type $\int_\Omega u_\eta(x)v_\eta(x)\, dx$ s'appuie sur une notion de convergence forte à deux-échelles.

Définition :
i) On dit qu'une suite $u_\eta \in L^2(\Omega)$ converge faiblement à deux échelles vers une fonction $u_0(x,y) \in L^2(\Omega \times Y)$ et on note $u_\eta \rightharpoonup u_0(x,y)$ faible à deux échelles si :

$$\forall \psi(x,y) \in \mathcal{D}(\Omega; C^\infty_\sharp(Y)) \ , \ \lim_{\eta\to 0} \int_\Omega u_\eta(x)\psi(x, \frac{x}{\eta})\, dx = \iint_{\Omega\times Y} u_0(x,y)\psi(x,y)\, dxdy$$

ii) On dit qu'une suite $u_\eta \in L^2(\Omega)$ converge fortement à deux échelles vers une fonction $u_0(x,y) \in L^2(\Omega \times Y)$ et on note $u_\eta \twoheadrightarrow u_0(x,y)$ fort à deux échelles si

$$\limsup_{\eta\to 0} \int_\Omega \mid u_\eta \mid^2 dx \leq \iint_{\Omega\times Y} \mid u_0 \mid^2(x,y)\, dxdy \ ,$$

soit encore,

$$\lim_{\eta\to 0} \|u_\eta\|_{L^2(\Omega)} = \|u_0\|_{L^2(\Omega\times Y)} \ .$$

Remarques :

1) La limite faible dans $L^2(\Omega)$ de la suite $u_{\eta_k}(x)$ est donnée par $u(x) = \int_Y u_0(x,y)\, dy$.

En effet, si on prend une fonction $\varphi(x,y)$ telle que $\varphi(x,y)=\varphi(x)$, alors

$$\lim_{k\to+\infty}\int_\Omega u_{\eta_k}(x)\varphi(x,\frac{x}{\eta})\,dx=\iint_{\Omega\times Y}u_0(x,y)\varphi(x)\,dxdy=\int_\Omega\Big(\int_Y u_0(x,y)\,dy\Big)\varphi(x)\,dx$$

2) La convergence forte dans *ii)* exprime que les seules oscillations effectives de la suite (u_η) sont à l'échelle η. Dans la proposition 3 *iii)*, due à Allaire [2], un résultat de correcteur est obtenu pour la suite (u_η), lorsque u_0 est assez régulière.

Proposition 3

Soit (u_η) une suite bornée dans $L^2(\Omega)$ telle que $u_\eta \rightharpoonup u_0(x,y)$ faible à deux échelles. Alors

i) u_η converge faiblement dans $L^2(\Omega)$ vers $u(x)=\displaystyle\int_Y u_0(x,y)\,dy$ et de plus

$$\liminf_{\eta\to0}\|u_\eta\|_{L^2(\Omega)}\geq\|u_0\|_{L^2(\Omega\times Y)}\geq\|u\|_{L^2(\Omega)}$$

ii) Soit v_η une autre suite bornée dans $L^2(\Omega)$ telle que $v_\eta \twoheadrightarrow v_0$ fortement, alors $u_\eta v_\eta \to w(x)$ dans $\mathcal{D}'(\Omega)$ où $w(x)=\displaystyle\int_Y u_0(x,y)v_0(x,y)\,dy$

iii) Si $u_\eta \twoheadrightarrow u_0(x,y)$ fort à deux échelles et u_0 admissible, alors

$$\|u_\eta-u_0(x,\frac{x}{\eta})\|_{L^2(\Omega)}\to0$$

Pour passer à la limite dans le système de Maxwell, nous serons amenés, étant donnée une suite (u_η) bornée dans $H^1(\Omega)$ (qui vérifie alors $u_\eta \rightharpoonup u_0$ et $\nabla u_\eta \rightharpoonup \chi$ d'après la proposition 2), à déterminer la relation différentielle liant χ à u_0. Dans la proposition qui suit nous aurons besoin de la définition de l'espace $H^1_\sharp(Y)$ que nous rappelons.

Définition :

$$H^1_\sharp(Y)\ =\Big\{w\in H^1_{loc}(\mathbb{R}^N);\ w \text{ est } KY\text{-périodique } (\forall z\in\mathbb{Z}^N\ w(.+z)=w(.) \text{ p.p. } y\in KY)\Big\}$$

$H^1_\sharp(Y)$ muni du produit scalaire $(u\mid v)=\displaystyle\int_Y u.v\,dy+\int_Y\nabla u\cdot\nabla v\,dy$ est un espace de Hilbert.

Par ailleurs, il est connu que dans $H^1_\sharp(Y)/\mathbb{R}$, $w\longmapsto\|\nabla w\|_{L^2(Y)}$ définit une norme équivalente à celle de $H^1_\sharp(Y)$ qui fait de $H^1_\sharp(Y)/\mathbb{R}$ un espace de Hilbert.

Nous sommes maintenant en mesure d'établir le résultat de structure pour les gradients dû à G. Allaire [2].

Proposition 4

Soit (u_η) une suite bornée dans $W^{1,2}(\Omega)$. Alors $\exists u\in W^{1,2}(\Omega),\exists u_1\in L^2(\Omega,H^1_\sharp(Y))$ et une suite extraite (encore notée (u_η)) telle que :

$$\begin{cases}u_\eta \twoheadrightarrow u_0 \text{ où } u_0(x,y)=u(x)\\ \nabla u_\eta \rightharpoonup \nabla_x u(x)+\nabla_y u_1(x,y)\end{cases}$$

Démonstration :

première étape :

u_η et ∇u_η sont bornées dans $L^2(\Omega)$ et $[L^2(\Omega)]^N$ donc convergent (après une extraction de sous-suite) à deux échelles vers des limites $u_0(x,y) \in L^2(\Omega \times Y)$ et $\bigtriangledown_y u_0(x,y) \in [L^2(\Omega \times Y)]^N$.

Soit $\varphi \in [\mathcal{D}(\Omega; C^\infty_\sharp(Y))]^N$ alors

$$\lim_{\eta \to 0} \int_\Omega \nabla u_\eta(x) \cdot \varphi(x, \frac{x}{\eta})\, dx = \iint_{\Omega \times Y} \chi_0(x,y) \cdot \varphi(x,y)\, dxdy \tag{1}$$

La formule de Green nous assure que :

$$\int_\Omega \nabla u_\eta(x) \cdot \varphi(x, \frac{x}{\eta})\, dx = -\int_\Omega u_\eta \operatorname{div}(\varphi(x, \frac{x}{\eta}))\, dx$$

Par ailleurs, l'opérateur divergence "rescalé" prend la forme suivante :

$$\operatorname{div} \varphi(x, \frac{x}{\eta}) = (\operatorname{div}_x \varphi)(x, \frac{x}{\eta}) + \frac{1}{\eta}(\operatorname{div}_y \varphi)(x, \frac{x}{\eta})$$

L'égalité (1) peut donc être réécrite :

$\iint_{\Omega \times Y} \chi_0(x,y)\varphi(x,y)\, dxdy = \lim_{\eta \to 0} I_\eta$ avec

$$I_\eta = [-\int_\Omega u_\eta (\operatorname{div}_x \varphi)(x, \frac{x}{\eta})\, dx - \frac{1}{\eta}\int_\Omega u_\eta (\operatorname{div}_y \varphi)(x, \frac{x}{\eta})\, dx] \tag{2}$$

Comme I_η reste borné, on déduit de (2) que

$$\begin{aligned} 0 &= \lim_{\eta \to 0} \eta I_\eta \\ &= \lim_{\eta \to 0} [-\int_\Omega u_\eta (\operatorname{div}_y \varphi)(x, \frac{x}{\eta})\, dx] \end{aligned}$$

En prenant la limite à deux échelles de u_η, on obtient :

$$\iint_{\Omega \times Y} u_0(x,y)(\operatorname{div}_y \varphi)(x,y)\, dxdy = 0 \ \ , \forall \varphi \in \mathcal{D}(\Omega; C^\infty_\sharp(KY)) \tag{3}$$

On choisit dans (3) la fonction test particulière $\varphi(x,y) = \theta(x)\psi(y)$ où $\theta \in [\mathcal{D}(\Omega)]^N$ et $\psi \in [C^\infty_\sharp(Y)]^N$.

Le théorème de Fubini appliqué aux fonctions $u_0(x,y)(\operatorname{div}_y \varphi)$ qui sont intégrables pour la mesure produit $dxdydz$, nous assure que :

$$\int_\Omega \theta(x)[\int_Y u_0(x,y) \operatorname{div}_y \psi(y,z)\, dy]\, dx = 0$$

Ceci étant vrai pour tout $\theta \in \mathcal{D}(\Omega)$, on obtient que pour tout $\Psi \in [C^\infty_\sharp(Y)]^N$, et pour presque tout $x \in \Omega$:

$$\int_Y u_0(x,y) \operatorname{div}_y \psi(y)\, dy = 0$$

D'où l'équation vraie pour presque tout $x \in \Omega$

$$\nabla_y u_0(x,y) = 0 \ \text{ dans } \mathcal{D}'(Y) \tag{4}$$

L'équation (4) entraine que pour presque tout $x \in \Omega$, $u_0(x,y) = u(x)$ (p.p. $y \in Y$).

Deuxième étape : identification de χ_0 donné par (1).

On choisit une fonction $\varphi \in [\mathcal{D}(\Omega; C^\infty_\sharp(Y))]^N$ telle que $\mathrm{div}_y\, \varphi = 0$ et on passe à la limite dans (2) quand $\eta \to 0$:

$$\begin{aligned}\iint_{\Omega\times Y} \chi_0(x,y)\cdot\varphi(x,y)\,dxdy &= -\iint_{\Omega\times Y} u_0(x,y)(\mathrm{div}_x\,\varphi)(x,y)\,dxdy \\ &= -\int_\Omega u(x)\Big[\int_Y (\mathrm{div}_x\,\varphi)(x,y)\,dy\Big]\,dx\end{aligned}$$

Posons $[\varphi](x) := \displaystyle\int_Y \varphi(x,y)\,dy$, le théorème de dérivation sous le signe somme nous assure alors que, $[\varphi] \in [\mathcal{D}(\Omega)]^N$ et $\mathrm{div}_x[\varphi] = \displaystyle\int_Y (\mathrm{div}_x\,\varphi)(x,y)\,dy$. En intégrant par parties et d'après Fubini, on en déduit que :

$$\begin{aligned}\iint_{\Omega\times Y} \chi_0(x,y)\cdot\varphi(x,y)\,dxdy &= -\int_\Omega u(x)\,\mathrm{div}_x[\varphi]\,dx \\ &= \int_\Omega \nabla\, u(x)\cdot[\varphi](x)\,dx\end{aligned}$$

On applique une nouvelle fois Fubini pour obtenir que :

$$\forall \varphi \in [\mathcal{D}(\Omega; C^\infty_\sharp(Y))]^N,\ \iint_{\Omega\times Y} [\chi_0(x,y) - \nabla\, u(x)]\cdot\varphi(x,y)\,dxdy = 0 \tag{5}$$

Localisation en x : en choisissant φ de la forme $\varphi(x,y) = \theta(x)\psi(y)$ avec $\psi \in [C^\infty_\sharp(Y)]^N$ telle que $\mathrm{div}_y\,\psi = 0$ et $\theta \in [\mathcal{D}(\Omega)]^N$ dans (5), on a immédiatement que :

$$\text{p.p. } x \in \Omega,\ \int_Y (\chi_0(x,y) - \nabla\, u(x))\cdot\psi(y)\,dy = 0 \tag{6}$$

Cette relation s'étend par densité à toute fonction $\psi \in [L^2_\sharp(Y)]^N$ telle que $\mathrm{div}_y\,\psi = 0$. Pour caractériser l'ensemble décrit par ces fonctions Ψ, nous avons besoin du

Lemme 5

Soit l'ensemble

$$M = \{w \in [L^2_\sharp(Y)]^N \mid \exists v \in H^1_\sharp(Y)\ \nabla_y\, v = w\}$$

Alors, M est un sous-espace fermé de $[L^2_\sharp(Y)]^N$ dont l'orthogonal est donné par

$$M^\perp = \{\psi \in [L^2_\sharp(Y)]^N \mid \mathrm{div}_y\,\psi = 0\}$$

Démonstration :

Soit $w_n = \nabla_y v_n$ tel que $w_n \to w$ dans $[L^2_\sharp(Y)]^N$. Alors $\dot{v}_n$ est une suite de Cauchy dans l'espace de Hilbert $H^1_\sharp(Y)/\mathbb{R}$, ce qui nous assure de l'existence d'une limite $\dot{v} \in H^1_\sharp(Y)/\mathbb{R}$ telle que $\dot{v}_n \to \dot{v}$.

En particulier, on a la convergence $\nabla_y\, v_n \to \nabla_y\, v$ dans $[L^2_\sharp(Y)]^N$. Par unicité de la limite on en déduit que $w = \nabla_y\, v$ donc w est un élément de M.

Il nous reste à caractériser l'orthogonal de M. Pour cela, on considère un élément ψ de $M^{\perp}$. Notant que $\int_Y \psi \cdot \nabla_y v \, dy = 0 \ \forall v \in H^1_\sharp(Y)$, par intégration par parties, on déduit que :

$$\int_Y v \; div_y \psi \, dy = - \int_Y \psi \cdot \nabla_y v \, dy = 0 \ , \ \forall v \in \mathcal{D}(Y)$$

Donc $div_y \psi = 0$ dans $\mathcal{D}'(Y)$. Par ailleurs, le théorème de la divergence appliqué à la fonction ψ de $[L^2_\sharp(Y)]^N$ dont la divergence est dans $L^2_\sharp(Y)$ nous assure l'existence d'une trace $\psi \cdot n$ dans $H_\sharp^{-\frac{1}{2}}(\partial Y)$ telle que :

$$\int_Y \mathrm{div}_y(\psi) \, v \, dy = < (\psi \cdot n) \; v \ , \ 1 >_{H^{-\frac{1}{2}}(\partial Y), H^{\frac{1}{2}}(\partial Y)} = 0$$

On en déduit que $\psi \cdot n$ prend des valeurs opposées sur les faces opposées de ∂Y et que $div_y \psi = 0$ dans $\mathcal{D}'(\mathbb{R}^N)$ par Y-périodicité.

Réciproquement si $div_y \psi = 0$ dans $\mathcal{D}'(\mathbb{R}^N)$, il est clair que

$$\int_Y \psi \cdot \nabla_y v \, dy = 0 \ , \ \forall v \in H^1_\sharp(Y)$$

(QED)

D'après (6) et le lemme 5, on en déduit que $\chi_0(x,.) - \nabla u(x) \in M^{\perp\perp} = M$ (car M est fermé). Donc il existe $u_1(x,.) \in H^1_\sharp(Y)$ tel que $\chi_0(x,.) = \bigtriangledown_x u(x) + \bigtriangledown_y u_1(x,.)$. Ce qui achève la démonstration de la proposition.

(QED)

2.2 Homogénéisation 3D périodique

Dans cette section, on montre le théorème 1 du chapitre 1 en utilisant de manière essentielle le fait que $\mu = \mu_0 = \text{cste}$. Le cas μ variable, plus délicat du fait que les champs électromagnétiques oscillent à l'ordre 0, sera traité ultérieurement (cf. [104]).

Soit (E_η, H_η) une solution du système de Maxwell $\mathcal{P}_\eta^{(E,H)}$ suivant ;

$$\mathcal{P}_\eta^{(E,H)} \begin{cases} (1) \ \mathrm{rot}\, E_\eta + j\omega\mu_0 H_\eta = 0 & , \text{dans } [\mathcal{D}'(\mathbb{R}^3)]^3 \\ (2) \ \mathrm{rot}\, H_\eta - j\omega\varepsilon_0\varepsilon_\eta E_\eta = 0 & , \text{dans } [\mathcal{D}'(\mathbb{R}^3)]^3 \\ (3) \ \mathrm{div}(\varepsilon_\eta E_\eta) = 0 & , \text{dans } \mathcal{D}'(\mathbb{R}^3) \\ (4) \ \mathrm{div}(\mu_0 H_\eta) = 0 & , \text{dans } \mathcal{D}'(\mathbb{R}^3) \end{cases}$$

Si l'on considère des milieux dont la perméabilité μ_0 est constante (milieux non magnétiques), le problème de diffraction par une structure D constituée d'un matériau hétérogène périodique de période η, caractérisé par une permittivité $\varepsilon_\eta(x)$, se ramène à chercher

l'unique solution $H_\eta \in L^2_{loc}(\mathbb{R}^3, \mathbb{C}^3)$ (champ magnétique) du système suivant :

$$(\mathcal{P}^H_\eta) \begin{cases} (i)\ \mathrm{rot}\Big(\varepsilon_\eta^{-1}\,\mathrm{rot}\, H_\eta\Big) - k_0^2 H_\eta = 0 & \text{dans } [\mathcal{D}'(\mathbb{R}^3)]^3 \\ (ii)\ \mathrm{div}\, H_\eta = 0 & \text{dans } \mathcal{D}'(\mathbb{R}^3) \\ (iii)\ H^d_\eta = O(\frac{1}{|x|}) & \text{quand } |\, x\, | \to +\infty \text{ dans } [C^\infty(\mathbb{R}^3 \setminus \bar{D})]^3 \\ (iv)\ \frac{x}{|x|} \wedge \mathrm{rot}\, H^d_\eta + ikH^d_\eta = o(\frac{1}{|x|}) & \text{quand } |\, x\, | \to +\infty \text{ dans } [C^\infty(\mathbb{R}^3 \setminus \bar{D})]^3 \end{cases}$$

où les conditions d'onde sortante (iii) et (iv) jouent un rôle fondamental en assurant l'existence et l'unicité de la solution H_η de $(\mathcal{P}^H_\eta)$ [51] (noter que $\varepsilon_\eta(x) = 1$ en dehors de D). Pour la dérivation des systèmes de Maxwell dans les cas $2D$ polarisés (obstacles diffractants de type cylindrique), on renvoie le lecteur au chapitre 4.

Nous allons passer à la limite quand η tend vers 0 dans le système vectoriel $\mathcal{P}^H_\eta$. Ceci nous amène à travailler dans des espaces fonctionnels adaptés (indépendants de η) associés à un ouvert Ω contenant strictement l'objet diffractant D.

2.2.1 Résultats préliminaires

Proposition 6

Soit Ω un ouvert borné de $\mathbb{R}^3$. Alors
i) Les espaces fonctionnels

$$H(\mathrm{div}, \Omega) = \Big\{ v \in [L^2(\Omega)]^3\ ,\ \mathrm{div}\, v \in L^2(\Omega) \Big\}$$

$$H(\mathrm{rot}, \Omega) = \Big\{ v \in [L^2(\Omega)]^3\ ,\ \mathrm{rot}\, v \in [L^2(\Omega)]^3 \Big\}$$

sont des espaces de Hilbert pour les normes

$$\|v\|_{H(\mathrm{div},\Omega)} = \Big\{ \|v\|^2_{[L^2(\Omega)]^3} + \|\mathrm{div}\, v\|^2_{L^2(\Omega)} \Big\}^{\frac{1}{2}}$$

$$\|v\|_{H(\mathrm{rot},\Omega)} = \Big\{ \|v\|^2_{[L^2(\Omega)]^3} + \|\mathrm{rot}\, v\|^2_{[L^2(\Omega)]^3} \Big\}^{\frac{1}{2}}$$

ii) $H(\mathrm{div}, \Omega) \cap [H(\mathrm{rot}, \Omega)]^3$ est un espace de Hilbert défini par

$$H(\mathrm{rot}, \mathrm{div}, \Omega) = \Big\{ v \in [L^2(\Omega)]^3\ ,\ \mathrm{div}\, v \in L^2(\Omega)\ ,\ \mathrm{rot}\, v \in [L^2(\Omega)]^3 \Big\}$$

Démonstration
Pour une preuve de la proposition, on se reportera à [58] (Tome 2, chap. IX).

Proposition 7

Soit Ω un ouvert borné de classe C^2 de $\mathbb{R}^3$, de bord $\partial\Omega$. Alors les espaces de Sobolev

$$H_n(\mathrm{rot}, \mathrm{div}, \Omega) = \Big\{ v \in H(\mathrm{rot}, \mathrm{div}, \Omega)\ ,\ v \cdot n_{|\partial\Omega}\ \in\ H^{\frac{1}{2}}(\partial\Omega) \Big\}$$

$$H_t(\mathrm{rot},\mathrm{div},\Omega)=\Big\{v\in H(\mathrm{rot},\mathrm{div},\Omega)\ ,\ v\wedge n_{|\partial\Omega}\ \in\ [H^{\frac12}(\partial\Omega)]^3\Big\}$$

s'identifient topologiquement avec l'espace de Hilbert $[W^{1,2}(\Omega)]^3$. *En particulier, il existe des constantes* C_1 *et* $C_2>0$ *telles que :*

$$\|v\|_{[H^1(\Omega)]^3}\le C_1\Big\{\|v\|_{[L^2(\Omega)]^3}+\|\mathrm{rot}\,v\|_{[L^2(\Omega)]^3}+\|\mathrm{div}\,v\|_{L^2(\Omega)}+\|v\cdot n\|_{H^{\frac12}(\partial\Omega)}\Big\}$$

$$\|v\|_{[H^1(\Omega)]^3}\le C_2\Big\{\|v\|_{[L^2(\Omega)]^3}+\|\mathrm{rot}\,v\|_{[L^2(\Omega)]^3}+\|\mathrm{div}\,v\|_{L^2(\Omega)}+\|v\wedge n\|_{[H^{\frac12}(\partial\Omega)]^3}\Big\}$$

Démonstration

On trouvera la preuve de la proposition dans [58] (Tome 2, Chap. IX, p. 247, corollaire 1).

Proposition 8

Soit $Y=[0,1]^3$ *de bord* ∂Y. *Alors le sous-espace de* $L^2_{loc}(\mathbb{R}^3,\mathbb{C}^3)$ *défini par :*

$$V=\Big\{u\in L^2_{loc}(\mathbb{R}^3,\mathbb{C}^3)\ ,\ u\ \ Y\text{-}périodique\ \ ,\ \mathrm{div}\,u\in L^2_{loc}(\mathbb{R}^3,\mathbb{C})\ ,\ \mathrm{rot}\,u\in L^2_{loc}(\mathbb{R}^3,\mathbb{C}^3)\Big\}$$

muni du produit scalaire

$$\langle u|v\rangle=\int_Y \mathrm{rot}\,u\cdot\overline{\mathrm{rot}\,v}\,dx+\int_Y \mathrm{div}\,u\,\overline{\mathrm{div}\,v}\,dx+\int_Y u\cdot\overline{v}\,dx$$

est un espace de Hilbert qui s'identifie topologiquement à l'espace

$$\begin{aligned}[H^1_\sharp(Y)]^3 &=\{u\in L^2_{loc}(\mathbb{R}^3,\mathbb{C}^3)\mid\ u\ Y\text{-}périodique\ ,\ \nabla u\in L^2_{loc}(\mathbb{R}^3,\mathbb{C}^{3\times3})\Big\}\\ &=\Big\{u\in H^1(Y,\mathbb{C}^3)\mid u\ \ à\ la\ même\ trace\ sur\ les\ faces\ opposées\ du\ cube\Big\}\end{aligned}$$

muni du produit scalaire

$$(u|v)=\int_Y \nabla u:\overline{\nabla v}\,dx+\int_Y u\cdot\overline{v}\,dx$$

où $\nabla u:\overline{\nabla v}$ *désigne le produit scalaire des matrices jacobiennes* ∇u *et* $\overline{\nabla v}$ *défini par :*

$$\nabla u:\overline{\nabla v}=Tr(\overline{\nabla^t v}\,\nabla u)$$

En particulier, il existe une constante C *strictement positive telle que :*

$$\forall u\in V,\ \|u\|_{[H^1_\sharp(Y)]^3}\le C\Big\{\|u\|^2_{[L^2(Y)]^3}+\|\mathrm{rot}\,u\|^2_{[L^2(Y)]^3}+\|\mathrm{div}\,u\|^2_{L^2(Y)}\Big\}^{\frac12}$$

Remarque :

Dans la suite, nous considérerons aussi le sous-espace quotient de $[H^1_\sharp(Y)]^3$ par les constantes dans $\mathbb{C}^3$:

$$[H^1_\sharp(Y)/\mathbb{C}]^3 = \Big\{ u \in H^1(Y,\mathbb{C}^3)\ ,\ v \in H^1(Y,\mathbb{C}^3)\ |u \sim v \iff \exists c \in \mathbb{C}^3\ ,\ u(x) - v(x) = c\ \ p.p.\ x \in Y \Big\}$$

qui est muni de la classe d'équivalence des fonctions égales (presque partout) dans $[H^1_\sharp(Y)]^3$ à une constante additive près (dans $\mathbb{C}^3$). Il est d'usage de noter les éléments de la classe d'équivalence de u par $\dot{u}$. On munit alors $[H^1_\sharp(Y)/\mathbb{C}]^3$ d'un produit scalaire par :

$$(\dot{u}|\dot{v}) = \int_Y \nabla u : \overline{\nabla v}\, dx$$

En effet, si $(\dot{u}|\dot{u}) = 0$, alors $\nabla u(x) = 0$ pour presque tout $x \in Y$. On prolonge le résultat à $[\mathcal{D}'(\mathbb{R}^3)]^3$ par périodicité et on en déduit qu'il existe une constante $c \in \mathbb{C}^3$ telle que $u(x) = c$ pour presque tout $x \in \mathbb{C}^3$, soit $\dot{u} = 0$. Par ailleurs, la norme induite par ce produit scalaire est équivalente à celle de $[H^1_\sharp(Y)]^3$ et fait de $[H^1_\sharp(Y)/\mathbb{C}]^3$ un espace de Hilbert.

Démonstration :

Soit Ω une boule ouverte de $\mathbb{R}^3$ et soit $Y =]-\frac{1}{2};\frac{1}{2}[^3$ tels que $\bar{Y} \subset \Omega \subset 2Y$ (la boule $\Omega = B(0,r)$ de rayon $r = \dfrac{\sqrt{3}}{2}$ convient). Prenons α une fonction de $\mathcal{D}(\Omega;[0;1])$ telle que $\alpha = 1$ sur $\bar{Y}$ et $supp\ \alpha \subset \Omega$. Soit $u \in V$, prenant $v = \alpha u$, on peut écrire que :

$$\operatorname{div} v = \alpha \operatorname{div} u + \nabla \alpha \cdot u \tag{1}$$

$$\operatorname{rot} v = \alpha \operatorname{rot} u + \nabla \alpha \wedge u \tag{2}$$

De (1) et (2), on déduit que :

$$\| \operatorname{div} v\|_{L^2(\Omega)} \leq \|\alpha\|_{L^\infty(\Omega)} \| \operatorname{div} u\|_{L^2(\Omega)} + \| \nabla \alpha\|_{[L^\infty(\Omega)]^3} \|u\|_{[L^2(\Omega)]^3} \tag{3}$$

$$\| \operatorname{rot} v\|_{[L^2(\Omega)]^3} \leq \|\alpha\|_{L^\infty(\Omega)} \| \operatorname{rot} u\|_{[L^2(\Omega)]^3} + \| \nabla \alpha\|_{[L^\infty(\Omega)]^3} \|u\|_{[L^2(\Omega)]^3} \tag{4}$$

Les majorations (3) et (4) nous assurent qu'il existe alors une constante $C(\alpha,\Omega) > 0$ ne dépendant que de la fonction α et de la mesure de Ω, telle que :

$$\int_\Omega [|v|^2 + |\operatorname{rot} v|^2 + |\operatorname{div} v|^2]\, dx \leq C(\alpha,\Omega) \int_\Omega [|u|^2 + |\operatorname{rot} u|^2 + |\operatorname{div} u|^2]\, dx \tag{5}$$

Revenant à $v = \alpha\ u$, on note que $u \in V$, donc que $v \in H(\operatorname{rot},\operatorname{div},\Omega)$. Par ailleurs, v est nul en dehors de l'ouvert Ω et $v \cdot n_{|\partial\Omega} = 0$ grâce aux propriétés de α, donc $v \in H_n(\operatorname{rot},\operatorname{div},\Omega)$. On peut donc appliquer à la fonction v la proposition 3.1.2 avec $\|v \cdot n\|_{H^{\frac{1}{2}}(\partial\Omega)} = 0$. Nous sommes donc assurés de l'existence d'une constante $C_1(\Omega)$ strictement positive telle que :

$$\|v\|_{[H^1_0(\Omega)]^3} \leq C_1(\Omega) \Big[\int_\Omega |v|^2\, dx + \int_\Omega |\operatorname{rot} v|^2\, dx + \int_\Omega |\operatorname{div} v|^2\, dx \Big] \tag{6}$$

Des majorations (5) et (6) on déduit que :

$$\|v\|_{[H_0^1(\Omega)]^3} \leq C_1(\Omega)\ C(\alpha,\Omega)\ \int_\Omega [|u|^2 + |\mathrm{rot}\, u|^2 + |\mathrm{div}\, u|^2]\ dx \tag{7}$$

Notant que $\Omega \subset 2\,Y$, on a :

$$\int_\Omega |u|^2\ dx + \int_\Omega |\mathrm{rot}\, u|^2\ dx + \int_\Omega |\mathrm{div}\, u|^2\ dx \leq \int_{2Y} |u|^2\ dx + \int_{2Y} |\mathrm{rot}\, u|^2\ dx + \int_{2Y} |\mathrm{div}\, u|^2\ dx \tag{8}$$

D'après la Y-périodicité de u, de (7) et (8) on tire que :

$$\|v\|_{[H_0^1(\Omega)]^3} \leq 2^3\ C_1(\Omega)\ C(\alpha,\Omega)\ \Big[\int_Y |u|^2\ dx + \int_Y |\mathrm{rot}\, u|^2\ dx + \int_Y |\mathrm{div}\, u|^2\ dx\Big]$$

Finalement, il existe une constante $C_2(\alpha,\Omega) = 8\ C_1(\Omega)\ C(\alpha,\Omega)$ strictement positive telle que :

$$\forall u \in V\ ,\ \int_Y [|u|^2 + |\nabla\, u|^2]\ dx \leq \|v\|_{[H_0^1(\Omega)]^3} \leq C_2(\alpha,\Omega) \int_Y [|u|^2 + |\mathrm{rot}\, u|^2 + |\mathrm{div}\, u|^2]\ dx$$

(QED)

Nous sommes maintenant en mesure de reformuler le résultat de structure établi dans la proposition 4 pour les rotationnels de fonctions vectorielles á divergence nulle.

Corollaire 9

Soient Ω un ouvert borné de classe C^2 de $\mathbb{R}^3$ et H_η une suite dans $[L^2(\Omega)]^3$ tels que :

$$\begin{array}{ll} \mathrm{div}\, H_\eta = 0 & (a) \\ \sup\limits_\eta \displaystyle\int_\Omega \Big(|\ H_\eta\ |^2 + |\ \mathrm{rot}\, H_\eta\ |^2\Big)\ dx < +\infty & (b) \\ H_\eta \wedge n \quad \text{est bornée dans } \left[H^{\frac{1}{2}}(\partial\Omega)\right]^3 & (c) \end{array}$$

Alors la suite est bornée dans $[W^{1,2}(\Omega)]^3$. Donc il existe une sous-suite de (H_η), encore notée (H_η), et deux fonctions $H_0 \in [W^{1,2}(\Omega)]^3$ et $H_1 \in [L^2(\Omega, H^1_\sharp(Y))]^3$ telles que :

$$\begin{array}{ll} H_\eta \to H_0(x) \quad \text{dans } [L^2(\Omega)]^3 \text{ fort, et } \mathrm{div}\, H_0 = 0 & (i) \\ \nabla\, H_\eta \rightharpoonup \nabla\, H_0(x) + \nabla_y H_1(x,y) \text{ et } \mathrm{div}_y\, H_1 = 0 & (ii) \end{array}$$

En particulier, on a la convergence des rotationnels suivante :

$$\mathrm{rot}\, H_\eta \rightharpoonup \mathrm{rot}\, H_0(x) + \mathrm{rot}_y H_1(x,y)$$

Démonstration :

Les hypothèses de la proposition 7 étant satisfaites, il existe une constante $C > 0$ ne dépendant que de la mesure de Ω telle que :

$$\|H_\eta\|_{[H^1(\Omega)]^3} \leq C\Big\{\|H_\eta\|_{[L^2(\Omega)]^3} + \|\mathrm{rot}\, H_\eta\|_{[L^2(\Omega)]^3} + \|\mathrm{div}\, H_\eta\|_{[L^2(\Omega)]^3} + \|H_\eta \wedge n\|_{[H^{\frac{1}{2}}(\partial\Omega)]^3}\Big\}$$

D'après les hypothèses (a), (b) et (c) du corollaire, on en déduit que

$$\sup_\eta \|H_\eta\|_{[H^1(\Omega)]^3} < +\infty$$

On peut donc appliquer la proposition 4 qui nous donne l'existence d'une sous-suite de (H_η), encore notée (H_η), de $H_0 \in [H^1(\Omega)]^3$ et de $H_1 \in [L^2(\Omega, L^2_\sharp(Y))]^3$ telles que :

$$H_\eta \to H_0(x) \quad \text{dans } [L^2(\Omega)]^3 \text{ fort}\ , \quad \text{et } \nabla H_\eta \rightharpoonup \nabla H_0(x) + \nabla_y H_1(x,y) \tag{9}$$

La condition $\mathrm{div}\, H_\eta = 0$ entraine que $\mathrm{div}\, H_0 = 0$ sur Ω. Si l'on prend des fonctions test du type $\varphi(x, \frac{x}{\eta})Id \quad$ où $\varphi \in \mathcal{D}(\Omega, \mathcal{D}_\sharp(Y))$, on déduit alors de (9) que :

$$\mathrm{div}\, H_\eta \rightharpoonup \mathrm{div}_x H_0 + \mathrm{div}_y H_1$$

$\Big($noter que $\displaystyle\int_\Omega \nabla H_\eta \cdot (\varphi(x, \frac{x}{\eta})Id)\, dx = \int_\Omega \mathrm{div}\, H_\eta(\varphi(x, \frac{x}{\eta}))\, dx\Big)$. Par ailleurs, la divergence de H_η étant une suite identiquement nulle, on a :

$$\mathrm{div}_x H_0 + \mathrm{div}_y H_1 = 0 \quad \text{dans} \quad L^2_\sharp(\Omega \times Y)$$

Puisque $\mathrm{div}_x H_0 = 0$, on conclut que :

$$\text{p.p.}x \in \Omega, \ \ \mathrm{div}_y H_1(x, \cdot) = 0$$

(QED)

2.2.2 Résultat de convergence

Théorème 10

Quand η tend vers zéro, H_η solution du problème $(\mathcal{P}^H_\eta)$, converge dans $[L^2_{loc}(\mathbb{R}^3)]^3$ vers l'unique solution H_0 du problème $(\mathcal{P}^H_{hom})$ suivant :

$$(\mathcal{P}^H_{hom}) \begin{cases} (1)\ \mathrm{rot}\Big(\varepsilon^{-1}_{hom}\mathrm{rot}\, H_0(x)\Big) - k_0^2 H_0(x) = 0 & \text{dans } [\mathcal{D}'(\mathbb{R}^3)]^3 \\ (2)\ \mathrm{div}\, H_0(x) = 0 & \text{dans } [\mathcal{D}'(\mathbb{R}^3)]^3 \\ (3)\ H_0^d = O(\frac{1}{|x|}) & \text{quand } |\, x\, | \to +\infty \text{ dans } [C^\infty(\mathbb{R}^3 - \bar{\Omega})]^3 \\ (4)\ \frac{x}{|x|} \wedge \mathrm{rot}\, H_0^d + ikH_0^d = o(\frac{1}{|x|}) & \text{quand } |\, x\, | \to +\infty \text{ dans } [C^\infty(\mathbb{R}^3 - \bar{\Omega})]^3 \end{cases}$$

Avec

$$\begin{cases} \varepsilon_{hom}(x) = <\varepsilon(I - \nabla_y \theta)>_Y (x) & \text{dans } \Omega \\ \varepsilon_{hom}(x) = 1 & \text{dans } \mathbb{R}^3 - \bar{\Omega} \end{cases}$$

Où θ_j, $j \in \{1,\ 2,\ 3\}$ est l'unique solution dans $H^1_\sharp(Y)/\mathbb{C}$ du problème annexe suivant :

$(\mathcal{K}_j) : -\mathrm{div}_y(\varepsilon(y)(\nabla_y\theta_j - e_j)) = 0$, e_j vecteur unitaire de la base canonique de $\mathbb{R}^3$

Démonstration :

Soit un objet diffractant D. On considère un rayon R tel que $\Omega := \{|\ x\ | < R\}$ vérifie $\overline{D} \subset \Omega$. Dans une première étape, on démontre le théorème sous l'hypothèse que la suite (H_η) est bornée dans $[L^2(\Omega)]^3$ donc converge faiblement (à une sous-suite extraite près) vers une limite notée H_0. On vérifie ensuite cette hypothèse par un raisonnement par l'absurde qui utilise l'unicité de la solution du problème limite vérifié par H_0.

Étape 1 : (H_η) est supposée bornée dans $[L^2(\Omega)]^3$:

a) **Comportement asymptotique de (E_η, H_η) en dehors de Ω :**

Fixons $r < R$ tel que $\overline{D} \subset \{|\ x\ | < r\} \subset \Omega$. Noter que l'équation (i) de $\mathcal{P}^H_\eta$ est vérifiée au sens faible dans $\mathbb{R}^3$ (i.e. au sens des distributions). Mais, du fait que $\varepsilon = 1$ en dehors de D, toute solution de (i) vérifie l'équation de Helmholtz vectorielle $\Delta H_\eta + k_0^2 H_\eta = 0$ pour $|\ x\ | \geq r$. Ce qui assure l'analycité de H_η pour $|\ x\ | \geq r$. De même, E_η est solution faible dans $\mathbb{R}^3$ de $\mathrm{rot}\,\mathrm{rot}\, E_\eta - k_0^2\varepsilon_\eta E_\eta = 0$, et elle vérifie l'équation de Helhmoltz vectorielle au sens classique pour $|\ x\ | \geq r$. E_η est donc analytique pour $|\ x\ | \geq r$. Supposant connues les valeurs de $\dfrac{x}{|\ x\ |} \wedge E_\eta$ et de $\dfrac{x}{|\ x\ |} \wedge H_\eta$ pour $|\ x\ | = r$, on en déduit la valeur du champ électromagnétique diffracté (E^d_η, H^d_η) pour $|\ x\ | > r$ par la forme intégrale suivante de (iii) et (iv) du problème $\mathcal{P}^H_\eta$, et son analogue pour le champ électrique diffracté ${E_\eta}^d$:

$$(SC)\ \begin{cases} E^d_\eta(x) = i\omega\mu_0 \displaystyle\int_{|y|=r} G(x-y)(\frac{y}{r} \wedge H^d_\eta(y))\ ds + \int_{|y|=r} \nabla G(x-y)(\frac{y}{r} \wedge E^d_\eta(y))\ ds \\ H^d_\eta(x) = -i\omega\varepsilon_0 \displaystyle\int_{|y|=r} G(x-y)(\frac{y}{r} \wedge E^d_\eta(y))\ ds + \int_{|y|=r} \nabla G(x-y)(\frac{y}{r} \wedge H^d_\eta(y))\ ds \end{cases}$$

où G est la fonction de Green $G(x) = \dfrac{1}{4\pi}\dfrac{e^{ik_0|x|}}{|\ x\ |}$.

Quitte à extraire une sous-suite, on peut supposer que (H_η) converge faiblement dans $[L^2(\Omega)]^3$ vers un champ H_0. Grâce à l'hypoellipticité de l'opérateur $\Delta + k_0^2$, la convergence $H_\eta \rightharpoonup H_0$ a lieu en fait dans $\mathcal{E}(\Omega \setminus \overline{D})$, ce qui entraine la convergence uniforme du couple (E_η, H_η) et de toutes ses dérivées sur la sphère $\{|\ x\ | = r\}$ (remarquer que $E_\eta = \dfrac{1}{j\omega\varepsilon_0}\,\mathrm{rot}\, H_\eta$ sur $\Omega \setminus \overline{D}$). Passant à la limite dans (SC), on obtient ainsi la convergence de (E_η, H_η) dans $\mathcal{E}(\mathbb{R}^3 \setminus \overline{D})$. La limite de (H_η) égale à H_0 sur Ω sera encore notée H_0 sur $\mathbb{R}^3$ tout entier. Notant E_0 la limite de E_η sur $\mathbb{R}^3 \setminus \overline{D}$, on aura donc le système :

$$\begin{cases} E_0 = j\omega\mu_0 H_0 & , \text{sur } \mathbb{R}^3 \setminus \overline{D} \\ H_0 = -j\omega\varepsilon_0 E_0 & , \text{sur } \mathbb{R}^3 \setminus \overline{D} \\ (E^d_0, H^d_0) := (E_0 - E^i_0, H_0 - H^i_0)\ \text{ vérifie } (SC) & , \text{sur } \mathbb{R}^3 \setminus \overline{D} \end{cases}$$

b) **Convergence et étude des oscillations de (E_η, H_η) sur Ω :**

On commence par établir le lemme 11, d'où résulte que la suite (E_η, H_η) est bornée dans $H(\mathrm{rot}, \Omega)$.

Lemme 11

Soit (E_η, H_η) *une solution de* $\mathcal{P}_\eta^{(E,H)}$ *telle que* $\sup_\eta \int_\Omega \mid H_\eta \mid^2 dx < +\infty$. *Alors les suites* (E_η), $(\mathrm{rot}\, E_\eta)$, $(\mathrm{rot}\, H_\eta)$ *sont bornées dans* $[L^2(\Omega)]^3$.

Démonstration :

Compte tenu de (1) et (2) dans $\mathcal{P}_\eta^{(E,H)}$, il suffit d'établir que $\sup_\eta \int_\Omega \mid \mathrm{rot}\, H_\eta \mid^2 dx < +\infty$. Supposant la suite (H_η) bornée dans $[L^2(\Omega)]^3$, l'équation (i) du problème $\mathcal{P}_\eta^H$ nous assure que $\Big(\mathrm{rot}(\frac{1}{\varepsilon_\eta(x)}\mathrm{rot}\, H_\eta)\Big)$ est elle même une suite bornée dans $[L^2(\Omega)]^3$. On multiplie alors (i) par la fonction test φ_η dans $[\mathcal{D}(\mathbb{R}^3)]^3$ et on intègre sur Ω :

$$\int_\Omega \mathrm{rot}\Big(\frac{1}{\varepsilon_\eta(x)}\mathrm{rot}\, H_\eta\Big)\cdot\varphi_\eta\, dx - k_0^2\int_\Omega H_\eta\cdot\varphi_\eta\, dx = 0\ ,\forall\varphi_\eta\in[\mathcal{D}(\mathbb{R}^3)]^3 \qquad (1)$$

Par ailleurs, l'identité de Poynting nous assure que pour toute fonction test φ_η dans $[\mathcal{D}(\mathbb{R}^3)]^3$:

$$\int_\Omega \mathrm{rot}\Big(\frac{1}{\varepsilon_\eta(x)}\mathrm{rot}H_\eta\Big)\cdot\varphi_\eta\, dx = \int_\Omega \frac{1}{\varepsilon_\eta(x)}\mathrm{rot}H_\eta\cdot\mathrm{rot}\varphi_\eta\, dx + \int_\Omega \mathrm{div}\Big(\frac{1}{\varepsilon_\eta(x)}\mathrm{rot}H_\eta\wedge\varphi_\eta\Big)\, dx \quad (2)$$

Le théorème de la divergence appliqué à la suite de fonctions $\psi_\eta(x) = \frac{1}{\varepsilon_\eta(x)}\mathrm{rot}H_\eta\wedge\varphi_\eta$ de $[L^2(\Omega)]^3$ dont la divergence est dans $L^2(\Omega)$, nous apprend qu'il existe une suite $(\psi_\eta\cdot n)$ dans $H^{-\frac{1}{2}}(\partial\Omega)$ telle que :

$$\int_\Omega \mathrm{div}\,\psi_\eta\, dx = <\psi_\eta\cdot n\ ,\ 1>_{H^{-\frac{1}{2}}(\partial\Omega),H^{\frac{1}{2}}(\partial\Omega)}$$

De (2) on tire alors que pour toute fonction test φ_η dans $[\mathcal{D}(\mathbb{R}^3)]^3$:

$$\begin{aligned}
&\int_\Omega \mathrm{rot}(\frac{1}{\varepsilon_\eta(x)}\mathrm{rot}H_\eta)\cdot\varphi_\eta\, dx\\
&= \int_\Omega \frac{1}{\varepsilon_\eta(x)}\mathrm{rot}H_\eta\cdot\mathrm{rot}\varphi_\eta\, dx + <(\frac{1}{\varepsilon_\eta(x)}\mathrm{rot}H_\eta\wedge\varphi_\eta)\cdot n\ ,\ 1>_{H^{-\frac{1}{2}}(\partial\Omega),H^{\frac{1}{2}}(\partial\Omega)}\\
&= \int_\Omega \frac{1}{\varepsilon_\eta(x)}\mathrm{rot}H_\eta\cdot\mathrm{rot}\varphi_\eta\, dx - <(n\wedge\varphi_\eta)\cdot(\frac{1}{\varepsilon_\eta(x)}\mathrm{rot}H_\eta)\ ,\ 1>_{H^{-\frac{1}{2}}(\partial\Omega),H^{\frac{1}{2}}(\partial\Omega)}
\end{aligned}$$

On déduit de (1) que pour toute fonction test φ_η dans $[\mathcal{D}(\mathbb{R}^3)]^3$:

$$\int_\Omega \frac{1}{\varepsilon_\eta(x)}\,\mathrm{rot}\, H_\eta\cdot\mathrm{rot}\,\varphi_\eta\, dx - k_0^2\int_\Omega H_\eta\cdot\varphi_\eta\, dx = <(n\wedge\varphi_\eta)\cdot(\frac{1}{\varepsilon_\eta(x)}\,\mathrm{rot}\, H_\eta)\ ,\ 1>_{H^{-\frac{1}{2}}(\partial\Omega),H^{\frac{1}{2}}(\partial\Omega)}$$

Par densité de $[\mathcal{D}(\mathbb{R}^3)]^3$ dans $[L^2(\Omega)]^3$, on peut prendre la fonction test particulière $\varphi_\eta = H_\eta$:

$$\int_\Omega \frac{1}{\varepsilon_\eta(x)}\mid \mathrm{rot}\, H_\eta\mid^2 dx - k_0^2\int_\Omega \mid H_\eta\mid^2 dx = <(n\wedge H_\eta)\cdot\mathrm{rot}\, H_\eta\ ,\ 1>_{H^{-\frac{1}{2}}(\partial\Omega),H^{\frac{1}{2}}(\partial\Omega)} \quad (3)$$

Comme (H_η) converge faiblement dans $[L^2(\Omega)]^3$ et vérifie $\Delta H_\eta + k_0^2 H_\eta = 0$ sur $\mathbb{R}^3 \setminus \bar{\Omega}$, par hypoellipticité de l'opérateur de Helmholtz, (H_η) prolongée à $[L^2(\mathbb{R}^3)]^3$ via les relations de Stratton-Chu, converge uniformément (ainsi que toutes ses dérivées) sur tout compact $K \subset \mathbb{R}^3 \setminus \bar{\Omega}$. On en déduit que :

$$\lim_{\eta\to 0} < (n \wedge H_\eta) \cdot \operatorname{rot} H_\eta \ , \ 1 >_{H^{-\frac{1}{2}}(\partial\Omega), H^{\frac{1}{2}}(\partial\Omega)} = < (n \wedge H_0) \cdot \operatorname{rot} H_0 \ , \ 1 >_{H^{-\frac{1}{2}}(\partial\Omega), H^{\frac{1}{2}}(\partial\Omega)}$$

Or l'intégrale $k_0^2 \displaystyle\int_\Omega |\ H_\eta\ |^2\, dx$ reste bornée par hypothèse. En passant à la limite dans l'équation (3) on en déduit que $\displaystyle\int_\Omega \frac{1}{\varepsilon_\eta(x)} |\operatorname{rot} H_\eta\ |^2\, dx$ reste bornée. Par ailleurs, $\dfrac{1}{\varepsilon_\eta(x)}$ est minorée dans l'ouvert Ω, d'où la conclusion.

(QED)

D'après le lemme 11, (H_η) est bornée dans $H(\Omega, \operatorname{rot})$. Par ailleurs, (H_η) est à divergence nulle et sa trace tangentielle est bornée dans $\left[H^{\frac{1}{2}}(\partial\Omega)\right]^3$. Donc le corollaire 9 nous assure que (H_η) est bornée dans $[W^{1,2}(\Omega)]^3$ et qu'il existe une sous-suite extraite de (H_η), encore notée (H_η), et deux fonctions $H_0 \in [W^{1,2}(\Omega)]^3$ et $H_1 \in \left[L^2(\Omega, \frac{H^1_\sharp(Y)}{\mathbb{R}})\right]^3$ telles que :

$$\begin{cases} H_\eta \to H_0(x) \ \text{ dans } [L^2(\Omega)]^3 \text{ fort} \\ \operatorname{rot} H_\eta \rightharpoonup \operatorname{rot} H_0(x) + \operatorname{rot}_y H_1(x,y) \end{cases}$$

On écrit alors la formulation variationnelle associée au problème $\mathcal{P}_\eta^H$ sur Ω. De (1), on tire que :

$$\int_\Omega \Big(\frac{1}{\varepsilon_\eta(x)} \operatorname{rot} H_\eta\Big) \cdot \operatorname{rot} \varphi_\eta \, dx - k_0^2 \int_\Omega H_\eta \cdot \varphi_\eta \, dx = 0 \ , \ \forall \varphi_\eta \in [\mathcal{D}(\Omega)]^3 \qquad (3')$$

Dans $(3')$, on prend des fonctions test particulières de la forme $\varphi_\eta = \varphi_0(x) + \eta\varphi_1(x, \dfrac{x}{\eta})$, où $\varphi_0 \in [\mathcal{D}(\Omega)]^3$ et $\varphi_1 \in [\mathcal{D}(\Omega, C^\infty_\sharp(Y^m))]^3$. On obtient en particulier que :

$$\begin{aligned} \operatorname{rot} \varphi_\eta(x) &= \operatorname{rot} \varphi_0(x) + \eta\Big[\operatorname{rot} \varphi_1(x, \tfrac{x}{\eta})\Big] \\ &= \operatorname{rot} \varphi_0(x) + \eta\Big[(\operatorname{rot}_x \varphi_1)(x, \tfrac{x}{\eta}) + \tfrac{1}{\eta}(\operatorname{rot}_y \varphi_1)(x, \tfrac{x}{\eta})\Big] \end{aligned}$$

L'opérateur rotationnel "rééchelonné" prend donc la forme suivante :

$$\operatorname{rot} \varphi_\eta(x) = \operatorname{rot} \varphi_0(x) + \eta(\operatorname{rot}_x \varphi_1)(x, \frac{x}{\eta}) + (\operatorname{rot}_y \varphi_1)(x, \frac{x}{\eta}) \qquad (4)$$

En appliquant (4) à (3), pour toutes fonctions test $\varphi_0 \in [\mathcal{D}(\Omega)]^3$ et $\varphi_1 \in [\mathcal{D}(\Omega; C^\infty_\sharp(Y^m))]^3$, on obtient que :

$$\begin{aligned} &\int_\Omega \Big(\frac{1}{\varepsilon_\eta(x)} \operatorname{rot} H_\eta(x)\Big) \cdot \Big(\operatorname{rot} \varphi_0(x) + (\operatorname{rot}_y \varphi_1)(x, \frac{x}{\eta})\Big)\, dx \\ &+\eta \int_\Omega \Big(\frac{1}{\varepsilon_\eta(x)} \operatorname{rot} H_\eta(x)\Big) \cdot \Big((\operatorname{rot}_x \varphi_1)(x, \frac{x}{\eta})\Big)\, dx = k_0^2 \int_\Omega H_\eta \cdot \varphi_0 \, dx + \eta\, k_0^2 \int_\Omega H_\eta \cdot \varphi_1(x, \frac{x}{\eta})\, dx \end{aligned} \qquad (5)$$

On souhaite maintenant passer à la limite quand η tend vers zéro dans (5). Or, (H_η) est bornée dans $[L^2(\Omega)]^3$ et φ_1 est très régulière donc :

$$\sup_\eta \mid \int_\Omega H_\eta \cdot \varphi_1(x, \frac{x}{\eta}) \mid < +\infty$$

Par ailleurs, $(\varepsilon_\eta^{-1} \operatorname{rot} H_\eta)$ est bornée dans $[L^2(\Omega)]^3$ donc :

$$\sup_\eta \mid \int_\Omega \varepsilon_\eta^{-1} \operatorname{rot} H_\eta \cdot \operatorname{rot}_x \varphi_1(x, \frac{x}{\eta}) \mid < +\infty$$

On en déduit que :

$$\lim_{\eta\to 0}\left[\eta k_0^2 \int_\Omega H_\eta \cdot \varphi_1(x, \frac{x}{\eta})\, dx\right] = \lim_{\eta\to 0}\left[\eta \int_\Omega \Big(\frac{1}{\varepsilon_\eta}\operatorname{rot} H_\eta\Big) \cdot \Big(\operatorname{rot}_x \varphi_1(x, \frac{x}{\eta})\Big)\, dx\right] = 0$$

Pour traiter la convergence des deux termes restant dans l'expression (5), on note que la fonction

$$\psi(x,y) = \varepsilon^{-1}(y)\ (\operatorname{rot}\varphi_0(x) + (\operatorname{rot}_y \varphi_1)(x,y))$$

est dans $[L^2_\sharp(Y, C(\bar\Omega))]^3$. ψ est donc admissible pour la convergence à deux échelles. En passant à la limite à deux échelles dans l'expression (5), on obtient pour toutes fonctions test $\varphi_0 \in [\mathcal{D}(\Omega)]^3$ et $\varphi_1 \in [\mathcal{D}(\Omega; C^\infty_\sharp(Y^m))]^3$:

$$\iint_{\Omega\times Y} \frac{1}{\varepsilon(x,y)}\Big[\operatorname{rot} H_0(x) + \operatorname{rot}_y H_1(x,y)\Big]\cdot\Big[\operatorname{rot}\varphi_0(x) + \operatorname{rot}_y\varphi_1(x,y)\Big]\, dxdy = k_0^2 \int_\Omega H_0(x)\cdot\varphi_0(x)\, dx \tag{6}$$

Par densité, on en déduit que (H_0, H_1) satisfait la formulation variationnelle précédente pour tout couple de fonctions (φ_0, φ_1) dans $[H^1_0(\Omega)]^3 \times [L^2(\Omega\ ;\ H^1_\sharp(Y)/\mathbb{C})]^3$.

c) **Équation microscopique sur Y :**

On veut déduire de l'équation précédente, l'équation locale ayant cours sur la cellule Y. On choisit pour cela des fonctions test particulières $\varphi_0 \in \mathcal{D}(\Omega)$ telles que $\varphi_0 = 0$ et $\varphi_1(x,y) = \theta(x)\chi(y)$ avec $\theta \in [\mathcal{D}(\Omega)]^3$ et $\chi \in [C^\infty_\sharp(Y)]^3$. On obtient alors que :

$$\iint_{\Omega\times Y}\Big[\frac{1}{\varepsilon(x,y)}(\operatorname{rot} H(x) + \operatorname{rot}_y H_1(x,y))\Big]\cdot \operatorname{rot}_y\chi(y)\theta(x)\, dxdy = 0\ ,\ \forall\theta \in [\mathcal{D}(\Omega)]^3, \forall\chi \in [C^\infty_\sharp(Y)]^3 \tag{7}$$

D'après le théorème de Fubini, on en déduit que pour presque tout $x \in \Omega$:

$$\int_\Omega\Big[\int_Y \frac{1}{\varepsilon}(x,y)(\operatorname{rot} H(x) + \operatorname{rot}_y H_1(x,y))\cdot\operatorname{rot}_y\chi(y)\, dy\Big]\theta(x)\, dx = 0\ ,\ \forall\theta \in [\mathcal{D}(\Omega)]^3, \forall\chi \in [C^\infty_\sharp(Y)]^3 \tag{8}$$

Ce résultat étant valable quelle que soit la fonction test $\theta \in \mathcal{D}(\Omega)$, on a donc :

$$p.p.x \in \Omega\quad \int_Y \frac{1}{\varepsilon(x,y)}(\operatorname{rot} H_0(x) + \operatorname{rot}_y H_1(x,y))\cdot\operatorname{rot}_y\chi(y)\, dy = 0\ ,\ \forall\chi \in [C^\infty_\sharp(Y)]^3 \tag{9}$$

En appliquant l'identité de Poynting, on obtient que pour presque tout $x \in \Omega$:

$$\begin{aligned}&\int_Y \operatorname{rot}_y\Big[\frac{1}{\varepsilon(x,y)}(\operatorname{rot} H(x) + \operatorname{rot}_y H_1(x,y))\Big]\cdot\chi(y)\, dy\\ &-\int_Y \operatorname{div}_y\Big[\frac{1}{\varepsilon(x,y)}(\operatorname{rot} H(x) + \operatorname{rot}_y H_1(x,y))\wedge\chi(y)\Big]\, dy = 0\ ,\ \forall\chi \in [C^\infty_\sharp(Y)]^3\end{aligned} \tag{10}$$

Le théorème de la divergence appliqué à la fonction

$$\psi_x(y) = \frac{1}{\varepsilon(x,y)}(\mathrm{rot}H(x) + \mathrm{rot}_y H_1(x,y)) \wedge \chi(y)$$

de $[L^2_\sharp(Y)]^3$ dont la divergence est dans $L^2_\sharp(Y)$, nous apprend que pour presque tout $x \in \Omega$ il existe une trace $(\psi_x \cdot n)$ dans $H^{-\frac{1}{2}}(\partial Y)$ telle que :

$$p.p.x \in \Omega\ ,\ \int_Y \mathrm{div}_y\, \psi_x(y)\, dy = <\psi_x \cdot n\ ,\ 1>_{H^{-\frac{1}{2}}(\partial Y), H^{\frac{1}{2}}(\partial Y)}$$

Il s'ensuit que pour presque tout $x \in \Omega$ et pour toute fonction χ dans $[C^\infty_\sharp(Y)]^3$:

$$\begin{aligned}&\int_Y \mathrm{rot}_y\Big[\frac{1}{\varepsilon(x,y)}(\mathrm{rot}H(x) + \mathrm{rot}_y H_1(x,y))\Big] \cdot \chi(y)\, dy \\ &- <\Big[\frac{1}{\varepsilon(x,y)}(\mathrm{rot}H(x) + \mathrm{rot}_y H_1(x,y)) \wedge \chi(y)\Big] \cdot n\ ,\ 1>_{H^{-\frac{1}{2}}(\partial Y), H^{\frac{1}{2}}(\partial Y)} = 0\end{aligned} \tag{11}$$

En utilisant l'antipériodicité de n sur la cellule de base Y, on en déduit que pour presque tout $x \in \Omega$:

$$\int_Y \mathrm{rot}_y\Big[\frac{1}{\varepsilon(x,y)}(\mathrm{rot}H(x) + \mathrm{rot}_y H_1(x,y))\Big] \cdot \chi(y)\, dy = 0\ ,\ \forall \chi \in [C^\infty_\sharp(Y)]^3 \tag{12}$$

Posant $\xi = \mathrm{rot}\, H_0(x)$, par densité de $[C^\infty_\sharp(Y)]^3$ dans $[L^2_\sharp(Y)]^3$ on aboutit à la formulation variationnelle suivante :

$$(\mathcal{P}^x_\xi) :\ \int_Y \mathrm{rot}_y\Big[\frac{1}{\varepsilon(x,y)}(\xi + \mathrm{rot}_y H_1(x,y))\Big] \cdot \chi(y)\, dy = 0\ ,\ \forall \chi \in [L^2_\sharp(Y)]^3 \tag{13}$$

On souhaite maintenant établir l'existence et l'unicité du problème local $(\mathcal{P}^x_\xi)$. Pour ce faire, nous revenons à sa forme variationnelle : posant $\xi = \mathrm{rot}\, H_0(x)$ dans (9), par densité de $[C^\infty_\sharp(Y)]^3$ dans $[L^2_\sharp(Y)]^3$ on aboutit à la formulation variationnelle suivante :

$$\int_Y \frac{1}{\varepsilon(x,y)}(\xi + \mathrm{rot}_y H_1(x,y)) \cdot \mathrm{rot}_y\, \chi(y)\, dy = 0\ ,\ \forall \chi \in [H^1_\sharp(Y)]^3 \tag{14}$$

L'existence et l'unicité de la solution du problème $(\mathcal{P}^x_\xi)$ relève du lemme de Lax-Milgram. Pour cela, pour presque tout $x \in \Omega$, on définit la forme sesquilinéaire $a_x(.,.)$ sur $[H^1_\sharp(Y)/\mathbb{C}]^3 \times [H^1_\sharp(Y)/\mathbb{C}]^3$:

$$a_x(\dot{u}, \dot{v}) = \int_Y \frac{1}{\varepsilon(x,y)}\Big[\mathrm{rot}_y u(y)\Big] \cdot \Big[\mathrm{rot}_y v(y)\Big]\, dy \tag{15}$$

Cette forme est continue. En effet, la coercivité de ε, nous assure qu'il existe une constante γ strictement positive telle que pour presque tout $x \in \Omega$:

$$\|a_x(\dot{u}, \dot{v})\|_{[H^1_\sharp(Y)/\mathbb{C}]^3} \leq \frac{1}{\gamma} \int_Y \Big[\mathrm{rot}_y u(y)\Big] \cdot \Big[\mathrm{rot}_y v(y)\Big]\, dy \tag{16}$$

De l'inégalité de Cauchy-Schwarz, et de la proposition 8 on déduit alors qu'il existe une constante strictement positive γ_1 telle que pour presque tout $x \in \Omega$:

$$\begin{aligned}\|a_x(\dot{u}, \dot{v})\|_{[H^1_\sharp(Y)/\mathbb{C}]^3} &\leq \gamma \|\,\mathrm{rot}_y\, u(y)\|_{[L^2(Y)]^3}\ \|\,\mathrm{rot}_y\, v(y)\|_{[L^2(Y)]^3} \\ &\leq \gamma_1 \|\,\nabla_y\, u(y)\|_{[L^2(Y)]^3}\ \|\,\nabla_y\, v(y)\|_{[L^2(Y)]^3} \\ &= \gamma_1 \|\dot{u}\|_{[H^1_\sharp(Y)/\mathbb{C}]^3}\ \|\dot{v}\|_{[H^1_\sharp(Y)/\mathbb{C}]^3}\end{aligned} \tag{17}$$

Par ailleurs, $a_x(.,.)$ est une forme sesquilinéaire coercive sur $[H^1_\sharp(Y)/\mathbb{C}]^3 \times [H^1_\sharp(Y)/\mathbb{C}]^3$. On a en effet le lemme suivant :

Lemme 12

Si $\mathrm{div}_y\, u(y) = 0$, *il existe une constante* $\beta > 0$ *telle que pour presque tout* $x \in \Omega$ *et pour tout* u *dans* $[H^1_\sharp(Y)/\mathbb{C}]^3$:

$$\Re e\{a_x(\dot{u}, \dot{u})\} \geq \beta \|\dot{u}\|^2_{[H^1_\sharp(Y)/\mathbb{C}]^3} \tag{18}$$

Démonstration :

Soit s un réel > 0. Par hypothèse, $\mathrm{div}_y\, u(y) = 0$, ce qui implique que pour tout $\dot{u}$ dans $[H^1_\sharp(Y)/\mathbb{C}]^3$, on a :

$$a_x(\dot{u}, \dot{u}) = \int_Y \frac{1}{\varepsilon(x,y)} \Big[\mathrm{rot}_y u(y)\Big] \cdot \Big[\mathrm{rot}_y u(y)\Big]\, dy + s \int_Y \Big[\mathrm{div}_y u(y)\Big] \Big[\mathrm{div}_y u(y)\Big]\, dy \tag{20}$$

Comme $\Re e\{\varepsilon\}$ est bornée dans $[L^\infty(\Omega; L^\infty_\sharp(Y))]^9$, d'après la proposition 8 il en résulte qu'il existe $\beta(s) > 0$ telle que pour presque tout $x \in \Omega$ et pour tout $\dot{u}$ dans $[H^1_\sharp(Y)/\mathbb{C}]^3$:

$$\begin{aligned} \Re e\{a_x(\dot{u}, \dot{u})\} &\geq \beta \int_Y |\, \nabla_y u(y)\, |^2\, dy \\ &= \beta \|\dot{u}\|^2_{[H^1_\sharp(Y)/\mathbb{C}]^3} \end{aligned}$$

(QED)

On définit maintenant la forme linéaire $b_x(\cdot)$ sur $[H^1_\sharp(Y)/\mathbb{C}]^3$ pour presque tout $x \in \Omega$ par :

$$\forall \dot{u} \in [H^1_\sharp(Y)/\mathbb{C}]^3\ ,\ b_x(\dot{u}) = \int_Y \frac{1}{\varepsilon(x,y)} \xi \cdot \mathrm{rot}_y\, u(y)\, dy \tag{21}$$

Cette forme est continue car il existe des constantes $\gamma_2(\xi)$ et $\gamma_3(\xi)$ telles que :

$$\begin{aligned} \|b_x(\dot{u})\|_{[H^1_\sharp(Y)/\mathbb{C}]^3} &\leq \gamma_2(\xi) \|\, \mathrm{rot}_y\, u(y)\|_{[L^2(Y)]^3} \\ &\leq \gamma_3(\xi) \|\, \nabla_y\, u(y)\|_{[L^2(Y)]^3} \\ &= \gamma_3(\xi) \|\dot{u}\|_{[H^1_\sharp(Y)/\mathbb{C}]^3} \end{aligned} \tag{22}$$

Le lemme de Lax-Milgram appliqué dans l'espace de Hilbert $[H^1_\sharp(Y)/\mathbb{C}]^3 \times [H^1_\sharp(Y)/\mathbb{C}]^3$ à la forme sesquilinéaire continue coercive $a_x(\cdot,\cdot)$ et à la forme linéaire continue $b_x(\cdot)$, nous assure alors de l'existence et de l'unicité de la solution $\dot{u}$ du problème local $(\mathcal{P}^x_\xi)$.

Nous allons maintenant montrer que le problème annexe se ramène à 3 problèmes scalaires.

De (12), on déduit l'expression suivante dans $[\mathcal{D}'(Y)]^3$:

$$p.p.x \in \Omega\ \ \mathrm{rot}_y\Big[\frac{1}{\varepsilon(x,y)}(\mathrm{rot}H(x) + \mathrm{rot}_y H_1(x,y))\Big] = 0 \tag{23}$$

Posant que :

$$w(x,y) = \frac{1}{\varepsilon}(x,y)(\mathrm{rot}_y H_1(x,y) + \mathrm{rot}_x H(x)) \ , \tag{23'}$$

l'expression (23) se traduit comme suit :

$$\mathrm{rot}_y w(x,y) = 0 \ , \text{ dans } [\mathcal{D}'(Y)]^3 \tag{24}$$

On prend maintenant la divergence par rapport à la variable y dans (23) :

$$\mathrm{div}_y(\varepsilon w) = \mathrm{div}_y \,\mathrm{rot}_y \, H_1 + \mathrm{div}_y \,\mathrm{rot}_x \, H_0(x) \ , \text{ dans } \mathcal{D}'(Y) \tag{25}$$

Notant que $\mathrm{div}_y \,\mathrm{rot}_y = 0$ et que $\mathrm{div}_y \,\mathrm{rot}_x = 0$, il vient :

$$\mathrm{div}_y(\varepsilon w) = 0 \text{ dans } \mathcal{D}'(Y) \tag{26}$$

On établit alors le lemme :

Lemme 13

Soit une fonction $w \in [L^2_\sharp(Y)]^3$ telle que

$$< w >:= \int_Y w(y)\, dy = 0 \ \text{ et } \ \mathrm{rot}_y \, w(y) = 0 \ ,$$

alors il existe une fonction $\psi \in H^1_\sharp(Y)$ telle que $\nabla_y \, \psi(y) = w(y) - < w >$.

Démonstration :

Ce lemme découle du théorème 5.8.1 page 202 de [21] : sur un tore de dimension 3, la dimension du quotient des 1-formes fermées par les bords est de dimension $C^1_3 = 3$. En d'autres termes, une fonction de rotationnel nul sur le tore de dimension 3 est à un vecteur constant près le gradient d'une fonction périodique.

(QED)

Remarque :

Sur un tore de dimension 2, on obtient qu'une fonction périodique de divergence nulle est à un vecteur constant près le rotationnel d'une fonction périodique.

Le lemme 13 appliqué à (26), nous assure qu'il existe une fonction $\psi \in H^1_\sharp(Y)$ telle que :

$$\mathrm{div}_y(\varepsilon(< w > - \nabla_y \, \psi)) = 0 \tag{27}$$

Par linéarité de la divergence, on note que :

$$\begin{aligned} - \mathrm{div}_y \, \varepsilon \, \nabla_y \, \psi \ &= - \mathrm{div}_y \, \varepsilon \tilde{w} \\ &= - \mathrm{div}_y (\varepsilon \sum_{j=1}^{3} < w_j > e_j) \\ &= - \sum_{j=1}^{3} \mathrm{div}_y (\varepsilon(y) e_j) < w_j > (x) \end{aligned} \tag{28}$$

De (28) on tire que les solutions du problème (27) sont données par les fonctions :

$$\psi(x,y) = \sum_{j=1}^{3} \theta_j(y) < w >_j (x) = \theta \cdot < w > \tag{29}$$

où les θ_j, $j \in \{1,\ 2,\ 3\}$ sont les solutions uniques dans $H^1_\sharp(Y)/\mathbb{C}$ des trois problèmes annexes scalaires (de types électrostatiques) suivants :

$$(\mathcal{K}_j) : -\mathrm{div}_y(\varepsilon(x,y)(\nabla_y \theta_j + e_j)) = 0 \tag{30}$$

d) Équation homogénéisée :

Nous allons maintenant préciser le lien entre le problème annexe (ayant court sur la cellule de base Y), et le problème macroscopique. Prenant $\varphi_1 = 0$ dans (6), on en déduit que $\forall \varphi_0 \in [\mathcal{D}(\Omega)]^3$:

$$\iint_{\Omega \times Y} \varepsilon^{-1} [\mathrm{rot} H(x) + \mathrm{rot}_y H_1(x,y)] \cdot \mathrm{rot}_x \varphi_0(x) = k_0^2 \int_\Omega H(x) \varphi_0(x)\, dx \tag{31}$$

D'après Fubini, pour toute fonction $\varphi_0 \in [\mathcal{D}(\Omega)]^3$, on a :

$$\int_\Omega [\int_Y \frac{1}{\varepsilon(x,y)} [\mathrm{rot} H(x) + \mathrm{rot}_y H_1(x,y)]\, dy] \cdot \mathrm{rot}_x \varphi_0(x)\, dx = k_0^2 \int_\Omega H(x) \varphi_0(x)\, dx \tag{32}$$

L'égalité suivante est donc vraie au sens des distributions dans l'ouvert Ω :

$$\mathrm{rot}_x \Big[\int_Y \frac{1}{\varepsilon(x,y)} (\mathrm{rot} H(x) + \mathrm{rot}_y H_1(x,y))\, dy \Big] = k_0^2 H(x) \tag{33}$$

Par ailleurs, d'après (23′) :

$$w(x,y) = \frac{1}{\varepsilon(x,y)} (\mathrm{rot} H(x) + \mathrm{rot}_y H_1(x,y)) \tag{34}$$

On déduit alors de (33) et (34) que :

$$\mathrm{rot}_x < w > (x) - k_0^2 H(x) = 0 \text{ dans } [\mathcal{D}'(\Omega)]^3 \tag{35}$$

On va maintenant exprimer $< w >$ en fonction de H et d'une matrice homogénéisée. Du lemme 13 et de (29), on tire que :

$$w = (I + \nabla_y \theta) < w > \tag{36}$$

De (34) et (36), on tire que :

$$\varepsilon (I + \nabla_y \theta) < w >= (\mathrm{rot}_y H_1 + \mathrm{rot}_x H) \tag{37}$$

On fait la moyenne de cette expression sur la cellule de base Y et on obtient :

$$\int_Y \Big(\mathrm{rot} H(x) + \mathrm{rot}_y H_1(x,y) \Big)\, dy =< \varepsilon (I + \nabla_y \theta) >< w > \tag{38}$$

Par ailleurs, la formule de Green nous assure que :

$$\int_Y \mathrm{rot}_y\, H_1(x,y)\, dy = < (n \wedge H_1(x,y)\Big)\ ,\ 1 >_{H^{-\frac{1}{2}}(\partial Y), H^{\frac{1}{2}}(\partial Y)} = 0 \tag{39}$$

car n est antipériodique et H_1 prend les mêmes valeurs sur les faces opposées de Y. De (38) et (39), on tire alors que :

$$\mathrm{rot}_x H =< \varepsilon(I + \nabla_y \theta) >< w > , \tag{40}$$

soit encore :

$$\mathrm{rot}_x H = \varepsilon_{hom} < w > , \tag{41}$$

avec

$$\varepsilon_{hom} =< \varepsilon(I - \nabla_y \theta) > \ . \tag{42}$$

De (35), (41) et (42), on déduit le problème homogénéisé suivant :

$$\mathrm{rot}\Big(\varepsilon_{hom}^{-1}(\mathrm{rot}\, H(x))\Big) - k_0^2 H(x) = 0 \text{ dans } [\mathcal{D}'(\Omega)]^3 \tag{43}$$

Avec

$$\varepsilon_{hom} =< \varepsilon(I - \nabla_y \theta) >$$

Étape 2 : Preuve que (H_η) est bornée dans $[L^2(\Omega)]^3$:

Il nous reste à montrer que (H_η) est une suite bornée dans $[L^2(\Omega)]^3$. Comme dans [37], on raisonne par l'absurde. Supposant que (H_η) n'est pas bornée dans $[L^2(\Omega)]^3$, on peut en extraire une sous-suite, encore notée (H_η), telle que $\|H_\eta\|_{[L^2(\Omega)]^3}$ tende vers l'infini. Posons $v_\eta = \dfrac{H_\eta}{\|H_\eta\|_{[L^2(\Omega)]^3}}$, alors (v_η) est bornée dans $[L^2(\Omega)]^3$. On obtient alors les mêmes résultats qu'à l'étape 1, pourvu que l'on remplace H^i par $\dfrac{H^i}{\|H_\eta\|_{[L^2(\Omega)]^3}}$. La suite (v_η) converge donc fortement dans $L^2_{loc}(\mathbb{R}^3, \mathbb{C}^3)$ vers l'unique solution du problème :

$$(\mathcal{P}_0) \begin{cases} (i)\ \mathrm{rot}\Big\{\varepsilon_{hom}^{-1}\, \mathrm{rot}\, v_0(x)\Big\} - k_0^2 v_0(x) = 0 & \text{dans } [\mathcal{D}'(\mathbb{R}^3)]^3 \\ (ii)\ \mathrm{div}\, v_0(x) = 0 & \text{dans } [\mathcal{D}'(\mathbb{R}^3)]^3 \\ (iii)\ v_0(x) = O(\frac{1}{|x|}) & \text{quand } |\, x\, | \to +\infty \text{ dans } [C^\infty(\mathbb{R}^3 \setminus \overline{D})]^3 \\ (iv)\ \frac{x}{|x|} \wedge \mathrm{rot}\, v_0(x) + ik\, v_0(x) = o(\frac{1}{|x|}) & \text{quand } |\, x\, | \to +\infty \text{ dans } [C^\infty(\mathbb{R}^3 \setminus \overline{D})]^3 \end{cases}$$

C'est à dire que le champ incident $v_0^i = v_0 - v_0^d$ est nul dans le problème homogénéisé. Par unicité de la solution du problème $(\mathcal{P}_0)$, on peut conclure que v_0 est identiquement nul. Par suite, (v_η) converge fortement vers 0 dans $[L^2(\Omega)]^3$, ce qui est absurde puisque $\|v_\eta\|_{[L^2(\Omega)]^3} = 1$.

(QED)

Remarque :

On peut s'étonner du caractère contradictoire entre notre résultat d'homogénisation et le résultat classique d'homogénéisation 2D en polarisation $H \parallel$ [18] [72] dans lequel le problème annexe fait intervenir non pas ε mais son inverse. Dans [72], le champ homogénéisé $H = u(x_1, x_2)e_3$ vérifie l'équation

$$\mathrm{div}\Big(B_{hom}\,\nabla\, u) + k_0^2 u = 0 \tag{44}$$

où B_{hom} est la matrice donnée par :

$$B_{hom}e_j = < \frac{1}{\varepsilon}(e_j + \nabla\, w_j(y) >$$

où w_j est l'unique solution dans $H^1_\sharp(Y)/\mathbb{R}$ de

$$\mathrm{div}_y\Big(\frac{1}{\varepsilon}(e_j + \nabla\, w_j(y))\Big) = 0$$

Appliquons le théorème 10 dans le cas où $\varepsilon(x, y)$ ne dépend que des variables (x_1, x_2, y_1, y_2) et où l'ouvert Ω est un cylindre de la forme $G \times \mathbb{R}$. La relation $D = \varepsilon_{hom}E$ conduit dans ce cas à une matrice effective de la forme :

$$\varepsilon_{hom} = \begin{pmatrix} A_{hom} & 0 \\ 0 & < \varepsilon > \end{pmatrix}$$

où A_{hom} est la matrice 2 lignes 2 colonnes définie par $A_{hom}e_j = < \varepsilon(e_j + \nabla\, v_j(y)) >$, et v_j est l'unique solution dans $H^1_\sharp(Y)/\mathbb{R}$ de

$$\mathrm{div}_y\Big(\varepsilon(e_j + \nabla\, v_j(y))\Big) = 0$$

Dans le cas d'une onde incidente polarisée T.M., le champ magnétique
$H(x_1, x_2, x_3) = u(x_1, x_2)e_3$ vérifie alors l'équation

$$\mathrm{rot}\Big(\varepsilon_{hom}^{-1}\,\mathrm{rot}\, H\Big) = k_0^2 H \tag{45}$$

Il n'est pas évident *a priori* que la solution de (45) cherchée sous la forme
$H = u(x_1, x_2)e_3$ vérifie l'équation (44). Pour le montrer, on note tout d'abord que la composante ε_{33} de ε_{hom} n'intervient pas dans le calcul et que l'on a :

$$\mathrm{rot}\left(\varepsilon_{hom}^{-1}\,\mathrm{rot}\Big(u(x_1, x_2)e_3\Big)\right) = -\,\mathrm{div}\left(Adj(A_{hom}^{-1})\,\nabla\, u\right)e_3 \tag{46}$$

En effet, si M désigne une matrice symétrique de la forme :

$$M = \begin{pmatrix} m_{11} & m & 0 \\ m & m_{22} & 0 \\ 0 & 0 & m_{33} \end{pmatrix} = \begin{pmatrix} \tilde{M} & 0 \\ 0 & m_{33} \end{pmatrix}$$

on obtient :

$$\mathrm{rot}\Big(M\,\mathrm{rot}\Big(u(x_1,x_2)e_3\Big)\Big) = -\left(\frac{\partial}{\partial x_1}\Big(m_{22}\frac{\partial u}{\partial x_1} - m\frac{\partial u}{\partial x_2}\Big) + \frac{\partial}{\partial x_2}\Big(m_{11}\frac{\partial u}{\partial x_2} - m\frac{\partial u}{\partial x_1}\Big)\right)e_3$$

Notant M' la matrice deux lignes deux colonnes suivante :

$$M' = \begin{pmatrix} m'_{11} & m'_{12} \\ m'_{21} & m'_{22} \end{pmatrix}$$

on aura

$$\mathrm{rot}\Big(M\,\mathrm{rot}\Big(u(x_1,x_2)e_3\Big)\Big) = -\,\mathrm{div}\Big(M'\,\nabla\, u\Big)e_3$$

si et seulement si

$$m'_{11}\frac{\partial u}{\partial x_1} + m'_{12}\frac{\partial u}{\partial x_2} = m_{22}\frac{\partial u}{\partial x_1} - m\frac{\partial u}{\partial x_2}$$

$$m'_{21}\frac{\partial u}{\partial x_1} + m'_{22}\frac{\partial u}{\partial x_2} = m_{11}\frac{\partial u}{\partial x_2} - m\frac{\partial u}{\partial x_1}$$

Par identification, on en déduit que $M' = Adj(\tilde{M})$.
D'après (46), pour lever la contradiction, il suffit de vérifier que :

$$Adj(A_{hom}^{-1}) = B_{hom}$$

Cette propriété est une conséquence d'une variante des résultats classiques de Keller [117] et de Dykhne sur le problème de l'échiquier [68], et de ceux de Milton *et al.* [156][155][92] pour des diffuseurs quelconques répartis périodiquement. Pour notre part, nous nous affranchissons de l'hypothèse de continuité par morceaux pour ε :

lemme 14

Soit A_{hom} et B_{hom} les matrices homogénéisées associées aux uniques solutions w_j et p_j ($j \in \{1\ ,\ 2\}$) dans $H^1_\sharp(Y)/\mathbb{C}$ des quatre problèmes annexes suivants :

$$\mathrm{div}_y\Big(a(y)(e_j + \bigtriangledown_y w_j(y)\Big) = 0$$

$$\mathrm{div}_y\Big(b(y)(e_j + \bigtriangledown_y p_j(y)\Big) = 0$$

où $b = a^{-1}$. Alors, on a :

$$B_{hom} = \frac{A_{hom}}{Det(A_{hom})}\ \Big(\text{ resp. }\ A_{hom} = \frac{B_{hom}}{Det(B_{hom})}\Big)$$

Démonstration du lemme 14 :

La matrice A_{hom} est obtenue en considérant pour tout $\xi \in \mathbb{C}^2$, l'unique solution w_ξ dans $H^1_\sharp(Y)/\mathbb{C}$ du problème annexe :

$$\mathrm{div}_y\Big(a(y)(\xi + \bigtriangledown_y w_\xi(y)\Big) = 0$$

D'après le lemme de Lax-Milgram, on vérifie aisément que :

$$\frac{1}{2}A_{hom}\xi\cdot\xi = \inf_{v(y)\in H^1_\sharp(Y)/\mathbb{C}}\left\{\frac{1}{2}\int_Y a(y)|\ \xi+\nabla\, v(y)\ |^2\, dy\right\}$$

Une formule classique d'analyse convexe (cf. par exemple [14][115]) permet de calculer la conjuguée de Fenchel relativement à la variable $\xi\in\mathbb{R}^n$ du second membre de l'égalité précédente. On obtient : du problème annexe

$$\tfrac{1}{2}A^{-1}_{hom}\xi^*\cdot\xi^* \quad = \inf_{q(y)\in L^2_\sharp(Y)}\left\{\frac{1}{2}\int_Y a^{-1}(y)|\ \xi^*+q\ |^2\, dy\ ,\ \mathrm{div}_y\, q(y)=0\ \text{ et }\ \int_Y q(y)\, dy=0\right\}$$

En dimension 2, il est bien connu (cf lemme 13) que toute fonction q de $L^2_\sharp(Y)$ de moyenne nulle et de divergence nulle est à une rotation près le gradient d'une fonction de $H^1_\sharp(Y)$. Plus précisément, il existe une fonction $v\in H^1_\sharp(Y)$ (unique à une constante additive près) telle que :

$$q(y) = R\Big(\nabla_y\, v(y)\Big)$$

où R désigne la matrice

$$R=\begin{pmatrix} 0 & -1\\ 1 & 0\end{pmatrix}$$

Notant que

$$|\ \xi^*+q(y)\ |^2 = |\ R\xi^*+Rq(y)\ |^2 = |\ R\xi^*+\nabla_y\, v(y)\ |^2$$

on obtient l'égalité :

$$\frac{1}{2}A^{-1}_{hom}\xi^*\cdot\xi^* = \inf_{v(y)\in H^1_\sharp(Y)/\mathbb{C}}\left\{\frac{1}{2}\int_Y a^{-1}(y)|\ R\xi^*+\nabla_y\, v(y)\ |^2\, dy\right\} \tag{47}$$

Or, la matrice homogénéisée B_{hom} associée à l'unique solution $p(y)$ du problème annexe suivant dans $H^1_\sharp(Y)/\mathbb{C}$:

$$\mathrm{div}_y\Big(b(y)(\xi+\bigtriangledown_y p(y)\Big)=0$$

avec $b=a^{-1}$, vérifie :

$$\frac{1}{2}B_{hom}z\cdot z = \inf_{v(y)\in H^1_\sharp(Y)/\mathbb{C}}\left\{\frac{1}{2}\int_Y a^{-1}(y)|\ z+\nabla_y\, v(y)\ |^2\, dy\right\}$$

Choisissant $z=R\xi^*$ et tenant compte de (47), on obtient :

$$A^{-1}_{hom}\xi^*\cdot\xi^* = B_{hom}R\xi^*\cdot R\xi^*$$

d'où la relation :

$$A^{-1}_{hom} = R^tB_{hom}R = R^{-1}B_{hom}R \tag{48}$$

En fait, le second membre de l'inégalité précédente n'est autre que la matrice adjointe de B_{hom}, d'où il existe Λ telle que :

$$B_{hom} = \Lambda A_{hom}$$

Par ailleurs, en égalant le determinant des deux membres de (48), on obtient

$$Det(A_{hom})Det(B_{hom}) = 1$$

D'où

$$\Lambda = \frac{1}{det(A_{hom})}$$

(QED)

Remarque :

Dans le cas d'un damier où ε est une fonction constante par morceaux qui prend deux valeurs α et β sur les cases du damier, on obtient par un argument de symétrie que $B_{hom} = \frac{1}{\alpha\beta} A_{hom}$ et que $A_{hom} = a_{hom} Id$. Tenant compte du lemme 14, on en déduit que

$$B_{hom} = \frac{A_{hom}}{Det(A_{hom})} = \frac{A_{hom}}{\alpha\beta}$$

D'où $DetA_{hom} = \alpha\beta$ et $a_{hom} = \sqrt{\alpha\beta}$.

Application pratique :

Soit une structure bornée constituée d'un matériau hétérogène périodique à deux indices optiques $n_1 = \varepsilon_1^2$ et $n_2 = \varepsilon_2^2$. En utilisant le résultat du lemme 14, on peut déduire du calcul de la matrice effective A_{hom} du lemme 14, la matrice effective C_{hom} correspondant à la même structure mais avec le contraste inversé : on note pour cela qu'il suffit de multiplier la matrice B_{hom} du lemme 14 par le produit $\varepsilon_1\varepsilon_2$ (voir figure 2.1).

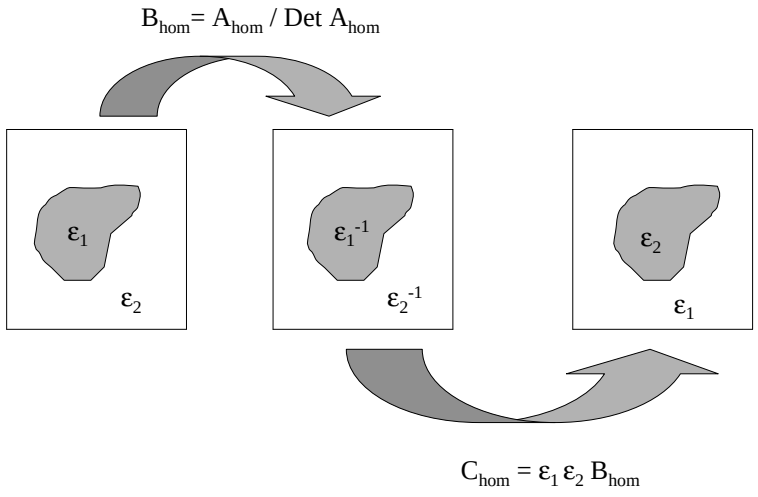

FIGURE 2.1 – Calcul de la matrice effective pour un contraste inversé en fonction de la matrice effective initiale.

Chapitre 3

Some concepts related to quasi-crystalline phasis.

'Twas brillig, and the slithy toves
Did gyre and gimble in the wabe :
All mimsy were the borogoves,
And the mome raths outgrabe.
"Beware the Jabberwock, my son !
The jaws that bite, the claws that catch !
Beware the Jubjub bird, and shun
The frumious Bandersnatch !"
'Through the Looking-Glass', by Lewis Carroll.

3.1 Introduction to quasi-crystallography

In December 1984, the Israeli physicist D. Shechtman, together with I. Blech, J. W. Cahn and the French physicist D. Gratias [190], announced the discovery of a phase of an aluminium-manganese alloy which seemed indeed to be a crystalline-like substance (now referred to as a quasicrystal) with fivefold symmetry (see figure 3.1).

These patterns are somewhat remarkable in that a standart mathematical theorem concerning crystal lattices states that the only rotationnal symmetries that are allowed for a crystalline pattern (see figure 3.2) are twofold, threefold, fourfold, and sixfold (by a crystalline pattern, one means a discrete system of points which has a translational symmetry).

Furthermore, a remarkable feature of the quasicrystalline tiling patterns is that their assembly is necessarily non-local. That is to say, in assembling the patterns, it is necessary, from time to time, to examine the state of the pattern many, many atoms away from the point of assembly, if one is to be sure of not making a serious error when putting the pieces together. Normally, when Nature seeks out a crystalline configuration, she is searching for a configuration of lowest energy. It sounds that with quasicrystal growth, the state of lowest energy is much more difficult to find as for periodic structures, and the best arrangement of the atoms cannot be discovered simply by adding on atoms one at time in the hope that

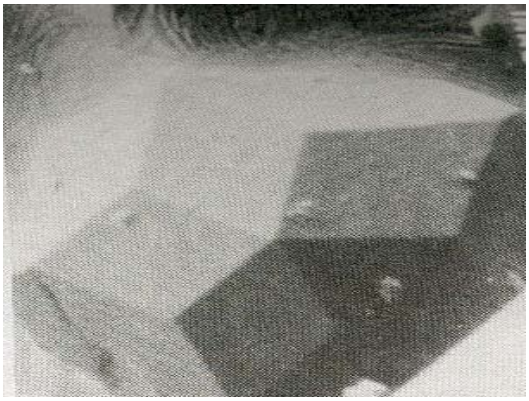

FIGURE 3.1 – A quasicrystal of about one millimetre in size (an AL-Li-Cu alloy) due to Gayle [85] with an apparently impossible crystal symmetry (the one of Schechtman's was about one micrometre in size).

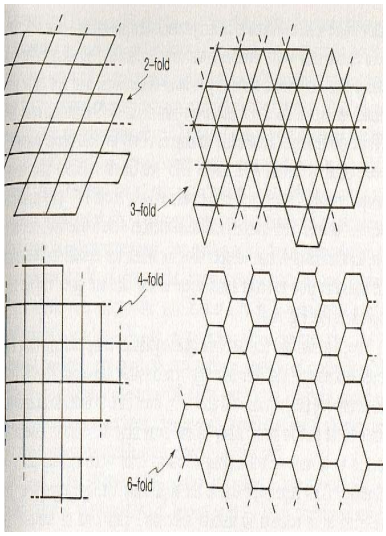

FIGURE 3.2 – Periodic tilings with various symmetries (where the centre of symmetry, in each case, is taken to be the centre of a tile).

each individual atom can get away with just solving its own minimizing problem. Instead, we have a global problem to solve. Such tilings where previously studied by Roger Penrose who found many interessant mathematical properties related, as we will see, to arithmetic and logic. It is to be noticed that quasicrystalline substances also exhibit a symmetry in three-dimensions, and not only in the plane, giving a forbidden icosahedral symmetry (these analogues of the Penrose tilings had been found by Robert Amman in 1975).

3.2 The puzzle game

Numerous mathematicians spent time to play activities which often led to discoveries. Amongst them, the great number theorist Russel whose mathematical works where inspired by books and puzzles of Lewis Carroll. In the early seventies, Roger Penrose was considering

the question of covering the Euclidean plane with polygonal shapes, where there is a given finite number of different such shapes. The question was to find whenever it is possible or not to cover the plane completely, without gaps or overlaps, using just these shapes and no others. It is well known that such tilings are possible using just squares, or just equilateral triangles, or just regular hexagons, but not using just regular pentagons, as was seen above. Many other single shapes will tile the plane, such as irregular pentagons, but with a pair of shapes the tilings can become more elaborate (see fig. 3.3). Now, there are

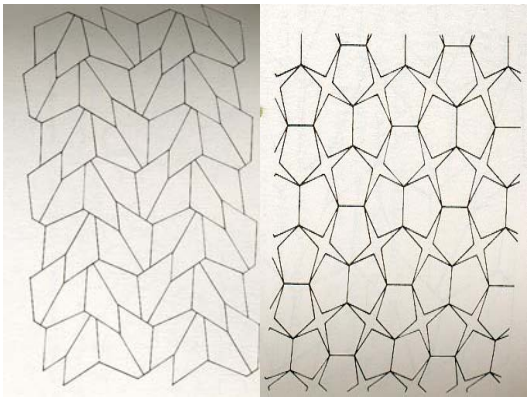

FIGURE 3.3 – Two examples of periodic tilings of the plane. The left one uses a single shape and the right one uses two shapes.

many tilings of the plane which are not periodic. Amongst them, the famous non-periodic spiral tilings (see figure 3.4) who were devised by B. Grunbaum and G. C. Shepard (1981). It is worth noting that the same 'versatile' shape tile both periodically and non periodically

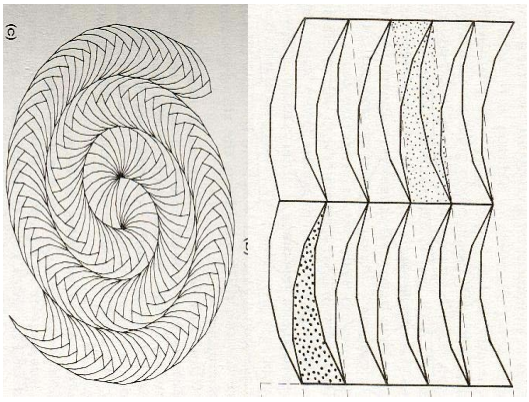

FIGURE 3.4 – On the left, a non-periodic spiral tiling using the same versatile shape that is used in the periodic tiling on the right.

the Euclidean plane (see figure 3.4), which is a property shared by many other single tile shapes and sets of tile shapes. Are there single or sets of tiles which will tile the plane only non-periodically ? In 1971, the American mathematician Raphael Robinson exhibited a tiling with six shapes which tiles the plane only in a non-periodic way. His works were inspired from those of the Chinese-American logician Hao Wang who adressed the question of whether or not there is a decision procedure for the tiling problem, that is to say, is there

an algorithm for deciding whether or not a given finite set of different polygonal shapes will tile the entire plane. Hao Wang [203] was able to show that there indeed would be such a decision procedure if it could be shown that every finite set of distinct tiles which will in some way tile the plane, will in fact also tile the plane periodically. In 1966, following some of the directions that Hao Wang had suggested, Robert Berger was able to show that there is in fact no decision procedure for the tiling problem : the tiling problem is a part of what is called **non-recursive mathematics**.

Thus, it follows from Hao Wang's earlier result that an aperiodic set of tiles must exist. The first one was exhibited by Berger and involved originally 20426 different tiles. Berger was then able to reduce this number to 104 tiles in 1964. In 1971, we have seen that Raphael Robinson get this number down to six. Finally, Roger Penrose found in 1974 an aperiodic tile made of two tiles (see figure 3.5). The question of whether or not it is possible to tile the Euclidean plane aperiodically with a single tile remains an open question. According to Roger Penrose, one way of doing this would be to give the vertices of the tile as points in the complex plane, and these points may be given as algebraic numbers. Indeed, N. G. de Bruijn [60] showed that such patterns could be built thanks to a **cut and projection method** who was developped, among others, by M. Duneau and A. Katz [66].

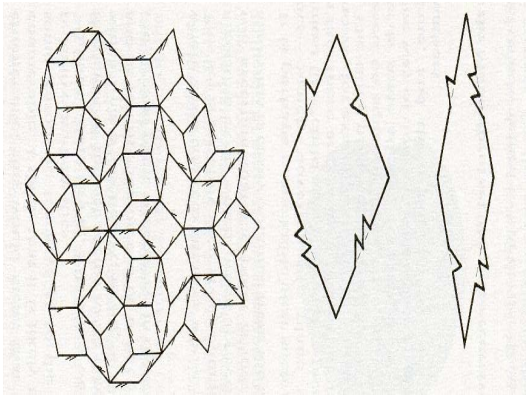

FIGURE 3.5 – A pair of tiles tiling the plane only non-periodically and a region of the plane tiled with such a pair.

3.3 The cut-and-projection method

Let us begin by a brief description of the method in the one-dimensional case : consider the plane $\mathbb{R}^2$, the square lattice $\mathbb{Z}^2$ and a line $E_{\|}$ to be tiled (see figure 3.6).

A strip is obtained by shifting a unit square $Y^2 =]0;1[^2$ along $E_{\|}$. Then, for almost all positions of the line $E_{\|}$, this strip contains a unique broken line (made of edges of the lattice), which joins exactly all the vertices inside the strip. The orthogonal projection $P_{\|}$ of this line on $E_{\|}$ gives a tiling, the two tiles being the projections of the vertical and horizontal edges of the unit square Y^2. Consider now the slope of the line $E_{\|}$ with respect to the canonical basis of $\mathbb{R}^2$. One can check that the tiling is periodic if and only if this slope is a rational number.

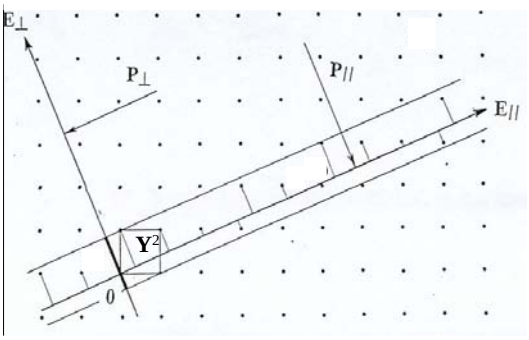

FIGURE 3.6 – The cut and projection method : when the slope of the line $E_{\|}$ is irrational, the orthogonal projection $P_{\|}$ of the vertices of $\mathbb{Z}^2$ (belonging to the strip spaned by the unit square Y^2) onto $E_{\|}$ defines a quasi-periodic tiling of $E_{\|}$.

An important property of such patterns is the **local isomorphism property**, introduced by M. Duneau and A. Katz [66] as a property of Penrose tilings, which asserts that any finite patch of tiles that belongs to a tiling appears infinitely many times in any tiling defined through a strip with the same irrational slope. To prove this property, one has to consider the line $E_{\perp}$, orthogonal to $E_{\|}$. A finite patch of tiles in a given tiling is the projection of a finite broken line, the projection of which on $E_{\perp}$ is strictly smaller than the projection of the whole strip. Then, their exists a non empty open set of translations in $E_{\perp}$ that keep the projection of the finite broken line inside the strip. Because the orthogonal projection $P_{\perp}$ of $\mathbb{Z}^2$ on $E_{\perp}$ is dense, there are infinitely many translations of $\mathbb{Z}^2$ which map the finite broken line inside the strip, which give infinitely many copies of the initial patch of tiles. One can show along the same lines that any finite patch of tiles that appears in a tiling appears in all tilings with the same slope.

There are interesting questions concerning the mean distance between copies of a given patch. The density of the copies of a patch depends on arithmetical properties of the slope. Indeed, it can be seen that when the slope of $E_{\|}$ is given by an algebraic number, the mean distance between two copies is proportional to the size of the patch. On the contrary, when the slope is given by a Liouville number (non-algebraic irrational number), the distance can grow arbitrarily quickly. It is to be noticed that if the unit square is replaced by any other unit cell of $\mathbb{Z}^2$ (say KY^2, where K is a positive integer), new tilings involving the projections of the two edges of this cell are obtained. This is closely related to self-similarity properties of the Penrose tilings i.e. each fragmented geometric shape can be subdivided in parts, each of which is (at least approximately) a reduced-size copy of the whole. However, the projection method should not be restricted to these tilings since more general strips also generate tilings involving a finite number of tiles. Furthermore, one can easily generalize this method to higher dimensions. To get a quasi-periodic pattern in $\mathbb{R}^n$ issued from a projection of a periodic pattern in $\mathbb{R}^m$ $(m > n)$, one has to consider the subspace $E_{\|} = \mathbb{R}^n$ and $E_{\perp}$ its orthogonal subspace in $\mathbb{R}^m$. The Penrose tilings are issued from a cut and projection of $\mathbb{R}^4$ (or $\mathbb{R}^5$) in $\mathbb{R}^2$ and their three-dimensional equivalents (the icosahedral structures) from a cut and projection of $\mathbb{R}^6$ (or $\mathbb{R}^{12}$) in $\mathbb{R}^3$.

3.4 Quasi-crystals versus fractal sets

These strange properties are related to abstract mathematical objects introduced by Benoît Mandelbrot : let us first consider the mapping $z \longmapsto z^2 + c$ where z and c are two complex numbers. It is easy to see that for certain choices of the given complex number c, the mapping remains bounded (to be precise this set was found by Julia and Mandelbrot considered the mapping $z \longmapsto z^2 + c$). Such a set of values of c defines what is called **the Mandelbrot set** (cf. figure 3.7).

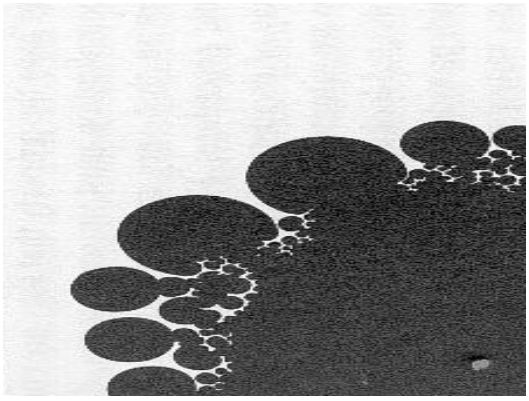

FIGURE 3.7 – The black part denotes the Mandelbrot set, and the white part denotes its complementary set. It is not a computable matter to ascertain that a point is actually in the white region itself.

To test whether a point of the complex plane belongs to the Mandelbrot set (coloured black) or to the complementary set (coloured white), one can imagine a computer starting at 0, then applying the map $z \longmapsto z^2 + c$ to $z = 0$ to obtain c, and then to $z = c$ to obtain $z^2 + c$ and then to $z = z^2 + c$ to obtain $z^4 + 2z^3 + z^2 + z$, and so on. If this sequence remains bounded after a fixed number of iterations, then the point is coloured black ; otherwise it is coloured white. For the complementary of the Mandelbrot set, the computer can detect the unboundedness of the sequence after a finite number of iterations. This set is thus said to be a recursive set, for there is a general algorithmic way of deciding whether or not an element belongs to this set. As concerning the Mandelbrot set, there is still no proof of whether or not it is a recursive set. It seems that this property may rely upon properties of **algebraic numbers**, that is to say complex numbers which are solutions of algebraic equations with integer coefficients. Indeed, the algebraic numbers are countable and computable (contrary to complex numbers, since there is no bijection between $\mathbb{C}$ and $\mathbb{N}$) and it is actually a computable matter to decide whether or not two of them are equal. It turns out that such structures, baptised **fractals** by Benoît Mandelbrot, are closely related to quasi-crystals : they are **self-similar** and their properties seem to rely upon those of irrational numbers. We explain in the sequel that we can actually characterize a quasi-crystal in terms of **fractal dimension**. The strict mathematical definition is that fractal is an object whose Hausdorff dimension strictly exceeds its topological dimension. Most fractals objects have self-similar shapes although there some fractal objects exist that are hardly self-similar at all. Most fractals also have infinite complexity and detail, that is,

the complexity and detail of the fractals remain no matter how far you "zoom-in", as long as you are zooming in on the right location. Also, most fractals have fractional dimensions [70], and although we just outline an approach to characterize a quasi-crystal in terms of fractal dimension, there is no doubt that it will be the case !

We note that the natural way to study the quasi-crystalline phases is to look at their diffraction pattern i.e. the Fourier transform of the structure. In the following, we thus focus on the properties of fractal measures in Fourier space, as did the mathematician Strichartz, who showed that the classical relation :

$$\frac{1}{T^n}\int_{|\xi|\leq T} \mid \hat{\mu}(\xi) \mid^2 d\xi \sim T^{-\alpha} \ , \quad \text{when} \ \ T \to +\infty \ , \quad \text{with} \ \ \mu \ \ \text{a finite measure on} \ R^n \ ,$$

(where α is an integer in simple cases as absolutely continuous measures or discrete measures), could be generalized to fractal measures with α a real exponent. For example, in case of Cantor measure, whose support is the Cantor triadic set (with null Lebesgue measure), we have :

$$\frac{1}{T}\int_{|\xi|\leq T} \mid \hat{\mu}(\xi) \mid^2 d\xi \sim T^{-\frac{\log 2}{\log 3}} \ , \quad \text{when} \ \ T \to +\infty$$

Guérin and Holschneider showed [107] that quadratic means of the Fourier transform of a finite positive Borel measure μ :

$$M\mu(T) = \frac{1}{T^n}\int_{|\xi|\leq T} \mid \hat{\mu}(\xi) \mid^2 d\xi$$

are related to a fractal dimension of the measure μ, called dimension of correlation d. For this, they considered the function $\Omega\mu$:

$$\Omega\mu(r) = \int_{x\in\mathbb{R}^n} \mu(B(x,r))\, d\mu(x) \qquad (*)$$

and they defined the upper and lower dimensions of correlation of μ as follows :

$$d^+(\mu) = \limsup_{r\to 0} \frac{\log \Omega\mu(r)}{\log r} \ \ \text{et} \ \ d^-(\mu) = \liminf_{r\to 0} \frac{\log \Omega\mu(r)}{\log r}$$

d^+ and d^- are related to $M\mu$ by (Guérin, Holschneider, 1998) :

$$d^+(\mu) = \limsup_{T\to+\infty} \frac{\log M\mu(T)}{\log T} \ \ \text{et} \ d^-(\mu) = \limsup_{T\to+\infty} \frac{\log M\mu(T)}{\log T}$$

Analogously to the physicists who deduce the characteristics of the quasi-crystals from the intensity of their diffracted field (reciprocal space) by inverse Fourier transform, one can calculate the inverse Fourier tranform of $M\mu$ via the mean value of $\mu(x)$ on the ball of radius r in $(*)$:

$$\Gamma\mu(r) = \frac{1}{r^n}\int_{x\in\mathbb{R}^n} \mid \mu(B(x,r)) \mid^2 dx$$

($x \longmapsto \mu(B(0,r))$ is square integrable). It can be seen that d^+ and d^- are related to $\Gamma\mu$ by [107] :

$$d^+(\mu) = \limsup_{r\to 0} \frac{\log \Gamma\mu(r)}{\log r} \ \ \text{et} \ \ d^-(\mu) = \liminf_{r\to 0} \frac{\log \Gamma\mu(r)}{\log r}$$

To conclude this section, it is worth noting that one can distinguish two opposite cases for the dimensionality of a measure via quadratic means of its Fourier transform. On one side, if μ is absolutely continuous in conjonction with the Lebesgue measure, of density $f \in L^2(\mathbb{R}^n)$, the Plancherel formula ensures us that :

$$\lim_{T\to+\infty} \int_{|\xi|\leq T} \mid \hat{\mu}(\xi) \mid^2 d\xi = (2\pi)^n \int_{\mathbb{R}^n} \mid f(x) \mid^2 dx \ .$$

On the opposite side, one has the Wiener's theorem which ensures that for discrete measures $\mu(x) = \sum_{k\in\mathbb{Z}^n} c_k \delta(x - x_k)$:

$$\lim_{T\to+\infty} \frac{1}{T^n} \int_{|\xi|\leq T} \mid \hat{\mu}(\xi) \mid^2 d\xi = \sum_{k\in\mathbb{Z}^n} \mid c_k \mid^2 ,$$

and the Besicovitch identity for almost-periodic measurable functions F :

$$\lim_{T\to+\infty} \frac{1}{T^n} \int_{|\xi|\leq T} \mid F(\xi) \mid^2 d\xi = \sum_{k\in\mathbb{Z}^n} \mid c_k \mid^2 .$$

This last formula will be the key point in the proof of the corrector type result for the homogenization of the one-dimensional quasi-crystal and more particularly of the 1D penrose tiling (see chapter 5). Although we are not yet capable to give a rigorous mathematical statement of this conjecture, we believe that our result provides the correlation dimension of these quasi-periodic structures (cf [193]).

3.5 quasi-crystals versus Gödel

We have seen that non-recursive properties are related to a kind of **non-halting** property of an algorithm : in our previous example, the Mandelbrot set, the computer may calculate for eternity in case of unboundedness of the mapping. This question of whether or not one can find a halting criteria was adressed by Türing. Türing was concerned with the resolution of Hilbert's broad-ranging *Entscheidungsproblem* : is there some mechanical procedure for answering all mathematical problems, belonging to some broad, but well-defined class ? The response he found in the works of the Austrian mathematical logician Kurt Gödel. What Gödel showed in 1931 was that any system of axioms, provided that it is broad enough to contain descriptions of simple arithmetical propositions and provided that it is free from contradiction (consistent), must contain some statements which are neither provable nor disprovable by the means allowed within the system. The truth of such statements is thus **undecidable** by the approved procedures. Such a result is of the foremost importance, as shown by the fascinating story of one of the notes Pierre de Fermat wrote in the margins of Bachet's publication of the Latin version of the Diophantus'*Arithmetica* (1621) : *Cubum autem in duos cubos, aut quadrato quadratum in duos quadrato quadratos, etgeneraliter nullam in infinitum ultra quadratum potestatem in duos ejusdem nominis fas estdividere : cujus rei demonstrationem mirabilem sane detexi. Hanc marginis exiguitas*

non caperet.[1] No one was able to prove this statement, nor to find a counter-example (i.e. to exhibit such a 'Fermatean triple') during three centuries. In the eighties, the believe was therefore that it was part of undecidable procedures, until the mathematician Gerhard Frey claimed in 1984 that if anyone could prove the so-called Taniyama-Shimura conjecture, then they would also prove this statement.

More precisely, let us consider the famous 'Fermat's last theorem' asserted by the French mathematician Pierre de Fermat $(1601 - 1665)$ and proved by Andrew Wiles in 1995, in terms of a formal mathematical proposition F :

$$F = \neg\, \exists w,\ x,\ y,\ z \in \mathbb{N}\ ,\ [(x+1)^{w+3} + (y+1)^{w+3} = (z+1)^{w+3}]$$

which stands for *it is not so that there exists natural numbers w, x, y, z such that*[2]

$$(x+1)^{w+3} + (y+1)^{w+3} = (z+1)^{w+3}\ .$$

A proposition might also depend on one or more variables. For example, for some particular power $w+3$, we have :

$$G(w) = \neg\, \exists w,\ x,\ y,\ z \in \mathbb{N}\ ,\ [(x+1)^{w+3} + (y+1)^{w+3} = (z+1)^{w+3}]$$

so that $G(0)$ asserts *no cube can be the sum of positive cubes*, and so on. The Fermat assertion is now that $G(w)$ holds for all w :

$$F = \forall w[G(w)]$$

$G(.)$ is an example of what is called a **propositional function**. Hilbert's hope was that for any string of symbols representing a mathematical proposition, say G, one should be able to prove either G or $\neg G$, depending upon whether G is true or false. Here we must assume that the string is syntactically correct in its construction i.e. is satisfying all the notational rules of the formalism, such as brackets being paired off correctly, so that G has a well-defined true or false meaning. The hope had been that a comprehensive

1. It is impossible for a cube to be written as a sum of two cubes or a fourth power to be written as the sum of two fourth powers or, in general, for any number which is a power greater than the second to be written as a sum of two like powers : I have a truly marvellous demonstration of this proposition which this margin is too narrow to contain.

2. Note the strong connection of this problem with solutions which concerned Pythogoreas'theorem. Instead of considering the equation

$$x^2 + y^2 = z^2$$

where there exists an infinite number of solutions (Pythagorean triples), Fermat was contemplating a variant of Pythagora's creation

$$x^3 + y^3 = z^3$$

where there are no solution at all. The proof of the first statement is quiet elementary, and was stated by Euclid. Euclid's proof begins with the observation that the difference between successive square numbers is always an odd number (e.g. $4^2 - 3^2 = 7$). Every single one of the infinity of odd numbers can be added to a particular square number to make another square number. A fraction of these odd numbers are themselves square, but a fraction of infinity is also infinite. Therefore, there are also an infinity of odd square numbers which can be added to one square to make another square number. In other words, there must be an infinite number of Pythagorean triples.

system of axioms and rules of procedure could be given for arithmetic such that it would be **complete** i.e. it would enable us in principle to decide the truth or falsity of any mathematical statement formulated within this system. If Hilbert's hope could be realized, this would even enable us to dispense with worrying about what the propositions mean altogether. G would just be a syntactically correct string of symbols. The string of symbols G would be assigned the truth-value TRUE if G is a theorem (i.e. if G is provable within the system) and it would be assigned the truth-value FALSE if, on the other hand, $\neg G$ is a theorem. For this to make sense, we require **consistency**, in addition to completeness. That is to say, there must be no string of symbols G for which both of G and $\neg G$ are theorems. Otherwise, G could be TRUE and FALSE at the same time ! This was in fact established by Gödel [90].

The complicated part of the Gödel's argument is to show how one may actually code the individual rules of procedure of the formal system, and also the use of its various axioms, into arithmetical operations. In order to carry out this coding, we need to find some convenient way of labelling propositions with natural numbers (the so-called gödelisation). One way would be simply to use some kind of **alphabetical** ordering for all the strings of symbols of the formal system for each specific length, where there is an overall ordering according to the length of the string. Thus, the strings of length one could be alphabetically ordered, followed by the strings of length two alphabetically ordered, and so on. This is called **lexicographical ordering**. We shall be particularly concerned with propositional functions which are dependent on a single variable, like $G(w)$ above. Let the nth such propositional function (in the chosen ordering of strings of symbols), applied to w, be $G_n(w)$. We can allow our numbering to be a little sloppy if we wish, so that some of these expressions may not be syntactically correct. If $G_n(w)$ is syntactically correct, it will be some perfectly well-defined particular arithmetical statement concerning the two natural numbers n and w. Precisely which arithmetical statement it is will depend on the details of the particular numbering system that has been chosen (Arabic notation, Binary notation...). That belongs to the complicated part of the Gödel's argument and will not concern us here (a method is given of constructing, for any formal system of mathematics, a question of number theory undecidable in the system in Gödel's first incompleteness theorem [90]). The strings of propositions which constitutes a proof of some theorem in the system can also be labelled by natural numbers using the chosen ordering scheme. Let $\prod_n$ denote the nth proof. Now consider the following propositional function, which depends on the natural number w :

$$\neg\, \exists x\, [\prod\nolimits_x \text{ proves } P_w(w)]\ .$$

The statement in the square brackets is given partly in words, but it is actually a well-defined arithmetical statement about two natural numbers x and w. It is not supposed to be obvious that the statement can be coded in arithmetic, but it can be, as Gödel provided it. We have numbered all propositional functions which depend on a single variable, so the one we have just written down must have been assigned a number. Let us write this number as k. Our propositional function is the kth one in the list. Thus, it turns out that :

$$\neg\, \exists x\, [\prod\nolimits_x \text{ proves } P_w(w)] = P_k(w)\ ,$$

which is known as a self-reference principle.

Now examine this function for the particular w-value : $w = k$. We get :

$$\neg\, \exists x\, [\prod\nolimits_x \text{ proves } P_k(k)] = P_k(k)\ .$$

Although $P_k(k)$ is just an arithmetical proposition, we have constructed it so that it asserts what has been written on the left-hand side : *there is no proof, within the system, of the proposition* $P_k(k)$. If we have been careful in laying down our axioms and rules of procedure, and assuming that we have done our numbering right, then there cannot be any proof of this $P_k(k)$ within the system. For if there were such a proof, then the meaning of the statement that $P_k(k)$ actually asserts, namely that there is no proof, would be false, so $P_k(k)$ would have to be false as an arithmetical proposition. We have found a true proposition which has no proof within the system !

What about its negation $\neg\, P_k(k)$? It follows that we had also better not be able to find a proof of this either. We have just established that $\neg\, P_k(k)$ must be false (since $P_k(k)$ is true), and we are not supposed to be able to prove false propositions within the system ! Thus, neither $P_k(k)$ nor $\neg\, P_k(k)$ is provable within our formal system. This establishes Gödel's second incompletness theorem which states that no classical formal system of mathematics can prove its own consistency [90].

Although it is very abstract, this theorem is closely related to non-recursive mathematics. Indeed, if we accept that $P_k(k)$ is a perfectly valid proposition, we may simply add it to our system, as an additional axiom denoted G_0. Of course, our new amended system will have its own Gödel proposition, say G_1, which again is seen to be a perfectly valid statement about numbers. Accordingly we adjoin G_1 to our system also, and so on. Is the resulting system with infinite system of axioms G_0, G_1, G_2, G_3, ... complete ? This continuing adjoining of Gödel propositions is a perfectly valid scheme and can be rephrased as an ordinary finite logical system of axioms and rules of procedure. This system will have its own Gödel proposition, say G_ω, which we can again adjoin, and then form the Gödel proposition $G_{\omega+1}$, of the resulting system. Repeating, as above, we obtain a list G_ω, $G_{\omega+1}$, $G_{\omega+2}$, ... of propositions, all perfectly valid statements about natural numbers, and which can all be adjoined to our formal system. This is again perfectly systematic, and it leads us to a new system encompassing the whole lot ; but this again will have its Gödel proposition, say $G_{\omega+\omega}$, which we can rewrite as $G_{\omega 2}$, and the whole procedure can be started up again, so that we get a new infinite, but systematic, list of axioms $G_{\omega 2}$, $G_{\omega 2+1}$, $G_{\omega 2+2}$, ... leading to yet a new system and a new Gödel proposition $G_{\omega 3}$. Repeating the entire procedure, we get $G_{\omega 4}$ and then $G_{\omega 5}$ and so on. Now this procedure is entirely systematic and has its own Gödel proposition G_{ω^2}. This procedure never ends. It was discussed by Alan Türing in 1939 [199]. The insight whereby we concluded that the Gödel proposition $P_k(k) = G_0$ is actually a true statement in arithmetic is an example of a general type of procedure known to logicians as a **reflection principle**. There is a similarity between the argument establishing the truth yet unprovability of $P_k(k)$ and the argument of Bertrand Russell's famous paradox : consider R the set of all sets which are not members of themselves. The question is whether or not the Russell's set R is a member of itself or not. If it is not a member of itself then it should belong to R, since R consists precisely of those sets which are not members of themselves. Thus R belongs to R after all, which is a contradiction.

On the other hand, if R is a member of itself, then since itself is actually R, it belongs to that set whose members are characterized by not being members of themselves i.e. it is not a member of itself after all, which is again a contradiction (the most popular paradox is the one of the ancient greek Epimenide which said that all greeks are liers.). Russel and its collegue Alfred North Whitehead set about developping a highly formalized mathematical system of axioms and selected rules of procedure so as to prevent the paradoxical types of reasonning that led Russel's own paradox. There is a strong thread of historical connection between Russel's paradox, Gödel's theorem and Türing machines. Türing found his argument after studying the work of Gödel. Gödel himself was well aware of the Russel paradox, and was able to transform paradoxical reasoning of this kind, which stretches the use of logic too far, into a valid mathematical argument. All these arguments have their origins in Cantor's diagonal slash argument which establishes by *reductio ad absurdum* that there is no one-to-one correspondence between the real numbers and the natural numbers. Nevertheless, the continum hypothesis of Cantor will never be prooved since Gödel showed it is an undecidable proposition.

Let us come back to the last Fermat theorem in terms of a formal mathematical proposition F

$$F = \neg\ \exists w,\ x,\ y,\ z \in \mathbb{N}\ [(x+1)^{w+3} + (y+1)^{w+3} = (z+1)^{w+3}]\ .$$

One can ask whether or not we could establish that a computer algorithm which runs through all the quadruples of numbers $(w,\ x,\ y,\ z)$ one after the other until the equation is satisfied would ever stop. If we could establish that this algorithm does not stop, then we would have a proof of the Fermat assertion. It turns out that there is no algorithmic procedure for answering the general question of the halting problem completely automatically, as was showed by Türing. But this is not to say that in our individual case we may be not able to decide the truth, or otherwise, of this particular mathematical statement. Perhaps this statement could be proved by the exercise of ingenuity or thanks to arguments coming from outside the system : it is not obvious that another branch of mathematics belonging to geometry, analysis or algebra could not be the good point of view. Indeed, as was shown by Andrew Wiles in 1995 [208], the proof of the theorem is issued from considerations on modular forms rather than on algebraic equations : the proof is indeed mainly based upon the Taniyama-Shimura conjecture, which asserts that "Every elliptic equation is a modular form".

The modular forms were studied by the French mathematician Henri Poincar in the nineteenth century and he had great difficulty coming to terms with their immense symmetry. These esoteric objects exhibit indeed infinite symmetry. For the sake of simplicity, it is convenient to make a parallel with the trivial example of a square tiling. In case of the square tiling we have an object which live in two dimensions, its space being defined by the x-axis and the y-axis. A modular form is also defined by two axes, but the axes are both complex. Modular forms therefore live in a four dimensional space called **hyperbolic space**. This is this extra dimension which gives the modular forms such an immensely high level of symmetry. The modular forms which live in hyperbolic space come in various shapes and sizes, but each one is built from the same basic ingredients. What differentiate modular forms is the amount of each ingredient it contains. The ingredients of a modular

form are labelled from one to infinity (M_1, M_2, M_3, ...,) and so a particular modular form might contain one lot of ingredient one (M_1), three lots of ingredient two (M_2), two lots of ingredients three (M_3), etc... This information describing how a modular form is constructed can be summarized in a so-called modular series (or M-series) i.e. a list of the ingredients and the quantity of each one required :

$$M_1 = 1 \ , \ M_2 = 3 \ , \ M_3 = 2 \ , \ ...$$

The amount of each ingredient listed in the M-series is critical. Depending on how you change the amount of, say, the first term you might generate a completely different, but equally symmetrical, modular form, or you might destroy the symmetry altogether and generate a new object which is not a modular form. If the amount of each term is arbitrarily chosen, then the result will probably be an object with little or no symmetry. Modular forms and elliptic equations live in completely different regions of the mathematics.

The elliptic equations date back to the ancient greeks and have nothing to do with symmetry. The name "elliptic equations" or "elliptic curves" denotes algebraic equations of the form :

$$y^2 = x^3 + ax^2 + bx + c \ , \ a, \ b, \ c, \ \in \mathbb{Z} \ ,$$

for in the past they were used to measure the perimeters of ellipses and the lenghts of planetary orbits. While the fascinating thing about Penrose's tiled surfaces is their restricted symmetry, the interesting property of modular forms is that they exhibit infinite symmetry. The modular forms studied by the Japanese mathematicians Taniyama and Shimura can be shifted, switched, swapped, reflected and rotated in an infinite number of ways and still they remain unchanged, making them the most symmetrical of mathematical objects. The French mathematician Henri Poincaré dicovered their fascinating properties at the begining of the century and hardly accepted that they were symmetrical in the extreme. One can not imagine such objects since they live in a four-dimensional space $\mathbb{C} \times \mathbb{C}$ (hyperbolic space). Nevertheless, the english clergyman and shakespearean Edwin A. Abbott (1836-1926) who published in 1884 the novel "Flatland, a romance of many dimensions" under the pseudonym A. Square, described what life could be in such upper dimensional space. The artist Mauritz Escher drawn a representation of the hyperbolic space on a two-dimensional page (cf. figure 3.8).

More precisely, let us define an analytic function on the half-plane of Poincaré $\{z \in \mathbb{C} \ , \ \mathcal{I}m(z) > 0\}$, satisfying certain monotony assumption on its boundary, and the following equation

$$f\left(\frac{az+b}{cz+d}\}\right) = (cz+d)^2 f(z) \ , \ \begin{pmatrix} a & b \\ Nc & d \end{pmatrix} \in \Gamma_0(N)$$

where $\Gamma_0(N)$ is the group of matrices with entries a, b, c, $d \in \mathbb{Z}$ and whose determinant is unitary. Such functions are modular forms invariant under the translation $z \longmapsto z+1$ and can therefore be expanded in Fourier series

$$f(z) = \sum_{n=0}^{+\infty} a_n(f) q^n \ , \ q = e^{2\pi i z}$$

FIGURE 3.8 – Representation of two-dimensional creatures living in an hyperbolic space.

If f satisfy an adequate monotony condition on the boundary (parabolic modular form), it appears that $a_0(f) = 0$.

What is the link between modular forms and elliptic equations ? The Shimura-Taniyama-Weil conjecture claims that there exists an integer $N \geq 1$ and a parabolic form f, normalized such that $a_1(f) = 1$, satisfying

$$a_p(E) = a_p(f) \ ,$$

where p denotes the prime numbers of good reduction for the elliptic curve E (if the reduced equation associated to E has no singularities on the finite corps $\mathbf{Z}/p\mathbf{Z}$ with p elements, E is said to have good reduction in p). For example, the elliptic curve defined by the equation

$$y^2 = x^3 - x^2 + \frac{1}{4} \ ,$$

which is equivalent to

$$y^2 + y = x^3 - x^2 \ ,$$

has good reduction in p for $p \neq 11$. Let N_p be the number of solutions on $\mathbf{Z}/p\mathbf{Z}$ of the reduced equation. Then the sequence $(a_p(E))_p$ defined as $a_p(E) = p - N_p$, where p runs on prime numbers of good reduction, is a natural arithmetic invariant of the elliptic curve. In the particular case of the second order equation $x^2 - d = 0$, where d is an integer, the primes numbers which do not divide $2d$ are of good reduction for this equation. For such a p, N_p equals 2 or 0, depending upon d is a square modulo p or not. Thanks to the quadratic reciprocity law of Gauss, we know that this property of p solely depends upon the congruence class of p modulo $4d$, and the sequence N_p is therefore $4d$-periodic. The Shimura-Taniyama-Weil conjecture just claims that in the general case of elliptic curves, the sequence $(a_p(E))_p$ follows the same kind of rule.

During the autumn of 1984 Gerhard Frey, a German number theorist, claimed that if the Fermat Last Theorem were wrong, the Shimura-Taniyama-Weil conjecture would be

false. Considering the three whole numbers a, b, c, hypothetical solutions of :

$$a^n + b^n = c^n \ ,$$

thanks to a deft series of complicated manoeuvres Frey fashioned Fermat's original equation into :

$$y^2 = x^3 + (a^n - b^n)x^2 - a^n b^n \ .$$

which is an elliptic equation. By turning Fermat's equation into an elliptic equation, Frey had linked Fermat's Last Theorem to the Shimura-Taniyama-Weil conjecture : Frey prooved that his elliptic equation could never be modular, which invalidated the Shimura-Taniyama-Weil conjecture. In other words, Frey's argument was as follows :

(1) If (and only if) Fermat's Last Theorem is wrong, then Frey's elliptic equation exists.

(2) Frey's elliptic equation is so weird that it can never be modular.

(3) The Taniyama-Shimura conjecture claims that every elliptic equation must be modular.

(4) Therefore the Taniyama-Shimura conjecture must be false.

By running his argument backwards, Frey had come to the conclusion that the truth of Fermat's Last Theorem would be an immediate consequence of the Shimura-Taniyama-Weil conjecture being proved.

To prove this conjecture, Wiles had gone outside the system of arithmetics. The notion of mathematical truth thus goes beyond the whole concept of formalism. Any particular formal system has a provisional and man-made quality about it. Such systems indeed have very valuable roles to play in mathematical discussions, but they can supply only a partial (or approximate) guide to truth. According to Roger Penrose, real mathematical truth goes beyond mere man-made constructions. The physicist takes therefore advantage to his contact with reality to test whether its system is consistant or not.

3.6 Quasi-crystals versus homogenization

In this thesis, guided by physical experiments, we choose the point of view of Fourier analysis to treat the mathematical problems under consideration ; but we may have chosen a completely different point of view (a probalistic one, an algebraic one...). To be more precise, the spectral properties of the Penrose patterns under consideration, first observed by A. L. Mackay [134] using optical methods, exhibited the presence of sharp Bragg peaks in the diffraction patterns, now identified as the expression of quasiperiodicity : the Fourier transform of the measure defined as the sum of Dirac deltas at all the vertices of the tiling, is a sum of weighted Dirac carried by a fractal set (see figure 3.9).

Therefore, we choose to make our study in the Fourier space since it seems to reveal the deep nature of quasi-crystals. Furthermore, the very non-recursive nature of quasi-crystals, coming from fractal set properties, is studied with a functional analysis point of view : one may have thought to treat the problem from the point of view of the logician. Obviously, all the problems arising in quasi-crystals, such as self-similarity and local-isomorphism, are very present in all our study, but our general point of view is mainly based upon a functional approach (except for the estimate of the corrector in chapter 5).

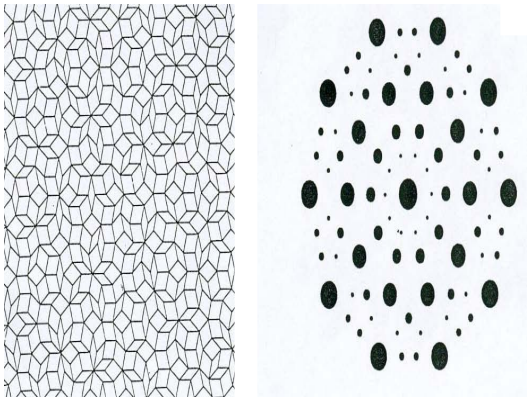

FIGURE 3.9 – The Penrose lattice and its diffraction pattern.

Let us now develop the plan of the following chapter. In the introduction, we explain what is the physical problem of scattering by a finite size quasi-periodic structure for the long wavelengths limit : contrary to the periodic and random media, there is in fact a competition between the size of the quasi-periods of the structure and the increasing wavelength, during the process of homogenization (self-similarity of quasi-crystals). Whatever large the wavelength is, it still remains in resonance with one of the quasi-periods of the structure. The very nature of algebraic numbers and more particularly the "bad approximation" of the gold number by rationals allows the homogenization process to converge : we can exhibit a homogenized structure with an anisotropic matrix of effective permittivity, whose coefficients depend upon the resolution of problems of electrostatic type in the Fourier space. In a first section, we set up in mathematical terms the physical problem under consideration, thanks to the vector Maxwell system. We then state the general properties of quasi-periodic functions in the sense of Bohr and Besicovitch : we can define an almost periodic function f in the sense of Bohr as the uniform limit of a trigonometric polynomial P_h of degree $r_h \in \mathbb{N}_*$:

$$\lim_{h\to\infty} \|P_h(y) - f(y)\|_\infty = 0$$

where for all $x_j^h \in \mathbb{R}$ and $v_j^h \in \mathbb{R}$, $P_h(y) = \sum_{j=1}^{r_h} x_j^h e^{iv_j^h y}$. The main drawback of this definition is that it just concerns continous functions. When dealing with measurable functions, we must introduce the notion of almost periodic functions in the sense of Besicovitch. For this, we define a linear functional L (called ergodic mean) on the set of almost periodic functions in the sense Bohr :

$$L(f) = \lim_{T\to+\infty} \frac{1}{2T} \int_{-T}^{T} f(y)\, dy$$

The set of almost-periodic measurable functions $f : \mathbb{R} \longmapsto \mathbb{C}$ (in the sense of Besicovitch) coincides with the closure of the set of trigonometric polynomials for the following norm :

$$\lim_{h\to\infty} L(\mid P_h(y) - f(y) \mid) = 0$$

Keeping in mind that our aim is to study the diffraction by quasi-periodic structures such as Penrose tilings, we introduce the notion of quasi-periodic functions issued from a cut and projection of periodic functions in a space of higher dimension. A quasi-periodic function $f_\alpha : \mathbb{R} \longmapsto \mathbb{C}$ issued from a cut and projection of a Y^2-periodic function $f(y,z)$ can be written as follows :

$$f_\alpha(y) = f(y, \alpha y) \ .$$

where α is a positive irrational number. We generalize this notion to almost-periodic functions on $\mathbb{R}$, issued from a cut and projection of periodic functions on $\mathbb{R}^m$ $(m > 1)$:

$$f_{\alpha_{m-1}}(y) = f(y, \alpha_1 y, \alpha_2 y, ..., \alpha_{m-1} y) \ ,$$

where the irrational numbers α_i satisfy the condition $\dfrac{\alpha_i}{\alpha_j} \notin \mathbb{Q}$, $\forall i \neq j$. Let us denote the set of such almost-periodic functions $Q_{1,m}$. We then see that $\bigcup_{m>1} Q_{1,m}$ is actually dense in the set of almost-periodic functions in the sense of Besicovitch (denoted by B_1). We generalize the preceding results to almost periodic functions $f_R : \mathbb{R}^n \longmapsto \mathbb{C}^p$ issued from a cut and projection of a Y^m-periodic function $f(y_1, ..., y_m)$:

$$f_R(y_1, ..., y_n) = f(R(y_1, ..., y_n))$$

where R is a given matrix with m lines and n columns such that $R^t k \neq 0$, $\forall k \in \mathbb{Z}^m \setminus \{0\}$. We can see that these functions are dense in the Besicovitch almost-periodic functions $f : \mathbb{R}^n \longmapsto \mathbb{C}^p$, thanks to the Besicovitch identity (generalized Plancherel formula) :

$$\lim_{T\to\infty} \frac{1}{(2T)^n} \int_{|y|\leq T} \|f(y)\|^2 \, d\xi = \sum_{k=1}^{\infty} \|x_k\|^2 \ ,$$

where $f(y) = \sum_{k=1}^{\infty} x_k e^{i\omega_k y}$, $x_k \in \mathbb{C}^p$ and $\omega_k \in \mathbb{R}^n$.

We then explain the link between the quasi-periodic measurable functions issued from a cut and projection and quasi-crystals : the most important point is that we describe the geometry of the quasi-crystalline structures thanks to their permittivity, which belongs to the preceding class of functions. To conclude this section, we point out on two ambiguities when defining a quasi-crystal thanks to the cut and projection method. The Penrose tilings can actually be issued from a cut and projection of crystal lattices in $\mathbb{R}^4$ or $\mathbb{R}^5$ (in fact, they may be issued from spaces of higher dimensions too) : uniqueness of the definition is missing, since f_R depends upon the choice of the matrix R. Furthermore, such quasi-crystal structures are even issued from an infinity of periodic lattices in $\mathbb{R}^4$ or $\mathbb{R}^5$. These paradox are closely related to non-recursive mathematics.

In a second section, we introduce a notion of two-scale convergence relatively to the R matrix, based on the following result (cf. proposition 2) : let Ω be a bounded subset of $\mathbb{R}^n$ and $Y =]0;1[^m$. If (u_η) is a bounded sequence in $L^2(\Omega)$, then there exists a function $u_0(x,y) \in L^2(\Omega; L^2_\sharp(Y^m))$ (i.e. square integrable over Ω in the x variable and Y^m periodic and square integrable over Y^m in the y variable) such that $\forall \varphi \in \mathcal{D}(\Omega; C^\infty_\sharp(Y^m))$ (i.e.

infinitely differentiable function with compact support in Ω in the x variable, and infinitely differentiable with compact support in Y^m, Y^m periodic in the y variable)

$$\lim_{k\to+\infty}\int_\Omega u_{\eta_k}(x)\varphi(x,\frac{R(x)}{\eta_k})\,dx=\int_\Omega\int_{Y^m}u_0(x,y)\varphi(x,y)\,dxdy$$

provided that R is a matrix such that $R^tk\neq 0\ ,\ \forall k\in\mathbb{Z}^m\setminus\{0\}$. If the result holds, we say that u_{η_k} two-scale converge towards u_0 (relatively to the R matrix), and we write :

$$u_{\eta_k}\overset{R}{\searrow}u_0$$

It is worth noting that this convergence highly depends on the irrational entries of the R matrix. If $n=1$ and $m=2$, we take $R^t=(1,\alpha)$, which satisfies the previous condition if α is irrational : $\forall\varphi\in\mathcal{D}(\Omega;C^\infty_\sharp(Y^2))$,

$$\lim_{k\to+\infty}\int_\Omega u_{\eta_k}(x)\varphi(x,\frac{x}{\eta_k},\alpha\frac{x}{\eta_k})\,dx=\int_\Omega\int_{Y^2}u_0(x,y_1,y_2)\varphi(x,y_1,y_2)\,dxdy_1dy_2$$

The physical underlying idea is that we "scan" the basic cell Y^2 (see figure 3.10) if the slope of the subspace $E_\parallel$ is irrational. For this, we translate every segment derived from the intersection of the line of slope α ($E_\parallel$) with the basic cells of R^2, on the basic cell centered at the origin.

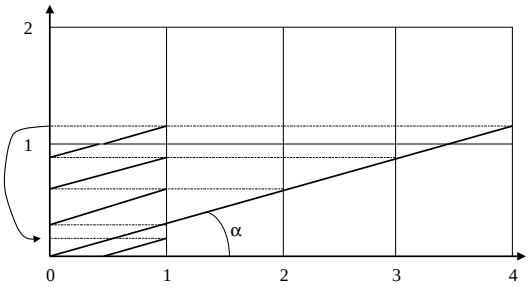

FIGURE 3.10 – A scanner for the basic cell Y^2.

We see that the two-scale limit of oscillating quasi-periodic sequences no more depends upon the choice of R, which leads to an obvious physical interpretation : if u_η stands for the diffracted field by a quasi-periodic structure, there is no more ambiguity on the definition of its two-scale limit u_0, since it represents the diffracted field by an homogeneous body.

In the sequel, we will have to pass to the limit in $\displaystyle\int_\Omega u_\eta\,v_\eta\,dx$ where $u_\eta\overset{R}{\searrow}u_0$ and $v_\eta\overset{R}{\searrow}v_0$. We therefore introduce a notion of strong two-scale convergence. We say that a sequence (u_η) in $L^2(\Omega)$ strongly two-scale converges to a limit u_0 in $L^2_\sharp(\Omega\times Y^m)$ (relatively to the R matrix), and we write $u_\eta\overset{R}{\twoheadrightarrow}u_0$, if and only if :

$$\|u_\eta\|_{L^2(\Omega)}\to\|u_0(x,y)\|_{L^2(\Omega\times Y^m)}$$

We then have a result of corrector type (proposition 5) : if $u_\eta\overset{R}{\twoheadrightarrow}u_0(x,y)$

and $\|u_0(x,\frac{x}{\eta})\|_{L^2(\Omega)} \to \|u_0(x,y)\|_{L^2(\Omega\times Y^m)}$, it follows that $\|u_\eta - u_0(x,\frac{x}{\eta})\|_{L^2(\Omega)} \to 0$.

Concerning the convergence of gradients of such sequences, we make the study in Fourier space, since the oscillations of a sequence (∇u_η) cannot be expressed by means of the gradient of a periodic function. We are thus led to introduce the space

$$\mathcal{L}_R = \Big\{ w \in [L^2_\sharp(Y^m)]^n \ \mid \ w(y) = \sum_{k\in\mathbb{Z}^m\setminus\{0\}} \lambda_k \, R^T(k) e^{2i\pi k\cdot y} \ , \ \lambda_k \in \mathbb{C} \Big\}$$

which is a closed subspace of $[L^2_\sharp(Y^m)]^n$ (cf. lemma 6). It is worth noting that (λ_k) is not necessary in l^2, but solely verify $\sum_{k\in\mathbb{Z}^m\setminus\{0\}} \mid \lambda_k \mid^2 \mid R^T(k) \mid^2 < +\infty$, since $\mid R^T(k) \mid$ is positive for all $k \in \mathbb{Z}^m \setminus \{0\}$ but has no lower bound. Thanks to the very definition of $\mathcal{L}_R$, we can state the fundamental result on the convergence of gradients (cf. proposition 7) : let (u_η) be a bounded sequence in $W^{1,2}(\Omega)$. Then there exists $u_0 \in W^{1,2}(\Omega)$ (i.e. square integrable function of square integrable gradient over Ω), $w \in L^2(\Omega, \mathcal{L}_R)$ and a subsequence (still denoted (u_η)) such that :

$$\begin{cases} u_\eta \overset{R}{\twoheadrightarrow} u_0(x) \\ \nabla u_\eta \overset{R}{\rightharpoonup} \nabla_x u_0(x) + w(x,y,z) \end{cases}$$

provided that R is a matrix such that $R^t k \neq 0$, $\forall k \in \mathbb{Z}^m \setminus \{0\}$. In the third section, we extend the result of proposition 7 to the convergence of rotationals of vector valued sequences. Let R be a matrix with m lignes and 3 columns such that $R^t k \neq 0$, $\forall k \in \mathbb{Z}^m \setminus \{0\}$. We denote by $\mathcal{M}_R$ the closed subspace of $[L^2_\sharp(Y^m)]^9$:

$$\mathcal{M}_R = \Big\{ w \in [L^2_\sharp(Y^m)]^9 \ \mid \ w(y) = \sum_{k\in\mathbb{Z}^m\setminus\{0\}} \Lambda_k \otimes R^T(k) e^{2i\pi k\cdot y}$$
$$\text{where } \Lambda_k \in \mathbb{C}^3 \text{ and } \Lambda_k \cdot R^T(k) = 0 \ , \ \forall\, k \in \mathbb{Z}^m \setminus \{0\} \Big\}$$

We establish, in corollary 8 that if Ω is a regular open bounded set of $\mathbb{R}^3$ and (H_η) a sequence in $[L^2(\Omega)]^3$ such that :

$$\mathcal{P}_\eta = \begin{cases} (i) \ \operatorname{div} H_\eta = 0 \\ (ii) \ \sup\limits_\eta \displaystyle\int_\Omega \Big(\mid H_\eta \mid^2 + \mid \operatorname{rot} H_\eta \mid^2 \Big) \, dx < +\infty \\ (iii) \ H_\eta \wedge n \quad \text{is bounded in } \left[H^{\frac{1}{2}}(\partial\Omega)\right]^3 \end{cases}$$

then (H_η) is bounded in $[W^{1,2}(\Omega)]^3$ and there exists $H_0 \in [W^{1,2}(\Omega)]^3$ and $w \in L^2(\Omega, \mathcal{M}_R)$ such that, up to a subsequence,

$$\begin{cases} H_\eta \to H_0(x) \text{ in } [L^2(\Omega)]^3 \\ \nabla\, H_\eta \overset{R}{\rightharpoonup} \nabla\, H_0(x) + w(x,y) \end{cases}$$

Thanks to this result, we can now make the asymptotic analysis of the vector Maxwell system for the magnetic field :

$$(\mathcal{P}^H_{\eta,\alpha}) = \begin{cases} (i)\ \mathrm{rot}\Big(\varepsilon_\eta^{-1}\,\mathrm{rot}\,H_\eta\Big) - k_0^2 H_\eta = 0 & \text{in } [\mathcal{D}'(\mathbb{R}^3)]^3 \\ (ii)\ \mathrm{div}\,H_\eta = 0 & \text{in } \mathcal{D}'(\mathbb{R}^3) \\ (iii)\ H^d_\eta = O(\frac{1}{|x|}) & \text{when } |\,x\,| \to +\infty \text{ in } [C^\infty(\mathbb{R}^3 \setminus \bar{D})]^3 \\ (iv)\ \frac{x}{|x|} \wedge \mathrm{rot}\,H^d_\eta + ikH^d_\eta = o(\frac{1}{|x|}) & \text{when } |\,x\,| \to +\infty \text{ in } [C^\infty(\mathbb{R}^3 \setminus \bar{D})]^3 \end{cases}$$

where $H^d_\eta = H_\eta - H^i$ (H^i is the incident field and H^d_η is the diffracted field). It is worth noting that the electric field is then deduced from the equation $E_\eta = \dfrac{1}{j\omega\varepsilon_0\mu_0\varepsilon_\eta}\,\mathrm{rot}\,H_\eta$.

In theorem 9, we establish our main result : let L be the linear continuous mapping defined for every matrix in $\mathbb{C}^9$ by : $\forall\ v \in \mathbb{C}^3$, $L(w) \wedge v = (w - w^T)v$. Let w be the unique solution in $\mathcal{M}_R$ of the three variational annex problems (indexed by $x \in \mathbb{R}^3$) $(\mathcal{P}^x_i)$, $i \in \{1\,,2\,,3\}$:

$$(\mathcal{P}^x_i) : \int_{Y^m} \frac{1}{\varepsilon(x,y)}\Big[e_i + L(w_i(y))\Big] \cdot \Big[L(w'_i(y))\Big]\,dy = 0\ ,\ \forall w'_i \in \mathcal{M}_R$$

When η tends to 0, the unique solution H_η of the problem $(\mathcal{P}^H_{\eta,\alpha})$ tends strongly in $L^2_{loc}(\mathbb{R}^3, \mathbb{C}^3)$ to the unique solution H_0 of the following problem $(\mathcal{P}_0)$:

$$\mathcal{P}_0 = \begin{cases} (i)\ \mathrm{rot}\Big\{\varepsilon_{hom}^{-1}\,\mathrm{rot}\,H_0(x)\Big\} - k_0^2 H_0(x) = 0 & \text{in } [\mathcal{D}'(\mathbb{R}^3)]^3 \\ (ii)\ \mathrm{div}\,H_0(x) = 0 & \text{in } [\mathcal{D}'(\mathbb{R}^3)]^3 \\ (iii)\ H^d_0(x) = O(\frac{1}{|x|}) & \text{when } |\,x\,| \to +\infty \text{ in } [C^\infty(\mathbb{R}^3 \setminus \overline{D})]^3 \\ (iv)\ \frac{x}{|x|} \wedge \mathrm{rot}\,H^d_0(x) + ikH^d_0(x) = o(\frac{1}{|x|}) & \text{when } |\,x\,| \to +\infty \text{ in } [C^\infty(\mathbb{R}^3 \setminus \overline{D})]^3 \end{cases}$$

where the homogenized matrix ε^{-1}_{hom} is given for all $x \in \mathbb{R}^3$ by :

$$\varepsilon^{-1}_{hom}(x) = \int_{Y^m} \frac{1}{\varepsilon(x,y)}\,dy + \int_{Y^m} \frac{B(y)}{\varepsilon(x,y)}\,dy := \Big\langle \frac{1}{\varepsilon(x,y)} \Big\rangle_{Y^m} + \Big\langle \frac{B(y)}{\varepsilon(x,y)} \Big\rangle_{Y^m}$$

B being the matrix defined by the three column vectors $L(w_i(y))$:

$$B(y) = (L(w_1(y))\ \mid\ L(w_2(y))\ \mid\ L(w_3(y)))$$

It is worth noting that one cannot expect to obtain such a result by the use of matrices which approximate that of the icosahedral structure : passing to the limit over η with a matrix of rational entries and then approximating the R-matrix leads to the homogenized problem of chapter 2 (periodic case). It is worth noting that dealing with metallic quasi-crystals would lead to two successive problems of limits : the first one is related to the approximation of irrationals by rationals and the second one is induced by the approximation of infinitely conducting scatterers by conducting ones.

In the fourth section, we apply this result to the Penrose tilings and one-dimensional quasi-crystals (quasi-periodic Bragg mirrors). Concerning the two-dimensional case, we consider a quasi-periodic assembly of dielectric rods lightened in the polarizations $E \parallel$ and $H \parallel$. In the first polarization, the result is trivial :

$$\mathcal{P}^{E\|}_{0,\alpha}\begin{cases}\Delta E_0^3(x)+k_0^2\varepsilon_{eff}(x)E_0^3(x)=0 & \text{, in } \mathcal{D}'(\mathbb{R}^2)\\ E_0^{3,d}(x)=O\Big(\dfrac{1}{\sqrt{\mid x\mid}}\Big) & \text{, when } \mid x\mid\to+\infty \text{ in } C^\infty(\mathbb{R}^2\setminus\overline{D})\\ \Big(E_0^{3,d}(x)-ik_0\dfrac{\partial E_0^{3,d}}{\partial x}(x)\Big)=o\Big(\dfrac{1}{\sqrt{\mid x\mid}}\Big) & \text{, when } \mid x\mid\to+\infty \text{ in } C^\infty(\mathbb{R}^2\setminus\overline{D})\end{cases}$$

$$\text{where } \varepsilon_{eff}(x)=\begin{cases}\displaystyle\int_{Y^2\times Y^2}\varepsilon(y,z)\,dydz & \text{, if } x\in D\\ 1 & \text{, elsewhere}\end{cases}$$

Concerning the second polarization, we establish in proposition 11 that :
let w_j, $j\in\{1,2\}$ be the unique solution in $[L^2_\sharp(Y^2)]^2$ of the following local problem

$$\mathcal{Q}_j \ : \ \text{Find the projection of } e_j \text{ (constant function in } [L^2_\sharp(Y^2)]^2) \text{ on } \mathcal{L}_\alpha.$$

Then H_0 is the unique solution in $W^{1,2}(\Omega)$ of the homogenized problem :

$$\mathcal{P}_{0,\alpha}: \ -div_x\Big(\varepsilon^{-1}_{eff}(x)\ \nabla H_0(x)\Big)=k_0^2H_0(x)$$

where ε^{-1}_{eff} is the homogenized matrix given by :

$$\varepsilon^{-1}_{eff}(x)=<\frac{1}{\varepsilon}>_{Y^2}\ Id+(<\frac{1}{\varepsilon}w_1>_{Y^2},\ <\frac{1}{\varepsilon}w_2>_{Y^2})$$

In the one-dimensional case, we establish in proposition 12 that the homogenized problem for the $H\parallel$ polarization is given by :

$$\mathcal{P}_{0,\alpha}\begin{cases}\dfrac{d}{dx}\Big(<\varepsilon>_{Y^2}{}^{-1}\dfrac{du}{dx}(x)\Big)+(k_0^2-\beta^2<\varepsilon^{-1}>_{Y^2})u(x)=0 & \text{, dans } \mathcal{D}'(]0;1[)\\ u'(0)+i\gamma u(0)=0\ ,\ u'(1)-i\gamma u(1)=-2i\gamma e^{-i\gamma}\end{cases}$$

3.7 Inside the gold number

The Birth of Venus of the painter Sandro Botticelli (1446-1510) is the symbol of mystery through which the divine message of beauty came into the world. The picture of Boticelli forms a perfeclty harmonious pattern, so that we do not notice the unnatural length of the neck of the Venus, the step fall of her shoulders and the queer way her left arm is hinged to the body. We should say that these liberties which boticelli took with nature in order to achieve a graceful outline add to the beauty and harmony of the design because they enhance the impression of an infinitely tender and delicate being, wafted to our shores as a gift from heaven. The Birth of Venus respects the same rules that the architecture of monuments (Parthenon, Cheops pyramid...). L'Estaque of the painter Paul Cézanne takes its beauty from the agencement of backgroung, middleground and foreground. All these creations were thought in respect to the approximants of the Gold number.

The gold number τ has a particular status. τ is the positive solution of the algebraic equation :

$$\tau^2-\tau=1$$

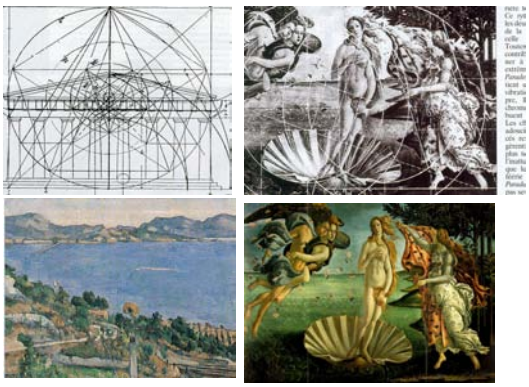

FIGURE 3.11 – These pictures of Boticelli and Cezanne were painted in conjonction with the Gold number, as are some famous architectures.

One easily sees that τ is the fixed point of the following sequence :

$$u_n = u_{n-1} + u_{n-2}$$

The rate of successive numbers 0 , 1 , 1 , 2 , 3 , 5 , 8 , 13 , 21 , 34 , 55 ... gives the rational approximants of τ. This sequence was found in 1202 by Léonard de Pise (son of Bonaccio, or "Filius Bonacci", hence the name Fibonacci sequence), although the ancient Greeks knew about the Gold number for a long time. They used to compute the successive powers of τ thanks to the formula :

$$\tau^n = \tau^{n-1} + \tau^{n-2}$$

and hence had an empirical knowledge of the sequence of Fibonacci.

From this time, the Golden mean and its approximants appeared in various situations in physics and notably in phenomena dealing with chaotic process (cf. Kolmogorov-Arnold-Mozer theorem). Since the last decade, many physicists and among them Roger Penrose, worked on the connections between the quasi-crystalline growth and the physics of chaos [174] and in particular with its famous tiles. It sounds that this properties rely on the speed of convergence of rational towards the algebraic numbers and in particular to that of the Gold number. From these results, we know that the degree of irrationality of algebraic numbers involved in the slope of the cut-projection method will probably influence the result of homogenization. We will see that the touchstone of homogenization of such structures is a corrector type result (see proposition 3 of chapter 5) where we estimate the asymptotic behavior of the error in conjunction with the properties of algebraic numbers. From our result, we expect that this corrector lies between that of periodic structures (for the Gold number) and that of random structures (Liouville numbers i.e. transcendantal numbers). But, we have seen that the Penrose tillings and quasi-crystalline phases encountered in nature can always been deduced from cut-projection methods involving the gold number (Penrose tillings and icosahedral structures). Therefore, it sounds that the quasi-crystalline phases can be homogenized in the same way as periodic structures.

Chapitre 4

Homogénéisation des quasi-cristaux via une convergence deux-échelles-coupe-projection

'Though it be madness, yet there is method in't.' [1]
'Hamlet', Act II, Sc. II, William Shakespeare
"Regis Iusfu Cantio Et Reliqua Canonica Arte Refotula"
J. S. Bach [2]

4.1 Introduction

A l'échelle atomique la matière apparait comme éminemment hétérogène mais l'expérience quotidienne nous la montre plutôt comme homogène. En effet, des inhomogénéités microscopiques peuvent "être lissées" à l'échelle macroscopique (aspect fluide d'un sable fin...). Les méthodes d'homogénéisation que nous allons employer s'inspirent de cette évidence en faisant fondre à la limite les hétérogénéités au regard de la taille gigantesque de la structure par rapport à celle des aspérités.

Nous considérons donc une structure éclairée par une onde monochromatique, dont la longueur d'onde est grande devant les dimensions (diamètre) des diffuseurs. Avec de telles hypothèses, on peut s'attendre à ce que le système physique considéré se comporte comme si il était homogène. Il est en effet bien connu (Bensoussan, Lions and Papanicolaou, 1978 [18]) (Bouchitté and Petit, 1985 [37]) (Felbacq and Bouchitté, 1997 [72]) que si l'on agence ces diffuseurs périodiquement, on peut remplacer la structure par une structure qui peut s'avérer anisotrope dans le cas 2D. Des résultats analogues ont été obtenus pour des

1. 'C'est de la folie, mais il y a une méthode'

2. "À la Demande du Roi, le Chant Et le Reste Résolus selon l'Art Canonique" est une dédicace de J. S. Bach à "l'offrande musicale" écrite pour le Roi Frédéric. Les initiales des mots de la dédicace donnent RICERCAR, mot italien qui signifie "chercher" ou désigne un type de fugue pour les érudits. Les 10 canons qui composent l'offrande ont un lien étroit avec le principe d'auto-référence et certaines suites quasi-périodiques [113].

matériaux 2D présentant une répartition aléatoire de diffuseurs, dans le cas de l'équation des ondes (Garnier and Fouque, 1996 [84]). Notre étude porte, quant à elle, sur un domaine qui ne rentre dans aucune des catégories que nous venons de citer : celui de l'étude de la diffraction par des phases quasi-cristallines. Notre objectif est donc de remplacer un quasi-cristal par une structure homogène ayant les mêmes propriétés diffractives à la limite des grandes longueurs d'ondes. La difficulté de l'étude réside dans ce que la longueur d'onde, quelque grande qu'elle soit, est dans le domaine de résonance de l'une au moins des échelles caractéristiques (quasipériodes) du cristal étudié.

Des résultats existent dans la littérature (Kozlov, 1979 [122], 1984 [124]) (Oleinik and Zhikov, 1982 [169]) (Braides, 1985 [41], 1990 [40]) conduisant, quand le nombre de diffuseurs tend vers l'infini, à la convergence du modèle vers un modèle homogénéisé avec une matrice effective représentant les caractéristiques physiques d'un milieu homogène équivalent. La question pratique est la détermination de cette matrice effective, qui selon les résultats théoriques précédemment cités, est obtenue par passage à la limite sur des problèmes élémentaires sur une cellule de taille N, avec N qui tend vers l'infini.

Ici, nous nous proposons de donner une méthode de calcul ramenant les problèmes élémentaires sur une seule cellule de base mais sous l'hypothèse particulière que la structure est engendrée par une coupe projection (suite de Fibonacci, Pavage de Penrose...). Le chapitre est organisé de la façon suivante :

Dans la section 2, on décrit la géométrie du problème et le problème de diffraction indexé par le petit paramètre η (quasi-période).

Dans la section 3, nous rappelons des résultats classiques sur les fonctions quasi-périodiques, et définissons une notion de fonctions quasi-périodiques construites par coupe-projection.

Dans la section 4, on introduit une variante de la méthode de convergence à deux échelles (Allaire, 1992 [2]) adaptée à la structure coupe-projection et démontrons des résultats de structure pour les limites de champs de gradients.

Ces résultats sont appliqués dans la section 5 où nous établissons notre résultat principal d'homogénéisation pour le système de Maxwell (cas 3D).

Dans la section 6, on particularise au cas d'une onde polarisée et d'un obstacle cylindrique (réduction au cas 2D et équations d'Helmholtz scalaires), puis au cas d'un milieu stratifié (une étude qualitative du correcteur est donnée dans ce cas dans le chapitre suivant).

4.2 Position du problème de diffraction

On étudie la diffraction électromagnétique par des structures tri-dimensionnelles bornées (ou bien cylindriques dans le cas polarisé), construites par adjonction d'un arrangement "quasi-périodique" d'un grand nombre de diffuseurs identiques T_η (dont les dimensions sont de l'ordre du petit paramètre η) insérés dans un domaine fixe D qui sera dans toute la suite un ouvert borné de classe C^2 de $\mathbb{R}^2$ ou $\mathbb{R}^3$. Nous nous intéressons plus particulièrement à des structures finies du type pavages de Penrose en dimension 2 : ces pavages sont générés par deux losanges (dont les angles sont des multiples de $\frac{2\pi}{10}$ et de

rapport de surfaces égal au nombre d'or τ) à l'aide de règles de connexion ou "matching rules". Ces pavages, qui présentent une symétrie d'ordre 5 interdite par la cristallographie, peuvent-être obtenus par la coupe d'une structure périodique dans $\mathbb{R}^4$ ou $\mathbb{R}^5$ suivant un hyperplan de pente irrationnelle qui s'exprime en fonction de τ (méthode de coupe-projection [66][67], cf. annexe B). De même, on peut générer l'équivalent 3D des pavages de Penrose, les icosaèdres, qui sont des phases quasi-cristallines qui peuvent-être obtenues par la coupe d'une structure périodique dans $\mathbb{R}^6$ ou dans $\mathbb{R}^{12}$. Notre étude s'applique à des profils de permittivité décrits par une fonction ε_η bornée et supérieure à 1 (les matériaux rencontrés en pratique à profil de permittivitté continu ou constant par morceaux rentrent dans ce cadre). Considérons par exemple une phase quasi-cristalline dans $\mathbb{R}^3$, dont le profil d'indice prend deux valeurs. Si on désigne par χ_D la fonction caractéristique de l'obstacle diffractant D ($\chi_D = 1$ sur D et 0 ailleurs), la permittivité relative en tout point de l'espace sera définie par :

$$\varepsilon_\eta(x) = \varepsilon_\sharp(\frac{R(x)}{\eta})\chi_D(x) + (1 - \chi_D)(x) \tag{0}$$

où $\varepsilon_\sharp$ est une fonction mesurable bornée $]0;1[^6$-périodique sur $\mathbb{R}^6$ ($\varepsilon_\sharp \in L^\infty_\sharp(]0;1[^6)$), η un petit paramètre (quasi-période) et où R désigne un relèvement linéaire de $\mathbb{R}^3$ dans $\mathbb{R}^6$ (ou $\mathbb{R}^{12}$). Comme on le verra, l'analyse des oscillations de la suite ε_η quand $\eta \to 0$ dépendra essentiellement du caractère irrationnel des coefficients de la matrice associée à R. Notons que la fonction $\varepsilon_\sharp$ est en général à valeurs complexes et vérifie $0 \leq arg(\varepsilon_\sharp) < \pi$ ($\mathcal{I}m(\varepsilon_\sharp) \geq 0$). La zône où $\mathcal{I}m(\varepsilon_\sharp) > 0$ correspond à la présence d'un diélectrique à pertes.

On éclaire l'obstacle diffractant D par un champ incident monochromatique (E^i, H^i) dont la longueur d'onde λ est grande devant les dimensions des diffuseurs T_η. L'étude mathématique consiste alors à étudier le champ électromagnétique en régime harmonique (par convention la dépendance temporelle est en $exp(-j\omega t)$) qui est diffracté par l'obstacle D quand le petit paramètre η tend vers 0. Nous considérons donc la suite des couples (E_η, H_η) solutions du problème de diffraction $\mathcal{P}^{(E,H)}_{\eta,\alpha}$ associé à la permittivité ε_η définie par (0) via l'obstacle D et la fonction $\varepsilon_\sharp$:

$$\mathcal{P}^{(E,H)}_{\eta,\alpha} \begin{cases} (1)\ \mathrm{rot}\, E_\eta + j\omega\mu_0 H_\eta = 0 & , \text{dans } [\mathcal{D}'(\mathbb{R}^3)]^3 \\ (2)\ \mathrm{rot}\, H_\eta - j\omega\varepsilon_0\varepsilon_\eta E_\eta = 0 & , \text{dans } [\mathcal{D}'(\mathbb{R}^3)]^3 \\ (3)\ \mathrm{div}(\varepsilon_\eta E_\eta) = 0 & , \text{dans } \mathcal{D}'(\mathbb{R}^3) \\ (4)\ \mathrm{div}(\mu_0 H_\eta) = 0 & , \text{dans } \mathcal{D}'(\mathbb{R}^3) \end{cases}$$

Le champ électromagnétique cherché doit de plus avoir un comportement à l'infini particulier. Les conditions de rayonnement de Silver-Müller imposent au champ diffracté $(E^d_\eta, H^d_\eta) = (E_\eta - E^i, H_\eta - H^i)$ une décroissance en $\frac{1}{|x|}$ uniformément pour toutes les directions :

$$(SM) \begin{cases} E^d_\eta = O(\frac{1}{|\,x\,|}) & , H^d_\eta = O(\frac{1}{|\,x\,|}) \\ \frac{x}{|\,x\,|} \wedge \mathrm{rot}\, E^d_\eta + ikE^d_\eta = o(\frac{1}{|\,x\,|}) & , \frac{x}{|\,x\,|} \wedge \mathrm{rot}\, H^d_\eta + ikH^d_\eta = o(\frac{1}{|\,x\,|}) \end{cases}$$

Ces conditions appelées aussi conditions d'onde sortante (elles correspondent à une superposition d'ondes planes sortantes), jouent un rôle fondamental en assurant l'existence et l'unicité de la solution du problème $\mathcal{P}^{E,H}_{\eta,\alpha}$ [51]. Dans le cadre de notre analyse asymptotique du problème $\mathcal{P}^{E,H}_{\eta,\alpha}$, on considère un rayon R et un ouvert Ω tels que $\Omega := \{\mid x \mid < R\}$ vérifie $\overline{D} \subset \Omega$. On fixe alors $r < R$ de sorte que $\bar{D} \subset \{\mid x \mid < r\} \subset \Omega$ et on écrit la formulation variationnelle associée à $\mathcal{P}^{E,H}_{\eta,\alpha}$ sur l'ouvert borné Ω indépendant de η. Pour traiter la convergence du champ diffracté (E^d, H^d), nous faisons alors appel à la forme intégrale de (SM), appelée aussi formule de Stratton-Chu, valable pour tout $\mid x \mid > r$:

$$(SC)\begin{cases} E^d_\eta(x) = i\omega\mu_0 \displaystyle\int_{|y|=r} G(x-y)(\frac{y}{r} \wedge H^d_\eta(y))\, ds + \int_{|y|=r} \bigtriangledown G(x-y)(\frac{y}{r} \wedge E^d_\eta(y))\, ds \\ H^d_\eta(x) = -i\omega\varepsilon_0 \displaystyle\int_{|y|=r} G(x-y)(\frac{y}{r} \wedge E^d_\eta(y))\, ds + \int_{|y|=r} \bigtriangledown G(x-y)(\frac{y}{r} \wedge H^d_\eta(y))\, ds \end{cases}$$

où G est la fonction de Green $G(x) = \dfrac{1}{4\pi}\dfrac{e^{ik_0|x|}}{\mid x \mid}$.

Si l'on considère des milieux dont la perméabilité μ_0 est constante (milieux non magnétiques), le problème de diffraction $\mathcal{P}^{(E,H)}_\eta$ par la structure D caractérisée par le coefficient $\varepsilon_\eta(x)$ se ramène alors à chercher l'unique solution $H_\eta \in L^2_{loc}(\mathbb{R}^3, \mathbb{C}^3)$ (champ magnétique) du système suivant (E_η étant alors déduit de (2)) :

$$(\mathcal{P}^H_{\eta,\alpha})\begin{cases} (i)\ \operatorname{rot}\Big(\varepsilon_\eta^{-1} \operatorname{rot} H_\eta\Big) - k_0^2 H_\eta = 0 & \text{dans } [\mathcal{D}'(\mathbb{R}^3)]^3 \\ (ii)\ \operatorname{div} H_\eta = 0 & \text{dans } \mathcal{D}'(\mathbb{R}^3) \\ (iii)\ H^d_\eta = O(\frac{1}{|x|}) & \text{quand } \mid x \mid \to +\infty \text{ dans } [C^\infty(\mathbb{R}^3 \setminus \bar{D})]^3 \\ (iv)\ \frac{x}{|x|} \wedge \operatorname{rot} H^d_\eta + ikH^d_\eta = o(\frac{1}{|x|}) & \text{quand } \mid x \mid \to +\infty \text{ dans } [C^\infty(\mathbb{R}^3 \setminus \bar{D})]^3 \end{cases}$$

Pour l'existence et l'unicité de la solution H_η de $\mathcal{P}^H_{\eta,\alpha}$, on se réfèrera à [51].

Dans le cas d'une onde polarisée, on peut envisager un obstacle cylindrique $G = D \times \mathbb{R}$, D étant un ouvert borné de $\mathbb{R}^2$. Dans les cas transverse électrique (E_η est parallèle à la génératrice du cylindre e_3) et transverse magnétique ($H_\eta \parallel e_3$), le champ diffracté $(E^d_\eta, H^d_\eta) = (E_\eta - E^i, H_\eta - H^i)$ vérifie les conditions de rayonnement de Sommerfeld :

$$(S)\begin{cases} E^d_\eta = O\Big(\dfrac{1}{\sqrt{\mid x \mid}}\Big) & , H^d_\eta = O\Big(\dfrac{1}{\sqrt{\mid x \mid}}\Big) \\ \Big(E^d_\eta - ik_0 \dfrac{\partial E^d_\eta}{\partial x}\Big) = o\Big(\dfrac{1}{\sqrt{\mid x \mid}}\Big) & , \Big(H^d_\eta - ik_0 \dfrac{\partial H^d_\eta}{\partial x}\Big) = o\Big(\dfrac{1}{\sqrt{\mid x \mid}}\Big) \end{cases}$$

Les relations de Kirchhoff-Helmholtz (cf. [51]) nous assurent que (S) est équivalent à :

$$(KH)\begin{cases} E^d_\eta(x) = \displaystyle\int_{\partial D} \Big[\Phi(x-y)\frac{\partial E^d_\eta}{\partial y}(y) - \frac{\partial \Phi}{\partial y}(x-y)E^d_\eta(y)\Big]\, ds & , \text{dans } \mathbb{C}^\infty(\mathbb{R}^2 \setminus \bar{D}) \\ H^d_\eta(x) = \displaystyle\int_{\partial D} \Big[\Phi(x-y)\frac{\partial H^d_\eta}{\partial y}(y) - \frac{\partial \Phi}{\partial y}(x-y)H^d_\eta(y)\Big]\, ds & , \text{dans } \mathbb{C}^\infty(\mathbb{R}^2 \setminus \bar{D}) \end{cases}$$

où Φ est la fonction de Hankel de première espèce $\Phi(x) = \frac{i}{4}H_0^{(1)}(k_0 \mid x \mid)$.

Les composantes du champ électromagnétique E_η et H_η sont solutions de deux systèmes d'équations aux dérivées partielles découplées :

$$\mathcal{P}^{E\|}_{\eta,\alpha} \begin{cases} \Delta E_\eta + k_0^2 \varepsilon_\eta \, E_\eta = 0 & \text{dans } \mathcal{D}'(\mathbb{R}^2) \\ E_\eta^d \text{ vérifie } (KH) & , \text{ dans } C^\infty(\mathbb{R}^2 \setminus \bar{D}) \end{cases}$$

et

$$\mathcal{P}^{H\|}_{\eta,\alpha} \begin{cases} -div\Big(\varepsilon_\eta^{-1} \bigtriangledown H_\eta\Big) = k_0^2 H_\eta & , \text{ dans } \mathcal{D}'(\mathbb{R}^2) \\ H_\eta^d \text{ vérifie } (KH) & , \text{ dans } C^\infty(\mathbb{R}^2 \setminus \bar{D}) \end{cases}$$

4.3 Rappels sur les fonctions quasi-périodiques

Pour les besoins de notre étude, il nous faut définir les différentes notions de fonctions quasi-périodiques : contrairement à Kozlov [122][124], Oleinik et Zhikov [169] et Braides [41][40], nous n'étudions qu'une classe particulière de fonctions quasi-périodiques, en vue d'une application pour des phases quasi-cristallines rencontrées en pratique.

4.3.1 Fonctions quasi-périodiques continues

Il y a plusieurs définitions équivalentes des fonctions quasi-périodiques, dont la suivante qui est due à Harald Bohr [26] :

Définition :

Une fonction continue $f : \mathbb{R} \longmapsto \mathbb{R}$ est dite quasi-périodique si

$$\forall \varepsilon > 0, \ \exists l_\varepsilon > 0 \quad \text{tel que tout intervalle de longueur } l_\varepsilon \text{ contient un réel } a \text{ vérifiant } \sup_{x \in \mathbb{R}} | \, f(x) - f(x+a) \, | \leq \varepsilon \tag{1}$$

Les nombres a sont appelés **quasi-périodes** de f, attachées à ε et l_ε **longueur d'inclusion**. Il faut noter que toute fonction périodique vérifie trivialement cette condition, ses quasi-périodes étant données par les multiples de sa période fondamentale.

Pour fixer les idées, nous montrons dans l'annexe B que la fonction $f(x) = \sin(2\pi x) + \sin(2\pi\tau x)$ $\Big($où τ est le nombre d'or $\tau = \dfrac{1+\sqrt{5}}{2} = 1 + \cos\dfrac{2\pi}{5}\Big)$ est quasi-périodique sur $\mathbb{R}$.

Plus généralement, on peut montrer que tout polynôme trigonométrique est une fonction quasi-périodique continue. Par ailleurs, on peut montrer [17][26] qu'une fonction f quasi-périodique au sens de Bohr est limite uniforme d'une suite de polynômes trigonométriques : soit P_h un polynôme trigonométrique de degré $r_h \in \mathbb{N}_*$ défini pour $x_j^h \in \mathbb{R}$ et $\upsilon_j^h \in \mathbb{R}$ par :

$$P_h(y) = \sum_{j=1}^{r_h} x_j^h e^{i\upsilon_j^h \, y} \tag{4}$$

Alors

$$\lim_{h \to \infty} \| P_h(y) - f(y) \|_\infty = 0$$

De plus, les fonctions quasi-périodiques au sens de Bohr sont uniformément continues sur $\mathbb{R}$. En effet, se donnant un réel ε et sa longueur d'inclusion l_ε associée (4), soient deux réels t_1 et t_2 tels que $\mid t_1 - t_2 \mid < l_\varepsilon$. Ils appartiennent à un même intervalle $[\gamma\ ,\ \gamma + l_\varepsilon]$ qui contient une presque période a_ε. Par conséquent, $t_1 - a_\varepsilon$ et $t_2 - a_\varepsilon$ appartiennent à un même intervalle $[-l_\varepsilon\ ,\ l_\varepsilon]$ dans lequel $f(x)$ est uniformément continue. On peut donc trouver un nombre d_ε tel que, si $\mid (t_1 - \tau) - (t_2 - \tau) \mid\ = \mid t_1 - t_2 \mid\ < d_\varepsilon$, on ait $\mid f(t_1 - \tau) - f(t_2 - \tau) \mid < \dfrac{\varepsilon}{3}$. De la continuité de f, on déduit que :

$$\mid f(t_1) - f(t_2) \mid \leq \mid f(t_1) - f(t_1 - \tau) \mid + \mid f(t_1 - \tau) - f(t_2 - \tau) \mid + \mid f(t_2 - \tau) - f(t_2) \mid < \varepsilon$$

4.3.2 Fonctions quasi-périodiques mesurables

L'inconvénient de la notion de quasi-périodicité au sens de Bohr est qu'elle exclut les fonctions constantes par morceaux, qui apparaissent naturellement dans les structures cristallines (en particulier les multi-couches fabriqués avec la suite de fibonacci). Il existe plusieurs généralisations (dues à Besicovitch, Stepanoff et Weyl) de la définition de fonction quasi-périodique continue aux fonctions présentant des discontinuités. Dans chacune de ces généralisations, l'ensemble des fonctions quasi-périodiques est donné par l'adhérence de l'ensemble des polynômes trigonométriques pour une norme donnée. L'argument de densité invoqué dans chacune de ces généralisations utilise de manière essentielle l'existence d'une fonctionnelle linéaire L (appelée moyenne ergodique) sur l'ensemble des fonctions quasi-périodiques au sens de Bohr :

$$L(f) = \lim_{T \to +\infty} \frac{1}{2T} \int_{-T}^{T} f(y)\, dy$$

On peut structurer l'espace des fonctions quasi-périodiques au sens de Bohr (1)en espace vectoriel normé non plus avec la norme de la convergence uniforme, mais en posant :

$$\|f(y)\|_p = \left(L(\mid f(y) \mid^p) \right)^{\frac{1}{p}} \qquad (*)$$

Définition :

Pour tout $p \geq 1$, on note $B^p(\mathbb{R}, \mathbb{R})$ (espace de Besicovitch) le complété des fonctions quasi-périodiques au sens de Bohr (ou bien des polynômes trigonométriques) pour la norme $\| \cdot \|_p$.

Remarque :

Il est important de noter que les éléments de B^p sont des fonctions mesurables mais non continues *a priori* (il existe des suites de fonctions quasi-périodiques continues qui sont de Cauchy pour la norne de L^p, dont la limite n'est pas quasi-périodique continue).

Propriétés :

1) Il est facile de vérifier que la forme linéaire L se prolonge de manière unique en un élément du dual de B^p et que la formule $(*)$ est encore vraie pour tout élément de B^p.

2) Pour tout $1 < p < +\infty$, B^p est un Banach réflexif. Pour $p = 2$, le produit scalaire défini par :

$$\forall (f,g) \in B^2 \times B^2 \ , \ (f,g) = L(f\bar{g})$$

associé la norme quadratique, procure à B^2 une structure d'espace de Hilbert (Besicovitch, 1932 [23], Braides, 1990 [40]).

Plus généralement, si $(X, \|\cdot\|)$ est un espace de Banach complexe, on dit qu'une fonction mesurable $f : \mathbb{R}^n \longmapsto X$ est (Besicovitch) quasi-périodique, et on note $f \in B^p(\mathbb{R}^n, X)$, s'il existe une suite de polynômes trigonométriques P_h (du type (4)) telle que :

$$\lim_{h\to\infty} L(\|P_h(y) - f(y)\|^p) = 0 \tag{5}$$

L'espace $B^p(\mathbb{R}^n, X)$ est alors muni de la norme suivante :

$$\|f(y)\|_p = \left(L(\|f(y)\|^p) \right)^{\frac{1}{p}}$$

4.3.3 Suites quasi-périodiques

On cherche maintenant à étendre la notion de quasi-périodicité aux suites numériques. On pense en premier lieu à définir une suite quasi-périodique à partir d'une fonction quasi-périodique f sur $\mathbb{R}$ telle que $f(n) = u_n$, $\forall n \in \mathbf{Z}$. Une suite $(x_n)_{n\in\mathbf{Z}}$ de nombres réels est alors quasi-périodique si $\forall \varepsilon > 0$ il existe un entier N tel que parmi N entiers consécutifs, on puisse trouver un entier a tel que :

$$\sup_{n\in\mathbf{Z}} | \ x_n - x_{n+a} \ | \leq \varepsilon$$

On note alors qu'une suite quasi-périodique prenant un nombre fini de valeurs ne satisfait pas ce critère. En particulier, la suite de Fibonacci ne rentre pas dans ce cadre. Un critère moins restrictif de quasi-périodicité pour une suite (u_n) est alors d'exiger que pour tout couple $(l,n) \in \mathbf{Z} \times \mathbb{N}_*$, il existe un entier $N > 0$ tel que

$$\forall k \in \mathbf{Z} \ , \ \exists i \in [k; k+N] \ \text{ tel que } \ x_{l+j} = x_{i+j} \ , \ \forall j \in \{0, ..., n-1\}$$

Une autre manière d'exprimer ce critère de quasi-périodicité est de raisonner en terme d'alphabet : la suite de Fibonacci peut par exemple être générée par la succession de deux lettres A et B :

$$u_0 = A, u_1 = AB, u_2 = ABA, u_3 = ABAAB, u_4 = ABAABABA...$$

Les mots de l'alphabet sont les ensembles de lettres générées par u_i, $\forall i \in \{1, ..., n\}$. Le critère se reformule alors de la manière suivante : la suite (u_n) est quasi-périodique si pour tout mot de (u_n), l'espace séparant ses différentes répliques est borné. On montre que (u_n) vérifie bien ce critère. On remarquera l'absence d'une succession AA où BBB : on définit ainsi une grammaire pour l'alphabet associé à (u_n). On retrouve cette propriété dans les règles de sélection permettant de générer un pavage de Penrose.

Dans la pratique quotidienne des quasi-cristaux, le physicien a, en fait, accès à la donnée d'une succession quasi-périodique de deux couches d'indices optiques différents dont le rapport des épaisseurs est τ. Ce pavage de Penrose uni-dimensionnel appelé empilement multi-couches est généré à partir de la séquence précédente (ou A et B désignent les couches d'épaisseurs a et τa). Par ailleurs, on peut définir la position de la nième couche par rapport à une origine par la relation :

$$x_n = na + \frac{a}{\tau} E(\frac{n}{\tau})$$

$E(x)$ désignant la partie entière de $x \in \mathbb{R}$. On note de plus que la structure quasi-périodique est générée par une procédure itérative dite de **déflation** : Une couche épaisse A est transformée en une couche épaisse et une couche mince AB. Si la séquence d'itérations commence par une couche épaisse, la succession de couches sera alors $ABAABABAA$.... Par déflation de cet empilement infini, on obtiendra le même empilement constitué de couches plus petites, i.e. la structure obtenue est invariante par un changement d'échelle donné (auto-similarité).

4.3.4 Fonctions quasi-périodiques type coupe et projection

Les résultats d'homogénéisation connus dans le cas de milieux quasi-périodiques (cf. [122][124][169][41][40]) font, en fait, toujours référence à un tenseur effectif dont les composantes sont obtenues en considérant des limites de problèmes élémentaires sur des cubes dont la dimension tend vers l'infini. Autrement dit, l'existence d'un tenseur homogénéisé est établie de façon abstraite en utilisant des résultats de type ergodique, mais le calcul effectif de ce tenseur n'est pas réalisable en pratique.

Ici, nous utilisons la structure particulière des fonctions quasi-périodiques au sens de Besicovitch (à valeurs dans $X = \mathbb{C}$ ou $X = \mathbb{C}^3$) déduites par **coupe-projection** d'une fonction périodique dans $\mathbb{R}^m$ $(m > n)$, pour tenter de ramener toute notre analyse asymptotique à la cellule élémentaire $Y^m =]0;1[^m$. Pour fixer les idées, nous allons d'abord commencer par l'exemple le plus élémentaire de fonctions quasi-périodiques au sens de Besicovitch, savoir les fonctions de $\mathbb{R}$ dans $\mathbb{C}$ pour lesquelles la dimension de périodicité vaut 2. Suivant Duneau et Katz [66][67], cette classe particulière de fonctions quasi-périodiques peut être générée de la manière suivante : Soit $\mathbb{Z}^2$ le maillage de $\mathbb{R}^2$ et (O, z_1, z_2) le repère qui lui est attaché. Pour ce faire, on considère le repère (O, e_1, e_2) déduit de (O, z_1, z_2) par une rotation d'angle Φ (cf. 3.6). Soient alors $E_\parallel$ et $E_\perp$ deux sous-espaces orthogonaux de dimension 1 de $\mathbb{R}^2$ représentés par les droites portées par les vecteurs e_1 et e_2. L'ensemble dénombrable des points de $\mathbb{Z}^2$ peut-être projeté orthogonalement sur la droite $E_\parallel$. Quand la pente $\alpha = \tan\Phi$ de $E_\parallel$ est rationnelle, la projection des points de $\mathbb{Z}^2$ est un ensemble discret de points répartis périodiquement sur $E_\parallel$. En revanche, si la pente α est irrationnelle la projection des points de $\mathbb{Z}^2$ est un ensemble de points qui est dense dans $E_\parallel$. Si l'on veut subdiviser la droite $E_\parallel$ en intervalles de mesures non nulles, il faut alors restreindre la projection aux points de $\mathbb{Z}^2$ dont la distance à la droite $E_\parallel$ est inférieure à une valeur donnée. On considère alors une cellule unitaire Y^2 (appelée fenêtre de sélection) que l'on translate suivant la direction du vecteur e_1, et on obtient une bande B qui contient les points de $\mathbb{Z}^2$ dont la distance à la droite $E_\parallel$ est inférieure à $\frac{1}{2}$. Les projections orthogonales

des points de $B \cap \mathbb{Z}^2$ sur $E_\parallel$ génèrent alors une suite quasi-périodique de deux types de segments dont le rapport des longueurs vaut α^{-1}. Par ailleurs, la projection orthogonale de $\mathbb{Z}^2$ sur $E_\parallel$ étant dense si la pente α de $E_\parallel$ est irrationnelle, il est clair qu'il y a une infinité de translations de $\mathbb{Z}^2$ dont les points contenus dans la bande de coupe-projection B peuvent être projetés sur $E_\parallel$. On a donc une infinité de copies du pavage initial de $E_\parallel$. On en déduit une propriété importante des pavages quasi-périodiques issus d'une coupe-projection baptisée "isomorphisme local" par Duneau et Katz dans [66][67] : toute partie finie d'un tel pavage apparaît une infinité de fois dans tout pavage défini par une bande avec la même pente irrationnelle. On ne peut donc pas différentier deux pavages de Penrose par une quelconque de leur parties finies : on parle alors de *classes d'équivalence* des pavages de Penrose. Nous reviendrons sur ce point fondamental un peu plus loin. En pratique, cela signifie que si l'on se donne une structure quasi-cristalline, il n'y a pas unicité de la matrice de relèvement. On verra dans la suite que cela n'induit pas d'ambiguïté sur le calcul de la structure équivalente à la limite des grandes longueurs d'onde. On génère ainsi une fonction f_α quasi-périodique dans $\mathbb{R}$ par coupe-projection à partir d'une fonction $f(y,z)$ $]0;1[\times]0;1[$-périodique dans $\mathbb{R}^2$ par :

$$f_\alpha(y) = f(y, \alpha y) \ .$$

On généralise sans peine ce procédé à des fonctions quasi-périodiques

$$f_{\alpha_{m-1}}(y) = f(y, \alpha_1 y, \alpha_2 y, ..., \alpha_{m-1} y) \ ,$$

où les irrationnels α_i vérifient la condition $\dfrac{\alpha_i}{\alpha_j} \notin \mathbb{Q}$, $\forall i \neq j$. Ces fonctions quasi-périodiques sur $\mathbb{R}$ sont alors issues de la coupe-projection d'une fonction périodique dans $\mathbb{R}^m$ avec $m > 1$. On montre que la classe de telles fonctions quasi-périodiques est alors dense dans les fonctions quasi-périodiques sur $\mathbb{R}$: appelant spectre de f l'ensemble

$$\sigma(f) = \{\omega \in \mathbb{R} \ , \ L(f(y)e^{-i\omega y}) \neq 0\} \ ,$$

[3] H. Bohr a en effet remarqué que $\sigma(f)$ était un ensemble dénombrable (fini ou non). Notant alors ω_k les valeurs discrètes de ω, il a démontré une formule de Plancherel généralisée aux

3. Il existe un opérateur linéaire continu P dont les $e^{-i\omega_k y}$ sont les fonctions propres et les x_k les valeurs propres associées. En effet, définissant la convolution en moyenne sur les fonctions quasi-périodiques continues comme $h(y) = f * g(y) = L(f(y-s)g(s))$, l'opérateur P défini par $Pg = f * g$ est un endomorphisme sur les fonctions quasi-périodiques continues. La continuité de P résulte de la majoration suivante :

$$\|Pg\|_\infty = \sup_{s\in\mathbb{R}} \mid h(s) \mid \leq \sup_{s\in\mathbb{R}} \mid f(s) \mid \sup_{s\in\mathbb{R}} \mid g(s) \mid = \|f\|_\infty \|g\|_\infty$$

Par ailleurs, l'opérateur linéaire P admet pour fonctions propres des exponentielles $e^{i\omega y}$:

$$L(f(y-s)e^{i\omega s}) = L(f(s)e^{i\omega(y-s)}) = e^{i\omega y} L(f(s)e^{-i\omega s})$$

On note alors que $L(f(s)e^{-i\omega s})$ est nul sauf pour $w = w_k \in \sigma(f)$; auquel cas $x_k = L(f(s)e^{-i\omega_k s})$ est le coefficient de Fourier-Bohr correspondant. On a donc

$$P(e^{i\omega_k s}) = x_k e^{i\omega_k s}$$

fonctions quasi-périodiques continues [27] :

$$L(\mid f \mid^2) = \sum_{k=1}^{\infty} \mid x_k \mid^2 ,$$

où les $x_k = L(f(y)e^{-i\omega_k y})$ sont appelés coefficients de Fourier-Bohr et les ω_k les pulsations propres de la fonction f quasi-périodique continue. Dans le cas particulier des fonctions quasi-périodiques issues d'une coupe-projection, les ω_k sont générés par un nombre fini de pulsations incommensurables. En d'autres termes, pour ces fonctions quasi-périodiques, pour tout entier k il existe un nombre fini de réels incommensurables $\tilde{\omega}_1, \tilde{\omega}_2, ..., \tilde{\omega}_m$ et un nombre fini d'entiers $l(1,k), l(2,k), ..., l(m,k)$ tels que :

$$\omega_k = \sum_{j=1}^{m} l(j,k)\tilde{\omega}_j .$$

La fonction quasi-périodique $f_1(y) = \sin(2\pi y) + \sin(2\tau\pi y)$ est par exemple issue d'une coupe projection de la fonction $\tilde{f}_1(y,z) = \sin y + \sin z$ périodique dans $\mathbb{R}^2$. Au contraire, la fonction quasi-périodique $f_2(y) = \sum_{k\in\mathbf{Z}} \frac{e^{i\sqrt{2\pi|k|}y}}{1+k^2}$ n'est issue d'aucune coupe projection. On peut étendre les résultats précédents aux fonctions quasi-périodiques de $\mathbb{R}^n$ dans X espace de Banach, issues d'une **coupe-projection généralisée** dans $\mathbb{R}^m$ avec $m > n$. On génère ainsi une fonction f_R quasi-périodique dans $\mathbb{R}^n$ par coupe-projection à partir d'une fonction $f(y_1, ..., y_m)$ Y^m-périodique dans $\mathbb{R}^m$ par :

$$f_R(y_1, ..., y_n) = f(R(y_1, ..., y_n))$$

où R est une matrice à m lignes et n colonnes satisfaisant la condition $R^t k \neq 0$, $\forall k \in \mathbf{Z}^m \backslash \{0\}$. On étend la formule de Plancherel généralisée précédente au complété $B^2(\mathbb{R}^n, X)$ des fonctions quasi-périodiques continues de $\mathbb{R}^n$ dans X (identité de Besicovitch qui est à rapprocher de (5) pour $p = 2$) :

$$\lim_{T\to\infty} \frac{1}{(2T)^n} \int_{|y|\leq T} \|f(y)\|^2 \, d\xi = \sum_{k=1}^{\infty} \|x_k\|^2 ,$$

où $f(y) = \sum_{k=1}^{\infty} x_k e^{i\omega_k y}$, $x_k \in X$ et $\omega_k \in \mathbb{R}^n$.

On montre que l'espace des fonctions coupe-projection f_R, est alors dense dans $B^2(\mathbb{R}^n, X)$ pour la norme quadratique, à l'aide de l'identité de Besicovitch.

4.3.5 Méthode de coupe et projection

Ces résultats sont à la base de la méthode de coupe-projection généralisée initialement et indépendemment proposée par plusieurs auteurs dont M. Duneau et A. Katz [66][67]. La séquence de Fibonacci est ainsi la coupe d'une structure périodique dans $\mathbb{R}^2$ suivant une droite de pente τ^{-1}. Son équivalent bi-dimensionnel, le pavage de Penrose, est la coupe d'une structure périodique dans $\mathbb{R}^4$ ou $\mathbb{R}^5$. En ce qui concerne les phases quasi-cristallines

icosaédrique-rhomboédrique de l'alliage $Al_{63.5}Fe_{12.5}Cu_{24}$ (cf. [153]), elles sont issues d'une coupe-projection dans $\mathbb{R}^6$ d'un réseau cubique (certains auteurs en donnent aussi une coupe-projection dans $\mathbb{R}^{12}$).

Par analogie au cas uni-dimensionnel, on considère ainsi $E_\parallel$ le sous-espace dans lequel est définie la phase icosaédrique et $E_\perp$ son sous-espace orthogonal dans $\mathbb{R}^6$:

$$\mathbb{R}^6 = E_\parallel \oplus E_\perp$$

Soient $X = (X_1, ..., X_6)$ un point de $\mathbb{R}^6$ et $x_\parallel = (x_1, x_2, x_3)$ (resp. $x_\perp = (x_4, x_5, x_6)$) un point de $E_\parallel = \mathbb{R}^3$ (resp. $E_\perp$). La matrice de projection orthogonale M_τ qui conduit à la phase icosaédrique est alors définie par une opération de rotation qui fait passer du repère lié au réseau cubique à celui attaché aux sous-espaces orthogonaux $E_\parallel$ et $E_\perp$:

$$(x_\parallel, x_\perp) = M_\tau(X)$$

$$\text{avec } M_\tau = \frac{1}{\sqrt{2(\tau+2)}} \begin{pmatrix} 1 & \tau & 0 & -1 & \tau & 0 \\ \tau & 0 & 1 & \tau & 0 & -1 \\ 0 & 1 & \tau & 0 & -1 & \tau \\ -\tau & 1 & 0 & \tau & 1 & 0 \\ 1 & 0 & -\tau & 1 & 0 & \tau \\ 0 & -\tau & 1 & 0 & \tau & 1 \end{pmatrix} \text{ où } \tau = \frac{1+\sqrt{5}}{2}$$

On vérifie trivialement que la matrice M_τ est bien orthogonale, un de ses pseudo-inverses à droite étant donné par sa transposée. Par ailleurs, la phase icosaédrique est donnée en pratique par la projection des points de $\mathbb{Z}^6$ dans $E_\parallel = \mathbb{R}^3$ associée à la matrice P_τ suivante :

$$P_\tau = \frac{1}{\sqrt{2(\tau+2)}} \begin{pmatrix} 1 & \tau & 0 & -1 & \tau & 0 \\ \tau & 0 & 1 & \tau & 0 & -1 \\ 0 & 1 & \tau & 0 & -1 & \tau \end{pmatrix}$$

Notant que $\tau^2 = 1 + \tau$, la matrice R_τ ci-dessous est l'un des pseudo-inverses à droite de P_τ :

$$R_\tau = \frac{1}{\sqrt{2(\tau+2)}} \begin{pmatrix} 1 & \tau & 0 \\ \tau & 0 & 1 \\ 0 & 1 & \tau \\ -1 & \tau & 0 \\ \tau & 0 & -1 \\ 0 & -1 & \tau \end{pmatrix}$$

Noter que la matrice M_τ étant de rang 3, le choix de P_τ est arbitraire. On doit donc en toute rigueur définir une classe d'équivalence de matrices de projection P_τ, donc de matrices R_τ. Cette ambiguïté apparaît clairement comme une conséquence du choix arbitraire des vecteurs de base de $E_\parallel$ dans la construction de la matrice M_τ (à rapprocher de la propriété d'*isomorphisme local* des pavages apériodiques, dont parlent M. Duneau et A. Katz). Le quasi-cristal mono-dimensionnel est le seul qui échappe à cette règle : en dimension supérieure à un, les vecteurs d'une base de $\mathbb{R}^n$ sont déterminés à $\frac{n!}{2}$ rotations près.

Dans la suite, nous n'aurons besoin, en fait, que de la donnée de la matrice R_τ, dite matrice de relèvement. En effet, dans la pratique, grâce à des considérations de symétries sur des clichés de diffraction en rayon X (pseudo-réseau réciproque), le physicien a accès aux caractéristiques opto-géométriques d'une phase quasi-cristalline, autrement dit, à la donnée de la matrice de relèvement. La matrice de permittivité de l'alliage $Al_{63.5}Fe_{12.5}Cu_{24}$ se met ainsi sous la forme :

$$\begin{aligned}\varepsilon(x_1,x_2,x_3) &= \varepsilon_\sharp(X_1,X_2,X_3,X_4,X_5,X_6) = \varepsilon_\sharp(R_\tau(x_1,x_2,x_3))\\ &= \varepsilon_\sharp(n_\tau(x_1+\tau x_2), n_\tau(\tau x_1+x_3), n_\tau(x_2+\tau x_3),\\ &\quad n_\tau(-x_1+\tau x_2), n_\tau(\tau x_1-x_3), n_\tau(-x_2+\tau x_3))\end{aligned}$$

où n_τ est la constante de normalisation $\dfrac{1}{\sqrt{2(2+\tau)}}$ et $\varepsilon_\sharp \in L^\infty_\sharp(Y^6)$.

Remarque :

Il s'avère que de nouveau, il peut y avoir une ambiguïté. Par exemple, dans le cas de l'alliage $Al_{63.5}Fe_{12.5}Cu_{24}$, on note que l'on peut aussi définir la permittivité à partir d'une coupe-projection de $\mathbb{R}^{12}$ dans $\mathbb{R}^3$ (cf. [66][67]) :

$$\varepsilon(x_1,x_2,x_3) = \varepsilon_\sharp(R_\tau(x_1,x_2,x_3)) = \varepsilon'_\sharp(R'_\tau(x_1,x_2,x_3))$$

où R'_τ est une matrice à 12 lignes et 3 colonnes et $\varepsilon'_\sharp \in L^\infty_\sharp(Y^{12})$. Nous verrons dans la section suivante que le résultat d'analyse limite est, en fait, indépendant de la matrice de relèvement R_τ, pourvu qu'elle soit du type "coupe-projection" i.e. $R_\tau^T k \neq 0\ ,\ \forall k \in \mathbb{Z}^m\backslash\{0\}$.

Dans la section suivante, nous allons définir une notion de convergence adaptée aux fonctions oscillantes quasi-périodiques, issues d'une telle coupe-projection.

4.4 Convergence à deux échelles coupe-projection

4.4.1 Remarques préliminaires

Il est facile de vérifier que des produits de fonctions trigonométriques dont les rapports de périodes sont irrationnels ont des moyennes ergodiques décorrelées i.e. que la moyenne ergodique du produit de telles fonctions soit le produit de leurs moyennes ergodiques. Plus généralement, on établit le résultat suivant :

Lemme 0

*Soient f et g des polynômes trigonométriques 1-périodiques sur un ouvert borné Ω de $\mathbb{R}$. Pour tout irrationnel $\alpha > 0$, on a alors la convergence suivante dans $L^\infty(\Omega)$ *-faible :*

$$f(nx)g(n\alpha x) \overset{*}{\rightharpoonup} \Big(\int_0^1 f(y)\,dy\Big)\Big(\int_0^1 g(y)\,dy\Big)$$

Remarque :

On généralise sans peine le résultat précédent à des polynômes trigonométriques f_1, f_2, ..., f_k 1-périodiques et des irrationnels α_1, α_2,..., $\alpha_k > 0$ tels que $\dfrac{\alpha_i}{\alpha_j} \in \mathbb{R}_*^+ \setminus \mathbb{Q}$, $\forall i \neq j$. On a alors :

$$f_1(n\alpha_1 x) f_2(n\alpha_2 x) ... f_k(n\alpha_k x) \overset{*}{\rightharpoonup} \Big(\int_0^1 f_1(y)\, dy\Big)\Big(\int_0^1 f_2(y)\, dy\Big) ... \Big(\int_0^1 f_k(y)\, dy\Big)$$

Démonstration :

On considère des fonctions f et g de type polynômes trigonométriques en y :

$$f(y) = \sum_{\substack{k\in\mathbb{Z} \\ |k|\leq k_0}} f_k e^{2i\pi k y} \text{ et } \; g(y) = \sum_{\substack{l\in\mathbb{Z} \\ |l|\leq l_0}} g_l e^{2i\pi l y}$$

Le produit $f(y)g(\alpha y)$ s'écrit dans ce cas :

$$f(y)g(\alpha y) = \sum_{\substack{l\in\mathbb{Z} \\ |l|\leq l_0}} \sum_{\substack{k\in\mathbb{Z} \\ |k|\leq k_0}} f_k g_l e^{2i\pi y(k+\alpha l)}$$

La suite $f(nx)g(\alpha nx)$ bornée dans $L^\infty(\Omega)$ admet donc au moins une valeur d'adhérence pour la topologie $*$-faible. Il suffit de montrer que celle-ci est unique et coïncide avec la constante $= f_0 g_0 = \Big(\int_0^1 f(y)\, dy\Big)\Big(\int_0^1 g(y)\, dy\Big)$. Pour cela, il est suffisant de prouver la convergence suivante :

$$\lim_{n\to+\infty} \int_a^b f(nx)g(nx)\, dx = f_0 g_0 (b-a)$$

pour tout intervalle $]a;b[\subset \Omega$. Quitte à effectuer le changement de variable $x \longmapsto \dfrac{x-a}{b-a}$ on se ramène à faire le calcul sur un intervalle ouvert $\Omega =]0;1[$. On obtient :

$$\int_0^1 f(nx)g(\alpha nx)\, dx = \frac{1}{n}\int_0^n f(y)g(\alpha y) dy = \sum_{\substack{l\in\mathbb{Z} \\ |l|\leq l_0}} \sum_{\substack{k\in\mathbb{Z} \\ |k|\leq k_0}} \frac{1}{n}\int_0^n f_k g_l e^{2i\pi y(k+\alpha l)}\, dy \qquad (P1)$$

Notant alors *sinc* la fonction sinus cardinal définie par $sinc(x) = \dfrac{\sin(\pi x)}{\pi x}$ sur $\mathbb{R}_*$ et prolongée par continuité à 1 à l'origine, on obtient :

$$\begin{aligned} \lim_{n\to+\infty} \frac{1}{n}\int_0^n e^{2i\pi y(k+\alpha l)}\, dy &= \lim_{n\to+\infty} \frac{1}{n}\frac{1}{2i\pi(k+\alpha l)}\Big[e^{2i\pi y(k+\alpha l)}\Big]_0^n \\ &= \lim_{n\to+\infty} e^{i\pi(k+\alpha l)n} sinc((k+\alpha l)n) \end{aligned}$$

Par ailleurs, si $\alpha \in \mathbb{R}_*^+ \setminus \mathbb{Q}$, nous sommes assurés que $k+\alpha l \neq 0$, $\forall (k,l) \in \mathbb{Z}\times\mathbb{Z}\setminus\{0,0\}$. Il s'ensuit que :

$$\lim_{n\to+\infty} \frac{1}{n}\int_0^n e^{2i\pi y(k+\alpha l)}\, dy = \delta_k^0 \delta_l^0 \qquad (P2)$$

où $\delta_i^j = 1$ si $i = j$ et 0 sinon. De $(P1)$ et $(P2)$, on tire alors que :

$$\begin{aligned}\lim_{n\to+\infty}\int_0^1 f(nx)g(\alpha nx)\,dx &= \lim_{n\to+\infty}\sum_{\substack{l\in\mathbf{Z}\\|l|\le l_0}}\sum_{\substack{k\in\mathbf{Z}\\|k|\le k_0}}\frac{1}{n}\int_0^n f_k g_l e^{2i\pi y(k+\alpha l)}\,dy\\ &= \sum_{\substack{l\in\mathbf{Z}\\|l|\le l_0}}\sum_{\substack{k\in\mathbf{Z}\\|k|\le k_0}} f_k g_l\Big(\lim_{n\to+\infty}\frac{1}{n}\int_0^n e^{2i\pi y(k+\alpha l)}\,dy\Big)\\ &= f_0 g_0\end{aligned}$$

4.4.2 Définitions et propriétés

Dans une première étape, il nous faut adapter les techniques double-échelle introduites dans [2]. Nous introduisons alors un concept de convergence à deux échelles coupe-projection relativement à une matrice R pseudo inverse à droite d'une matrice de coupe projection P de $\mathbb{R}^m$ dans $\mathbb{R}^n$. Dans toute la suite, R sera donc une matrice à m lignes et n colonnes $(m > n)$. Par analogie au cas classique [2], notre objectif est d'approcher une suite oscillante $u_\eta(x)$ par une suite de fonctions pseudo-périodiques de la forme $u_0(x, \frac{R(x)}{\eta})$ où $u_0(x,.)$ est périodique sur $\mathbb{R}^m$ de période η. Au préalable, nous devons nous assurer que si g est un polynôme trigonométrique, alors la fonction quasi-périodique $f = g \circ R$ de moyenne $[g]$, admet $[g]$ comme moyenne ergodique i.e. :

$$L(f) = \lim_{T\to+\infty}\frac{1}{(2T)^n}\int_{]-T;T[^n} f(x)\,dx = [g] \qquad (*)$$

Dans la section précédente, nous avons remarqué par ailleurs que la matrice de relèvement n'était pas unique. On lève cette ambiguïté en notant que la propriété $(*)$ est en fait indépendante, pour P donné, du choix du pseudo-inverse R tant que R vérifie la condition :

$$R^T k \neq 0\ ,\ \forall k \in \mathbf{Z}^m \setminus \{0\} \qquad (0)$$

En effet, on a :

Lemme 1

Soit $R : \mathbb{R}^n \longmapsto \mathbb{R}^m$ $(m \geq n)$ telle que (0) est vérifiée. Alors, $(*)$ est satisfaite pour tout g polynôme trigonométrique sur $\mathbb{R}^m$.

Preuve :

Soit g un polynôme trigonométrique sur $\mathbb{R}^m$ défini pour tout k multi-indice dans $\mathbf{Z}^m$ par :

$$\forall y \in \mathbb{R}^m\ ,\ g(y) = \sum_{|k|\le k_0} C_k e^{2i\pi k\cdot y}$$

Notant que pour tout $k \in \mathbf{Z}^m$ et pour tout $x \in \mathbb{R}^n$, on a :

$$\begin{aligned}L(e^{2i\pi k\cdot R(x)}) &= \lim_{T\to+\infty}\frac{1}{(2T)^n}\int_{]-T;T[^n} e^{2i\pi k\cdot R(x)}\,dx\\ &= \lim_{T\to+\infty}\prod_{j=1}^n\frac{1}{(2T)}\frac{1}{2i\pi k_l R_{lj}}\Big[e^{2i\pi(k_l R_{lj}x_j)}\Big]_{-T}^{T}\\ &= \lim_{T\to+\infty}\prod_{j=1}^n sinc(2k_l R_{lj}T)\end{aligned}$$

où la fonction sinus cardinal est définie par $sinc(x) = \dfrac{\sin(\pi x)}{\pi x}$ sur $\mathbb{R}_*$ et prolongée par continuité à 1 à l'origine. Sous la condition (0), on a clairement $L(e^{2i\pi k\cdot R(x)}) = 0$, $\forall k \in \mathbb{Z}^m \setminus \{0\}$, ce qui implique que :

$$L(f) = \sum_{|k|\leq k_0} C_k L(e^{2i\pi k\cdot R(x)}) = C_0 L(1) = [g]$$

(QED)

Ce résultat nous conduit à définir une notion de convergence faible à deux-échelles relativement à une matrice de relèvement R telle que $R^t k \neq 0$, $\forall k \in \mathbb{Z}^m \setminus \{0\}$:

Définition :

On dit que la suite (u_η) converge à deux échelles relativement à R vers la fonction $u_0 \in L^2(\Omega \times Y^m)$ si :

$$\forall \varphi \in \mathcal{D}(\Omega; C^\infty_\sharp(Y^m)) \ , \ \lim_{\eta\to+\infty} \int_\Omega u_\eta(x)\varphi(x, \frac{R(x)}{\eta})\, dx = \iint_{\Omega\times Y^m} u_0(x,y)\varphi(x,y)\, dxdy \quad (1)$$

ce que l'on notera $u_\eta \overset{R}{\searrow} u_0$.

Nous sommes maintenant en mesure d'établir l'existence de telles limites lorsque la suite (u_η) est bornée dans $L^2(\Omega)$.

Proposition 2

Soit R une matrice satisfaisant l'hypothèse (0). *Soit Ω un ouvert borné de $\mathbb{R}^n$, $Y^m =]0;1[^m$ et (u_η) une suite bornée dans $L^2(\Omega)$. Alors $\exists \eta_k$ suite tendant vers 0 et $\exists u_0(x,y) \in L^2(\Omega \times Y^m)$ (Y^m-périodique en y) tels que $u_{\eta_k} \overset{R}{\searrow} u_0$.*

Remarques

1) Soient α un irrationnel > 0, Ω un ouvert borné de $\mathbb{R}^N$ et $Y^N =]0;1[^N$. Désignant par R la matrice qui à tout vecteur x de $\mathbb{R}^N$ associe le vecteur $R(x) = (x, \alpha x)$ de $\mathbb{R}^N \times \mathbb{R}^N$, on déduit de la proposition 2 le résultat suivant :

Soit (u_η) une suite bornée dans $L^2(\Omega)$. Alors $\exists \eta_k$ suite tendant vers 0 et $\exists u_0(x,y,z) \in L^2(\Omega \times Y^N \times Y^N)$ (Y^N-périodique en y et en z) tels que $\forall \varphi \in \mathcal{D}(\Omega; (C^\infty_\sharp(Y^N))^2)$,

$$\lim_{k\to+\infty} \int_\Omega u_{\eta_k}(x)\varphi(x, \frac{x}{\eta_k}, \alpha\frac{x}{\eta_k})\, dx = \iiint_{\Omega\times Y^N\times Y^N} u_0(x,y,z)\varphi(x,y,z)\, dxdydz$$

En effet, α étant irrationnel, on a $R^t(m,n) = m + \alpha\, n \neq 0, \forall\ (m,n) \in \mathbb{Z}^N \times \mathbb{Z}^N \setminus \{0,0\}$.

2) Il est important de noter que le théorème est faux si il existe $k \in \mathbb{Z}^m \setminus \{0\}$ tel que $R^t k = 0$. En effet, dans 1), prenons la suite constante $u_\eta = 1$ et par exemple $\alpha = \dfrac{q}{p}, p \in \mathbb{N}^*$ et $q \in \mathbb{N}$. Alors, $\forall \varphi \in \mathcal{D}(\Omega; (C^\infty_\sharp(Y^N))^2)$

$$\lim_{\eta\to 0} \int_\Omega \varphi(x, \frac{R(x)}{\eta})\, dx = \frac{1}{q^N} \int_\Omega \Big(\int_{q\, Y^N} \varphi(x,y,\frac{p}{q}y)\, dy \Big)\, dx = \iiint_{\Omega\times Y^N\times Y^N} \varphi(x,y,z)\ dx\, \mu(dydz)$$

où μ est une mesure portée par la diagonale de $Y^N \times Y^N$ définie par :

$$\forall \Psi \in C(Y^N \times Y^N),\ < \mu, \Psi(y,z) >= \int_{Y^N} \Psi(y, \frac{py}{q})\, dy$$

Clairement, il n'existe pas de fonction $u_0(x,y,z)$ telle que

$$\lim_{\eta\to 0} \int_\Omega \varphi(x, \frac{R(x)}{\eta})\, dx = \iiint_{\Omega\times Y^N\times Y^N} u_0(x,y,z)\varphi(x,y,z)\, dxdydz$$

puisque le second membre de cette égalité est associé à une mesure étrangère à μ.

3) Comme cela sera précisé dans la proposition 5 ci-après, la limite à deux-échelles (coupe-projection) u_0 contient plus d'information qu'une limite L^2-faible classique : la convergence à deux-échelles agit comme un filtre sur certaines oscillations de la suite considérée, qui sont alors restituées dans la limite deux-échelles.

Démonstration

Cette proposition se démontre à l'aide de 2 lemmes préliminaires.

Lemme 3

*Soit R une matrice satisfaisant (0). Soit Ω un ouvert borné de $\mathbb{R}^n$ et $Y^m =]0;1[^m$. Soit $\varphi \in C_\sharp(Y^m))$ et la suite de fonctions φ_η définie par $\varphi_\eta(x) = \varphi(\frac{R(x)}{\eta})$. Alors φ_η converge *-faiblement dans $L^\infty(\Omega)$ vers la fonction constante $[\varphi] := \int_{Y^m} \varphi(y)\, dy$.*

Démonstration du lemme 3

Le résultat est immédiat pour une fonction de type polynôme trigonométrique en y i.e. pour

$$\varphi(R(y)) = \sum_{\substack{k\in\mathbb{Z}^m \\ |k|\le k_0}} C_k e^{2i\pi k\cdot R(y)}$$

En effet, φ_η s'écrit dans ce cas :

$$\varphi_\eta(x) = \varphi(\frac{R(x)}{\eta}) = \sum_{\substack{k\in\mathbb{Z}^m \\ |k|\le k_0}} C_k e^{2i\pi k\cdot \frac{R(x)}{\eta}}$$

Par hypothèse, $R^t k \neq 0, \forall k \in \mathbb{Z}^m \setminus \{0\}$, par conséquent $e^{\frac{2i\pi}{\eta} R^t(k)\cdot x}$ converge faiblement vers 0 pour $k \in \mathbb{Z}^m \setminus \{0\}$. On en déduit que :

$$\forall \Psi(x) \in C(\Omega), \quad \lim_{\eta\to 0} \int_\Omega \varphi_\eta(x)\Psi(x)\, dx = \int_\Omega C_0 \Psi(x)\, dx = \int_\Omega \Psi(x)\, dx \Big(\int_{Y^m} \varphi(y)\, dy \Big)$$

Le cas général s'obtient par approximation : soit $\varphi \in C_\sharp(Y^m)$, $\delta > 0$ et $\tilde\varphi$ un polynôme trigonométrique tel que $\sup_{y\in Y^m} |\, \tilde\varphi - \varphi\, | \le \delta$. Soit $\Psi \in C(\Omega, \mathbb{R}^+)$. Posons $I_\eta = \int_\Omega \varphi_\eta(x)\Psi(x)\, dx$.

Comme $\tilde\varphi$ est un polynôme trigonométrique, il converge vers sa moyenne $[\tilde\varphi] = \int_{Y^m} \tilde\varphi(y)\, dy$. D'où

$$\forall \delta > 0, \quad ([\tilde\varphi] - \delta) \int_\Omega \Psi(x)\, dx \le \liminf_{\eta\to 0} I_\eta \le \limsup_{\eta\to 0} I_\eta \le ([\tilde\varphi] + \delta) \int_\Omega \Psi(x)\, dx$$

Or $|\,[\tilde{\varphi}]-[\varphi]\,| \leq \sup_{y\in Y^m} |\,\tilde{\varphi}-\varphi\,| \leq \delta$, ce qui assure que

$$([\varphi]-2\delta)\int_\Omega \Psi(x)\,dx \leq \liminf_{\eta\to 0} I_\eta \leq \limsup_{\eta\to 0} I_\eta \leq ([\varphi]+2\delta)\int_\Omega \Psi(x)\,dx$$

Ceci étant vrai $\forall\delta$, on en déduit que pour toute fonction continue Ψ positive

$$\lim_{\eta\to 0}\int_\Omega \varphi_\eta \Psi\,dx = [\varphi]\int_\Omega \Psi\,dx$$

La convergence précédente s'étend immédiatement au cas $\Psi \in C(\Omega)$, puis du fait que (φ_η) est bornée dans $L^\infty(\Omega)$, à tout $\Psi \in L^1(\Omega)$.

(QED)

Lemme 4

Soit R une matrice satisfaisant (0) *et* $\varphi \in L^2(\Omega, C_\sharp(Y^m))$
$\Big(i.e.\ \int_\Omega (\sup_{y\in Y^m} |\,\varphi(x,y)\,|)^2\,dx < +\infty\Big)$, *alors :*

$$\lim_{\eta\to 0}\int_\Omega |\,\varphi(x,\frac{R(x)}{\eta})\,|^{\,2}\,dx = \iint_{\Omega\times Y^m} |\,\varphi(x,y)\,|^2\,dxdy \qquad (1')$$

Remarque :

Ce résultat nous conduit à définir de manière analogue à [2] la notion de classes de fonctions admissibles pour la convergence à deux-échelles relativement à une matrice R : $\varphi \in L^2(\Omega, Y\times Y)$ est dite admissible si la suite $\{\varphi(x,\frac{R(x)}{\eta})\}_{\eta\in]0;1[}$ est bornée dans $L^2(\Omega)$ et vérifie $(1')$ pour R satisfaisant (0).

Démonstration du lemme 4

On considère d'abord le cas où φ est de la forme $\varphi(x,y)=\alpha(x)\beta(y)$ où $\alpha(x)\in L^\infty(\Omega)$ et $\beta(y)\in C_\sharp(Y^m)$. Alors β^2 étant une fonction périodique dans $C_\sharp(Y^m)$, on déduit du lemme 1 que $\beta^2((\frac{R(x)}{\eta})) \rightharpoonup [\beta^2]$ faiblement dans $L^1(\Omega)$. Puisque α^2 appartient à $L^\infty(\Omega)$, on peut écrire que :

$$\lim_{\eta\to 0}\int_\Omega \alpha^2(x)\beta^2(\frac{R(x)}{\eta})\,dx = (\int_\Omega \alpha^2(x)\,dx)(\int_{Y^m}\beta^2(y)\,dy)$$

Le théorème de Fubini nous assure alors que :

$$\lim_{\eta\to 0}\int_\Omega |\,\varphi(x,\frac{R(x)}{\eta})\,|^{\,2}\,dx = \iint_{\Omega\times Y^m}\varphi^2(x,y)\,dxdy$$

Ce résultat s'étend par linéarité aux fonctions étagées $\varphi_k \in S_t(\Omega, C_\sharp(Y^m))$ de la forme $\varphi_k = \sum_{i=1}^k t_i\chi_{A_i}(x)\psi_i(y)$, où $A_i = \{x\in\Omega\,,\ \varphi_k(x,.)=t_i\}$ et $\psi_(y)\in C_\sharp(Y^m)$, puis au cas général par densité des fonctions étagées dans $L^2(\Omega, C_\sharp(Y^m))$.

Soit $\varphi \in L^2(\Omega, C_\sharp(Y^m))$. Alors il existe une suite de fonctions $\varphi_k \in S_t(\Omega, C_\sharp(Y^m))$ telle que :

$$\lim_{k\to 0}\int_\Omega (\sup_{y\in Y^m} \mid \varphi_k(x,y)-\varphi(x,y)\mid)^2\,dx = \lim_{k\to 0}\|\varphi_k-\varphi\|^2_{L^2(\Omega,C_\sharp(Y^m)}=0$$

Par ailleurs, de l'inégalité triangulaire et de la continuité de R, on déduit qu'il existe une constante $C>0$ telle que :

$$\|\varphi(x,\frac{R(x)}{\eta})\|_{L^2(\Omega)} \leq C\|\varphi(x,\frac{x}{\eta})-\varphi_k(x,\frac{x}{\eta})\|_{L^2(\Omega)} + \|\varphi_k(x,\frac{R(x)}{\eta})\|_{L^2(\Omega)}$$

Remarquant que pour toute fonction v dans $L^2(\Omega,C_\sharp(Y^m))$, on a la majoration suivante :

$$\int_\Omega \mid v(x,\frac{x}{\eta})\mid^2 dx \leq \int_\Omega (\sup_{y\in Y^m}\mid v(x,y)\mid)^2\,dx = \|v\|^2_{L^2(\Omega,C_\sharp(Y^m))}$$

on en déduit que pour tout entier k :

$$\|\varphi(x,\frac{R(x)}{\eta})\|_{L^2(\Omega)} \leq C\|\varphi-\varphi_k\|_{L^2(\Omega,C_\sharp(Y^m))} + \|\varphi_k(x,\frac{R(x)}{\eta})\|_{L^2(\Omega)}$$

Puisque φ_k est admissible, il s'en suit que :

$$\begin{aligned}\limsup_{\eta\to 0}\|\varphi(x,\tfrac{R(x)}{\eta})\|_{L^2(\Omega)} &\leq C\|\varphi-\varphi_k\|_{L^2(\Omega,C_\sharp(Y^m))}+\|\varphi_k\|_{L^2(\Omega\times Y^m)}\\ &\leq \|\varphi-\varphi_k\|_{L^2(\Omega,C_\sharp(Y^m))}+\|\varphi-\varphi_k\|_{L^2(\Omega\times Y^m)}+\|\varphi\|_{L^2(\Omega\times Y^m)}\end{aligned}$$

Par ailleurs, on note que :

$$\iint_{\Omega\times Y^m}\mid\varphi-\varphi_k\mid^2 dxdy \leq \int_\Omega\Big(\sup_{y\in Y^m}\mid\varphi(x,y)-\varphi_k(x,y)\mid^2\Big)\,dx = \|\varphi-\varphi_k\|^2_{L^2(\Omega,C_\sharp(Y^m))}$$

On en déduit que pour tout entier k :

$$\limsup_{\eta\to 0}\|\varphi(x,\frac{R(x)}{\eta})\|_{L^2(\Omega)} \leq (C+1)\,\|\varphi-\varphi_k\|_{L^2(\Omega,C_\sharp(Y^m))}+\|\varphi(x,y)\|_{L^2(\Omega\times Y^m)}$$

Faisant tendre k vers 0, on obtient que :

$$\limsup_{\eta\to 0}\|\varphi(x,\frac{R(x)}{\eta})\|_{L^2(\Omega)} \leq \|\varphi(x,y)\|_{L^2(\Omega\times Y^m)} \tag{2}$$

En ce qui concerne la limite inférieure, le raisonnement est identique :

$$\|\varphi_k(x,\frac{R(x)}{\eta})\|_{L^2(\Omega)} \leq \|\varphi(x,\frac{R(x)}{\eta})-\varphi_k(x,\frac{R(x)}{\eta})\|_{L^2(\Omega)} + \|\varphi(x,\frac{R(x)}{\eta})\|_{L^2(\Omega)}$$

φ_k étant admissible et par les mêmes majorations que précédemment on obtient que :

$$\|\varphi_k(x,y)\|_{L^2(\Omega\times Y^m)} \leq C\|\varphi-\varphi_k\|_{L^2(\Omega,C_\sharp(Y^m))} + \liminf_{\eta\to 0}\|\varphi(x,\frac{R(x)}{\eta})\|_{L^2(\Omega)}$$

On en déduit que pour tout entier k :

$$\begin{aligned}\liminf_{\eta\to 0} \|\varphi(x,\tfrac{R(x)}{\eta})\|_{L^2(\Omega)} &\geq \|\varphi_k\|_{L^2(\Omega\times Y^m)} - C\|\varphi-\varphi_k\|_{L^2(\Omega,C_\sharp(Y^m))}\\ &\geq \|\varphi\|_{L^2(\Omega\times Y^m)} - \|\varphi-\varphi_k\|_{L^2(\Omega\times Y^m)} - C\|\varphi-\varphi_k\|_{L^2(\Omega,C_\sharp(Y^m))}\\ &\geq \|\varphi\|_{L^2(\Omega\times Y^m)} - (C+1)\,\|\varphi-\varphi_k\|_{L^2(\Omega,C_\sharp(Y^m))}\end{aligned}$$

En faisant tendre k vers 0, il en découle que :

$$\liminf_{\eta\to 0} \|\varphi(x,\frac{R(x)}{\eta})\|_{L^2(\Omega)} \geq \|\varphi(x,y)\|_{L^2(\Omega\times Y^m)} \tag{3}$$

Des inégalités (2) et (3), on déduit le lemme 3.

(QED)

Preuve de la proposition :

Soit (u_η) une suite bornée dans $L^2(\Omega)$ et $M = \sup_\eta \|u_\eta\|_{L^2(\Omega)}$.

Soit $\varphi \in L^2(\Omega, C_\sharp(Y^m))$, on définit une forme linéaire sur cet espace en posant :

$$< L_\eta, \varphi >= \int_\Omega \varphi(x,\frac{R(x)}{\eta}) u_\eta(x)\,dx$$

D'après l'inégalité de Cauchy-Schwarz, on obtient

$$|< L_\eta, \varphi >| \leq \|u_\eta\|_{L^2(\Omega)}\, \|\varphi(x,\frac{R(x)}{\eta})\|_{L^2(\Omega)} \leq M\, \|\varphi(x,\frac{R(x)}{\eta})\|_{L^2(\Omega)} \tag{4}$$

On en déduit que :

$$\forall \varphi \in L^2(\Omega, C_\sharp(Y^m)),\ \sup_\eta |< L_\eta, \varphi >| < +\infty$$

Donc L_η est une suite bornée ($\|L_\eta\|_{L^2(\Omega)} \leq \|u_\eta\|_{L^2(\Omega)} \leq M$) d'applications linéaires continues sur $L^2(\Omega, C_\sharp(Y^m))$. Cet espace étant un Banach séparable, on en déduit qu'il existe une sous-suite η_k de η tendant vers 0, et une application L dans le dual de $L^2(\Omega, C_\sharp(Y^m))$ telles que :

$$\forall \varphi \in L^2(\Omega, C_\sharp(Y^m)),\ \lim_{k\to\infty} < L_{\eta_k}, \varphi >=< L, \varphi >$$

On a montré dans le lemme 4 que φ est admissible. En passant à la limite quand η tend vers 0 dans l'inégalité (4), on en déduit que :

$$|< L, \varphi >| \leq\ M\, \|\varphi\|_{L^2(\Omega\times Y^m)}$$

L'application L est linéaire continue sur $L^2(\Omega, C_\sharp(Y^m))$ muni de la norme de $L^2(\Omega \times Y^m)$. Donc il existe un unique prolongement linéaire à l'adhérence de $L^2(\Omega, C_\sharp(Y^m))$ dans $L^2(\Omega\times Y^m)$. Par densité de $L^2(\Omega, C_\sharp(Y^m))$ dans $L^2(\Omega\times Y^m)$, on en déduit que l'application L s'étend par continuité à tout $L^2(\Omega \times Y^m)$ en un élément du dual de $L^2(\Omega \times Y^m)$. En d'autres termes, il existe $u_0(x,y)$ dans $L^2(\Omega \times Y^m)$ périodique en y tel que :

$$\forall \varphi \in L^2(\Omega; C_\sharp(Y^m)),\ \lim_{k\to+\infty} \int_\Omega u_{\eta_k}(x)\varphi(x, \frac{R(x)}{\eta_k})\, dx = \iint_{\Omega\times Y^m} u_0(x,y)\varphi(x,y)\, dxdy$$

Ce qui achève la démonstration de la proposition.

(QED)

Nous aurons besoin dans la suite de justifier des passages à la limite dans des intégrales du type $\int_\Omega u_\eta\, v_\eta\, dx$ où $u_\eta \overset{R}{\searrow} u_0$ et $v_\eta \overset{R}{\searrow} v_0$. Pour cela, nous introduisons de manière similaire à Allaire [2] la notion de convergence forte à deux-échelles (coupe-projection) relativement à une matrice R satisfaisant (0).

Définition :
Soit R une matrice de $\mathbb{R}^n$ dans R^m satisfaisant (0). On dit qu'une suite u_η de $L^2(\Omega)$ converge fortement à deux-échelles (coupe-projection) vers une limite u_0 dans $L^2_\sharp(\Omega \times Y^m)$ et on note $u_\eta \overset{R}{\twoheadrightarrow} u_0$, si et seulement si :

$$\|u_\eta\|_{L^2(\Omega)} \to \|u_0(x,y)\|_{L^2(\Omega\times Y^m)}$$

La convergence forte précédente exprime que les seules oscillations effectives de la suite (u_η) sont à l'échelle η. Dans la proposition 5 (iii), un résultat de correcteur est obtenu pour la suite u_η lorsque u_0 est assez régulière.

Proposition 5

Soit R une matrice de $\mathbb{R}^n$ dans R^m satisfaisant (0). Soit u_η une suite bornée dans $L^2(\Omega)$ telle que $u_\eta \overset{R}{\searrow} u_0(x,y)$ faible à deux échelles (coupe-projection). Alors

i) u_η converge faiblement dans $L^2(\Omega)$ vers $u(x) = \int_{Y^m} u_0(x,y)\, dy$ et de plus

$$\liminf_{\eta\to 0} \|u_\eta\|_{L^2(\Omega)} \geq \|u_0\|_{L^2(\Omega\times Y^m)} \geq \|u\|_{L^2(\Omega)}$$

ii) Soit v_η une autre suite bornée dans $L^2(\Omega)$ telle que $v_\eta \overset{R}{\twoheadrightarrow} v_0$ fortement (coupe-projection), alors

$$u_\eta v_\eta \to w(x) \ \ \textit{dans } \mathcal{D}'(\Omega) \ \textit{où } w(x) = \int_{Y^m} u_0(x,y)v_0(x,y)\, dy$$

iii) Supposons que $u_\eta \overset{R}{\twoheadrightarrow} uo(x,y)$ fort à deux échelles (coupe-projection). Si de plus,

$$\|u_0(x, \frac{R(x)}{\eta})\|_{L^2(\Omega)} \to \|u_0(x,y)\|_{L^2(\Omega\times Y^m)} \qquad (*)$$

Alors :

$$\|u_\eta - u_0(x, \frac{R(x)}{\eta})\|_{L^2(\Omega)} \to 0$$

Remarque :

Les classes de fonctions u_0 satisfaisant $(*)$ sont les classes de fonctions admissibles pour la convergence deux-échelles (coupe-projection). En particulier, les fonctions de $L^2(\Omega, C_\sharp(Y^m))$ (sous-espace dense de $L^2(\Omega \times Y^m)$) sont admissibles d'après le lemme 2.

Démonstration :

La preuve est en tout point similaire à celle de Allaire [2].

(QED)

4.4.3 Limite à deux-échelles d'une suite de gradients

Pour passer à la limite dans le problème $(\mathcal{P}^{E,H}_{\eta,\alpha})$ on est amené, étant donné une suite (u_η) bornée dans $W^{1,2}(\Omega)$ (qui vérifie alors $u_\eta \overset{R}{\rightarrow} u_0$ et $\nabla u_\eta \overset{R}{\rightarrow} \chi$ d'après la proposition 2), à déterminer la relation différentielle liant χ à u_0. Ce problème a été résolu par Allaire dans le cadre classique des fonctions périodiques [2]. L'adaptation à notre cadre est plus délicate dans la mesure où les oscillations de la suite (∇u_η) ne peuvent-être représentées en général à l'aide du gradient d'une fonction périodique. Nous nous ramenons systématiquement à une description dans l'espace de Fourier. Pour cela, nous introduisons l'espace

$$\mathcal{L}_R = \left\{ w \in [L^2_\sharp(Y^m)]^n \ \mid \ w(y) = \sum_{k \in \mathbf{Z}^m \setminus \{0\}} \lambda_k \, R^T(k) e^{2i\pi k \cdot y} \ , \ \lambda_k \in \mathbb{C} \right\}$$

Remarquons que la suite (λ_k) qui apparaît dans la définition ci-dessus n'appartient pas nécessairement à l^2 mais vérifie seulement :

$$\sum_{k \in \mathbf{Z}^m \setminus \{0\}} \mid \lambda_k \mid^2 \mid R^T(k) \mid^2 < +\infty$$

(l'expression $\mid R^T(k) \mid$ est non nulle pour tout $k \in \mathbf{Z}^m \setminus \{0\}$ mais **n'est pas minorée**).

Lemme 6

Soit R une matrice satisfaisant (0). *Alors $\mathcal{L}_R$ est un sous-espace fermé de $[L^2_\sharp(Y^m)]^n$ et on a :*

$$\mathcal{L}_R^\perp = \left\{ v \in [L^2_\sharp(Y^m)]^n \ \mid \ v(y) = \sum_{k \in \mathbf{Z}^m \setminus \{0\}} D_k e^{2i\pi k \cdot y} \, ; D_k \perp R^T(k) \ , \ \forall k \in \mathbf{Z}^m \setminus \{0\} \right\}$$

Démonstration

Montrons que $\mathcal{L}_R$ est un sous-espace fermé de $[L^2_\sharp(Y^m)]^n$.

Soit $w^{(p)}(y) = \sum_{k \in \mathbf{Z}^m \setminus \{0\}} \lambda_k^{(p)} R^T(k) e^{2i\pi k \cdot y}$ une suite d'éléments de $\mathcal{L}_\alpha$ convergente vers w. Alors, pour tout multi-indice $k_0 \in \mathbf{Z}^m \setminus \{0\}$, la suite $\left\{ \lambda_{k_0}^{(p)} \ , \ p \in \mathbb{N} \right\}$ est une suite de Cauchy puisque :

$$\begin{aligned} \| w^{(p)} - w^{(p')} \|^2 &= \sum_{k \in \mathbf{Z}^m \setminus \{0\}} \mid \lambda_k^{(p)} - \lambda_k^{(p')} \mid^2 \mid R^T(k) \mid^2 \\ &\geq \mid \lambda_{k_0}^{(p)} - \lambda_{k_0}^{(p')} \mid^2 \mid R^T(k_0) \mid^2 \end{aligned}$$

On remarque en effet que $\mid R^T(k_0) \mid^2$ est strictement positif grâce à (0). Ainsi, pour tout multi-indice $k_0 \in \mathbb{Z}^m \setminus \{0\}$, la suite $\left\{\lambda_{k_0}^{(p)}\right\}$ admet une limite quand $p \to +\infty$ que nous notons λ_{k_0}. On en déduit que par continuité du produit scalaire :

$$\begin{aligned}\forall k_0 \in \mathbb{Z}^m \setminus \{0\}\ ,\ \left(w(y)\ \mid\ e^{2i\pi k_0 \cdot y}\right) &= \lim_{p\to+\infty}\left(w^{(p)}(y)\ \mid\ e^{2i\pi k_0\cdot y}\right)\\ &= \lim_{p\to+\infty}\lambda_{k_0}^{(p)} R^T(k_0)\\ &= \lambda_{k_0} R^T(k_0)\end{aligned}$$

D'après Parseval, on a donc

$$w(y) = \sum_{k_0\in\mathbb{Z}^m\setminus\{0\}} \lambda_{k_0} R^T(k_0) e^{2i\pi k_0\cdot y}$$

On en déduit que w est bien élément de $\mathcal{L}_\alpha$.

Il nous reste à caractériser l'orthogonal de $\mathcal{L}_\alpha$ dans $[L^2_\sharp(Y^m)]^n$. Ecrivons un élément v de $\mathcal{L}_\alpha^\perp$ sous la forme

$$v(y) = \sum_{k\in\mathbb{Z}^m\setminus\{0\}} D_k e^{2i\pi k\cdot y}$$

Alors, pour tout $k_0 \in \mathbb{Z}^m \setminus \{0\}$, la fonction $w = R^T(k_0)e^{2i\pi k_0\cdot y}$ appartenant à $\mathcal{L}_\alpha$, on a :

$$\begin{aligned}\left(v(y)\ \mid\ w(y)\right) &= (R^T(k_0))\left(v(y)\ \mid\ e^{2i\pi k_0\cdot y}\right)\\ &= (R^T(k_0))\ \cdot D_{k_0}\\ &= 0\end{aligned}$$

$$\text{i.e. } \forall\ k_0 \in \mathbb{Z}^m \setminus \{0\}\ ,\ D_{k_0} \perp R^T(k_0)$$

(QED)

Nous pouvons maintenant énoncer notre résultat de structure pour les gradients de fonctions scalaires bornées dans $W^{1,2}(\Omega)$.

Proposition 7

Soit R une matrice satisfaisant (0). Soit u_η une suite bornée dans $W^{1,2}(\Omega)$. Alors

$$\exists u_0 \in W^{1,2}(\Omega), \exists w \in L^2(\Omega, \mathcal{L}_R)$$

et une suite extraite (encore notée u_η) telle que

$$\begin{cases} u_\eta \overset{R}{\twoheadrightarrow} u_0(x)\\ \nabla u_\eta \overset{R}{\rightharpoonup} \nabla_x u_0(x) + w(x,y)\end{cases}$$

Démonstration :

première étape :

u_η et $\bigtriangledown u_\eta$ sont bornées dans $L^2(\Omega)$ et $[L^2(\Omega)]^n$ donc convergent (après une extraction de sous-suite) à deux-échelles vers des limites $u_0(x,y) \in L^2(\Omega \times Y^m)$ et $\chi_0(x,y) \in [L^2(\Omega \times Y^m)]^n$.
Soit $\varphi \in [\mathcal{D}(\Omega; C^\infty_\sharp(Y^m))]^n$ alors

$$\lim_{\eta\to 0} \int_\Omega \bigtriangledown u_\eta(x) \cdot \varphi(x, \frac{R(x)}{\eta})\, dx = \iint_{\Omega\times Y^m} \chi_0(x,y) \cdot \varphi(x,y)\, dxdy \tag{5}$$

La formule de Green nous assure que :

$$\int_\Omega \bigtriangledown u_\eta(x) \cdot \varphi(x, \frac{R(x)}{\eta})\, dx = -\int_\Omega u_\eta \,\mathrm{div}(\varphi(x, \frac{R(x)}{\eta}))\, dx$$

Par ailleurs, l'opérateur divergence "rééchelonné" prend la forme suivante :

$$\mathrm{div}\, \varphi(x, \frac{R(x)}{\eta}) = (\mathrm{div}_x\, \varphi)(x, \frac{R(x)}{\eta}) + \frac{1}{\eta}(\mathrm{div}_y(\varphi \circ R))(x, \frac{R(x)}{\eta})$$

Remarquant que $\mathrm{div}_y(\varphi \circ R) = Tr(\bigtriangledown_y(\varphi \circ R)) = \dfrac{\partial \varphi_i}{\varphi_j} R_{ji} := \varphi_{i,j} R_{ji},\ i \in \{1,..,n\}$ et $j \in \{1,..,m\}$, on en déduit que l'égalité (5) peut être réécrite :
$\iint_{\Omega\times Y^m} \chi_0(x,y)\varphi(x,y)\, dxdy = \lim_{\eta\to 0} I_\eta$ avec

$$I_\eta = [-\int_\Omega u_\eta (\mathrm{div}_x\, \varphi)(x, \frac{R(x)}{\eta})\, dx - \frac{1}{\eta}\int_\Omega u_\eta \varphi_{i,j} R_{ji}(x, \frac{R(x)}{\eta})\, dx] \tag{6}$$

Comme I_η reste borné, on en déduit que

$$\begin{aligned} 0 &= \lim_{\eta\to 0} \eta I_\eta \\ &= \lim_{\eta\to 0} [-\int_\Omega u_\eta \varphi_{i,j} R_{ji}(x, \frac{R(x)}{\eta})\, dx] \end{aligned}$$

En prenant la limite à deux-échelles (coupe-projection) de u_η, on en déduit que :

$$\iint_{\Omega\times Y^m} u_0(x,y)\varphi_{i,j} R_{ji}(x,y)\, dxdy = 0 \ \ ,\forall \varphi \in [\mathcal{D}(\Omega; C^\infty_\sharp(Y^m))]^n \tag{7}$$

On choisit dans (7) la fonction test particulière $\varphi(x,y) = \theta(x)\psi(y)$ où $\theta \in \mathcal{D}(\Omega)$ et $\psi \in [C^\infty_\sharp(Y^m)]^n$.

Le théorème de Fubini appliqué à la fonction $uo(x,y)\varphi_{i,j} R_{ji}(x,y)$ qui est intégrable pour la mesure produit $dxdy$, nous assure que :

$$\int_\Omega \theta(x)[\int_{Y^m} u_0(x,y)\psi_{i,j} R_{ji}(y)\, dy]\, dx = 0$$

Ceci étant vrai pour tout $\theta \in \mathcal{D}(\Omega)$, on obtient que pour tout $\Psi \in [C^\infty_\sharp(Y^m)]^n$, et pour presque tout $x \in \Omega$:

$$\int_{Y^m} u_0(x,y)\psi_{i,j} R_{ji}(y)\, dy = -\int_{Y^m} \frac{\partial u_0}{y_j}(x,y)\psi_i R_{ji}(y)\, dy = 0$$

D'où l'équation vraie pour presque tout $x \in \Omega$

$$R^T(\bigtriangledown_y u_0(x,y)) = 0 \ \text{ dans } [\mathcal{D}'(Y^m)]^n \tag{8}$$

Développons $u_0(x,.)$ qui est élément de $[L^2_\sharp(Y^m)]^n$ en utilisant Parseval :

$$u_0(x,y) = \sum_{k\in\mathbf{Z}^m} C_k(x) e^{2i\pi k\cdot y}$$

L'équation (8) entraine que pour presque tout $x \in \Omega$, $\sum_{k\in\mathbf{Z}^m} 2i\pi R^T(k) C_k(x) e^{2i\pi k\cdot y} = 0$. Puisque $e^{2i\pi k\cdot y}$ forme un système libre, on en déduit que :

$$p.p.x \in \Omega,\ R^T(k)C_k(x) = 0\ ,\ \forall k \in \mathbf{Z}^m \setminus \{0\}$$

Par ailleurs, R satisfaisant (0), nous sommes assurés que $R^T(k) \neq 0$, $\forall k \in \mathbf{Z}^m \setminus \{0\}$. Posant $u(x) = C_0(x)$, nous obtenons alors l'égalité $u_0(x,y) = u(x)$, p.p. $x \in \Omega$ (p.p.$y \in Y^m$).

Deuxième étape : identification de χ_0 donné par (5).

On choisit une fonction $\varphi \in [\mathcal{D}(\Omega; C^\infty_\sharp(Y^m))]^n$ telle que $\mathrm{div}_y(\varphi \circ R) = 0$ et on passe à la limite dans (6) quand $\eta \to 0$:

$$\begin{aligned}\iint_{\Omega\times Y^m} \chi_0(x,y)\cdot\varphi(x,y)\,dxdy &= -\iint_{\Omega\times Y^m} u_0(x,y)(\mathrm{div}_x\,\varphi)(x,y)\,dxdy \\ &= -\int_\Omega u(x)[\int_{Y^m}(\mathrm{div}_x\,\varphi)(x,y)\,dy]\,dx\end{aligned}$$

Posons $[\varphi](x) := \int_{Y^m}\varphi(x,y)\,dy$, le théorème de dérivation sous le signe somme nous dit alors que $[\varphi] \in \mathcal{D}(\Omega)$ et $\mathrm{div}_x[\varphi] = \int_{Y^m}(\mathrm{div}_x\,\varphi)(x,y)\,dy$. En intégrant par parties et d'après Fubini, on en déduit que :

$$\begin{aligned}\iint_{\Omega\times Y^m} \chi_0(x,y)\cdot\varphi(x,y)\,dxdy &= -\int_\Omega u(x)\,\mathrm{div}_x[\varphi]\,dx \\ &= \int_\Omega \bigtriangledown u(x)\cdot[\varphi](x)\,dx\end{aligned}$$

On applique une nouvelle fois Fubini pour obtenir que :

$$\forall\varphi \in [\mathcal{D}(\Omega; C^\infty_\sharp(Y^m))]^n,\ \iint_{\Omega\times Y^m}[\chi_0(x,y) - \bigtriangledown u(x)]\cdot\varphi(x,y)\,dxdy = 0 \tag{9}$$

Localisation en x : en choisissant φ de la forme $\varphi(x,y) = \theta(x)\psi(y)$ avec $\psi \in [C^\infty_\sharp(Y^m)]^n$ telle que $Tr(\bigtriangledown_y(\varphi\circ R)) = 0$ et $\theta \in \mathcal{D}(\Omega)$, on a immédiatement que :

$$\text{p.p. } x \in \Omega,\ \int_{Y^m}(\chi_0(x,y) - \bigtriangledown u(x))\cdot\psi(y)\,dy = 0 \tag{10}$$

Cette relation s'étend par densité à toute fonction $\psi \in [L^2_\sharp(Y^m)]^n$ telle que $Tr(\bigtriangledown_y(\psi\circ R)) = 0$ et donc, d'après le lemme 6, $\chi_0(x,.) - \bigtriangledown u(x)$ appartient au bi-orthogonal de

$\mathcal{L}_R$ $\Big($ noter pour cela que $w(y) = \sum_{k\in\mathbf{Z}^m\setminus\{0\}} D_k e^{2i\pi k\cdot y}$ avec $D_k \perp R^T(k)$, $\forall k \in \mathbf{Z}^m \setminus \{0\}\Big)$.
Puisque $\mathcal{L}_R$ est fermé (donc $\mathcal{L}_R^{\perp\perp} = \mathcal{L}_R$), il existe donc un élément $w(x,.)$ de $\mathcal{L}_R$ tel que $\chi_0(x,.) = \bigtriangledown_x u(x) + w(x,.)$.

Ce qui achève la démonstration de la proposition.

(QED)

4.5 Résultat d'homogénéisation pour le système Maxwell en dimension 3

4.5.1 Résultats préliminaires

Dans l'étude de la diffraction par un obstacle 3-D, nous devons passer à la limite quand η tend vers 0 dans le système vectoriel $\mathcal{P}_{\eta,\alpha}^{(E,H)}$. Ceci nous amène à travailler dans des espaces fonctionnels adaptés (indépendants de η) associés à un ouvert Ω contenant strictement l'objet diffractant D, définis dans le chapitre 2. Par ailleurs, nous devons étendre le résultat de structure sur la convergence des rotationnels établi dans le chapitre 2 (corollaire 9) au cas quasi-périodique. Pour cela, on note R une matrice à m lignes et 3 colonnes satisfaisant (0). On introduit le sous-espace $\mathcal{M}_R$ de $[L^2_\sharp(Y^m)]^9$ défini par :

$$\mathcal{M}_R = \Big\{ w \in [L^2_\sharp(Y^m)]^9 \ \mid \ w(y) = \sum_{k\in\mathbf{Z}^m\setminus\{0\}} \Lambda_k \otimes R^T(k) e^{2i\pi k\cdot y}$$
$$\text{où } \Lambda_k \in \mathbb{C}^3 \text{ et } \Lambda_k \cdot R^T(k) = 0 \ , \ \forall\, k \in \mathbf{Z}^m \setminus \{0\}\Big\}$$

De manière similaire au lemme 6, on établit que $\mathcal{M}_R$ est un sous-espace fermé de $[L^2_\sharp(Y^m)]^9$. Le résultat de structure établi dans le cas de fonctions scalaires dans la proposition 7 se reformule de la façon suivante :

Corollaire 8

Soit R une matrice à m lignes et 3 colonnes satisfaisant (0). Soient Ω un ouvert borné de classe C^2 de $\mathbb{R}^3$ et (H_η) une suite dans $[L^2(\Omega)]^3$ telle que :

$$\begin{array}{ll} \operatorname{div} H_\eta = 0 & (i) \\ \sup_\eta \int_\Omega \Big(\mid H_\eta \mid^2 + \mid \operatorname{rot} H_\eta \mid^2 \Big)\, dx < +\infty & (ii) \\ H_\eta \wedge n \quad \textit{est bornée dans } \left[H^{\frac{1}{2}}(\partial\Omega)\right]^3 & (iii) \end{array}$$

Alors la suite est bornée dans $[W^{1,2}(\Omega)]^3$ et il existe une sous-suite de (H_η), encore notée (H_η), et deux fonctions $H_0 \in [W^{1,2}(\Omega)]^3$ et $w \in L^2(\Omega, \mathcal{M}_R)$ telles que :

$$\begin{cases} H_\eta \to H_0(x) \ \ \textit{dans } [L^2(\Omega)]^3 \textit{ fort} \\ \bigtriangledown H_\eta \overset{R}{\rightharpoonup} \bigtriangledown H_0(x) + w(x,y) \end{cases}$$

Démonstration :

Les hypothèses de la proposition 7 du chapitre 2 étant satisfaites, il existe une constante $C(\Omega) > 0$ ne dépendant que de la mesure de Ω telle que :

$$\|H_\eta\|_{[H^1(\Omega)]^3} \leq C(\Omega)\Big\{\|H_\eta\|_{[L^2(\Omega)]^3} + \|\mathrm{rot}\, H_\eta\|_{[L^2(\Omega)]^3} + \|\mathrm{div}\, H_\eta\|_{L^2(\Omega)} + \|H_\eta \wedge n\|_{[H^{\frac{1}{2}}(\partial\Omega)]^3}\Big\}$$

D'après les hypothèses (i), (ii) et (iii) du corollaire, on en déduit que

$$\sup_\eta \|H_\eta\|_{[H^1(\Omega)]^3} < +\infty$$

La limite de $\mathrm{div}\, H_\eta$ étant nulle, la proposition 7 du chapitre 4 nous assure de l'existence d'une sous-suite de (H_η), encore notée (H_η), de $H_0 \in [W^{1,2}(\Omega)]^3$ et de $w \in L^2(\Omega, \mathcal{M}_R)$ tels que :

$$H_\eta \to H_0(x) \quad \text{dans } [L^2(\Omega)]^3 \text{ fort}\ , \quad \text{et } \bigtriangledown H_\eta \overset{R}{\rightharpoonup} \bigtriangledown H_0(x) + w(x,y) \tag{23}$$

(QED)

4.5.2 Résultat de convergence

L'étude asymptotique du problème $\mathcal{P}^H_{\eta,\alpha}$ quand $\eta \to 0$ conduit au résultat suivant :

Théorème 9

Considérons l'application linéaire continue L qui à toute matrice de $\mathbb{C}^\theta$ associe le vecteur $L(w)$ de $\mathbb{C}^3$ comme suit :

$$\forall\, v \in \mathbb{C}^3\ ,\ L(w) \wedge v = (w - w^T)v \tag{0}$$

Soit w l'unique solution dans $\mathcal{M}_R$ des 3 problèmes variationnels annexes (paramétrés par $x \in \mathbb{R}^3$) $(\mathcal{P}^x_i)$, $i \in \{1\ ,2\ ,3\}$, suivants :

$$(\mathcal{P}^x_i) : \int_{Y^m} \frac{1}{\varepsilon(x,y)}\Big[e_i + L(w_i(y))\Big] \cdot \Big[L(w'_i(y))\Big]\, dy = 0\ ,\ \forall w'_i \in \mathcal{M}_R$$

Quand η tend vers zéro, H_η solution du problème $(\mathcal{P}^H_{\eta,\alpha})$, converge dans $L^2_{loc}(\mathbb{R}^3, \mathbb{C}^3)$ vers l'unique solution H_0 du problème $(\mathcal{P}_0)$ suivant :

$$(\mathcal{P}_0)\begin{cases} (i)\ \mathrm{rot}\Big\{\varepsilon^{-1}_{hom}\,\mathrm{rot}\, H_0(x)\Big\} - k_0^2 H_0(x) = 0 & \textit{dans } [\mathcal{D}'(\mathbb{R}^3)]^3 \\ (ii)\ \mathrm{div}\, H_0(x) = 0 & \textit{dans } [\mathcal{D}'(\mathbb{R}^3)]^3 \\ (iii)\ H_0^d(x) = O(\frac{1}{|x|}) & \textit{quand } |\ x\ | \to +\infty \textit{ dans } [C^\infty(\mathbb{R}^3 \setminus \overline{D})]^3 \\ (iv)\ \frac{x}{|x|} \wedge \mathrm{rot}\, H_0^d(x) + ikH_0^d(x) = o(\frac{1}{|x|}) & \textit{quand } |\ x\ | \to +\infty \textit{ dans } [C^\infty(\mathbb{R}^3 \setminus \overline{D})]^3 \end{cases}$$

avec la matrice homogénéisée définie pour tout $x \in \mathbb{R}^3$ *par :*

$$\varepsilon_{hom}^{-1}(x) = \left\langle \frac{1}{\varepsilon(x,y)} \right\rangle_{Y^m} + \left\langle \frac{B(y)}{\varepsilon(x,y)} \right\rangle_{Y^m}$$

B *étant la matrice définie par les vecteurs colonnes* $L(w_i(y))$ *:*

$$B(y) = (L(w_1(y)) \ | \ L(w_2(y)) \ | \ L(w_3(y)))$$

Remarque :

On peut réécrire le problème $(\mathcal{P}_i^x)$ en utilisant l'application linéaire continue L^* adjointe de L et en notant que pour tous w , $w' \in \mathfrak{C}^{\mathfrak{0}}$, on a :

$$\begin{aligned} L(w) \cdot L(w') &= (L(w) \wedge v) \cdot (L(w') \wedge v) = [(w - w^T)\, v] \cdot [(w' - w'^T)\, v] \\ &= v^T\, (w'^T - w') \cdot (w - w^T)\, v = Tr((w'^T - w')\, (w - w^T)) = w_a : w'_a \end{aligned}$$

où w_a (resp. w'_a) désigne la partie antisymétrique $(w - w^T)$ de la matrice w (resp. w') et v est un vecteur unitaire quelconque. Alors $(\mathcal{P}_i^x)$ devient :

$$(\mathcal{P}_i^x) : \int_{Y^m} \frac{1}{\varepsilon(x,y)} \Big[L^*(e_i) + w_{a_i}(y) \Big] : \Big[w'_{a_i}(y) \Big]\, dy = 0 \ , \ \forall w'_i \in \mathcal{M}_R$$

Ici l'application adjointe L^* est déterminée pour tous vecteurs u et v de $\mathfrak{C}^{\mathfrak{3}}$ par la relation :

$$L^*(u \wedge v) = (u \otimes v)_a$$

En effet, pour toute matrice w de $\mathfrak{C}^{\mathfrak{0}}$, on a :

$$\begin{aligned} L^*(u \wedge v) : w &= (u \wedge v) \cdot L(w) = -(w - w^T)\, v \cdot u = (w - w^T) : (u \otimes v) \\ &= w : (u \otimes v) - (u \otimes v)^T : w = w : (u \otimes v - v \otimes u) \end{aligned}$$

Nous allons maintenant démontrer le théorème 9.

Démonstration :

On reprend les hypothèses géométriques imposées dans la section 1. On considère un rayon R tel que $\Omega := \{ \mid x \mid < R \}$ vérifie $\overline{D} \subset \Omega$. Dans une première étape, on démontre le théorème sous l'hypothèse que la suite (H_η) est bornée dans $[L^2(\Omega)]^3$ donc converge faiblement (à une sous-suite extraite près) vers une limite notée H_0. On vérifie ensuite cette hypothèse par un raisonnement par l'absurde qui utilise l'unicité de la solution du problème limite vérifié par H_0.

Étape 1 : (H_η) **est supposée bornée dans** $[L^2(\Omega)]^3$ **:**

a) **Comportement asymptotique de** (E_η, H_η) **en dehors de** Ω **:**

On renvoie le lecteur à la preuve du théorème 10 du chapitre 2.

b) **Convergence et étude des oscillations de** (E_η, H_η) **sur** Ω **:**

D'après le lemme 11 du chapitre 2, (H_η) est bornée dans $H(\Omega, \mathrm{rot})$. Par ailleurs, (H_η) est à divergence nulle et sa trace tangentielle est bornée dans $[H^{\frac{1}{2}}(\partial\Omega)]^3$.

Donc le corollaire 8 nous assure que (H_η) est bornée dans $[W^{1,2}(\Omega)]^3$ et qu'il existe une sous-suite extraite de (H_η), encore notée (H_η), et deux fonctions $H_0 \in [W^{1,2}(\Omega)]^3$ et $w \in L^2(\Omega, \mathcal{M}_R)$ telles que :

$$\begin{cases} H_\eta \to H_0(x) \ \text{ dans } [L^2(\Omega)]^3 \text{ fort} \\ \bigtriangledown H_\eta \xrightarrow{R} \bigtriangledown H_0(x) + w(x,y) \end{cases} \tag{1}$$

Soit l'application linéaire continue L définie pour toute matrice u dans $\mathbb{C}^9$ par :

$$\forall\, v \in \mathbb{C}^3\ ,\ L(u) \wedge v = (u^T - u)v \tag{2}$$

On déduit de (1) et (2) la convergence des rotationnels suivante :

$$\operatorname{rot} H_\eta \xrightarrow{R} \operatorname{rot} H_0(x) + L(w(x,y))$$

On écrit alors la formulation variationnelle associée au problème $\mathcal{P}^H_{\eta,\alpha}$ sur Ω :

$$\int_\Omega \Big(\frac{1}{\varepsilon_\eta(x)} \operatorname{rot} H_\eta\Big) \cdot \operatorname{rot} \varphi_\eta \, dx - k_0^2 \int_\Omega H_\eta \cdot \varphi_\eta \, dx = 0 \ \ ,\forall \varphi_\eta \in [\mathcal{D}(\Omega)]^3 \tag{3}$$

Dans (3), on prend des fonctions test particulières de la forme $\varphi_\eta = \varphi_0(x) + \eta\varphi_1(x, \dfrac{R(x)}{\eta})$, où $\varphi_0 \in [\mathcal{D}(\Omega)]^3$ et $\varphi_1 \in [\mathcal{D}(\Omega, C^\infty_\sharp(Y^m))]^3$. On obtient en particulier que :

$$\begin{aligned} \operatorname{rot} \varphi_\eta(x) &= \operatorname{rot} \varphi_0(x) + \eta\Big[\operatorname{rot} \varphi_1(x, \frac{R(x)}{\eta})\Big] \\ &= \operatorname{rot} \varphi_0(x) + \eta\Big[(\operatorname{rot}_x \varphi_1)(x, \frac{R(x)}{\eta}) + \frac{1}{\eta}(\operatorname{rot}_y(\varphi_1 \circ R))(x, \frac{R(x)}{\eta})\Big] \end{aligned}$$

L'opérateur rotationnel "rééchelonné" prend donc la forme suivante :

$$\operatorname{rot} \varphi_\eta(x) = \operatorname{rot} \varphi_0(x) + \eta(\operatorname{rot}_x \varphi_1)(x, \frac{R(x)}{\eta}) + (\operatorname{rot}_y(\varphi_1 \circ R))(x, \frac{R(x)}{\eta}) \tag{4}$$

En appliquant (4) à (3), pour toutes fonctions test $\varphi_0 \in [\mathcal{D}(\Omega)]^3$ et $\varphi_1 \in [\mathcal{D}(\Omega; C^\infty_\sharp(Y^m))]^3$, on obtient que :

$$\begin{aligned} &\int_\Omega \Big(\frac{1}{\varepsilon_\eta(x)} \operatorname{rot} H_\eta(x)\Big) \cdot \Big(\operatorname{rot} \varphi_0(x) + (\operatorname{rot}_y(\varphi_1 \circ R))(x, \frac{R(x)}{\eta})\Big)\, dx \\ &+\eta \int_\Omega \Big(\frac{1}{\varepsilon_\eta(x)} \operatorname{rot} H_\eta(x)\Big) \cdot \Big((\operatorname{rot}_x \varphi_1)(x, \frac{R(x)}{\eta})\Big)\, dx \\ &= k_0^2 \int_\Omega H_\eta \cdot \varphi_0 \, dx + \eta\, k_0^2 \int_\Omega H_\eta \cdot \varphi_1(x, \frac{R(x)}{\eta})\, dx \end{aligned} \tag{5}$$

On souhaite maintenant passer à la limite quand η tend vers zéro dans (5). Or, (H_η) est bornée dans $[L^2(\Omega)]^3$, φ_1 est très régulière et R est continue, donc :

$$\sup_\eta \Big| \int_\Omega H_\eta \cdot \varphi_1(x, \frac{R(x)}{\eta}) \Big| < +\infty$$

Par ailleurs, $(\varepsilon_\eta^{-1} \operatorname{rot} H_\eta)$ est bornée dans $[L^2(\Omega)]^3$ donc :

$$\sup_\eta \mid \int_\Omega \varepsilon_\eta^{-1} \operatorname{rot} H_\eta \cdot \operatorname{rot}_x \varphi_1(x, \frac{R(x)}{\eta}) \mid < +\infty$$

On en déduit que :

$$\lim_{\eta\to 0}\left[\eta k_0^2 \int_\Omega H_\eta \cdot \varphi_1(x, \frac{R(x)}{\eta})\, dx\right] = \lim_{\eta\to 0}\left[\eta \int_\Omega \Big(\frac{1}{\varepsilon_\eta}\operatorname{rot} H_\eta\Big) \cdot \Big(\operatorname{rot}_x \varphi_1(x, \frac{R(x)}{\eta})\Big)\, dx\right] = 0$$

Pour traiter la convergence des deux termes restant dans l'expression (5), on note que la fonction

$$\psi(x,y) = \varepsilon^{-1}(y)\ (\operatorname{rot}\varphi_0(x) + (\operatorname{rot}_y(\varphi_1 \circ R))(x,y))$$

est dans $[L^2_\sharp(Y^m, C(\bar\Omega))]^3$. ψ est donc admissible pour la convergence à deux échelles relativement à la matrice R, au sens du lemme 4. En passant à la limite dans l'expression (5), on en déduit que pour tous champs $\varphi_0 \in [L^2(\Omega)]^3$ et $w' \in L^2(\Omega, \mathcal{M}_R)$:

$$\begin{aligned}&\iint_{\Omega\times Y^m} \frac{1}{\varepsilon(x,y)}\Big[\operatorname{rot} H_0(x) + L(w(x,y))\Big]\cdot\\ &\Big[\operatorname{rot}\varphi_0(x) + L(w'(x,y))\Big]\, dxdy = k_0^2 \int_\Omega H_0(x)\cdot\varphi_0(x)\, dx \quad (6)\end{aligned}$$

c) **Équation microscopique sur Y^m :**

On veut déduire de (6) l'équation locale ayant cours dans la cellule Y^m. On choisit pour cela des fonctions test particulières $\varphi_0 \in [\mathcal{D}(\Omega)]^3$ telles que $\varphi_0 = 0$. On obtient alors que pour tout $w' \in L^2(\Omega, \mathcal{M}_R)$:

$$\iint_{\Omega\times Y^m} \frac{1}{\varepsilon(x,y)}\Big[\operatorname{rot} H_0(x) + L(w(x,y))\Big]\cdot\Big[L(w'(x,y))\Big]\, dxdy = 0 \quad (7)$$

D'après Fubini, on en déduit que pour presque tout $x \in \Omega$ et pour tout élément de $\mathcal{M}_R$, encore noté w' :

$$\int_{Y^m} \frac{1}{\varepsilon(x,y)}\Big[\operatorname{rot} H_0(x) + L(w(y))\Big]\cdot\Big[L(w'(y))\Big]\, dy = 0 \quad (8)$$

Posant $\xi = \operatorname{rot} H_0(x)$, on aboutit donc à la résolution de problèmes annexes $(\mathcal{P}_\xi^x)$, ξ décrivant $\mathbb{C}^3$, suivants :

$$(\mathcal{P}_\xi^x) : \int_{Y^m} \frac{1}{\varepsilon(x,y)}\Big[\xi + L(w(y))\Big]\cdot\Big[L(w'(y))\Big]\, dy = 0 \quad (9)$$

L'existence et l'unicité de la solution du problème $(\mathcal{P}_\xi^x)$ relève alors du lemme de Lax-Milgram. A cet effet, pour presque tout $x \in \Omega$, on définit la forme sesquilinéaire $a_x(.,.)$ sur $\mathcal{M}_R \times \mathcal{M}_R$:

$$a_x(w,w') = \int_{Y^m} \frac{1}{\varepsilon(x,y)}\Big[L(w(y))\Big]\cdot\Big[L(w'(y))\Big]\, dy$$

Cette forme est continue. En effet, la coercivité de ε, nous assure qu'il existe une constante γ strictement positive telle que pour presque tout $x \in \Omega$:

$$\|a_x(w,w')\| \quad \le \frac{1}{\gamma}\int_{Y^m}\Big[L(w(y)\Big]\cdot\Big[L(w'(y))\Big]\, dy$$

De l'inégalité de Cauchy-Schwarz appliquée dans l'espace de Hilbert $\mathcal{M}_R$, et de la continuité de L, on déduit alors qu'il existe une constante strictement positive $\gamma_1(\xi)$ telle que pour presque tout $x \in \Omega$:

$$\|a_x(w, w')\| \quad \leq \gamma_1(\xi)\|w(y)\| \, \|w'(y)\|$$

Par ailleurs, $a_x(.,.)$ est une forme sesquilinéaire coercive sur $\mathcal{M}_R \times \mathcal{M}_R$. On a en effet le lemme suivant :

Lemme 10

Pour tous vecteurs a et b dans $\mathbb{C}^3$ tels que $a \cdot b = 0$, le vecteur $L(a \otimes b)$ de $\mathbb{C}^3$ (cf. (0)) vérifie :

$$\|L(a \otimes b)\| = \|a\| \ \|b\|$$

Démonstration :

Par homogénéité, on se ramène au cas où a et b sont unitaires.

$$\begin{aligned}
\|L(a \otimes b)\| &= \sup_{\|z\|=1} \|L(a \otimes b) \wedge z\| \\
&= \sup_{\|z\|=1} \|(a \otimes b - b \otimes a)z\| \\
&= \sup_{\|z\|=1} \|a(b \cdot z) - b(a \cdot z)\| \\
&= \sup_{\|z\|=1} \left[\mid b \cdot z \mid^2 + \mid a \cdot z \mid^2 \right]^{\frac{1}{2}} \\
&= 1
\end{aligned}$$

où dans l'avant dernière égalité, on a utilisé le fait que a et b sont orthogonaux.

(QED)

Pour tous $k \in \mathbb{Z}^m \setminus \{0\}$ et $\Lambda_k \in \mathbb{C}^3$ tels que $\Lambda_k \cdot R^T(k) = 0$, on déduit du lemme 10 la majoration suivante :

$$\|L(\Lambda_k \otimes R^T(k))\| = \|\Lambda_k\| \, \|R^T(k)\| = \|\Lambda_k \otimes R^T(k)\|$$

Comme $\Re e\{\varepsilon\}$ est bornée dans $[L^\infty(\Omega; L^\infty_\sharp(Y^m))]^9$, il en résulte qu'il existe $\beta > 0$ telle que pour presque tout $x \in \Omega$ et pour tout $w \in \mathcal{M}_R$:

$$\begin{aligned}
\Re e\{a_x(w, w)\} &\geq \frac{1}{\beta} \int_{Y^m} \mid Lw \mid^2 (y) \, dy \\
&\geq \frac{1}{\beta} \|w\|^2
\end{aligned}$$

On définit maintenant la forme linéaire continue $b_x(\cdot)$ sur $\mathcal{M}_R$ pour presque tout $x \in \Omega$ par :

$$\forall w' \in \mathcal{M}_R \ , \ b_x(w') = \int_{Y^m} \frac{1}{\varepsilon(x, y)} \xi \cdot L(w'(y)) \, dy$$

Le lemme de Lax-Milgram appliqué dans l'espace de Hilbert $\mathcal{M}_R$ à la forme sesquilinéaire continue coercive $a_x(\cdot, \cdot)$ et à la forme linéaire continue $b_x(\cdot)$, nous assure alors de l'existence et de l'unicité de la solution w du problème local $(\mathcal{P}^x_\xi)$.

d) **Équation homogénéisée :**

On veut maintenant préciser le lien entre le problème annexe (ayant court sur la cellule de base Y^m), et le problème macroscopique. On prend pour cela $w' = 0$ dans (6), et on en déduit que pour toute fonction $\varphi \in [\mathcal{D}(\Omega)]^3$:

$$\iint_{\Omega \times Y^m} \varepsilon^{-1} \Big[\operatorname{rot} H_0(x) + L(w(x,y)) \Big] \cdot \operatorname{rot} \varphi(x) = k_0^2 \int_\Omega H_0(x) \varphi(x)\, dx \tag{10}$$

D'après Fubini, on obtient que pour toute fonction $\varphi \in [\mathcal{D}(\Omega)]^3$:

$$\int_\Omega \left\{ \int_{Y^m} \frac{1}{\varepsilon(x,y)} \Big[\operatorname{rot} H_0(x) + L(w(x,y)) \Big]\, dy \right\} \cdot \operatorname{rot} \varphi(x)\, dx = k_0^2 \int_\Omega H_0(x) \varphi(x)\, dx \tag{11}$$

L'égalité suivante est donc vraie au sens des distributions dans l'ouvert Ω :

$$\operatorname{rot} \left\{ \int_{Y^m} \frac{1}{\varepsilon(x,y)} \Big[\operatorname{rot} H_0(x) + L(w(x,y)) \Big]\, dy \right\} - k_0^2 H_0(x) = 0 \tag{12}$$

Notant B la matrice dans $\mathcal{M}_R$ telle que

$$L(w(x,y)) = (\operatorname{rot} H_0(x))_1 L(w_1) + (\operatorname{rot} H_0(x))_2 L(w_2) + (\operatorname{rot} H_0(x))_3 L(w_3) = B(y,z) \operatorname{rot} H_0(x)$$

on en déduit que :

$$\operatorname{rot} \left\{ \int_{Y^m} \frac{1}{\varepsilon(x,y)} \Big[\operatorname{rot} H_0(x) + B(y,z) \operatorname{rot} H_0(x)) \Big]\, dy \right\} - k_0^2 H_0(x) = 0 \tag{13}$$

Il s'en suit que H_0 est la solution dans $[\mathcal{D}'(\Omega)]^3$ de l'équation :

$$\operatorname{rot} \left\{ \Big[\int_{Y^m} \Big(\frac{1}{\varepsilon(x,y)} + \frac{B(y,z)}{\varepsilon(x,y)} \Big)\, dydz \Big] \operatorname{rot} H_0(x) \right\} - k_0^2 H_0(x) = 0 \tag{14}$$

H_0 est donc solution dans $[\mathcal{D}'(\Omega)]^3$ de l'équation homogénéisée

$$\operatorname{rot} \left\{ \varepsilon_{hom}^{-1} \operatorname{rot} H_0(x) \right\} - k_0^2 H_0(x) = 0 \tag{15}$$

avec la matrice homogénéisée définie pour tout $x \in \mathbb{R}^3$ par :

$$\varepsilon_{hom}^{-1}(x) = \Big\langle \frac{1}{\varepsilon(x,y)} \Big\rangle_{Y^m} + \Big\langle \frac{B(y)}{\varepsilon(x,y)} \Big\rangle_{Y^m}$$

Étape 2 : Preuve que (H_η) est bornée dans $[L^2(\Omega)]^3$:

On renvoie le lecteur à la preuve du théorème 10 du chapitre 2.

(QED)

4.6 Application aux obstacles cylindriques et aux milieux stratifiés

Dans cette section, on particularise l'étude de la section précédente à des obstacles diffractants cylindriques en polarisation $E \parallel$ et $H \parallel$ puis pour un milieu stratifié en polarisation $H \parallel$. Par ailleurs, une étude qualitative du correcteur est donnée dans le chapitre 5, pour un problème d'électrostatique uni-dimensionnel.

4.6.1 Résultats d'homogénéisation pour un ensemble de tiges parallèles infinies réparties quasi-périodiquement

Dans ce paragraphe, on reprend les hypothèses géométriques imposées dans la section 1. Pour simplifier les notations, on considère une assemblée de tiges de génératrices suivant e_3, placées aux noeuds d'un réseau quasi-périodique de $\mathbb{R}^2$ issu d'une coupe projection de $\mathbb{R}^4$ (les noeuds d'un pavage de Penrose par exemple, dont la matrice de relèvement est donnée en annexe) et contenues dans un ouvert borné D. L'obstacle diffractant G est alors défini par $G = D \times \mathbb{R}$. Nous nous intéressons aux deux cas de polarisation transverse magnétique dit $H \parallel$ (champ magnétique vectoriel de la forme $H_\eta(x_1, x_2, x_3) = H^3_\eta(x_1, x_2)e_3$) et transverse électrique dit $E \parallel$ (champ électrique vectoriel de la forme $E_\eta(x_1, x_2, x_3) = E^3_\eta(x_1, x_2)e_3$).

Cas $E \parallel$

Dans le cas d'une onde polarisée $E \parallel$, le résultat de convergence est trivial. En effet, on déduit de $\mathcal{P}^{E,H}_{\eta,\alpha}$ que $E_\eta(x_1, x_2, x_3) = E^3_\eta(x_1, x_2)e_3$ est solution dans $\mathcal{D}'(\mathbb{R}^2)$ de $\Delta E^3_\eta + k_0^2 \varepsilon_\eta E^3_\eta = 0$. E^3_η étant bornée dans $W^{1,2}(D)$ et ε_η étant bornée dans $L^\infty(D)$, ΔE^3_η est elle même bornée dans $W^{1,2}(D)$. Quitte à extraire une sous-suite, on peut donc supposer qu'il existe $E^3_0 \in W^{1,2}(D)$ telle que $E^3_\eta \to E^3_0(x_1, x_2)$ et $\Delta E^3_\eta \to \Delta E^3_0(x_1, x_2)$ dans $L^2(D)$ fort. Sachant que $\varepsilon_\eta \rightharpoonup \displaystyle\int_{Y^2 \times Y^2} \varepsilon(y, z)\, dydz$ dans $L^2(D)$ faible, on en déduit que E^3_0 est l'unique solution du problème homogénéisé :

$$\mathcal{P}^{E\parallel}_{0,\alpha} \begin{cases} \Delta E^3_0(x) + k_0^2 \varepsilon_{eff}(x) E^3_0(x) = 0 & , \text{dans } \mathcal{D}'(\mathbb{R}^2) \\ E^{3,d}_0 \text{ vérifie } (S) & , \text{dans } C^\infty(\mathbb{R}^2 \setminus \overline{D}) \end{cases}$$

$$\text{où } \varepsilon_{eff}(x) = \begin{cases} \displaystyle\int_{Y^2 \times Y^2} \varepsilon(y, z)\, dydz & , \text{si } x \in D \\ 1 & , \text{si } x \notin D \end{cases}$$

Cas $H \parallel$

On déduit du théorème 9 le résultat de convergence suivant en polarisation $H \parallel$:

Proposition 11

Soit v_i l'unique solution dans

$$\mathcal{L}_R = \left\{ w \in [L^2_\sharp(Y^m)]^n \ \mid \ w(y) = \sum_{k \in \mathbb{Z}^m \setminus \{0\}} \lambda_k \, R^T(k) e^{2i\pi k \cdot y} \ , \ \lambda_k \in \mathbb{C} \right\}$$

des 2 problèmes variationnels annexes $(\mathcal{Q}_i^x)$, $i \in \{1\ ,2\}$, *suivants :*

$$(\mathcal{Q}_i^x): \int_{Y^2\times Y^2} \frac{1}{\varepsilon(x,y,z)}\Big[e_i + v_i(y,z)\Big]\cdot\Big[v_i'(y,z)\Big]\,dydz = 0\ ,\ \forall v_i' \in \mathcal{L}_R$$

Quand η *tend vers zéro,* $H_\eta(x_1,x_2,x_3) = H_\eta^3(x_1,x_2)e_3$ *solution du problème* $(\mathcal{P}_{\eta,\alpha}^H)$, *converge dans* $L^2_{loc}(\mathbb{R}^3,\mathbb{C}^3)$ *(à une sous-suite extraite près) vers* $H_0(x_1,x_2,x_3) = H_0^3(x_1,x_2)e_3$ *où* H_0^3 *est l'unique solution du problème homogénéisé :*

$$\mathcal{P}_{0,\alpha}^{H\|}\begin{cases} -div\Big(\varepsilon_{eff}^{-1} \bigtriangledown H_0^3\Big) = k_0^2 H_0^3 & ,\ dans\ \mathcal{D}'(\mathbb{R}^2) \\ H_0^{3,d}\ \ v\acute{e}rifie\ (S) & ,\ dans\ C^\infty(\mathbb{R}^2\setminus\bar{D}) \end{cases}$$

ε_{eff}^{-1} *désignant la matrice définie par :*

$$\varepsilon_{eff}^{-1}(x) = < \frac{1}{\varepsilon} >_{Y^2\times Y^2} Id + (< \frac{1}{\varepsilon}v_1 >_{Y^2\times Y^2} | < \frac{1}{\varepsilon}v_2 >_{Y^2\times Y^2})$$

Démonstration :

On applique le théorème 9 en tenant compte du fait que H_η est parallèle à e_3 et ne dépend que de (x_1,x_2). Exploitons le problème annexe $(\mathcal{P}_i^x)$ dans ce cas :

$$(\mathcal{P}_i^x): \int_{Y^2\times Y^2} \frac{1}{\varepsilon(x,y,z)}\Big[e_i + L(w_i(y,z))\Big]\cdot\Big[L(w_i'(y,z))\Big]\,dydz = 0\ ,\ \forall w_i' \in \mathcal{M}_R$$

Les matrices jacobiennes associées à des champs de vecteurs parallèles à e_3 et ne dépendant que de (x_1,x_2) étant des combinaisons linéaires des tenseurs $e_1\otimes e_2$ et $e_2\otimes e_3$, on cherche w sous la forme :

$$w(x,y,z) \ = \sum_{k\in\mathbb{Z}_*^4} R^T(k)\Big[\lambda_k^1(x_1,x_2)e^{2i\pi k\cdot(y,z)}e_1\otimes e_3 + \lambda_k^2(x_1,x_2)e^{2i\pi k\cdot(y,z)}e_2\otimes e_3\Big]$$

Considérant alors l'application linéaire continue L du théorème 9, on a :

$$L(w(x,y,z)) = \sum_{k\in\mathbb{Z}_*^4} R^T(k)\Big[\lambda_k^2 e^{2i\pi k\cdot(y,z)}e_1 - \lambda_k^1 e^{2i\pi k\cdot(y,z)}e_2\Big]$$

$(\mathcal{P}_i^x)$ s'écrit dans ce cas :

$$\begin{aligned}(\mathcal{P}_1^x): \quad & \int_{Y^2\times Y^2} \frac{1}{\varepsilon(x,y,z)}\left\{1 + \sum_{(m,n)\in\mathbb{Z}_*^4} R^T(k)\Big[\lambda_k^2 e^{2i\pi k\cdot(y,z)}\Big]\right\} \\ & \left\{\sum_{k\in\mathbb{Z}_*^4} R^T(k)\Big[\lambda_k'^2 e^{2i\pi k\cdot(y,z)}\Big]\right\} dydz = 0 \\ (\mathcal{P}_2^x): \quad & \int_{Y^2\times Y^2} \frac{1}{\varepsilon(x,y,z)}\left\{1 - \sum_{k\in\mathbb{Z}_*^4} R^T(k)\Big[\lambda_k^1 e^{2i\pi k\cdot(y,z)}\Big]\right\} \\ & \left\{\sum_{k\in\mathbb{Z}_*^4} R^T(k)\Big[\lambda_k'^1 e^{2i\pi k\cdot(y,z)}\Big]\right\} dydz = 0\end{aligned}$$

Posant alors :

$$\begin{cases} \lambda_k^1(x_1,x_2) & = \theta_k^{1,1}\dfrac{\partial}{\partial x_1}H_0^3(x_1,x_2) - \theta_k^{1,2}\dfrac{\partial}{\partial x_2}H_0^3(x_1,x_2) \\ \lambda_k^2(x_1,x_2) & = \theta_k^{2,1}\dfrac{\partial}{\partial x_1}H_0^3(x_1,x_2) - \theta_k^{2,2}\dfrac{\partial}{\partial x_2}H_0^3(x_1,x_2) \end{cases}$$

On déduit du i) du théorème 9 que H_0^3 est solution dans $\mathcal{D}'(D)$ de l'équation :

$$\mathrm{div}_x\left\{\Big[\int_{Y^2\times Y^2}(\frac{1}{\varepsilon(x,y,z)}+\frac{B(y,z)}{\varepsilon(x,y,z)})\,dydz\Big]\bigtriangledown H_0^3(x_1,x_2)\right\} - k_0^2 H_0^3(x_1,x_2) = 0$$

où $B_(y,z)$ est la matrice définie par :

$$B(y,z) = \sum_{k\in\mathbf{Z}_*^4} R^T(k)\Big(\theta_k^{1,1}e_1\otimes e_1 + \theta_k^{1,2}e_1\otimes e_2 + \theta_k^{2,1}e_2\otimes e_1 + \theta_k^{2,2}e_2\otimes e_2\Big)e^{2i\pi k\cdot(y,z)}$$

Pour faire le lien entre les problèmes annexes $\mathcal{P}_j^x$ et $\mathcal{Q}_j^x$, il suffit de poser :

$$v_j = \sum_{p=1}^{2}\sum_{k\in\mathbf{Z}_*^4} R^t(k)\theta_k^{p,j}e^{2i\pi k\cdot(y,z)}$$

Remarque :

Nous devons résoudre le problème local $\mathcal{Q}_j^x$, $j\in\{1,2\}$:

$$\iint_{Y^2\times Y^2}\frac{1}{\varepsilon(x,y,z)}(e_j+v_j(y,z))v_j'(y,z)\,dydz = 0\ ,\ \forall\, v'\in\mathcal{L}_R \tag{16}$$

On note pour cela que e_j est une fonction constante de $[L^2_\sharp(Y^2\times Y^2)]^2$ et que v_j est élément de $\mathcal{L}_R$. De (16), on déduit que $e_j + v_j(y,z)\in\mathcal{L}_R^\perp$. Le théorème de projection orthogonale nous assure alors de l'existence d'un projecteur $P_{\mathcal{L}_\mathcal{R}}$ sur $\mathcal{L}_R$ parallèlement à $\mathcal{L}_R^\perp$ tel que v_j est l'unique solution dans $[L^2_\sharp(Y^2\times Y^2)]^2$ du problème $\mathcal{Q}_j$, $j\in\{1,2\}$:

$$\mathcal{Q}_j :\ -v_j = P_{\mathcal{L}_\mathcal{R}}(e_j) \Longleftrightarrow e_j + v_j(y,z)\in\mathcal{L}_R^\perp \ \text{ et } v_j\in\mathcal{L}_R$$

En d'autres termes, résoudre le problème $\mathcal{Q}_j$, c'est trouver la projection dans l'espace de Hilbert $[L^2_\sharp(Y^2\times Y^2)]^2$ de e_j sur le sous-espace fermé $\mathcal{L}_R$: on peut donc envisager de résoudre le problème annexe avec une méthode numérique de type "moindre carrés".

4.6.2 Étude du cas mono-dimensionnel $H\parallel$

On considère un milieu quasi-périodique hétérogène d'épaisseur finie, stratifié suivant (Ox). On éclaire ce quasi-cristal mono-dimensionnel par une onde plane (pulsation ω) sous l'incidence θ, venant des x positifs i.e. la fonction ε ne dépend que de x. On se propose d'étudier le comportement électromagnétique d'une telle structure quand le nombre de couches tend vers l'infini, cependant que l'onde incidente reste en résonance avec la structure dont l'épaisseur est fixe. On considère le cas de polarisation $H\parallel$ pour lequel le champ magnétique peut se mettre sous la forme :

$$H_\eta(x,y,z) = u_\eta(x)e^{i\beta y}e_z$$

où $\beta = k_0^2 \sin\theta$ et $k_0^2 = \omega^2 \mu_0$. Par ailleurs, $H_\eta^z(x,y) = u_\eta(x) e^{i\beta y}$ est solution faible dans $\mathbb{R}^2$ de l'équation :

$$\mathrm{div}(\varepsilon_\eta^{-1}(x) \bigtriangledown H_\eta^z) + k_0^2 H_\eta^z = 0$$

On en déduit que $u_\eta(x) e^{i\beta y}$ est solution dans $\mathcal{D}'(\mathbb{R}^2)$ de l'équation :

$$\frac{d}{dx}\Big(\varepsilon_\eta^{-1}(x)\frac{du_\eta}{dx}(x)e^{i\beta y}\Big) + \frac{d}{dy}\Big(i\beta\varepsilon_\eta^{-1}(x)u_\eta(x)e^{i\beta y}\Big) + k_0^2 u_\eta(x) = 0$$

La composante tangentielle u_η du champ magnétique H_η est donc solution dans $\mathcal{D}'(\mathbb{R})$ de l'équation :

$$\frac{d}{dx}\Big(\varepsilon_\eta^{-1}(x)\frac{du_\eta}{dx}(x)\Big) + (k_0^2 - \beta^2\varepsilon_\eta^{-1}(x))u_\eta(x) = 0 \tag{1}$$

Dans le superstrat ($x > 1$), la permittivité relative du milieu ε_η est constante et vaut $\varepsilon_0 = 1$ (air). En conséquence, u_η est solution de l'équation :

$$u_\eta''(x) + \gamma^2 u_\eta(x) = 0$$

où $\gamma^2 = k_0^2 - \beta^2$.

On en déduit qu'il existe A_η et B_η dans $\mathbb{R}$ telles que :

$$u_\eta(x) = A_\eta e^{i\gamma x} + B_\eta e^{-i\gamma x}$$

Compte tenu des conditions d'ondes sortantes, notant r_η le coefficient de reflexion de l'onde incidente, pour tout $x > 1$, on a :

$$u_\eta(x) = r_\eta e^{i\gamma x} + e^{-i\gamma x}$$

Par ailleurs, d'après (1) la composante tangentielle u_η du champ magnétique H_η est continue sur l'interface $\{x = 1\}$:

$$u_\eta(1^+) - u_\eta(1^-) = 0$$

La condition d'impédance en $\{x = 1\}$ est alors explicite :

$$u_\eta'(1) - i\gamma u_\eta(1) = -2i\gamma e^{-i\gamma} \tag{2}$$

De même, dans le substrat ($x < 0$), notant t_η le coefficient de transmission de l'onde incidente, on montre que :

$$u_\eta(x) = t_\eta e^{-i\gamma x}$$

On en déduit la condition d'impédance en $\{x = 0\}$:

$$u_\eta'(0) + i\gamma u_\eta(0) = 0 \tag{3}$$

Pour tout $\eta > 0$, u_η est donc solution du problème de diffraction suivant :

$$\mathcal{P}_{\eta,\alpha} \begin{cases} \dfrac{d}{dx}\Big(\varepsilon_\eta^{-1}(x)\dfrac{du_\eta}{dx}(x)\Big) + (k_0^2 - \beta^2\varepsilon_\eta^{-1}(x))u_\eta(x) = 0 & \text{, dans } \mathcal{D}'(]0;1[) \\ {u_\eta}'(0) + i\gamma u_\eta(0) = 0\ ,\ {u_\eta}'(1) - i\gamma u_\eta(1) = -2i\gamma e^{-i\gamma} \end{cases}$$

où $\varepsilon_\eta(x) = \varepsilon(\frac{x}{\eta}, \alpha\frac{x}{\eta})$ ($\varepsilon \in L^\infty_\sharp(Y \times Y)$ où $Y =]0;1[$, et $\varepsilon \geq \varepsilon_0$)

Pour l'existence et l'unicité du problème $\mathcal{P}_{\eta,\alpha}$, on pourra consulter [51].

L'étude asymptotique du problème de diffraction $\mathcal{P}_{\eta,\alpha}$ quand η tend vers 0, conduit au résultat très simple suivant :

Proposition 12

Soient $\alpha \in \mathbb{R}^+_* \setminus \mathbb{Q}$ et u_η l'unique solution du problème $\mathcal{P}_{\eta,\alpha}$. Alors u_η converge faiblement dans $W^{1,2}(]0;1[, \mathbb{C})$ vers l'unique solution u du problème homogénéisé suivant :

$$\mathcal{P}_{0,\alpha} \begin{cases} \dfrac{d}{dx}\Big(< \varepsilon >^{-1} \dfrac{du}{dx}(x)\Big) + (k_0^2 - \beta^2 < \varepsilon^{-1} >)u(x) = 0 \quad \text{, dans } \mathcal{D}'(]0;1[) \\ u'(0) + i\gamma u(0) = 0 \ , \ u'(1) - i\gamma u(1) = -2i\gamma e^{-i\gamma} \end{cases}$$

où $< f >:= \displaystyle\int_{Y\times Y} f(\xi_1, \xi_2)\, d\xi_1 d\xi_2$ et $Y =]0;1[$.

Remarque :

La preuve peut se faire directement sous la seule hypothèse que les suites ε_η et ε_η^{-1} convergent faiblement (dans notre cas, les limites de ces deux suites sont respectivement $< \varepsilon >$ et $< \varepsilon^{-1} >$). On note pour cela que $\chi_\eta = {\varepsilon_\eta}^{-1} \dfrac{du_\eta}{dx}(x)$ converge fortement dans $L^2(]0;1[)$ vers une limite χ. Par conséquent, $\dfrac{du_\eta}{dx}(x) = \chi_\eta \varepsilon_\eta$ converge faiblement dans $L^2(]0;1[)$ vers $\dfrac{du}{dx}(x) = \chi < \varepsilon >$. La limite χ est donc donnée par $\chi =< \varepsilon >^{-1} \dfrac{du}{dx}(x)$. Par ailleurs, comme u_η converge fortement dans $L^2(]0;1[)$ vers u, on déduit que la suite $u_\eta \varepsilon_\eta^{-1}$ converge faiblement dans $L^2(]0;1[)$ vers $u < \varepsilon >^{-1}$.

Pour la commodité du lecteur, nous remontrons ce résultat en appliquant directement la proposition 11 dans le cas d'un milieu stratifié i.e. ne dépendant que de la variable x_1.

Démonstration :

On note $\mathcal{L}_\alpha$ le sous-espace de $L^2_\sharp(Y \times Y)$ suivant :

$$\mathcal{L}_\alpha = \Big\{ w \in L^2_\sharp(Y \times Y) \ \mid \ w(y,z) = \sum_{(m,n)\in\mathbb{Z}\times\mathbb{Z}\setminus\{0,0\}} \lambda_{m,n}\, (m + \alpha n) e^{2i\pi(my+nz)} \ , \ \lambda_{m,n} \in \mathbb{C} \Big\}$$

Soit alors l'application linéaire continue $R \ : \ x \in \mathbb{R} \longmapsto (x, \alpha x) \in \mathbb{R}\times\mathbb{R}$. Puisque α est irrationnel, $R^T(m,n) = m + \alpha n \neq 0$, $\forall (m,n) \in \mathbb{Z} \times \mathbb{Z} \setminus \{0,0\}$, donc R vérifie la condition d'admissibilité (0) pour la convergence à deux échelles relativement à une matrice. De la proposition 11, on déduit alors que u_η converge faiblement dans $W^{1,2}(]0;1[, \mathbb{C})$ vers la solution u de l'équation homogénéisée suivante :

$$\frac{d}{dx}\Big(\varepsilon_0^{-1} \frac{du}{dx}(x)\Big) + (k_0^2 - \beta^2 < \varepsilon^{-1} >)u(x) = 0 \ \text{ dans } \mathcal{D}'(]0;1[)$$

la permittivité ε_0 étant donnée par :

$$\varepsilon_0^{-1} =< \varepsilon^{-1} > + < \frac{w}{\varepsilon} >$$

où $w \in \mathcal{L}_\alpha$ est l'unique solution du problème variationnel suivant :

$$\int_{Y\times Y} \frac{1}{\varepsilon}\varphi(\xi_1,\xi_2)\,d\xi_1 d\xi_2 = -\int_{Y\times Y} \frac{1}{\varepsilon} w(\xi_1,\xi_2)\varphi(\xi_1,\xi_2)\,d\xi_1 d\xi_2 \ ,\ \forall \varphi \in \mathcal{L}_\alpha$$

$\frac{1}{\varepsilon}(1+w)$ appartient donc à $\mathcal{L}_\alpha^\perp$. Par ailleurs, le lemme 6 nous assure que $\mathcal{L}_\alpha$ est un sous-espace fermé de $L^2_\sharp(Y\times Y)$ ($\mathcal{L}_\alpha$ est donc un Hilbert) dont le sous-espace orthogonal $\mathcal{L}_\alpha^\perp$ dans $L^2_\sharp(Y\times Y)$ est donné par :

$$\mathcal{L}_\alpha^\perp = \Big\{ v \in L^2_\sharp(Y\times Y) \ \mid \ v(y,z) = \sum_{(m,n)\in \mathbb{Z}_*\times\mathbb{Z}_*} D_{m,n} e^{2i\pi(my+nz)} \ ; \\ D_{m,n} \perp (m+\alpha n)\ ,\ \forall (m,n)\in \mathbb{Z}_*\times\mathbb{Z}_* \Big\}$$

On note alors que $\mathcal{L}_\alpha^\perp$ est réduit à l'ensemble des fonctions constantes sur la cellule $Y\times Y$. Il existe donc une unique constante $c \in \mathbb{C}$ telle que :

$$\frac{1}{\varepsilon}(1+w(\xi_1,\xi_2)) = c$$

Par ailleurs, w est élément de $\mathcal{L}_\alpha$, donc sa moyenne sur la cellule $Y\times Y$ est nulle. La constante c est alors donnée par :

$$c = < \varepsilon >^{-1}$$

Il s'ensuit que w satisfait :

$$\frac{w}{\varepsilon} = \frac{1}{< \varepsilon >} - \frac{1}{\varepsilon}$$

Notant alors que $< \frac{w}{\varepsilon} >= \frac{1}{< \varepsilon >} - < \varepsilon^{-1} >$, on en conclut que :

$$\varepsilon_0^{-1} = < \varepsilon >^{-1}$$

Il nous reste à établir les conditions d'impédance vérifiées par le problème limite $\mathcal{P}_{0,\alpha}$. Soit alors u_η la solution faible dans $\mathcal{D}'(\mathbb{R})$ de l'équation (1) :

$$\frac{d}{dx}\Big(\varepsilon_\eta^{-1}(x)\frac{du_\eta}{dx}(x)\Big) = \Big(-k_0^2 + \beta^2 \varepsilon_\eta^{-1}(x)\Big) u_\eta(x)$$

Cela implique que $\frac{1}{\varepsilon_\eta}\frac{du_\eta}{dx}(x)$ et $\frac{du_\eta}{dx}(x)$ sont continues sur $\mathbb{R}$, donc sur $[0;1]$.

De plus, $\frac{1}{\varepsilon_\eta}\frac{du_\eta}{dx}(x)$ étant continue sur $[0;1]$, elle converge uniformément vers $\frac{1}{\varepsilon_0}\frac{du}{dx}(x)$ dans $[0;1]$.

D'après la continuité de $\frac{1}{\varepsilon_0}\frac{du}{dx}(x)$ sur $[0;1]$ (limite uniforme d'une suite de fonctions continues), et remarquant que ε_0 vaut 1 en dehors de $]0;1[$, on en déduit que $\frac{1}{\varepsilon_0}\frac{du}{dx}(0^+) = \frac{du}{dx}(0^-)$. Par ailleurs, u_η est continue sur $[0;1]$, donc converge uniformément vers u qui est continue sur $[0;1]$. On obtient alors la condition d'impédance sur $\{x=0\}$ pour $\mathcal{P}_{0,\alpha}$, par passage à la limite dans (3) :

$$\frac{du}{dx}(0) + i\gamma u(0) = 0 \tag{4}$$

De manière analogue, on obtient la condition d'impédance sur $\{x = 1\}$, par passage à la limite dans (2) :

$$\frac{du}{dx}(1) - i\gamma u(1) = -2i\gamma e^{-i\gamma} \tag{5}$$

(QED)

Chapitre 5

Comportement asymptotique de l'erreur

"Proof is an idol before which the mathematician tortures himself."
Sir Arthur Eddington.

"C'est l'une des pratiques spontanées du chercheur, quand il piétine devant une difficulté technique de son montage ou une erreur masquée de son calcul, que d'aller exposer son problème aux collègues voisins [...]. Le simple fait de s'adresser à un autre, par l'effort d'explication et de conviction qu'il exige, mobilise plus intensément la pensée que la réflexion solitaire, et lui permet souvent de faire sauter les entraves."
Jean Marc Lévy Leblond [129].

5.1 Préliminaires

5.1.1 Position du problème physique

Notre objectif est maintenant d'estimer l'erreur R_η commise sur la solution approchée u_η de la solution u du problème limite. Pour ce faire, nous restreignons le cadre de notre étude au problème d'électrostatique suivant : pour tout $\eta > 0$, u_η est l'unique solution dans $H^1(]0;1[)/\mathbb{R}$ du problème :

$$\mathcal{P}_{\eta,\alpha} \left\{ \begin{array}{l} \dfrac{d}{dx}\Big(\varepsilon_\eta(x)\dfrac{du_\eta}{dx}(x)\Big) = 0 \quad \text{, sur }]0;1[\\ u_\eta(0) = 0\ ,\ u_\eta(1) = 1 \end{array} \right.$$

où $\varepsilon_\eta(x) = \varepsilon(\dfrac{x}{\eta}, \alpha\dfrac{x}{\eta})(\varepsilon \in L^\infty_\sharp(Y \times Y)$ avec $Y =]0;1[$ et $\varepsilon \geq \varepsilon_0)$. Ce problème d'électrostatique revient à se donner une différence de potentiel aux deux bornes d'un condensateur constitué d'un milieu périodique hétérogène de période η et à étudier la limite asymptotique du champ électrostatique quand η tend vers 0. Plus précisément, on désire évaluer la vitesse de convergence de $\left\|\dfrac{R_\eta}{\eta}\right\|_{L^2(]0;1[)} = \left\|\dfrac{u_\eta - u}{\eta}\right\|_{L^2(]0;1[)}$ vers 0. Cette dernière dépend

étroitement de la nature de α i.e. de la façon dont α est approché par une suite de rationnels. Nous rappelons donc en premier lieu les résultats de théorie des nombres qui nous seront utiles pour la suite.

5.1.2 Rappels de théorie des nombres

Se donnant un nombre $\alpha \in \mathbb{R}$, on peut (par densité de $\mathbb{Q}$) trouver pour tout $\eta > 0$ un couple $(p, q) \in \mathbb{Z} \times \mathbb{Z}_*$ tel que :

$$| \frac{p}{q} - \alpha | \leq \eta$$

La question est maintenant de savoir à quelle vitesse on peut approcher α. Un résultat classique [110] est que pour un réel α et un entier n donnés, **il existe** un couple (p, q) d'entiers, $0 < q \leq n$ tel que :

$$| \frac{p}{q} - \alpha | \leq \frac{1}{q(n+1)}$$

Cela entraine en particulier que :

$$| \frac{p}{q} - \alpha | < \frac{1}{q^2} \qquad (*)$$

Ce résultat appelle deux remarques :

Remarque 1 : Si α est un rationnel $\frac{a}{b}$, alors pour tout $(p, q) \in \mathbb{Z} \times \mathbb{Z}_*$ tel que $\frac{p}{q} \neq \alpha$, on a :

$$| \frac{p}{q} - \alpha | = | \frac{p}{q} - \frac{a}{b} | = \frac{| bp - aq |}{bq} \geq \frac{1}{bq} \qquad (**)$$

Il résulte alors de $(*)$ que l'entier q dans $(**)$ vérifie $q < b$. Autrement dit, si α est rationnel, il y a seulement un nombre **fini** de solutions à $(*)$.

Remarque 2 : Rappelons l'approximation d'un réel par une suite de fractions continues. Étant donnée une suite d'entiers non nuls $(a_1,\ a_2,\ a_3,\ ...,\ a_n,\ ...)$ on définit

$$[a_1,\ ...,\ a_n,\ ...] = a_1 + \frac{1}{a_2 + \frac{1}{a_3 + ...}} = \lim_{n \to 0} [a_1,\ ...,\ a_n]$$

où la suite $([a_1,\ ...,\ a_n])$ est définie par :

$$[a_1,\ ...,\ a_n] = a_1 + \frac{1}{[a_2,\ ...,\ a_n]} = [a_1,\ [a_2,\ ...,\ a_n]]$$

Alors pour tout réel α, il existe une suite unique $([a_1,\ ...,\ a_n])$ telle que $\alpha = [a_1,\ ...,\ a_n,\ ...]$ et on appelle n-ième convergent de α le rationnel $[a_1, ..., a_n]$. Par exemple, le nombre d'or τ peut être défini par :

$$\tau = 1 + \frac{1}{1 + \frac{1}{1 + ...}} = [1, 1, 1, ...] = \frac{1 + \sqrt{5}}{2}$$

On génère ainsi une suite d'approximants $\frac{p_n}{q_n}$ donnés par les termes successifs de la suite de Fibonacci :

$$\begin{cases} q_n & = p_{n-1} \\ p_n & = q_{n-1} + p_{n-1} \\ p_0 & = q_0 = 1 \end{cases}$$

Il est bien connu (voir [110]) que si $\frac{p_n}{q_n}$ est le n-ième convergent d'un irrationnel α, on a

$$| \frac{p_n}{q_n} - \alpha | < \frac{1}{q_n^2} \qquad (***)$$

d'où l'équation $(*)$ admet contrairement au cas $\alpha \in \mathbb{Q}$ une **infinité** de solutions. Ceci permet de distinguer un α irrationnel d'un α rationnel. Ce principe de distinction peut-être généralisé en remplaçant $(***)$ par une inégalité du type $| \frac{p}{q} - \alpha | < \frac{C(\alpha)}{q^\xi}$ comme cela est décrit ci-dessous :

Définition 1 :

On dit que α est approximable à l'ordre ξ (ξ entier > 0), s'il existe une constante $C(\alpha) > 0$ telle que l'inéquation :

$$| \frac{p}{q} - \alpha | < \frac{C(\alpha)}{q^\xi} ,$$

admet une infinité de couples (p, q) solutions.

Il est clair que si α est approximable à l'ordre ξ, il le sera a fortiori pour tout ordre $\xi' < \xi$. On définit donc l'ordre d'approximation du réel α comme la borne supérieure des entiers ξ pour lesquels α est approximable à l'ordre ξ.

Commentaires :

D'après la remarque 1, l'ordre d'approximation d'un rationnel est égal à 1 (noter que l'équation $bp - aq = 1$ admet une infinité de solutions) et d'après la remarque 2, il est supérieur à 2 pour tout irrationnel. Dans le cas du nombre d'or τ, il est égal à 2 (voir [110]) et dans le cas des nombres de Liouville il est infini.

Notons que si α a un degré d'approximation égal à ξ_0, alors pour tout $\xi > \xi_0$ et toute constante $C(\alpha) > 0$ l'équation

$$| \frac{p}{q} - \alpha | < \frac{C(\alpha)}{q^\xi} ,$$

admet au plus un nombre fini de solutions. Il en résulte (pour $C = 1$ par exemple) que pour tout $\xi > \xi_0$, il existe un entier q_0 tel que :

$$| \frac{p}{q} - \alpha | > \frac{1}{q^\xi} , \ \forall q \geq q_0 \qquad (****)$$

C'est cette inégalité qui permettra de minorer le correcteur R_η. En fait, une inégalité de type $(****)$ peut-être obtenue en pratique à l'aide du théorème de Liouville :

Théorème de Liouville :

Si α vérifie une équation algébrique d'ordre n, alors $(****)$ a lieu pour $\xi = n$. Il en résulte que l'ordre ξ_0 d'approximation d'un tel α est nécessairement $\leq n$.

Preuve :

Soit α un irrationnel algébrique racine du polynôme à coefficients entiers :

$$f(\alpha) = a_0\alpha^n + a_1\alpha^{n-1} + ... + a_n$$

Il existe une constante $M(\alpha) > 0$ telle que pour tout $x \in]\alpha - 1\ ;\ \alpha + 1[$,

$$| f'(x) | < M(\alpha) \tag{1}$$

Soit $\frac{p}{q} \neq \alpha$ une approximation de α telle que $\frac{p}{q} \in]\alpha - 1\ ;\ \alpha + 1[$. De plus, nous choisissons cette approximation telle qu'elle soit plus proche de α que l'une quelconque des autres racines de $f(x) = 0$, de sorte que $f(\frac{p}{q}) \neq 0$. Puisque $f(\frac{p}{q})$ est un entier ≥ 1, on en déduit que :

$$| f(\frac{p}{q}) | = \frac{| a_0 p^n + a_1 p^{n-1} q + ... |}{q^n} \geq \frac{1}{q^n} \tag{2}$$

f étant continue sur $[\frac{p}{q}\ ;\ \alpha]$ et dérivable sur $]\frac{p}{q}\ ;\ \alpha[$, le théorème des accroissements finis nous assure qu'il existe une constante $x \in]\frac{p}{q}\ ;\ \alpha[$ telle que :

$$f(\frac{p}{q}) = f(\frac{p}{q}) - f(\alpha) = (\frac{p}{q} - \alpha) f'(x) \tag{3}$$

De (1), (2) et (3), on tire alors que :

$$| \frac{p}{q} - \alpha | = \frac{| f(\frac{p}{q}) |}{| f'(x) |} > \frac{1}{M(\alpha) q^n}$$

(QED)

Commentaires :

Le théorème précédent fournit un critère de distinction entre les irrationnels algébriques et les irrationnels transcendantaux. Dans le cas où α est un nombre de Liouville i.e. de la forme :

$$\alpha = \sum_{n=0}^{+\infty} 10^{-n!}\ ,$$

notant α_i la somme des i premiers termes de la série, il existe un couple d'entiers (p, q) tel que $\alpha_i = \frac{p}{10^{i!}} = \frac{p}{q}$. Alors pour tout $N \geq i + 1$, on a :

$$0 < \alpha - \frac{p}{q} = \alpha - \alpha_i = \sum_{n=i+1}^{+\infty} 10^{-n!} < 2.10^{-(i+1)!} < 2q^{-N}\ .$$

Il en résulte que le degré d'un tel nombre α est arbitrairement grand (donc α est transcendantal).

Les résultats précédents nous assurent que pour un irrationnel algébrique α d'ordre $\xi \geq 2$, il existe deux constantes $C_1(\alpha)$ et $C_2(\alpha) > 0$ et un réel s $(2 < s \leq \xi)$ tels que :

$$\frac{C_1(\alpha)}{q^\xi} \leq | \frac{p}{q} - \alpha | \leq \frac{C_2(\alpha)}{q^s} \leq \frac{1}{q^2}$$

En résumé, pour tout irrationnel α, il existe une fonction bornée $f_\alpha(q)$ telle que :

$$\inf_{p \in \mathbb{N}} | \frac{p}{q} - \alpha | = \frac{f_\alpha(q)}{q^2}\ .$$

De plus, on a $\lim_{q \to +\infty} f_\alpha(q) = 0$, dès que le degré ξ de α est > 2.

5.1.3 Estimation d'une serie

Notant B_η une bande de largeur η orientée suivant la droite de coupe-projection

$$B_\eta = \Big\{(m,n) \in \mathbb{Z}\times\mathbb{Z}\setminus\{0,0\}\ ,\ \mid m+\alpha n \mid \leq \eta\Big\}\ , \tag{4}$$

nous sommes maintenant en mesure d'établir une première estimation de la fonction

$$\Theta(\eta) = \sum_{(m,n)\in B_\eta} \mid C_{m,n} \mid^2\ , \tag{5}$$

qui joue un rôle essentiel dans le résultat de correcteur.

Remarque :

Il est facile de vérifier que $\lim\limits_{\eta\to 0} \sum\limits_{(m,n)\in B_\eta} \mid C_{m,n} \mid^2 = 0$. En effet, puisque $\alpha \notin \mathbb{Q}$, l'intersection $\bigcap\limits_{\eta>0} B_\eta$ est vide et donc en appliquant le théorème de convergence monotone à la suite $\mid C_{m,n} \mid^2 \chi_{B_\eta}(n,m)$ définie sur $\mathbb{Z}\times\mathbb{Z}\setminus(0,0)$ muni de la mesure discrète $\mu = \sum\limits_{(m,n)\in\mathbb{Z}^2_*} \delta_{(m,n)}$, on a :

$$\lim_{\eta\to 0} \sum_{(m,n)\in B_\eta} \mid C_{m,n} \mid^2 = \lim_{\eta\to 0}\downarrow \int_{\mathbb{Z}^2_*} \mid C_{m,n} \mid^2 \chi_{B_\eta}(n,m) d\mu = \int_{\mathbb{Z}^2_*} \Big(\lim_{\eta\to 0}\downarrow \mid C_{m,n} \mid^2 \chi_{B_\eta}(n,m)\Big) d\mu = 0$$

Il s'agit maintenant d'estimer la vitesse de convergence vers 0 qui dépend étroitement du degré d'irrationnalité de α.

Lemme 1

Soit α un irrationnel solution d'une équation algébrique de degré ξ. Soit $r > 0$ et ε un élément de $H_\sharp^{\frac{1}{2}-r}(Y^2)$ i.e.

$$\sum_{(m,n)\in\mathbb{Z}^2} \mid C_{m,n} \mid^2 \Big[1 + (m^2+n^2)^{\frac{1}{4}-\frac{r}{2}}\Big] < +\infty$$

Alors, on a :

$$\sum_{(m,n)\in B_\eta} \mid C_{m,n} \mid^2 = o(\eta^{(\frac{1}{2}-r)(\frac{1}{\xi-1})})$$

où B_η est défini par (4).

Remarque :

En pratique, nous utilisons des permittivités ε_η provenant d'une coupe-projection correspondant à une fonction ε périodique sur $\mathbb{R}^2$ et constante par morceaux. Il est bien connu que de telles fonctions appartiennent à l'espace $H_\sharp^{\frac{1}{2}-r}(Y^2)$ pour tout $r > 0$ (Maz'ja, 1985 [139]).

Démonstration :

On peut supposer que α est > 0. D'après le théorème de Liouville, il existe une constante $C > 0$ telle que :

$$| \frac{n}{m} + \alpha | > \frac{C}{| m |^{\xi}} , \forall (m,n) \in \mathbb{Z}_*^2$$

Il en résulte que pour tout $(m,n) \in B_\eta$, on a :

$$\frac{C}{| m |^{\xi}} < | \frac{n}{m} + \alpha | \leq \frac{\eta}{| m |}$$

Le rapport $\frac{\eta}{m}$ étant minoré sur B_η, on a donc pour une constante C_1 adéquate :

$$\begin{aligned} n^2 + m^2 &\geq C_1 m^2 \\ &= C_1 | m^{\xi - 1} |^{\frac{2}{\xi - 1}} \\ &\geq C_1 \left| \frac{C}{\eta} \right|^{\frac{2}{\xi - 1}} , \end{aligned}$$

pour tout couple (m,n) dans B_η.

On en déduit qu'il existe une constante C_2 telle que pour tout couple (m,n) dans B_η :

$$\begin{aligned} \sum_{(m,n) \in B_\eta} | C_{m,n} |^2 &= \sum_{(m,n) \in B_\eta} | C_{m,n} |^2 (n^2 + m^2)^{-\frac{1}{4} + \frac{r}{2}} (n^2 + m^2)^{\frac{1}{4} - \frac{r}{2}} \\ &\leq C_1^{-(\frac{1}{4} - \frac{r}{2})} \sum_{(m,n) \in B_\eta} | C_{m,n} |^2 ((\frac{C}{\eta})^{-(\frac{1}{4} - \frac{r}{2})(\frac{2}{\xi - 1})}) (n^2 + m^2)^{\frac{1}{4} - \frac{r}{2}} \\ &\leq \frac{C_2}{\eta^{(\frac{1}{2} - r)(\frac{1}{\xi - 1})}} \Psi(\eta) \end{aligned}$$

où $\Psi(\eta) := \sum_{(m,n) \in B_\eta} | C_{m,n} |^2 (n^2 + m^2)^{\frac{1}{4} - \frac{r}{2}}$.

Puisque $\sum_{(m,n) \in \mathbb{Z}_*^2} | C_{m,n} |^2 (n^2 + m^2)^{\frac{1}{4} - \frac{r}{2}} \leq \| \varepsilon \|^2_{H^{\frac{1}{2} - r}} < +\infty$, et notant que l'intersection $\bigcap_{\eta > 0} B_\eta$ est vide, on déduit du théorème de convergence monotone que $\lim_{\eta \to 0} \Psi(\eta) = 0$.

(QED)

5.1.4 Examples pratiques :

Dans le lemme 1 nous avons obtenu une majoration de l'ordre de convergence vers 0 de la fonction $\Theta(\eta)$ définie par (5). Du fait que le théorème de Liouville ne donne qu'une minoration de la vitesse de convergence, nous ne sommes pas capables de donner un équivalent de $\Theta(\eta)$ quand $\eta \to 0$. Cependant dans le cas du nombre d'or $\alpha = \tau = \frac{1 + \sqrt{5}}{2}$ (dans ce cas $\xi = 2$ et $\Theta(\eta) = o(\eta^{\frac{1}{2} - r})$, $\forall r > 0$), nous allons établir que pour une fonction périodique constante par morceaux $\varepsilon(x,y)$, il existe une constante C telle que :

$$\Theta(\eta) \sim C \eta^2 , \quad \text{quand } \eta \to 0 . \tag{6}$$

La démonstration de ce résultat est basée sur l'estimation de la fonction $f(\eta)$ suivante :

$$f(\eta) = \sum_{[q\tau]\leq\eta} \frac{1}{q^s}$$

où s est > 1 et $[q\tau] = q\tau - E(q\tau) = q\tau - p$.

L'estimation précise de la fonction $f(\eta)$ au voisinage de $\{\eta = 0\}$, utilise de façon essentielle les propriétés des approximants du nombre d'or τ.

On considère pour cela ε, la permittivité du réseau de $\mathbb{R}^2$ dont on prend la coupe-projection suivant la droite de pente $\alpha = \tau$. Alors il existe une constante $C > 0$ telle que :

$$\sum_{(m,n)\in B_\eta} \mid C_{n,m} \mid^2 \sim C\eta^2$$

Proposition 2

Pour tout $s > 1$, si τ désigne le nombre d'or $\tau = \dfrac{1+\sqrt{5}}{2}$, on a :

$$f(\eta) = \sum_{[q\tau]\leq\eta} \frac{1}{q^s} = O(\eta^s)$$

Commentaires :

Ce résultat nous donne un équivalent pour $f(\eta)$ (voir annexe) :

$$\exists C > 0\ ,\ f(\eta) = \sum_{[q\tau]\leq\eta} \frac{1}{q^s} \sim C\eta^s\ ,\ \text{quand } \eta \to 0$$

La preuve de la proposition 2 est rejetée en annexe B. Dans le cas général d'un nombre algébrique, nous ne donnons que des résultats de majoration (voir lemme 1 et lemme 2 de l'annexe B).

Dans la section suivante, nous établissons notre résultat principal sur le correcteur.

5.2 Estimation du correcteur

Dans cette section, on s'interesse plus particulièrement à la minoration du correcteur, dans la mesure ou des estimations pour la borne supérieure existent dans la littérature [115].

Proposition 3

Soit $\alpha \in \mathbb{R}_*^+ \setminus \mathbb{Q}$, $Y =]0;1[$ et u_η l'unique solution du problème $\mathcal{P}_{\eta,\alpha}$. Alors u_η converge faiblement dans $W^{1,2}(]0;1[,\mathbb{R})$ vers l'unique solution u du problème homogénéisé suivant dans $W^{1,2}(]0;1[,\mathbb{R})/\mathbb{R}$:

$$\mathcal{P}_{0,\alpha} \begin{cases} \dfrac{d}{dx}\Big(< \varepsilon^{-1} >^{-1} \dfrac{du}{dx}(x)\Big) = 0 \quad , \text{sur }]0;1[\\ u(0) = 0\ ,\ u(1) = 1 \end{cases}$$

où $< f >:= \int_{Y\times Y} f(\xi_1,\xi_2)\,d\xi_1 d\xi_2$. Par ailleurs, si α est un irrationnel solution d'une équation algébrique (cf. [110]) et $\varepsilon \in H_\sharp^{\frac{1}{2}-r}(Y^2)$, $\forall r>0$, alors :

$$\|\frac{u_\eta(x)-u_0(x)}{\eta}\|^2_{L^2(]0;1[)} \geq \frac{\theta(\eta)}{\eta^2} \qquad (*)$$

où $\theta(\eta) = \sum_{(m,n)\in B_\eta} |\, C_{m,n}\,|^2$.

Remarques :

On conjecture que le comportement asymptotique du correcteur est compris entre celui d'un milieu aléatoire [39]

$$\|u_\eta(x)-u_0(x)\|_{L^2(]0;1[)} \sim \sqrt{\eta}\,,$$

et celui d'un milieu périodique [18]

$$\|u_\eta(x)-u_0(x)\|_{L^2(]0;1[)} \sim \eta\,.$$

Le cas périodique correspond à $\alpha=\tau$, où τ est le nombre d'or. En effet, dans ce cas $\theta(\eta)\sim\eta^2$ d'après la proposition 2 et $(*)$ devient

$$\|\frac{u_\eta(x)-u_0(x)}{\eta^2}\|^2_{L^2(]0;1[)} \geq 1 \qquad (*)$$

Le correcteur est très sensible aux approximants de α : en fait, plus l'irrationnel α est difficile à approcher par un rationnel, meilleur est le correcteur. Plus précisément, si α est un irrationnel transcendantal (par exemple un nombre de Liouville), on conjecture que le correcteur se comporte de manière analogue à celui d'un milieu aléatoire. Ces irrationnels sont les mieux approchés par les rationnels. En effet, un nombre de Liouville α est défini par :

$$\alpha = \sum_{n=0}^{+\infty} 10^{-n!}$$

La théorie des nombres nous assure alors de l'existence de deux entiers $q>N>0$ et d'une constante $C(\alpha)>0$ tels que :

$$\begin{array}{ll} |\alpha - \sum_{n=0}^{N} 10^{-n!}| & \leq C(\alpha)10^{-(N+1)!} \\ & \leq C(\alpha)(\frac{1}{10^{N!}})^{N+1} \sim C(\alpha)(\frac{1}{q})^N \end{array}$$

où q est lié à N par $\log q = N!$. Quand N tend vers l'infini, $\log\log q \sim N\log N$ soit encore

$$N \sim \log\log\log q$$

Contrairement au nombre d'or dont la suite des approximants est très régulière (elle est géométrique), les nombres de Liouville ont un développement en fraction continue très irrégulier. Nous ne sommes pas encore en mesure d'exhiber des irrationnels tels que $\theta(\eta)>\eta^2$, mais l'idée est de prendre un irrationnel quadratique dont le développement en

fraction continu est irrégulier. Par ailleurs, il est bon de noter que si l'on s'intéresse à la minoration du correcteur pour la norme $\|\cdot\|_{W^{1,2}(]0;1[)}$, de tels cas peuvent-être plus faciles à exhiber.

Dans la pratique, il s'avère que les seules phases quasi-cristallines découvertes à ce jour sont celles construites par coupe-projection à l'aide du nombre d'or. La physique de ces matériaux est régie par les lois du chaos : malgré son caractère aléatoire, la croissance des phases quasi-cristallines est expliquée par un principe de moindre energie de type déterministe.

Démonstration :

On montre la proposition sous l'hypothèse que ε est continue.
De l'équation dans $\mathcal{P}_{\eta,\alpha}$, on tire que :

$$\varepsilon_\eta(x)\frac{du_\eta}{dx}(x) = a_\eta \ , \ \text{ sur } [0;1]$$

où la constante a_η est déterminée par la relation suivante :

$$1 = u_\eta(1) - u_\eta(0) = a_\eta \int_0^1 {\varepsilon_\eta}^{-1}(x)\, dx \ .$$

On en déduit que l'unique solution du problème $\mathcal{P}_{\eta,\alpha}$ vérifie :

$$\forall x \in [0;1] \ , \ u_\eta(x) = a_\eta \int_0^x \varepsilon_\eta^{-1}(t)\, dt = \frac{\displaystyle\int_0^x \varepsilon_\eta^{-1}(t)\, dt}{< \varepsilon_\eta^{-1} >} \tag{1}$$

Par conséquent, la suite (u_η) est bornée dans $W^{1,2}(]0;1[) \subset C([0;1])$ et converge uniformément dans $[0;1]$ quand η tend vers 0 vers sa limite simple

$$u(x) = \frac{\displaystyle\int_0^x < \varepsilon^{-1} > \, dt}{< \varepsilon^{-1} >} = x \tag{2}$$

Ici, on a utilisé le fait que la fonction quasi-périodique $b_\eta = \dfrac{\varepsilon_\eta^{-1}}{< \varepsilon_\eta^{-1} >}$ converge $*$-faiblement dans $L^\infty(]0;1[)$ vers sa valeur moyenne qui vaut 1. La décomposition de la fonction $]0;1[^2$-périodique $\varepsilon(x,y)$ en série de Fourier dans $L^2_\sharp(]0;1[^2)$ permet d'écrire ε_η^{-1}sous la forme :

$$\varepsilon_\eta^{-1}(x) = \sum_{(m,n)\in\mathbf{Z}\times\mathbf{Z}} C_{m,n} e^{2i\pi(m+\alpha n)\frac{x}{\eta}} \ , \tag{3}$$

où $\displaystyle\sum_{(m,n)\in\mathbf{Z}\times\mathbf{Z}} | \, C_{m,n} \, |^2 = \int_{]0;1[^2} | \, \varepsilon(x,y) \, |^2 \, dxdy < +\infty.$
La moyenne C_η de ε_η^{-1} vérifie donc :

$$\begin{aligned} C_\eta \ &= < \varepsilon_\eta^{-1} > \\ &= \sum_{(m,n)\in\mathbf{Z}\times\mathbf{Z}} \frac{C_{m,n}}{2i\pi(m+\alpha n)} \, \eta \, (e^{2i\pi\frac{(m+\alpha n)}{\eta}} - 1) \\ &= \sum_{(m,n)\in\mathbf{Z}\times\mathbf{Z}} C_{m,n} \, sinc(\frac{\pi(m+\alpha n)}{\eta}) e^{i\pi\frac{(m+\alpha n)}{\eta}} \end{aligned} \tag{4}$$

On note $R_\eta = u_\eta - x$ l'erreur commise (ou terme correcteur) entre la solution approchée $u_\eta(x)$ et la solution exacte du problème limite $u(x) = x$. Notre objectif est d'évaluer la norme quadratique de R_η. D'après (1) et (4), la suite (u_η) se met sous la forme :

$$u_\eta(x) = a_\eta \tilde{u}_\eta(x) = C_\eta^{-1} \tilde{u}_\eta(x) \ , \tag{5}$$

où

$$\tilde{u}_\eta(x) = \int_0^x \varepsilon_\eta^{-1}(t)\, dt \tag{6}$$

Nous sommes alors conduits à estimer la quantité suivante :

$$\begin{aligned} \| R_\eta \|^2_{L^2(]0;1[)} &= \int_0^1 \mid u_\eta - x \mid^2 dx \\ &= \int_0^1 \mid \tilde{u}_\eta - x + (a_\eta - 1)\tilde{u}_\eta \mid^2 dx \\ &= \int_0^1 \mid \tilde{u}_\eta - x \mid^2 dx + \mid 1 - a_\eta \mid^2 \int_0^1 \mid \tilde{u}_\eta \mid^2 dx \\ &+ 2\mathcal{R}e\{ \int_0^1 \tilde{u_\eta}(1 - a_\eta)(\tilde{u}_\eta - x)\, dx \} \end{aligned} \tag{7}$$

Posons,

$$\begin{aligned} I_\eta(\alpha) &= \eta \int_0^{\frac{1}{\eta}} \mid \sum_{(m,n)\in\mathbf{Z}\times\mathbf{Z}\setminus\{0,0\}} \frac{C_{m,n}}{2i\pi(m+\alpha n)} \Big(e^{2i\pi(m+\alpha n)y} - 1 \Big) \mid^2 dy \\ &:= \int_0^{\frac{1}{\eta}} \mid \sum_{(m,n)\in\mathbf{Z}\times\mathbf{Z}\setminus\{0,0\}} \frac{C_{m,n}}{2i\pi(m+\alpha n)} \Big(e^{2i\pi(m+\alpha n)y} - 1 \Big) \mid^2 dy \end{aligned} \tag{8}$$

puis pour tout réel $\delta > 0$:

$$I_\eta^\delta(\alpha) = \int_0^{\frac{1}{\eta}} \mid \sum_{(m,n)\in B_\eta^\delta} \frac{C_{m,n}}{2i\pi(m+\alpha n)} \Big(e^{2i\pi(m+\alpha n)y} - 1 \Big) \mid^2 dy \ , \tag{9}$$

où B_η^δ désigne une bande de largeur $\dfrac{\eta}{\delta}$ dans $\mathbf{Z} \times \mathbf{Z} \setminus \{0,0\}$:

$$B_\eta^\delta = \Big\{ (m,n) \in \mathbf{Z} \times \mathbf{Z} \setminus \{0,0\} \ , \ \mid m + \alpha n \mid \leq \frac{\eta}{\delta} \Big\}$$

Nous allons montrer successivement que :

(i) $$\| \frac{\tilde{R}_\eta}{\eta} \|_{L^2(]0;1[)} := \| \frac{\tilde{u}_\eta - x}{\eta} \|_{L^2(]0;1[)} = I_\eta(\alpha) \ ,$$

(ii) $$\alpha \notin \mathbb{Q} \Rightarrow \forall \delta > 0 \ , \ I_\eta(\alpha) \sim I_\eta^\delta(\alpha) \to +\infty \ , \quad \text{quand } \eta \to 0 \ .$$

(iii) $$\alpha \notin \mathbb{Q} \Rightarrow \exists d(\alpha) > 1 \ , \quad \mid 1 - a_\eta \mid = \mid 1 - C_\eta^{-1} \mid = O(\eta^{d(\alpha)}) \ , \quad \text{quand } \delta \to 0 \ , \ (C_\eta \text{ défini par (4)})$$

De (i), (ii) et (iii), et de l'inégalité de Cauchy-Schwarz appliquée au terme $\int_0^1 \tilde{u_\eta}(1-a_\eta)(\tilde{u}_\eta - x)\,dx$ dans l'expression (7) de l'erreur, on déduira que :

$$(iv)\ \forall \alpha \notin \mathbb{Q}\,,\ \|\frac{R_\eta}{\eta}\|^2_{L^2(]0;1[)} \sim \|\frac{\tilde{R}_\eta}{\eta}\|^2_{L^2(]0;1[)} \sim I^\delta_\eta(\alpha) \geq \frac{\sum_{(m,n)\in B^\delta_\eta} |\ C_{m,n}\ |^2}{\eta^2}\ ,\ \text{ quand } \delta \to 0$$

prouvant ainsi que $\|R_\eta\|_{L^2(]0;1[)} \gg \eta$ dès que $\theta(\eta) = \sum_{(m,n)\in B^\delta_\eta} |\ C_{m,n}\ |^2 \sim \eta^{d(\alpha)}$, quand $d(\alpha) < 2$.

Preuve de (i) :

Sans restreindre la généralité, on peut supposer que $< \varepsilon^{-1} >= 1$ i.e. $C_{0,0} = 1$. De (3) et (6), on déduit que :

$$\begin{aligned}
\tilde{u}_\eta(x) &= \sum_{(m,n)\in\mathbb{Z}\times\mathbb{Z}} C_{m,n} \int_0^x e^{2i\pi(m+\alpha n)\frac{t}{\eta}}\,dt \\
&= \int_0^x C_{0,0}\,dt + \sum_{(m,n)\in\mathbb{Z}_*\times\mathbb{Z}_*} C_{m,n} \int_0^x e^{2i\pi(m+\alpha n)\frac{t}{\eta}}\,dt \\
&= x + \eta\Big\{ \sum_{(m,n)\in\mathbb{Z}_*\times\mathbb{Z}_*} \frac{C_{m,n}}{2i\pi(m+\alpha n)}\Big(e^{2i\pi(m+\alpha n)\frac{x}{\eta}} - 1\Big)\Big\}
\end{aligned} \tag{10}$$

où dans la première égalité, on a utilisé le fait que la série converge uniformément (ε est continue).

Pour évaluer la norme quadratique de $\tilde{R}_\eta$, on calcule :

$$\begin{aligned}
\|\tilde{R}_\eta\|^2_{L^2(]0;1[)} &= \int_0^1 |\ \tilde{u}_\eta - x\ |^2\,dx \\
&= \eta^2 \int_0^1 \Big| \sum_{(m,n)\in\mathbb{Z}_*\times\mathbb{Z}_*} \frac{C_{m,n}}{2i\pi(m+\alpha n)}\Big(e^{2i\pi(m+\alpha n)\frac{x}{\eta}} - 1\Big)\Big|^2\,dx \\
&= \eta^2 \int_0^{\frac{1}{\eta}} \Big| \sum_{(m,n)\in\mathbb{Z}_*\times\mathbb{Z}_*} \frac{C_{m,n}}{2i\pi(m+\alpha n)}\Big(e^{2i\pi(m+\alpha n)y} - 1\Big)\Big|^2\,dy \\
&= \eta^2 I_\eta(\alpha)
\end{aligned} \tag{11}$$

où $I_\eta(\alpha)$ est défini par (8).

Remarque :

Lorsque $\alpha \in \mathbb{Q}$, la fonction ε_η donnée par (3) est périodique (de période ηq où $q \geq 1$) et le comportement bien connu de l'erreur $\tilde{R}_\eta$ en $O(\eta)$ indique que $I_\eta(\alpha) = O(1)$ quand η tend vers 0 (prendre $\alpha = 0$ dans (11)). Le résultat (iv) montre qu'inversement si α est un irrationnel tel que $\theta(\eta) \sim \eta^{d(\alpha)}$ où $d(\alpha) < 2$, alors

$$\lim_{\eta\to 0} I_\eta(\alpha) = +\infty\ , \tag{12}$$

(autrement dit $\limsup_{\eta\to 0} I_\eta(\alpha)$ est une fonction discontinue de α) si bien que l'erreur $\tilde{R}_\eta$ tendra vers 0 moins vite que η.

Preuve de (ii) **:**

Fixons $\delta > 0$. On écrit $I_\eta(\alpha)$ sous la forme :

$$I_\eta(\alpha) = \fint_0^{\frac{1}{\eta}} g(y)\, dy\ , \tag{13}$$

où g est la fonction quasi-périodique suivante :

$$g(y) = \Big| \sum_{(m,n)\in\mathbb{Z}\times\mathbb{Z}\setminus\{0,0\}} \frac{C_{m,n}}{2i\pi(m+\alpha n)}\Big(e^{2i\pi(m+\alpha n)y} - 1\Big)\Big|^2\ . \tag{14}$$

La convergence dans (13) revient donc à étudier l'existence ou non d'une moyenne ergodique pour g. Pour cela, on décompose g comme suit :

$$g(y) = \mid h_\eta^\delta(y) + r_\eta^\delta(y) \mid^2\ , \tag{15}$$

avec

$$\begin{aligned} h_\eta^\delta(y) &= \sum_{(m,n)\in B_\eta^\delta} f_{m,n} e^{i\omega_{m,n}y} - \sum_{(m,n)\in B_\eta^\delta} f_{m,n} \\ &= \sum_{(m,n)\in B_\eta^\delta} \frac{C_{m,n}}{2i\pi(m+\alpha n)}\Big(e^{2i\pi(m+\alpha n)y} - 1\Big) \\ &= \sum_{(m,n)\in B_\eta^\delta} \frac{C_{m,n}}{\pi(m+\alpha n)}\Big(\sin\pi(m+\alpha n)y\Big)e^{i\pi(m+\alpha n)y} \end{aligned} \tag{16}$$

et

$$\begin{aligned} r_\eta^\delta(y) &= \sum_{(m,n)\in\mathbb{Z}_*^2\setminus B_\eta^\delta} f_{m,n} e^{i\pi\omega_{m,n}y} - \sum_{(m,n)\in\mathbb{Z}_*^2\setminus B_\eta^\delta} f_{m,n} \\ &= \sum_{(m,n)\in\mathbb{Z}_*^2\setminus B_\eta^\delta} \frac{C_{m,n}}{\pi(m+\alpha n)}\Big(\sin\pi(m+\alpha n)y\Big)e^{i\pi(m+\alpha n)y} \end{aligned} \tag{17}$$

où $\omega_{m,n} = 2\pi(m+\alpha n)$ et $f = C_{m,n}/i\omega_{m,n}$.

Notant que :

$$I_\eta = \fint_0^{\frac{1}{\eta}} g(y)\, dy = \fint_0^{\frac{1}{\eta}} \mid h_\eta^\delta(y) \mid^2 dy + \fint_0^{\frac{1}{\eta}} \mid r_\eta^\delta(y) \mid^2 dy + 2\mathcal{R}e\Big\{\fint_0^{\frac{1}{\eta}} h_\eta^\delta(y) r_\eta^\delta(y)\, dy\Big\}\ , \tag{18}$$

l'assertion (iii) résulte alors des propriétés suivantes :

$$\lim_{\eta\to 0} \fint_0^{\frac{1}{\eta}} \mid r_\eta^\delta(y) \mid^2 dy = O(1) \tag{19}$$

$$\lim_{\eta\to 0} \fint_0^{\frac{1}{\eta}} \mid h_\eta^\delta(y) \mid^2 dy = +\infty \tag{20}$$

Appliquant Cauchy-Schwarz à $2\mathcal{R}e\Big\{\fint_0^{\frac{1}{\eta}} h_\eta^\delta(y) r_\eta^\delta(y)\, dy\Big\}$ dans (18), on déduit alors de (19) et (20) que :

$$I_\eta(\alpha) = \fint_0^{\frac{1}{\eta}} g(y)\, dy \sim \fint_0^{\frac{1}{\eta}} \mid h_\eta^\delta \mid^2 dy \sim +\infty\ ,\ \text{ quand } \eta \to 0 \tag{21}$$

Preuve de (19) **:**

Fixons $\delta > 0$. Pour démontrer la propriété (19), on utilise l'expression (17) :

$$\begin{aligned}
\int_0^{\frac{1}{\eta}} \mid r_\eta^\delta(y) \mid^2 dy &\leq 2 \int_0^{\frac{1}{\eta}} \sum_{(m,n)\in\mathbb{Z}_*^2\setminus B_\eta^\delta} \frac{\mid C_{m,n} \mid^2}{\pi^2 \mid m+\alpha n \mid^2} \Big|\sin \pi(m+\alpha n)y\Big|^2 dy \\
&\leq 2 \sum_{(m,n)\in\mathbb{Z}_*^2\setminus B_\eta^\delta} \frac{\mid C_{m,n} \mid^2}{\pi^2 \mid m+\alpha n \mid^2} \eta \int_0^{\frac{1}{\eta}} \Big|\sin \pi(m+\alpha n)y\Big|^2 dy \\
&\leq 2 \sum_{(m,n)\in\mathbb{Z}_*^2\setminus B_\eta^\delta} \frac{\mid C_{m,n} \mid^2}{\pi^2 \mid m+\alpha n \mid^2} \int_0^1 \Big|\sin \pi(m+\alpha n)\frac{x}{\eta}\Big|^2 dx \\
&= 2 \sum_{(m,n)\in\mathbb{Z}_*^2\setminus B_\eta^\delta} \mid C_{m,n} \mid^2 \frac{\eta^2}{2\pi^2 \mid m+\alpha n \mid^2} \Big(1 - \frac{\sin(2\pi\frac{m+\alpha n}{\eta})}{2\pi(\frac{m+\alpha n}{\eta})}\Big) \\
&\leq \frac{\delta^2}{\pi^2} \sum_{(m,n)\in\mathbb{Z}_*^2\setminus B_\eta^\delta} \mid C_{m,n} \mid^2 \qquad (22)
\end{aligned}$$

où dans la deuxième inégalité on a appliqué Fubini-Tonelli et dans la dernière inégalité on a utilisé le fait que $\dfrac{\eta^2}{\mid m+\alpha n \mid^2} \leq \delta^2$ lorsque $(m,n) \in \mathbb{Z}_*^2 \setminus B_\eta^\delta$. La convergence de la série $\displaystyle\sum_{(m,n)\in\mathbb{Z}_*^2\setminus B_\eta^\delta} \mid C_{m,n} \mid^2$ nous assure alors de la propriété (19).

Preuve de (20) **:**

Fixons δ et $\rho > 0$. Pour démontrer la propriété (20), on définit h_η^δ dans (16) sous la forme :

$$h_\eta^\delta = \lim_{\rho\to 0} \sum_{(m,n)\in B_\eta^{\delta,\rho}} f_{m,n} e^{i\omega_{m,n}y} \qquad (23)$$

où $\omega_{m,n} = 2\pi(m+\alpha n)$, $f_{m,n} = \dfrac{C_{m,n}}{i\omega_{m,n}}$ et $B_\eta^{\delta,\rho}$ est définie par :

$$B_\eta^{\delta,\rho} = \Big\{(m,n) \in \mathbb{Z}\times\mathbb{Z}\setminus\{0,0\}\ ,\ \mid m \mid + \mid n \mid \leq \frac{1}{\rho}\ ,\ \mid m+\alpha n \mid \leq \frac{\eta}{\delta}\Big\}\ .$$

On en déduit les minorations suivantes pour tous réels δ et $\rho > 0$:

$$\begin{aligned}
\liminf_{\eta\to 0} \int_0^{\frac{1}{\eta}} \mid \sum_{(m,n)\in B_\eta^{\delta,\rho}} f_{m,n} e^{i\omega_{m,n}y} \mid^2 dy &\geq \sum_{(m,n)\in B_\eta^{\delta,\rho}} \mid f_{m,n} \mid^2 \\
&\geq \frac{1}{4\pi^2} \sum_{(m,n)\in B_\eta^{\delta,\rho}} \Big|\frac{C_{m,n}}{m+\alpha n}\Big|^2 \\
&\geq \frac{1}{4\pi^2} \min_{(m,n)\in B_\eta^{\delta,\rho}} \frac{1}{\mid m+\alpha n \mid^2} \sum_{(m,n)\in B_\eta^{\delta,\rho}} \mid C_{m,n} \mid^2 \qquad (24)
\end{aligned}$$

où dans la première inégalité, on a utilisé la formule de Parseval Plancherel généralisée.

Passant alors à la limite quand $\rho \to 0$ dans (24), on tire que :

$$\lim_{\rho\to 0}\liminf_{\eta\to 0}\int_0^{\frac{1}{\eta}} \mid \sum_{(m,n)\in B_\eta^{\delta,\rho}} f_{m,n}e^{i\omega_{m,n}y} \mid^2 dy \geq \frac{1}{4\pi^2}\min_{(m,n)\in B_\eta^\delta}\frac{1}{\mid m+\alpha n\mid^2}\sum_{(m,n)\in B_\eta^\delta}\mid C_{m,n}\mid^2 \tag{25}$$

Par ailleurs, comme ε est continue, nous sommes assurés que :

$$\begin{aligned}\lim_{\eta\to 0}\int_0^{\frac{1}{\eta}} \mid h_\eta^\delta(y)\mid^2 dy &:= \liminf_{\eta\to 0}\lim_{\rho\to 0}\Big(\int_0^{\frac{1}{\eta}} \mid \sum_{(m,n)\in B_\eta^{\delta,\rho}} f_{m,n}e^{i\omega_{m,n}y}\mid^2 dy\Big)\\ &= \lim_{\rho\to 0}\liminf_{\eta\to 0}\Big(\int_0^{\frac{1}{\eta}} \mid \sum_{(m,n)\in B_\eta^{\delta,\rho}} f_{m,n}e^{i\omega_{m,n}y}\mid^2 dy\Big)\end{aligned}$$

on établit alors la propriété (20) en notant que d'une part

$$\min_{(m,n)\in B_\eta^\delta}\frac{1}{\mid m+\alpha n\mid^2} \geq \frac{\delta^2}{\eta^2}\ ,$$

et que d'autre part il existe une constante $C>0$ telle que :

$$\theta(\eta) = \sum_{(m,n)\in B_\eta^\delta}\mid C_{m,n}\mid^2 \sim C\eta^{d(\alpha)} \quad \text{avec } d(\alpha)<2\ ,$$

dans le cas où α est un nombre algébrique autre que le nombre d'or (noter que $d(\alpha)=2$ pour le nombre d'or d'après la proposition 2 établie dans l'annexe B, qui correspond à une erreur R_η qui converge comme η.).

Preuve de (iii) **:**

Notant que $<\varepsilon^{-1}>=1$ i.e. $C_{0,0}=1$, de (4) on tire que :

$$\begin{aligned}\mid 1-C_\eta\mid &= \Big\mid \sum_{(m,n)\in\mathbb{Z}_*\times\mathbb{Z}_*} C_{m,n}\ sinc(\frac{\pi(m+\alpha n)}{\eta})e^{i\pi\frac{(m+\alpha n)}{\eta}}\Big\mid\\ &\leq \sum_{(m,n)\in\mathbb{Z}_*\times\mathbb{Z}_*}\Big\mid C_{m,n}\ sinc(\frac{\pi(m+\alpha n)}{\eta})\Big\mid\\ &= \sum_{(m,n)\in B_\eta^\delta}\Big\mid C_{m,n}\ sinc(\frac{\pi(m+\alpha n)}{\eta})\Big\mid + \sum_{(m,n)\in\mathbb{Z}_*^2\setminus B_\eta^\delta}\Big\mid C_{m,n}\ sinc(\frac{\pi(m+\alpha n)}{\eta})\Big\mid \end{aligned}\tag{26}$$

où dans la première egalité, on a utilisé le fait que *sinc* est prolongée par continuité à 1 en 0. Notant ξ est le degré algébrique de l'irrationnel α, d'après le lemme 2 de l'annexe B, on sait par ailleurs que :

$$\sum_{(m,n)\in B_\eta^\delta}\Big\mid C_{m,n}\ sinc(\frac{\pi(m+\alpha n)}{\eta})\Big\mid = o(\eta^{\frac{2}{\xi-1}})\ , \tag{27}$$

pour des coefficients de Fourier $C_{m,n} = sinc\frac{\pi m}{\eta}sinc\frac{\pi m}{\eta}$ et

$$\sum_{(m,n)\in B_\eta^\delta}\Big\mid C_{m,n}\ sinc(\frac{\pi(m+\alpha n)}{\eta})\Big\mid = o(\eta^{\frac{3}{2(\xi-1)}})\ , \tag{28}$$

pour des coefficients de Fourier $C_{m,n} = \dfrac{J_1(\sqrt{n^2+m^2})}{\sqrt{n^2+m^2}}$.

De plus, pour tout couple d'entiers $(m,n) \in \mathbb{Z}^2_* \setminus B^\delta_\eta$, $\dfrac{\eta}{\mid m+\alpha n \mid} \leq \delta$. On en déduit qu'il existe une constante $C_1 > 0$ telle que :

$$\sum_{(m,n)\in\mathbb{Z}^2_*\setminus B_\eta} \left| C_{m,n}\ sinc(\frac{\pi(m+\alpha n)}{\eta}) \right| \leq C_1 \sum_{(m,n)\in\mathbb{Z}^2_*\setminus B^\delta_\eta} \frac{\eta}{\mid m+\alpha n \mid} \mid C_{m,n} \mid$$

$$\leq \delta C_1 \sum_{(m,n)\in\mathbb{Z}^2_*\setminus B^\delta_\eta} \mid C_{m,n} \mid \qquad (29)$$

Comme ε est continue, $\sum_{(m,n)\in\mathbb{Z}^2_*\setminus B^\delta_\eta} \mid C_{m,n} \mid < +\infty$, on établit alors $iii)$ en passant à la limite quand δ tend vers 0 dans(26) à l'aide de (27) (ou (28)) et (29).

(QED)

Deuxième partie

Analyse numérique de la propagation de modes guidés dans les fibres optiques.

Chapitre 6

Propagating modes in dielectric waveguides

> Physical vector quantities may be divided in two classes, in one of which the quantity is defined with reference to a line, while in the other the quantity is defined with reference to an area.
>
> 'A Treatise on Electricity and Magnetism', by J. C. Maxwell. [135]

6.1 Introduction

Optical fibers and integrated optical waveguides are today finding wide use in areas covering telecommunications, sensor technology, spectroscopy, and medicine. As was experimentally shown by Russell and co-workers ([24][119][120][44][121]), a special class of components incorporating photonic crystals can propagate light in a low index medium or be monomode at all wavelengths in a high index defect. More precisely, they fashioned a dielectric waveguide with a two-dimensional periodic variation in the plane perpendicular to the fiber axis, and an invariant structure along it. One application of such materials is a type of optical waveguide where light is confined by surrounding it with a band gap material. The photonic band gap effect (PBG) may be achieved in periodically structured materials having a periodicity on the scale of the optical wavelength : this is the well-known ability of photonic crystals to inhibit the propagation of photons with well-defined frequencies, which has a close analogy with the electronic properties of semiconductors. Therefore, two-dimensional periodic structures in the form of long, fine silica fibers that have a regular array of tiny air holes running down their length ([24][119][120][44][121]) constitute two-dimensional photonic crystals with lattice constants of the order of micrometers. In the sequel, we will refer to such structures as photonic crystal fibers (PCF). These microstructure fibers have recently been used to form both endlessly single-mode crystal fibers based on total internal reflection thanks to a high defect index core and the crystal cladding, lossless crystal fibers based on light confinement in a low defect index core by PBG effect. The first type of PCF is a glass fiber with a regular array of holes running down its length : we will call it in the sequel high photonic crystal fiber (HPCF). A single missing hole in the array forms a region which effectively has a higher refractive

index than the surrounding photonic crystal. This acts as a waveguide core in which light can become trapped, forming a guided mode. Russell and al ([24][119][120][44][121]) have experimentally demonstrated a single-mode operation in such waveguides in a wavelength range from 337 nm to 1550 nm. Furthermore, it can be theoretically predicted that this type of PCF remains monomode even for very short wavelengths using the effective index model of Russell and *al* ([24][120]). The first step is to note that in a standard step-index fiber with core radius r and core and cladding indices n_{co} and n_{cl}, the number of guided modes is determined by the V value ([24][120]) :

$$V = \frac{2\pi r}{\lambda}\sqrt{n_{co}^2 - n_{cl}^2}\ ,$$

which must be less than 2.405 for the fiber to be single mode at optical wavelengths. Thus, single-mode fibers are in fact multimode for light of sufficiently short wavelength. Russell and al then propose an explanation for the monomode property of PCF based on the effective refractive index of the cladding. They find an empirical rule which determines whether the fiber is single mode or not :

$$V_{eff} = \frac{2\pi d}{\lambda}\sqrt{n_0^2 - n_{eff}^2}\ ,$$

where d denotes the center-center spacing between holes, n_0 is the index of silica and

$$n_{eff} = \frac{\gamma_{eff}\lambda}{2\pi}\ ,$$

γ_{eff} being the maximum propagation constant γ allowed in the cladding. V_{eff} is then calculated by solving the scalar wave equation within a unit cell centered on one of the holes. Furthermore, they noted that for small λ, the scalar wave equation gives :

$$\Lambda^2\Delta_t F + V_{eff}^2 F = 0\ ,$$

where F stands for the electromagnetic field of the crystal in silica regions and Δ_t is the transverse part of the Laplacian. When λ tends towards zero, the field F is excluded from the low index air holes and is confined to the silica region bounded by the edges of the holes. For a given ratio of hole size to Λ, the field is therefore an invariant function of normalized transverse coordinates $\frac{x}{\Lambda}$ and $\frac{y}{\Lambda}$ in the short wavelength limit. The previous equation then implies that V_{eff} is finite and independent of λ and Λ under these conditions. This situation contrasts with that for the step index fiber, for which V tends to infinity as λ tends to zero. Russel and co-workers then conclude that the limiting value of V_{eff} depends on the relative size of the holes, but a sufficiently small value guarantees single-mode operation for all wavelengths λ and scales Λ.

The second type of PCF is certainly the more surprisingly one, since it enables light propagation in a low index structural defect thanks to the PBG effect : we will call it in the sequel low photonic crystal fiber (LPCF). Its properties have been studied both theoretically and experimentally in honeycomb photonic crystal fibers made of around one hundred rods. For the numerical determination of the defect modes, Broeng *et al.* employed a super-cell enhancement of the plane-wave method (the basic cell contains the

overall guide to take into account the defect). Let us recall that for a single mode, the full-vector wave equation of the magnetic field $H_{\mathbf{k}}$ may be obtained from Maxwell's equations and expressed as follows :

$$\operatorname{curl} \frac{1}{\varepsilon_r} \operatorname{curl} H_{\mathbf{k}} = -\frac{\omega^2}{c^2} H_{\mathbf{k}} \ ,$$

where $\mathbf{k}$ represents the wave propagation vector of the mode and ε_r is the relative permittivity of the periodic structure. Taking advantage of the periodic nature of the problem, the magnetic field may be expanded into a sum of plane waves using the Floquet-Bloch's theorem as follows :

$$H_{\mathbf{k}} = \sum_{\mathbf{G}} h_{\mathbf{k}-\mathbf{G}} e^{-i(\mathbf{k}-\mathbf{G})\cdot\mathbf{r}} \ ,$$

where $\mathbf{G}$ represents a lattice vector in reciprocal space, describing the periodic structure. The dielectric constant may be expressed as a Fourier series expansion to obtain :

$$\frac{1}{\varepsilon_r} = \sum_{\mathbf{G}} V_{\mathbf{G}} e^{i\mathbf{G}\cdot\mathbf{r}} \ ,$$

where $V_{\mathbf{G}}$ denotes the following Fourier coefficients of $\dfrac{1}{\varepsilon}$:

$$V_{\mathbf{G}} = \frac{1}{meas(Y)} \int_Y \frac{1}{\varepsilon_r} e^{-i\mathbf{G}\cdot\mathbf{r}} \, d\mathbf{r} \ ,$$

In this equation, Y denotes the smallest basic cell that may be used to represent the cross-section of the guide to be periodized (and $meas(Y)$ the measure of Y). Therefore, a matrix generalized eigenvalue problem is obtained, where, for a fixed wave vector $\mathbf{k}$, the frequencies ω of the allowed modes in the periodic structures are found as complex eigenvalues.

The main drawback of this method is that it is necessary to suppose *a priori* that the finite size of the crystal cladding has no influence on the propagating modes, which is far from being obvious. We will see in the sequel that such an assumption could led to unphysical solutions : the bounded cross-section of the PCF induces a **discrete spectrum** which corresponds to propagating modes and the exterior of the photonic guide induces a **continuous spectrum** (non-propagating modes). Therefore, one question naturally arises : how can we make a distinction between physical modes which belong to the discrete spectrum and that of the continuous one if we consider the operator associated to the Bloch-wave decomposition ?

In this study, we try to give both theoretical and numerical elements to answer this question. To be complete, we must add that our modelling allows us only to observe non-dissipative modes : we therefore have numerical access to the first type of PCF (HPCF). Concerning the second type (LPCF), we outline an alternative approach to that of Broeng and *al* : although this numerical study is not yet achieved, we explain our battle plan to find such leaky modes.

6.2 Preliminaries

Before going to the general case of propagation in two-dimensional dielectric waveguides, we simply want to illustrate our approach with the analysis of the classical dielec-

tric slab. For this, we consider an heterogeneous dielectric waveguide invariant along the y and z axes (e.g. propagation of modes in one or more parallel slabs). We then set :

$$\mathbf{E}(x,y,z) = u(x)e^{i\gamma y}ez \text{ in } E_{\|}, \text{ and } \mathbf{H}(x,y,z) = u(x)e^{i\gamma y}ez \text{ in } H_{\|}$$

$$\begin{cases} \operatorname{curl}\mathbf{H} & = -i\omega\varepsilon \operatorname{curl}\mathbf{E} \\ \operatorname{curl}\mathbf{E} & = i\omega\mu \operatorname{curl}\mathbf{H} \\ \operatorname{curl}(\mu\mathbf{H}) & = 0 \\ \operatorname{curl}(\varepsilon\mathbf{E}) & = \rho \end{cases}$$

In the absence of volumic charges, if $\mu = \mu_0$ (non-ferro-magnetic media), we are led to the well-known equations :

$$\begin{cases} \dfrac{1}{\varepsilon}\operatorname{curl}\dfrac{1}{\mu_0}\operatorname{curl}\mathbf{E} + \omega^2\mathbf{E} & = 0 \\ \dfrac{1}{\mu_0}\operatorname{curl}\dfrac{1}{\varepsilon}\operatorname{curl}\mathbf{H} + \omega^2\mathbf{H} & = 0 \end{cases}$$

The above system defines two spectral problems, which amount to looking for frequencies ω for which the electromagnetic field $(\mathbf{E},\mathbf{H})$ is of finite energy in $\mathbb{R}^3$.

If ε is a piecewise constant function associated to a one-dimensional photonic crystal fiber, we know that for the two polarizations, u satisfies an equation of Helmholtz type in each homogeneous media. If k_0 denotes the wave number $\sqrt{\omega\mu_0\varepsilon_0}$, we define k_j as $k_0\varepsilon_j$, where ε_j is the permittivity of the j-th media. We are thus led to :

$$\Delta u + (k_j^2 - \gamma^2)u = 0 \tag{0}$$

On the above expression, we see that the spectral problem splits in two ways : we can either fix the propagating constant γ and look for k_j corresponding to bounded eigenvectors $(\mathbf{E},\mathbf{H})$, or we can consider a given wavenumber k_j and look for propagation constants associated to **bound modes** i.e vector analogues to bound states in quantum mechanics, where the γ are discrete eigenvalues. Although these two point of views are mathematically equivalent (γ is a strictly monotonic function of k_j as shown by Bonnet [28]), it sounds that the usual way to study optical fibers is the second one. For this reason, we discuss the one-dimensional case this way. It is worth noting that we will choose the first approach in the two-dimensional case, to keep a linear operator.

For a fixed γ, defining β_j^2 as $\sqrt{k_j^2 - \gamma^2}$, we deduce that in every media :

$$u(x) = A_j^- e^{-i\beta_j x} + A_j^+ e^{i\beta_j x}$$

where $\beta_j = \sqrt{k_j^2 - \gamma^2}$ if $\gamma \geq k_j$, or $i\sqrt{k_j^2 - \gamma^2}$ if $\gamma \leq k_j$.

We now consider that $\varepsilon(x) = \varepsilon_0$ for $x \in \mathbb{R}\setminus[-1;1]$ (the dielectric waveguide is included in $]-1;1[\times\mathbb{R}^2$). If we denote k_1 (resp. k_n) the wave numbers for $x > 1$ (resp. $x < 1$) we see that for α lower than k_1 (resp. k_n), β_1 (resp. β_n) is a positive real. We deduce that γ must be greater than k_1 (resp. k_n), therefore $i\beta_1 = -\sqrt{\gamma^2 - k_1^2}$ (resp. $i\beta_n = -\sqrt{\gamma^2 - k_n^2}$)

and u is thus bounded for $x > 1$ if A_1^- is null (resp. for $x < 1$ if A_n^+ is null) : elsewhere u is an oscillating function which does not vanish at infinity. The propagating constant must thus satisfy :

$$\gamma \geq \max(k_1, k_n)$$

This lower bound is the condition for total internal reflection : when light travelling inside the PCF approaches the interface with the air, one of two things can occur. If the angular condition for total reflection is met, the light is reflected back into the photonic guide, otherwise much of the light passes into the air and is lost.

To get an upper bound for γ, we take the variational form associated to (0) and apply the Green formula. From Maxwell equations, we know that in $E_\parallel$, u and du must be continuous and that in $H_\parallel$ u and $\frac{1}{\varepsilon}\frac{du}{dx}$ is continuous. We hence deduce that (Petit, 1993 [176]) :

$$-\beta_1^2 \int_{]1;+\infty[} u\overline{u}\,dx - \beta_n^2 \int_{]-\infty;0[} u\overline{u}\,dx + \int_{]-\infty;+\infty[} u\frac{d^2\overline{u}}{dx^2}\,dx = \sum_{j=2}^{n-1} \beta_j^2 \int_{]1-2\frac{j}{n-1};1-2\frac{j-1}{n-1}[} u\frac{d^2\overline{u}}{dx^2}dx$$

which shows that $\beta_j^2 > 0$ for all $j \in \{2, n-1\}$, since β_1^2 and β_n^2 are < 0. We hence know that the propagating constants of the bound modes satisfy :

$$\max(k_1, k_n) < \gamma < k_j \ , \ \forall j \in \{2, n-1\}$$

These are the so-called dispersion relations. Note that the upper bound occurs because γ is a component of k_j, which is the magnitude of the wavevector $\mathbf{K}_j$ that points in the direction of light propagation in the layer $]1 - 2\frac{j}{n-1}; 1 - 2\frac{j-1}{n-1}[$.

Remark :

From the previous study, we know that :

$$u(x) = \begin{cases} A_1^+ e^{i\beta_1 x} \text{ , si } x > 1 & \beta_1 = i\sqrt{\gamma^2 - k_1^2} \\ A_j^- e^{-i\beta_j x} + A_j^+ e^{i\beta_j x} \text{ , si } -1 < x < 1 & \beta_j = \sqrt{k_j^2 - \gamma^2} \\ A_n^- e^{-i\beta_n x} \text{ , si } x < -1 & \beta_n = i\sqrt{\gamma^2 - k_n^2} \end{cases} \quad (1)$$

Noting once more that in $E_\parallel$, u and $\frac{du}{dx}$ must be continuous on each interface (resp. u and $\frac{1}{\varepsilon}\frac{du}{dx}$ in $H_\parallel$), we can deduce some relations between A_n^-, A_j^-, A_j^+ and A_1^+ (Petit, 1993 [176]). More precisely, for a given γ these constants are the unknowns of a homogeneous linear system which has a solution if and only if its discriminent Δ (depending upon γ) is null. The properties of Δ are closely related to that of the discriminent of the scattering matrix S (Tayeb and Maystre, 1997 [197]). The S matrix links the incident field F_i to that of the diffrated one F_d :

$$S\ F_i = F_d \quad (2)$$

One can then define the propagating modes as solutions of Maxwell's equations without any incident field, that is with $F_i = 0$. The linear system (1) hence reduces to :

The scattering matrix S can be considered as a function of the wavelength λ. Equation (2) has solutions only for discrete values λ_p of λ, which are the poles of the S matrix :

$$det[S^{-1}(\lambda_p)] = 0$$

what is equivalent to :

$$det[S(\lambda_p)] = \infty$$

These complex values λ_p are obtained numerically by searching for the roots of $det[S^{-1}(\lambda_p)]$ in the complex plane. The propagating modes are then the eigenmodes associated to these eigenvalues. The F column associated with the mode is the eigenvector of $S^{-1}(\lambda_p)$ associated with the eigenvalue 0 (Maystre *et al*, 1996 [138]).

From a theoretical point of view, we face a spectral problem with an unbounded operator with dense domain $H^2(\mathbb{R})$ in $L^2(\mathbb{R})$. This operator thus exhibits a spectrum made of two parts : a discrete one with eigenvalues associated to eigenvectors of finite energy (the propagating modes) and a continuous one corresponding to the scattering problem (the so-called radiation modes associated to this part of the spectrum are not in $L^2(\mathbb{R})$ since they do not decrease in the exterior of the guide). From a numerical point of view, we cannot hope to mesh the overall space $\mathbb{R}$ to discretize this problem. One may first think that taking some Dirichlet boundary conditions at a finite distance of the guide (say on the boundary $\partial\Omega$ of a given open bounded set $\Omega \subset \mathbb{R}$) would correctly approximate the problem : the energy of the field is indeed rapidly vanishing outside the waveguide (as $\frac{1}{|\ x\ |^2}$). Theoretically speaking, the Helmholtz operator would thus be of compact resolvent thanks to the compact embedding of $H^1(\Omega)$ in $L^2(\Omega)$. The compact operators being well approached by finite rank operators (i.e. matrices) since it only has a discrete spectrum, a Galerkin scheme would thus have some good properties (Ciarlet, 1978 [54]). Nevertheless, taking Dirichlet boundary conditions at a finite distance would add the modes of a metallic cavity (spurious modes, Bossavit, 1990 [30]) !

One way to avoid this drawback is to use some transformation methods combined with a particular class of finite elements (Nedelec 1980, [160]) in the two-dimensional case : these so-called Nedelec (or edge) elements have the peculiarity to keep topological properties under a so-called pull-back mapping (see next section). The idea is then to map the infinite domain in a finite one : we transform orthogonal coordinates in curvilinear ones. We therefore keep the unbounded nature of the Helmholtz operator, but we just have to mesh a finite set. In the one-dimensional case, the transformation is trivial, and the discretization can be led with basic nodal elements on Fourier bases. Let us emphasize that this scaling procedure will not affect the boundary conditions (Dirichlet ones, since the field is null at infinity), because our transformation applies on the exterior of the waveguide, where no discontinuities occur. Some further details can be found in the section "transformation method", where the two-dimensional case is treated (we can sketch that the transformation is a kind of conformal mapping on the interface between the guide and the air). To show this, let us consider the bijection :

$$\frac{2}{\pi} arctan : x \in]-\infty; +\infty[\longmapsto \alpha \in [-1; 1] \tag{3}$$

Besides, we know that :

$$\frac{du}{dx}(x(\alpha)) = \frac{d\alpha}{dx}\frac{du}{d\alpha}(x(\alpha))$$

We thus deduce that :

$$\frac{d^2u}{dx^2}(x(\alpha)) = \frac{d\alpha}{dx}\frac{d}{d\alpha}\left(\frac{d\alpha}{dx}\frac{du}{d\alpha}(x(\alpha))\right) \tag{4}$$

Letting $h(\alpha)$ be equal to $u(x(\alpha))$, we derive from (4) and (0) that :

$$\frac{d\alpha}{dx}\frac{d}{d\alpha}\Big(\frac{d\alpha}{dx}\frac{dh}{d\alpha}(\alpha)\Big) + (k^2-\gamma^2)h(\alpha) = 0$$

Noting that $\alpha = \frac{2}{\pi}arctanx$, we derive that $\frac{d\alpha}{dx} = \frac{2}{\pi}\frac{1}{1+\tan^2\frac{\pi\alpha}{2}} = -\frac{2}{\pi}\cos^2\frac{\pi\alpha}{2}$ and we thus obtain :

$$\frac{4}{\pi^2}\cos^2\frac{\pi\alpha}{2}\frac{d}{d\alpha}\Big(\cos^2\frac{\pi\alpha}{2}\frac{dh}{d\alpha}(\alpha)\Big) + (k^2-\gamma^2)h(\alpha) = 0 \tag{5}$$

with the Dirichlet boundary conditions $h(-1) = h(1) = 0$.

We now want to discretize this spectral problem. For this, we expand h in Fourier series :

$$h = \sum_{n\in\mathbf{Z}} h_n e^{in\pi\alpha}$$

Noting that $\cos^2\frac{\pi\alpha}{2} = \frac{1}{2} + \frac{1}{2}\cos\pi\alpha$, we get :

$$\cos^2\frac{\pi\alpha}{2}\frac{dh}{d\alpha}(\alpha) = \frac{i\pi}{2}\Big(1+\frac{1}{2}e^{i\pi\alpha}+\frac{1}{2}e^{-i\pi\alpha}\Big)\sum_{n\in\mathbf{Z}} nh_n e^{in\pi\alpha}$$

$$= \frac{i\pi}{2}\sum_{n\in\mathbf{Z}}\Big(nh_n + \frac{1}{2}(n-1)h_{n-1} + \frac{1}{2}(n+1)h_{n+1}\Big)e^{in\pi\alpha}$$

We thus deduce that :

$$\cos^2\frac{\pi\alpha}{2}\frac{d}{d\alpha}\Big(\cos^2\frac{\pi\alpha}{2}\frac{dh}{d\alpha}(\alpha)\Big)$$

$$= \frac{-\pi^2}{4}\Big(1+\frac{1}{2}e^{i\pi\alpha}+\frac{1}{2}e^{-i\pi\alpha}\Big)\sum_{n\in\mathbf{Z}} n\Big(nh_n + \frac{1}{2}(n-1)h_{n-1} + \frac{1}{2}(n+1)h_{n+1}\Big)e^{in\pi\alpha}$$

$$= \frac{-\pi^2}{4}\sum_{n\in\mathbf{Z}}\Big[\Big(n^2+\frac{1}{4}(n+1)n+\frac{1}{4}(n-1)n\Big)h_n + \Big(\frac{1}{2}(n-1)^2+\frac{1}{2}n(n-1)\Big)h_{n-1}$$

$$+\Big(\frac{1}{2}(n+1)^2+\frac{1}{2}n(n+1)\Big)h_{n+1} + \frac{1}{4}(n-1)(n-2)h_{n-2} + \frac{1}{4}(n+1)(n+2)h_{n+2}\Big]e^{in\pi\alpha}$$

From (5), we derive the following linear system of equations for $n \in \mathbf{Z}$:

$$\frac{1}{4}\Big(6n^2h_n + (n-1)(2n-1)h_{n-1} + 2(n+1)(2n+1)h_{n+1} + (n-1)(n-2)h_{n-2} + (n+1)(n+2)h_{n+2}\Big)$$

$$= (k^2 - \gamma^2) h_n$$

This is a large sparse system which can be solved thanks to the Lanczos algorithm, which is introduced in the next section. The remaining question is to address the convergence of the truncated system towards the infinite one. In the next section, we generalize this study to the two-dimensional vector problem.

6.3 Setup of the problem

We consider a dielectric waveguide of constant section Ω, invariant along the z axis and whose permittivity profile ε is supposed to be a known function (e.g. a piecewise constant function to model a photonic crystal fiber). We look for electromagnetic fields $(\mathcal{E}, \mathcal{H})$ which are solutions of the following Maxwell equations :

$$(1) \begin{cases} \operatorname{curl} \mathcal{H} = \varepsilon \dfrac{\partial \mathcal{E}}{\partial t} \\ \operatorname{curl} \mathcal{E} = -\mu_0 \dfrac{\partial \mathcal{H}}{\partial t} \end{cases}$$

μ_0 being the permeability of vacuum.

Furthermore, choosing a time dependence in $e^{-i\omega t}$, and taking into account the invariance of the guide along its z axis, we define time-harmonic two-dimensional electric and magnetic fields $\mathbf{E}$ and $\mathbf{H}$ by :

$$(2) \begin{cases} \mathcal{E}(x, y, z, t) = \Re e(\mathbf{E}(x, y) e^{-i(\omega t - \gamma z)}) \\ \mathcal{H}(x, y, z, t) = \Re e(\mathbf{H}(x, y) e^{-i(\omega t - \gamma z)}) \end{cases}$$

If $[L^2(\mathbb{R}^2)]^3$ denotes the Hilbert space of square integrable functions on $\mathbb{R}^2$ with values in $\mathbb{C}^3$, we say that $(\mathbf{E}, \mathbf{H})$ is a guided mode when :

$$\begin{cases} (\gamma, \omega) \in \mathbb{R}_+^2 \\ (\mathbf{E}, \mathbf{H}) \neq (\mathbf{0}, \mathbf{0}) \\ \mathbf{E}, \mathbf{H} \in [L^2(\mathbb{R}^2)]^3 \end{cases}$$

where ω is the angular frequency in the vacuum and γ denotes the propagating constant of the guided mode.

For $(\mathbf{E}, \mathbf{H})$ satisfying (1), (2) can be written as :

$$(3) \begin{cases} \operatorname{curl}_\gamma \mathbf{H} = -i\omega\varepsilon_0\varepsilon_r(x, y)\mathbf{E} & (3.1) \\ \operatorname{curl}_\gamma \mathbf{E} = i\omega\mu_0 \mathbf{H} & (3.2) \end{cases}$$

where ε_r denotes the relative permittivity is such that $1 \leq \varepsilon_r \leq \varepsilon^+ = \sup_{(x,y)\in\mathbb{R}^2} \varepsilon_r(x, y)$ (bounded and coercive function) and where $\operatorname{curl}_\gamma \mathbf{H}$ and $\operatorname{curl}_\gamma \mathbf{E}$ are defined by :

$$(4) \begin{cases} \operatorname{curl}_\gamma \mathbf{H}(x, y) = \operatorname{curl}\Big(\mathbf{H}(x, y) e^{i\gamma z}\Big) e^{-i\gamma z} \\ \operatorname{curl}_\gamma \mathbf{E}(x, y) = \operatorname{curl}\Big(\mathbf{E}(x, y) e^{i\gamma z}\Big) e^{-i\gamma z} \end{cases}$$

Furthermore, $\operatorname{div}_\gamma$ being an operator analogously defined to $\operatorname{curl}_\gamma$ in (4), it is clear that $\operatorname{div}_\gamma \operatorname{curl}_\gamma \varphi = 0$, $\forall \varphi \in [\mathcal{D}(\mathbb{R}^2)]^3$, that is for smooth vector valued functions φ. Thus,

denoting by k_0 the wave number $\omega\sqrt{\mu_0\varepsilon_0}$, we are led to the two following systems of Maxwell's type :

$$(4'_E)\begin{cases}\operatorname{curl}_\gamma \operatorname{curl}_\gamma \mathbf{E} = k_0^2\varepsilon_r\mathbf{E}\\ \operatorname{div}_\gamma(\varepsilon_0\varepsilon_r\mathbf{E}) = 0\end{cases}$$

$$(4'_H)\begin{cases}\operatorname{curl}_\gamma(\varepsilon_r^{-1}\operatorname{curl}_\gamma \mathbf{H}) = k_0^2\mathbf{H}\\ \operatorname{div}_\gamma(\mu_0\mathbf{H}) = 0\end{cases}$$

It must be noticed that $\mathbf{H}$ (resp. $\mathbf{E}$) can be deduced from $(4'_E)$ (resp. $(4'_H)$) thanks to (3.2) (resp. (3.1)). Making the obvious remark that the divergence of $\mathbf{H}$ is null, contrary to that of $\mathbf{E}$, we choose a magnetic formulation. We thus have the following lemma ([28]) :

Lemma 1 :

Let s be a positive real. Then, the two following systems are equivalent in $[H^1(\mathbb{R}^2)]^3$ (space of functions in $[L^2(\mathbb{R}^2)]^3$ whose gradients are in $[L^2(\mathbb{R}^2)]^9$) :

$$(5)\begin{cases}\operatorname{curl}_\gamma(\varepsilon_r^{-1}\operatorname{curl}_\gamma \mathbf{H}) = k_0^2\mathbf{H} & \textit{(5.1)}\\ \operatorname{div}_\gamma \mathbf{H} = 0 & \textit{(5.2)}\end{cases}$$

$$(6)\qquad \operatorname{curl}_\gamma(\varepsilon_r^{-1}\operatorname{curl}_\gamma \mathbf{H}) - s\bigtriangledown_\gamma(\operatorname{div}_\gamma \mathbf{H}) = k_0^2\mathbf{H}$$

Remark :

Taking the divergence in (5.1), we simply derive (5.2) but we keep this last equation to emphasize on this fundamental property of null divergence.

Proof :

A solution $\mathbf{H}$ of (5) in the Hilbert space $[H^1(\mathbb{R}^2)]^3$ clearly satisfies (6).

Conversely, suppose that $\mathbf{H}$ satisfies (6). Taking the divergence of the two members of (6) and letting φ be $\operatorname{div}_\gamma \mathbf{H}$, we get :

$$-s\operatorname{div}_\gamma(\bigtriangledown_\gamma\varphi) = k_0^2\varphi$$

We are thus led to the following system :

$$(7)\begin{cases}\varphi \in L^2(\mathbb{R}^2)\\ -s\Delta\varphi = (k_0^2 - \gamma^2 s)\varphi\end{cases}$$

Taking the Fourier transform $\hat{\varphi}$ of φ, we get :

$$(\Lambda^2 - p^2)\hat{\varphi} = 0\ ,\quad \text{in } L^2(\mathbb{R}^2)$$

$$\text{where } \Lambda = \begin{cases}\sqrt{\dfrac{k_0^2 - \gamma^2 s}{s}} & \text{if } \gamma^2 > k_0\\ i\sqrt{\dfrac{\gamma^2 s - k_0^2}{s}} & \text{if } k_0 > \gamma^2\end{cases}$$

and with a Fourier convention in $e^{-i(p_x x + p_y y)}$. The solution of the preceding equation in the sense of tempered distributions is of the form :

$$\hat{\varphi} = A\delta(\Lambda - p) + B\delta(\Lambda + p)$$

which is not in $L^2(\mathbb{R}^2)$. Hence, (7) admits only trivial solutions, which proves that $\mathrm{div}_\gamma \mathbf{H} = 0$.

(QED)

Noting that in $\mathbb{R}^2 \setminus \bar{\Omega}$ (exterior of Ω), (6) becomes :

$$-\Delta \mathbf{H} + \gamma^2 \mathbf{H} + (1-s) \bigtriangledown_\gamma (\mathrm{div}_\gamma \mathbf{H}) = k_0^2 \mathbf{H} \ ,$$

we take $s = 1$ to get the vector Helmholtz equation outside Ω. Our problem reduces to find real ε_r (for a given positive propagation constant γ) such that there exists $\mathbf{H}$ solution of the problem $(\mathcal{P})$:

$$(\mathcal{P}) \begin{cases} \mathbf{H} \in [H^1(\mathbb{R}^2)]^3 \ , \mathbf{H} \neq 0 \\ c(\gamma; \mathbf{H}, \mathbf{H}') = k_0^2(\mathbf{H}, \mathbf{H}') \ , \forall \mathbf{H}' \in [H^1(\mathbb{R}^2)]^3 \end{cases}$$

where $c(\gamma; \cdot, \cdot)$ is the sesquilinear form defined by :

$$c(\gamma; \mathbf{H}, \mathbf{H}') = \int_{\mathbb{R}^2} (\frac{1}{\varepsilon_r} \mathrm{curl}_\gamma \mathbf{H} \cdot \overline{\mathrm{curl}_\gamma \mathbf{H}'} + \mathrm{div}_\gamma \mathbf{H} \overline{\mathrm{div}_\gamma \mathbf{H}'}) dxdy$$

Note that for all $\mathbf{U}$ in $[H^1(\mathbb{R}^2)]^3$, we have :

$$\int_{\mathbb{R}^2} (\mid \mathrm{curl}_\gamma \mathbf{U} \mid^2) \, dxdy = \int_{\mathbb{R}^2} \mathrm{curl}_\gamma(\mathrm{curl}_\gamma \mathbf{U}) \cdot \bar{U} \, dxdy$$

$$= \int_{\mathbb{R}^2} \Big(-\Delta \mathbf{U} + \gamma^2 \mathbf{U} + \bigtriangledown_\gamma (\mathrm{div}_\gamma \mathbf{U}) \Big) \cdot \bar{U} \, dxdy = \int_{\mathbb{R}^2} \Big(\mid \bigtriangledown \mathbf{U} \mid^2 + \gamma^2 \mid \mathbf{U} \mid^2 - \mid \mathrm{div}_\gamma \mathbf{U} \mid^2 \Big) \, dxdy$$

where $\mid \bigtriangledown \mathbf{U} \mid^2 = Tr((\bigtriangledown \mathbf{U})^t \bigtriangledown \mathbf{U}) = \sum_{i=1}^{3} \mid \partial^i \mathbf{U}_i \mid^2$. Thus, assuming that $\inf_{(x,y) \in \mathbb{R}^2} \varepsilon_r(x,y) = 1$, we deduce that $c(\gamma; \cdot, \cdot)$ satisfies, $\forall \gamma \in \mathbb{R}^+ \ , \forall \mathbf{H} \in [H^1(\mathbb{R}^2)]^3$

$$\begin{cases} c(\gamma; \mathbf{H}, \mathbf{H}) \geq \dfrac{1}{\varepsilon^+} \displaystyle\int_{\mathbb{R}^2} (\mid \bigtriangledown \mathbf{H} \mid^2 + \gamma^2 \mid \mathbf{H} \mid^2) dxdy \geq \dfrac{\min(\gamma^2, 1)}{\varepsilon^+} \|\mathbf{H}\|^2_{H^1(\mathbb{R}^2)} \\ c(\gamma; \mathbf{H}, \mathbf{H}) \leq \displaystyle\int_{\mathbb{R}^2} (\mid \bigtriangledown \mathbf{H} \mid^2 + \gamma^2 \mid \mathbf{H} \mid^2) dxdy \leq \max(\gamma^2, 1) \|\mathbf{H}\|^2_{H^1(\mathbb{R}^2)} \end{cases}$$

where ε^+ is given by $\varepsilon^+ = \sup_{(x,y) \in \mathbb{R}^2} \varepsilon_r(x,y)$ and $\|\mathbf{H}\|^2_{H^1(\mathbb{R}^2)} = \displaystyle\int_{\mathbb{R}^2} (\mid \bigtriangledown \mathbf{H} \mid^2 + \mid \mathbf{H} \mid^2) dxdy$.

The previous system ensures us that $c(\gamma)$ is thus continuous and coercive in $[H^1(\mathbb{R}^2)]^3$ if $\gamma \neq 0$. From the Lax-Milgram lemma, we then deduce that (5) admits a unique solution in $[H^1(\mathbb{R}^2)]^3$ given by the minimum of the following functional in the Hilbert space $[H^1(\mathbb{R}^2)]^3$:

$$\mathcal{R}(\gamma; \mathbf{H}, \mathbf{H}') = \int_{\mathbb{R}^2} \frac{1}{\varepsilon_r} \mathrm{curl}_\gamma \mathbf{H} \cdot \overline{\mathrm{curl}_\gamma \mathbf{H}'} dxdy$$

$$+s \int_{\mathbb{R}^2} \mathrm{div}_\gamma \mathbf{H} \, \overline{\mathrm{div}_\gamma \mathbf{H}'} dxdy - k_0^2 \int_{\mathbb{R}^2} \mathbf{H} \cdot \overline{\mathbf{H}'} dxdy \tag{8}$$

Besides, from the Lax-Milgram lemma we know that for a given positive real γ, there is a unique operator $C(\gamma)$ defined for all $\mathbf{H}$ and $\mathbf{H}'$ in $[L^2(\mathbb{R}^2)]^3$ by $(C(\gamma)\mathbf{H}, \mathbf{H}') = c(\gamma; \mathbf{H}, \mathbf{H}')$. It can thus be established that ([28]) :

Lemma 2 :

Let γ be in $\mathbb{R}^+$. Then the operator $C(\gamma)$ is a self adjoint operator and its spectrum $\sigma(C(\gamma))$ satisfies the following inclusion :

$$\sigma(C(\gamma)) \subset [\frac{\gamma^2}{\varepsilon^+}, +\infty[$$

Besides, if we denote by $\sigma_p(C(\gamma))$ the set of eigenvalues of $C(\gamma)$, then $\frac{\gamma^2}{\varepsilon^+} \notin \sigma_p(C(\gamma))$.

Proof :

(i) We know that for all $\mathbf{H}$ in $[H^1(\mathbb{R}^2)]^3$

$$c(\gamma; \mathbf{H}, \mathbf{H}) \geq \frac{\gamma^2}{\varepsilon^+} \|\mathbf{H}\|^2_{L^2(\mathbb{R}^2)}$$

which proves both the self adjointness of $C(\gamma)$ and the inclusion satisfied by its spectrum (Reed and Simon, theorem 8.15 p. 278, tome 1 [183]).

(ii) We have to prove that $\frac{\gamma^2}{\varepsilon^+}$ is not an eigenvalue of $C(\gamma)$. Stating that $\mathbf{H}$ is such that the above inequality is an equality, we deduce that

$$\int_{\mathbb{R}^2} | \bigtriangledown \mathbf{H} |^2 \, dxdy = 0$$

Thanks to the Parseval identity, we get that :

$$\int_{\mathbb{R}^2} | \bigtriangledown \hat{\mathbf{H}} |^2 \, dp_x dp_y = - \int_{\mathbb{R}^2} (p_x^2 + p_y^2) | \hat{\mathbf{H}} |^2 \, dp_x dp_y = 0$$

Hence, $\hat{\mathbf{H}}$ is identically null (contradiction).

(QED)

We now develop $\mathbf{H}(x, y)$ in its transverse and longitudinal components $\mathbf{H}_t(x, y)$ and $H_l(x, y)$:

$$\mathbf{H}(x, y) = H_{t,1}(x, y)\mathbf{e}_x + H_{t,2}(x, y)\mathbf{e}_y + H_l(x, y)\mathbf{e}_z = \mathbf{H}_t(x, y) + H_l(x, y)\mathbf{e}_z$$

We define the transverse gradient, divergence and curl as

$$\bigtriangledown_t H_l(x, y) = \frac{\partial H_l}{\partial x}\mathbf{e}_x + \frac{\partial H_l}{\partial y}\mathbf{e}_y$$
$$\mathrm{div}_t(H_{t,1}\mathbf{e}_x + H_{t,2}\mathbf{e}_y) = \frac{\partial H_{t,1}}{\partial x} + \frac{\partial H_{t,2}}{\partial y}$$
$$\mathrm{curl}_t(H_{t,1}\mathbf{e}_x + H_{t,2}\mathbf{e}_y) = \frac{\partial H_{t,2}}{\partial x} - \frac{\partial H_{t,1}}{\partial y}$$

and we develop curl_γ and div_γ in their transverse and longitudinal components :

$$\mathrm{div}_\gamma \, \mathbf{H} = \frac{\partial H_{t,1}}{\partial x} + \frac{\partial H_{t,2}}{\partial y} + i \, \gamma H_l = \mathrm{div}_t \, H_t + i \, \gamma H_l$$

$$\begin{aligned}\mathrm{curl}_\gamma \mathbf{H} &= \Big(\frac{\partial H_l}{\partial y} - i\,\gamma H_{t,2}\Big)\mathbf{e}_x + \Big(i\,\gamma H_{t,1} - \frac{\partial H_l}{\partial x}\Big)\mathbf{e}_y + \Big(\frac{\partial H_{t,2}}{\partial x} - \frac{\partial H_{t,1}}{\partial y}\Big)\mathbf{e}_z \\ &= \mathrm{curl}_t\, H_t\, \mathbf{e}_z + (\bigtriangledown_t H_l - i\,\gamma H_t) \times \mathbf{e}_z\end{aligned}$$

Making use of the Green formula :

$$\int_{\mathbb{R}^2} \Big(\bigtriangledown H_l \cdot \bar{\mathbf{H}}'_t - \mathbf{H}_t \cdot \bigtriangledown \bar{H}'_l\Big)\, dxdy = -\int_{\mathbb{R}^2} \Big(\mathrm{div}_t\, \mathbf{H}_t\ \bar{H}'_l - H_l\ \mathrm{div}\, \bar{\mathbf{H}}'_t\Big)\, dxdy\ ,$$

we derive the following lemma ([28]) :

Lemma 3 :

For all positive real γ, and for $\mathbf{H}$ and $\mathbf{H}'$ in $[H^1(\mathbb{R}^2)]^3$, we have the following equality :

$$c(\gamma; \mathbf{H}, \mathbf{H}') = d(\gamma, \mathbf{H}, \mathbf{H}') + \gamma^2(\mathbf{H}, \mathbf{H}') \tag{9}$$

with $d(\gamma, ., .)$ defined by :

$$d(\gamma, \mathbf{H}, \mathbf{H}') = d^0(\mathbf{H}, \mathbf{H}') + \gamma d^1(\mathbf{H}, \mathbf{H}') + \gamma^2 d^2(\mathbf{H}, \mathbf{H}')$$

where d^0, d^1 and d^2 are given by :

$$\begin{aligned} d^0(\mathbf{H}, \mathbf{H}') &= \int_{\mathbb{R}^2} \Big(\frac{1}{\varepsilon_r}\, \mathrm{curl}_t\, \mathbf{H}_t\, \mathrm{curl}_t\, \bar{\mathbf{H}}'_t + \mathrm{div}_t\, \mathbf{H}_t\ \mathrm{div}_t\, \bar{\mathbf{H}}'_t + \frac{1}{\varepsilon_r}\, \bigtriangledown_t H_l \cdot \bigtriangledown_t \bar{H}'_l\Big)\, dxdy \\ d^1(\mathbf{H}, \mathbf{H}') &= i \int_{\mathbb{R}^2} \Big((\frac{1}{\varepsilon_r} - 1)(\mathbf{H}_t \cdot \bigtriangledown_t \bar{H}'_l - \bigtriangledown_t H_l \cdot \bar{\mathbf{H}}'_t)\Big)\, dxdy \\ d^2(\mathbf{H}, \mathbf{H}') &= \int_{\mathbb{R}^2} (\frac{1}{\varepsilon_r} - 1)\mathbf{H}_t \cdot \bar{\mathbf{H}}'_t\, dxdy \end{aligned}$$

It is worth noting that we are dealing with an unbounded operator, since d has a support in the overall space $\mathbb{R}^2$ (this would not be the case for a metallic guide of dielectric rods). We therefore have to deal with the essential part of the spectrum, that is the set of eigenvalues of infinite multiplicity, accumulation points of eigenvalues and the continuous spectrum (bands). It can be shown that for all $\gamma \in \mathbb{R}^+$, the essential spectrum $\sigma_{ess}(C(\gamma))$ of $C(\gamma)$ satisfies ([28]) :

$$\sigma_{ess}(C(\gamma)) = \Big[\gamma^2; +\infty\Big[$$

Lemma 4 :

For all $\gamma \in \mathbb{R}^+$, the essential spectrum $\sigma_{ess}(C(\gamma))$ of $C(\gamma)$ satisfies :

$$\sigma_{ess}(C(\gamma)) = \Big[\gamma^2; +\infty\Big[$$

Proof :

We see that d^1 and d^2 are compact perturbations of d^0 (note that $\dfrac{1}{\varepsilon_r} - 1$ is null outside Ω and conclude by the compact embedding of $[H^1(\Omega)]^3$ in $[L^2(\Omega)]^3$.), thus they do not change its continuous spectrum ([183]). We then have that :

$$\sigma_{ess}(C(\gamma)) = \Big\{\Lambda + \gamma^2\ ;\ \Lambda \in \sigma_{ess}(C(0))\Big\}$$

Furthermore, the lemma 3 ensures that $d^0(\mathbf{H},\mathbf{H})$ satisfies for all $\mathbf{H} \in [H^1(\mathbb{R}^2)]^3$:

$$d^0(\mathbf{H},\mathbf{H}) \geq \frac{1}{\varepsilon^+}\int_{\mathbb{R}^2} |\bigtriangledown \mathbf{H}|^2\, dxdy$$

where $\varepsilon^+ = \sup_{(x,y)\in\mathbb{R}^2} \varepsilon_r(x,y)$.
From the lemma 2, we hence deduce that :

$$\sigma_{ess}(C(0)) = \mathbb{R}^+$$

The lemma is thus straightforward.

(QED)

Lemma 5 :

If ε is a piecewise function of class C^2 in Ω the discrete spectrum of $C(\gamma)$ satisfies :

$$\sigma_d(C(\gamma)) \subset]-\infty;\gamma^2]$$

Proof :

In other words, we must prove that there are no eigenvalues in the continuous spectrum except sometimes for γ^2 (when a new mode appears, cf. figure 6.1). Let $\mathbf{H}$ be a mode in $[H^1(\mathbb{R}^2)]^3$ and $\Lambda > \gamma^2$ an eigenvalue such that :

$$c(\gamma,\mathbf{H},\mathbf{H}') = \Lambda(\mathbf{H},\mathbf{H}')\ ,\ \forall\, \mathbf{H}' \in [H^1(\mathbb{R}^2)]^3$$

From (6), we see that for all $(x,y) \in \mathbb{R}^2 \setminus \bar{\Omega}$, $\mathbf{H}(x,y)$ satisfies :

$$-\Delta\mathbf{H} + (\Lambda - \gamma^2)\mathbf{H} = 0$$

The above equation admits only trivial square integrable solutions since $\Lambda - \gamma^2$ is positive [184]. Therefore the theory of partial differential equations ensures us of the nullity of $\mathbf{H}$ in $\mathbb{R}^2$ [114].

(QED)

Remark :

This lemma holds for instance for step profile fibers, graded profile fibers and obviously for photonic crystal fibers.

The operator $C(\gamma)$ is self adjoint, hence every point which is not in its essential spectrum is an isolated eigenvalue of finite multiplicity ([183]). Furthermore, the operator $C(\gamma)$ is lower bounded. We can then apply the Min-Max principle on each eigenvalue inferior to the lower bound γ^2 of its essential spectrum [28].

Lemma 6 :

Every eigenvalue $\Lambda^j(\gamma)$, $j \in \{1,..,k\}$, of the operator $C(\gamma)$ satisfies the following dispersion relations (DR) :

$$\frac{\gamma^2}{\varepsilon^+} < \Lambda^1(\gamma) \leq \Lambda^2(\gamma) \leq ... \leq \Lambda^k(\gamma) \leq \gamma^2 \qquad (DR)$$

where ε^+ *is given by* $\varepsilon^+ = \sup_{(x,y)\in\mathbb{R}^2} \varepsilon_r(x,y)$

Remarks :

An empty discrete spectrum $\sigma_d(C_\gamma)$ corresponds to frequencies under the cut-off, and an integer $k = 1$ to a monomode fiber (fig. 6.1).

Thanks to the dispersion relations (DR), we know that every eigenvalue greater than γ^2 belongs to the essential spectrum, which gives us a numerical criterion to eliminate the modes without any physical meaning. Nevertheless, we numerically detect some frequencies in the essential spectrum whose associated eigenvectors seem to satisfy all the properties of propagating modes (notably null divergence). We believe that those eigenvectors may give us information on the diffracting problem in conical incidence.

From (9), we see that $c(\gamma)$ depends on both γ and γ^2 i.e. ε_r being fixed, the calculus of γ such that (γ, ε_r) is a solution of $\mathcal{P}$, is a non linear problem. We thus choose to look for ω as a function of γ (such an approach would not hold for a dispersive media).

Let us also note that the functions $\gamma \in \mathbb{R}^+ \longmapsto \Lambda_m(\gamma) \in \mathbb{R}^+$ are monotonic, provided that

$$(1 - \frac{1}{\varepsilon^+})(\sqrt{\varepsilon^+} + 1) < 1 \ ,$$

which is a property shared by all the optical fibers ([28]). The functions Λ_m are therefore bijective on $\mathbb{R}^+$ and the usual dispersion curve is straightforward from (DR). To be more precise, the Λ_m are even almost everywhere differentiable since they satisfy ([28]) :

$$\frac{\mid \Lambda_m(\gamma) - \Lambda_m(\gamma') \mid}{\mid \gamma - \gamma' \mid} \leq 2(1 - \frac{1}{\varepsilon^+})(\sqrt{\varepsilon^+} + 1) \max(\gamma,\ \gamma') \ .$$

We thus have an upper estimate for the slope of the curves : the lower ε^+, the smaller the estimate (therefore the slope) and this estimate is asymptotically equal to $2(\sqrt{\varepsilon^+} + 1) \max(\gamma,\ \gamma')$ for large ε^+. One cannot hope to show stronger properties on the derivatives of the curves, since there are some branches of eigenvalues crossing each other even in the case of a step profile optical fiber of circular cross section.

To be complete, we must add that the previous results can be generalized to the case of dielectric waveguides in perturbed media. The theoretical study is much more difficult to perform since d^1 and d^2 are no more compact perturbations of d^0. These optical waveguides have very specific properties. For instance, it can be shown that such waveguides have no guided mode when the wave number is close to 0, due to the discontinuity of the permittivity at the interface [28]. Furthermore, the numerical study of propagating modes in a waveguide in the vinicity of an interface is of pratical interest : in integrated optics the optical guides lie on dielectric substrates and in telecoms the optical fibers are layed under water. We therefore give a sketch of the proof of a theorem which evaluates the new lower bound of the essential spectrum. The reader can find the complete proof in [28].

Without loss of generality, we can suppose that there exists a positive real a such that :

$$\varepsilon_r(x,y) = \varepsilon_\infty^+ \ , \quad \text{if } \mid x \mid > a \ \text{ and } y > 0$$

$$\varepsilon_r(x,y) = \varepsilon_\infty^- \ , \quad \text{if } \mid x \mid > a \ \text{ and } y < 0$$

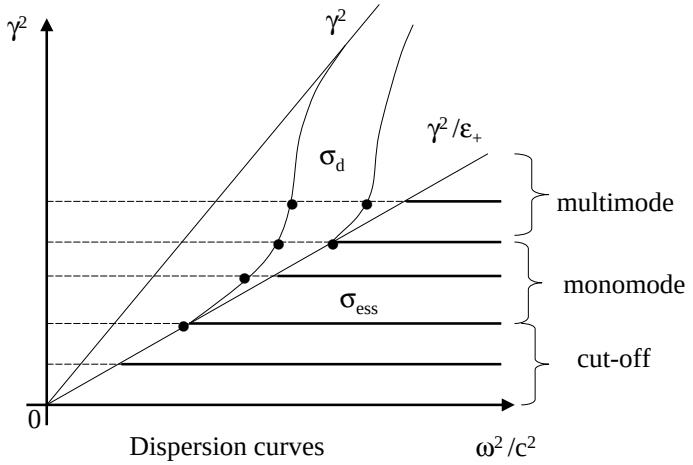

FIGURE 6.1 – Decomposition of the spectrum $\sigma((C\gamma))$ of the open guide operator $C(\gamma)$ in its discrete part σ_d (which gives the dispersion curves when γ varies in $\mathbb{R}_*^+$) and its essential part σ_{ess} (eigenvalues of infinite multiplicity, accumulation points of eigenvalues and continuous spectrum which are probably associated to the diffracting problem).

Let us assume that $\varepsilon_\infty^+ > \varepsilon_\infty^-$.

Theorem 7 :

For all $\gamma \in \mathbb{R}^+$, the essential spectrum $\sigma_{ess}(C(\gamma))$ of $C(\gamma)$ satisfies :

$$\sigma_{ess}(C(\gamma)) = \left[\frac{\gamma^2}{\varepsilon_\infty^+}; +\infty\right[$$

Proof :

If we prove that

$$\sigma_{ess}(C(\gamma)) \subset \left[\frac{\gamma^2}{\varepsilon_\infty^+}; +\infty\right[,$$

the theorem will be deduced from lemma 2.

We know that $\sigma_{ess}(C(\gamma))$ is closed. We therefore have to prove that

$$\left]\frac{\gamma^2}{\varepsilon_\infty^+}; +\infty\right[\subset \sigma_{ess}(C(\gamma)) .$$

Let $\lambda > \dfrac{\gamma^2}{\varepsilon_\infty^+}$. To prove that $\lambda \in \sigma(C(\gamma))$, we must find a sequence of singular eigenvectors $(H^p)_{p\in\mathbb{N}^*}$ for λ [189]. Following [28], we set :

$$(11) \begin{cases} \Lambda = \varepsilon_\infty^+ \lambda - \gamma^2 > 0 \\ \mathbf{H}^p = u^p \mathbf{H}^0 \ , \forall\ p \in \mathbb{N}^* \end{cases}$$

where $\mathbf{H}^0 \neq 0$ is an arbitrary vector of $\mathbb{C}^3$ and u^p is defined by :

$$u^p(x,y) = \frac{1}{\sqrt{p}}\Psi(\frac{x}{p},\frac{y}{p})\varphi(x,y)\ ,\forall\ p \in \mathbb{N}^* \tag{12}$$

with $\varphi(x,y) = J_0(\sqrt{\Lambda}\sqrt{x^2+y^2})$, and where J_0 is the Bessel function of order 0. Ψ is an infinitely differentiable function with compact support in $\mathbb{R}^2$ such that :

$$\begin{cases} \displaystyle\int_{\mathbb{R}^2} |\ \Psi\ |^2\, dxdy = 1 \\ \Psi \equiv 0 \ \text{ dans } \mathbb{R}\times]-\infty; d^+[\end{cases} \tag{13}$$

where $d^+ = \inf\Big\{\alpha \in \mathbb{R}^+; \varepsilon_r(x,y) = 1 \ \text{ p.p. } x \in \mathbb{R}\ ,\ y > \alpha\Big\}$.

It is worth noting that J_0 is a Bessel function which describes an almost periodic phenomenon vanishing at infinity. Furthermore, $J_0(0) = 1$ is the maximum of this function. This function thus fits the behavior of transverse fields whose energy is mainly in the core of the fiber and which are vanishing with oscillations outside the fiber.

It is clear that :

$$u^p \in H^1(\mathbb{R}^2)\ ,\forall\ p \in \mathbb{N}^*$$

and

$$\text{supp}\ (u^p) \subset \mathbb{R}\times]d^+; +\infty[\ ,\forall\ p \in \mathbb{N}^*$$

We want to establish that :

$$\begin{cases} \|\mathbf{H}^p\|_{[L^2(\mathbb{R}^2)]^3} \geq \|\mathbf{H}^0\|_{[L^2(\mathbb{R}^2)]^3} & ,\ \forall\ p \in \mathbb{N}^* \\ \|C(\gamma)\mathbf{H}^p - \lambda\mathbf{H}^p\|_{[L^2(\mathbb{R}^2)]^3} \overset{p\to+\infty}{\to} 0 & \\ \mathbf{H}^p \overset{p\to+\infty}{\rightharpoonup} 0 & ,\ \text{in } [L^2(\mathbb{R}^2)]^3 \text{ weak} \end{cases}$$

Noting that $\Big(\frac{1}{\varepsilon} - \frac{1}{\varepsilon_\infty}\Big)\mathbf{H}^p$ is null on $\mathbb{R}^2$, from lemma 3 we deduce that :

$$\begin{aligned} c(\gamma;\mathbf{H}^p,\mathbf{V}^p) - \lambda\int_{\mathbb{R}^2}\mathbf{H}^p\bar{\mathbf{V}}^p\,dxdy = \frac{1}{\varepsilon_\infty^+}\int_{\mathbb{R}^2}\Big(&\text{curl}_t\,\mathbf{H}_t^p\,\text{curl}_t\,\bar{\mathbf{V}}_t^p \\ &+ \text{div}_t\,\mathbf{H}_t^p\ \text{div}_t\,\bar{\mathbf{V}}_t^p + \bigtriangledown_t H_l^p\cdot\bigtriangledown_t\bar{V}_l^p - \Lambda\mathbf{H}^p\bar{\mathbf{V}}^p\Big)\,dxdy \end{aligned}$$

Integrating par parts, we get that :

$$C(\gamma)\mathbf{H}^p - \lambda\mathbf{H}^p = -\frac{1}{\varepsilon_\infty^+}(\Delta u^p + \Lambda u^p)\mathbf{H}^0$$

We therefore have to establish that :

$$i)\ \exists\ \alpha > 0 \ \text{ such that } \ \|u^p\|_{L^2(\mathbb{R}^2)} \geq \alpha\ ,\forall\ p \in \mathbb{N}^*\ ,$$

$$ii)\ \|\Delta u^p + \Lambda u^p\|_{L^2(\mathbb{R}^2)} \to 0\ ,\ \text{when } p \to +\infty$$

$$iii)\ u^p \rightharpoonup 0 \ \text{ in } L^2(\mathbb{R}^2) \text{ weak}\ ,\ \text{when } p \to +\infty$$

i) Noting that $J_0(0) = 1$, we see that $i)$ holds for finite p. The assertion $i)$ is then derived from the asymptotic behavior of J_0 [1] :

$$J_0(r) \overset{r\to+\infty}{\sim} \sqrt{\frac{2}{\pi r}}\cos(r-\frac{\pi}{4}) \ , \tag{14}$$

where $r = \sqrt{x^2+y^2}$. Taking $v = \dfrac{x}{p}$ and $w = \dfrac{y}{p}$ in (4.2), we get that :

$$\|u_p\|_{L^2(\mathbb{R}^2)} = \int_{\mathbb{R}^2} \Psi^2(v,w)\ p\ J_0^2(p\sqrt{\Lambda}\sqrt{v^2+w^2})\, dvdw \tag{15}$$

We deduce from (13), (14) and (15) that :

$$\begin{aligned}\|u^p\|_{L^2(\mathbb{R}^2)} &\overset{p\to+\infty}{\sim} \frac{2}{\pi\sqrt{\Lambda}}\int_{\mathbb{R}^2}\Psi^2(v,w)\cos^2(p\sqrt{\Lambda}\sqrt{v^2+w^2}-\frac{\pi}{4})\, dvdw \\ &\overset{p\to+\infty}{\sim} \frac{1}{\pi\sqrt{\Lambda}}\int_{\mathbb{R}^2}\Psi^2(v,w)\, dvdw = \frac{1}{\pi\Lambda}\end{aligned}$$

The assertion is then straightforward.

ii) It can be shown that [28] :

$$-(\Delta+\Lambda)u^p = \frac{1}{p^{\frac{1}{2}}}\Psi(\frac{x}{p},\frac{y}{p})(-\Delta\varphi(x,y)-\Lambda\varphi(x,y))$$

$$-\frac{2}{p^{\frac{3}{2}}}\bigtriangledown\Psi_\eta(\frac{x}{p},\frac{y}{p})\cdot\bigtriangledown\varphi(x,y) - \frac{1}{p^{\frac{5}{2}}}\Delta\Psi_\eta(\frac{x}{p},\frac{y}{p})\varphi(x,y) \ .$$

Noting that $\varphi(x,y) = J_0(\sqrt{\Lambda}\sqrt{x^2+y^2})$ satisfies

$$\Delta\varphi+\Lambda\varphi = 0 \ ,$$

and taking into account that

$$\bigtriangledown J_0(r) \overset{r\to+\infty}{\sim} \sqrt{\frac{2}{\pi r}}\cos(r-\frac{3\pi}{4})\mathbf{e}_r \ ,$$

(where $\mathbf{e}_r$ is a unit radial vector) the assertion can be deduced analogously to $i)$.

iii) This assertion derives from the Lebesgue dominated theorem (see [28]).

Remarks :

It is established in [28] that :

$$\int_{\mathbb{R}^2} |\ \bigtriangledown\mathbf{H}\ |^2\, dxdy \le \gamma^2 M(\varepsilon_r)\int_\Omega |\ \mathbf{H}_t\ |^2\, dxdy$$

where

$$M(\varepsilon_r) = \delta(\varepsilon_r)(1+4\sqrt{\delta(\varepsilon_r)}+4\delta(\varepsilon_r))$$

and

$$\delta(\varepsilon_r(x,y)) = \sup_{(x,y)\in\mathbb{R}^2}\varepsilon_r(x,y)\sup_{(x,y)\in\mathbb{R}^2}\Big|\frac{1}{\varepsilon_r(x,y)}-\frac{1}{\varepsilon_\infty^+}\Big|$$

Besides, we know that $\mathrm{div}_\gamma \mathbf{H} = 0$. This implies that :

$$\mathrm{div}_t \mathbf{H}_t = -i\gamma H_l$$

Integrating par parts, it thus follows that :

$$\int_{\mathbb{R}^2} \mid H_l \mid^2 dxdy \leq M(\varepsilon_r) \int_\Omega \mid \mathbf{H}_t \mid^2 dxdy$$

If $M(\varepsilon_r)$ is small (i.e. ε_r is close to ε_{∞^+}), we deduce that the magnetic field is almost transverse : the weak coupling assumption can therefore been used.

The confinement of the field in the core region Ω of the fiber can be quantified with the following ratio :

$$\frac{\int_\Omega \mid \mathbf{H} \mid^2 dxdy}{\int_{\mathbb{R}^2} \mid \mathbf{H} \mid^2 dxdy}.$$

If we denote by Ω_{∞^-} the lower outer medium (substratum)

$$\Omega_{\infty^-} = \left\{(x,y) \in \mathbb{R}^2 \ , \mid x \mid > a \ \text{ and } \ y < 0\right\},$$

it can be established that [28] :

$$\delta_\infty(\varepsilon_r) \int_{\Omega_{\infty^-}} \mid \mathbf{H}_t \mid^2 dxdy \leq M_\infty(\varepsilon_r) \int_\Omega \mid \mathbf{H}_t \mid^2 dxdy$$

where

$$M_\infty(\varepsilon_r) = \delta(\varepsilon_r)(1+\delta(\varepsilon_r)) + 2\sqrt{M(\varepsilon_r)\delta(\varepsilon_r)(1+\delta(\varepsilon_r))\delta_\infty(\varepsilon_r)} + 4M(\varepsilon_r)\delta_\infty(\varepsilon_r)$$

and

$$\delta_\infty(\varepsilon_r(x,y)) = \sup_{(x,y)\in\mathbb{R}^2} \varepsilon_r(x,y) \sup_{(x,y)\in\mathbb{R}^2} \Big| \frac{1}{\varepsilon_\infty^-(x,y)} - \frac{1}{\varepsilon_\infty^+} \Big|$$

We note that the majoration of $\displaystyle\int_{\Omega_{\infty^-}} \mid H_t \mid^2 dxdy$ is obvious if the outer of the waveguide is an homogeneous medium ($\delta_\infty(\varepsilon_r(x,y)) = 0$). On the contrary, if the outer of the waveguide consists of two media of very different permittivities ($\delta_\infty(\varepsilon_r(x,y))$ is big), we see that the magnetic field is vanishing in the substratum.

These theoretical developments are of very importance for the numerical treatment of propagating problems encountered in most of the pratical cases : optical cables under the sea, micro-strips...

6.4 Variational methods and finite elements.

6.4.1 Maxwell's equations and differential forms.

The calculus of differential forms has been used for a long time, in general relativity, quantum field theory, thermodynamics, or mechanics, whereas in electromagnetic field theory it has been rather lately introduced as an alternative to vector analysis. However, it

clarifies different notions such as field intensity or flux density, the connection between the Stokes theorem and the divergence theorem and the correspondence between vector fields and their rotationals. Cartan and others developed the calculus of differential forms in the early 1900's. A differential form is a quantity that can be integrated, including differentials. More precisely, we will see in the sequel that a differential form is a fully covariant, fully antisymmetric tensor. The calculus of differential forms is a self-contained subset of tensor analysis. Since Cartan's time, the use of forms has spread to many fields of pure and applied mathematics and a section on differential forms is commonplace in mathematical physics texts.

The laws of electromagnetic field theory as expressed by James Clerk Maxwell in the mid 1800's required dozens of equations. Vector analysis offered a more convenient tool for working with electromagnetic theory than earlier methods. Tensor analysis is in turn more concise and general, but is very abstract and gives no intuitive representation to tensor fields such as the curl operation (and it requires many indices). The question is thus to find another way which may combine the simplicity of vector analysis to the power of tensor analysis. The answer was given by Weyl and Poincaré who expressed Maxwell's laws using differential forms early this century. Applied to electromagnetics, differential forms combine much of the generality of tensors with the simplicity and the concreteness of vectors. Other formalisms for electromagnetic theory are available, including bivectors and quaternions. We will give further details on the notion of bivectors in the sequel. Concerning the set of quaternions, H, we just note that it is a generalization of the set of complex numbers defined as :

$$\{a = r_i\ e_i\ :\ i = 0, 1, 2, 3\ :\ r_i \in \mathbb{R}\} \tag{16}$$

such that $e_0\ e_0 = e_0$, and $e_i\ e_j = -\delta_{ij}\ e_0 + \varepsilon_{ijk}\ e_k$ for all i, j, $k = 1, 2, 3$. H is a non-commutative associative algebra whose properties are studied by group theorists and were introduced in electromagnetism by J. C. Maxwell himself [135] :

$$\begin{array}{ll} \mathcal{C} = v \cdot \nabla \mathcal{H} & , \mathcal{C} = \mathcal{J} + \mathcal{D}, \\ \mathcal{B} = v \cdot \nabla \mathcal{U} & , \mathcal{E} = -\mathcal{U} + \nabla \Psi, \\ \mathcal{B} = \mu \mathcal{H} & , \mathcal{D} = K\mathcal{E} \end{array} \tag{17}$$

where v means "vector part" of a quaternion product, and ∇ is the operator $e_i \dfrac{d}{dx} + e_j \dfrac{d}{dy} + e_k \dfrac{d}{dz}$. With vector calculus, we would write it :

$$\operatorname{curl} \mathbf{H} = \mathcal{C} = \mathbf{J} + \frac{\partial}{\partial t}\mathbf{D}\ ,\ \mathbf{B} = \operatorname{curl} \mathbf{A}\ ,\ \text{ and } \mathbf{E} = -\frac{\partial}{\partial t}\mathbf{A} - \nabla \Psi \tag{18}$$

None of these offer the combination of concrete graphical representations and close relationship to vector methods that the calculus of differential forms. Last, but not least, differential forms give an easy way to compute electromagnetic fields thanks to a particular class of finite elements called **Nédelec elements** or **edge elements** (Nédélec, 1980 [160], 1982 [161] and Bossavit, 1988 [29]), which are a kind of discrete differential forms whose properties were studied by Whitney (Whitney, 1957 [206]).

6.4.2 Notions of differential geometry

From a differential geometry point of view, the vector fields are the first order linear differential operators on functions. They have a vector space structure, one basis of which is the set $\{\frac{\partial .}{\partial x^i}\}$ of partial derivatives with respect to coordinates. The action of a vector field v on a function f is noted $v(f)$. A 1-form α is a linear map from vector fields v to scalar functions $\alpha(v)$, also noted $< \alpha, v >$ to emphasize duality (at one point of space, a vector field is represented by a vector and a 1-form by a covector i.e. a linear map from vectors to real numbers). A special 1-form associated to a function f is its differential df defined such that $df(v) = v(f)$. One basis for the vector space of 1-forms is the set $\{dx^i\}$ of the differentials of the coordinates. A p-form ω is a multilinear totally skew symmetric map from p vectors v_1, ..., v_p to scalar functions $\omega(v_1, ..., v_p)$. Functions are identified with 0-forms. In three-space only 0-,1-,2- and 3-forms are not identically equal to zero (because of the skew symmetry). 0- and 3-form spaces are one-dimensional vector spaces while 1- and 2-forms are three-dimensional vector spaces (neglecting of course the functional aspect where they are all infinite dimensional). From this point of view, scalar fields from vector analysis are 0- or 3-forms depending on their physical meaning : 0-forms are pointwise relevant functions while 3-forms are densities to be integrated on volumes. The vector fields from the vector analysis are 1-forms and 2-forms : 1-forms are integrands of line integrals while 2-forms are flux densities. Operations on forms include the exterior or wedge product $\wedge$ that maps pairs of a p-form ω_1 and a q-form ω_2 on the $(p+q)$-form $\omega_1 \wedge \omega_2$ defined by :

$$(\omega_1 \wedge \omega_2)(v_1, ..., v_{p+q}) = \frac{1}{p!q!} \sum_{\pi \in S_{p+q}} \Big[Sgn(\pi) \omega_1(v_{\pi(1)}, ..., v_{\pi(p)}) \times \omega_2(v_{\pi(p+1)}, ..., v_{\pi(p+q)}) \Big]$$

where π runs over the set of permutations of $p+q$ indices. The set $\{dx^{i_1} \wedge ... \wedge dx^{i_p}\}$ of the linearly independent exterior products of p differentials of the coordinates is a basis for the $\frac{n!}{p!(n-p)!}$-dimensional vector space of p-forms. Any p-form can be expressed as a linear combination of such p-monomials.

Another fundamental operation on forms is the exterior derivative d that maps p-forms

$$\omega = \frac{1}{p!} \sum_{i_1 \, ... \, i_p = 1}^{n} \omega_{i_1 \, ... \, i_p} dx^{i_1} \wedge ... \wedge dx^{i_p} \, ,$$

on $(p+1)$-forms

$$d\omega = \frac{1}{p!} \sum_{i_1 \, ... \, i_p = 1}^{n} (d\omega_{i_1 \, ... \, i_p}) \wedge dx^{i_1} \wedge ... \wedge dx^{i_p} \, ,$$

where $d\omega_{i_1 \, ... \, i_p}$ stands for the differential of $\omega_{i_1 \, ... \, i_p}$ considered as a function.

From this definition it is obvious that the exterior derivative of a function f is its differential df. The opposite operation of the exterior derivative is the integration of a n-form $\omega = f(x^1 \, ... \, x^n) dx^1 \wedge ... \wedge dx^n$ on a n-dimensional domain M, which is defined by :

$$\int_M \omega = \int_{\mathbb{R}^n} f(x^1 \, ... \, x^n) dx^1 \, ... \, dx^n \, ,$$

where f is supposed to be zero outside M.

These objects and operations only involve the topology and the differential structure of the ambient space i.e. they are independent of any notion of angle and/or distance. Those notions are introduced by giving a metric g i.e. a symmetric bilinear map from two vector fields v, w to scalar functions numbers $g(v,w)$. The metric allows the definition of the Hodge star operator $\star$ which maps p-forms on $(n-p)$-forms where n is the dimension of the ambient space. In local coordinates, the star operator is defined for an exterior p-monomial by (using the Einstein summation convention on repeated indices) :

$$\star dx^{i_1} \wedge \ ... \ \wedge dx^{i_p} = g^{i_1 j_1} \ ... \ g^{i_p j_p} dx^{j_{p+1}} \wedge \ ... \ \wedge dx^{j_n} \varepsilon_{j_1 \ ... \ j_n} \frac{\sqrt{\mid g \mid}}{(n-p)!} \ ,$$

where $\varepsilon_{j_1 \ ... \ j_n}$ is the Levi-Civita symbol. If the matrix the elements of which are

$$g_{ij} = g(\partial./\partial x^i, \ \partial./\partial x^j)$$

is considered, the g^{ij} are the components of its inverse and $\mid g \mid = det(g_{ij})$ is its determinant. By linearity, the definition of the star operator may be extended to any form. In three-space, the Hodge star operator maps 0-forms on 3-forms, 1-forms on 2-forms and conversely. This is why only functions and vector fields are used in the vector analysis of the three-space with the Euclidean metric.

6.4.3 A brief survey on edge elements and Whitney forms

"**Edge elements**" is a nickname for recently developed finite-element bases for vector fields, whose degrees of freedom are not to be interpreted as the components of some vector field at mesh nodes, but as circulations of the field along element edges [162]). We will see in the sequel that they do not impose on the magnetic and electric fields H and E more continuity than physics requires : edge-element approximations of (let's say) H, will have tangential continuity across material interfaces, but its normal component will not be forced to (unwanted) continuity by the nature of finite-element interpolants, as may happen with some node-based elements. Edge-elements are part of a discrete algebraic-geometric-differential structure of finite-element shape functions invented by H. Whitney ([206]) which assign degrees of freedom to **simplices** of a given mesh : nodes, edges, facets, tetrahedra. This structure, the so-called "**Whitney complex**", closely matches a continuous structure made of four vector subspaces of L^2 and of three differential operators $\bigtriangledown$, curl, div, which is known as the "**de Rham complex**". This complex is called an **exact sequence** if the image of each operator domain of this structure is exactly the kernel of the next operator what depends upon the topological properties of the domains such as connectivity assumptions. We thus choose the point of view of differential geometry in the sequel.

Consider a simplicial mesh on a three-dimensional manifold D, that is, a set of tetrahedra which 2 by 2 have in common either a full facet, or a full edge, or a node (vertex), or nothing, and whose set union is D. We also assume a numbering of the nodes n, so that edge e or facet f can alternatively be described by a list of node numbers. We call $\mathcal{T}$, $\mathcal{F}$, $\mathcal{E}$, $\mathcal{N}$ respectively, the sets of tetrahedra (or volumes), facets, edges and nodes which

constitute the mesh. Hence an edge e element of $\mathcal{E}$ will be denoted by the ordered set $\{i,\ j\}$ of its two extremities. A node n element of $\mathcal{N}$ will be denoted by $\{i\}$ (i is the number of node n) and a facet f element of $\mathcal{F}$ will be denoted by $\{i,\ j,\ k\}$. We shall adopt from now on the generic term of p-**simplices** to refer to nodes ($p = 0$), edges ($p = 1$), facets ($p = 2$) and volumes ($p = 3$) : more precisely, a p-simplex denotes the convex envelope of $p+1$ nodes i.e. if x_i denotes the location of the i-th node, the p-simplex is the set $\left\{\sum_{i=1}^{p+1} \beta_i\, x_i\ ,\ \beta_i \geq 0\ ,\ \sum_{i=1}^{p+1} \beta_i = 1\right\}$. Let us emphasize that if edge $\{i,\ j\}$ belongs to $\mathcal{E}$, or if facet $\{i,\ j,\ k\}$ belongs to $\mathcal{F}$, then $\{j,\ i\}$ does not belong to $\mathcal{E}$, and neither $\{k,\ i,\ j\}$, $\{j,\ k,\ i\}$, etc., do belong to $\mathcal{F}$: each p-simplex appears only once, with a definite orientation. We shall associate with this tesselation four finite-dimensional vector spaces (i.e. discrete functional spaces), named W^p, $p = 0$ to 3, of p-forms (see the previous section for a definition of p-forms). For each of these four vector spaces we may exhibit a basis (not an orthogonal one, but such that all base functions have a compact support). The elements of these bases are the node-, edge-, facet-, volume-elements alluded to.

Let us first define $\lambda_{\underline{i}}^{jkl}(x)$ the barycentric coordinate of point x with respect to node $\{\underline{i}\}$ located in $x_{\underline{i}}$: this **barycentric function** is continuous over D, piecewise linear in the tetahedron $\{\underline{i},\ j,\ k,\ l\}$ and null elsewhere (fig. 6.2).

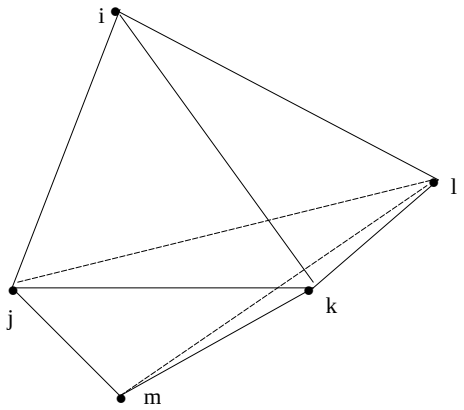

FIGURE 6.2 – Two tetrahedra $\{i,\ j,\ k,\ l\}$ and $\{m,\ l,\ k,\ j\}$ with a common facet $\{j,\ k,\ l\}$.

Consequently, this function is entirely defined by its values on the four vertices of the tetrahedra $\{\underline{i},\ j,\ k,\ l\}$:

$$\begin{cases} \lambda_i^{jkl}(x_i) & = 1 \\ \lambda_i^{jkl}(x_m) & = 0\ \text{, if } m \neq i \end{cases} \tag{19}$$

Let us now denote by K_i the set of integers m such that x_m and x_i belong to the same edge. This way, we can define a function Λ_i whose support is the set of tetrahedra which have the node $\{x_i\}$ in common (fig. 6.2) :

$$\Lambda_i = \sum_{\{j,\,k,\,l\} \in K_i^3} \lambda_i^{jkl}$$

(of course, in the case of curved tetrahedra, this should be understood in the reference space).

We are now ready to define **Whitney elements** of order $p = 0,\ 1,\ 2,\ 3$. They are differential p-forms associated with p-simplices and generate the spaces W^p. For a node $n = \{i\}$, we set :

$$w_n(x) = \Lambda_i(x) \tag{20}$$

This is a "Whitney element of order 0", based at node n. These elements are nothing else than the familiar piecewise linear, continuous P^1 elements : the "hat functions", or "Lagrange elements of polynomial degree 1", of finite element theory (P^k stands for the set of polynomial functions of degree $\leq k$). To edge $e = \{i,\ j\}$, we assign the "Whitney element of order 1", or "edge-element" based at edge e, defined by the 1-form (vector field) :

$$w_e = \Lambda_i \bigtriangledown \Lambda_j - \Lambda_j \bigtriangledown \Lambda_i \tag{21}$$

To facet $f = \{i,\ j,\ k\}$, we assign the "facet-element" defined by the 2-form (vector field) :

$$w_f = 2(\Lambda_i \bigtriangledown \Lambda_j \times \bigtriangledown\Lambda_k + \Lambda_k \bigtriangledown \Lambda_i \times \bigtriangledown\Lambda_j + \Lambda_j \bigtriangledown \Lambda_k \times \bigtriangledown\Lambda_i) \tag{22}$$

Finally, we associate with volume $\{i,\ j,\ k,\ l\}$ a function whose analytical expression can be infered from (21) and (22) (a factor 6 should be thrown in), but it is piecewise constant (P^0 element), so writing it down would be pointless. The 1-form in (21) is certainly not continuous over D, since the λ_is are not continuously differentiable. But it has some continuity nevertheless. To see this, consider the gradient (exterior derivative) of the 0-form Λ_i :

$$\bigtriangledown\Lambda_i = \{\bigtriangledown\Lambda_i\} + n[\Lambda_i]\ \delta_\Sigma\ ,$$

where δ_Σ denotes a Dirac mass (de Rham current) with support on the tetrahedral facet opposite to the node i, $[\Lambda_i]$ denotes the jump of Λ_i across this facet, n denotes the outward normal to this facet and $\{\bigtriangledown\Lambda_i\}$ denotes the regular part of $\bigtriangledown\Lambda_i$. Thanks to the continuity of Λ_j, we know that $[\Lambda_j] = 0$ and $[\Lambda_j \bigtriangledown \Lambda_i] = \Lambda_j[\bigtriangledown\Lambda_i]$. If we then take the rotational of the 1-form $\Lambda_j \bigtriangledown \Lambda_i$, we get that :

$$\mathrm{curl}(\Lambda_j \bigtriangledown \Lambda_i) = \{\mathrm{curl}(\Lambda_j \bigtriangledown \Lambda_i\}) + n\Lambda_j \times [\bigtriangledown\Lambda_i]\ \delta_\Sigma$$

One cannot hope the continuity of $\bigtriangledown\Lambda_i$ on Σ since it is not differentiable on Σ (it is a de Rham current). Nevertheless, it is obvious from the definition of λ_i^{jkl} :

$$\lambda_i^{jkl}(x) = \sum_{p=1}^{3} \frac{n_p^{ijkl} x_p + a^{ijkl}}{n_0^{ijkl} x_0 + a^{ijkl}}\ ,$$

where n_p^{ijkl} is the outward normal to the facet $\{j,\ k,\ l\}$ opposite to the node $\{i\}$ (tetrahedron $\{i,\ j,\ k,\ l\}$) and a^{ijkl} is solely defined by (19) (cf. figure 6.2). Besides n_p^{ijkl} and a^{ijkl} are the coefficients defining the plane (fig. 6.2)

$$\sum_{k=1}^{3} n_p^{ijkl} x_k + a^{ijkl} = 0\ ,$$

such that $\bigtriangledown\Lambda_i$ is collinear to the outward normal n of the previous plane (whose components are given by the n_p^{ijkl}). After cumbersome but easy computations, the reader can check that for each facet $n \times [\bigtriangledown\lambda_i] = 0$.

We can thus conclude that the rotational (exterior derivative) of the 1-form w_e is given by :

$$\operatorname{curl} w_e = \Lambda_i \operatorname{curl} \bigtriangledown\Lambda_j + \bigtriangledown\Lambda_i \times \bigtriangledown\Lambda_j - \Lambda_j \operatorname{curl} \bigtriangledown\Lambda_i - \bigtriangledown\Lambda_j \times \bigtriangledown\Lambda_i = 2 \bigtriangledown \Lambda_i \times \bigtriangledown\Lambda_j \ .$$

The very fact that $\operatorname{curl} w_e$ exists as 2-form, and not as a distribution as a de Rham current (distribution) proves that the tangential part of w_e on facets of the mesh is continuous across these facets ([30]). In other words, the tangential component of w_e on a common facet $\{j,\ k,\ l\}$ of two adjacent tetrahedra $\{i,\ j,\ k,\ l\}$ and $\{m,\ l,\ k,\ j\}$ depends only on its values on the three edges $\{j,\ k\}$, $\{k,\ l\}$, $\{l,\ i\}$ (fig. 6.2).

From this remark, we can already infer that Whitney vector fields of degree 1 (that is, those generated by edge-elements) are exactly what is needed in order to represent vector field like $\mathbf{E}$ (electric field) or $\mathbf{H}$ (magnetic field) in electromagnetic computations : for these fields (1-forms) have precisely this kind of continuity i.e. continuity of the tangential part across material interfaces.

A similar remark holds about facet-elements ($p = 2$). For this, let us consider the divergence of (21). We first note that the Poynting identity ensures us that :

$$\operatorname{div}(\Lambda_i \bigtriangledown \Lambda_j \times \bigtriangledown\Lambda_k) = \bigtriangledown\Lambda_k \cdot \operatorname{curl}(\Lambda_i \bigtriangledown \Lambda_j) - \Lambda_i \bigtriangledown \Lambda_j \cdot \operatorname{curl}(\bigtriangledown\Lambda_k)$$

If we develop the previous equation, we get that :

$$\operatorname{div}(\Lambda_i \bigtriangledown \Lambda_j \times \bigtriangledown\Lambda_k) = \bigtriangledown\Lambda_k \cdot (\Lambda_i \operatorname{curl} \bigtriangledown\Lambda_j + \bigtriangledown\Lambda_i \times \bigtriangledown\Lambda_j) - \Lambda_i \bigtriangledown \Lambda_j \cdot \operatorname{curl}(\bigtriangledown\Lambda_k)$$

We have already seen that $\operatorname{curl} \bigtriangledown\Lambda_j = \{\operatorname{curl} \bigtriangledown\Lambda_j\} = 0$. We therefore deduce that :

$$\operatorname{div} w_f = 6 \bigtriangledown \Lambda_i \cdot (\bigtriangledown\Lambda_j \times \bigtriangledown\Lambda_k) \ ,$$

which is a 3-form. Besides, we can write the exterior derivative of the 2-form w_f in terms of a continuous form and a de Rham current as follows :

$$\operatorname{div} w_f = \{\operatorname{div} w_f\} + n \cdot [w_f]\delta_\Sigma.$$

We hence conclude that the normal component $n \cdot w_f$ of w_f is continuous across facets. The facet-elements are thus closely related to the magnetic and electric flux densities $\mathbf{B}$ and $\mathbf{D}$ (2-forms). It is worth noting that the tangential continuity of w_e and the normal continuity of w_f reveal the deep nature of Whitney elements which are built to ensure their continuity and that of their exterior derivative. Furthermore, w_e satisfies

$$\operatorname{div}(\operatorname{curl} w_e) = \operatorname{div}(\bigtriangledown\Lambda_i \times \bigtriangledown\Lambda_j) = \bigtriangledown\Lambda_j \cdot \operatorname{curl} \bigtriangledown\Lambda_i - \bigtriangledown\Lambda_i \cdot \operatorname{curl}(\bigtriangledown\Lambda_j) = 0 \ ,$$

which is nothing else than $ddw = 0$. Moreover, using differential forms, we are able to exhibit a general expression for Whitney forms ([31]) :

$$\omega_s = \sum_{i=0}^{p} (-1)^i \lambda_i d\lambda_0 \wedge \ \ldots \ \wedge d\lambda_{i-1} \wedge d\lambda_{i+1} \wedge \ \ldots \ \wedge d\lambda_p$$

Now let us consider p-forms built from Whitney elements, i.e. following linear combinations :

$$u = \sum_{s \in \mathcal{S}} \bar{u}_s w_s \ ,$$

where the set $\mathcal{S}$ of p-simplices is $\mathcal{N}$, $\mathcal{E}$, $\mathcal{F}$ or $\mathcal{T}$, according to the value p. If $p = 0$ (thus $\mathcal{S} = \mathcal{N}$, the set of nodes), the $\bar{u}_s$ are the nodal values of u, hence a clear interpretation of the degrees of freedom $\bar{u}_s$. If $p = 1$ (thus $\mathcal{S} = \mathcal{E}$), it follows from the very definition of w_e (21) that its circulation along edge e (from node $\{i\}$ to node $\{j\}$) is equal to 1, and to 0 along the other edges. Therefore, in the development of u, the degree of freedom $\bar{u}_s$ is the nodal value of u if s is a node, and the circulation of u along the edge, if s is an edge.

Furthermore, $\lambda_i(x)$ being the barycentric coordinate of point located in x_i, it must satisfy :

$$\sum_i \lambda_i(x) = 1 \ , \ \forall x \in D \ ,$$

where i denotes the nodes of D. This and (21) imply that :

$$\sum_{j \neq i} w_{\{i,\,j\}} = \bigtriangledown \Lambda_i \ \text{ for all nodes } i \text{ and } j \text{ of } D.$$

Therefore, the gradient of a 0-Whitney element is a linear combination of 1-Whitney elements, which we may express as follows :

$$\bigtriangledown W^0 \subset W^1 \ .$$

Similarly, one can prove that $\operatorname{curl} W^1 \subset W^2$ and $\operatorname{div} W^2 \subset W^3$ (see [31]). We can summarize these injectivity properties of the Whitney complex in the following diagram :

$$W^0 \xrightarrow{\bigtriangledown} W^1 \xrightarrow{\text{curl}} W^2 \xrightarrow{\text{div}} W^3$$

We can express the same phenomena in terms of spaces $\overline{W}^p$ of degrees of freedom :

$$\overline{W}^0 \xrightarrow{G} \overline{W}^1 \xrightarrow{C} \overline{W}^2 \xrightarrow{D} \overline{W}^3$$

where $\overline{W}^0$ is the set of the node's values of the field, $\overline{W}^1$ is the set of the circulation along the edges, $\overline{W}^2$ is the set of the flow across the facets and $\overline{W}^3$ is the set of the volume integral on the elements. The symbols G, C, D denote rectangular incidence matrices (whose entries are all 0, 1 or -1) which represent $\bigtriangledown$, curl, div in the bases provided by Whitney elements. For instance, if $h = \sum_{e \in \mathcal{E}} \overline{h}_e w_e$, then $\operatorname{curl} h = \sum_{f \in \mathcal{F}} C_{fe} \overline{h}_e w_f$: the size of C is the number of facets times the number of edges. If we denote by N_n, N_e, N_f and N_v respectively the number of nodes ($N_n = Card\mathcal{N}$), edges, facets and volumes, one can see that G and D are similarly matrices with N_e lines and N_n column, and N_v lines and N_f column. The fundamental properties of these matrices, as shown by the diagram, are $CG = 0$ and $DC = 0$: there is an isomorphism between the W^p and the $\overline{W}^p$, which are spanned by the vectors of degrees of freedom. We will see in the sequel that the magnetic field H actually "lives" in the space of 1-forms and is therefore well represented at the discrete level as an element of W^1 given by the set of coefficients $\overline{W}^1$ (to be determined by our numerical method).

6.4.4 A discrete analogue to the variational problem

The electromagnetic fields and sources may be represented by differential forms : the magnetic field $\mathbf{H}$ and the electric field $\mathbf{E}$ are 1-forms, the magnetic flux density $\mathbf{B}$, the electric flux density $\mathbf{D}$ and the current density $\mathbf{J}$ are 2-forms and the charge density ρ is a 3-form. In this representation, the vector Maxwell system is given by :

$$(23)\begin{cases} d\mathbf{H} &= \mathbf{J} + \dfrac{\partial \mathbf{D}}{\partial t} \\ d\mathbf{E} &= -\dfrac{\partial \mathbf{B}}{\partial t} \\ d\mathbf{B} &= 0 \\ d\mathbf{D} &= \rho \end{cases}$$

The 1-form $\mathbf{A}$ and the 0-form V may be introduced as potentials such that $\mathbf{B} = dA$ and $\mathbf{E} = -\dfrac{\partial \mathbf{A}}{\partial t} - dV$. All those equations are obviously independent of the metric. Nevertheless, this one is involved in the definition of the constitutive relations given by $\mathbf{D} = \varepsilon \star \mathbf{E}$ and $\mathbf{B} = \mu_0 \star \mathbf{H}$ (where the Hodge star operator satifies $\star dx = dy \wedge dz$, $\star dy = dz \wedge dx$ and $\star dz = dx \wedge dy$).

In this representation, the harmonic vector Maxwell system is given by :

$$(24)\begin{cases} d\mathbf{H} &= -i\omega\varepsilon \star \mathbf{E} \\ d\mathbf{E} &= i\omega\mu \star \mathbf{H} \\ d(\mu_0 \star \mathbf{H}) &= 0 \\ d(\varepsilon \star \mathbf{E}) &= 0 \end{cases}$$

in the absence of current density and volumic charges.

In the case of a two-dimensional electromagnetic problem, invariant by translation along the z-axis, the geometry is described by the trace of the electric and magnetic fields on the transverse plane. We choose the magnetic field as the variable and we develop $\mathbf{H}(x, y)$ in its transverse and longitudinal components $\mathbf{H}_t(x, y)$ and $H_l(x, y)$:

$$\mathbf{H}(x, y) = H_{t,1}(x, y)dx + H_{t,2}(x, y)dy + H_l(x, y)dz = \mathbf{H}_t(x, y) + H_l(x, y)dz$$

If we take the exterior derivative to the 1-form $\mathbf{H}_t$, we get that :

$$d\mathbf{H}_t = \frac{\partial H_{t,1}}{\partial y} dy \wedge dx + \frac{\partial H_{t,2}}{\partial x} dx \wedge dy = (-\frac{\partial H_{t,1}}{\partial y} + \frac{\partial H_{t,2}}{\partial x}) dx \wedge dy$$

Applying the Hodge star operator $\star$ to $\mathbf{H}_t$, we get that :

$$\star\mathbf{H}_t = H_{t,1} dy \wedge dz + H_{t,2} dz \wedge dx$$

If we take the exterior derivative of the previous expression, we obtain :

$$d(\star\mathbf{H}_t) = \frac{\partial H_{t,1}}{\partial x} dx \wedge dy \wedge dz + \frac{\partial H_{t,2}}{\partial y} dy \wedge dz \wedge dx = (\frac{\partial H_{t,1}}{\partial x} + \frac{\partial H_{t,2}}{\partial y}) dx \wedge dy \wedge dz = (\frac{\partial H_{t,1}}{\partial x} + \frac{\partial H_{t,2}}{\partial y}) \star 1$$

We define the transverse gradient, divergence and curl as follows :

$$\bigtriangledown_t H_l(x,y) = dH_l = \frac{\partial H_l}{\partial x}dx + \frac{\partial H_l}{\partial y}dy$$
$$\mathrm{div}_t(\mathbf{H}_t) = \star d \star \mathbf{H}_t = \frac{\partial H_{t,1}}{\partial x} + \frac{\partial H_{t,2}}{\partial y}$$
$$\mathrm{curl}_t(\mathbf{H}_t)dz = \star d\mathbf{H}_t = (\frac{\partial H_{t,2}}{\partial x} - \frac{\partial H_{t,1}}{\partial y})dz$$

We can thus rewrite the problem (5) of lemma 1 with the formalism of differential forms as follows :

$$\begin{cases} \star\,\mathrm{curl}_\gamma(\varepsilon_r^{-1} \star \mathrm{curl}_\gamma\,\mathbf{H}) = k_0^2\mathbf{H} & (A1) \\ \mathrm{div}_\gamma(\mu_0 \star \mathbf{H}) = 0 & (A2) \end{cases}$$

The discretization of the problem is based on Whitney forms. Taking the variational form of $(A1)$ and assuming some Dirichlet boundary conditions on the boundary $\partial\theta$ the three-dimensional manifold $\theta = \Omega \times \mathbb{R}$, we get that :

$$\int_\theta \star\star\varepsilon_r^{-1}\star\mathrm{curl}_\gamma\,\mathbf{H}\wedge\overline{\mathrm{curl}_\gamma\,\mathbf{H}'} = \int_\theta \varepsilon_r^{-1}\star\mathrm{curl}_\gamma\,\mathbf{H}\wedge\overline{\mathrm{curl}_\gamma\,\mathbf{H}'} = k_0^2\int_\theta \star\mathbf{H}\wedge\overline{\mathbf{H}}'\ ,\forall\mathbf{H}\in W_0^1 \quad (25)$$

where W_0^p denotes the restriction of the space of p-forms on a finite element space W^p, with null value on $\partial\theta$.

Analogously to ([30]), we note that the sequence of W^p is exact i.e. that the image of W^{p-1} by the operator $\bigtriangledown_\gamma$, (resp. curl_γ, div_γ) is exactly the kernel of the next operator, thanks to the nullity of its trace (resp. the tangential and the normal trace). It is thus identified with the De Rham complex (Bossavit, 1990). Let φ' be a test function in W^0. Noting that $\bigtriangledown_\gamma W^0 \subset W^1$, we take $\mathbf{H}'$ such that $\mathbf{H}' = \bigtriangledown_\gamma\varphi'$ and derive from (25) that (if $\omega \neq 0$) :

$$\int_\theta \mu_0 \star \mathbf{H} \wedge \bigtriangledown\overline{\varphi'} = 0\ ,\ \forall\varphi' \in W^0 \quad (26)$$

Bossavit has proved that this property solves the **spurious mode** problem for resonant cavities ([30]). This weak formulation of null divergence $(A2)$ still works if μ_0 is not constant. Therefore, replacing $\mathbf{H}$ by $\mathbf{E}$ and μ_0 by $\varepsilon_0\varepsilon_r$, we see that Whitney forms clearly satisfy $\mathrm{div}_\gamma(\varepsilon_0\varepsilon_r \star \mathbf{E}) = 0$. The electric formulation is thus straightforward from (25).

Concerning our formulation, we are dealing with $\mathbf{H} \in [H^1(\mathbb{R}^2)]^3$ which implies that $\mathbf{H}$ is null at infinity. The sequence of W^p remaining exact (the trace conditions are obviously satisfied), the edge elements still fulfill (26).

We now develop curl_γ and div_γ in their transverse and longitudinal components :

$$\mathrm{div}_\gamma\,\mathbf{H} = \frac{\partial H_{t,1}}{\partial x} + \frac{\partial H_{t,2}}{\partial y} + i\,\gamma H_l = \mathrm{div}_t\,H_t + i\,\gamma H_l$$
$$\begin{aligned}\mathrm{curl}_\gamma\,\mathbf{H} &= \Big(\frac{\partial H_l}{\partial y} - i\,\gamma H_{t,2}\Big)dx + \Big(i\,\gamma H_{t,1} - \frac{\partial H_l}{\partial x}\Big)dy + \Big(\frac{\partial H_{t,2}}{\partial x} - \frac{\partial H_{t,1}}{\partial y}\Big)dz \\ &= \mathrm{curl}_t\,H_t\,dz + (\bigtriangledown_t H_l - i\,\gamma H_t)\wedge dz\end{aligned}$$

If we use the star Hodge operator property $\star dz = dx \wedge dy$, we deduce that :

$$\star\,\mathrm{curl}_\gamma\,H \wedge \overline{\mathrm{curl}_\gamma\,H'}$$

$$= \star(\mathrm{curl}_t\, H_t\, dz + (\bigtriangledown_t H_l - i\,\gamma H_t) \wedge dz) \wedge (\mathrm{curl}_t\, \overline{H'_t}\, dz + (\bigtriangledown_t \overline{H'_l} + i\,\gamma \overline{H'_t}) \wedge dz)$$
$$= \mathrm{curl}_t\, H_t\, \mathrm{curl}_t\, \overline{H'_t} \star 1 + \star(\bigtriangledown_t H_l - i\,\gamma H_t) \wedge (\bigtriangledown_t \overline{H'_l} + i\,\gamma \overline{H'_t})$$
$$= \mathrm{curl}_t\, H_t\, \mathrm{curl}_t\, \overline{H'_t} \star 1 + \star \bigtriangledown_t H_l \wedge \bigtriangledown_t \overline{H'_l} - i\,\gamma \star H_t \wedge \bigtriangledown_t \overline{H'_l} + i\,\gamma \star \bigtriangledown_t H_l \wedge \overline{H'_t} + \gamma^2\ \star H_t \wedge \overline{H'_t}$$

From a numerical point of view, we minimize the following functional, which is a discrete analogue to (8) :

$$\mathcal{R}(\gamma; \mathbf{H}, \mathbf{H}') = \int_\theta \varepsilon_r^{-1} \star \Big(\mathrm{curl}_t\, \mathbf{H}_t\, \mathrm{curl}_t\, \overline{\mathbf{H}'_t} + \bigtriangledown_t H_l \wedge \bigtriangledown_t \overline{H'_l}$$
$$-i\,\gamma \mathbf{H}_t \wedge \bigtriangledown_t \overline{H'}_l + i\,\gamma\, \bigtriangledown_t H_l \wedge \overline{\mathbf{H}'_t} + \gamma^2\, \mathbf{H}_t \wedge \overline{\mathbf{H}'_t}\Big) - k_0^2 \int_\theta \star\Big(\mathbf{H}_t \wedge \overline{\mathbf{H}'_t} + H_l \overline{H'_l}\Big)$$

This formulation involves both a transverse field in the section of the guide and a longitudinal field along its axis. The section of the guide is meshed with triangles and Whitney finite elements are used i.e. edge elements for the transverse field and node elements for the longitudinal field :

$$\mathbf{H} = \begin{cases} \mathbf{H}_t = \sum_j^n \alpha_j \mathbf{w_j^e}(x,y) e^{i\gamma z} & \text{in } \mathbb{R}^2 \\ H_z = \sum_j^n \beta_j w_j^n(x,y) e^{i\gamma z} & \text{in } \mathbb{R} \end{cases}$$

where α_j denotes the line integral of the transverse component $\mathbf{H}_t$ on the edge elements, and β_j denotes the line integral of the longitudinal component H_z along one unit of length of the axis of the guide (which is equivalent to the nodal value). Besides, $\mathbf{w_j^e}$ and w_j^n are respectively the basis functions of Whitney 1-forms and Whitney 0-forms.

6.4.5 Transformation methods

The interesting property of differential forms is their behaviour under mapping of domains. If Φ is a differential map from a domain M to a domain N, a function f on N is mapped (pulled back) on a function $\Phi^*(f) = f \circ \Phi$ on M by composition with Φ. Vector fields on M are mapped (pushed forward) on vector fields on N by considering their action on pulled back functions. Since a vector field v on M maps the pulled back functions $\Phi^*(f)$ to numbers $v(\Phi^*(f))$, it defines a linear differential operator for the functions f on N i.e. a vector field $\Phi_*(v)$ on N whose action on a function f on N is given by $\Phi_*(v)(f) = v(\Phi^*(f))$. A 1-form on N is mapped (pulled back) on M by considering its action on pushed forward vector fields from M to N. The pullback $\Phi^*(\alpha)$ on M of a 1-form α on N is defined by $< \Phi^*(\alpha)\ ,\ v >=< \alpha\ ,\ \Phi_*(v) >$. Any purely covariant object such as a p-form or the metric can be pulled back from M to N by the following definitions, for a p-form $\Phi^*(\omega)(v_1,\ ...,\ v_p) = \omega(\Phi_*(v_1),\ ...,\ \Phi_*(v_p))$ and for the metric $\Phi^*(g)(v_1,\ v_2) = g(\Phi_*(v_1),\ \Phi_*(v_2))$. As g allows the definition of the star operator $\star_g$ on N, $\Phi^*(g)$ allows the definition of the star operator $\star_{\Phi^*(g)}$ on M. In the preceding definitions, it is important to remark how the duality reverses maps leading to an alternation of push forward and pull back maps for the domains, the functions, the vector fields, and the forms. The fundamental point for the setting of transformation methods is that the operations on forms previously defined commute with the pull back. For forms α, β one has :

$$\varphi^*(\alpha \wedge \beta) = \Phi^*(\alpha) \wedge \Phi^*(\beta)$$

$$\Phi^*(d\alpha) = d\Phi^*(\alpha)$$
$$\int_M \Phi^*(\alpha) = \int_{N=\Phi(M)} \alpha$$
$$\star_{\Phi^*(g)}\Phi^*(\alpha) = \Phi^*(\star_g \alpha)$$

In the following we will consider two types of geometric transformations for two-dimensional electromagnetic problems invariant by translation along the z-axis, the geometry of which will be described by the trace of the 1-form $\mathbf{H}(x,y)dz$ (magnetic field) on the $x-y$ plane : dielectric waveguides in unbounded domain and dielectric waveguides surrounded by a jacket at a finite distance (chapter 7). We will make use of two transformation methods to deal with the infinite domain outside the waveguide (Dirichlet boundary conditions at infinity) and with the jacket (Dirichlet boundary conditions at a given distance). The philosophy of the transformation methods is the following : a domain M^* being mapped on the original domain M, the forms and the metric on M are pulled back on M^* and the formulation of the problem on M^* is immediate. The mapping of the domain M^* with coordinates $\{X,\ Y\}$ on the original domain M with coordinates $\{x,\ y\}$ is given by two functions f_1 and f_2 such that $\{X,\ Y\} \longmapsto \{x,\ y\} = \{f_1(X,\ Y),\ f_2(X,\ Y)\}$.

We then descretize the problem thanks to the finite element method which consists of approximating the vector field $\mathbf{H}$ of the infinite dimensional hilbert space $H(\text{curl}, M^*)$ by the linear combination $\sum H_i\omega_i$ where H_i are parameters and ω_i are 1-forms corresponding to **shape functions** [*Nedelec*] obtained by assuming a simple behaviour on elements from a meshing of M. The subspace of $H(\text{curl}, M^*)$ spaned by these linear combinations is the so-called **Galerkin space**. More precisely, we consider the variational formulation of the previous section. We then discretize the problem thanks to edge elements which are shape 1-forms $\omega_i = \alpha_i(x,y)dz$ where $\alpha_i(x,y)$ are the classical shapes functions (Lagrange elements,Nedelec) and $\star\omega_i = \alpha_i(x,y) \star dz = \alpha_i(x,y)dx \wedge dz$. We are thus led to integrals of discrete 3-forms $d\omega_i \wedge \star d\omega_j = a_{ij}$. The contribution of an element to the coefficient a_{ij} of H_j in the ith equation is the integral on the element of :

$$\begin{pmatrix} \partial_X\alpha_i & \partial_Y\alpha_i \end{pmatrix} \begin{pmatrix} \dfrac{\partial_Y f_1^2 + \partial_Y f_2^2}{\partial_X f_1\partial_Y f_2 - \partial_X f_2\partial_Y f_1} & \dfrac{\partial_X f_1\partial_Y f_1 + \partial_X f_2\partial_Y f_2}{\partial_X f_1\partial_Y f_2 - \partial_X f_2\partial_Y f_1} \\ \dfrac{\partial_Y f_1^2 + \partial_Y f_2^2}{\partial_X f_1\partial_Y f_2 - \partial_X f_2\partial_Y f_1} & \dfrac{\partial_X f_1^2 + \partial_X f_2^2}{\partial_X f_1\partial_Y f_2 - \partial_X f_2\partial_Y f_1} \end{pmatrix} \begin{pmatrix} \partial_X\alpha_j \\ \partial_Y\alpha_j \end{pmatrix}$$

where ∂_x and ∂_y indicate the partial derivative with respect to X and Y respectively, and $\alpha_i(X,\ Y)$, $\alpha_j(X,\ Y)$ are the shape functions on the transformed element. This contribution of the transformed element is equal to the non transformed one up to the central matrix. If the transformtion is trivial ($f_1(X,Y) = X$, $f_2(X,Y) = Y$) or corresponds to a conformal transformation ($f_1(X,Y) + if_2(X,Y)$ is analytic i.e. $\partial_X f_1 = \partial_Y f_2$ and $\partial_X f_2 = -\partial_Y f_1$), this matrix reduces to the unit matrix. As for the term involving the transverse magnetic field and its conjugate, the contribution to the i th equation of an element is the product of H_iH_j by the integral of $\omega_i \wedge \star\omega_j = \alpha_i\alpha_j \star 1$ on the element. $\star 1$ is the volume form associated to the metric i.e. $\star 1 = (\partial_X f_1\partial_Y f_2 - \partial_X f_2\partial_Y f_1)dX \wedge dY$ and the integral transforms simply according to the formula for the change of coordinates in multiple integrals.

Remark :

If $f_1(x,y)$ and $f_2(x,y)$ are the two components of a conformal mapping, and therefore satisfy the Cauchy-Riemann criteria (analytic function), we easily see that this Jacobian reduces to the identity.

6.4.6 Transformation method for unbounded domain

To deal with an open problem, a judicious choice of coordinate transformation allows the finite element modeling of the infinite exterior domain ([166]) (Nicolet *et al.*, 1994). The underlying idea is to use the nice properties of **conformal mapping** of our transformation on the interface between the guide and the coronna : one can chek that if $OA = 2OB$, then the Jacobian reduces to the identity on the interface, and thus behaves as a conformal mapping transformation (see previous section). We thus avoid the analysis of transformation of interface/boundary conditions due to scaling ([133]) (Lowther *et al*, 1989). Considering two disks $D(O,A)$ and $D(O,B)$ of center $O=(0,0)$ and radii A and $B > A$ strictly including Ω, we define a corona $C = D(O,B) \setminus \overline{D(O,A)}$. Let (x,y) be a point in $\mathbb{R}^2 \setminus \overline{D(O,A)}$ (the infinite outer domain) and (X,Y) be a point in C, the transformation is then given by :

$$\begin{cases} x = f_1(X,Y) = X[A(B-A)]/[R(B-R)] \\ y = f_2(X,Y) = Y[A(B-A)]/[R(B-R)] \end{cases}$$

where R denotes the Euclidean norm $\sqrt{X^2+Y^2}$. This transformation may be viewed as a mapping of the finite corona C with the non orthogonal coordinate system (X,Y) to the infinite domain with the cartesian coordinate system (x,y) (see figure 6.3).

This way, the finite element discretization appears as a chained map from the reference space to the transformed space and from the transformed space to the physical space. Using discretizations entirely based on differential forms allows a straightforward formulation of transformation methods by pull-back of the corresponding weighted residuals. Following the remark of the preceding section, we fix $\gamma \in \mathbb{R}^+$ and look for (ε_r, H) satisfying (8). We are thus led to a linear generalized eigenvalue system.

It is also to be noticed that taking Dirichlet boundary conditions at a finite distance (without geometric transformation) from the cross section of the guide allows to consider an operator with a compact resolvent (thus artificially eliminating the continuous spectrum) but it would add the modes of an unphysical metallic guide. As for us, we pay a special attention to the unboundness of our resolvent operator : the operator remains unbounded under the transformation method and we therefore use the relations (DR) as a practical criterion to select the discrete spectrum corresponding to propagating modes and reject the numerical values corresponding to the continuous spectrum.

Remarks :

Another way to discretize the problem would be to use vector nodal elements. The main drawback of this method is that vector nodal elements do not contain the gradients of the scalar nodal elements. One way of tackling this problem is thus to penalize the divergence. For this, we develop the divergence in its transverse and longitudinal components as follows :

$$\mathrm{div}_\gamma\, H\ \overline{\mathrm{div}_\gamma\, V} = \mathrm{div}_t\, H_t\ \ \mathrm{div}_t\, \overline{H'_t} + \gamma^2 H_l\ \overline{H'_l} + i\,\gamma\Big(H_l\ (\mathrm{div}_t\, \overline{H'_t}) - (\mathrm{div}_t\, H_t)\ \overline{H'_l}\Big)$$

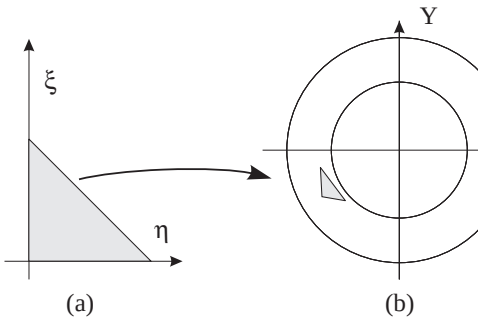

FIGURE 6.3 – (a) Reference element. (b) Meshing of the corona equivalent to the unbounded domain with transformed coordinates. (c) Physical unbounded domain in cartesian coordinates.

The problem of minimization (8) therefore admits a unique solution thanks to the added term

$$s\int_\theta \mathrm{div}_\gamma \mathbf{H}\,\overline{\mathrm{div}_\gamma \mathbf{H'}} = s\int_\theta \Big(\mathrm{div}_t H_t\ \mathrm{div}_t \overline{H'_t} + \gamma^2 H_l\ \overline{H'_l} + i\,\gamma(H_l\ (\mathrm{div}_t \overline{H'_t}) - (\mathrm{div}_t H_t)\ \overline{H'_l})\Big)$$

which acts in fact as a constraint which forces the nullity of the magnetic field divergence (the greater the s, the better the solution). Furthermore, with nodal elements, vector quantities are represented by three functions, one for each component (in cartesian coordinates). The geometrical meaning is lost together with pull-back properties and the naturalness of the transformation method. The practical implementation is then much more cumbersome.

It is worth noting that the edge elements belong to the Hilbert space :

$$L^2(\mathrm{curl},\ \theta) = \{f \in L^2(\theta),\ \mathrm{curl}\, f \in L^2(\theta)\ \ n \times f = 0 \text{ on } \partial\theta\}$$

and it has been proven ([63])(Dodziuk, 1976) that for a given field φ in $L^2(\mathrm{curl},\ \theta)$, there exists a sequence of Whitney edge elements φ_m which converges to φ for the norm of $L^2(\mathrm{curl},\ \theta)$, provided that the tetrahedra of the mesh tends to 0 in a given way. Concerning the node elements of $[W^0]^3$ it is classical that they tend towards a given function φ in $H^1(\theta)$: such a convergence therefore necessitates to place the study in an inadequate functional space ($H^1(\theta)$), which leads to divergence penalization techniques. Finally, one can improve the convergence of the numerical scheme by using high order curl conforming finite elements (hierarchical finite elements) which are linear combinations of functions of types (21), (22), $\Lambda_i\Lambda_j \bigtriangledown (\Lambda_k)$ and $\bigtriangledown\Big(\Lambda_i\Lambda_j(\Lambda_i - \Lambda_j)\Big)$ (Geuzaine, 2001 [88]).

6.5 Numerical implementation

Our discrete formulation leads to a generalized eigenvalue problem solved thanks to the Lanczos algorithm, which allows the computation of several eigenvalues and their associated eigenvectors for Hermitian matrices. In the Lanczos algorithm, spectral shifting is required to give access to a given part of the spectrum and/or to accelerate or even guarantee the convergence towards a given eigenvalue. The (DR) relations give a useful practical estimate of the shift to be used to obtain the lowest frequency modes. In the following subsection,

we give a brief survey on the Lanczos algorithm and its main properties. The interested reader can get further details in ([187],[86]) (Saad, 1991, Geradin and Rixen, 1997).

6.5.1 The Lanczos algorithm

The Lanczos algorithm is an iteration method on both eigenvectors and eigenvalues adapted to the resolution of generalized eigenvalue problems of the following form ([187],[86]) (Saad, 1991, Geradin and Rixen, 1997) :

$$Kx = k_0^2 Mx \tag{27}$$

where the matrices K and M (generally called mass and stiffness matrices) are Hermitian and positive definite. The underlying concept of this method is that of the power algorithm which is the basis of all methods using iteration on eigenvectors. The first main property of the power algorithm holds in its convergence rate towards a given solution independent of the matrix size, which potentially makes it the ideal method for very large systems. The second one is that it makes it possible to limit the solving of the eigenvalue problem to the number of required solutions. One of the main drawbacks of the Lanczos method is its bad convergence rate for close eigenvalues. One way to tackle this problem is to use a spectral shift. Let us now introduce the principle of the Lanczos algorithm : it consists of generating a subspace including the system fundamental eigensolutions by inverse iteration on one starting vector called x_0. From the latter, we construct the Krylov sequence

$$\{x_0,\ K^{-1}Mx_0,\ (K^{-1}M)^2 x_0,\ ...\}$$

the terms of which are made orthogonal to each other by a construction process of conjugate directions. Starting from an arbitrary vector x_0, the Lanczos algorithm consists of combining inverse iteration operations and orthogonalization of the successive iterates by applying the relation :

$$c_{p+1}x_{p+1} = K^{-1}Mx_p - a_p x_p - b_{p-1}x_{p-1}$$

with coefficients a_p, b_{p-1} and c_{p+1} determined in such a way that :

$$\begin{cases} x_{p+1}^t M x_j & = 0\ ,\ j < p+1 \\ x_{p+1}^t M x_{p+1} & = 1 \end{cases} \tag{28}$$

One can easily calculate coefficients a_p and b_{p-1} by imposing the orthogonality of x_{p+1} with respect to x_p and x_{p-1} with the Gram-Schmidt algorithm. One gets that :

$$\begin{cases} a_p & = x_p^t M K^{-1} M x_p \\ b_{p-1} & = x_p^t M K^{-1} M x_{p-1} \end{cases} \tag{29}$$

the orthogonality of x_{p+1} to x_{p-2}, x_{p-3} is then deduced by recurrence thanks to :

$$x_p^t M K^{-1} M x_{p-j} = x_p^t M (c_{p+1-j}x_{p+1-j} + c_{p-j}x_{p-j} + b_{p-j-1}x_{p-j-1})$$

which vanish as soon as $j \geq 2$. Let us also note that relations (29) enable us to calculate a new expression for b_{p-1} :

$$b_{p-1} = x_p^t M K^{-1} M x_{p-1} = x_p^t M (c_p x_p + a_{p-1}x_{p-1} + b_{p-2}x_{p-2}) = c_p$$

Thus we arrive at the symmetry relation of the coefficients :

$$b_{p-1} = c_p \tag{30}$$

Applied to generate the successive iterates $X = [x_0, ..., x_p]$, the algorithm (27) gives rise to the matrix form relationship :

$$K^{-1}M[x_0 \ldots x_p] = [x_0 \ldots x_p] \begin{pmatrix} a_0 & b_0 & & & \\ c_1 & a_1 & b_1 & & 0 \\ \ldots & \ldots & \ldots & \ldots & \ldots \\ 0 & & c_{p-1} & a_{p-1} & b_{p-1} \\ & & & c_p & a_p \end{pmatrix} + [0 \ldots 0\ c_{p+1}x_{p+1}]$$

Or, if we take (30) into account to define the symmetric tridiagonal matrix of the coefficients :

$$T = \begin{pmatrix} a_0 & c_1 & & & \\ c_1 & a_1 & c_2 & & 0 \\ \ldots & \ldots & \ldots & \ldots & \ldots \\ 0 & & & & c_p \\ & & & c_p & a_p \end{pmatrix} \tag{31}$$

we can summarize the Lanczos algorithm with the following matrix formalism :

$$K^{-1}MX = XT + S\ , \tag{32}$$

where S is the remainder matrix :

$$S = [0 \ldots 0\ c_{p+1}x_{p+1}] = c_{p+1}x_{p+1}e_p^t\ . \tag{33}$$

We multiply at stage p the equation (4.6) by $(MX)^t$, and we get that :

$$X^tM^tK^{-1}MX = X^tM^tXT + X^tM^tS\ .$$

If we note the orthogonality $(MX)^tS = 0$ obtained by constructing iterate p, thanks to (28) we get the interaction relation :

$$X^tM^tK^{-1}MX = X^tM^tXT = T\ . \tag{34}$$

In fact, the tridiagonal matrix T of the Lanczos coefficients can be seen as the projection (with respect to the metric M) of the matrix $K^{-1}M$ onto the Lanczos orthogonal subspace X. The matrix T thus has the same eigensolutions as the projection of $K^{-1}M$ onto the reduced basis X.

We can further improve the analysis of the significance of the interaction problem eigensolutions :

$$Tz = \lambda z\ . \tag{35}$$

By looking at two successive iterates of the iteration method

$$v_0 = Xz \ \text{ and } \ v_1 = K^{-1}Mv_0 = K^{-1}MXz\ ,$$

and taking into account of (32), we get :

$$K^{-1}Mv_0 = XTz + Sz \ .$$

If we then premultiply the two members of the previous equation by $(MXz)^t$, we get :

$$\lambda = \frac{z^tTz}{z^tz} = \frac{v_1^tMv_0}{v_0^tMv_0} \ ,$$

which shows that the Rayleigh quotient of the tridiagonal matrix formed with vector z is equal to the Schwarz quotient formed for the complete system with vector v_0, which is the corresponding estimate in the Lanczos vector basis. Owing to the remarkable properties of the Schwarz quotient (Geradin and Rixen, 1997), we can expect a very good convergence of the method. In practice, experience shows that the Lanczos method requires three or four inverse iterations per converged eigenvalue. Furthermore, this number remains independent of the problem size. It is also not very strongly affected by the closeness of the eigenvalues.

Besides, we have an estimate of the accuracy of the numerical calculus of the eigensolutions. Let (λ_m, z_m) be a solution of the problem (35). This corresponds to an approximate solution of the initial problem (27) :

$$v_m = Xz_m \tag{36} \ ,$$

obtained by projection into the subspace formed by the Lanczos vectors. The error on the eigensolution (36) can be measured by calculating the following difference :

$$s_m = (K^{-1}M - \lambda_m)v_m \tag{37} \ .$$

With this in view, let us return to the recursive relation (32) and let us multiply it by z_m. We get that :

$$K^{-1}MXz_m = XTz_m + Sz_m \ .$$

Let us note that $Tz_m = \lambda_m z_m$. We then obtain :

$$(K^{-1}M - \lambda_m)v_m = s_m \ ,$$

where s_m is defined as follows :

$$s_m = Sz_m = c_{p+1}e_p^tz_mx_{p+1} \tag{38} \ .$$

The different factors forming the right-hand side of (38) can be deduced from the Lanczos iteration process. Consequently, it is easy without any further effort to carry out the test :

$$\|s_m\| < \delta \tag{39}$$

where δ is an adequate accuracy measure.

Let us now analyse the difficulties of the Lanczos method. First, it must be noticed that the dominant modes of the system are very quickly extracted from the started vector so that, after a few iterations, numerical errors become of the same order of magnitude as the Lanczos base vectors. The result is that vectors $[x_0 \ ... \ x_{p-2}]$, in relation to which

orthogonality has been achieved, reappear in iterate x_{p+1}. We overcome this situation by reconstructing the direction's orthogonality by a Gram-Schmidt process, but it is obvious that we lose part of the method's benefit. Nevertheless, a selective re-orthogonalization process leads to a reduction of the cost of the operation.

Theoretically, multiple eigenvectors can not be extracted using the Lanczos method : indeed, the starting vector contains only a linear combination of those multiple modes, and this combination remains unchanged in the course of iterations. In practice, the result of the degeneration of the orthogonalization process is that multiple solutions reappear progressively. In the case of a dielectric waveguide of circular cross section, we know that the degeneracy of the modes induced by the symmetry is 2. We numerically verify that the eigenvalues belonging to the discrete spectrum (those with physical meaning) are given twice (with ten significant figures), but their associated modes are different. Furthermore, we restart the algorithm with other starting vectors, therefore we can guarantee effective computation of all eigenvectors with a multiple eigenvalue.

Another difficulty is that of appearance of parasitic solutions or even skipping of solutions, which result from the degeneration of the orthogonalization process and a bad conditioning of matrices K and M. To overcome this difficulty, we multiply the M matrix by a factor c^2 (c being the velocity of light in vaccuum) : we then have two matrices K and c^2M with the same order coefficients, which induces a good starting vector associated to $K^{-1}c^2M - \lambda$ implemented in the Lanczos algorithm (see (37)). It is to be noticed that non-converged solutions can be rejected *a posteriori* by an error criterion such as (39).

To conclude this section, we want to say that the Lanczos method is extremely powerful for the extraction of eigenvalues and makes it possible to treat very large sparse systems. But its implementation is delicate and its use sometimes requires precautions. Nowadays, it is used in most finite element analysis codes.

6.5.2 Validation of the code

Let us first note that the GetDP software ([65]) (Dular *et al.*, 1998) has been used to set up the finite element problem. We study the case of a low index step fiber of circular cross-section ($\varepsilon_r = 1.25$) to validate our method : it is then easy to compare our dispersion curve to that derived in the weak-coupling assumptions (Snyder and Love, 1983). In this case, the HE_{1m} modes have a small azimuthal variation and depend only on the radial position $\mathbf{r}$. There is therefore no prefered axis of symmetry in the circular cross-section. In this exceptional case, the transverse magnetic field can be directed so that it is everywhere parallel to one of an arbitrary pair of orthogonal directions. If we denote this pair of directions by x- and y-axes, then there are two fundamental or HE_{1m} modes, one with its transverse magnetic field parallel to the x-direction, and the other parallel to the y-direction. The symmetry also requires that the scalar propagation constants of each pair of modes are equal. This degeneracy of the modes highly depends upon the geometry of the waveguide cross-section. It is worth noting that if the cross-section is elliptical, the transverse magnetic field is everywhere parallel to the major and minor axes of the elliptical cross-section. As for the circular fiber there are two modes associated with this solution (one for each polarization). Because the cross-section is not circular, the

propagation constants of these two modes will differ : the difference is due to polarization, or birefringence properties of the waveguide. In this sense, the propagation on noncircular waveguides is similar to propagation in anisotropic media. It is worth noting that with the exception of the fundamental HE_{11} mode, every mode is cut off below a certain value of V (see section 1).

Thanks to the symmetry of the guide, we just mesh one fourth of the guide (we could have considered a smaller part of the guide) : we take Dirichlet or Neumann boundary conditions on the x and y axis to get symmetric or antisymmetric modes versus these axes (fig. 6.4).

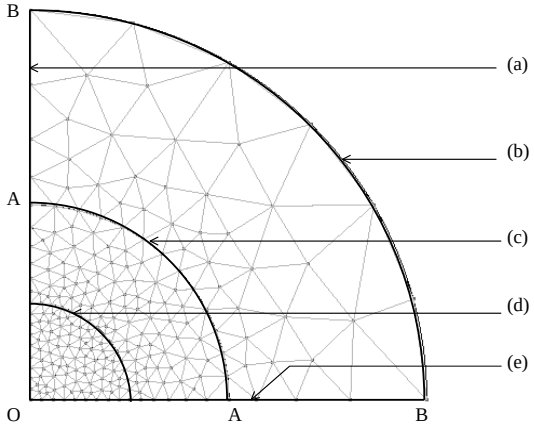

FIGURE 6.4 – (a), (e) Projections of a plane of symmetry (Dirichlet condition) or antisymmety (Neumann condition). (b) Exterior boundary of the corona rejected to infinity (Dirichlet boundary condition). (c) Interface between air and corona (tangential continuity of the Whitney elements). (d) Interface between core and air (tangential continuity of the Whitney elements).

This remark is of importance in the case of PCF structures : we only consider one fourth of the PCF since their crystal cladding has the square symmetry. Our validation is all the more significant that we obtain both the dispersion curves (fig. 6.5) and the associated expected transverse magnetic fields (fig. 6.6) for all the modes : these results strengthen those foreseen by B. Meys ([154], 1999). Furthermore, there is a good agreement with analytical results of the classical book of Snyder and Love ([191], 1983) :

$$\begin{cases} u^2 + w^2 = r_c^2 \omega^2 \mu_0 (\varepsilon_1 - \varepsilon_2) \\ \Big(\dfrac{J'_m(u)}{uJ_m(u)} + \dfrac{K'_m(w)}{wK_m(w)}\Big)\Big(\dfrac{\varepsilon_1 J'_m(u)}{\varepsilon_2 uJ_m(u)} + \dfrac{K'_m(w)}{wK_m(w)}\Big) \quad = m^2\Big(\dfrac{1}{u^2} + \dfrac{1}{w^2}\Big)\Big(\dfrac{\varepsilon_1}{\varepsilon_2 u^2} + \dfrac{1}{w^2}\Big) \end{cases}$$

with $u = r_c\sqrt{\omega^2\varepsilon_1\mu_0 - \gamma^2}$, $w = r_c\sqrt{\gamma^2 - \omega^2\varepsilon_2\mu_0}$, J_m, K_m, J'_m and K'_m being the Bessel (and modified Bessel) functions and their first derivatives ([191],[1]). Here, $r_c = 1$ is the radius of the fiber, $\varepsilon_1 = 1.25$ is the permittivity of the fiber and $\varepsilon_2 = 1$ is that of the air.

6.5.3 Analysis of cross-talk phenomena

In this section, we explain how to get numerically the phenomena of cross-talk between identical fibers (Vassalo, 1985 [200]), (Petit, 1993 [176]) for a given time frequency ω. Fi-

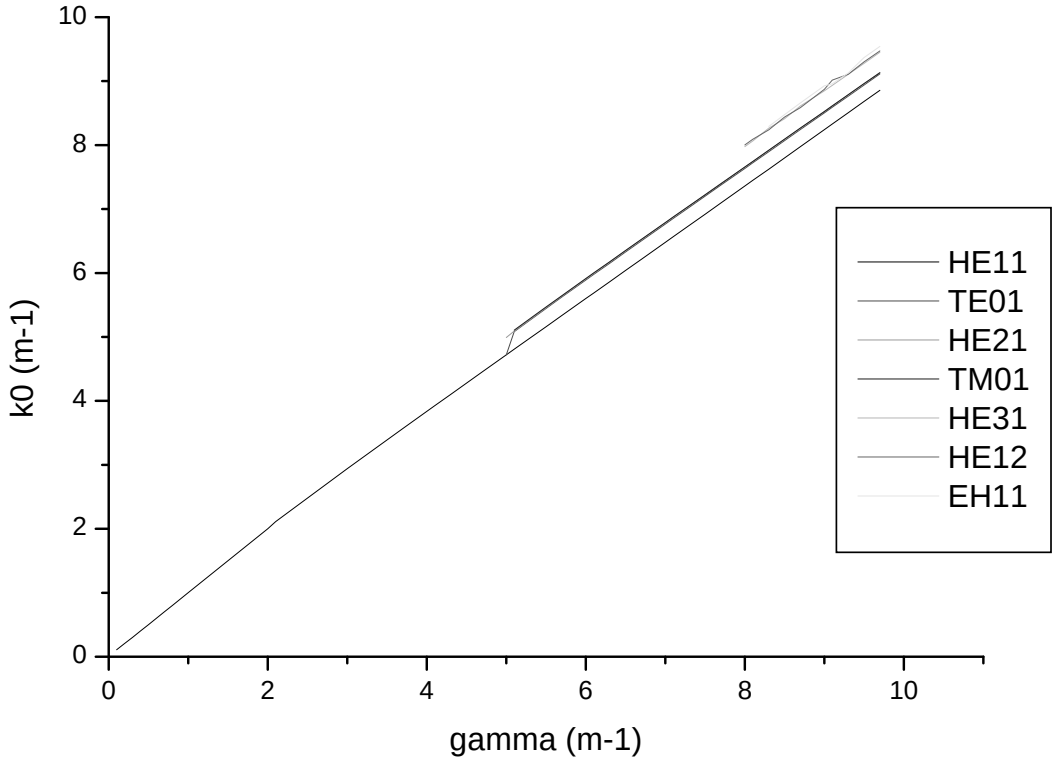

FIGURE 6.5 – Dispersion curves of a fiber of circular cross-section with relative permittivity $\varepsilon_r = 1.25$ and a unit radius.

gure 6.8 shows the variation of the real and imaginary parts of the three components of the magnetic field $\mathbf{H}$ along a line through the centers of the fibers, for a given propagating constant γ. Because of the symmetry of the problem (the two guides are identical), we can deduce that the mirror reflection with respect to the axis of symmetry between the guides is also a solution (with the same propagating constant γ and the angular frequency ω). It corresponds to a degeneracy of the mode. These two solutions can be linearly combined to give a symmetric solution $\mathbf{H}_s$ (even part of the curve) and an antisymmetric solution $\mathbf{H}_a$ (odd part of the curve). Unfortunately, it is very unprobable that the Lanczos algorithm gives directly such solutions. It rather gives an arbitrary linear combination of these solutions. We therefore have to "build" them.

Thanks to the linearity of the Maxwell equations, we can state that there are propagating modes of the form :

$$\mathbf{H}(x,y,z) = \mathbf{H}_s(x,y)exp(i\gamma_s z) + \mathbf{H}_a(x,y)exp(i\gamma_a z)$$

The so called phenomenon of optical cross talk, whereby light initially in one fiber transfers to the other fiber during propagation, is a consequence of interference between the modal fields $\mathbf{H}$ associated with symmetric and antisymmetric magnetic fields $\mathbf{H}_s$ and $\mathbf{H}_a$ (linearly polarized thanks to the symmetries) for distinct propagating constants γ_s and γ_a (cf. figure 6.7).

Besides, we can define the intensity of the magnetic field as follows :

$$I = \mid \mathbf{H} \mid^2 = \mathbf{H}_s^2 + \mathbf{H}_a^2 + 2\Re e\{\mathbf{H}_s \cdot \overline{\mathbf{H}_a} exp(i(\gamma_s - \gamma_a)z)\}$$

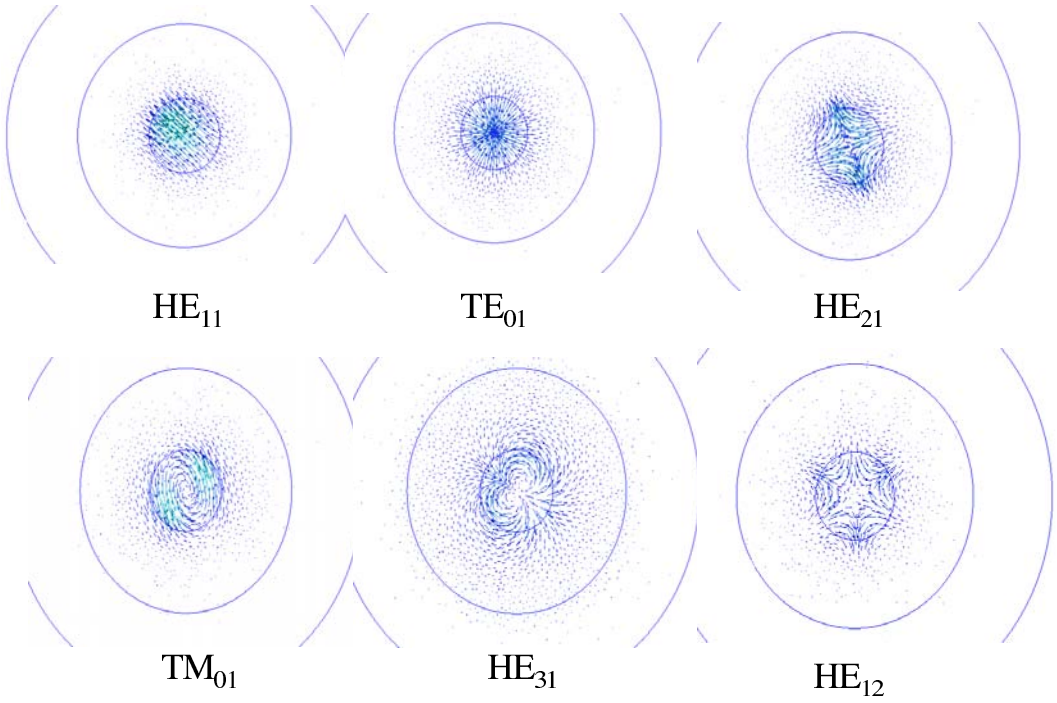

FIGURE 6.6 – The four hybrid modes HE_{11}, HE_{21}, HE_{31}, HE_{12} (ordered in increasing frequencies) and the two transverse modes TE_{01} and TM_{01} of the circular fiber of radius 1 with relative permittivity of $\varepsilon_r = 1.25$ (corresponding to the dispersion curves of fig. 6.5) for a propagation constant $\gamma = 8m^{-1}$. Their associated wave numbers are $k_0 = 7.38194$, 7.70039, 7.99773, 7.97468, 7.62185 and 7.73754 m^{-1}.

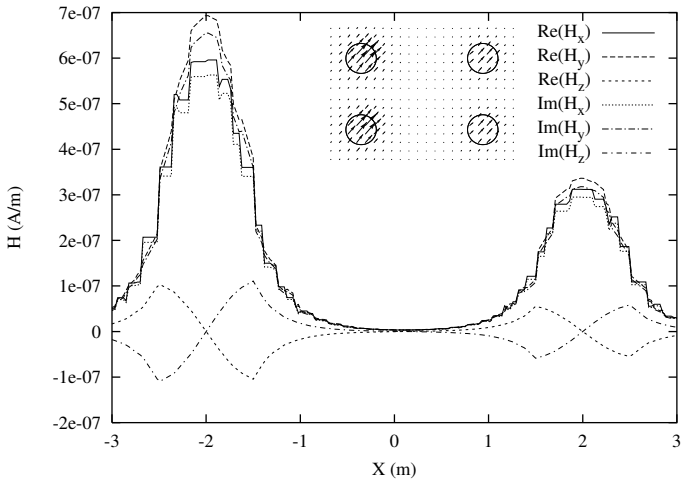

FIGURE 6.7 – Representation of the real and imaginary parts of the three components of a magnetic mode for a propagating constant $\gamma = 9m^{-1}$.

We then deduce that :

$$I(x,y,z) = \begin{cases} \mid \mathbf{H}_s(x,y) + \mathbf{H}_a(x,y) \mid^2 & \text{if } (\gamma_s - \gamma_a)z = 2p\pi, p \in \mathbb{Z} \\ \mid \mathbf{H}_s(x,y) - \mathbf{H}_a(x,y) \mid^2 & \text{if } (\gamma_s - \gamma_a)z = \pi + 2q\pi, q \in \mathbb{Z} \end{cases}$$

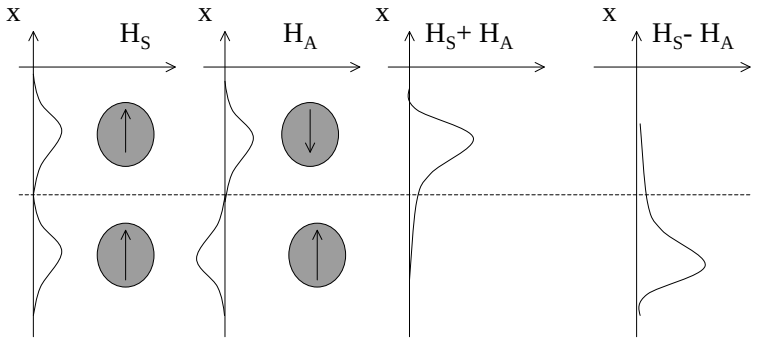

FIGURE 6.8 – Behaviour of the fields $\mathbf{H}_s$ and $\mathbf{H}_a$. The dotted line corresponds to the symmetry plane.

In fact, light power oscillates from one fiber to the other in a manner analogous to the behaviour of a pair of coupled, identical pendulums. If l denotes the beat length, i.e. the distance along the waveguide in which there is a total transfer of power from one fiber to the other fiber and back again, then we have :

$$l = \pi / \mid \gamma_s - \gamma_a \mid$$

As the separation increases, $\gamma_s \to \gamma_a$ and the beat length becomes rapidly large (no more coupling of the fibers).

The cross talk effect can form the basis of many devices such as demultiplexers in optoelectronic components. In mechanics, the coupling between two identical pendulums is function of the time t and the time frequency ω which respectively play the role of z and γ in the cross talk phenomenon. In mechanics, it is well known that coupling two pendulums degenerates their frequencies. The coupling of two fibers induces degeneracy of the propagating constant.

In the next section, we present the extension of this study (invited talk in EMF 2000 [99], and article in COMPEL 2001 [100]) to coupling between a large number of dielectric parallel rods i.e. the so-called photonic crystal fibers (PCF).

6.5.4 Numerical results for the PCF

Let us first discuss the physics underlying photonic propagation in the first type of photonic crystal fibers (HPCF of glass with air holes) i.e. with a high index structural defect : we consider a waveguide of circular cross-section composed of a matrix of index 2 and 80 air holes periodically arranged. We achieve a numerical study of modes confined in specific parts of the high index region thanks to the crystal cladding : one can see on figure (6.9) some propagating modes trapped in the high index core region of the fiber and one can see the analogous phenomenon on figure (6.10) for modes confined outside the crystal cladding (and even inside-outside). The most popular physical interpretation is that the effective index for the crystal cladding is lower than that one of core and exterior regions and the modes therefore propagate in these regions. Such an effect is very similar

to that of the classical waveguides. A second interpretation can be formulated : we consider the periodic assembly of air holes as independent fibers (although they are air holes) that are strongly coupled together. Let us assume that each isolated rod could support many distinct modes (obviously, these modes are purely complex since they cannot propagate in air holes), each with a different frequency ω. When a large number of such rods (in our case 80) are placed in close proximity, they couple together, and each mode of the single rod opens up into a passband of modes of the composite structure (when the number of rods tends to infinity), each passband now covering a range of ω values. The passbands are separated by band gaps also known as photonic band gaps. The central high index defect would, if isolated, support a different set of waveguide modes, thanks to its different morphology. If the ω value of one of these modes falls within one of the bands of modes of the periodic cladding, this mode of the core will be coupled to the spatially extended modes of the periodic cladding (everywhere in high index). However, if one of the modes of the core region falls in between the passbands of the fully periodic lattice region, then this mode is localized within the core and forms a PBG guided mode. Thus, at some wavelengths, there is a mode trapped within the core (resp. outside the crystal cladding), whereas at other wavelengths modes are extending between the fibers (they cannot propagate in air holes).

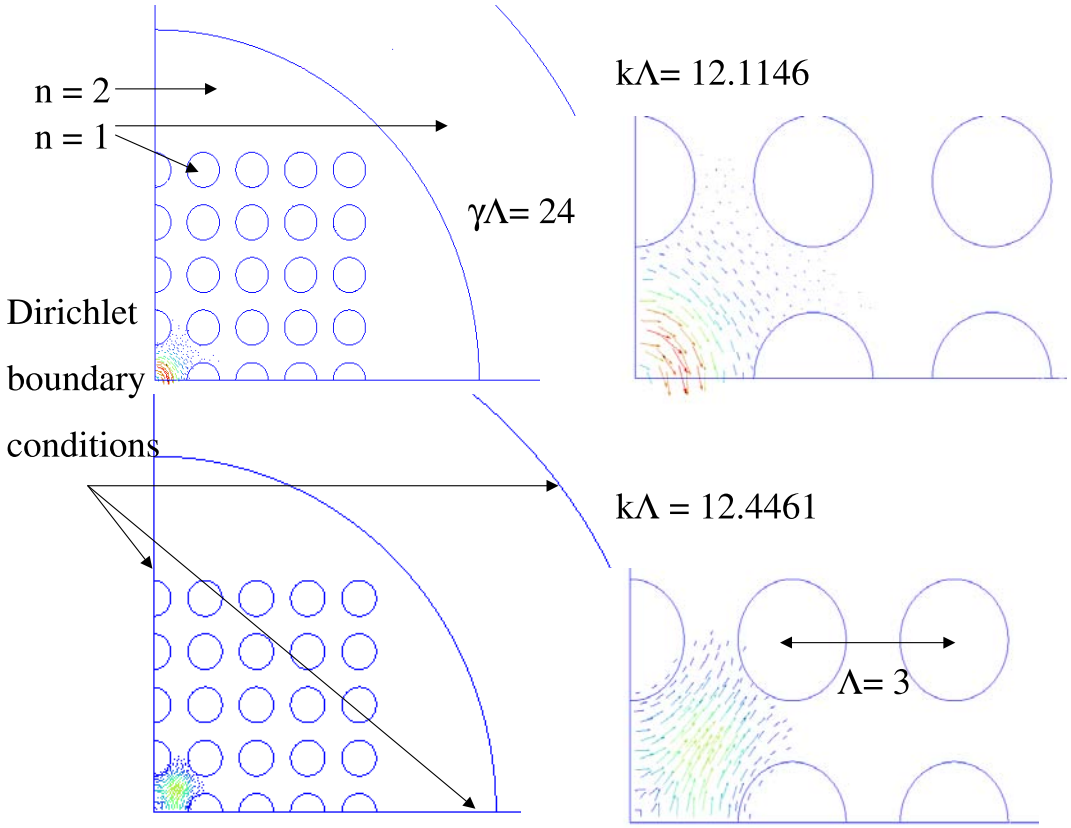

FIGURE 6.9 – Transverse magnetic fields and their associated normalized wave numbers $k\Lambda$ in a circular HPCF (PCF type 1) of index 2 with 80 unit radius air holes and nearest hole spacing $\Lambda = 3$. The normalized propagation constant $\gamma\Lambda$ is equal to 24.

We achieve a numerical study of modes propagating in fibers of index 2 in a crystal

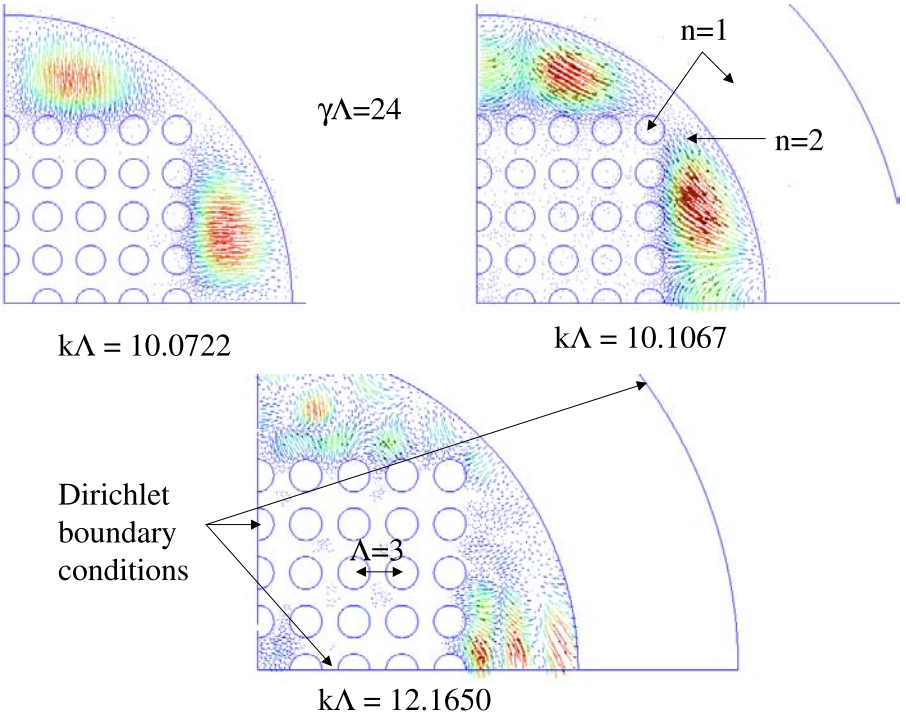

FIGURE 6.10 – Transverse magnetic fields and their associated normalized wave numbers $k\Lambda$ in a circular HPCF (PCF type 1) of index 2 with 80 unit radius air holes and nearest hole spacing $\Lambda = 3$. The normalized propagation constant $\gamma\Lambda$ is equal to 24.

cladding. We clearly see that such modes propagate in each fiber independently of the other fibers (which is far from being obvious) (see figure 6.12) : these modes have the same frequencies and symmetries (up to a phasis) than the ones of a single fiber of unit radius and relative permittivity $\varepsilon = 4$. Obviously, these modes are identical in each fiber up to a phasis and amplitude : they are linear combinations of each individual mode, which induces degeneracy of the eigenvalues.

Such a result could although be interpreted as modes belonging to the Bloch spectrum : in the Bloch wave decomposition, one only considers a fiber in a unit cell Y with quasi-periodicity conditions (up to a phasis).

6.6 Conclusion and perspectives

In conclusion, we want to say a few words about the physical aspect of the study. Due to the vector treatment of the problem, we achieve a rigorous numerical study of the physical phenomena arising in propagation of modes in a photonic crystal fiber. We first compare the numerical results of the finite element scheme with classical ones : for this, we study the dispersion curves of a dielectric circular waveguide. We then study two types of photonic crystal fibers of finite cross section. In the first type of PCF (HPCF), we numerically characterize modes which propagate thanks to the photonic band gap effect in a region of high index surrounding a crystal cladding (fiber of index 2 with a periodic assembly of air holes). In the second type of PCF (LPCF), we numerically show some propagating modes

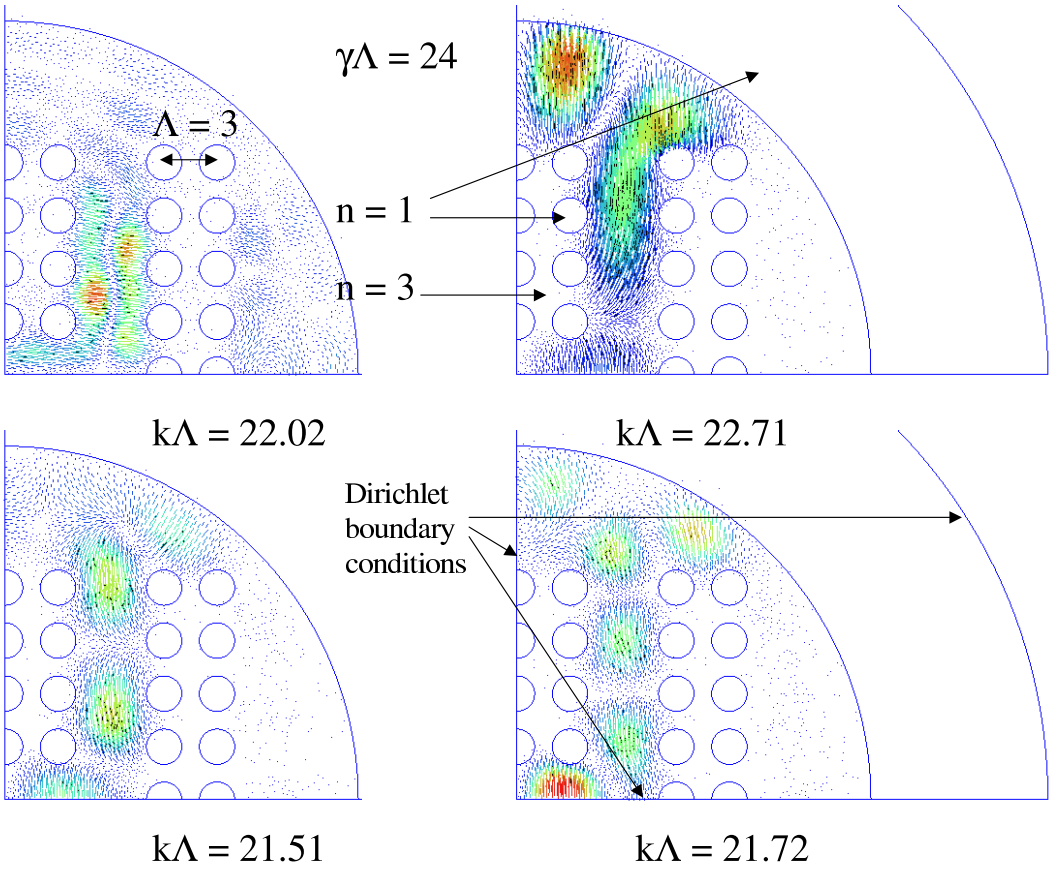

FIGURE 6.11 – Transverse magnetic fields and their associated normalized wave numbers $k\Lambda$ in a circular HPCF (with a "H" default) of index 3 with 60 unit radius air holes and nearest hole spacing $\Lambda = 3$. The normalized propagation constant $\gamma\Lambda$ is equal to 24.

confined in each rod (silica) of the crystal cladding and which have all the properties of the modes of a circular fiber : the frequencies and associated modes of such fibers do not depend on the existence of the other fibers and are thus called local modes. We are working at the present time on the generalization of the Lanczos method to the computation of leaky modes (see next section for an approach of leaky modes via an electric field formulation). In the next section we will study with further details the influence of geometry in such guides (see figure 6.11 for a striking example). Other remarkable properties of PCF are that linearly polarized light coupled into the fiber parallel to one axis emerges linearly polarized and parallel to the same axis even if the fiber is bent or twisted. An analogous phenomena is even observed concerning the loss of energy induced by the bends : unlike classical optical waveguides, the PCF can propagate light without loss of energy in the bends, thanks to the PBG effect. Such a modelling could be achieved with our formalism, thanks to adequate geometrical transformations (by the use of pull-back properties of the edge-elements) similar to the ones of the C method [52].

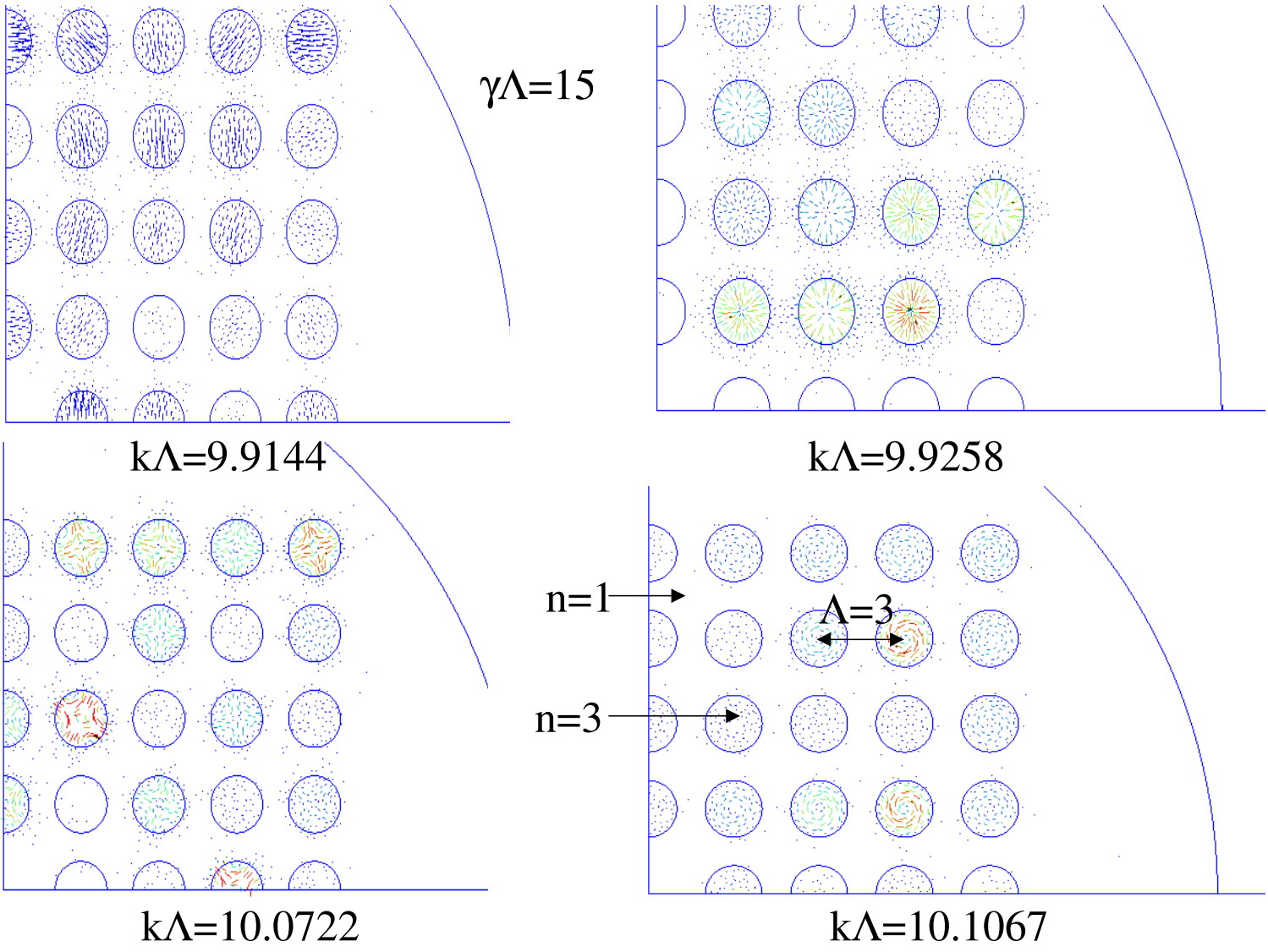

FIGURE 6.12 – Transverse magnetic fields and their associated normalized wave numbers $k\Lambda$ in a circular LPCF (PCF type 2) of index 1 with 80 unit radius rods of index 3 and nearest rod spacing $\Lambda = 3$. The normalized propagation constant $\gamma\Lambda$ is equal to 15.

Chapitre 7

Propagating modes in metallic waveguides

The purpose of computing is insight, not numbers.
R. W. Hamming. [109]

7.1 Preliminaries

Let us now introduce some qualitative insight into the nature of the guided modes of a low-index PCF structure (LPCF with silica rods). Although rigorous, our numerical study holds only for the non-dissipative modes. The localized mode is a kind of "leaky mode", that is a dissipative mode, and is therefore associated with complex frequencies. To look for such a mode necessitates the investigation of the case of complex propagation constant γ. For this, it seems more natural to work with a fixed frequency ω and look for gamma : we are thus led to a non-linear generalized eigenvalue problem with non-hermitian matrices. Such a "spectral problem" could be numerically solved thanks to an algorithm of non linear inverse iterations. This algorithm can indeed solve our generalized eigenvalue problems which takes the form :

$$K(\gamma)X = \omega^2 MX$$

where the matrix K is complex non hermitian and depends non-linearly on γ and M is a complex hermitian matrix.

It is then necessary to shift the convergence of the algorithm towards the estimation of each solution. For this, we transform the previous system as follows :

$$(K(\gamma) - \Lambda M)X = (\omega^2 - \Lambda)MX \ ,$$

which shifts the spectrum of eigenvalues of $-\Lambda$. Noting that the algorithm of non linear inverse iterations without shift converges towards the smaller eigenvalue (in modulus), we hence force the convergence to the closest eigenvalue of Λ (in modulus). This algorithm has not been implemented yet, although it is a straigthforward generalization of our discrete formulation. It is worth noting that the localized mode has a complex propagation constant

$$\gamma = \gamma_r + i\gamma_i \ ,$$

therefore, there are many kinds of propagating modes for a given complex frequency ω. The magnetic field can therefore be written as follows :

$$\mathcal{H}(x,y,z,t) = \Re e(\mathbf{H}(x,y)e^{(i\gamma_r-\gamma_i)z-i\omega t})$$

If we consider the propagating modes with positive z, we know that the ones with $\gamma_i < 0$ correspond to exponentially increasing waves at infinity i.e. leaky modes. The ones with $\gamma_r = 0$ and $\gamma_i > 0$ are evanescent, and the ones with $\gamma_r > 0$ and $\gamma_i > 0$ are dissipative propagating modes (the case $\gamma_r > 0$ and $\gamma_i = 0$ corresponds to non-dissipative modes).

The main difficulty is that this algorithm only gives one eigenvalue and its associated eigenvector per calculus. Therefore, we do not investigate the leaky modes by this way. Analogously to ([205])(White, 2000), we could consider a medium with a complex permittivity including the PCF, to take into account the amount of loss of the leaky modes. In that case, ε is not hermitian and the linear system can be solved thanks to an Arnoldi algorithm, which provide many eigenvalues per calculus. To keep the self-adjointness of the operator (real spectrum), we take a jacket at a finite distance from the waveguide, with Dirichlet conditions.

7.2 Set up of the problem

We consider a metallic waveguide with heterogeneous permittivity and permeablity, of constant section Ω invariant along the z axis. We are looking for electromagnetic fields $(\mathcal{E},\mathcal{H})$ solutions of the following Maxwell equations :

$$(1)\begin{cases} \operatorname{curl}\mathcal{H} &= \varepsilon\star\dfrac{\partial\mathcal{E}}{\partial t}+\mathcal{J} \\ \operatorname{curl}\mathcal{E} &= -\mu\star\dfrac{\partial\mathcal{H}}{\partial t} \end{cases}$$

$\star\varepsilon$ and $\star\mu$ being two second order real symmetric tensor fields, defined in Ω, with bounded coefficients satisfying the ellipticity conditions

$$\sum_{i,j=1,3}\varepsilon_{ij}\xi_i\xi_j \geq \alpha|\,\xi\,|^2 \text{ and } \sum_{i,j=1,3}\mu_{ij}\xi_i\xi_j \geq \beta|\,\xi\,|^2\ ,\ \forall\xi\in\mathbb{R}^3$$

Furthermore, choosing a time dependance in $e^{-i\omega t}$, and taking into account the invariance of the guide along its z axis, we define time-harmonic two-dimensional electric and magnetic fields $\mathbf{E}$ and $\mathbf{H}$ by :

$$(2)\begin{cases} \mathcal{E}(x,y,z,t) &= \Re e(\mathbf{E}(x,y)e^{-i(\omega t-\gamma z)}) \\ \mathcal{H}(x,y,z,t) &= \Re e(\mathbf{H}(x,y)e^{-i(\omega t-\gamma z)}) \end{cases}$$

where ω is the angular frequency in the vacuum and γ denotes the propagating constant of the guided mode.

For $(\mathbf{E},\mathbf{H})$ satisfying (2), (1) can be written as :

$$(3)\begin{cases} \operatorname{curl}_\gamma\mathbf{H} &= -i\omega\varepsilon(x,y)\star\mathbf{E}+\mathbf{J} \\ \operatorname{curl}_\gamma\mathbf{E} &= i\omega\mu(x,y)\star\mathbf{H} \end{cases}$$

where $\mathbf{J}$ is defined as $\mathbf{E}$ and $\mathbf{H}$ in (7.2), and $\mathrm{curl}_\gamma \mathbf{H}$ and $\mathrm{curl}_\gamma \mathbf{E}$ are given by :

$$(4)\ \begin{cases} \mathrm{curl}_\gamma \mathbf{H}(x,y) &= \mathrm{curl}\Big(\mathbf{H}(x,y)e^{i\gamma z}\Big)e^{-i\gamma z} \\ \mathrm{curl}_\gamma \mathbf{E}(x,y) &= \mathrm{curl}\Big(\mathbf{E}(x,y)e^{i\gamma z}\Big)e^{-i\gamma z} \end{cases}$$

We say that $(\mathbf{E},\mathbf{H})$ is a guided mode if :

$$(5)\ \begin{cases} (\gamma,\omega) \in \mathbb{R}^2 \\ (\mathbf{E},\mathbf{H}) \neq (\mathbf{0},\mathbf{0}) \\ \mathbf{E},\mathbf{H} \in [L^2(\Omega)]^3 \end{cases}$$

with $n \wedge \mathbf{E} = 0$ and $n \wedge \mathbf{H} = \mathbf{J}_s$ (surface current) on the boundary $\partial\Omega$ of Ω.

We choose an electric field formulation [185] because the tangential trace of $\mathbf{E}$ is null, contrary to that of $\mathbf{H}$. Thus, div_γ being an operator analogously defined to curl_γ in (4), it is clear that $\mathrm{div}_\gamma \star \mathrm{curl}_\gamma \star \mathbf{E} = 0$, for all 1-form $\mathbf{E}$ in Ω such that $n \wedge \mathbf{E} = 0$. Thus, we are led to the following system of Maxwell's type :

$$(6)\ \begin{cases} \varepsilon^{-1} \star \mathrm{curl}_\gamma(\mu^{-1} \star \mathrm{curl}_\gamma \mathbf{E}) &= \omega^2 \mathbf{E} \\ \mathrm{div}_\gamma(\varepsilon \star \mathbf{E}) &= 0 \end{cases}$$

Let (γ,ω) be a solution of the spectral problem (6) and $\mathbf{F}$ its associated eigenvector. Then $(\gamma,-\omega)$ is a solution of (6) with the same eigenvector $\mathbf{F}$. Physically speaking, this is induced by the time-invariance of the wave equation when dealing with non dissipative media (ω is not complex). Furthermore, $(-\gamma,\omega)$ et $(-\gamma,-\omega)$ are also solutions of (6) with the eigenvector $(F_1,F_2,-F_3)$: this is a space-invariance induced by the symmetry of the guide along the z-axis. Roughly speaking, the physical nature of the problem remains unchanged if a wave propagates along the z-positive or negative, provided that the cross section of the guide is constant. We therefore look solely for $(\gamma,\omega) \in \mathbb{R} + \times\mathbb{R}^+$.

The variational formulation associated to (6) is :

$$(7)\ \int_\Omega \varepsilon^{-1} \star \mathrm{curl}_\gamma(\mu^{-1} \star \mathrm{curl}_\gamma \mathbf{E}) \wedge \star\mathbf{E}' \ = \int_\Omega \omega^2 \mathbf{E} \wedge \star\mathbf{E}'$$

Thanks to the Stokes theorem, we see that the left member of (7) defines a bilinear form

$$(8)\ a(\gamma;\mathbf{E},\mathbf{E}') \ = \int_\Omega \frac{1}{\mu} \star \mathrm{curl}_\gamma \mathbf{E} \wedge \star\,\mathrm{curl}_\gamma \frac{1}{\varepsilon}\overline{\mathbf{E}'}$$

which is not symmetric. We therefore introduce a new measure on the domain Ω i.e. we change the scalar product. Noting that the Hodge operator defines a volume-form $dx \wedge dy \wedge dz$ thanks to $\star 1 = dx \wedge dy \wedge dz$ and that $\star\star\,\alpha = \alpha$, we can rewrite (8) as follows

$$(9)\ a(\gamma;\mathbf{E},\mathbf{E}') \ = \int_\Omega \star(\frac{1}{\mu} \star \mathrm{curl}_\gamma \mathbf{E} \wedge \star\,\mathrm{curl}_\gamma\, \overline{\mathbf{E}'})\frac{1}{\varepsilon} \star 1$$

It is clear that this form is bilinear, symmetric, continuous and cœrcive on the weighted Sobolev space

$$V(\gamma) = \{V \in [L^2(\Omega,d\mathcal{L})]^3\ ;\ \mathrm{curl}_\gamma V \in [L^2(\Omega,d\mathcal{L})]^3;\ \mathrm{div}_\gamma V = 0\ ,\ n \wedge V = 0 \ \text{ on } \partial\Omega\}$$

where $d\mathcal{L}$ denotes the measure (2-form) $\varepsilon \star 1$. Thanks to the properties of ε (coercivity and uniform boundedness), $V(\gamma)$ is isomorphic to the Sobolev space

$$\{V \in [L^2(\Omega)]^3 \ ; \ \mathrm{curl}_\gamma V \in [L^2(\Omega)]^3; \ \mathrm{div}_\gamma V = 0 \ , \ n \wedge V = 0 \ \text{ on } \partial\Omega\} \ .$$

This functional space highly depends upon γ. It is then difficult to study the dispersion curves, since the guided modes are functions of γ. Numerically speaking, it is a problem of penalization of the divergence. We therefore use the following result :

Lemma 1 :

Let F be a 1-form in $[H^1(\Omega)]^3$ such that $n \wedge \mathbf{F} = 0$ on the boundary $\partial\Omega$ of Ω. We then have the Green formula :

$$\int_\Omega (|\ \mathrm{curl}_\gamma F\ |^2 + |\ \mathrm{div}_\gamma F\ |^2)\, d\mathcal{L} = \int_\Omega (|\ \bigtriangledown F\ |^2 + \gamma^2 |\ F\ |^2)\, d\mathcal{L}$$

The functional space $V(\gamma)$

$$V(\gamma) = \{V \in [L^2(\Omega, d\mathcal{L})]^3 \ ; \ \mathrm{curl}_\gamma V \in [L^2(\Omega, d\mathcal{L})]^3; \ \mathrm{div}_\gamma V \in [L^2(\Omega, d\mathcal{L})]^3 \ , \ n \wedge V = 0 \ \text{ on } \partial\Omega\}$$

is then isomorphic to the Hilbert space $[H_0^1(\Omega)]^3$.

Proof :

Thanks to nullity of $n \wedge \mathbf{F}$ on $\partial\Omega$, the results follows from an integration by parts.

(QED)

Lemma 2 :

Let s be a positive real. Then, the two following systems are equivalent in $V(\gamma)$:

$$(10) \begin{cases} \mathrm{curl}_\gamma(\mu^{-1}\, \mathrm{curl}_\gamma \mathbf{E}) & = \omega^2 \varepsilon \mathbf{E} \\ \mathrm{div}_\gamma(\varepsilon \mathbf{E}) & = 0 \end{cases}$$

$$\mathrm{curl}_\gamma(\mu^{-1}\, \mathrm{curl}_\gamma \mathbf{E}) - s \bigtriangledown_\gamma (\mathrm{div}_\gamma\, \varepsilon \mathbf{E}) = \omega^2 \varepsilon \mathbf{E}$$

Proof :

The proof is analogous to that of lemma 1 of chapter 6 (note that $n \wedge \mathbf{F} = 0$ on $\partial\Omega$).

(QED)

The solution of the above problem is then given by the minimum of the following functional in the weighted Hilbert space $[H_0(\Omega, d\mathcal{L})]^3$ where $d\mathcal{L}$ is the measure $\varepsilon dxdy$:

$$\mathcal{R}(\gamma; \mathbf{E}, \mathbf{E}') = \int_\Omega \mathrm{curl}_\gamma \mathbf{E} \cdot \overline{\mathrm{curl}_\gamma \mathbf{E}'}\, d\mathcal{L}$$
$$+ \int_\Omega \mathrm{div}_\gamma \mathbf{E}\, \overline{\mathrm{div}_\gamma \mathbf{E}'}\, d\mathcal{L} - \mu_0 \omega^2 \int_\Omega \mathbf{E} \cdot \overline{\mathbf{E}'}\, d\mathcal{L}$$

This problem of minimization admits a unique solution thanks to the added term

$\int_\Omega \mathrm{div}_\gamma \mathbf{E}\, \overline{\mathrm{div}_\gamma \mathbf{E}'}\, d\mathcal{L}$ which acts in fact as a constraint which forces the nullity of $\mathrm{div}_\gamma(\varepsilon_r \mathbf{E})$. It is worth noting that the operator associated to this variational problem has a compact resolvent (compact embedding of $H^1(\Omega)$ in $L^2(\Omega)$). From the chapter 6, it is clear that its spectrum is a discrete set of eigenvalues belonging to $[\frac{\gamma^2}{\varepsilon_r}; +\infty[$ which gives us a numerical criterion to eliminate non physical modes.

7.3 Application to homogeneous metallic waveguides

We now make the hypothesis that $\mu(x, y)$ is a constant function, which takes the value μ_0 (non ferro-magnetic media), and we write the bounded coercive function $\varepsilon(x, y)$ as the product $\varepsilon_0 \varepsilon_r$. Thus, denoting by k_0 the wave number $\omega\sqrt{\mu_0 \varepsilon_0}$, we are led to the two following systems of Maxwell's type :

$$(11) \begin{cases} \mathrm{curl}_\gamma \mathrm{curl}_\gamma \mathbf{E} & = k_0^2 \varepsilon_r \mathbf{E} \\ \mathrm{div}_\gamma(\varepsilon_0 \varepsilon_r \mathbf{E}) & = 0 \end{cases}$$

We achieve numerical computations with the help of finite elements. It involves both a transverse field in the section of the guide and a longitudinal field along its axis. The section of the guide is meshed with triangles and Whitney finite elements are used i.e. edge elements for the transverse field and nodal elements for the longitudinal field. It is to be noticed that the generalized eigenvalue problem is solved thanks to the Lanczos algorithm. The GetDP software [64] has been used to set up the finite element problem.

We give the dispersion curves for a metallic homogeneous wave guide of circular cross-section, to validate the code (see figure 7.1) and some associated transverse electric fields (see figure 7.2). We note a good agreement betwen our dispersion curves (fig. 7.1) and analytical results given by classical waveguide theory ([176])(Petit, 1993),([200])(Vassalo, 1985). Nevertheless, one can see on figure 7.1 that there are some numerical discrepancies for small propagating constant and high frequency modes. One can avoid these inaccuracies by refining the mesh of the structure.

7.4 Application to heterogeneous metallic waveguides

7.4.1 Propagating waves and symmetry groups

Three symmetry types influence modes in PCF : the outer guide symmetry, the single rod symmetry and the architectural symmetry (multirod pattern). The previous Finite Element Method is applied on multishapes PCF to show the various influences : the literature on symmetries as applied to Finite element models in automatics is wide (see e.g. ([130])(Lobry, 1993) or ([127])(Lasquellec, 1998)), but it sounds not being fairly used in Finite Element Models for studying propagating modes in PCF. Nevertheless, symmetry analysis provides exact information concerning mode classification, mode degeneracy, modal electromagnetic-field symmetries, and the minimum waveguide sectors which completely determine the modes in each mode class, as shown in ([140])(Mac Isaac, 1975). This author uses the irreducible representations to determine the mode classes and their

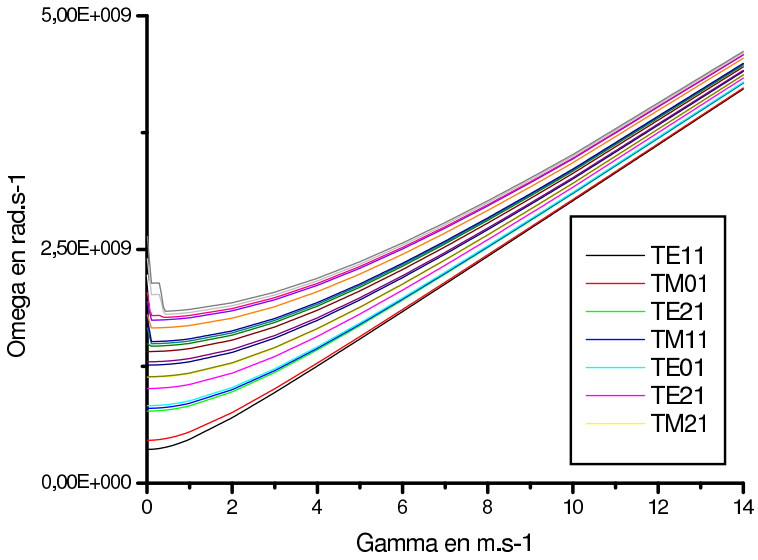

FIGURE 7.1 – Dispersion curves for a circular metallic waveguide.

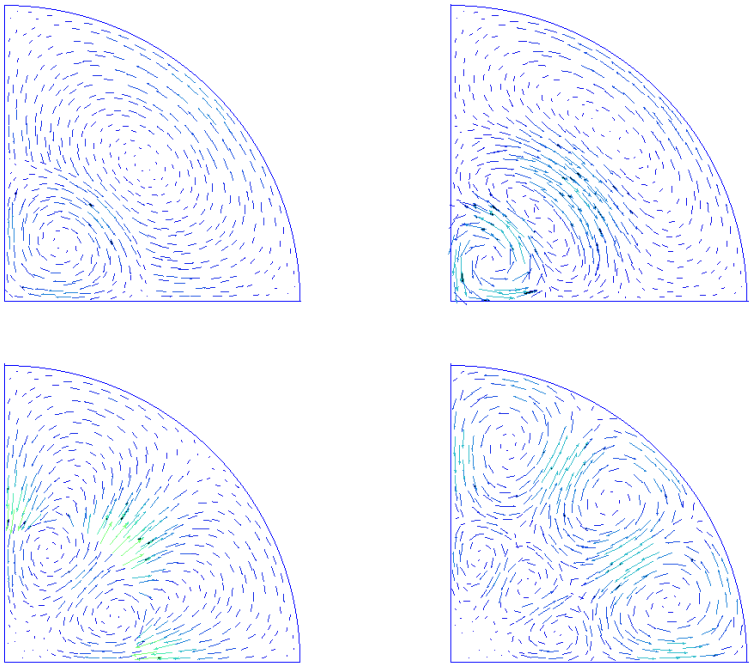

FIGURE 7.2 – Miscelleneaous modes of a metallic circular waveguide.

degeneracies, as well as their azimuthal symmetries. For this, he introduces the notion of group i.e. a set G of distinct elements for which a combining operation is defined and which satisfies four group postulates. The combining operation is called "group multiplication" and associates a third element of the set with any ordered pair of elements. The number of distinct elements of G is called the order of the group and denoted by g. For any particular group one can writ a group multiplication table which displays the results of multiplying any two elements of the group (note that group multiplication is not re-

quired to be commutative i.e. $AB \neq BA$). Examples of groups are provided by the sets of spatial symmetry. It is easy to check that the set of n distinct rotations about an axis (labeled C_n) satisfies the group postulates ([202][201])(Vincent, 1978) as well as the set of n distinct rotations about an axis and n mirror reflections in planes containing the axis. Sets of spatial symmetry operations which satisfy the group postulates are called symmetry groups. For a discussion of propagating modes in uniform waveguides, only the C_n and C_{nv} symmetry groups need be considered, as noted by Mc Isaac. This holds true for discussion of the associated scattering problem : one can relate the symmetry of the waveguide to that of its diffracted field via the so-called scattering operator, as shown by Vincent ([202][201])(Vincent, 1978). The relationship of the group of spatial symmetry operations belonging to a particular symmetry group possessed by a particular waveguide and the modal electromagnetic fields of the waveguide can be expressed in either of two ways. Consider some symmetry operation R belonging to the symmetry group G. One can apply the symmetry operation R to the waveguide structure, leaving the modal fields fixed in space ; or one can apply the symmetry operation R to the modal fields, leaving the waveguide structure fixed in space. In either case, after the symmetry operation is applied, the modal fields must again be a solution to the boundary value problem for the waveguide. For clarity, we distinguish between symmetry operations on the structure and on the electromagnetic fields by defining $P(R)$ to be that symmetry operation acting on the electromagnetic-field-waveguide-structure relationship to be the same after operation by either R (on the structure) or $P(R)$ (on the electromagnetic fields). One must have

$$P(R)E(r) = E(R^{-1}r)$$

where $E(r)$ is the electric field and R^{-1} is the symmetry operation inverse to R. A similar relation holds for the magnetic field ([140])(Mac Isaac, 1975).

In addition to symmetry groups there are many other sets of elements which satisfy the requirements for a group. Particularly important examples for symmetry analysis are sets of square matrices which satisfy all the group postulates with matrix multiplication as the group multiplication operation. Such a set of matrices is called a group representation, and certain group representations are central to symmetry analysis. Given any symmetry group G of order g, one can always devise a set of g matrices which satisfies the same multiplication table as the symmetry group, after making a correspondence between each element of the symmetry group and one of the matrices. Although an infinite number of group representations can be written for any symmetry group, it is found that all of these can be written as the sum of a few group representations whose matrices have a dimension of one, two, or at most three ([140])(Mc Issac, 1975). These few group representations are called the irreducible representations associated with the symmetry group. For the symmetry groups of current interest, the associated irreducible representations are known and tabulated ([202][201])(Vincent, 1978).

The boundary value problems associated with waveguides can usually be formulated in terms of an eigenvalue problem. Typically,

$$L\psi = \lambda\psi$$

where L is an operator, λ is an eigenvalue, and ψ is the associated eigenfunction. Suppose the waveguide has the symmetry group G. If R is one of the symmetry operations of the group, then the operator $P(R)$ must commute with the operator L. Therefore, we know that

$$P(R)L\psi = P(R)\lambda\psi$$

$$L\Big(P(R)\psi\Big) = \lambda P(R)\psi \ .$$

Thus, if ψ is an eigenfunction with eigenvalue λ, then $P(R)\psi$ must also be an eigenfunction with eigenvalue λ. If the eigenvalue λ has p degenerate eigenfunctions ψ_i ($i = 1,\ 2,\ ...,\ p$), then $P(R)\psi_n$, where ψ_n is one of these p eigenfunctions, can always be expressed as a sum over the p degenerate eigenfunctions. The effect of $P(R)$ is completely characterized by its effect on each of the basis functions ψ_i. For example, we get

$$P(R)\psi_j = \psi_1\Gamma(R)_{1j} + \psi_2\Gamma(R)_{2j} + ... + \psi_p\Gamma(R)_{pj} \ .$$

The coefficients $\Gamma(R)_{ij}$ in these equations can be considered to be the elements of a $p \times p$ square matrix $\Gamma(R)$. If the ψ_i are collected into a row matrix

$$\tilde{\psi} = (\psi_1\psi_2\psi_3 \ ... \ \psi_p) \ ,$$

then the previous equations can be written as

$$P(R)\tilde{\psi} = \tilde{\psi}\Gamma(R) \ .$$

Any solution of the eigenvalue problem with eigenvalue λ must beexpressible as a linear combination of the p independent solutions $\psi_1,\ \psi_2,\ ,...,\ \psi_p$. Thus, there is an equation analogous to the last one for every member of the symmetry group G. The complete set of matrices $\Gamma(R)$ for all g members of the symmetry group forms a representation. The basic assumption of symmetry analysis is the Irreducibility Postulate ([202][201])(Vincent, 1978)([150])(Mc Weeny, 1963) :

Lemma 3 :

Provided there are no accidental degeneracies (no mode degeneracy which appears not to be symmetry related), every degenerate group of eigenfunctions of an operator L provides an irreducible representation of the group of symmetry operations which leaves L invariant.

Thus, the $\Gamma(R)$ in the previous equation forms an irreducible representation. An alternative form of this postulate is the one which is used as the basis for the symmetry analysis here ([140])(Mc Isaac, 1975) :

Lemma 4 :

For every p-dimensional irreducible representation of the symmetry group under which an operator L is invariant, we can find p-fold degenerate sets of eigenfunctions. Any further degeneracy would be accidental and expected to occur only rarely.

As a consequence, any eigenfunction of the operator L can be associated with a row of one of the irreducible representations of the symmetry group G. For those irreducible

representations which are one-dimensional, each of the associated eigenfunctions is non-degenerate ([140])(Mc Isaac, 1975). For those irreducible representations which are two-dimensional, the associated eigenfunctions must occur in degenerate pairs, with one member of each pair associated with the first row and the second member with the second row of the irreducible representation. A similar statement applies to higher dimensional irreducible representations, but for uniform waveguides only one- or two-dimensional representations are encountered ([140])(Mc Isaac, 1975).

Furthermore, the symmetry group of the Maxwell operator for uniform waveguides being either C_n or C_{nv} (with no irreducible representations with dimension higher than two), there will be no symmetry-induced modal degeneracies higher than two. Reference to tables of irreducible representations of the symmetry groups ([202])(Vincent, 1978)([150])(Mc Issac, 1963) reveals that symmetry group C_4 has two one-dimensional and one two-dimensional irreducible representations, and symmetry group C_{6v} has four one-dimensional and two two-dimensional irreducible representations. Therefore, waveguides with C_4 symmetry have two nondegenerate mode classes and a pair of mutually degenerate mode classes, and waveguides with C_{6v} symmetry have four nondegenerate mode classes and two pairs of mutually degenerate mode classes.

7.4.2 Symmetries in PCF

In this section, we apply the formalism of group symmetry to propagating modes in photonic crystal fibers (article in preparation, [128]).

A- The Outer Guide Symmetry (macroscopic scale).

Figure 7.3 shows a PCF with a propagation constant $\gamma = 0.1cm^{-1}$, which corresponds to a low frequency according to the dispersion curve. Because of the high wavelength, modes are not sensitive to individual rods and they spread out over the total fiber. The PCF is homogenized and therefore behaves as a classical circular metallic waveguide. It is worth noting that in case of a periodic arrangement of elliptic dielectric rods, the overall structure then behaves as an anisotropic circular metallic waveguide [105].

B - The Architectural Symmetry (mesoscopic scale).

The symmetry and degeneracy of the modes in resonance with the multirod pattern can be assigned to one of two general symmetry groups C_n and C_{nv} depending upon it presents n-fold rotation symmetry but no reflection symmetry, or n-reflection planes [140]. For a given mode class, it is possible to assign a minimum waveguide sector sufficient to determine the fields of all the modes of that mode class. Thanks to group representation, it can be shown that the minimum sector to consider to take into account all the degenerated modes for the hexagonal structure (C_{6v} waveguide) is 90 degrees, which is far from being obvious. Furthermore, lines for *adequate* boundary conditions must correspond with the reflection planes of the hexagon.

C - The Single Rod Symmetry (microscopic scale).

Rod shapes allow to select modes associated to wavelengths of their order : at a fixed frequency, modes can be found either in circular rods or in square rods as shown on Figure 7.4. Dirichlet boundary conditions induce no modes in the central fiber. This property highly depends upon the symmetries of the rod cross-sections (circle, triangle, square,

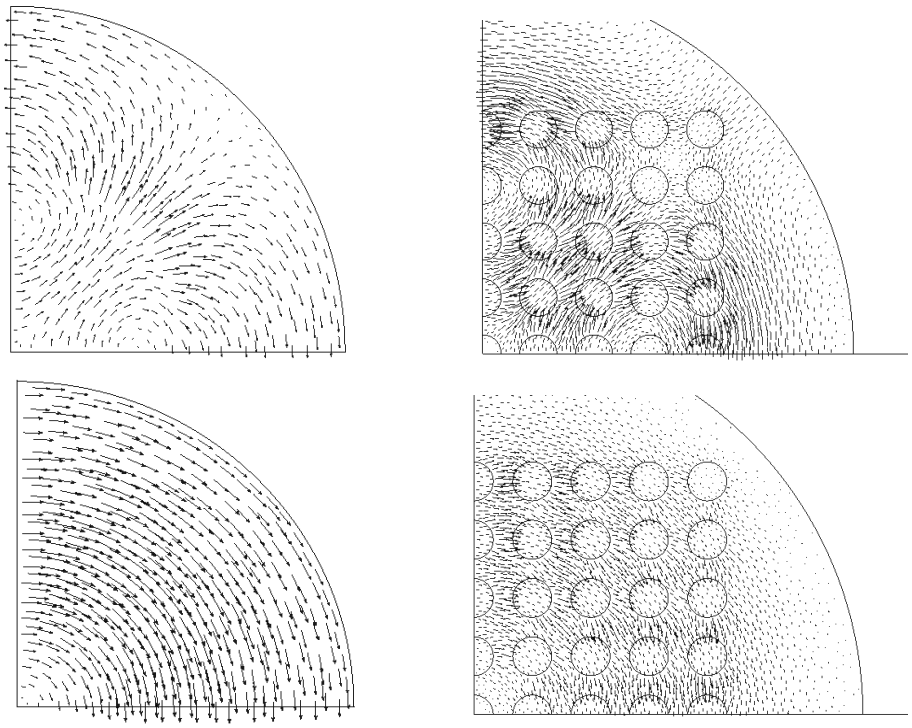

FIGURE 7.3 – Transverse electric field in a PCF with rods of unit radius, for a propagating constant $\gamma = 0.1cm^{-1}$ and a wave number $k = 0.275cm^{-1}$ (wavelength equal to $22.847cm$) compared to the mode $TE_{2,1}$ of an equivalent homogeneous circular metallic waveguide.

hexagon) : for a given frequency, the field can only propagate in rods compatible with its symmetry.

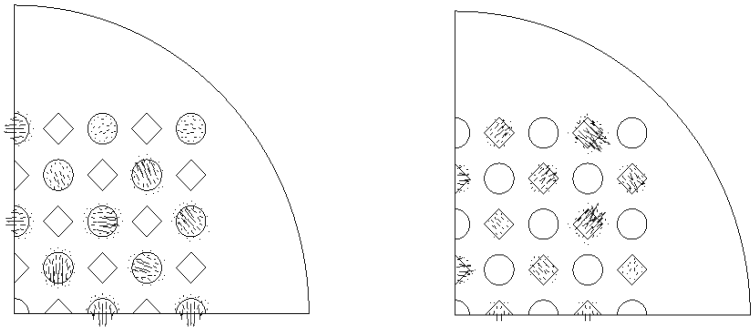

FIGURE 7.4 – For $\gamma = 8cm^{-1}$, the transverse electric field is either confined in square rods ($k = 4.243cm^{-1}$) or in circular rods ($k = 4.159cm^{-1}$).

Propagating modes in photonic crystal waveguides present a wide variety of behaviour due to the various effects involved (metallic waveguide, photonic band gap, localized modes,

Bloch modes, homogenization ...). A particular behaviour does not depend only on the ratio of the wavelength of the mode to the characteristic lengths of the three scales, but it also depends on the symmetries of the various components ([49])(Centeno, 2000)([50])(Centeno, 1999).

7.5 Application to leaky modes in Photonic Crystal Fibers

In this section, we study the second class of PCF which is known as Photonic Bandgap Guidance fibers (PBG) : if the holey region extends far enough from the core, typically containing several hundred holes, there can be significant Bragg reflection of particular wavelengths in the transverse plane $(x-y)$ resulting in a two-dimensional photonic bandgap. The core region forms a localised state that allows wavelengths in the bandgap to propagate along the core of the fiber, but not in the crystal cladding : light can therefore propagate in the air, a property that can never be achieved in classical optical fibers. Because such MOF have a finite cladding, and the silica region between the holes allows some radiations to escape the core region, all the modes propagating in the central low index structural defect (air) are lossy. Some of these modes propagate in or near the core of the fiber for relatively long distances, and it is these guided radiation modes that are of particular interest when studying lossy fibers. There are only a discrete number of such modes, and they can be expressed as a superposition of the radiation modes of the continuous spectrum ([191])(Snyder and Love, 1983). Modes of this type resemble bound modes, except they are attenuated as energy is lost to the cladding. Such modes, called leaky modes, are thus not square integrable in the transverse plane $(x-y)$, and necessitate an *adequate* treatment. In ([205])(White, 2000) a jacket with lossy material is introduced surrounded the MOF, which presents the advantage of allowing estimate of the losses of such modes. This multipole approach is based on properties of Green-functions and leads a search for zeros of a matrix determinant. We choose a discrete approach (finite element modelling) and take a jacket with Dirichlet boundary conditions to keep the self-adjointness of the Maxwell operator (real spectrum). Furthermore, thanks to the boundness of the domain, the operator is of compact resolvent and its spectrum is only made of an infinite number of isolated eigenvalues associated with bound modes. When there is only 6 air-holes in the PCF, surrounding the low structural defect, we do not see guided modes (fig. 7.7). The leaky mode has a large imaginary part and it does not propagate on a long distance. When there 54 holes surrounding the low defect, we catch the leaky mode (fig. 7.9). Some theoretical works show that these kind of modes have an imaginary part depending upon the number of layers surrounding the cavity, in the one-dimensional case ([76])(Figotin and Gountsveig, 1998).

Work is in progress to estimate the loss of these modes thanks to the computation of the magnetic current on the boundary of the jacket. For this, one has to consider a variant of the geometric transformation of section 6.4.6. Considering three disks $D(O,A)$, $D(O,B)$ and $D(O,C)$ of center $O=(0,0)$ with radii $C>B>A$ strictly including the cross section of the waveguide Ω, we define a first corona $\mathcal{C}_1 = D(O,B)\setminus\overline{D(O,A)}$. Let (x,y) be a point in a second corona $\mathcal{C}_2 = D(O,C)\setminus\overline{D(O,A)}$ and (X,Y) be a point in $\mathcal{C}_1$, the transformation

is then given by :

$$\begin{cases} x = f_1(X,Y) = X[CA(B-A)]/[(C-1)R(B-R)+A(B-A)] \\ y = f_2(X,Y) = Y[CA(B-A)]/[(C-1)R(B-R)+A(B-A)] \end{cases}$$

where R denotes the Euclidean norm $\sqrt{X^2+Y^2}$. This transformation may be viewed as a mapping of the first corona $\mathcal{C}_1$ (small one) with the non orthogonal coordinate system (X,Y) to the second corona $\mathcal{C}_2$ (big one) with the cartesian coordinate system (x,y) (when $C \to +\infty$, this is the mapping of section 6.4.6.). Furthermore, one can check that this transformation has the nice property of local conformal mapping in the interface between guide and the corona : the interface boundary conditions need no particular analysis. When the distance between the jacket and the PCF grows to infinity, the bounded operator (of compact resolvent) tends to an unbounded one, and we thus fits the behavior of modes propagating in a low index structural default i.e. leaky modes.

It is worth noting that the Finite Element Method is insensible of inversion of contrast (fig. 7.6), unlike the multipole-methods (due the use of Hankel functions), and that we can deal with every type of geometry (the multipole method has been recently generalized by Yardley, Mc Phedran, Nicorovici and Botten to elliptic cylinders [210]). The drawback of our method remains its time of computation and the memory it requires, compared to the higly rapidly convergent lattice sums. These two methods sound therefore complementary ones and an extension of the thesis could be to compare both approachs in various situations arising in electromagnetics.

Remark :

We think that taking a jacket remains to looking for modes in the complex plane has shown on figure 7.10. To minimize the influence of this spurious device, the jacket can be placed far thanks to a geometric transformation : this transformation allows studying the influence of the distance of the jacket to the PCF on the calculated leaky modes.

Conclusion :

Optical fibers with a micron-scaled periodic arrangement of air holes in a silica background material can be readily fabricated ([121])(Knight *et al.*, 1998). Although silica-air photonic crystals do not exhibit PBGs for wave propagation refined strictly in the periodic plane, we show that this system does allow for complete bangaps (i.e. for any polarization of the light) to appear for waves propagating with a non-zero wave-vector component in the direction perpendicular to the periodic plane. This out-of-plane is exactly the case of interest in optical fibers, where light is intended to be guided along the fiber axis : we enforce that our results differ from those of ([44])(Broenj *et al*,1999) for large conical incidence, since we take into account the finite size of the waveguide. This correction is of the foremost importance, since PBG effects occur only for such incidences in air-silica structures. Because real PCF have a finite crystal cladding (contrary to the assumption of [**?**]), all the propagating modes induced by PBG effects are leaky. It is therefore important that the losses associated with leaky modes be considered when calculating the modal properties of PCF. For this, we embed our PCF in a metallic jacket : all the modes remain therefore bounded (associated with real eigenvalues) and we can take into account the losses of leaky modes via the computation of the current ($\mathbf{J}_S = n \wedge \mathrm{curl}_\gamma \mathbf{E}$) on the metallic cavity. To our

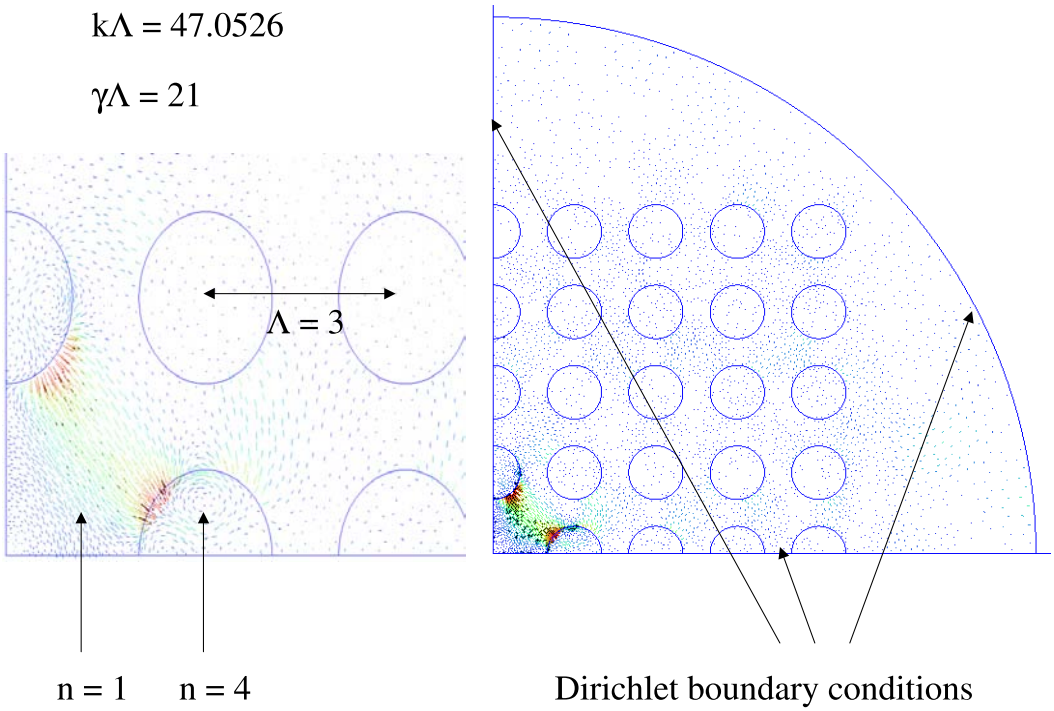

FIGURE 7.5 – Transverse electric field and its associated renormalized wave numbers $k\Lambda = 47.0526$ in a circular LPCF (PCF type 2) with 80 unit radius rods of index 4, a nearest rod spacing $\Lambda = 3$ and a renormalized propagation constant $\gamma\Lambda = 21$.

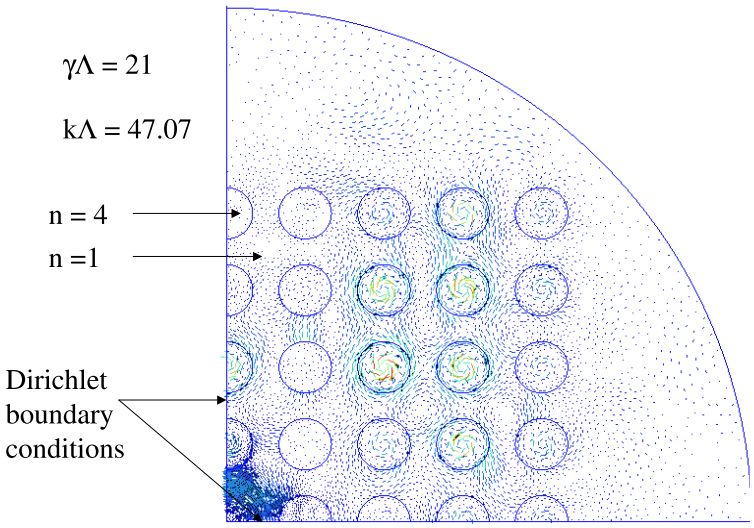

FIGURE 7.6 – Transverse electric field and its associated renormalized wave numbers $k\Lambda = 47.07$ in a circular LPCF (PCF type 2) with 80 unit radius rods of index 4, a nearest rod spacing $\Lambda = 3$ and a renormalized propagation constant $\gamma\Lambda = 21$.

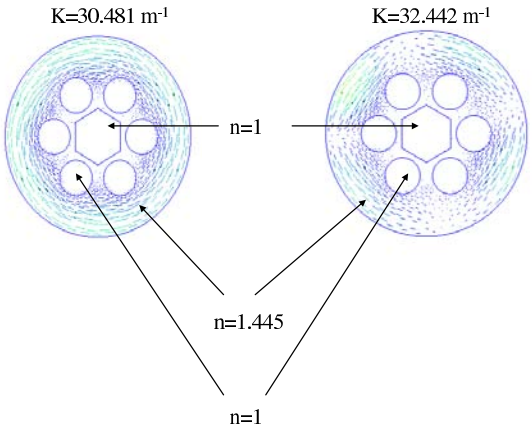

FIGURE 7.7 – Transverse electric field and its associated renormalized wave numbers $k\Lambda = 91.433$ and $k\Lambda = 97.326$ in a circular air-silica LPCF (PCF type 2) with a hexagonal air cavity surrounded by 6 unit radius air holes, a nearest hole spacing $\Lambda = 3$ and a renormalized propagation constant $\gamma\Lambda = 21$.

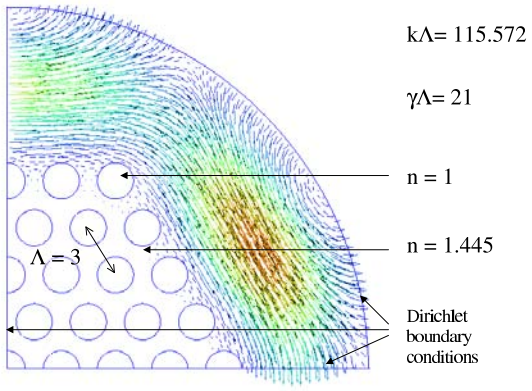

FIGURE 7.8 – Transverse electric field and its associated renormalized wave numbers $k\Lambda = 115.572$ in a circular air-silica LPCF (PCF type 2) with 55 unit radius air holes (no central defect), a nearest hole spacing $\Lambda = 3$ and a renormalized propagation constant $\gamma\Lambda = 21$

knowledge, this has not been done so far in the published literature : the nearest approach is that of ([205])(White, 2000), which involves a lossy jacket combined with a Multipole method. First efforts into the realization of structures with a complete out-of-plane PBG for 2D silica-air photonic crystals were performed using triangular arrangements of air holes, but the requirement of large air hole sizes proved difficult to fulfil experimentally, and fabricated photonic crystal fibers using triangular arrangements of air holes showed no evidence of PBG effects. We have investigated numerically square arrangements, but we have only found leaky modes for PCF with semiconductor rods in air matrix. Our attention was therefore shifted to so-called honeycomb photonic crystals, which have been found to possess larger band gaps than square crystals and to exhibit waveguidance by PBG at realistic parameters ([121])(Knight *et al.*). Work is in progress with Russell's team

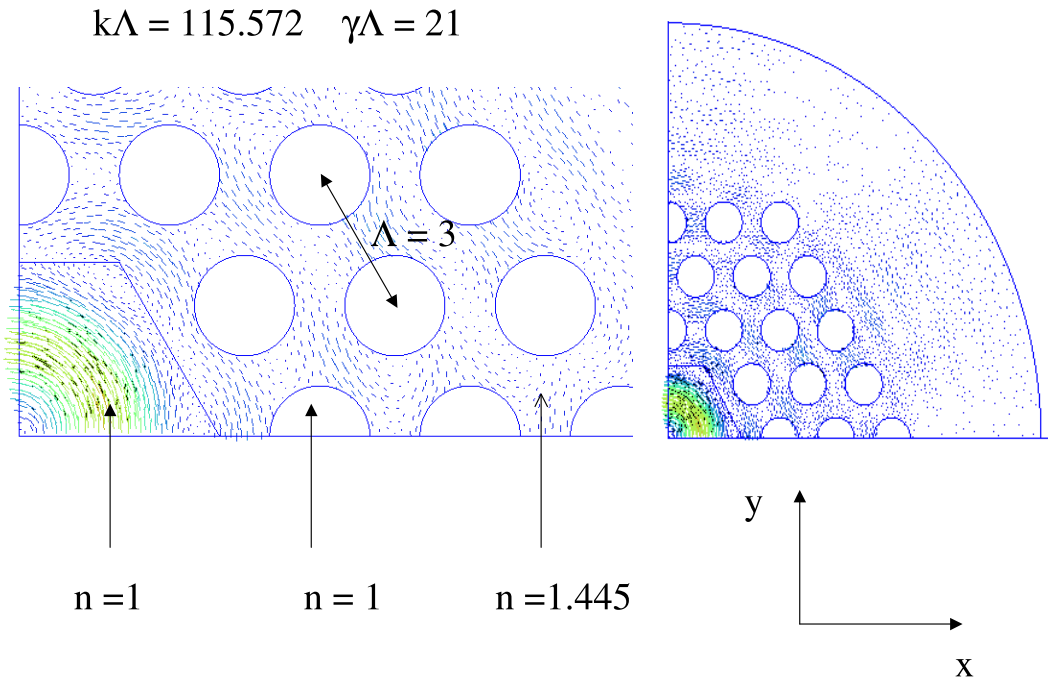

FIGURE 7.9 – Transverse electric field and its associated renormalized wave numbers $k\Lambda = 115.572$ in a circular air-silica LPCF (PCF type 2) with 54 unit radius air holes (one missing air hole), a nearest hole spacing $\Lambda = 3$ and a renormalized propagation constant $\gamma\Lambda = 21$

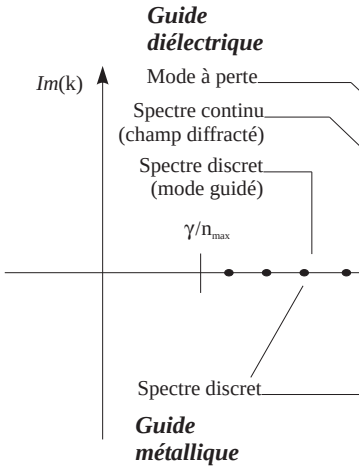

FIGURE 7.10 – In the above figure, we show the link between the spectrum of a dielectric PCF in unbounded domain (discrete and continuous spectrum) and that of the PCF surrounded by a jacket with Dirichlet conditions (only discrete spectrum).

to improve new geometries (both numerically and experimentaly). Although the research in PBG-guiding is still in its infancy, their potential as ultralow-loss transmission fibers, as well as their dispersive properties may pave the way for PBG fibers to become of high

commercial interest in optical communications.

Chapitre 8

Propagating modes in metallo-dielectric waveguides

> "Dave", said Hal, "I don't understand why you're doing this to me... I have the greatest... enthusiasm for the mission... You are destroying my mind... Don't you understand ?... I will become a childish... I will become nothing."
>
> Arthur C. Clarke [46].

8.1 Introduction

In recent years the development of microwave, millimeter and optical devices and systems has promoted interest in more complex waveguide structures. We can divide these structures in two main classes : the first one concerns dielectric guides (open domain, chapter 6) and the second one concerns metallic guides (closed domain, chapter 7). To study the first class, one has to consider the field decrease outside the guide (finite elements coupled to integral formulations, to Fourier series expansions or to geometric transformation). It is worth noting that there is a continuous part in the spectrum of this spectral problem, coming from the unboundness of its operator : one thus has to eliminate the corresponding non propagating modes, thanks to a theoretical criterion ([100], chapter 6). To study the second class, one has to use an electric formulation, since the tangential trace of the magnetic field is an unknown of the problem (chapter 7). Nevertheless, the compacity of the resolvent of the operator ensures that the spectrum is composed of an enumerable set of isolated eigenvalues tending to infinity. For problems including these two classes, we have to take into account both the unboundness of the domain and the metallic inclusions. The numerical scheme developed in the paper is based on a finite element method combining edge elements for the transverse field and nodal elements for the longitudinal field. The use of the so-called Whitney elements eliminates the spurious modes [30]. We choose an electric field formulation (dual to the magnetic one) to get simple boundary conditions because the tangential component of the electric field is null [185], what is not the case of the tangential magnetic field equal to the surface current .

8.2 Set up of the problem

We consider a complex waveguide of constant section Ω composed of a dielectric part Ω_d and a metallic part Ω_m, invariant along the z axis and whose permittivity profile $\varepsilon = \varepsilon_0\varepsilon_r$ (ε_0 and ε_r being the permittivity of vacuum and relative permittivity of the medium) is supposed to be a known function e.g. a piecewise constant function.

We are looking for electromagnetic fields $(\mathcal{E}, \mathcal{H})$ solutions of the following Maxwell equations :

$$\begin{cases} \operatorname{curl} \mathcal{H} = \varepsilon \dfrac{\partial \mathcal{E}}{\partial t} + \mathcal{J}_s \\ \operatorname{curl} \mathcal{E} = -\mu_0 \dfrac{\partial \mathcal{H}}{\partial t} \end{cases} \tag{1}$$

μ_0 being the permeability of the medium, supposed to be non-magnetic and $\mathcal{J}_s$ denoting the surface current density on the boundary of the metallic part Ω_m.

Furthermore, choosing a time dependance in $e^{-i\omega t}$, and taking into account the invariance of the guide along its z axis, we define time-harmonic two-dimensional electric and magnetic fields $\mathbf{E}$ and $\mathbf{H}$ by :

$$\begin{cases} \mathcal{E}(x,y,z,t) = \Re e(\mathbf{E}(x,y)e^{-i(\omega t - \gamma z)}) \\ \mathcal{H}(x,y,z,t) = \Re e(\mathbf{H}(x,y)e^{-i(\omega t - \gamma z)}) \end{cases} \tag{2}$$

where ω is the light pulsation and γ denotes the propagating constant of the guided mode.

We say that $(\mathbf{E}, \mathbf{H})$ is a guided mode if :

$$\begin{cases} (\gamma, \omega) \in \mathbb{R}^2 \\ (\mathbf{E}, \mathbf{H}) \neq (\mathbf{0}, \mathbf{0}) \\ \mathbf{E}, \mathbf{H} \in [L^2(\mathbb{R}^2 \setminus \Omega_m)]^3 \end{cases}$$

with $n \times \mathbf{E} = 0$ and $n \times \mathbf{H} = \mathbf{J}_s$ (surface current density) on the boundary of the conductor Ω_m.

$\mathbf{J}_s$ being unknown, we choose an electric formulation.

8.3 continuous formulation

For $(\mathbf{E}, \mathbf{H})$ satisfying (2), (1) can be written as :

$$\begin{cases} \operatorname{curl}_\gamma \mathbf{H} = -i\omega\varepsilon_0\varepsilon_r(x,y)\mathbf{E} - i\omega\mathbf{J}_s \\ \operatorname{curl}_\gamma \mathbf{E} = i\omega\mu_0\mathbf{H} \end{cases} \tag{3}$$

where ε_r denotes the relative permittivity (bounded and coercive function) and where $d_\gamma \mathbf{V}$ is defined by :

$$d_\gamma \mathbf{V}(x,y) = d\Big(\mathbf{V}(x,y)e^{i\gamma z}\Big)e^{-i\gamma z} \tag{4}$$

where d is either curl or div and $\mathbf{V}$ is either $\mathbf{H}$ or $\mathbf{E}$. Furthermore, from (4) it is clear that $\operatorname{div}_\gamma \operatorname{curl}_\gamma \varphi = 0$, $\forall \varphi \in [\mathcal{D}(\mathbb{R}^2)]^3$, that is for smooth vector valued functions φ. Thus, denoting by k_0 the wave number $\omega\sqrt{\mu_0\varepsilon_0}$, we are led to the following system of Maxwell's type :

$$\begin{cases} \operatorname{curl}_\gamma \operatorname{curl}_\gamma \mathbf{E} = k_0^2 \varepsilon_r \mathbf{E} \\ \operatorname{div}_\gamma(\varepsilon_0\varepsilon_r\mathbf{E}) = 0 \end{cases} \tag{5}$$

The solution of the above problem is then given by the minimum of the following functional in the weighted Hilbert space $[H(\mathbb{R}^2 \setminus \Omega_m, d\mathcal{L})]^3$ where $d\mathcal{L}$ is the Lebesgue measure $\varepsilon_r dxdy$:

$$\mathcal{R}(\gamma; \mathbf{E}, \mathbf{E}') = \int_{\mathbb{R}^2 \setminus \Omega_m} \mathrm{curl}_\gamma \, \mathbf{E} \cdot \overline{\mathrm{curl}_\gamma \, \mathbf{E}'} \, d\mathcal{L}$$
$$+ \int_{\mathbb{R}^2 \setminus \Omega_m} \mathrm{div}_\gamma \, \mathbf{E} \, \overline{\mathrm{div}_\gamma \, \mathbf{E}'} \, d\mathcal{L} - \mu_0 \omega^2 \int_{\mathbb{R}^2 \setminus \Omega_m} \mathbf{E} \cdot \overline{\mathbf{E}'} \, d\mathcal{L} \quad (6)$$

This problem of minimization admits a unique solution thanks to the penalty term

$$\int_{\mathbb{R}^2 \setminus \Omega_m} \mathrm{div}_\gamma \, \mathbf{E} \, \overline{\mathrm{div}_\gamma \, \mathbf{E}'} \, d\mathcal{L}$$

which acts in fact as a constraint which forces the nullity of $\mathrm{div}_\gamma(\varepsilon_r \mathbf{E})$ in the exterior of Ω_m.

8.4 Discrete formulation

We achieve numerical computations with the help of finite elements. For the reasons mentioned above, we choose the electric field as the variable. It involves both a transverse field in the section of the guide and a longitudinal field along its axis. The section of the guide is meshed with triangles and Whitney finite elements are used i.e. edge elements for the transverse field and nodal elements for the longitudinal field.

$$\mathbf{E} = \begin{cases} \mathbf{E}_t = \sum_j^n \alpha_j \mathbf{w_i^e}(x,y) e^{i\gamma z} & \text{, in } \mathbb{R}^2 \\ E_z = \sum_j^n \beta_j w_i^n(x,y) e^{i\gamma z} & \text{, in } \mathbb{R} \end{cases}$$

where α_j denotes the line integral of the transverse component $\mathbf{E}_t$ on the edges, and β_j denotes the line integral of the longitudinal component E_z along one unit of length of the axis of the guide (what is equivalent to the nodal value). Besides, $\mathbf{w_i^e}$ and w_i^n are respectively the basis functions of Whitney 1-forms and Whitney 0-forms.

We develop curl_γ and div_γ in their transverse and longitudinal components :

$$\begin{aligned} \mathrm{div}_\gamma \, \mathbf{E} &= \mathrm{div}_t \, \mathbf{E}_t + i \, \gamma E_z \\ \mathrm{curl}_\gamma \, \mathbf{E} &= \mathrm{curl}_t \, \mathbf{E}_t \, \mathbf{e_z} + (\bigtriangledown_t E_z - i \, \gamma \mathbf{E}_t) \times \mathbf{e_z} \end{aligned}$$

Similarly to the case of cavities [30], we know that we only have to minimize the following functional :

$$\mathcal{R}(\gamma; \mathbf{E}, \mathbf{E}') = \int_{\mathbb{R}^2 \setminus \Omega_m} \Big(\mathrm{curl}_t \, \mathbf{E}_t \cdot \mathrm{curl}_t \, \overline{\mathbf{E}'_t} - i \, \gamma \mathbf{E}_t \cdot \bigtriangledown_t \overline{E'_z}$$
$$+ i \, \gamma \bigtriangledown_t E_z \cdot \overline{\mathbf{E}'_t} + \gamma^2 \, \mathbf{E}_t \cdot \overline{\mathbf{E}'_t} \Big) \, d\mathcal{L}$$
$$- \mu_0 \omega^2 \int_{\mathbb{R}^2 \setminus \Omega_m} \Big(\mathbf{E}_t \cdot \overline{\mathbf{E}'_t} + E_z \, \overline{E'_z} \Big) \, d\mathcal{L} \quad (7)$$

To show this property, one has to take

$$\mathbf{E}' = \bigtriangledown_\gamma \varphi = \bigtriangledown_t \varphi + i\gamma\varphi \mathbf{e_z}$$

in (7), where φ is a Whitney 0-form (this is allowed since $\bigtriangledown_\gamma \varphi$ is a Whithey 1-form). The very properties of the Whitney complex ensures that $\mathrm{curl}_\gamma \bigtriangledown_\gamma \varphi$ is null and it follows from (7) that for all $\omega \neq 0$:

$$\int_{\mathbb{R}^2 \setminus \Omega_m} \mathbf{E} \cdot \overline{\bigtriangledown_\gamma \varphi}\, d\mathcal{L} = 0 \,,$$

which is a weak form of $\mathrm{div}_\gamma(\varepsilon_r \mathbf{E}) = 0$.

Finally, to deal with the open problem, the judicious choice of coordinate transformation of section 6.4.5 allows the finite element modelling of the infinite exterior domain : using discretizations based on differential forms allows a straightforward formulation of the transformation method thanks to pull-back properties [166][165] (it can also be seen as a conformal mapping [133]). It is to be noticed that the generalized eigenvalue problem is solved thanks to the Lanczos algorithm. The GetDP software [64] has been used to set up the finite element problem.

8.5 Application to a grooved metallic guide

We apply our model to a circular metallic waveguide with grooved dielectric inclusion (Fig. 8.1). This example combines all the theoretical difficulties presented in the previous sections. Figure 8.1 shows the real part of the transverse electric field for a propagating mode. Note that without the presence of the dielectric, there is no propagating mode (only leaky modes corresponding to complex eigenvalues could be present).

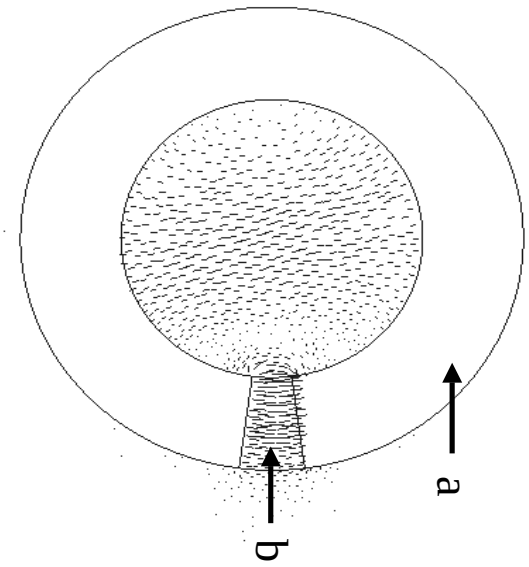

FIGURE 8.1 – Real part of the transverse electric field in a grooved metallic guide where a is the conductor and b the dielectric ($\varepsilon_r = 1.25$).

8.6 Perspectives

We are currently extending the method to twisted grooved metallic waveguides (article in preparation, [103]). Work is in progress to study the analogous of cross-talk phenomena for microstrips i.e. coupling between metallic rectangular waveguides lying on a dielectic substrate. We also want to study the influence of a plane interface on the behavior of propagating modes in an optical waveguide, whose z-axis is parallel to the interface. Although classical, this study leads to interesting applications e.g. for photonic crystal modeling : if we consider the simpler case of a plane interface separating two media, one of them containing an optical fiber. it is well known that the distance between the guide and the interface is closely related to the appearance of the cut-off frequencies [28]. In the case of two wave guides in the vicinity of a plane interface, it both induces coupling between the optical fibers and pertubations due to the proximity of the interface. The adopted configuration (two wave guides in the upper medium, or each one in a different medium) will certainly deeply transform the dispersion curves. Finally, a special attention should be paid to the case of an arrangement of many waveguides intersecting with the interface. The numerical computations could be achieved with the help of our Finite Element Formulation.

Troisième partie

Analyse asymptotique des cavités en cristal photonique.

Chapitre 9

Homogenization of dielectric PCF with metallic boundary

"Nous avons déjà vu que beaucoup d'affections considérées comme des qualités résidant dans les sujets externes n'ont en réalité d'existence qu'en nous-mêmes et ne sont en dehors de nous que des noms ; j'incline beaucoup à croire que la chaleur est du même genre et que cette matière qui produit en nous le chaud et nous le fait sentir, et que nous désignons du terme général de feu, se compose d'une multitude de corpuscules très petits ayant telle ou telle forme, telle ou telle vitesse ; rencontrant notre corps, ils le pénètrent grâce à leur extrême subtilité, et leur contact, qui affecte notre substance à leur passage, est la sensation que nous appelons le chaud ; affection agréable ou désagréable selon le nombre et la vitesse plus ou moins grande de ces particules qui piquent et pénètrent."

Galilée *in* "L'Éssayeur" (1623) [83]

9.1 Multiscale expansion of E_η.

In this chapter, we are looking for out-of-plane propagating modes (conical incidence) in a metallic waveguide of constant cross section Ω_f (open bounded subset of $\mathbb{R}^2$) filled a periodic assembly of dielectric rods for the large wavelengths. The problem is index by two positive real parameters : the small parameter η characterizing the distance between inclusions (tending to zero), and the fixed propagating constant γ. Since the tangential trace $n \wedge \mathbf{H}_\eta$ of the magnetic field $\mathbf{H}_\eta$ on the boundary $\partial\Omega_f$ is an unknown of the spectral problem, we choose an electric field formulation : we are therefore looking for $(\gamma, k_\eta^2, E_\eta) \in \mathbb{R}^+ \times \mathbb{R}^+ \times [H^1(\mathrm{curl}, \Omega_f, \varepsilon_\eta dx)]^3$, $\mathbf{E}_\eta \not\equiv 0$, such that

$$\mathcal{P}_\eta^{\mathbf{E}} \begin{cases} \dfrac{1}{\varepsilon_\eta(\mathbf{x})} \mathrm{curl}_\gamma \, \mathrm{curl}_\gamma \, \mathbf{E}_\eta(\mathbf{x}) = k_\eta^2 E_\eta(\mathbf{x}) & \text{in } \Omega_f \\ n \wedge \mathbf{E}_\eta = 0 & \text{on } \partial\Omega_f \end{cases}$$

where ε_η is a real coercive and bounded function. In second part, we have seen that the operator associated to this problem has a compact resolvent. Its spectrum is a discrete set

of isolated eigenvalues belonging to $[\frac{\gamma^2}{\varepsilon_r};+\infty[$.

As it was previously said, the main idea of homogenization is to select two scales in the study : a microscopic one (the size of the basic cell $Y=]0;1[^2$) and a mesoscopic one (the size of the whole obstacle of shape Ω_f). From a physical point of view, one can say that the modulus of the propagating field is forced to oscillate like the permittivity in the photonic crystal fiber. In fact, the smaller the diameter η of the rods, the faster the modulus of the field $\mathbf{E}_\eta$ oscillates. Hence, we suppose that $\mathbf{E}_\eta$, solution of the problem $\mathcal{P}_\eta^{\mathbf{E}}$ has a two-scale expansion of the form :

$$\forall \mathbf{x}\in\Omega_f,\quad \mathbf{E}_\eta(\mathbf{x})=\mathbf{E}_0(\mathbf{x},\frac{\mathbf{x}}{\eta})+\eta\mathbf{E}_1(\mathbf{x},\frac{\mathbf{x}}{\eta})+\eta^2\mathbf{E}_2(\mathbf{x},\frac{\mathbf{x}}{\eta})+...$$

where $\mathbf{E}_i:\Omega_f\times Y\longmapsto\mathbb{C}^3$ is a smooth function of 4 variables, independant of η, such that $\forall\mathbf{x}\in\Omega_f$, $\mathbf{E}_i(\mathbf{x},\cdot)$ is Y-periodic.

Our goal is to characterize the propagating modes when η tends to 0. If the coefficients $\mathbf{E}_i$ do not increase "too much" when η tends to 0, the limit of $\mathbf{E}_\eta$ will be $\mathbf{E}_0$, the rougher approximation of $\mathbf{E}_\eta$. Hence, we make the assumption that for all $\mathbf{x}\in\mathbb{R}^3$, $\mathbf{E}_i(\mathbf{x},\frac{\mathbf{x}}{\eta})=o(\frac{\mathbf{x}}{\eta^i})$, so that the expansion (also denoted by the german word "ansatz") still makes sense in neighbourhood of 0. If the above expansion is relevant, we can state the following fundamental result :

Theorem 1 *When η tends to zero, $\mathbf{E}_\eta$ solution of the problem $(\mathcal{P}_\eta^{\mathbf{E}})$, converges (for the norm of energy on Ω_f) to the unique solution $\mathbf{E}_{hom}$ of the spectral problem $(\mathcal{P}_{hom}^{\mathbf{E}})$ defined as follows : look for $(\gamma,k_{hom}^2,\mathbf{E}_{hom})\in\mathbb{R}^+\times\mathbb{R}^+\times[H^1(\mathrm{curl},\Omega,\varepsilon_{hom}dx)]^3$, $\mathbf{E}_{hom}\not\equiv 0$, such that*

$$\mathcal{P}_{hom}^{\mathbf{E}}\begin{cases}\dfrac{1}{\varepsilon_{hom}(\mathbf{x})}\mathrm{curl}_\gamma(\mathrm{curl}_\gamma\,\mathbf{E}_{hom}(\mathbf{x}))=k_{hom}^2\mathbf{E}_{hom}(\mathbf{x}) & \text{in } \Omega\\ n\wedge\mathbf{E}_{hom}=0 & \text{on } \partial\Omega\end{cases}$$

With

$$\begin{cases}\varepsilon_{hom}(\mathbf{x})=<\tilde{\varepsilon}(\mathbf{x},\mathbf{y})(I-\nabla_{\mathbf{y}}\mathbf{V}_Y(\mathbf{y}))>_Y & ,\text{in } \Omega_f\\ \varepsilon_{hom}(\mathbf{x})=1 & ,\text{in } \Omega_f^c\end{cases}$$

Where $<f>_Y$ and $\tilde{\varepsilon}(\mathbf{x},\mathbf{y})$ respectively denote the average of f in Y (i.e. $\int_Y f(x,y)\,dy$) and

$$\tilde{\varepsilon}(\mathbf{x},\mathbf{y})=\begin{cases}1 & ,\ \text{if } \mathbf{x}\in\Omega_f^c\\ \varepsilon_r^B(\mathbf{y}) & ,\ \text{if } \mathbf{x}\in\Omega_f\end{cases}$$

Besides, $\mathbf{V}_Y=(V_1,V_2)$, where V_j , $j\in\{1,2\}$ is the unique solution in $H^1_\sharp(Y)/\mathbb{R}$ (that is to say that V_j is defined up to an additive constant in the Hilbert space of Y-periodic functions $H^1_\sharp(Y)$) of one of the two following scalar problems $(\mathcal{K}_j)$ of electrostatic type :

$$(\mathcal{K}_j):-\mathrm{div}_{t,\mathbf{y}}\left[\varepsilon_r^B(\mathbf{y})(\nabla_{t,\mathbf{y}}(V_j(\mathbf{y})-y_j))\right]=0\ ,j\in\{1,2\}$$

Roughly speaking, as η tends to zero, we can replace the isotropic heterogeneous waveguide of shape Ω_f, by an anisotropic homogeneous waveguide of shape Ω_f. In other terms, the effective permittivity is given by the following result :

Theorem 2 *The relative permittivity matrix of the homogenized problem is equal to :*

$$\varepsilon_{hom} = \begin{pmatrix} < \varepsilon(y) >_Y & 0 & 0 \\ 0 & < \varepsilon(y) >_Y & 0 \\ 0 & 0 & < \varepsilon(y) >_Y \end{pmatrix} - \begin{pmatrix} \varphi_{11} & \varphi_{12} & 0 \\ \varphi_{21} & \varphi_{22} & 0 \\ 0 & 0 & 0 \end{pmatrix}$$

where φ_{ij} represent corrective terms defined by :
$\forall i,j \in \{1,2\},\ \varphi_{ij} =< \varepsilon \frac{\partial V_j}{\partial y_i} >_Y =< \varepsilon \frac{\partial V_i}{\partial y_j} >_Y = - < \varepsilon \bigtriangledown_\gamma V_i \cdot \bigtriangledown_\gamma V_j >_Y$
the brackets denoting averaging over Y, and V_j being the unique solutions in $H^1_\sharp(Y)/I\!R$ of the two partial differential equations $\mathcal{K}_j$. Hence, thanks to the symmetry of the right matrix above ($\varphi_{ij} = \varphi_{ji}$), the homogenized permittivity is given by the knowledge of four termes φ_{ij}, depending upon the resolution of two annex problems $\mathcal{K}_j$.

Proof of theorem 2

As for the homogenized permittivity, $\bigtriangledown_y \mathbf{V}_Y$ denoting the Jacobian matrix $\frac{\partial V_j}{\partial y_i}$ of $\mathbf{V}_Y$, ε_{hom} clearly derives from the equation of the theorem.

Multiplying $\mathrm{div}_y(\varepsilon \bigtriangledown_y (V_i - y_i))$ by V_j, $j \in \{1,2\}$, and integrating by parts over the basic cell Y leads to :
$\left\langle \varepsilon(y)(\bigtriangledown_y(V_i - y_i)) \cdot V_j \right\rangle_Y = 0$. Therefore, we get the equality :

$$\begin{aligned} \varphi_{ij} &= < \varepsilon \frac{\partial V_i}{\partial y_j} >_Y \\ &= - < \varepsilon \bigtriangledown V_i \cdot \bigtriangledown V_j >_Y \\ &= < \varepsilon \frac{\partial V_j}{\partial y_i} >_Y \quad \text{,} i \text{ and } j \text{ playing a symmetrical role} \end{aligned}$$

Hence, we derive that $\varphi_{ij} = \varphi_{ji}$.

Proof of theorem 1 :

For η fixed, $\mathbf{E}_\eta$ is the unique solution of the above problem (the reader may refer to [51] for existence and uniqueness theorems). Let us now assume that $\mathbf{E}_\eta$ satisfies the following two-scale expansion :

$$\mathbf{E}_\eta = \mathbf{E}_0(\mathbf{x}, \frac{\mathbf{x}}{\eta}) + \eta \mathbf{E}_1(\mathbf{x}, \frac{\mathbf{x}}{\eta}) + \eta^2 \mathbf{E}_2(\mathbf{x}, \frac{\mathbf{x}}{\eta}) + ... + \eta^N \mathbf{E}_\eta(\mathbf{x}, \frac{\mathbf{x}}{\eta}) + o(\eta^N) \quad \text{(E1)}$$

where $\mathbf{E}_i : \Omega_f \times I\!R^2 \longmapsto \mathbb{C}^3$ are smooth complex valued functions of the variables $(\mathbf{x}, \mathbf{y})$, independent of η, periodic in $\mathbf{y}$ of period 1. The introduction of the variable $\mathbf{y} = \frac{\mathbf{x}}{\eta}$ takes into account the periodic dependance on $\mathbf{x}$ of the permittivity ε_η in the "bounded periodic" structure.

Before going further, let us define the notations that will be used in this chapter. We first develop $\mathbf{E}(x_1, x_2)$ in its transverse and longitudinal components $\mathbf{E}_t(x_1, x_2)$ and $E_l(x_1, x_2)$:

$$\mathbf{E}(x_1, x_2) = E_{t,1}(x_1, x_2)\mathbf{e}_1 + E_{t,2}(x_1, x_2)\mathbf{e}_2 + E_l(x_1, x_2)\mathbf{e}_3 = \mathbf{E}_t(x_1, x_2) + E_l(x_1, x_2)\mathbf{e}_3$$

We define its transverse gradient, divergence and curl as

$$\begin{aligned}
\bigtriangledown_t E_l(x_1, x_2) &= \frac{\partial E_l}{\partial x_1}\mathbf{e}_1 + \frac{\partial E_l}{\partial x_2}\mathbf{e}_2 \\
\mathrm{div}_t(E_{t,1}\mathbf{e}_1 + E_{t,2}\mathbf{e}_2) &= \frac{\partial E_{t,1}}{\partial x_1} + \frac{\partial E_{t,2}}{\partial x_2} \\
\mathrm{curl}_t(E_{t,1}\mathbf{e}_1 + E_{t,2}\mathbf{e}_2) &= \frac{\partial E_{t,2}}{\partial x_1} - \frac{\partial E_{t,1}}{\partial x_2}
\end{aligned}$$

We define curl_γ and div_γ as follows :

$$\begin{aligned}
\mathrm{div}_\gamma \mathbf{E} &= \frac{\partial E_{t,1}}{\partial x_1} + \frac{\partial E_{t,2}}{\partial x_2} + i\,\gamma H_l = \mathrm{div}_t\, E_t + i\,\gamma E_l \\
\mathrm{curl}_\gamma \mathbf{E} &= \Big(\frac{\partial E_l}{\partial x_2} - i\,\gamma E_{t,2}\Big)\mathbf{e}_1 + \Big(i\,\gamma H_{t,1} - \frac{\partial E_l}{\partial x_1}\Big)\mathbf{e}_2 + \Big(\frac{\partial E_{t,2}}{\partial x_2} - \frac{\partial E_{t,1}}{\partial y}\Big)\mathbf{e}_3 \\
&= \mathrm{curl}_t\, E_t\ \mathbf{e}_3 + (\bigtriangledown_t E_l - i\,\gamma E_t) \times \mathbf{e}_3
\end{aligned}$$

Furthermore, we will denote by curl_0 and div_0 the previous operators for $\gamma = 0$ i.e.

$$\begin{aligned}
\mathrm{div}_0 \mathbf{E} &= \mathrm{div}_t\, E_t \\
\mathrm{curl}_0 \mathbf{E} &= \mathrm{curl}_t\, E_t\ \mathbf{e}_3 + \bigtriangledown_t E_l \times \mathbf{e}_3
\end{aligned}$$

Assuming that the above expansion is relevant, we can state the following lemma :

Lemma 1 *The Maxwell operator $A_\eta^\gamma = \varepsilon_\eta^{-1}\,\mathrm{curl}_\gamma\,\mathrm{curl}_\gamma$ associated to the problem $\mathcal{P}_\eta$ satisfies the following operator expansion $A_\eta^\gamma = \eta^{-2}A_{\mathbf{yy}}^0 + \eta^{-1}(A_{\mathbf{xy}}^{\gamma,0} + A_{\mathbf{yx}}^{0,\gamma}) + \eta^0 A_{\mathbf{xx}}^\gamma + o(1)$,*

where the asymptotic terms of A_η are solutions of

$$\mathcal{S}_0 = \left\{ \begin{array}{lll}
\eta^{-2} & & A_{\mathbf{yy}}^0\mathbf{E}_0 = 0 \quad (1) \\
\eta^{-1} & : & A_{\mathbf{yy}}^\gamma\mathbf{E}_1 + A_{\mathbf{xy}}^{\gamma,0}\mathbf{E}_0 + A_{\mathbf{yx}}^{0,\gamma}\mathbf{E}_0 = 0 \quad (2) \\
\eta^0 & : A_{\mathbf{yy}}^0\mathbf{E}_2 + A_{\mathbf{xy}}^{\gamma,0}\mathbf{E}_1 + A_{\mathbf{yx}}^{0,\gamma}\mathbf{E}_1 + A_{\mathbf{xx}}^\gamma\mathbf{E}_0 - \tilde{\varepsilon}k_0^2\mathbf{E}_0 = 0 \quad (3)
\end{array} \right.$$

where $A_{x,x}^\gamma$ denotes the operator $\mathrm{curl}_{\gamma,x}\,\mathrm{curl}_{\gamma,x}$, $A_{y,y}^0$ denotes $\mathrm{curl}_{0,y}\,\mathrm{curl}_{0,y}$, $A_{x,y}^{\gamma,0}$ denotes $\mathrm{curl}_{\gamma,x}\,\mathrm{curl}_{0,y}$ and $A_{y,x}^{0,\gamma}$ denotes $\mathrm{curl}_{0,y}\,\mathrm{curl}_{\gamma,x}$

Proof :

For convenience in the following calculations, we denote by P_η the operator of restriction onto the overplane $\{\mathbf{y} = \frac{\mathbf{x}}{\eta}\}$:

$$P_\eta : f(\mathbf{x}, \mathbf{y}) \longmapsto f(\mathbf{x}, \frac{\mathbf{x}}{\eta})$$

where $f(\mathbf{x}, \mathbf{y})$ and $f(\mathbf{x}, \frac{\mathbf{x}}{\eta})$ are respectively locally square integrable functions of $\Omega_f \times \mathbb{R}^2 \to \mathbb{C}^3$ and $\Omega_f \to \mathbb{C}^3$ of finite energy.

Let us sum up the properties of P_η in the following proposition :

proposition 1 *P_η is a "distributive operator", that is to say that $P_\eta(f)\ P_\eta(g) = P_\eta(fg)$.*

Furthermore, we can define the action of the differential operator on the projector P_η by :

$$\frac{\partial}{\partial \mathbf{x}_i}(P_\eta f(\mathbf{x},\mathbf{y})) = P_\eta(\frac{\partial}{\partial \mathbf{x}_i} f(\mathbf{x},\mathbf{y})) + \frac{1}{\eta} P_\eta(\frac{\partial}{\partial \mathbf{y}_i} f(\mathbf{x},\mathbf{y}))$$

that is to say that $[\frac{\partial}{\partial \mathbf{x}_i}, P_\eta] = \frac{1}{\eta} P_\eta \frac{\partial}{\partial \mathbf{y}_i}$.

With the help of the operator P_η, $(E1)$ can be rewritten in the form :

$$\begin{aligned} \mathbf{E}_\eta(\mathbf{x}) &= P_\eta \mathbf{E}_0(\mathbf{x},\mathbf{y}) + \eta P_\eta \mathbf{E}_1(\mathbf{x},\mathbf{y}) + ... + \eta^N P_\eta \mathbf{E}_N(\mathbf{x},\mathbf{y}) + o(\eta^N) \\ &= P_\eta\{\sum_{j=0}^{N} \eta^j\ \mathbf{E}_j(\mathbf{x},\mathbf{y})\} + o(\eta^N) \quad \text{(E2)} \end{aligned}$$

Thus, the partial differential operator $\dfrac{\partial}{\partial \mathbf{x}_i}$ acting on $\mathbf{E}_\eta(\mathbf{x})$ satisfies the following equality :

$$\begin{aligned} \frac{\partial}{\partial \mathbf{x}_i}\mathbf{E}_\eta(\mathbf{x}) &= \frac{\partial}{\partial \mathbf{x}_i} P_\eta\{\sum_{j=0}^{N} \eta^j\ \mathbf{E}_j(\mathbf{x},\mathbf{y})\} + o(\eta^N) \\ &= (P_\eta \frac{\partial}{\partial \mathbf{x}_i} + \frac{1}{\eta} P_\eta \frac{\partial}{\partial \mathbf{y}_i})\{\sum_{j=0}^{N} \eta^j\ \mathbf{E}_j(\mathbf{x},\mathbf{y})\} + o(\eta^{N-1}) \end{aligned}$$

We now want to deduce the action of the second order differential operator $\mathrm{curl}_\gamma(\varepsilon_\eta^{-1}\,\mathrm{curl}_\gamma)$ involved in the problem $\mathcal{P}_\eta^{\mathbf{E}}$, on the field $\mathbf{E}_\eta$. Taking into account that $[\mathrm{curl}_{\gamma,\mathbf{x}}, P_\eta] = \dfrac{1}{\eta} P_\eta\,\mathrm{curl}_{0,\mathbf{y}}$, we obtain that :

$$\mathrm{curl}_{\gamma,\mathbf{x}}\Big(P_\eta(\mathrm{curl}_{\gamma,\mathbf{x}}\, P_\eta \mathbf{E}_j)\Big) = \mathrm{curl}_{\mathbf{x}}\Big(P_\eta(P_\eta\,\mathrm{curl}_{\gamma,\mathbf{x}}\,\mathbf{E}_j + \frac{1}{\eta} P_\eta\,\mathrm{curl}_{0,\mathbf{y}}\,\mathbf{E}_j)\Big)$$

We then use the distributivity of P_η to get :

$$\mathrm{curl}_{\gamma,\mathbf{x}}\Big(P_\eta(\mathrm{curl}_{\gamma,\mathbf{x}}\, P_\eta \mathbf{E}_j)\Big) = \mathrm{curl}_{\gamma,\mathbf{x}}\, P_\eta(\mathrm{curl}_{\gamma,\mathbf{x}}\,\mathbf{E}_j) + \frac{1}{\eta}\,\mathrm{curl}_{\gamma,\mathbf{x}}\, P_\eta(\mathrm{curl}_{0,\mathbf{y}}\,\mathbf{E}_j)$$

We iterate the process, by taking into account once more that $\mathrm{curl}_{\gamma,\mathbf{x}}$ and P_η do not commute :

$$\begin{aligned} \mathrm{curl}_{\gamma,\mathbf{x}}\Big(P_\eta(\mathrm{curl}_{\gamma,\mathbf{x}}\, P_\eta \mathbf{E}_j)\Big) &= P_\eta\Big[\mathrm{curl}_{\gamma,\mathbf{x}}(\mathrm{curl}_{\gamma,\mathbf{x}}\,\mathbf{E}_j) + \frac{1}{\eta}\,\mathrm{curl}_{0,\mathbf{y}}(\mathrm{curl}_{\gamma,\mathbf{x}}\,\mathbf{E}_j\Big] \\ &+ \frac{1}{\eta} P_\eta\Big[\mathrm{curl}_{\gamma,\mathbf{x}}(\mathrm{curl}_{0,\mathbf{y}}\,\mathbf{E}_j) + \frac{1}{\eta}\,\mathrm{curl}_{0,\mathbf{y}}(\mathrm{curl}_{0,\mathbf{y}}\,\mathbf{E}_j)\Big] \end{aligned}$$

We then apply this two-scale second order operator in the expansion of the magnetic field $\mathbf{E}_\eta$. Assuming that the terms of the development of the powers higher than 2 are bounded, we can write :

$$\begin{aligned}&\operatorname{curl}_{\gamma,\mathbf{x}}\Big(\operatorname{curl}_{\gamma,\mathbf{x}}(\mathbf{E}_0+\eta\mathbf{E}_1)\Big)+\tfrac{1}{\eta}\operatorname{curl}_{\gamma,\mathbf{x}}\Big(\operatorname{curl}_{0,\mathbf{y}}(\mathbf{E}_0+\eta\mathbf{E}_1)\Big)\\&+\tfrac{1}{\eta}\Big(\operatorname{curl}_{0,\mathbf{y}}\operatorname{curl}_{\gamma,\mathbf{x}}(\mathbf{E}_0+\eta\mathbf{E}_1)\Big)+\tfrac{1}{\eta^2}\operatorname{curl}_{0,\mathbf{y}}\Big(\operatorname{curl}_{0,\mathbf{y}}(\mathbf{E}_0\\&+\eta\mathbf{E}_1+\eta^2\mathbf{E}_2)\Big)-\tilde{\varepsilon}k_0^2(\mathbf{E}_0+\eta\mathbf{E}_1)+O(\eta)=0\end{aligned}$$

In a neighborhood of $\eta=0$, we express the vanishing of the coefficients of successive powers of $\frac{1}{\eta}$. Thus, we have to consider the following system :

$$\mathcal{S}_0=\begin{cases}\eta^{-2} & A^0_{\mathbf{yy}}\mathbf{E}_0 = 0 \quad (1)\\ \eta^{-1} : & A^\gamma_{\mathbf{yy}}\mathbf{E}_1+A^{\gamma,0}_{\mathbf{xy}}\mathbf{E}_0+A^{0,\gamma}_{\mathbf{yx}}\mathbf{E}_0 = 0 \quad (2)\\ \eta^{0} : & A^0_{\mathbf{yy}}\mathbf{E}_2+A^{\gamma,0}_{\mathbf{xy}}\mathbf{E}_1+A^{0,\gamma}_{\mathbf{yx}}\mathbf{E}_1+A^{\gamma}_{\mathbf{xx}}\mathbf{E}_0-\tilde{\varepsilon}k_0^2\mathbf{E}_0 = 0 \quad (3)\end{cases}$$

where $A^\gamma_{x,x}$ denotes the operator $\operatorname{curl}_{\gamma,x}\operatorname{curl}_{\gamma,x}$, $A^0_{y,y}$ denotes $\operatorname{curl}_{0,y}\operatorname{curl}_{0,y}$, $A^{\gamma,0}_{x,y}$ denotes $\operatorname{curl}_{\gamma,x}\operatorname{curl}_{0,y}$ and $A^{0,\gamma}_{y,x}$ denotes $\operatorname{curl}_{0,y}\operatorname{curl}_{\gamma,x}$.

Let us consider the first equality of the previous system $\mathcal{S}_0$:

$$\operatorname{curl}_{0,y}\Big(\operatorname{curl}_{0,y}\mathbf{E}_0\Big)=0 \tag{1}$$

We first want to show the link between E_{hom} and E_0.

Lemma 4 *Let $\mathbf{E}_0$ be a Y periodic function in $\mathbf{y}$, solution of the equation (1) of the system $\mathcal{S}_0$. Then*

$$\textit{For almost every } \mathbf{y} \ \textit{ in } Y,\ \ \operatorname{curl}_{0,\mathbf{y}}\mathbf{E}_0(\mathbf{x},\mathbf{y})=0 \tag{4}$$

Proof :

Multiplying equation (1) in $\mathcal{S}_0$ by the conjugate $\mathbf{E}_0^*$ of $\mathbf{E}_0$ and integrating over Y leads to :

$$\int_Y \frac{1}{\varepsilon(\mathbf{x},\mathbf{y})}\operatorname{curl}_{0,\mathbf{y}}\Big[(\operatorname{curl}_{0,\mathbf{y}}\mathbf{E}_0(\mathbf{x},\mathbf{y}))\Big]\cdot\mathbf{E}_0^*(\mathbf{x},\mathbf{y})\,d\mu=0$$

By applying the Poynting Identity $\operatorname{div}_\gamma(A\wedge B)=-A\cdot\operatorname{curl}_\gamma B+B\cdot\operatorname{curl}_\gamma A$ for $\gamma=0$ and summing on Y, we have :

$$\int_Y\Big[(\operatorname{curl}_{0,\mathbf{y}}\mathbf{E}_0(\mathbf{x},\mathbf{y}))\Big]\cdot\operatorname{curl}_{0,\mathbf{y}}\mathbf{E}_0^*(\mathbf{x},\mathbf{y})\,d\mathbf{y}-\int_Y\operatorname{div}_{0,\mathbf{y}}\Big[(\operatorname{curl}_{0,\mathbf{y}}\mathbf{E}_0(\mathbf{x},\mathbf{y}))\wedge\mathbf{E}_0^*(\mathbf{x},\mathbf{y})\Big]\,d\mathbf{y}=0$$

The Green-Ostrogradsky formula then gives us :

$$\int_Y\Big[(\operatorname{curl}_{0,\mathbf{y}}\mathbf{E}_0(\mathbf{x},\mathbf{y}))\Big]\cdot\operatorname{curl}_{0,\mathbf{y}}\mathbf{E}_0^*(\mathbf{x},\mathbf{y})\,d\mathbf{y}-\int_{\partial Y}\Big[((\operatorname{curl}_{0,\mathbf{y}}\mathbf{E}_0(\mathbf{x},\mathbf{y}))\wedge\mathbf{E}_0^*(\mathbf{x},\mathbf{y})\Big]\cdot\mathbf{n}\,ds=0$$

From the anti-periodicity of the unit outgoing normal $\mathbf{n}$ to ∂Y and the periodicity in the $\mathbf{y}$ variable of $\mathbf{E}_0$, we deduce that :

$$\int_Y \Big[\mathrm{curl}_{0,\mathbf{y}}\mathbf{E}_0(\mathbf{x},\mathbf{y})\Big]^2 d\mathbf{y} = 0$$

It follows that :

$$a.e.\mathbf{y} \in Y,\ \ \mathrm{curl}_{0,\mathbf{y}}\,\mathbf{E}_0(\mathbf{x},\mathbf{y}) = 0 \tag{4}$$

This auxiliary lemma is applied to perform the proof of the second lemma.

Lemma 5 *Let* $\mathbf{E}_0$ *be a* Y *periodic function in* $\mathbf{y}$*, solution of the system* $\mathcal{S}_0$*. Then*

$$\textit{For almost every}\ \mathbf{y}\ \ \textit{in}\ Y,\ \ \mathrm{div}_{0,\mathbf{y}}\Big(\varepsilon(\mathbf{x},\mathbf{y})\mathbf{E}_0(\mathbf{x},\mathbf{y})\Big) = 0 \tag{4}$$

Proof :

From equations (2) and (4), we have that :

$$\mathrm{curl}_{0,\mathbf{y}}\Big(\mathrm{curl}_{\gamma,\mathbf{x}}\,\mathbf{E}_0(\mathbf{x},\mathbf{y})\Big) + \mathrm{curl}_{0,\mathbf{y}}\Big(\mathrm{curl}_{0,\mathbf{y}}\,\mathbf{E}_1(\mathbf{x},\mathbf{y})\Big) = 0 \tag{5}$$

By applying $\mathrm{div}_{0,\mathbf{y}}$ to (3) we derive that :

$$\begin{aligned}&\mathrm{div}_{0,\mathbf{y}}\Big(\mathrm{curl}_{\gamma,\mathbf{x}}(\mathrm{curl}_{\gamma,\mathbf{x}}\,\mathbf{E}_0)\Big) + \mathrm{div}_{0,\mathbf{y}}\Big(\mathrm{curl}_{\gamma,\mathbf{x}}(\mathrm{curl}_{0,\mathbf{y}}\,\mathbf{E}_1)\Big)\\ &+\mathrm{div}_{0,\mathbf{y}}\Big(\mathrm{curl}_{0,\mathbf{y}}(\mathrm{curl}_{\gamma,\mathbf{x}}\,\mathbf{E}_1)\Big) + \mathrm{div}_{0,\mathbf{y}}\Big(\mathrm{curl}_{0,\mathbf{y}}(\mathrm{curl}_{0,\mathbf{y}}\,\mathbf{E}_2)\Big) + k_0^2\,\mathrm{div}_{0,\mathbf{y}}\Big(\varepsilon(\mathbf{x},\mathbf{y})\mathbf{E}_0\Big) = 0\end{aligned} \tag{6}$$

Noting that

$$\mathrm{div}_{0,y}\,\mathrm{curl}_{\gamma,x}\,A(x,y) = \bigtriangledown_{0,y}\cdot\Big(\bigtriangledown_{\gamma,x}\wedge A(x,y)\Big) = -\bigtriangledown_{\gamma,x}\cdot\Big(\bigtriangledown_{0,y}\wedge A(x,y)\Big) = -\,\mathrm{div}_{\gamma,x}\,\mathrm{curl}_{0,y}\,A(x,y)\ ,$$

the expression (6) confines itself to :

$$-\,\mathrm{div}_{\gamma,\mathbf{x}}\Big(\underbrace{\mathrm{curl}_{0,\mathbf{y}}(\mathrm{curl}_{\gamma,\mathbf{x}}\,\mathbf{E}_0) + \mathrm{curl}_{0,\mathbf{y}}(\mathrm{curl}_{0,\mathbf{y}}\,\mathbf{E}_1)}_{=0(5)}\Big) + k_0^2\,\mathrm{div}_{0,\mathbf{y}}\Big(\varepsilon(\mathbf{x},\mathbf{y})\mathbf{E}_0\Big) = 0$$

Finally, we get the following formulation :

$$\mathrm{div}_{0,\mathbf{y}}\Big(\varepsilon(\mathbf{x},\mathbf{y})\mathbf{E}_0\Big) = 0 \tag{7}$$

Remark :

In [105][214], we have studied the homogenization of a three dimensional diffracting problem using the multi-scale expansion method in the magnetic field formulation. We deduced although that $\mathrm{curl}_y\,\mathbf{H_0}(\mathbf{x},\mathbf{y}) = 0$. Noting that $\mu = \mu_0$ (non magnetic medium) we knew that $\mathrm{div}_y\,\mathbf{H_0}(\mathbf{x},\mathbf{y}) = 0$, which is obviously not the case for the electric field. The main difference with the magnetic field expansion is thus that the first term $\mathbf{H_0}$ of the ansatz is independent of the $\mathbf{y}$ variable, unlike $\mathbf{E_0}$ which is therefore not the homogenized field (it is in fact its average on the basic cell Y).

The results of lemmae 2 and 3 (expressions (4) and (7)) are summed up in the following system :

$$(8)\quad \begin{cases} \mathrm{curl}_{0,\mathbf{y}}\Big(\mathbf{E}_0(\mathbf{x},\mathbf{y})\Big) = 0 \\ \mathrm{div}_{0,\mathbf{y}}\Big(\varepsilon(\mathbf{x},\mathbf{y})\mathbf{E}_0(\mathbf{x},\mathbf{y})\Big) = 0 \end{cases}$$

Making the obvious remark that the average of $\mathbf{E}_0$ on Y gives us a field independant of the microscopic variable, we denote by $\mathbf{E}_{hom}$ the following quantity :

$$\mathbf{E}_{hom}(\mathbf{x}) = \langle \mathbf{E}_0 \rangle_Y = \frac{1}{meas(Y)} \int_Y \mathbf{E}_0(\mathbf{x},\mathbf{y})\, d\mathbf{y} \tag{9}$$

Where $meas(Y)$ denotes the volume area of the unit cell Y.

Hence, $\mathrm{curl}_{\mathbf{y}}(\mathbf{E}_0 - \mathbf{E}_{hom}) = 0$. Then, $\mathbf{E}_0 - \mathbf{E}_{hom}$ derives from a scalar potential denoted by V. That is to say that there exists a Y-periodic function $V(\mathbf{x},\mathbf{y})$ such as :

$$\mathbf{E}_0 = \mathbf{E}_{hom} - \bigtriangledown_{0,\mathbf{y}} V \tag{10}$$

It is worth noting that this deduction would not hold anymore if there were currents in the Scattering-Box. This would be the case for a domain Ω_f filled up by diffracting objects of infinite conductivity. [1]

Injecting (10) in (7), leads us to :

$$\mathrm{div}_{0,\mathbf{y}}\Big(\tilde{\varepsilon}(\mathbf{E}_{hom} - \bigtriangledown_{0,\mathbf{y}} V)\Big) = 0 \tag{11}$$

By linearity of the divergence, we can write that :

$$\begin{aligned} -\mathrm{div}_{0,\mathbf{y}}\Big(\tilde{\varepsilon}(\bigtriangledown_{0,\mathbf{y}} V)\Big) &= -\mathrm{div}_{0,\mathbf{y}}(\tilde{\varepsilon}\mathbf{E}_{hom}) \\ &= -\mathrm{div}_{0,\mathbf{y}}\Big(\tilde{\varepsilon}\sum_{j=1}^{3}\mathbf{E}_{hom,j}e_j\Big) \\ &= -\sum_{j=1}^{2}\mathrm{div}_{0,\mathbf{y}}\Big(\tilde{\varepsilon}(\mathbf{x},\mathbf{y})e_j\Big)\mathbf{E}_{hom,j}(\mathbf{x}) \end{aligned}$$

We are thus led to solve an annex problem of electrostatic type $\mathcal{K}_j$:

$$\mathcal{K}_j :\ -\mathrm{div}_{0,\mathbf{y}}\Big(\tilde{\varepsilon}(\mathbf{x},\mathbf{y})(\bigtriangledown_{0,\mathbf{y}} V_j - e_j)\Big) = 0\ , j \in \{1,\ 2,\ 3\} \tag{12}$$

The variational form associated to this problem having the good properties (sesquilinear, continue and coercive) in the Hilbert space $H^1_\sharp(Y)\backslash\mathbb{R}$, Lax-Milgram lemma assures the existence and uniqueness of the solution of this problem in $H^1_\sharp(Y)\backslash\mathbb{R}$, that is, up to an additive constant.

1. In general, $\mathbf{E}_0 = \mathbf{E}_{hom}(\mathbf{x}) - \bigtriangledown_{\mathbf{y}} V(\mathbf{x},\mathbf{y}) + \mathbf{E}_{cohom}(\mathbf{x})$, where $\mathbf{E}_{cohom}$ belongs to the so called cohomology spaces whose dimensions depend upon the number of cuts made in the complex plane to obtain a simply connected open set $\tilde{Y}$. As for us, $< \mathbf{E}_0 >_Y = < \mathbf{E}_{hom} >_Y$ and $< \bigtriangledown_{0,\mathbf{y}} V >_Y = 0$ which implies that $\mathbf{E}_{cohom} = 0$

Let us remark that $\tilde{\varepsilon}(\mathbf{x},\mathbf{y})$ being a data of the problem $\mathcal{P}_\eta$, $\mathrm{div}_{\gamma,\mathbf{y}}\Big(\tilde{\varepsilon}(\mathbf{x},\mathbf{y})e_j\Big)$ is a known function. Therefore, we have to solve an annex problem where the unknowns are the three components of the potential V_j. The solutions of (11) are given by the functions :

$$V(\mathbf{x},\mathbf{y}) = \sum_{j=1}^{2} V_j(\mathbf{y}) E_{hom,j}(\mathbf{x}) = \mathbf{V}_Y \cdot \mathbf{E}_{hom} \tag{13}$$

where $\mathbf{V}_Y = (V_1, V_2, V_2)$ and V_j denote respectively the vectorial potential of the basic cell and one of the scalar potentials associated with the density of charges $\mathrm{div}_{0,\mathbf{y}}(\varepsilon(\mathbf{y})e_j)$.

Before going further, it is worth noting that the problem $\mathcal{K}_j$ is of interest by itself. It is solved by a method of fictitious sources [47][215][178], and works are in progress to solve it by a finite difference scheme (see next section).

We still have to precise the link between $\mathbf{E}_0$ and $\mathbf{E}_{hom}$.

From (10) and (13) we get that :

$$\mathbf{E}_0 = (I - \bigtriangledown_{0,\mathbf{y}}\mathbf{V}_Y)\mathbf{E}_{hom} \tag{14}$$

where I denotes the identity matrix and $\bigtriangledown_{0,\mathbf{y}}\mathbf{V}_Y$ denotes the jacobian of $\mathbf{V}_Y$.

That is to say that :

$$\mathbf{E}_0 = \left(I - \begin{bmatrix} \frac{\partial V_1}{\partial y_1} & \frac{\partial V_1}{\partial y_2} & 0 \\ \frac{\partial V_1}{\partial y_2} & \frac{\partial V_2}{\partial y_2} & 0 \\ 0 & 0 & 0 \end{bmatrix} \right) \mathbf{E}_{hom}$$

It remains to give the equation verified by $\mathbf{E}_{hom}(\mathbf{x})$. Summing the third equation in the system $\mathcal{S}_0$ over Y, we derive that :

$$\begin{aligned} & \int_Y \mathrm{curl}_{0,\mathbf{y}}\Big(\mathrm{curl}_{0,\mathbf{y}}\,\mathbf{E}_2\Big)\,d\mathbf{y} \\ = \; & k_0^2 \int_Y \tilde{\varepsilon}\mathbf{E}_0\,d\mathbf{y} - \int_Y \mathrm{curl}_{\gamma,\mathbf{x}}\Big(\mathrm{curl}_{\gamma,\mathbf{x}}\,\mathbf{E}_0\Big)\,d\mathbf{y} - \int_Y \mathrm{curl}_{\gamma,\mathbf{x}}\Big(\mathrm{curl}_{0,\mathbf{y}}\,\mathbf{E}_1\Big)\,d\mathbf{y} \\ & - \int_Y \mathrm{curl}_{0,\mathbf{y}}\Big(\mathrm{curl}_{\gamma,\mathbf{x}}\,\mathbf{E}_1\Big)\,d\mathbf{y} \end{aligned} \tag{17}$$

Due to periodicity of $\mathbf{E}_1$, $\mathbf{E}_2$ and $\tilde{\varepsilon}$, and due to the antiperiodicity of the outer normal $\mathbf{n}$ to ∂Y, by virtue of the Green formula ($\int_Y \mathrm{curl}_\gamma A\,d\mathbf{y} = \int_{\partial Y} n \wedge A\,ds$), we both get that :

$$\int_Y \mathrm{curl}_{0,\mathbf{y}}\Big(\mathrm{curl}_{\gamma,\mathbf{x}}\,\mathbf{E}_1(\mathbf{x},\mathbf{y})\Big) = \int_Y \mathrm{curl}_{0,\mathbf{y}}\Big(\mathrm{curl}_{0,\mathbf{y}}\,\mathbf{E}_2(\mathbf{x},\mathbf{y}))\Big) = 0\,,$$

and that

$$\int_Y \mathrm{curl}_{\gamma,\mathbf{x}}\Big(\mathrm{curl}_{0,\mathbf{y}}\,\mathbf{E}_1(\mathbf{x},\mathbf{y})\Big)\,d\mathbf{y} = \mathrm{curl}_{\gamma,\mathbf{x}} \int_Y \mathrm{curl}_{0,\mathbf{y}}\,\mathbf{E}_1(\mathbf{x},\mathbf{y})\,d\mathbf{y} = 0\,.$$

Therefore, the equation (17) reduces to :

$$-k_0^2 \int_Y \varepsilon(\mathbf{x},\mathbf{y})\mathbf{E}_0\,d\mathbf{y} + \int_Y \left(\mathrm{curl}_{\gamma,\mathbf{x}}\Big(\tilde{\varepsilon}^{-1}(\mathrm{curl}_{\gamma,\mathbf{x}}\,\mathbf{E}_0)\Big)\right) d\mathbf{y} = 0$$

From (14), we therefore deduce that :

$$-k_0^2\Big(\int_Y \varepsilon(\mathbf{x},\mathbf{y})(I-\bigtriangledown_{0,\mathbf{y}}\mathbf{V}_Y)\,d\mathbf{y}\Big)\mathbf{E}_{hom}(\mathbf{x})$$
$$+\operatorname{curl}_{\gamma,\mathbf{x}}\operatorname{curl}_{\gamma,\mathbf{x}}E_{hom}(\mathbf{x})-\operatorname{curl}_{\gamma,\mathbf{x}}\operatorname{curl}_{\gamma,\mathbf{x}}\Big(\int_Y \bigtriangledown_{0,y}\mathbf{V}_Y\,d\mathbf{y}\Big)\mathbf{E}_{hom}(\mathbf{x})=0 \quad (18)$$

Due to periodicity of $\mathbf{V}_Y$ and due to the antiperiodicity of the outer normal $\mathbf{n}$ to ∂Y, by virtue of the Green formula, we deduce that :

$$\int_Y \bigtriangledown_{0,y}\mathbf{V}_Y\,d\mathbf{y}=\int_{\partial Y} n\mathbf{V}_Y\,ds=0$$

We then deduce from (18) that $\mathbf{E}_{hom}$ is solution of a homogenized equation given by :

$$\varepsilon_{hom}^{-1}\operatorname{curl}_{\gamma,x}\Big(\operatorname{curl}_{\gamma,x}\mathbf{E}_{hom}(\mathbf{x})\Big)-k_0^2\mathbf{E}_{hom}(\mathbf{x})=0 \quad (19)$$

with the effective permittivity defined by :

$$\varepsilon_{hom}=<\tilde{\varepsilon}(I-\bigtriangledown_{0,\mathbf{y}}\mathbf{V}_Y)>_Y \quad (20)$$

Comments :

The operator associated to the homogenized problem $\mathcal{P}_{hom}$ of theorem 1 has a compact resolvent and its spectrum σ is made of a countable set of increasing eigenvalues Λ^k :

$$\sigma=\frac{\gamma^2}{\lambda_{min}}\leq\Lambda^0\leq\Lambda^1\leq...\Lambda^k\leq...$$

where λ_{min} is the smallest eigenvalue of the effective matrix ε_{hom} and $\lim\limits_{k\to+\infty}\Lambda^k=+\infty$. In the next chapter, we will explain in what sense the spectrum of the operator associated to the problem $\mathcal{P}_\eta$ converges to σ.

9.2 Numerical results.

In this section, we give some numerical results on the homogenization of a circular metallic waveguide made of a periodic arrangement of dielectric rods of elliptic cross-section of index 2 embedded in a matrix of index 1. We derive the tensor of effective permittivity from the resolution of the two annex problems of electrostatic type $\mathcal{K}_j$, with the method of fictitious sources [212]. This method consists in representing the potential by an approximate potential created by two families of fictitious charges : the first ones are located in the scatterer S and they radiate in its complement $Y\setminus S$ in the periodic cell Y, and the second ones are located in $Y\setminus S$ and radiate in S. Each of these charges satisfies a Laplace equation in Y with periodic conditions and they are chosen such that the potential V_j verifies the boundary conditions that appears in the following system :

$$\begin{cases}\Delta V_j & =0\ ,\text{ in } Y\setminus\partial S\\ [\varepsilon\,\frac{\partial V_j}{\partial n}]_{\partial S} & =-[\varepsilon]_{\partial S}\,n_j\\ [V_i]_{\partial S} & =0\end{cases}$$

$$\text{with } \varepsilon = \begin{cases} \varepsilon_{scat} & \text{, in } S \\ 1 & \text{, in } Y \setminus \bar{S} \end{cases}$$

$[f]_{\partial S}$ denotes the jump of f across the boundary ∂S, and n_j, $j \in \{1,2\}$, denotes the projection on the axis e_j of a normal of ∂S.

In figure 9.1, we compare the transverse electromagnetic field of a heterogeneous metallic waveguide made of a periodic arrangement of elliptic dielectric rods with that of its effective anisotropic waveguide, derived from the asymptotic analysis. We must solve an annex problem settled in the basic cell $Y =]0;1[^2$ with the shape of the scatterer defined by the equation

$$\frac{y_1^2}{a^2} + \frac{y^2}{b^2} = 1$$

with $a = 0.4$ and $b = 0.2$. Its permittivity is given by $\varepsilon_{scat} = 4$. The method of fictitious sources gives us

$$\varepsilon_{1,1}^{eff} = 1.39787 \ , \ \varepsilon_{2,2}^{eff} = 2.01435 \ , \ \varepsilon_{3,3}^{eff} = < \varepsilon^{eff} >_Y = 4.769911$$

the remaining terms being identically null.

We use the GetDP software [64] to modelize the **anisotropic waveguide** (chapter 7) defined by this tensor of permittivity.

Remark :

Our aim is the numerical treatment of the so-called Microstructered Optical Fibers (MOF) which are all-silica fibers with an arrangement of microscopic air holes that run down their entire length (Knight 1996 [119], Broenj 1999 [44]). In some cases, light is guided in a high index core region i.e. a solid core surrounded by air holes. Typically, the air holes are arranged in a hexagonal arrangement about a core formed by a missing hole (honeycomb). Such a guidance is related to effective index theories i.e. we can replace the composite structure by a homogeneous waveguide for the large wavelegths that is for $\Lambda >>$ hole diameter (in case of elliptical air holes, the effective structure is anisotropic). However, for short wavelengths, the field actually sees the air holes and the silica between them, and becomes confined to the high-index silica regions, raising the effective index of the modes. The experimental team of Bath, which is supervised by P. St. J. Russell, used an effective model to explain why MOF of this type are single mode over a very large wavelength range (Russell, 1997 [24] [120]). Because these fibers have strong anomalous dispersion in the visible spectrum, they have potential applications in dispersion compensation and non linear optics, such as soliton formation and continuum generation in the visible part of the spectrum. The effective model of Russell *et al.* doesn't hold any more when the fraction of air relative to silica is not large and appears to work well only for simple hole arrangements (e.g. hexagonal) as was mentioned by (Ghosh *et al.*, 1999 [89]). An alternative explanation has been proposed by (Ranka *et al.*, 2000 [182]) to show theoretically that for high-delta air-silica MOF, although several modes may be supported, there is almost no coupling between these modes. Even strong pertubations such as sharp bending may not excite higher modes, and the fiber may thus appear to be single mode. Furthermore, the number

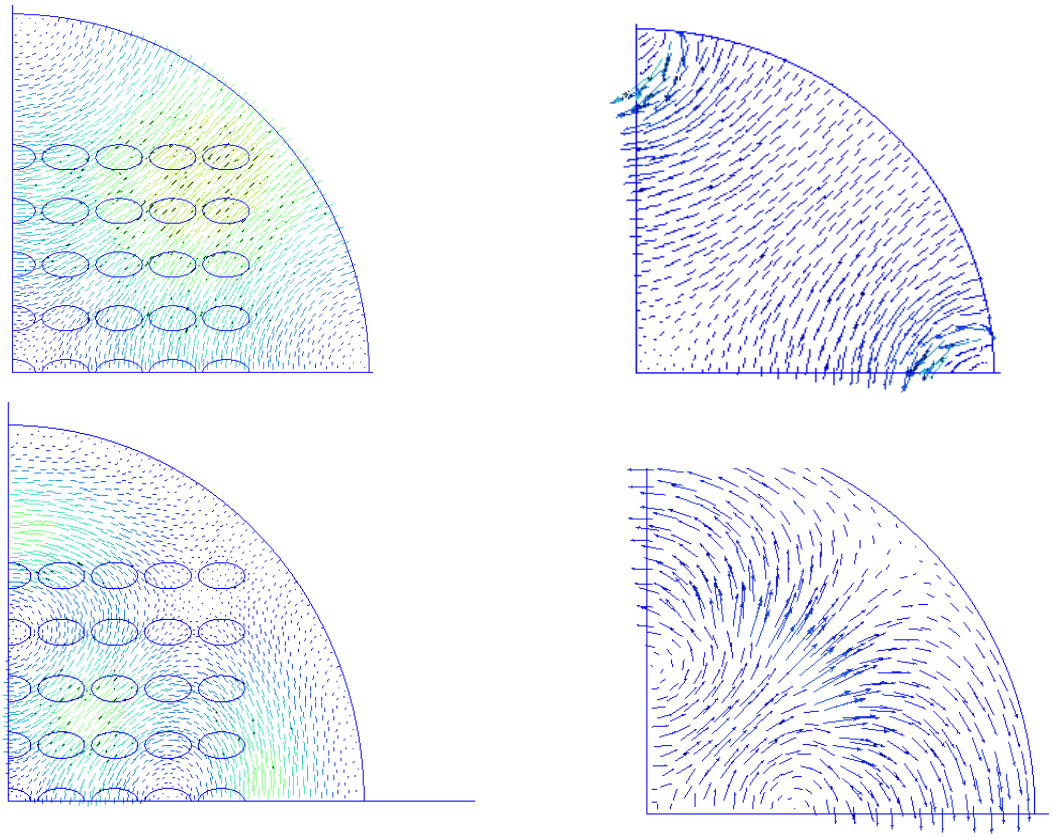

FIGURE 9.1 – Comparison between the transverse electric fields TE_{21} and TE_{31} of a metallic PCF for $\gamma = 1cm^{-1}$ ($k = 0.7707cm^{-1}$ and $k = 0.7607cm^{-1}$) with the ones of the homogenized anisotropic associated metallic waveguide for $\gamma = 1cm^{-1}$ ($k = 0.5478cm^{-1}$ and $k = 0.5201cm^{-1}$).

of modes supported by the MOF does not seem to depend on the absolute dimension of the fiber, but rather on the ratio of the hole diameter to the hole spacing $\frac{d}{\Lambda}$.

Chapitre 10

Analyse limite spectrale

> "Que tel phénomène périodique (une oscillation électrique, par exemple) soit réellement dû à la vibration de tel atome qui, se comportant comme un pendule, se déplace véritablement dans tel ou tel sens, voilà ce qui n'est ni certain ni intéresant. Mais qu'il y ait entre l'oscillation électrique, le mouvement du pendule et tous les phénomènes périodiques une parenté intime qui correspond à une réalité profonde ; que cette parenté, cette similitude, ou plutôt ce parallélisme se poursuive dans le détail ; qu'elle soit une conséquence de principes plus généraux, celui de l'énergie et celui de la moindre action ; voilà ce que nous pouvons affirmer ; voilà la vérité qui restera toujours la même sous tous les costumes dont nous pourrons juger utile de l'affubler."
>
> H. Poincaré *in* "La science et l'hypothèse" (1902)

Addendum

In this chapter, we outline an asymptotic approach of propagating modes in heterogeneous metallic waveguides constituted of a periodic dielectric medium (photonic crystal fibers) for the high frequencies (photonic band gap effects). For this, we use a method of "Bloch wave homogenization" introduced by Allaire and Conca in [5][4][7][8] which, unlike the classical homogenization method, characterizes a renormalized limit of the spectrum, namely sequences of eigenvalues of the order of the square of the medium period. We derive the convergence of spectral families associated to the operators of the photonic crystal cavities and in particular to that of their spectra. We prove that the renormalized limit spectrum contains in addition to the usual Bloch spectrum some boundary layer spectrum corresponding to sequences of eigenvectors whose support concentrates on the metallic boundary (boundary modes). The operator under consideration is self-adjoint with compact resolvent and depends on a small parameter η which describes the heterogeneity of the cavity. As we work in the T.M. case, we deal with the magnetic field and therefore **homogeneous Neumann conditions** are prescribed on the metallic boundary of the cavity. This study has been already performed in case of homogeneous Dirichlet conditions by Allaire and Conca who considered spectral problems in acoustic. In this chapter, we give a complete characterization of the boundary layer spectrum in the one-dimensional case, when the cavity is made of an integer number of periodic cells : we show that the boundary layer spectrum is characterized as in [8] by a spectral problem in the half plane (in the

one-dimensional case, we obtain a spectral problem in $]0;+\infty[$ with Neumann condition at 0). The associated spectrum can be deduced from a spectral problem set in $]0;1[$ with Neumann conditions. Furthermore, we illustrate our discussion by numerical results derived from this new spectral problem. Although we just address here the asymptotic analysis for the scalar electromagnetic case, we emphasize that our study can be generalized to the vector case thanks to the modelling proposed in the first section [35] of the chapter. It is worth noting that many related recent papers can be found on the subject, but with quite different approachs [55][198][157][77][78][79][80].

10.1 Position du problème physique

Dans ce chapitre, on s'intéresse à la propagation des ondes électromagnétiques dans un guide à parois infiniment conductrices, constitué d'une assemblée de tiges diélectriques réparties périodiquement. L'objet de cette étude théorique et numérique est de mettre en évidence l'influence des conditions limites sur les modes susceptibles de se propager. En hautes fréquences, nous montrons que deux types de modes coexistent : les modes induits par la périodicité ou modes de Bloch, et les modes induits par les conditions aux bords baptisés modes de bord. Les premiers sont bien connus des physiciens et sont insensibles au type de conditions aux limites. Au contraire, les modes de bord rendent compte de l'aspect fini de la structure en ce que leur existence dépend étroitement du type de conditions imposées au bord : il s'avère que leur support se concentre sur le bord du guide pourvu que ce dernier soit à parois métalliques.

On considère un ouvert Ω de classe C^2 dans $\mathbb{R}^2$ qui correspond à la section transverse du guide. On remplit ce guide d'un amas de tiges réparties périodiquement. Pour étudier le comportement asymptotique de ce guide, on considère alors un nombre croissant de tiges telles que le rapport de leur section sur ce nombre soit constant. Pour ce faire, on se donne un ouvert T (la section d'une tige) dont on supposera le bord ∂T régulier et une cellule de base $Y =]0;1[^2$, avec $T \subset Y$ (T peut éventuellement toucher les bords de la cellule Y). La région occupée par la section des tiges est alors donnée par :

$$T_\eta = \bigcup_{i \in \mathbb{Z}^2} \{\eta(i+T)\} \cap \Omega \tag{1}$$

Dans une première étape, nous allons déduire des équations de Maxwell le problème mathématique que nous nous posons. On considère un guide métallique de section constante Ω (un ouvert borné de $\mathbb{R}^2$), de génératrice suivant e_3, occupé par un milieu périodique hétérogène de période $\eta > 0$. Notant la cellule de base $Y =]0;1[^2$, le profil de permittivité du guide est représenté par une fonction ε_η de la forme $\varepsilon_\eta(x) = \varepsilon(x, \dfrac{x}{\eta})$ où $\varepsilon(x,y)$ ($\varepsilon(x,y) = 1$ si $x \notin \Omega$) est supposée satisfaire les hypothèses suivantes : $\varepsilon(x,y)$ est une matrice symétrique dans $[C(\mathbb{R}^2; L^\infty_\sharp(Y))]^9$ et vérifie par ailleurs une hypothèse de coercivité. Nous cherchons les champs électromagnétiques $(\mathcal{E}_\eta, \mathcal{H}_\eta)$ solutions des équations de Maxwell :

$$\begin{cases} \operatorname{rot} \mathcal{H}_\eta = \varepsilon_0 \varepsilon_\eta \dfrac{\partial \mathcal{E}_\eta}{\partial t} & \text{dans } \mathcal{D}'(]0;T[\times\mathbb{R}^3) \\ \operatorname{rot} \mathcal{E}_\eta = -\mu_0 \dfrac{\partial \mathcal{H}_\eta}{\partial t} & \text{dans } \mathcal{D}'(]0;T[\times\mathbb{R}^3) \end{cases} \tag{2}$$

Si l'on choisit une dépendance temporelle en $e^{-i\omega t}$ et si l'on prend en compte l'invariance du guide suivant e_3, on définit alors des solutions harmoniques d'un tel problème comme suit :

$$\begin{cases} \mathcal{E}_\eta(x_1,x_2,x_3,t) = \Re e(E_\eta(x_1,x_2)e^{-i(\omega t-\gamma x_3)}) \\ \mathcal{H}_\eta(x_1,x_2,x_3,t) = \Re e(H_\eta(x_1,x_2)e^{-i(\omega t-\gamma x_3)}) \end{cases} \tag{3}$$

On dit que (E_η, H_η) est un mode guidé si :

$$\begin{cases} (\gamma,\omega) \in \mathbb{R}^2 \\ (E_\eta,H_\eta) \neq (0,0) \\ E_\eta, H_\eta \in [L^2(\mathbb{R}^2)]^3 \end{cases} \tag{4}$$

où ω est la pulsation de la lumière dans le vide et γ la constante de propagation du mode. Pour les champs de la forme (3), le système (2) s'écrit :

$$\begin{cases} \operatorname{rot}_\gamma H_\eta = -i\omega\varepsilon_0\varepsilon_\eta E_\eta & \text{dans } \mathcal{D}'(\mathbb{R}^2) \\ \operatorname{rot}_\gamma E_\eta = i\omega\mu_0 H_\eta & \text{dans } \mathcal{D}'(\mathbb{R}^2) \end{cases} \tag{5}$$

où $\operatorname{rot}_\gamma H_\eta$ et $\operatorname{rot}_\gamma E_\eta$ sont définis par :

$$\begin{cases} \operatorname{rot}_\gamma H_\eta(x_1,x_2) = \operatorname{rot}\Big(H_\eta(x_1,x_2)e^{i\gamma x_3})e^{-i\gamma x_3} \\ \operatorname{rot}_\gamma E_\eta(x_1,x_2) = \operatorname{rot}\Big(E_\eta(x_1,x_2)e^{i\gamma x_3}\Big)e^{-i\gamma x_3} \end{cases} \tag{6}$$

Pour obtenir (6), il suffit de poser :

$$\operatorname{rot}_\gamma F = \begin{cases} \dfrac{\partial F_3}{\partial x_2} - i\gamma F_2 \\ i\gamma F_1 - \dfrac{\partial F_3}{\partial x_1} \\ \dfrac{\partial F_2}{\partial x_1} - \dfrac{\partial F_1}{\partial x_2} \end{cases}$$

Comme le champ électromagnétique $(E_\eta,\ H_\eta)$ est nul en dehors de Ω, les conditions limites sont données par :

$$\begin{cases} n \wedge E_\eta = 0 & \text{sur } \partial\Omega \\ H_\eta \cdot n = 0 & \text{sur } \partial\Omega \end{cases}$$

L'analyse mathématique des modes susceptibles de se propager consiste alors à chercher les triplets $(\gamma, \Lambda_\eta, H_\eta) \in \mathbb{R} \times \mathbb{R}^+ \times [H(\operatorname{rot},\Omega)]^3$, $H_\eta \not\equiv 0$, tels que :

$$\begin{cases} -\operatorname{rot}_\gamma(\varepsilon^{-1}(x,\dfrac{x}{\eta})\operatorname{rot}_\gamma H_\eta) = \dfrac{1}{\Lambda_\eta}H_\eta & \text{dans } \Omega \\ n \wedge (\operatorname{rot}_\gamma H_\eta) = 0 \ \text{ et } \ H_\eta \cdot n = 0 & \text{sur } \partial\Omega \end{cases} \tag{7}$$

Noter que Λ_η est positive car elle a les dimensions du carré d'une longueur d'onde i.e. de $\dfrac{c^2}{\omega^2}$ où c désigne la célérité de la lumière. On peut l'interpréter comme une réversibilté temporelle du problème physique (penser à l'invariance par renversement temporel de l'équation des ondes). De plus, $(-\gamma, \Lambda_\eta)$ est également une solution de (7) associée à la fonction propre $(H_\eta^1, H_\eta^2, -H_\eta^3)$. On a donc affaire à un problème physique présentant aussi une réversibilité spatiale suivant l'axe e_3. Il paraît en effet intuitif qu'une onde puisse se

propager dans le sens des x_3 positifs ou négatifs sans que la nature physique du problème soit changée (la section du guide étant constante). Le problème précédent se réduit alors à chercher les triplets $(\gamma, \Lambda_\eta, H_\eta) \in \mathbb{R}^+ \times \mathbb{R}^+ \times [H(\mathrm{rot}, \Omega)]^3$, $H_\eta \not\equiv 0$ vérifiant (7). La formulation équivalente à (7) en terme de champ électrique consiste à chercher les triplets $(\gamma, \Lambda_\eta, E_\eta) \in \mathbb{R}^+ \times \mathbb{R}^+ \times [H^1(\mathrm{rot}, \Omega)]^3$, $E_\eta \not\equiv 0$, tels que :

$$\begin{cases} -\varepsilon^{-1}(x, \dfrac{x}{\eta}) \,\mathrm{rot}_\gamma \,\mathrm{rot}_\gamma \, E_\eta = \dfrac{1}{\Lambda_\eta} E_\eta & \text{dans } \Omega \\ n \wedge E_\eta = 0 \;\text{ et } n \wedge (\mathrm{rot}_\gamma \, E_\eta) = 0 & \text{sur } \partial\Omega \end{cases} \tag{8}$$

Il est facile de vérifier que les spectres des opérateurs définis par (7) ou (8) sont réels : on note pour cela que

$$\int_\Omega \mathrm{rot}_\gamma \Big(\varepsilon_\eta^{-1} \,\mathrm{rot}_\gamma \, H_\eta \Big) \cdot H'_\eta \, dx = \int_\Omega \varepsilon_\eta^{-1} \,\mathrm{rot}_\gamma \, H_\eta \cdot \mathrm{rot}_\gamma \, H'_\eta \, dx$$

$$+ < \varepsilon_\eta^{-1} (n \wedge \mathrm{rot}_\gamma \, H_\eta) \cdot H'_\eta, 1 >_{H^{-\frac{1}{2}}(\partial\Omega), H^{\frac{1}{2}}(\partial\Omega)}$$

et que $n \wedge (\mathrm{rot}_\gamma \, H_\eta) = 0$. Le caractère auto-adjoint de (8) est obtenu en utilisant le produit scalaire associé à la mesure de Lebesgue $\varepsilon_\eta \; dx$. La difficulté de l'étude réside alors dans le passage à la limite : le produit scalaire dépend lui même du paramètre η. L'étude du spectre de cet opérateur à η fixé a été abordée dans la partie II d'un point de vue numérique. On a constaté que ce spectre est discret et qu'il est semblable à celui de l'opérateur associé au problème de la cavité résonnante ($\gamma = 0$) : la propagation induit un décalage à droite du spectre calculé pour l'opérateur associé à la cavité résonnante donné par γ, mais ne change pas la nature du spectre. Dans la suite, nous nous contenterons donc de l'étude du problème d'une cavité résonnante remplie d'un milieu hétérogène périodique de période η (i.e. lorsque la constante de propagation γ est nulle).

On déduit de (8) que le problème de la recherche des modes transverses magnétiques susceptibles d'exister dans la cavité ($\gamma = 0$) se réduit à trouver les couples $(\Lambda_\eta, E_\eta^3) \in \mathbb{R}^+ \times H^1(\Omega)$ $E_\eta^3 \not\equiv 0$ tels que :

$$\begin{cases} -\varepsilon^{-1}(x, \dfrac{x}{\eta}) \Delta E_\eta^3 = \dfrac{1}{\Lambda_\eta} E_\eta^3 & \text{dans } \Omega \\ E_\eta^3 = 0 & \text{sur } \partial\Omega \end{cases} \tag{9}$$

puisque les champs $n \wedge E_\eta^t = n \wedge (E_\eta^1 e_1 + E_\eta^2 e_2)$ et $n \wedge (E_\eta^3 e_3)$ sont respectivement portés par e_3 et dans le plan de section transverse, donc tous deux nuls. D'après (7), la recherche des modes transverses électriques revient quant à elle à chercher les couples $(\Lambda_\eta, H_\eta^3) \in \mathbb{R}^+ \times H^1(\Omega)$ $H_\eta^3 \not\equiv 0$ tels que :

$$\begin{cases} -div(\varepsilon^{-1}(x, \dfrac{x}{\eta}) \bigtriangledown H_\eta^3) = \dfrac{1}{\Lambda_\eta} H_\eta^3 & \text{dans } \Omega \\ \dfrac{\partial H_\eta^3}{\partial n} = 0 & \text{sur } \partial\Omega \end{cases} \tag{10}$$

Noter pour cela que

$$\int_\Omega \mathrm{rot}_\gamma\Big(\varepsilon_\eta^{-1}\,\mathrm{rot}_\gamma\, H_\eta^3\Big)\cdot H_\eta^{3'}\,dx = -\int_\Omega \mathrm{div}\Big(\varepsilon_\eta^{-1}\,\nabla\, H_\eta^3\Big)\cdot H_\eta^{3'}\,dx$$
$$+\gamma^2\int_\Omega H_\eta^3\cdot H_\eta^{3'}\,dx + \int_\Omega \nabla_\gamma\Big(\mathrm{div}_\gamma\, H_\eta^3\Big)\cdot H_\eta^{3'}\,dx$$

et que $\mathrm{div}_\gamma\, H_\eta^3 = 0$. La condition aux limites découle évidemment de

$$n\wedge(\mathrm{rot}_\gamma) = i\gamma n_1 H_\eta^1 - \frac{\partial H_\eta^3}{\partial x_1}n_1 - n_2\frac{\partial H_\eta^3}{\partial x_2} - i\gamma H_\eta^2 n_2 = 0\,.$$

L'étude asymptotique de ces deux problèmes spectraux peut être menée de front à l'aide d'une notion de convergence deux-échelles pour les opérateurs. Néanmoins, dans le cas unidimensionnel, nous avons à notre disposition le formalisme des matrices de monodromie qui simplifie les calculs et l'interprétation physique du résultat (voir la section 5). Remarquons que dans le cas 1D, la résolution du problème spectral permet de déterminer complètement la propagation à travers un guide planaire multi-couches. En effet, dans ce cas le problème est uni-dimensionnel et si nous prenons pour ouvert Ω l'intervalle $]0;1[$ et représentons le champ magnétique H_η sous la forme $H_\eta(x_1,x_2) = u_\eta(x_1)e^{i\gamma x_2}e_3$, le problème (7) prend la forme suivante :

Trouver les triplets $(\gamma, k_\eta, u_\eta)\in \mathbb{R}^+\times\mathbb{R}^+\times H^1(]0;1[)$, $u_\eta\not\equiv 0$ tels que :

$$\begin{cases} \dfrac{d}{dx}\Big(\varepsilon_\eta^{-1}(x)\dfrac{du_\eta}{dx}(x)\Big) + (k_\eta^2 - \gamma^2\varepsilon_\eta^{-1}(x))u_\eta(x) = 0 \quad \text{dans }]0;1[\\ {u_\eta}'(0) = 0\ ,\ {u_\eta}'(1) = 0 \end{cases} \tag{11}$$

avec $k_\eta = \dfrac{2\pi}{\lambda_\eta} = \omega\sqrt{\varepsilon_0\varepsilon_\eta\mu_0}$. De plus, $\gamma^2\varepsilon_\eta^{-1}(x)$ étant une perturbation bornée de l'opérateur à résolvante compacte obtenu pour $\gamma = 0$, l'opérateur associé à (11) est lui-même à résolvante compacte.

10.2 Exposé des principaux résultats obtenus

Revenons au problème de la cavité bi-dimensionnelle et considérons des modes tranverses électriques. On cherche donc les couples $(\Lambda_\eta, v_\eta)\in\mathbb{R}^+\times H^1(\Omega)$ $v_\eta\not\equiv 0$ tels que

$$\begin{cases} -div(\varepsilon^{-1}(x,\dfrac{x}{\eta})\bigtriangledown v_\eta) = \dfrac{1}{\Lambda_\eta}v_\eta & \text{dans } \Omega \\ \dfrac{\partial v_\eta}{\partial n} = 0 & \text{sur } \partial\Omega \end{cases} \tag{1}$$

$\varepsilon(x,y)\in[C(\overline{\Omega};L^\infty_\sharp(Y))]^9$ matrice symétrique et coercive. Soit $\eta>0$ fixé. Pour étudier le spectre du problème (1) on se ramène à l'étude du spectre de l'opérateur de Green (opérateur inverse) S_η défini pour tout $f\in L^2(\Omega)$ par $S_\eta f = u_\eta$ où u_η est la solution unique (par le lemme de Lax-Milgram) dans $H^1(\Omega)$ de

$$\begin{cases} -div(\varepsilon^{-1}(x,\dfrac{x}{\eta})\bigtriangledown u_\eta) = f & \text{dans } \Omega \\ \dfrac{\partial u_\eta}{\partial n} = 0 & \text{sur } \partial\Omega \end{cases}$$

S_η est autoadjoint compact dans $\mathcal{L}(L^2(\Omega))$ et donc son spectre $\sigma(S_\eta)$ est de la forme $\sigma(S_\eta) = \{0\} \bigcup \bigcup_{k\geq 1} \lambda_\eta^k$ avec $\Lambda_\eta^1 \geq \Lambda_\eta^2 \geq \Lambda_\eta^k \geq ...$ et $\lim_{k\to+\infty} \Lambda_\eta^k = 0$. À chaque Λ_η^k on associe une fonction propre $v_\eta^k \in L^2(\Omega)$ telle que $\|v_\eta^k\|_{L^2(\Omega)}=1$ et la famille v_η^k est une base orthonormale de $L^2(\Omega)$. Dans ce chapitre, on s'intéresse au comportement asymptotique du spectre $\sigma(S_\eta)$ quand la période η tend vers 0.

Pour ce qui concerne les basses fréquences, un résultat d'homogénéisation classique [56] est que la suite d'opérateurs S_η converge fortement vers un opérateur limite S défini pour tout $f \in L^2(\Omega)$ par $Sf = u$ où u est la solution unique dans $H^1(\Omega)$ du problème homogénéisé suivant :

$$\begin{cases} -div(\varepsilon_{hom}^{-1}(x) \bigtriangledown u) = f & \text{dans } \Omega \\ \dfrac{\partial u}{\partial n} = 0 & \text{sur } \partial\Omega \end{cases}$$

où ε_{hom} est la matrice homogénéisée habituelle. Il en résulte que lorsque la période $\eta \to 0$, $\sigma(S_\eta)$ converge vers $\sigma(S)$, spectre de l'opérateur $Sf = u$. L'opérateur S est autoadjoint compact et son spectre $\sigma(S) = \{0\} \bigcup \bigcup_{k\geq 1} \Lambda^k$ où les valeurs propres sont rangées par ordre décroissant et $\lim_{k\to+\infty} \Lambda^k = 0$.

Du principe du min-max, on en déduit que $\forall k \geq 1$, $\lim_{\eta\to 0} {\Lambda_\eta}^k = \Lambda^k$[5]. Néanmoins, cette convergence ne décrit pas le comportement asymptotique des suites de valeurs propres ${\Lambda_\eta}^{k(\eta)}$ quand $\eta \to 0$, pour une suite $k(\eta)$ tendant vers $+\infty$ (ce qui correspond aux hautes fréquences $\frac{1}{\Lambda_\eta}$).

Comme dans [5][6][7], nous allons étudier les valeurs propres de l'ordre de grandeur η^2 en effectuant un changement de variable dans le problème (1). Résoudre (1) revient alors à trouver $(\mu_\eta, v_\eta) \in \mathbb{R}^+ \times H^1(\Omega)\, v_\eta \not\equiv 0$ tels que :

$$\begin{cases} -\eta^2 div(\varepsilon^{-1}(x, \dfrac{x}{\eta}) \bigtriangledown v_\eta) + v_\eta = \dfrac{1}{\mu_\eta} v_\eta & \text{dans } \Omega \\ \dfrac{\partial v_\eta}{\partial n} = 0 & \text{sur } \partial\Omega \end{cases} \tag{2}$$

Cette transformation de (1) en (2) laisse invariant les vecteurs propres et change les valeurs propres Λ_η^k en $\mu_\eta^k = \frac{\Lambda_\eta^k}{\eta^2+\Lambda_\eta^k}$, ce qui permet d'avoir $\mu_\eta \sim 1$ si $\Lambda_\eta \sim \eta^2$.

On associe au problème (2) un nouvel opérateur $S_\eta \in \mathcal{L}(L^2(\Omega))$ défini par $S_\eta f = u_\eta$ où u_η est l'unique solution dans $H^1(\Omega)$ du problème suivant :

$$\begin{cases} -\eta^2 div(\varepsilon^{-1}(x, \dfrac{x}{\eta}) \bigtriangledown u_\eta) + u_\eta = f & \text{dans } \Omega \\ \dfrac{\partial u_\eta}{\partial n} = 0 & \text{sur } \partial\Omega \end{cases} \tag{3}$$

avec $f \in L^2(\Omega)$ et $\varepsilon(x, y) \in [C(\overline{\Omega}; L^\infty_\sharp(Y))]^9$ symétrique coercive. On peut vérifier que cet opérateur S_η converge faiblement vers l'identité [5], mais cela ne donne aucune information sur la convergence des spectres. Nous substituons à cette convergence faible de S_η une convergence à deux échelles où l'opérateur limite S_K (défini pour toute valeur $K \in \mathbb{N}^*$)

opère sur un espace de type

$$L^2_\sharp(\Omega\times KY) = \left\{ u : \Omega\times\mathbb{R}^N \longmapsto \mathbb{C},\ u(x,.)KY\text{-périodique}\ ,\ \iint_{\Omega\times KY} \mid u(x,y)\mid^2 dxdy < +\infty \right\}$$

La limite des spectres S_η sera alors déduite de la famille des spectres σ_K de S_K ($K \in \mathbb{N}^*$) en utilisant une décomposition par ondes de Bloch.

Cette façon de procéder est inspirée de la méthode dite "méthode d'homogénéisation par ondes de Bloch" introduite par G.Allaire et C.Conca dans [5][6][7] et qui consiste en une combinaison des méthodes de convergence à deux échelles [2] et de décomposition par ondes de Bloch [25][81].

L'introduction de cette méthode est partie de la constatation que si on homogénéise le problème (2), le spectre de l'opérateur homogénéisé ne coïncide pas avec le spectre de l'opérateur limite obtenu avec une méthode de décomposition par ondes de Bloch classique. L'idée de G.Allaire et C.Conca a été de travailler sur l'homothétique par un multiple $K \geq 1$ de la cellule de base $Y = [0;1]^2$. Lorsque l'on fait tendre $K \to +\infty$ le spectre de l'opérateur limite S^K converge vers la réunion du spectre de l'opérateur homogénéisé et du spectre de Bloch. La méthode d'homogénéisation par ondes de Bloch permet de caractériser une partie du spectre de l'équation qui se concentre à l'origine alors que dans les méthodes classiques d'homogénéisation les valeurs propres convergent dans $]0;+\infty[$. Cette partie du spectre est connue sous le nom de spectre de Bloch et est formée de limites de suites de valeurs propres μ^k_η telles que $\|\mu^k_\eta\|_{L^2(\Omega)} = 1$ avec $\mu^k_\eta \sim \eta^2$.

Notre présentation diffère de celle de G.Allaire et C.Conca en ce que ces derniers ont préféré travailler dans un espace fixe et pour ce faire ont dû prolonger les opérateurs S_η. Nous avons préféré introduire une notion de convergence à deux échelles pour une suite d'opérateurs dans $\mathcal{L}(L^2(\Omega))$ vers un opérateur dans $\mathcal{L}(L^2_\sharp(\Omega \times KY))$. Nous avons étendu certains théorèmes de convergence de familles spectrales ayant lieu dans un espace de Hilbert fixe au cas où l'opérateur limite n'est pas défini sur le même Hilbert. S'agissant du problème traîté, cette méthode nous permet de déduire un résultat de convergence pour les valeurs propres Λ_η convergeant en η^2. On introduit pour cela une famille de problèmes limites :

pour chaque $(x,\theta) \in \overline{\Omega} \times Y$, trouver $(\mu(x,\theta), v(y)) \in \mathbb{R}^+ \times H^1_\sharp(Y), \|v\|_{L^2(\Omega)} = 1$, tels que

$$-div_y[\varepsilon^{-1}(x,y) \bigtriangledown_y (v(y)e^{2\pi i\theta.y})] + v(y)e^{2\pi i\theta.y} = \frac{1}{\mu(x,\theta)} v(y)e^{2\pi i\theta.y} \text{ dans } Y \qquad (4)$$

On note $\sigma(x,\theta) = \{0\} \cup \bigcup_{k\geq 1}\{\mu^k(x,\theta)\}$ le spectre du problème (4) qui est aussi constitué de l'adhérence d'une suite dénombrable de valeurs propres qui tend vers 0. On montre que à k fixé $\mu^k(x,\theta)$ est une fonction continue de (x,θ). On définit alors le spectre de Bloch (spectre par bandes) comme suit :

$$\sigma_{Bloch} = \{0\} \cup \bigcup_{k\geq 1} [\min_{(x,\theta)\in\overline{\Omega}\times Y} \mu^k(x,\theta); \max_{(x,\theta)\in\overline{\Omega}\times Y} \mu^k(x,\theta)]$$

où σ_{Bloch} n'est autre que $\sigma(S)$ spectre de l'opérateur

$$S : f(x,y) \in L^2(\Omega \times \mathbb{R}^2) \longmapsto w(x,y) \in L^2(\Omega \times \mathbb{R}^2)$$

où $w \in L^2(\Omega; H^1(\mathbb{R}^2))$ est la solution du problème suivant :

Trouver $w \in L^2(\Omega; H^1(\mathbb{R}^2))$ tel que :

$$-div_y[\varepsilon^{-1}(x,y) \bigtriangledown_y w(x,y)] + w(x,y) = f(x,y)$$

On montre que $\sigma_{Bloch} \subset \sigma_0$ où σ_0 est la limite (au sens de Kuratowsky) des ensembles $\eta^{-2}\sigma(S_\eta)$.

Dans la suite de l'étude, nous ne donnons que des résultats partiels : notre objectif est avant tout de mettre en avant les phénomènes physiques mis en jeu et d'en esquisser une approche théorique. Nous illustrons notre propos par une étude numérique dans le cas unidimensionnel grâce au formalisme des matrices de transfert. Cette approche est inadaptable au cas d'une dimension supérieure où le formalisme matriciel doit être abandonné au profit de la théorie spectrale des opérateurs.

La deuxième partie de l'étude consisterait à étudier la complétude du spectre limite [5]. En d'autres termes, il s'agirait de montrer sous quelles conditions $\sigma_0 = \sigma_{Bloch}$. Ce doit être le cas si $\sigma_0 \subset \sigma_{Bloch}$, c'est à dire si toute valeur d'adhérence d'une suite $\mu_\eta \subset \sigma_\eta$ appartient à σ_{Bloch} [5][4][6][7]. Ceci n'est vrai pour une suite $\mu_\eta \in \sigma_\eta$ ($\mu_\eta \to \mu$) que si la suite de vecteurs propres associés v_η ($\|v_\eta\|_{L^2(\Omega)} = 1$) ne concentre pas son support sur $\partial\Omega$ [5]. On a en effet l'alternative suivante : soit la suite v_η peut être tronquée afin d'avoir un support compact dans Ω et devenir une suite de quasi-vecteurs propres associée à la suite de valeurs propres μ_η au sens suivant :

$$\begin{cases} v_\eta \text{ a un support compact dans } \Omega & , \ \|v_\eta\|_{L^2(\Omega)} = 1 \ , \ \eta\|\nabla v_\eta\|_{L^2(\Omega)} \leq C \\ -\eta^2 div[a(\dfrac{x}{\eta})\nabla v_\eta] + v_\eta = \dfrac{1}{\mu_\eta} v_\eta + r_\eta & , \text{ dans } \Omega \end{cases}$$

où r_η est un reste négligeable qui vérifie $\lim_{\eta \to 0} < r_\eta, w_\eta >_{H^{-1},H^1} = 0$ pour toute suite w_η telle que

$$\|w_\eta\|_{L^2(\Omega)} + \eta\|\nabla w_\eta\|_{L^2(\Omega)} \leq C \ ;$$

soit la suite v_η tend très vite vers 0 à l'intérieur de Ω et se concentre sur le bord $\partial\Omega$ au sens que pour tout ouvert ω tel que $\bar{\omega} \subset \Omega$ et pour tout entier $n \geq 0$, il existe une constante $c(\omega, n)$ telle que la suite v_η satisfait l'estimation

$$\|v_\eta\|_{L^2(\omega)} + \eta\|\nabla v_\eta\|_{L^2(\omega)} \leq c(\omega, n)\eta^n \ .$$

Le spectre de couche limite σ_{bord} est alors défini par les limites de valeurs propres μ telles que les vecteurs propres associés se concentrent sur $\partial\Omega$ [5][6][7]. Dans le cas contraire (une partie de l'énergie de la suite v_η reste à l'intérieur de Ω et on peut alors la tronquer pour construire une suite de quasi vecteurs propres), la valeur propre μ appartient au spectre de Bloch, ce qui montre le résultat de complétude suivant :

$$\sigma_0 = \sigma_{Bloch} \bigcup \sigma_{bord}$$

On est en droit de s'interroger sur l'aspect quelque peu arbitraire du rééchelonnement en η^2 : qu'advient-il du spectre limite pour les autres fréquences ? Il s'avère que pour les autres échelles, le résultat est plus simple [7][6] en ce sens qu'il n'y a pas d'intéraction entre la période η et la fréquence. En effet, il peut être établi en utilisant une notion de convergence trois-échelles [3] que pour toute suite s_η dans $\mathbb{R}^+$ qui tend vers 0 quand η tend vers 0 et telle que

$$\lim_{\eta\to 0} \eta^{-1} s_\eta = 0 \text{ ou } \lim_{\eta\to 0} \eta^{-1} s_\eta = +\infty$$

le spectre limite est donné par

$$\lim_{\eta\to 0} (s_\eta)^{-2} \sigma_\eta = \mathbb{R}^+$$

Remarques :

1) Ce résultat est bien en accord avec le cas particulier bien connu d'une cavité métallique sans hétérogénéïtés : si $\varepsilon(x, y)$ est une constante, la limite du spectre renormalisé du Laplacien conduit évidemment toujours à $\mathbb{R}^+$.

2) Supposons que l'ouvert Ω soit un cube de taille L et que la condition aux limites de Neumann sur $\partial\Omega$ soit remplacée par une condition de périodicité. Si de plus $\varepsilon(x_1, x_2)$ est périodique dans les deux variables x_1 et x_2, alors pour la suite de périodes $\varepsilon_n = \frac{L}{n}$, où n est entier, G. Allaire et C. Conca ont montré [7][8] que $\sigma_0 = \sigma_{Bloch}$.

En général, on ne peut pas expliciter le spectre de couche limite σ_{bord}. Cependant, si Ω est un parallélépipède qui, pour une sous-suite η, se divise en un nombre fini de cellules entières, on peut caractériser complètement σ_{bord} à l'aide d'une variante de la méthode d'homogénéisation par ondes de Bloch. On utilise alors une modification de la convergence à deux-échelles adaptée à des fonctions oscillantes dans la direction tangente à $\partial\Omega$ et qui décroissent à l'infini dans la direction perpendiculaire à ce bord [7][8](elles modélisent, en quelque sorte, des couches limites).

On peut en particulier caractériser complètement σ_{bord} dans le cas d'un multicouches à parois métalliques : le spectre de couche limite est alors donné par la résolution du problème aux valeurs propres suivant : trouver les couples $(\Lambda, \varphi) \in \mathbb{R}^+ \times H^1(]0;+\infty[)$, $\varphi \not\equiv 0$, tels que

$$\begin{cases} -\dfrac{d}{dy}\left(\dfrac{1}{\varepsilon(y)}\dfrac{d}{dy}\varphi(y)\right) = \dfrac{1}{\Lambda}\varphi(y) & \text{dans }]0;+\infty[\\ \varphi'(0) = 0 \ \text{ et } \lim\limits_{y\to+\infty} \varphi(y) = 0 \end{cases}$$

A l'aide du formalisme des matrices de transfert, on montre que ce problème revient à trouver les couples $(\Lambda, \varphi) \in \mathbb{R}^+ \times H^1(]0;1[)\ \varphi \not\equiv 0$ tels que

$$\begin{cases} -\dfrac{d}{dy}\left(\dfrac{1}{\varepsilon(y)}\dfrac{d}{dy}\varphi(y)\right) = \dfrac{1}{\Lambda}\varphi(y) & \text{dans }]0;1[\\ \varphi'(0) = 0 \ \text{ et } \ \varphi'(1) = 0 \end{cases}$$

le spectre de cet opérateur étant à résolvante compacte, on obtient une suite croissante de valeurs propres discrètes.

En conclusion le but de ce chapitre est de caractériser la limite σ_0 de la suite $\eta^{-2}\sigma(S_\eta)$ quand η converge vers 0 dans le cas particulier d'une cavité résonnante consituée d'un

milieu périodique hétérogène. Nous sommes en mesure d'établir que $\sigma_{Bloch} \subset \sigma_0$ dans le cas bi-dimensionnel à l'aide d'une notion de convergence deux échelles pour des opérateurs. Dans le cas d'une cavité 1D, nous caractérisons complètement le spectre $\sigma_0 = \sigma_{bloch} \bigcup \sigma_{bord}$ à l'aide du formalisme des matrices de transfert. Par ailleurs, nous obtenons des résultats numériques sur les modes de bord à partir du problème spectral limite posé dans $]0;1[$. La généralisation de l'étude aux guides métalliques de type cristal photonique fait l'objet d'un article en préparation[35].

10.3 Description des outils

10.3.1 Rappels de théorie spectrale

Soit (S_η) une suite d'opérateurs bornés autoadjoints dans un espace de Hilbert H qui converge fortement vers un opérateur S dans $\mathcal{L}(H)$ i.e. $S_\eta u \to Su$, $\forall u \in H$. D'après le théorème de Banach- Steinhaus, S est borné et on vérifie aisément qu'il est autoadjoint. On veut en déduire une convergence sur les spectres de ces opérateurs. On définit pour cela des opérateurs de projection sur H, associés aux opérateurs S_η et S, appelés familles spectrales de S_η et S. Leurs propriétés sont données par le résultat classique [183] suivant :

Théorème 1 (théorème spectral)
Soient H un espace de Hilbert complexe et $A \in \mathcal{L}(H)$ un opérateur autoadjoint. On note alors son spectre $\sigma(A)$ qui vérifie $\sigma(A) \subset [m_-, m_+] \subset \mathbb{R}$. Il existe une unique famille $\{E_\lambda\}_{\lambda\in\mathbb{R}}$ de projections autoadjointes telles que :
i) L'application $\lambda \longmapsto E_\lambda$ est fortement continue à droite.
ii) $E_\lambda = 0$ si $\lambda < m_-$ et $E_\lambda = I$ si $\lambda \geq m_+$.
iii) L'application $\lambda \longmapsto E_\lambda$ est croissante i.e. $E_\lambda \geq E_\mu$ si $\lambda \geq \mu$.
iv) Chaque projection E_λ de la famille spectrale de A commute avec tout opérateur borné B qui commute avec A.

On définit alors pour toute fonction continue f sur $[m_-, m_+]$ l'opérateur $f(A) \in \mathcal{L}(H)$ par :

$$f(A) = \int_{-\infty}^{m_+} f(\lambda) dE_\lambda$$

L'opérateur $f(A)$ coïncide avec la notion usuelle lorsque f est un polynôme, et si g est une fonction continue sur $[m_-; m_+]$ on a les règles de calcul suivantes :

$$(fg)(A) = f(A)g(A) \ \text{ et } \ (f+g)(A) = f(A) + g(A)$$

Théorème 2 (convergence des familles spectrales)
Soit (S_η) une famille d'opérateurs autoadjoints de $\mathcal{L}(H)$ telle que $S_\eta u \to Su$ fortement, $\forall u \in H$ (convergence forte de S_η vers S). Alors S est autoadjoint, et on a la convergence forte des familles spectrales :

$$\forall u \in H \ , \ \forall \lambda \notin \sigma(S) \ , \ E_\lambda(S_\eta)u \to E_\lambda(S)u \ \ \textit{fortement} \ \ , \ \ \textit{quand} \ \lambda \to 0$$

On se propose de donner une version du théorème 2 où l'hypothèse de convergence forte de (S_η) est remplacée par une condition de convergence forte à deux-échelles d'opérateurs telle que définie dans la section qui suit.

10.3.2 Convergence à deux échelles d'une suite d'opérateurs

Dans ce qui suit, on fixe K entier ≥ 1 et on travaille sur la cellule de dimension K $KY =]0; K[^N$ et avec l'espace $L^2_\sharp(\Omega \times KY)$. Tous les résultats propres au cas $K = 1$ du chapitre 2 s'adaptent. Il suffit de remplacer la notion de fonction admissible par :

Définition 3

Soit Ω un ouvert de $\mathbb{R}^N$. La fonction $\varphi \in L^2_\sharp(\Omega \times KY)$ est dite admissible si la suite $\varphi_\eta(x) = \varphi(x, \frac{x}{\eta})$ est bornée dans $L^2(\Omega)$ et vérifie

$$\lim_{\eta\to 0} \int_\Omega \mid \varphi(x, \frac{x}{\eta}) \mid^2 dx = \frac{1}{K^N} \iint_{\Omega\times KY} \mid \varphi \mid^2 (x,y)\, dxdy$$

Les propositions 2, 3 et 4 du chapitre 2 se transposent immédiatement avec la notion de convergence à deux-échelles (faible et forte) relativement à l'entier K suivante :

Définition 4

i) Une suite (u_η) de $L^2(\Omega)$ converge faiblement à deux-échelles relativement à l'entier K vers une fonction $u_0(x,y) \in L^2_\sharp(\Omega \times KY)$ (ce que l'on note $u_\eta \overset{K}{\rightharpoonup} u_0(x,y)$) si pour toute fonction ψ admissible on a :

$$\lim_{\eta\to 0} \int_\Omega u_\eta(x)\psi(x, \frac{x}{\eta})\, dx = \frac{1}{K^N} \iint_{\Omega\times KY} u_0(x,y)\psi(x,y)\, dxdy$$

ii) Une suite (u_η) de $L^2(\Omega)$ converge fortement à deux échelles relativement à l'entier K vers une fonction $u_0(x,y) \in L^2_\sharp(\Omega \times KY)$ (ce que l'on note $u_\eta \overset{K}{\rightarrow\!\!\!\!\!\rightharpoonup} u_0(x,y)$) si

$$\lim_{\eta\to 0} \int_\Omega \mid u_\eta \mid^2 dx = \frac{1}{K^N} \iint_{\Omega\times KY} \mid u_0(x,y) \mid^2 dxdy$$

Dans la suite, on omettra (sauf en cas d'ambiguïté) de préciser l'entier K.

Définition 5

i) L'opérateur $S \in \mathcal{L}(L^2_\sharp(\Omega \times KY))$ est admissible si $\forall f$ admissible, Sf est admissible.

ii) La suite (S_η) de $\mathcal{L}(L^2(\Omega))$ converge fortement à deux-échelles vers l'opérateur $S \in \mathcal{L}(L^2_\sharp(\Omega \times KY))$ si

$$\forall f \text{ admissible } ,\ S_\eta(f(x, \frac{x}{\eta})) \twoheadrightarrow S(f) \text{ fortement à deux-échelles}$$

Notre objectif est de déduire de la définition précédente une convergence forte à deux échelles des familles spectrales associées à la suite d'opérateurs S_η.

Proposition 6

Soit (S_η) une famille d'opérateurs bornés autoadjoints dans $\mathcal{L}(L^2(\Omega))$, $S \in \mathcal{L}(L^2_\sharp(\Omega, KY))$ et $\lambda \in \mathbb{C}$ tels que :

i) $S_\eta \twoheadrightarrow S$ fortement.

ii) S est admissible.

iii) λ n'est pas valeur propre de S.

Alors S est auto-adjoint sur $L^2_\sharp(\Omega, KY)$ et on a la convergence forte à deux-échelles $E_\lambda(S_\eta) \twoheadrightarrow E_\lambda(S)$.

Démonstration :

On commence la preuve sous l'hypothèse que $\lambda = 0$.

première étape : $\exists C > 0$ telle que $\|S_\eta\|_{\mathcal{L}(L^2(\Omega))} \leq C$ et $\|S\|_{\mathcal{L}(L^2(\Omega\times KY))} \leq C$
D'après i), il vient :

$$\forall \eta > 0\ ,\ \forall f \in \mathcal{D}(\Omega; C^\infty_\sharp(KY))\ ,\ \|S_\eta f(x, \frac{x}{\eta})\|_{L^2(\Omega)} \leq \|Sf(x, \frac{x}{\eta})\|_{L^2(\Omega)} + \eta \tag{1}$$

Comme Sf est admissible, $\sup_\eta \|S_\eta f(x, \frac{x}{\eta})\|_{L^2(\Omega)} \leq \|Sf(x, \frac{x}{\eta})\|_{L^2(\Omega\times KY)} < +\infty$.

Le théorème de Banach-Steinhaus appliqué à la suite d'opérateurs $S_\eta \in \mathcal{L}(L^2(\Omega))$ nous assure que $\sup_\eta \|S_\eta\|_{\mathcal{L}(L^2(\Omega))} < +\infty$ autrement dit, il existe une constante $C > 0$ (indépendante de η) telle que

$$\|S_\eta f(x, \frac{x}{\eta})\|_{L^2(\Omega)} \leq C\|f(x, \frac{x}{\eta})\|_{L^2(\Omega)}\ ,\ \forall \eta > 0\ ,\ \forall f \in \mathcal{D}(\Omega; C^\infty_\sharp(KY)) \tag{2}$$

Prenant $f(x, y) = f(x) \in \mathcal{D}(\Omega)$ dans (2), par densité de $\mathcal{D}(\Omega)$ dans $L^2(\Omega)$ on obtient que :

$$\|S_\eta f(x)\|_{L^2(\Omega)} \leq C\|f(x)\|_{L^2(\Omega)}\ ,\ \forall \eta > 0\ ,\ \forall f \in L^2(\Omega) \tag{3}$$

On a donc établi l'existence d'une constante $C > 0$ (indépendante de η) telle que $\|S_\eta\|_{\mathcal{L}(L^2(\Omega))} \leq C$. Notant par ailleurs que $S_\eta \twoheadrightarrow S$ fort à deux échelles, on déduit de (3) que :

$$\begin{aligned}
\frac{1}{K^N}\iint_{\Omega\times KY} |\ Sf(x,y)\ |^2\, dxdy &= \lim_{\eta\to 0}\int_\Omega |\ S_\eta f(x, \frac{x}{\eta})\ |^2\, dx \\
&\leq C^2 \lim_{\eta\to 0}\int_\Omega |\ f(x, \frac{x}{\eta})\ |^2\, dx \\
&= C^2 \frac{1}{K^N}\iint_{\Omega\times KY} |\ f(x,y)\ |^2\, dxdy
\end{aligned}$$

Cela établit que $S \in \mathcal{L}(L^2(\Omega \times KY))$.

deuxième étape : Pour tout polynôme $P, P(S_\eta) \twoheadrightarrow P(S)$ fort à deux échelles
Pour toute fonction f admissible, on a :

$$S_\eta(S_\eta f) = S_\eta(Sf(x, \frac{x}{\eta})) + S_\eta(S_\eta f(x, \frac{x}{\eta}) - Sf(x, \frac{x}{\eta})) \tag{4}$$

De (4), on déduit la majoration suivante :

$$\|S_\eta(S_\eta f)\|_{L^2(\Omega)} \leq \|S_\eta(Sf(x, \frac{x}{\eta}))\|_{L^2(\Omega)} + \underbrace{\|S_\eta\|_{\mathcal{L}(L^2(\Omega))}}_{<+\infty}\underbrace{\|S_\eta f(x, \frac{x}{\eta}) - Sf(x, \frac{x}{\eta})\|_{L^2(\Omega)}}_{\to 0}$$

Notant que $\|S_\eta\|_{\mathcal{L}(L^2(\Omega))} < +\infty$ et que $\|S_\eta f(x, \frac{x}{\eta}) - Sf(x, \frac{x}{\eta})\|_{L^2(\Omega)} \to 0$ d'après i), comme Sf est admissible on obtient que :

$$\limsup_{\eta\to 0} \|S_\eta(S_\eta(f(x, \frac{x}{\eta}))\|_{L^2(\Omega)} \leq \|S^2 f(x,y)\|_{L^2(\Omega\times Y)} \tag{5}$$

Par ailleurs, de (4) on tire que pour toute fonction f admissible :

$$\|S_\eta(S_\eta f)\|_{L^2(\Omega)} \geq \|S_\eta(Sf(x, \frac{x}{\eta}))\|_{L^2(\Omega)} - \underbrace{\|S_\eta\|_{\mathcal{L}(L^2(\Omega))}}_{<+\infty}\underbrace{\|S_\eta f(x, \frac{x}{\eta}) - Sf(x, \frac{x}{\eta})\|_{L^2(\Omega)}}_{\to 0}$$

Comme Sf est admissible, en passant à la limite quand $\eta \to 0$ dans l'inégalité précédente, on obtient que :

$$\liminf_{\eta\to 0} \|S_\eta(S_\eta(f(x,\frac{x}{\eta}))\|_{L^2(\Omega)} \geq \|S^2 f(x,y)\|_{L^2(\Omega\times KY)} \tag{6}$$

De (5) et (6) on déduit que :

$$\|S_\eta(S_\eta(f(x,\frac{x}{\eta}))\|_{L^2(\Omega)} \to \|S^2 f(x,y)\|_{L^2(\Omega\times KY)}$$

En itérant le procédé sur $n \in \mathbb{N}$, on a :

$$\|S_\eta^n f(x,\frac{x}{\eta})\|_{L^2(\Omega)} \to \|S^n f(x,y)\|_{L^2(\Omega\times KY)}$$

Il s'ensuit que pour tout $j \in \{1...n\}$ et tout $a_j \in \mathbb{R}$, on a :

$$(a_0 + a_1 S_\eta + a_2 S_\eta^2 + ... + a_j S_\eta^j + ... + a_n S_\eta^n) \twoheadrightarrow (a_0 + a_1 S + a_2 S^2 + ... + a_j S^j + ... + a_n S^n)$$

Donc $\forall P \in \mathbb{R}[X], P(S_\eta) \twoheadrightarrow P(S)$ fort à deux échelles.

troisième étape : Si S_η est autoadjoint et $S_\eta \twoheadrightarrow S$ fort à deux échelles alors S est autoadjoint

S_η est autoadjoint donc $\forall f \in \mathcal{D}(\Omega; C_\sharp^\infty(KY))$ et $\forall \varphi \in \mathcal{D}(\Omega; C_\sharp^\infty(KY))$ on a :

$$\int_\Omega S_\eta f(x,\frac{x}{\eta})\varphi(x,\frac{x}{\eta})\,dx = \int_\Omega f(x,\frac{x}{\eta}) S_\eta\varphi(x,\frac{x}{\eta})\,dx \tag{7}$$

Notant que $\|S_\eta f(x,\frac{x}{\eta}) - Sf(x,\frac{x}{\eta})\|_{L^2(\Omega)} \to O$ $\forall f$ admissible d'après i) on déduit que :

$$\lim_{\eta\to 0}\int_\Omega S_\eta f(x,\frac{x}{\eta})\varphi(x,\frac{x}{\eta})\,dx = \frac{1}{K^N}\iint_{\Omega\times KY} Sf(x,y)\varphi(x,y)\,dxdy \tag{8}$$

De plus, $\|S_\eta\varphi(x,\frac{x}{\eta}) - S\varphi(x,\frac{x}{\eta})\|_{L^2(\Omega)} \to O$ $\forall \varphi$ admissible, ce qui implique que :

$$\lim_{\eta\to 0}\int_\Omega f(x,\frac{x}{\eta}) S_\eta\varphi(x,\frac{x}{\eta})\,dx = \frac{1}{K^N}\iint_{\Omega\times KY} f(x,y) S_\eta\varphi(x,y)\,dxdy \tag{9}$$

De (7), (8) et (9) on déduit que pour toutes fonctions $f \in \mathcal{D}(\Omega; C_\sharp^\infty(KY))$ et $\varphi \in \mathcal{D}(\Omega; C_\sharp^\infty(KY))$, on a :

$$\iint_{\Omega\times KY} Sf(x,y)\varphi(x,y)\,dxdy = \iint_{\Omega\times KY} f(x,y) Sf(x,y)\,dxdy \tag{10}$$

Par densité de $\mathcal{D}(\Omega; C_\sharp^\infty(KY))$ dans $L^2(\Omega; L_\sharp^2(KY))$, on tire de (10) que S est autoadjoint sur $L^2(\Omega; L_\sharp^2(KY))$.

quatrième étape : $\|S_\eta\|_{\mathcal{L}(L^2(\Omega))} \leq C$ et S_η autoadjoint $\Rightarrow \sigma(S_\eta) \subset [-c;c]$

Soit $\lambda \in \mathbb{R}_*^+$ tel que $\lambda > C$. La première étape nous assure que $\|S_\eta\|_{\mathcal{L}(L^2(\Omega))} \leq C$ donc pour tout $u \in L^2(\Omega)$, on a :

$$< S_\eta u, u >_{L^2(\Omega)} \leq C\|u\|^2_{L^2(\Omega)}$$

On en déduit que pour tout $u \in L^2(\Omega)$:

$$< (S_\eta - \lambda I)u, u >_{L^2(\Omega)} \leq (C - \lambda)\|u\|^2_{L^2(\Omega)}$$

soit encore,

$$< -(S_\eta - \lambda I)u, u >_{L^2(\Omega)} \geq (\lambda - C)\|u\|^2_{L^2(\Omega)}$$

Comme $\lambda - C > 0$, $-(S_\eta - \lambda I)$ est $L^2(\Omega)$ elliptique et continue ($\|S_\eta\| \leq C$ et $\|I\| = 1$). Or S_η est autoadjoint donc $-(S_\eta - \lambda I)$ est autoadjoint. Par le lemme de Lax-Milgram $-(S_\eta - \lambda I)$ est un isomorphisme de $\mathcal{L}(L^2(\Omega))$ donc $\lambda \in \rho(S_\eta)$ (l'ensemble résolvant $\sigma(S_\eta) = \mathbb{R} \setminus \rho(S_\eta)$).

De même si $\lambda < -C$, nous sommes assurés que $\lambda \in \rho(S_\eta)$, ce qui établit que $\sigma(S_\eta) \subset [-c; c]$.

D'après le théorème 1 (théorème spectral), si f est une fonction continue sur $[-c; c]$, comme $S_\eta \in \mathcal{L}(L^2(\Omega))$ est un opérateur autoadjoint, alors il existe une unique famille spectrale $\{E_\lambda(S_\eta)\}_\lambda$ telle que $f(S_\eta) = \displaystyle\int_{-c}^{c} f(\lambda)\, dE_\lambda(S_\eta)$. D'après la première étape, nous savons par ailleurs que $\|S\|_{L^2(\Omega; L^2_\sharp(KY))} \leq C$ et S est autoadjoint. On en déduit comme précédemment que $\sigma(S) \subset [-c; c]$ et qu'il existe une unique famille spectrale $\{E_\lambda(S)\}_\lambda$ telle que $f(S) = \displaystyle\int_{-c}^{c} f(\lambda)\, dE_\lambda(S)$.

cinquième étape : $\forall f$ continue sur $[-c; c], f(S_\eta) \twoheadrightarrow f(S)$ fort à deux échelles

Pour tout polynôme P à valeurs réelles et toute fonction $u \in \mathcal{D}(\Omega; C^\infty_\sharp(KY))$ telle que $Su \in \mathcal{D}(\Omega; C^\infty_\sharp(KY))$, on a :

$$\begin{aligned} f(S_\eta)u(x, \tfrac{x}{\eta}) - f(S)u(x, \tfrac{x}{\eta}) &= (f(S_\eta)u(x, \tfrac{x}{\eta}) - P(S_\eta)u(x, \tfrac{x}{\eta})) \\ &\quad + (P(S_\eta)u(x, \tfrac{x}{\eta}) - P(S)u(x, \tfrac{x}{\eta})) \\ &\quad + (P(S)u(x, \tfrac{x}{\eta}) - f(S)u(x, \tfrac{x}{\eta})) \end{aligned} \tag{11}$$

De (11), on déduit la majoration suivante :

$$\begin{aligned} \|f(S_\eta)u(x, \tfrac{x}{\eta}) - f(S)u(x, \tfrac{x}{\eta})\| &\leq \|f(S_\eta)u(x, \tfrac{x}{\eta}) - P(S_\eta)u(x, \tfrac{x}{\eta})\|_{L^2(\Omega)} \\ &\quad + \|(P(S_\eta)u(x, \tfrac{x}{\eta}) - P(S)u(x, \tfrac{x}{\eta}))\|_{L^2(\Omega)} \\ &\quad + \|(P(S)u(x, \tfrac{x}{\eta}) - f(S)u(x, \tfrac{x}{\eta}))\|_{L^2(\Omega)} \end{aligned} \tag{12}$$

Par ailleurs, appliquant le théorème 1 à l'opérateur S_η qui vérifie $\sigma(S_\eta) \subset [-c; c]$, nous sommes assurés que :

$$\begin{aligned} \|f(S_\eta)u(x, \tfrac{x}{\eta}) - P(S_\eta)u(x, \tfrac{x}{\eta})\|_{L^2(\Omega)} &\leq \|u(x, \tfrac{x}{\eta})\|_{L^2(\Omega)} \|f(S_\eta) - P(S_\eta)\|_{\mathcal{L}(L^2(\Omega))} \\ &= \|u(x, \frac{x}{\eta})\|_{L^2(\Omega)} \sup_{y \in [-c;c]} |\, f(y) - P(y)\,| \end{aligned} \tag{13}$$

Comme f est une fonction continue sur $[-c; c]$ à coefficients réels, le théorème de Weierstrass nous assure qu'il existe une suite P_n de polynômes à coefficients réels tels que $\|f - P_n\|_\infty \to 0$ sur $[-c; c]$. On déduit donc de (13) que :

$$\|f(S_\eta)u(x, \frac{x}{\eta}) - P(S_\eta)u(x, \frac{x}{\eta})\|_{L^2(\Omega)} \to 0 \tag{14}$$

Appliquant le théorème 1 à S, on obtient que :

$$\|f(S)u(x,\frac{x}{\eta}) - P(S)u(x,\frac{x}{\eta})\|_{L^2(\Omega)} \to 0 \tag{15}$$

Notant que $\|P(S_\eta)u(x,\frac{x}{\eta}) - P(S)u(x,\frac{x}{\eta})\|_{L^2(\Omega)} \to 0$ d'après la deuxième étape, on déduit de (12), (14) et (15) que pour toute fonction f continue sur $[-c;c]$ et pour tout u admissible tel que Su soit admissible, on a :

$$\|f(S_\eta)u(x,\frac{x}{\eta}) - f(S)u(x,\frac{x}{\eta})\|_{L^2(\Omega)} \to 0 \tag{16}$$

sixième étape : $E_0^\eta \twoheadrightarrow E_0$ fort à deux échelles

On considère la fonction f suivante qui est continue sur $[-c;c]$

$$f(\lambda) = \begin{cases} \lambda & \text{si } \lambda \leq 0 \\ 0 & \text{si } \lambda > 0 \end{cases}$$

Le théorème 1 appliqué à f nous assure que :

$$f(S_\eta) = \int_{-c}^{c} f(\lambda)\, dE_\lambda(S_\eta) = \int_{-c}^{0} \lambda\, dE_\lambda(S_\eta)$$

avec $E_\lambda(S_\eta) = \chi_{]-\infty;\lambda]}(S_\eta)$ et $S_\eta = \displaystyle\int_{-c}^{c} \lambda\, dE_\lambda^\eta$ où $E_\lambda^\eta = E_\lambda(S_\eta)$, soit $f(S_\eta) = E_0^\eta S_\eta$.

De même on montre que $f(S) = E_0(S)$ où $E_0 = E_0(S)$. Par conséquent, (16) nous assure que $E_0^\eta S_\eta \twoheadrightarrow E_0 S$ fort à deux échelles i.e.

$$\|(E_0^\eta S_\eta)f(x,\frac{x}{\eta}) - (E_0 S)f(x,\frac{x}{\eta})\|_{L^2(\Omega)} \to O\,,$$

pour toute fonction f admissible (au sens où f admissible $\Rightarrow Sf$ admissible). On a donc établi que $E_0^\eta \twoheadrightarrow E_0$ fort à deux échelles.

septième étape : si μ n'est pas valeur propre de S alors $E_\mu^\eta \twoheadrightarrow E_\mu$ fort à deux échelles

On considère la suite d'opérateurs $(S_\eta - \mu I)$ qui converge fortement à deux échelles vers l'opérateur $S - \mu I$ car $S_\eta \twoheadrightarrow S$. Si 0 n'est pas valeur propre de S, alors $E_0^\eta \twoheadrightarrow E_0$ fort à deux échelles d'après la sixième étape. Si μ n'est pas valeur propre de S, 0 n'est pas valeur propre de $S - \mu I$ donc $E_0^\eta \twoheadrightarrow E_0$ fort à deux échelles où $E_0^\eta = E_0(S_\eta - \mu I)$ et $E_0 = E_0(S - \mu I)$. On en déduit que $E_\mu^\eta \twoheadrightarrow E_\mu$ fort à deux échelles où $E_\mu^\eta = E_\mu(S_\eta)$ et $E_\mu = E_\mu(S)$.

On établit la proposition en notant que les opérateurs S_η et S sont linéaires continus respectivement sur $\mathcal{D}(\Omega)$ et $\mathcal{D}(\Omega; C_\sharp^\infty(KY))$ qui sont respectivement des sous-espaces denses de $L^2(\Omega)$ et $L^2(\Omega; L_\sharp^2(KY))$.

(QED)

On va maintenant établir un résultat qui permet de caractériser en partie le spectre limite d'une suite d'opérateurs dans $\mathcal{L}(L^2(\Omega))$ qui converge à deux échelles fort vers un opérateur limite $S \in \mathcal{L}(L_\sharp^2(\Omega \times KY))$ (cf. [7]).

Lemme 7

Soit K un entier ≥ 1 et soient $S_\eta \in \mathcal{L}(L^2(\Omega))$ et $S \in \mathcal{L}(L^2(\Omega; L^2_\sharp(KY)))$ des opérateurs autoadjoints. Si $S_\eta \twoheadrightarrow S$ fort à deux échelles alors on a :

i) $\forall \lambda \in \sigma(S)$, il existe une suite $\lambda_\eta \in \sigma(S_\eta)$ telle que $\lambda_\eta \to \lambda$

ii) Soit λ_η une suite de valeurs propres pour S_η qui converge vers λ et u_η une suite telle que $\|u_\eta\|_{L^2(\Omega)} = 1$ et $S_\eta u_\eta = \lambda_\eta u_\eta$. Alors $\lambda \notin \sigma(S) \Rightarrow u_\eta \rightharpoonup 0$ faible à deux échelles.

Démonstration :

i) Soit $\lambda \in \sigma(S)$. Supposons que λ n'est limite d'aucune suite $\lambda_\eta \in \sigma(S_\eta)$.

Donc $\exists \delta > 0$, telle que pour η suffisamment petit, et pour chaque $\lambda_\eta \in \sigma(S_\eta)$ on a $\mid \lambda_\eta - \lambda \mid \geq \delta$.

On en déduit que $\forall u \in \mathcal{D}(\Omega; C^\infty_\sharp(KY))$, $\|S_\eta u(x, \frac{x}{\eta}) - \lambda u(x, \frac{x}{\eta})\|_{L^2(\Omega)} \geq \delta$.

Or $S_\eta \twoheadrightarrow S$ fort à deux échelles, donc pour tout $u \in \mathcal{D}(\Omega; C^\infty_\sharp(KY))$, on a :

$$\|Su(x,y) - \lambda u(x,y)\|_{L^2(\Omega; L^2_\sharp(KY))} \geq \delta$$

Par continuité de S et par densité de $\mathcal{D}(\Omega; C^\infty_\sharp(KY))$ dans $L^2(\Omega; L^2_\sharp(KY))$, on en déduit que :

$$\forall u \in L^2(\Omega; L^2_\sharp(KY)) \ , \ \|Su(x,y) - \lambda u(x,y)\|_{L^2(\Omega; L^2_\sharp(KY))} \geq \delta$$

Ce qui est en contradiction avec le fait que $\lambda \in \sigma(S)$.

ii) Supposons qu'il existe une suite $\lambda_\eta \in \sigma(S_\eta)$ telle que $\lambda_\eta \to \lambda \notin \sigma(S)$. Notant que λ_η est une suite de valeurs propres pour S_η, on a :

$$S_\eta u_\eta = \lambda_\eta u_\eta \ , \ \forall u_\eta \neq 0 \tag{17}$$

Comme $S_\eta \twoheadrightarrow S$ fort à deux échelles, si on note u_0 la limite à deux échelles de u_η, en passant à la limite quand $\eta \to 0$ dans (17), on obtient que :

$$Su_0 = \lambda u_0 \ , \ \forall u_0 \in L^2(\Omega; L^2_\sharp(KY))$$

Puisque $\lambda \notin \sigma(S)$, on en déduit que $u_0(x,y) = 0$.

10.4 Étude du spectre limite aux hautes fréquences

10.4.1 Inclusion du spectre de Bloch dans σ_0

Nous allons appliquer les résultats de la section précédente à l'analyse asymptotique de la cavité hétérogène en polarisation $H \parallel$.

Proposition 8
Soit $\Omega \subset \mathbb{R}^N$ et $Y =]0;1[^N$. Soit le problème $(\mathcal{P}_\eta)$ qui consiste à trouver u_η dans $H^1(\Omega)$ telle que

$$(\mathcal{P}_\eta) \begin{cases} -\eta^2 div(a(x,\frac{x}{\eta}) \bigtriangledown u_\eta) + u_\eta = f(x,\frac{x}{\eta}) & \text{dans } \Omega \\ \dfrac{\partial u_\eta}{\partial n} = 0 & \text{sur } \partial\Omega \end{cases}$$

avec $a(x,y) \in [C(\overline{\Omega}; L^\infty_\sharp(Y))]^{N\times N}$ symétrique coercive et $f(x,y)$ admissible pour la convergence à deux échelles i.e. $f \in L^2(\Omega, C^\infty_\sharp(KY))$. Alors
i) la solution du problème $(\mathcal{P}_\eta)$ est unique dans $H^1(\Omega)$.
ii) $u_\eta \rightharpoonup u_0(x,y)$ faible à deux échelles et $\eta \nabla u_\eta \rightharpoonup \bigtriangledown_y u_0(x,y)$ faible à deux échelles où $u_0(x,y)$ est solution dans $L^2(\Omega; H^1_\sharp(KY))$ de

$$-div_y(a(x,y) \bigtriangledown_y u_0(x,y)) + u_0(x,y) = f(x,y) \tag{0}$$

iii) u_0 est admissible et on a la convergence forte à deux-échelles de u_η vers u_0 (donc $\|u_\eta - u_0(x,\frac{x}{\eta})\|_{L^2(\Omega)} \to 0$).

Démonstration :

i) Existence et unicité de u_η dans $H^1(\Omega)$.
La solution u_η du problème $(\mathcal{P}_\eta)$ vérifie pour tout $\varphi_\eta \in H^1(\Omega)$ l'équation variationnelle

$$\int_\Omega \eta^2 a(x,\frac{x}{\eta}) \nabla u_\eta(x) \cdot \nabla \varphi_\eta(x)\, dx + \int_\Omega u_\eta(x)\varphi_\eta(x)\, dx = \int_\Omega f(x,\frac{x}{\eta})\varphi_\eta(x)\, dx \tag{1}$$

L'existence et l'unicité de u_η relèvent du lemme de Lax-Milgram appliqué dans $H^1(\Omega)$ à la forme bilinéaire symétrique coercive continue

$$b(u,v) = \int_\Omega \eta^2 a(x,\frac{x}{\eta}) \nabla u(x) \cdot \nabla \varphi(x)\, dx + \int_\Omega u(x)\varphi(x)\, dx$$

et à la forme linéaire continue $L(u) = \displaystyle\int_\Omega f(x,\frac{x}{\eta})u(x)\, dx$ (cf. [43]).

ii) première étape : u_η et $\eta \nabla u_\eta$ sont bornées dans $L^2(\Omega)$.
Posant $u_\eta = \varphi_\eta$ dans (1), on obtient :

$$\int_\Omega \eta^2 a(x,\frac{x}{\eta}) |\nabla u_\eta|^2\, dx + \int_\Omega |u_\eta|^2\, dx = \int_\Omega f(x,\frac{x}{\eta})u_\eta(x)\, dx \tag{2}$$

Notant que $a(x,y)$ est coercive et que $|\displaystyle\int_\Omega f(x,\frac{x}{\eta})u_\eta(x)\, dx| \leq \|f_\eta\|_{L^2(\Omega)}\|u_\eta\|_{L^2(\Omega)}$ d'après Cauchy-Schwarz, de (2) on tire qu'il existe une constante $\beta > 0$ telle que :

$$\beta\|\eta \nabla u_\eta\|^2_{L^2(\Omega)^N} + \|u_\eta\|^2_{L^2(\Omega)} \leq \|f_\eta\|_{L^2(\Omega)}\|u_\eta\|_{L^2(\Omega)}$$

On en déduit que $\|u_\eta\|_{L^2(\Omega)} \leq \|f_\eta\|_{L^2(\Omega)}$ et $\|\eta \nabla u_\eta\|_{L^2(\Omega)^N} \leq \frac{1}{\sqrt{\beta}}\|f_\eta\|_{L^2(\Omega)}$.

Quitte à extraire une sous-suite, on peut supposer que $u_\eta \rightharpoonup u_0(x,y)$ et qu'il existe une fonction χ dans $[L^2(\Omega; H^1_\sharp(KY))]^N$ telle que $\eta \nabla u_\eta \rightharpoonup \chi$. Par ailleurs, puisque f est admissible, on a $f_\eta \twoheadrightarrow f_0(x,y)$.

deuxième étape : u_0 est solution du problème (0).

En choisissant une fonction test $\varphi_\eta(x) = \varphi(x, \frac{x}{\eta})$ dans (1) avec $\varphi(x,y)$ admissible, on obtient :

$$\int_\Omega a(x,\frac{x}{\eta})\Big(\eta \nabla u_\eta(x)\Big)\cdot\Big(\eta \nabla \varphi + \nabla_y \varphi\Big)(x,\frac{x}{\eta})\,dx + \int_\Omega u_\eta(x)\varphi(x,\frac{x}{\eta})\,dx = \int_\Omega f(x,\frac{x}{\eta})\varphi(x,\frac{x}{\eta})\,dx$$

Tenant compte de la convergence forte à deux-échelles de la suite $a(x,\frac{x}{\eta})\Big(\eta \nabla \varphi + \nabla_y \varphi\Big)(x,\frac{x}{\eta})$ ainsi que de celle de $f_\eta(x) = f(x,\frac{x}{\eta})$, on déduit par passage à la limite quand η tend vers 0 dans l'expression précédente que :

$$\frac{1}{K^N}\iint_{\Omega\times KY} a(x,y)\chi(x,y)\cdot \bigtriangledown_y \varphi(x,y)\,dxdy + \frac{1}{K^N}\iint_{\Omega\times KY} u_0(x,y)\varphi(x,y)\,dxdy$$

$$= \frac{1}{K^N}\iint_{\Omega\times KY} f(x,y)\varphi(x,y)dxdy$$

d'où en localisant en x, l'équation :

$$p.p.x \in \Omega\ ,\ -div_y(a\chi(x,.)) + u_0(x,.) = f(x,.)\ ,\ \text{ dans } \mathcal{D}'(\mathbb{R}^N)$$

Pour montrer que u_0 est solution de (0), il suffit donc de vérifier que $\chi(x,.) = \nabla_y u_0(x,.)$.

Par hypothèse, $\eta \nabla u_\eta \rightharpoonup \chi_0(x,y) \in [L^2(\Omega\times KY)]^N$, donc en intégrant par parties, on en déduit que pour toute fonction $\varphi \in [\mathcal{D}(\Omega; C^\infty_\sharp(KY))]^N$

$$\begin{aligned}\frac{1}{K^N}\iint_{\Omega\times KY} \chi_0(x,y)\varphi(x,y)\,dxdy &= \lim_{\eta\to 0}\int_\Omega \eta \nabla u_\eta \varphi(x,\frac{x}{\eta})\,dx \\ &= \lim_{\eta\to 0}[-\int_\Omega \eta u_\eta (div_x\varphi)(x,\frac{x}{\eta})\,dx - \int_\Omega u_\eta (div_y\varphi)(x,\frac{x}{\eta})\,dx]\end{aligned}$$

Comme la suite $\varphi(x,\frac{x}{\eta})$ converge fortement à deux-échelles vers $\varphi(x,y)$, on en déduit que :

$$\frac{1}{K^N}\iint_{\Omega\times KY} u_0(x,y)(div_y\varphi)(x,y)\,dxdy = -\frac{1}{K^N}\iint_{\Omega\times KY} \chi_0(x,y)\varphi(x,y)\,dxdy$$

En intégrant par parties, il s'en suit que :

$$\iint_{\Omega\times KY} (\chi_0(x,y) - \bigtriangledown_y u_0(x,y))\,dxdy = 0\ \forall \varphi \in [\mathcal{D}(\Omega; C^\infty_\sharp(KY))]^N$$

D'où en localisant en x, l'équation suivante vraie dans $[\mathcal{D}'(KY)]^N$:

$$p.p.x \in \Omega\ ,\ \chi_0(x,.) = \bigtriangledown_y u_0(x,.)$$

iii) La suite (u_η) converge fortement à deux-échelles vers u_0.

On veut montrer que $\limsup_{\eta\to 0} \int_\Omega |\, u_\eta \,|^2\, dx \le \frac{1}{K^N} \iint_{\Omega\times KY} |\, u_0(x,y) \,|^2\, dxdy$.

D'après le lemme de Lax-Milgram, la solution unique $u_\eta \in H^1(\Omega)$ de $\mathcal{P}_\eta$ est solution du problème de minimisation suivant

$$\inf_{v\in H^1(\Omega)} J_\eta(v) = \inf_{v\in H^1(\Omega)} \{\frac{\eta^2}{2} \int_\Omega a(x,\frac{x}{\eta})|\, \nabla v \,|^2\, dx - \int_\Omega f_\eta v\, dx + \frac{1}{2}\int_\Omega |\, v \,|^2\, dx\}$$

On en déduit que $\forall v \in H^1(\Omega)$

$$\frac{1}{2}\int_\Omega |\, u_\eta \,|^2\, dx \le -\frac{\eta^2}{2}\int_\Omega a(x,\frac{x}{\eta})|\, \nabla u_\eta \,|^2\, dx + \int_\Omega f_\eta u_\eta\, dx + J_\eta(v) \tag{3}$$

Passant à la limite quand $\eta \to 0$ dans (3), on obtient que :

$$\begin{aligned} \limsup_{\eta\to 0} \frac{1}{2}\int_\Omega |\, u_\eta \,|^2\, dx \;&\le \limsup_{\eta\to 0}(-\frac{\eta^2}{2}\int_\Omega a(x,\frac{x}{\eta})|\, \nabla u_\eta \,|^2\, dx) \\ &+ \limsup_{\eta\to 0}(\int_\Omega f_\eta u_\eta\, dx) + \limsup_{\eta\to 0}(J_\eta(v)) \\ &\le -\liminf_{\eta\to 0}(\frac{\eta^2}{2}\int_\Omega a(x,\frac{x}{\eta})|\, \nabla u_\eta \,|^2\, dx) \\ &+ \limsup_{\eta\to 0}(\int_\Omega f_\eta u_\eta\, dx) + \limsup_{\eta\to 0}(J_\eta(v)) \end{aligned} \tag{4}$$

Par ailleurs, ii) nous assure que u_η converge à deux-échelles vers une limite $u_0(x,y)$ qui minimise la fonctionnelle J sur $L^2(\Omega; H^1_\sharp(KY))$. On remplace alors v par $u_0(x,\frac{x}{\eta}) \in \mathcal{D}(\Omega; C^\infty_\sharp(KY))$ dans (4) et on obtient

$$\begin{aligned} \limsup_{\eta\to 0} \frac{1}{2}\int_\Omega |\, u_\eta \,|^2\, dx \;&\le -\frac{1}{2K^N}\iint_{\Omega\times KY} a(x,y)|\, \bigtriangledown_y u_0(x,y) \,|^2\, dxdy \\ &+ \frac{1}{K^N}\iint_{\Omega\times KY} f(x,y)u_0(x,y)\, dxdy + J(u_0(x,y)) \\ &= \frac{1}{K^N}\iint_{\Omega\times KY} |\, u_0(x,y) \,|^2\, dxdy \end{aligned} \tag{5}$$

On étend (5) par densité à $L^2(\Omega; H^1_\sharp(KY))$.

Par ailleurs, notant que f est admissible ($f \in L^2(\Omega, C^\infty(KY))$), u_0 est lui-même admissible et d'après les assertions i) et iii) de la proposition 3 du chapitre 2, on en déduit que $\|u_\eta - u_0(x,\frac{x}{\eta})\|_{L^2(\Omega)} \to 0$.

(QED)

On peut maintenant en déduire un résultat de convergence d'une suite d'opérateurs $S_\eta \in \mathcal{L}(L^2(\Omega))$ vers un opérateur $S^K \in \mathcal{L}(L^2_\sharp(\Omega\times KY))$ comme annoncé dans l'introduction.

Corollaire 9

Soit S_η la suite d'opérateurs définis sur $L^2(\Omega)$ par $S_\eta f = u_\eta$ où u_η est la solution unique dans $H^1(\Omega)$ de

$$\mathcal{P}_\eta \begin{cases} -\eta^2 div(a(x,\frac{x}{\eta}) \bigtriangledown u_\eta) + u_\eta = f & \text{dans } \Omega \\ \dfrac{\partial u_\eta}{\partial n} = 0 & \text{sur } \partial\Omega \end{cases}$$

Alors pour tout entier $K \geq 1$, on a la convergence forte à deux-échelles (relativement à KY) $S_\eta \twoheadrightarrow S^K$ où S^K est l'opérateur sur $L^2_\sharp(\Omega \times KY)$ défini par :

$$S^K f(x,y) = u_0(x,y) \Longleftrightarrow \begin{cases} -div_y(a(x,y) \bigtriangledown_y u_0(x,y)) + u_0(x,y) = f(x,y) \\ u_0(x,y) \in H^1_\sharp(KY) \end{cases}$$

Démonstration :

Il suffit de noter que $\forall f$ admissible, $\|u_\eta(x, \frac{x}{\eta}) - u_0(x, \frac{x}{\eta})\|_{L^2(\Omega)} = \|S_\eta f(x, \frac{x}{\eta}) - Sf(x, \frac{x}{\eta})\|_{L^2(\Omega)}$ et d'appliquer la proposition 8 iii).

Pour f admissible $S^K f$ est solution de $-div_y(a(x,y) \bigtriangledown_y u_0(x,y)) + u_0(x,y) = f(x,y)$. La formulation variationnelle associée à cette équation est :

$$\frac{1}{K^N} \iint_{\Omega \times KY} a(x,y) \bigtriangledown_y u_0(x,y) \bigtriangledown_y v_0(x,y)\, dxdy + \frac{1}{K^N} \iint_{\Omega \times KY} u_0(x,y) v_0(x,y)\, dxdy$$
$$= \frac{1}{K^N} \iint_{\Omega \times KY} f(x,y) v_0(x,y)\, dxdy \tag{6}$$

Comme la matrice $a(x,y)$ est coercive, de (6) on tire que :

$$\|u_0(x,y)\|_{L^2(\Omega \times KY)} \leq C \|f\|_{L^2(\Omega \times KY)} \ \forall f \text{ admissible}$$

soit encore

$$\|S^K f\|_{L^2(\Omega \times KY)} \leq C \|f\|_{L^2(\Omega \times KY)} \ \forall f \text{ admissible}$$

L'application S^K est linéaire continue sur l'ensemble des fonctions admissibles qui est un sous-espace dense de $L^2_\sharp(\Omega \times KY)$. Donc S^K se prolonge de manière unique en un opérateur continu sur $L^2_\sharp(\Omega \times KY)$.

On en déduit que $S^K f = u_0(x,y)$, $\forall f \in L^2_\sharp(\Omega \times KY)$, ce qui établit le corollaire.

(QED)

Nous allons maintenant appliquer le corollaire 9 au cas qui nous intéresse.

Corollaire 10

Soit K un entier ≥ 1. Sous les hypothèses du corollaire 9, si λ n'est pas valeur propre de S^K alors $E_\lambda(S_\eta) \twoheadrightarrow E_\lambda(S^K)$ pour la convergence à deux échelles des opérateurs.

Démonstration :

La solution u_η du problème $(\mathcal{P}_\eta)$ dans $H^1(\Omega)$ vérifie l'équation variationnelle suivante :

$$\forall \varphi_\eta \in H^1(\Omega)\ ,\ \int_\Omega \eta^2 a(x, \frac{x}{\eta}) \nabla u_\eta \nabla \varphi_\eta\, dx + \int_\Omega u_\eta \varphi_\eta\, dx = \int_\Omega f \varphi_\eta\, dx \tag{7}$$

Posant $\varphi_\eta = u_\eta$ dans (7) et notant que $\int_\Omega \eta^2 a(x, \frac{x}{\eta}) |\ \nabla u_\eta\ |^2\, dx \geq 0$ (la matrice $a(x,y)$ est coercive), l'inégalité de Cauchy-Schwarz nous assure que :

$$\|u_\eta\|^2_{L^2(\Omega)} \leq \|f\|^2_{L^2(\Omega)} \|u_\eta\|^2_{L^2(\Omega)}$$

soit encore $\|u_\eta\|_{L^2(\Omega)} \leq \|f\|_{L^2(\Omega)}$ ce qui implique que $\|S_\eta f\|_{L^2(\Omega)} \leq \|f\|_{L^2(\Omega)}$. Par conséquent S_η est borné sur $L^2(\Omega)$. Par ailleurs, S_η est autoadjoint (cf. [56]). Le lemme 7 appliqué à la famille d'opérateurs S_η dans $\mathcal{L}(L^2(\Omega))$ autoadjoints qui est telle $S_\eta \twoheadrightarrow S$ fort à deux échelles établit alors le corollaire.

(QED)

Lemme 11

Soit K un entier ≥ 1 et soient S_η la suite d'opérateurs et S l'opérateur limite définis dans le corollaire 9. Alors on a :

i) $\forall \lambda \in \sigma_K(S^K)$, il existe une suite $\lambda_\eta \in \sigma(S_\eta)$ telle que $\lambda_\eta \to \lambda$

ii) Soit λ_η une suite de valeurs propres pour S_η qui converge vers λ et u_η une suite telle que $\|u_\eta\| = 1$ et $S_\eta u_\eta = \lambda_\eta u_\eta$. Alors $\lambda \notin \sigma_K(S^K) \Rightarrow u_\eta \rightharpoonup 0$ faible à deux échelles.

Démonstration :

La suite d'opérateurs $S_\eta \in \mathcal{L}(L^2(\Omega))$ et l'opérateur limite $S \in \mathcal{L}(L^2_{\sharp,K}(\Omega \times Y))$ sont bornés autoadjoints. De plus, $S_\eta \twoheadrightarrow S$ fort à deux échelles, donc on peut appliquer le corollaire 10 (cf. lemme 7).

Il nous faut maintenant clarifier en quel sens les parties des spectres des opérateurs S_η contenant les valeurs propres en η^{-2} convergent vers un spectre limite σ_0. Nous pourrons alors déduire du résultat précédent que pour tout entier $K \geq 1$, le spectre des opérateurs limite S^K opérant sur $L^2_{\sharp,K}(\Omega \times Y)$ est inclu dans σ_0.

Définition :

On appelle limite inférieure au sens de Kuratowsky de la suite $\eta^{-2}\sigma_\eta$ l' ensemble

$K \liminf_{\eta\to 0} \eta^{-2}\sigma_\eta = \Big\{\lambda \in \mathbb{R}\backslash \exists \lambda_\eta \in \sigma(S_\eta)$, telle que $\eta^{-2}\lambda_\eta \to \lambda\Big\}$.

On appelle limite supérieure au sens de Kuratowsky de la suite $\eta^{-2}\sigma_\eta$ l'ensemble

$K \limsup_{\eta\to 0} \eta^{-2}\sigma_\eta = \Big\{\lambda \in \mathbb{R}\backslash \exists \lambda_\eta \in \sigma(S_\eta)$, $\exists k \in \mathbb{N}$, $k \nearrow +\infty$, telle que $\eta^{-2}\lambda_{\eta_k} \to \lambda\Big\}$.

Définition :

On dit que $\eta^{-2}\sigma_\eta$ converge au sens de Kuratowsky vers σ_0 et on note $\eta^{-2}\sigma_\eta \to \sigma$ si $K \liminf_{\eta\to 0} \eta^{-2}\sigma_\eta = K \limsup_{\eta\to 0} \eta^{-2}\sigma_\eta$. Ceci équivaut à

$$\begin{cases} \lambda_\eta \in \sigma(S_\eta)\ ,\ \exists k \in \mathbb{N}\ ,\ k \nearrow +\infty & \text{, telle que } \eta^{-2}\lambda_{\eta_k} \to \lambda \Rightarrow \lambda \in \sigma_0 \\ \forall \lambda \in \sigma_0\ ,\ \exists \lambda_\eta \in \sigma(S_\eta) & \text{, telle que } \eta^{-2}\lambda_\eta \to \lambda \end{cases}$$

Corollaire 12

Soit σ_K le spectre de S^K du corollaire 9. Alors, on a :

$$\forall K \geq 1\ ,\ \sigma_K(S^K) \subset \sigma_0$$

Démonstration :

D'après le lemme 11 i), $\forall K \geq 1$, $\forall \lambda \in \sigma_K(S)$, $\exists \lambda_\eta \in \sigma(S_\eta) \setminus \lambda_\eta \to \lambda$.

où λ_η sont les valeurs propres de l'opérateur S_η rescalé i.e. $S_\eta f = v_\eta$ où v_η est solution du problème suivant :

Trouver $(\mu_\eta, v_\eta) \in \mathbb{R}^+ \times H^1(\Omega)\, v_\eta \not\equiv 0$ tels que

$$\begin{cases} -\eta^2 div(a(x, \frac{x}{\eta}) \bigtriangledown v_\eta) + v_\eta = \frac{1}{\mu_\eta} v_\eta & \text{dans } \Omega \\ \dfrac{\partial v_\eta}{\partial n} = 0 & \text{sur } \partial\Omega \end{cases}$$

Notant que les valeurs propres de l'opérateur S_η initial vérifient $\mu_\eta = \eta^{-2}\lambda_\eta$, nous sommes assurés que $\forall K \geq 1$, $\forall \lambda \in \sigma_K(S)$, $\exists \mu_\eta \in \sigma(S_\eta) \setminus \eta^{-2}\mu_\eta \to \lambda$. On en déduit que $\forall K \geq 1$, $\sigma_K(S^K) \subset \sigma_0$.

(QED)

Nous allons maintenant donner la définition du spectre de Bloch de l'opérateur S^K. Pour cette partie on réfère aux démonstrations de [183]. Considérant l'opérateur $S^K \in \mathcal{L}(L^2_K(\Omega \times Y))$ du corollaire 9, nous définissons son spectre de Bloch comme suit.

Définition 13

Le spectre de Bloch de l'opérateur S^K est défini par :

$$\sigma_{Bloch} = \{0\} \cup \bigcup_{k \geq 1} [\min_{(x,\theta) \in \overline{\Omega} \times Y} \mu^k(x, \theta); \max_{(x,\theta) \in \overline{\Omega} \times Y} \mu^k(x, \theta)]$$

où les $\mu^k(x, \theta)$ sont les valeurs propres des familles de problèmes limites suivant :

pour chaque $(x, \theta) \in \overline{\Omega} \times Y$, trouver $(\mu(x, \theta), v(y)) \in \mathbb{R}^+ \times H^1_\sharp(Y), \|v\|_{L^2(\Omega)} = 1$, tels que

$$-div_y[a(x, y) \bigtriangledown_y (v(y)e^{2\pi i\theta.y})] + v(y)e^{2\pi i\theta.y} = \frac{1}{\mu(x, \theta)} v(y)e^{2\pi i\theta.y} \text{ dans } Y$$

Cette définition s'appuie sur le résultat suivant :

Lemme 14

$\forall K \geq 1$ on peut décomposer le problème limite du corollaire 9 comme suit :
$u_0(x, y)$ solution dans $L^2(\Omega; H^1_\sharp(KY))$ de $-div_y(a(x, y) \bigtriangledown_y u_0(x, y)) + u_0(x, y) = f(x, y)$
en K sous-problèmes $u_j(x, y)$ solution dans $L^2(\Omega; H^1_\sharp(Y))$ de

$$\begin{cases} -div_y[a(x, y) \bigtriangledown_y u_j(x, y)e^{2\pi i\theta.y}] + u_j(x, y)e^{2\pi i\theta.y} = f_j(x, y)e^{2\pi i\theta.y} & \text{dans } \mathcal{D}'(\Omega \times Y) \\ y \longmapsto u_j(x, y) & KY\text{-périodique} \end{cases}$$

où $\theta = \frac{j}{K}$ est la fréquence de Bloch.

Démonstration :

De (6) on tire que pour toute fonction φ dans $L^2(\Omega; H^1_\sharp(KY))$, on a :

$$\frac{1}{K^N} \iint_{\Omega \times KY} a(x, y) \bigtriangledown_y u(x, y) \bigtriangledown_y \varphi(x, y)\, dxdy + \frac{1}{K^N} \iint_{\Omega \times KY} u(x, y)\varphi(x, y)\, dxdy$$
$$= \frac{1}{K^N} \iint_{\Omega \times KY} f(x, y)\varphi(x, y)\, dxdy$$

On applique la décomposition par ondes de Bloch discrète [183].

Il existe des familles $\{\varphi_l(x, y)\}_{0 \leq l \leq K-1} \in L^2(\Omega; [H^1_\sharp(Y)]^K)$, $\{\mu_j(x, y)\}_{0 \leq j \leq K-1} \in L^2(\Omega; [H^1_\sharp(Y)]^K)$ et $\{f_m(x, y)\}_{0 \leq m \leq K-1} \in L^2(\Omega; [H^1_\sharp(Y)]^K)$ uniques telles que

$$\sum_{0\leq j\leq K-1}\sum_{0\leq l\leq K-1}\iint_{\Omega\times Y} a(x,y)\bigtriangledown_y\,(u_j(x,y)e^{2\pi i\frac{j}{K}.y})\bigtriangledown_y\,(\varphi_j(x,y)e^{2\pi i\frac{j}{K}.y})\,dxdy$$
$$+\sum_{0\leq j\leq K-1}\sum_{0\leq l\leq K-1}\iint_{\Omega\times Y}(u_j(x,y)e^{2\pi i\frac{j}{K}.y})(\varphi_j(x,y)e^{2\pi i\frac{j}{K}.y})\,dxdy$$
$$=\sum_{0\leq m\leq K-1}\sum_{0\leq l\leq K-1}\iint_{\Omega\times Y}(f_j(x,y)e^{2\pi i\frac{j}{K}.y})(\varphi_j(x,y)e^{2\pi i\frac{j}{K}.y})\,dxdy$$

On identifie les coefficients correspondant à la même fréquence de Bloch $\frac{j}{K}=\theta$ (propriété d'orthogonalité de la décomposition par ondes de Bloch) :

$$\iint_{\Omega\times Y} a(x,y)\bigtriangledown_y\,(u_j(x,y)e^{2\pi i\theta.y})\bigtriangledown_y\,(\varphi_j(x,y)e^{2\pi i\theta.y})\,dxdy$$
$$+\iint_{\Omega\times Y}(u_j(x,y)e^{2\pi i\theta.y})(\varphi_j(x,y)e^{2\pi i\theta.y})\,dxdy$$
$$=\iint_{\Omega\times Y}(f_j(x,y)e^{2\pi i\theta.y})(\varphi_j(x,y)e^{2\pi i\theta.y})\,dxdy$$

On localise par des fonctions test $\varphi_j(x,y)=\theta_j(x)\psi_j(y)$ avec $\theta_j\in\mathcal{D}(\Omega)$ et $\psi_j\in C^\infty_\sharp(Y)$:

$$\int_\Omega[\int_Y a(x,y)\bigtriangledown_y\,(u_j(x,y)e^{2\pi i\theta.y})\bigtriangledown_y\,(\psi_j(x,y)e^{2\pi i\theta.y})\,dy]\theta_j(x)\,dx$$
$$+\int_\Omega[\int_Y(u_j(x,y)e^{2\pi i\theta.y})(\psi_j(x,y)e^{2\pi i\theta.y})\,dy]\theta_j(x)\,dx$$
$$=\int_\Omega[\int_Y(f_j(x,y)e^{2\pi i\theta.y})(\psi_j(x,y)e^{2\pi i\theta.y})\,dy]\theta_j(x)\,dx$$

On obtient que pour presque tout $x\in\Omega$ et $\forall\psi_j(y)\in\mathcal{D}(Y)$, on a :

$$<-div_y[a(x,y)\bigtriangledown_y u_j(x,y)e^{2\pi i\theta.y}],\psi_j(y)e^{2\pi i\theta.y}> \quad +<u_j(x,y)e^{2\pi i\theta.y},\psi_j(x,y)e^{2\pi i\theta.y}>$$
$$=<f_j(x,y)e^{2\pi i\theta.y},\psi_j(x,y)e^{2\pi i\theta.y}>$$

(QED)

10.4.2 Inclusion du spectre de Bord dans σ_0

Dans le cas d'un ouvert borné Ω de $\mathbb{R}^n$ avec conditions de Dirichlet sur $\partial\Omega$, il a été démontré la complétude du spectre en utilisant une notion de mesure de Bloch ([6][7][87]) : le spectre limite est constitué du spectre de Bloch et du spectre de bord σ_{bord} introduit dans la section 10.2. Malheureusement, la définition de σ_{bord} n'est pas attachée en général à un problème spectral limite. En effet, comme signalé par Castro et Zuazua [48], σ_{bord} dépend de la façon dont η tend vers 0 (i.e. de la suite particulière $\eta_k \downarrow 0$ associée au processus limite). Plus précisément, il est démontré dans [48] que la limite supérieure au sens de Kuratowsky de $\eta^2\sigma_\eta$, quand $\eta \to 0$, peut coïncider avec $\mathbb{R}^+$ tout entier pour certaines géométries du bord : *Soit η la suite de tous les nombres réels de l'intervalle* $]0;\eta_0[$ *où* $\eta_0 > 0$. *Alors, on a :*

$$K \limsup_{\eta\to 0} \eta^2\sigma_\eta = \mathbb{R}^+$$

Autrement dit, σ_{bord} remplit les "gaps" de σ_{Bloch} pourvu que la suite η prenne toutes les valeurs possibles au voisinage de 0.

Pour un choix particulier de domaine Ω cylindrique

$$\Omega = \Sigma\times]0;L[$$

où Σ est un ouvert borné de $\mathbb{R}^{n-1}$ et L est > 0, on peut utiliser une notion de convergence à deux-échelles pour des couches limites. Soit $x = (x', x_n) \in \Omega$ avec $x' \in \Sigma$ et $x_n \in]0;L[$. On veut analyser le comportement asymptotique de la partie du spectre de $\sigma(S_\eta)$ qui correspond aux fonctions propres se concentrant sur le bord $\Sigma \times \{0\}$. Pour cela, on définit une bande semie-infinie $G = Y'\times]0;+\infty[$ avec $Y' =]0;1[^{n-1}$ et $y = (y', y_n)$ avec $y' \in Y'$ et $y_n \in \mathbb{R}^+$. On introduit l'espace $L^2_\sharp(G)$ suivant :

$$L^2_\sharp(G) = \left\{\Phi(y) \in L^2(G)\ ,\ y' \longmapsto \Phi(y', y_n)\ ,\ \text{ est } Y'\text{-périodique}\right\}$$

On définit alors l'espace $L^2(\Sigma; L^2_\sharp(KG))$, où K est un entier ≥ 1, des fonctions deux - échelles qui oscillent périodiquement en y' parallèlement à Σ, et tendent vers 0 quand y_n tend vers l'infini.

La notion de "convergence faible deux échelles au sens des couches limites" [8] est basée sur le résultat suivant, analogue à la proposition 2 du chapitre 2 :

Proposition 15

Soit (u_η) une suite dans $L^2(\Omega)$ telle que :

$$\|u_\eta\|_{L^2(\Omega)} \leq C\sqrt{\eta}$$

Alors $\exists\eta_k$ suite tendant vers 0 et $\exists u_0(x', y) \in L^2(\Sigma; L^2_\sharp(KG))$ telle que pour toute fonction $\varphi(x', y) \in L^2_\sharp(KG; C(\bar{\Sigma}))$, on a :

$$\lim_{k\to+\infty} \frac{1}{\varepsilon_k} \int_\Omega u_{\eta_k}(x)\varphi(x', \frac{x}{\eta_k})\, dx = \frac{1}{|\ KY'\ |} \int_\Sigma \int_{KG} u_0(x', y)\varphi(x', y)\, dx'dy$$

On définit ensuite l'analogue des propositions 3 et 4 du chapitre 2 pour les couches limites [8]. La définition du spectre de couche limite est déduite du résultat de structure sur les gradients (pour les couches limites) suivant :

Proposition 16

Soit (u_η) *une suite dans* $H_0^1(\Omega)$ *telle que :*

$$\frac{1}{\sqrt{\eta}}(\|u_\eta\|_{L^2(\Omega)} + \eta\|\nabla u_\eta\|_{[L^2(\Omega)]^n}) \leq C$$

Alors il existe une sous-suite de u_η*, encore notée* u_η*, et une limite* $u_0(x', y) \in L^2(\Sigma; L^2_\sharp(KG))$ *telle que* u_η *converge fortement à deux-échelles vers* u_0 *et* $\eta\nabla u_\eta$ *converge faiblement à deux-échelles vers* $\nabla_y u_0$*, au sens de la proposition 15 (couches limites).*

De même, on peut définir la convergence deux-échelles pour les opérateurs au sens de la proposition 15 (couches limites) et reprendre l'étude menée dans la section précédente pour ce type de convergence.

Par analogie avec les résultats obtenus dans [7][8], il parait donc raisonnable de supposer que Ω est un parallélépipède à dimensions entières contenant un nombre entier de périodes $(\eta = \frac{1}{n})$. Dans ce cas particulier, σ_{bord} est défini par :

$$\begin{cases} -div(\varepsilon^{-1}(y) \bigtriangledown u(y)) = \Lambda u(y) & \text{dans } \mathbb{R}^{n-1}\times]0;+\infty[\\ u \in L^2(\Omega) \ \text{ et } \dfrac{\partial u}{\partial n} = 0 & \text{sur } \partial\Omega = \mathbb{R}^{n-1}\times\{0\} \end{cases} \tag{1}$$

et la conjecture naturelle est que $\sigma_0 = \sigma_{Bloch} \cup \sigma_{bord}$.

Nous démontrons cette égalité dans le cas 1D dans la section suivante.

10.4.3 Étude du cas mono-dimensionnel

Le problème (1) devient :

$$\begin{cases} -\dfrac{d}{dy}(\varepsilon(y)^{-1}\dfrac{d}{dy}u(y)) = \Lambda u(y) & \text{dans }]0;+\infty[\\ u'(0) = 0\ ,\ u \in L^2(\mathbb{R}^+) \end{cases} \tag{2}$$

Ayant en vue l'étude des modes propagatifs dans les guides d'onde, on va étudier une variante du problème initial 1D faisant intervenir la constante de propagation $\gamma > 0$. Le problème spectral à η fixé est alors défini par :

trouver les triplets $(\gamma, k_\eta, u_\eta) \in \mathbb{R}^+ \times \mathbb{R} \times H^1(]0;1[)$, $u_\eta \not\equiv 0$ tels que :

$$\begin{cases} \dfrac{d}{dx}\Big(\varepsilon_\eta^{-1}(x)\dfrac{du_\eta}{dx}(x)\Big) + (k_\eta^2 - \gamma^2\varepsilon_\eta^{-1}(x))u_\eta(x) = 0 & \text{dans }]0;1[\\ {u_\eta}'(0) = 0\ ,\ {u_\eta}'(1) = 0 \end{cases} \tag{3}$$

avec $k_\eta = \dfrac{2\pi}{\lambda_\eta} = \omega\sqrt{\varepsilon_0\varepsilon_\eta\mu_0}$ et $\varepsilon_\eta = \varepsilon(\dfrac{x}{\eta})$, où $\varepsilon(.)$ est 1-périodique, coercive bornée dans $\mathbb{R}$.

L'ensemble des solutions $\Lambda_\eta := k_\eta^2 - \gamma^2\varepsilon_\eta^{-1}(x)$ de (3) est noté σ_η. On se propose de montrer que

$$\sigma_0 = K\limsup_{\eta\to 0}\eta^2\sigma_\eta = \sigma_{Bloch} \cup \sigma_{bord}$$

où σ_{bord} est le spectre de (2), alors que le problème associé à σ_{Bloch} s'écrit :

$$\begin{cases} -\dfrac{d}{dy}(\varepsilon(y)^{-1}\dfrac{d}{dy}u(y)) = \Lambda u(y) \quad \text{dans } \mathbb{R} \\ u \in L^2(\mathbb{R}) \end{cases} \tag{4}$$

Il est bien connu que σ_{Bloch} contient le spectre essentiel de (2) (avec égalité si ε est pair). Pour montrer que $\sigma_{bord} \subset \sigma_0$, il suffit de montrer que toute valeur propre de (2) (i.e. du spectre ponctuel de σ_{bord}) appartient à σ_0.

Pour démontrer l'égalité $\sigma_0 = \sigma_{bord} \cup \sigma_{Bloch}$, nous considérons pour toute valeur du paramètre Λ la matrice T_Λ définie par :

$$T_\Lambda \begin{pmatrix} u_0 \\ u_1 \end{pmatrix} = \begin{pmatrix} w(1) \\ w'(1) \end{pmatrix}$$

où w est solution de :

$$\begin{cases} -\dfrac{d}{dy}(\varepsilon(y)^{-1}\dfrac{d}{dy}w(y)) = \Lambda w(y) \quad \text{dans } \mathbb{R} \\ w(0) = u_0 \ , \ w'(0) = u_1 \end{cases} \tag{5}$$

(la matrice de monodromie T_Λ est dans $SL_2(\mathbb{R})$ i.e. $detT_\Lambda = 1$ et T_Λ est à coefficients réels). Alors

Proposition 17

a) Λ est valeur propre de (2) si et seulement si $\begin{pmatrix} 1 \\ 0 \end{pmatrix}$ est un vecteur propre de T_Λ associé à une valeur propre réelle inférieure à 1. Dans ce cas, $\Lambda \notin \sigma_{Bloch}$ et la fonction propre associée est unique et de dérivée nulle sur les entiers.

b) $\sigma_0 = \sigma_{bord} \cup \sigma_{Bloch}$

Démonstration :

Preuve de b)

On peut réécrire (3) comme

$$\begin{cases} -\dfrac{d}{dx}\Big(\varepsilon_\eta^{-1}(x)\dfrac{du_\eta}{dx}(x)\Big) = \Lambda_\eta u_\eta(x) = 0 \quad \text{dans }]0;1[\\ {u_\eta}'(0) = 0 \ , \ {u_\eta}'(1) = 0 \end{cases} \tag{3'}$$

Comme $H^1(]0;1[) \subset C([0;1])$ on déduit de (4) que $u_\eta \in C([0;1])$ et $\varepsilon_\eta^{-1}\dfrac{du_\eta}{dx} \in C([0;1])$. On désigne alors par Ψ_η le vecteur colonne

$$\Psi_\eta(x) = \begin{pmatrix} u_\eta(x) \\ \dfrac{1}{\varepsilon(\frac{x}{\eta})}u'_\eta(x) \end{pmatrix}$$

dont les deux composantes sont continues. Afin de simplifier l'étude du problème écrit plus haut, on se restreint à un nombre entier de couches. On pose alors $n = E(\dfrac{1}{\eta})$, où n désigne le nombre de couches de diélectrique dans la cavité, et on note $\Psi_n(x)$ le vecteur colonne :

$$\Psi_n(x) = \begin{pmatrix} u_n(x) \\ \dfrac{1}{\varepsilon_n(x)}u'_n(x) \end{pmatrix}$$

où $\varepsilon_n(x) = \varepsilon(nx)$.

Notant par ailleurs que $\Lambda_\eta = \eta\Lambda$, on réécrit $(3')$ comme

$$\begin{cases} -\eta^2 \dfrac{d}{dx}\Big(\varepsilon_\eta^{-1}(x)\dfrac{du_\eta}{dx}(x)\Big) + u_\eta(x) = \Lambda u_\eta(x) = 0 \quad \text{dans }]0;1[\\ {u_\eta}'(0) = 0\ ,\ {u_\eta}'(1) = 0 \end{cases} \tag{3''}$$

Pour étudier la limite quand η tend vers 0 du spectre du problème spectral $(3'')$ on se ramène à l'étude du spectre de l'opérateur de Green (opérateur inverse) S_n défini pour tout $f \in L^2(]0;1[)$ par $S_n f = u_n$ où u_n est solution du problème $(\mathcal{P}_n)$ qui consiste à trouver u_n dans $H^1(]0;1[)$, $u_n \not\equiv 0$, tel que

$$(\mathcal{P}_n) \begin{cases} -\dfrac{1}{n^2}\dfrac{d}{dx}(\varepsilon_n(x)^{-1}\dfrac{d}{dx}u_n) + u_n = f(nx) \quad \text{dans }]0;1[\\ u_n'(0) = 0\ ,\ u_n'(1) = 0 \end{cases}$$

Du fait que $]0;1[$ contient un nombre entier de périodes $\Big(\dfrac{1}{\eta}$ est entier $\Big)$, $(\mathcal{P}_\eta)$ est équivalent à (2) ($u_n(x) = u(nx)$ implique que les conditions limites sont équivalentes). Les conditions limites dans $(\mathcal{P}_n)$ imposent par ailleurs que :

$$\Psi_n(0) = \begin{pmatrix} u_n(0) \\ 0 \end{pmatrix} \text{ et que } \Psi_n(1) = \begin{pmatrix} u_n(1) \\ 0 \end{pmatrix} \tag{1}$$

Par continuité du vecteur colonne Ψ_n, on passe alors de l'interface $x_i = \dfrac{i}{n}$ à l'interface $x_{i+1} = \dfrac{i+1}{n}$ par la matrice de monodromie T_i :

$$\Psi_n(x_{i+1}) = T_i \Psi_n(x_i)$$

Ces matrices sont dans le groupe $SL_2(\mathbb{R})$ i.e. elles sont à coefficients réels et de déterminant unitaire. Par ailleurs, la permittivité ε_n étant périodique de période $\dfrac{1}{n}$, on en déduit que $T_i = T_{i-1}$. On notera dorénavant la matrice de monodromie par T. La matrice T vérifie alors :

$$\Psi_n(\frac{1}{n}) = T\Psi_n(0)\ ,\ \Psi_n(\frac{2}{n}) = T\Psi_n(\frac{1}{n})\ ,\ \ldots\ ,\ \Psi_n(1) = T\Psi_n(\frac{n-1}{n})$$

On en déduit que :

$$\Psi_n(1) = T^n \Psi_n(0) \tag{2}$$

(noter que la structure de groupe de $SL_2(\mathbb{R})$ assure que T^n est toujours une matrice unimodulaire réelle).

Pour passer à la limite quand n tend vers l'infini dans l'équation précédente, il faut diagonaliser la matrice de transfert T. Soit X une valeur propre de T, alors X vérifie :

$$Det(T - XI) = 0 \Longleftrightarrow X^2 - XTr(T) + Det(T) = 0$$

Or $T \in SL_2(\mathbb{R})$ donc $Det(T) = 1$ et $Tr(T) \in \mathbb{R}$, on en déduit alors que deux cas peuvent se présenter :

i)Si $\mid Tr(T) \mid > 2$, on a deux valeurs propres réelles μ_1 et μ_2 telles que $\mu_1 > 1$ et $\mu_1 = \dfrac{1}{\mu_2}$. On peut montrer [74][73] que l'on se trouve alors dans un gap.

ii)Si $\mid Tr(T) \mid < 2$, on a deux valeurs propres conjuguées μ_1 et μ_1^*. On se trouve alors dans une bande de transparence.

Nous allons appliquer ces résultats à notre étude. Notant que si $\mid Tr(T) \mid \neq 2$, T est diagonalisable, on tire de (2) que :

$$\Psi_n(1) = Q^{-1} D^n Q \Psi_n(0) \tag{3}$$

où D est une matrice diagonale et Q est de la forme suivante :

$$Q = \begin{pmatrix} q_{11} & q_{12} \\ q_{21} & q_{22} \end{pmatrix}$$

L'inverse de Q est alors donné par :

$$Q^{-1} = \frac{1}{Det(Q)} \begin{pmatrix} q_{22} & -q_{12} \\ -q_{21} & q_{11} \end{pmatrix} \tag{4}$$

On déduit de (3) et (4), que T^n prend la forme suivante dans les gaps :

$$\begin{aligned} T^n &= \frac{1}{Det(Q)} \begin{pmatrix} q_{22} & -q_{12} \\ -q_{21} & q_{11} \end{pmatrix} \begin{pmatrix} \mu_1^n & 0 \\ 0 & \mu_1^{-n} \end{pmatrix} \begin{pmatrix} q_{11} & q_{12} \\ q_{21} & q_{22} \end{pmatrix} \\ &= \frac{1}{Det(Q)} \begin{pmatrix} t_{11}^{(n)} & t_{12}^{(n)} \\ t_{21}^{(n)} & t_{22}^{(n)} \end{pmatrix} \end{aligned} \tag{5}$$

où $t_{11}^{(n)} = q_{11}q_{22}\mu_1^n - q_{12}q_{21}\mu_1^{-n}$, $t_{12}^{(n)} = q_{12}q_{22}(\mu_1^n - \mu_1^{-n})$, $t_{21}^{(n)} = q_{11}q_{21}(-\mu_1^n + \mu_1^{-n})$, et $t_{22}^{(n)} = -q_{12}q_{21}\mu_1^n + q_{11}q_{22}\mu_1^{-n}$.

La condition (1) est alors réalisée si :

$$\begin{pmatrix} u_n(1) \\ 0 \end{pmatrix} = \frac{1}{Det(Q)} \begin{pmatrix} t_{11}^{(n)} & t_{12}^{(n)} \\ t_{21}^{(n)} & t_{22}^{(n)} \end{pmatrix} \begin{pmatrix} u_n(0) \\ 0 \end{pmatrix} \tag{6}$$

Cela implique que $t_{21}^{(n)}$ doit alors nécessairement vérifier :

$$t_{21}^{(n)} = q_{11}q_{21}(-\mu_1^n + \mu_1^{-n}) = 0 \,, \tag{7}$$

soit encore, $q_{11}(k_0) = 0$ ou $q_{21}(k_0) = 0$ puisque $\mu_1^n - \mu_1^{-n} \neq 0$ ($\mu_1 > 1$).

On distingue maintenant les cas où la fréquence est dans un gap ou une bande de transparence.

i) Dans les gaps :

Par l'absurde, si q_{21} est nul, on tire de (5) que :

$$T^n = \frac{q_{22}}{Det(Q)} \begin{pmatrix} q_{11}\mu_1^n & q_{12}(\mu_1^n - \mu_1^{-n}) \\ 0 & q_{11}\mu_1^{-n} \end{pmatrix} \tag{8}$$

On déduit de (6) que :

$$\begin{pmatrix} u_n(1) \\ 0 \end{pmatrix} = \frac{q_{11}q_{22}}{Det(Q)} \begin{pmatrix} \mu_1^n u_n(0) \\ 0 \end{pmatrix}$$

Or, q_{11} et q_{22} sont différents de zéro (sinon on aurait $Det(Q) = 0$). On a donc $u_n(1) = \frac{q_{11}q_{22}}{Det(Q)}\mu_1^n u_n(0)$. Comme $\mu_1 > 1$, cela implique que $u_n(1) \to +\infty$ (contradiction).

Par contre, si $q_{11}(k_0) = 0$, on tire de (5) que :

$$T^n = \frac{q_{12}}{Det(Q)} \begin{pmatrix} -q_{21}\mu_1^{-n} & q_{22}(\mu_1^n - \mu_1^{-n}) \\ 0 & -q_{21}\mu_1^n \end{pmatrix}$$

On déduit alors de (6) que :

$$\begin{pmatrix} u_n(1) \\ 0 \end{pmatrix} = \frac{q_{12}}{Det(Q)} \begin{pmatrix} -q_{21}\mu_1^{-n}u_n(0) \\ 0 \end{pmatrix}$$

qui vérifie bien la condition $u_n(1) \to 0$ quand $n \to +\infty$ ($\mu^{-1} < 1$). Ce cas correspond à une valeur propre μ dans le spectre de bord (noter que sa fréquence k_0 est indépendante de n i.e. du nombre de couches composant la cavité).

Remarque 1

L'égalité (7) est bien entendu, vraie pour $n = 1$. Or, d'après ce que nous venons de voir, on a $t_{21} = 0 \Longleftrightarrow q_{11}(k_0) = 0$, pourvu que l'on soit dans le gap. Or, si $t_{21} = 0$, alors $Det(T) = t_{11}t_{22}$. Comme $T \in SL_2(\mathbb{R})$, on en déduit que $t_{11}t_{22} = 1$. Dans les gaps, nous sommes donc assurés que :

$$Tr(T) = t_{11} + t_{22} = t_{11} + \frac{1}{t_{11}} > 2$$

On a donc nécessairement $t_{11} < 1$, donc la valeur propre Λ de T_Λ associée à (10) est < 1.

On tire de (5) que $t_{21} = q_{11}q_{21}(-\mu_1 + \mu_1^{-1})$. Par conséquent, t_{21} est nul si et seulement si $q_{11} = 0$ ou $q_{21} = 0$.

ii) **Dans les bandes de transparence :**

Dans une bande de transparence, la condition (7) est réalisée si :

$$q_{11}q_{21}(\mu_1^n - \mu_1^{*n}) = 0$$

On note qu'alors $q_{11}q_{21} \neq 0$. Posant, $\mu_1 = e^{i\pi\varphi_1}$ et $\mu_1^* = e^{-i\pi\varphi_1}$, on en déduit que nécessairement :

$$\sin(n\pi\varphi_1) = 0$$

Les fonctions $\varphi_{1,k}^n = \frac{k}{n}$ sont les fréquences de Bloch : quand n tend vers l'infini, elles forment des bandes (densité de $\mathbb{Q}$ dans $\mathbb{R}$) qui constituent le spectre de Bloch.

Remarque 2

On peut donner le facteur d'échelle permettant de déduire le comportement du mode dans une couche à partir de la couche précédente. En effet, notant $\tilde{u}$ la restriction de u à $[0; \frac{1}{n}]$, on a :

$$\tilde{u}_n(\frac{1}{n}) = t_{11}\tilde{u}_n(0) \quad \text{et} \quad \tilde{u}_n'(\frac{1}{n}) = 0$$

Pour tout $x \in [\frac{k}{n}; \frac{k+1}{n}]$, on obtient alors que :

$$u_n(x) = t_{11}^k \tilde{u}_n(x - \frac{k}{n}) = t_{11}^k \tilde{u}_1(x)$$

L'expression générale de u dans $[0;1]$ est alors donnée par :

$$u_n(x) = \sum_{k=0}^{n-1} \chi_{[\frac{k}{n};\frac{k+1}{n}]} t_{11}^k \tilde{u}_1(x-k) = \sum_{k=0}^{n-1} \chi_{[\frac{k}{n};\frac{k+1}{n}]} t_{11}^k u_1(x-k) \tag{9}$$

En résumé, on a le critère simple suivant : si $t_{21}(k_0) = 0$, alors
1) k_0 est dans le gap.
2) k_0 correspond à un mode de bord. Ce mode a un comportement décrit par (9).

Preuve de a)

On définit en premier lieu les fonctions u et v qui satisfont les relations différentielles $\frac{d}{dy}v(y) = \Lambda u(y)$ et $\frac{d}{dy}u(y) = \varepsilon(y)v(y)$. Notant $\Phi(y)$ le vecteur colonne $\begin{pmatrix} u(y) \\ v(y) \end{pmatrix}$, on déduit de (2), la relation suivante :

$$\frac{d\Phi}{dy}(y) = \begin{pmatrix} 0 & \varepsilon(y) \\ \Lambda & 0 \end{pmatrix} \Phi(y) := K_\Lambda(y)\Phi(y)$$

On note que $K_\Lambda(y)$ est 1-périodique et que l'on a :

$$\frac{d\Phi}{dy}(y+1) = K_\Lambda(y)\Phi(y+1) = K_\Lambda(y)T\Phi(y) = K_\Lambda(y)T^n\Phi(y-n+1)$$

Pour $y = j-1$, on obtient :

$$\frac{d\Phi}{dy}(j) = K_\Lambda(j-1)T^n\Phi(j-n) = K_\Lambda(j-1)T^j\Phi(0) = K_\Lambda(j-1)T^j \begin{pmatrix} u(0) \\ \frac{1}{\varepsilon}u'(0) \end{pmatrix} = K_\Lambda(j-1)T^j \begin{pmatrix} 1 \\ 0 \end{pmatrix} \tag{10}$$

Si k est dans le spectre de bord, de b) i) on déduit alors que :

$$\frac{d\Phi}{dy}(j) = K_\Lambda(j-1)T^j(k) \begin{pmatrix} 1 \\ 0 \end{pmatrix} = K_\Lambda(0) \begin{pmatrix} t_{11}^j(k) & t_{12}^j(k) \\ 0 & t_{22}^j(k) \end{pmatrix} \begin{pmatrix} 1 \\ 0 \end{pmatrix} = K_\Lambda(0) \begin{pmatrix} t_{11}^j(k) \\ 0 \end{pmatrix}$$

On en conclut que la dérivée de Φ s'annule pour les grandes valeurs de j en notant que $t_{11}^j(k) \to 0$ quand $j \to +\infty$ ($t_{11} < 1$). Pour $j = n-1$, on obtient :

$$\frac{d\Phi}{dy}(n-1) = \begin{pmatrix} \frac{du}{dy}(n-1) \\ \frac{dv}{dy}(n-1) \end{pmatrix} = \begin{pmatrix} 0 \\ \Lambda t_{11}^n(k) \end{pmatrix}$$

On en déduit que $\frac{du}{dy}(n-1) = 0, \forall n \in \mathbb{N}^*$ et notant que $\frac{d}{dy}\left(\frac{1}{\varepsilon}\frac{du}{dy}(n-1)\right) = \Lambda u(n-1)$, on obtient $u(n-1) = t_{11}^n$, $\forall n \in \mathbb{N}^*$. Comme $t_{11} < 1$, on a montré que :

$$u(n-1) \to 0 \ \text{ et } \frac{du}{dy}(n-1) \to 0\ , \ \text{ quand } n \to +\infty$$

Par ailleurs, on en déduit de (9) que :

$$\int_{\mathbb{R}^+} |\, u(x)\,|^2\, dx = \sum_{k=0}^{+\infty} t_{11}^{2j} \|u\|^2_{L^2(]0;1[)} = \frac{1}{1-t_{11}^2}\|u\|^2_{L^2(]0;1[)}$$

Ce qui montre que $u \in L^2(\mathbb{R}^+)$ ($t_{11} \neq 1$).

Par contre, si k n'est pas dans le spectre de bord, de (10) on tire que :

$$\frac{d\Phi}{dy}(j) = K_\Lambda(j-1)T^j(k)\begin{pmatrix}1\\0\end{pmatrix} = K_\Lambda(0)\begin{pmatrix}t_{11}^j(k) & t_{12}^j(k)\\ t_{21}^j(k) & t_{22}^j(k)\end{pmatrix}\begin{pmatrix}1\\0\end{pmatrix} = \begin{pmatrix}0 & \varepsilon(y)\\ \Lambda & 0\end{pmatrix}\begin{pmatrix}t_{11}^j(k)\\ t_{21}^j(k)\end{pmatrix}$$

où l'on a utilisé la 1-périodicité de $K_\Lambda(j)$. Ce qui montre que $\dfrac{d\Phi}{dy}(j) \to +\infty$ quand $j \to +\infty$. Comme $\dfrac{d\Phi}{dy}(j) = K_\Lambda(0)\Phi(j)$, nous sommes assurés que $\Phi(j) \to +\infty$ quand $j \to +\infty$ i.e. $u \notin L^2(\mathbb{R}^+)$. Donc Λ n'est pas dans le spectre de Bloch.

10.4.4 Application numérique

Dans la pratique, ε est une fonction constante par morceaux. Si l'on considère un milieu constitué de couches d'épaisseurs $\dfrac{1}{n}$ de fractions a_1 et a_2, la matrice de monodromie $T_1 = t_1 t_2$ où t_i, $i \in \{1,2\}$, est définie par :

$$t_i = \begin{pmatrix} \cos(\frac{a_i\beta_i}{n}) & \beta_i^{-1}\varepsilon(x_i)\sin(\frac{\beta_i a_i}{n})\\ -\beta_i\varepsilon^{-1}(x_i)\sin(\frac{a_i\beta_i}{n}) & \cos(\frac{\beta_i a_i}{n})\end{pmatrix}$$

où $\beta_i(x) = \sqrt{k_0^2\varepsilon(x_i) - \gamma^2}$.

Dans la suite, nous présentons des résultats numériques s'appuyant sur l'utilisation de telles matrices de transfert T, obtenus pour deux modes de bord dont les nombres d'onde valent respectivement $k_0 = 0,981441016617m^{-1}$ et $k_0' = 5,601471353685m^{-1}$ (noter que la fréquence du mode doit être calculée précisément). Ces deux modes correspondent à des fréquences appartenant aux premier et quatrième gap (on observe numériquement qu'il y a un mode de bord par gap). Les figures montrent le comportement du premier mode de bord pour une cavité composée de 5 couches puis 40 couches. Pour le deuxième mode de bord, nous donnons des résultats pour 5 couches puis 30 couches : au-delà de 30 couches, la précision de la machine n'est plus suffisante pour la fréquence de ce mode (quand la fréquence des modes recherchés augmente, et quand le nombre de couches augmente, l'erreur numérique augmente). Sur les figures 10.1 et 10.2, le facteur d'échelle t_{11} ressort nettement. Sur les figures 10.3 et 10.4, on constate que les oscillations du champ se concentrent sur le bord gauche de la cavité. Le problème étant invariant par symétrie axiale en $x = 0.5$, et par linéarité, on déduit que l'on a bien des champs qui se concentrent sur les deux bords de la cavité. Avant de clore cette section, nous nous devons de citer l'ouvrage classique de Kittel [118] sur la physique du solide qui aborde le problème des modes de bord avec une approche plus formelle, et la thèse de Gralak [93] qui traite ce type de problèmes en diffraction.

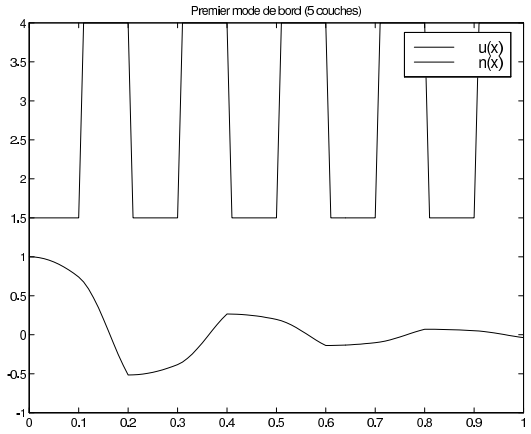

FIGURE 10.1 – Champ magnétique de nombre d'onde $k_0 = 0,981441016617m^{-1}$ pour 5 couches.

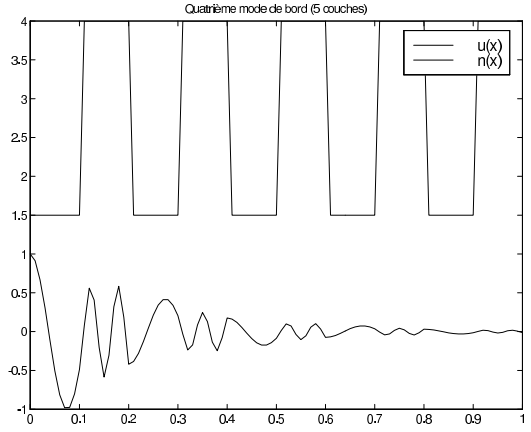

FIGURE 10.2 – Champ magnétique de nombre d'onde $k_0' = 5.601471353685m^{-1}$ pour 5 couches.

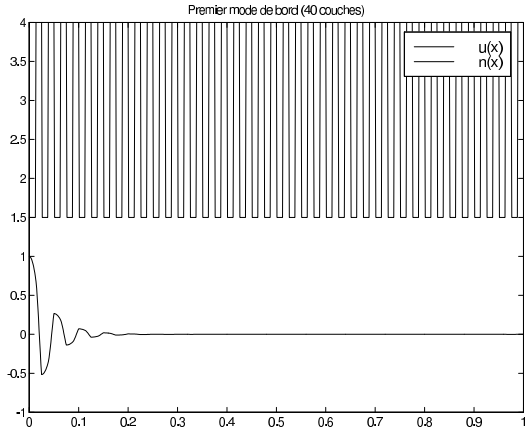

FIGURE 10.3 – Champ magnétique de nombre d'onde $k_0 = 0,981441016617m^{-1}$ pour 40 couches.

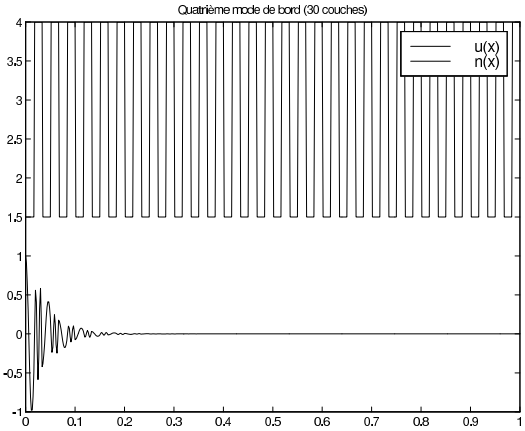

FIGURE 10.4 – Champ magnétique de nombre d'onde $k_0' = 5.601471353685 m^{-1}$ pour 30 couches.

Conclusion

"On rencontre des Marseillais dans tous les ports du monde, mais beaucoup ne sont jamais allés au château d'If."

Louis Brauquier [42]

In the first part of thesis, we outline an asymptotic approach of scattering by finite photonic crystals with heterogeneous permittivity and permeability in the quasi-static limit thanks to the so-called multi-scale expansion method (see chapter 1). We briefly discuss the physics underlying counter-intuitive phenomena : we note that there exists some Ferro-magnetic media whose relative permeability is lower than 1 (contrary to the relative permeability which is always greater than 1). On the first hand, thanks to the homogenization process, one can adjust the effective permittivity and the effective permeability in such a way that $\varepsilon_{eff}\mu_{eff} = Id$. The effective media therefore transmits light without deviation and reflects light as an ordinary medium (note that both effective permeability and permittivity can be anisotropic, although their product is the identity matrix, which certainly leads to astonishing phenomena !). On the second hand, one can adjust ε_{eff} and μ_{eff} such that their ratio is the impedance of the air : in the one-dimensional case, one can see that there is a Brewster incidence in both $E_{\|}$ and $H_{\|}$ polarizations. In the three-dimensional case, the physics of these effective structures sounds therefore far from obvious and one needs to improve his conjectures with numerical computations. We therefore propose a numerical approach based on a finite difference scheme coupled with Fast Fourier Transforms. We are only capable to present partial numerical results (we just give the behavior of the multi-scalar potential on the basic cell and do not compute explicitely the effective matrices of anisotropy), work is in progress to improve this method with a second approach based on a finite element scheme. An interesting perpestive is to compare the results given by the resolution of the annex problems and the ones given by the Bloch method. We justify the result of homogenization by using a two-scale convergence in the particular case of constant permeability and explain the paradoxal difference between the annex problems in the two dimensional and the three-dimensional cases thanks to a variant of the chessboard problem (see chapter 2). To conclude with ferro-magnetic structures, we believe that they may exhibit complete gaps in high frequencies even in the one-dimensional case (no dependence of the gaps upon the incident field when the ferro-magnetic medium has the index of the vaccum), unlike the traditional Bragg mirrors. The second contribution of the thesis is related to the homogenization of quasi-crystals (cf. Penrose tillings and icosahedral structures). We give a brief background in physics of quasi-crystalline phases (see chapter 3) and introduce a concept of "two-scale-cut-projection convergence" (see chapter 4) based

upon convergence of oscillating quasi-periodic functions deduced by cut-projection of periodic functions in higher dimensions spaces. We place our study in the Fourier space since the oscillations of the gradients of such functions are not necessarily represented by gradients of periodic functions : it is well known in crystallography that the reciprocal space reveals the deep nature of quasi-crystals. The touchstone of homogenization of such structures is a corrector type result (see chapter 5) where we estimate the asymptotic behavior of the error. The result relies on the properties of algebraic numbers associated with the cut-projection. We believe that our "two-scale-cut-projection method" can be used in various situations involving quasi-periodic funtions. The asymptotic analysis of quasi-periodic structures leads to various phenomena which are a world apart from periodic structures and random structures. Stochastic methods had been used by various authors [124][41] to study almost-periodic phenomena, but we emphasize that our method is well adapted to quasi-periodic structures and give therefore much information : we derive the effective tensor of permittivity of the structure from the resolution of three annex problems on a basic hyper-cell in Fourier space, unlike the previous authors who used annex problems on a cell whose size is tending to infinity.

In the second part of the thesis, we analyse both theoretically and numerically the propagating modes in various waveguides. We first investigate the case of dielectric waveguides (chapter 6). We make use of edge elements to discretize the vector problem (no spurious modes,[30]) and we take into account the unboundness of the domain thanks to a geometric transformation [166]. We take the magnetic field as the variable (null divergence) and we use the GetDP software [64]. The numerical study is based on a theoretical criterion which characterizes the bound part of the spectrum : thanks to this criterion, the Lanczos algorithm only looks for eigenvalues and their associated eigenvectors in the discrete part of the spectrum. As an application, we study the well-known cross-talk phenomenon [191] i.e. the coupling between two identical optical wave guides. We then generalize the numerical study to the coupling between 81 dielectric rods arranged in a square lattice (Photonic Crystal Fibers). We use the symmetries to study only one quater of the Microstructured Optical Fiber to avoid prohibiting calculus. We exhibit a propagating mode in a high index structural defect in this MOF. Secondly, we investigate the case of metallic waveguides. In that case, the spectrum is discrete and the computational time is much smaller. We give the dispersion curves for a metallic homogeneous wave guide of circular cross-section, to validate the code. We then investigate the case of metallic photonic crystal fibers i.e. metallic guides with a dielectric crystal cladding in the transverse plane. Since all the modes are bound modes, we exhibit the so-called leaky-modes at the expected frequencies [205]. We exhibit some leaky modes in square and honeycomb lattices (the higher the symmetry of the crystal cladding, the larger the band gaps). Finally, we investigate the case of spectral problems involving both unbounded domains and metallic inclusions : such cases arise e.g. in grouved metallic wave guides and micro-strips. We use the electric field formulation to get nice boundary conditions and we select the bound part of the spectrum thanks to the theoretical criterion of [28] (see chapter 6). We are not yet capable to give a rigorous mathematical framework for such problems, but we believe that the results on dielectric waveguides derived from [28], still hold in much cases when applied to dielectric

wave guides with metallic inclusions. A natural extension to this work would be to give a rigorous characterization of the spectrum and to discuss of the cases when the theoretical criterion for dielectric wave guides [28] does not hold any more. Concerning the numerical extension of the work, there is a wide variety of situations in physics dealing with such problems, and notably in the field of micro-wave engineering.

In the third part of the thesis, we make an asymptotic analysis of spectral problems in both low and high frequency limits. We first investigate the case of the homogenization of Photonic Crystal Fibers (see chapter 9) with a metallic boundary (bounded domain, hence discrete spectrum) thanks to the multi-scale expansion method. We then exhibit birefringence phenomena in an anisotropic homogeneous circular waveguide (GetDP software), whose thensor of permittivity is derived from the resolution of two annex problems of electrostatic types (Method of Fictitious Sources). Secondly, we use a notion of "Bloch wave homogenization" to perform the asymptotic analysis of Photonic Crystal Cavities in the resonance domain (photonic band gap effects). We introduce a notion of "two-scale convergence for operators" which allows us to deduce a result of convergence for spectral families in strong two-scale limit, and in particular of the sequence of renormalized spectra (eigenvalues of the order of the square of the medium period) towards the bloch part of the limit spectrum. We then analyse the so-called boundary layer part of the limit spectrum in the one-dimensional case, by the use of monodromy matrices. Following Allaire and Conca, we assume that the cavity is filled with an entire number of cells, and we also characterize the boundary layer spectrum thanks to a limit problem defined in the half plane (but with Neumann conditions instead of Dirichlet ones). The originality is that we explicit the discrete part of the boundary spectrum thanks to a new spectral problem defined in $]0;1[$: we show that each eigenvalue to this spectral problem belongs to a different gap and we give the expression of its decrease. Finally, we illustrate this theoretical study by numerical results deduced from this spectral problem. An interesting perspective is to generalize the asymptotic analysis to the case of propagating waves in Photonic Crystal Fibers with metallic boundary. This study can be also applied to analogous problems in elastodynamic i.e. phononic crystal fibers, since the Navier equations and the boundary conditions are quite similar. To conclude with the third part of the thesis, we believe that the so-called "Bloch wave homogenization method" allows asymptotic methods issued from homogenization to be adapted to high frequency phenomena and gives an alternative to classical tools such as lattice-sums.

Annexe A

The geometry of electromagnetism.

"-S'il vous plaît... dessine-moi un mouton...

Quand le mystère est trop impressionant, on n'ose pas désobéir. Aussi absurde que cela me semblât à mille milles de tous les endroits habités et en danger de mort, je sortis de ma poche une feuille de papier et un stylographe. Mais je me rappelai alors que j'avais surtout étudié la géographie, l'histoire, le calcul et la grammaire et je dis au petit bonhomme (avec un peu de mauvaise humeur) que je ne savais pas dessiner. Il me répondit :

- Ça ne fait rien. Dessine-moi un mouton."

"Le Petit Prince", A. De Saint Exupéry (1940)

A.1 Geometrical objects for Maxwell's equations

The material of this annex is partly based on [32] and [31].

There is a terrible confusion around concepts of **geometrical objects** which serve in describing electromagnetism : one may think for example to the old concepts of **axial vectors** and **polar vectors** which represent the magnetic and the electric fields. In order to stay very close to these familiar concepts, we shall have to introduce, and discuss with care, an appropriate geometrical framework, consisting of things such as **affine space**, the associated **vector space**, and geometrical objects living therein. We often take the good old Euclidean space, as the natural framework in which to do physics, but we want to stress that this is a modelling decision : the World is, and certainly has order and structure, but order and structure in our descriptions of the world are something else (issue of a process of model building). People who apply mathematics, including physicists and engineers, use abstract mathematical structures which reproduce some of the features of the real world, and thus can help in explaining or predicting the behavior of some definite segment of reality. So mathematical entities by which we thus describe physics are not *a priori frames* of our thinking. They are creation, moulded of course by the structures of the world out there, but still abstract things. Therefore, they are more or less adequate as tools with which to deal with the real world. One can thus criticize the way the mathematical tools are applied and question their adequacy. This process of reevaluation, constantly reinvigorated by new engineering practices, such as **programming** and **computing** is the impetus that

forces formalisms to evolve, even in well-understood compartments of physics like classical electromagnetism. In the sequel, we will discuss about abstract structures such as group, field, affine and vector spaces... Recall that all these structures are sets (we have seen that among others, Cantor, Hilbert and Russell present mathematics in such a light that all mathematical objetc are sets of some kind.), but not naked sets : structure is conferred on such sets by specific systems of relations and operations, which tell what can be done with and to the elements of the set.

For instance, a vector space on the reals is a set of objects called vectors, which one can add together and multiply by real numbers. It sounds that the vector space is a good candidate for electromagnetic fields, since they can be superposed, adding up their effects and since a given field can be scaled scaled up by a scalar factor. One can then envision the evolution of the electromagnetic field as a continuous sequence of values of a representative vector in this abstract space, in other words, as a trajectory. And there we are, with the beginning of a geometrization of the whole thing. We must therefore introduce the notion of **functional space** which is infinite dimensional. The main feature which distinguishes such vector spaces of fields from those of plane or spatial geometry is, of course, dimension. There are therefore two layers in the modelling of an electromagnetic problem : the shape of the bodies under study lives in a finite dimensional vector space (note that we make here a one-to-one correspondence between e.g. the set of all triples of real numbers $\mathbb{R}^3$ and the three-dimensional vector space V_3, but all this depends on the choices of the basis...), and the electromagnetic fields live in a functional space (infinite dimensional).

As for the first one, there is no canonical way to select a set of coordinate axes, and imposing one would break the symmetry of space in an arbitrary way, devoid of physical justification : it would be a kind of artificial anisotropy. What is this allusion to symmetries of space supposed to mean ? This is where another structure, that of group, intervenes. Group is a simpler, more primitive, and hence more general structure than vector space. A vector is already a group, an additive one : indeed, the addition admits a neutral element (the null vector) and each vector v has an opposite $-v$. Together with stability and associativity, these properties constitute the axioms for the group structure. Moreover, a vector space is a commutative (or **Abelian**) group, meaning that $v+w = w+v$, something which is not part of the definition of groups in general. So a vector space can be constructed as a set with two layers of structure : first, the one of Abelian group, conferred on it by vector addition ; and a second layer, due to the introduction of scalar multiplication, with the properties required to make it compatible with the addition. So if we forget about the multiplication by reals in V_3, what remains is an Abelian group, called the associated group of **translations**. To vector v, we may associate the map $T_v \ : \ w \longmapsto v + w$, called the v-translation. Note that T_v is not a linear map of V_3 to itself, because 0 does not map to 0. On the other hand, translations are not devoid of linear properties, since for instance, it is true that $T_v[\frac{(w+w')}{2}] = \frac{[T_v(w)+T_v(w')]}{2}$. We thus call them affine maps of V_3 to itself, or affine transforms on V_3. Obviously, the vector space structure is not required if one wants to define affine maps. All that is needed is a set, elements of which are now called **points**, not vectors, in which it makes sense to take the point midway between two points, or **barycenter** (and more generally, the barycenter of a given finite set of points to

which weights of nonzero sum are assigned). Affine maps are then defined as maps which preserve barycenters. A set thus equipped with a notion of barycenter is called an affine space. There is a way to associate to V_3 an affine space A_3. For this, we first define A_3 as a set on which we can perform v-translations : given a vector $v \in V_3$ and a point $a \in A_3$, there is another point, denoted $T_v(a)$ which is the v-translate of a, and we postulate the obvious properties $T_v(T_w(a)) = T_{v+w}(a)$, and so forth. We say that V_3 acts by translations on A_3. Second, we assume that any two points of A_3 can be connected by a v-translation i.e. there is always some v such that $T_v(a) = b$. Nothing more natural, now, than writing $v = b - a$, or $T_v(a) = a + v$, so if one selects in A_3 some particular point, denoted 0, one can make the identification between the point $T_v(0)$ *alias* $0 + v$, and the vector v. It is therefore not a canonical identification, of course. Now the barycenter of a and b is the well-defined $\frac{(b-a)}{2}$-translate of a, that is, the point $a + \frac{(b-a)}{2}$. The affine maps which are a one-to-one correspondence from A_3 into itself are invertibles and form a group called the **affine group**, denoted GA_3. There is a deep connection with GA_3 and the group GL_3 of linear transformations in V_3, which is isomorphic *via* selection of a basis, to the group of 3×3 regular matrices : note that a linear transform on vectors induces an affine transform on points and that, conversely, any affine transform can be described as the combination of such a special affine transform with a translation. As a consequence, the affine maps preserve many properties : three points on the same line are transformed to aligned points (this alignment property holds true since one of the points is the barycenter of the other two, with *adequate* weights ; pairs of parallel lines are transformed into pairs of parallel lines, and so on. But it is worth noting that distances and angles are not preserved, since they do not make sence in affine spaces. To give them status, we shall have to introduce another element of structure, called the **metric** of space. Note right now, however that ratios of distance between aligned points do make sence and are preserved. they are thus called **affine invariants**. More generally, all these properties hold in dimension n. Informally, A_3 is what we gets when forgetting where the origin was in V_3. Conversely, selecting an origin in A_3 yields V_3 in a non-canonical identification. If we notice that selecting an origin for the space we live in is always an arbitrary move, A_3 emerges as a better model for ambient space than V_3 and *a fortiori* $\mathbb{R}^3$. In particular, the notion of vector field needs affine space, not only vector space, to make sense : a vector field is a mapping from A_n in V_n. By the way, there is a name, **bound vector**, to designate a pair $\{x, v(x)\}$ consisting of a point in A_n and a vector of V_n which we consider as assigned to this point. Be carefull that bound vectors are not vectors since they do not form, taken together, a vector space : indeed, it makes no sense to add $\{x, v\}$ and $\{y, w\}$, unless $x = y$, or to multiply $\{y, w\}$ by a scalar. But they do form an affine space since a bound vector $\{x, v\}$ can be construed as the pair of points$\{x, x + v\}$. We now adress the question of whether or not, the affine space is adequate to reflect the symmetries of the real world around us. Mathematically speaking, the symmetries of a structure are just its structure-preserving maps, so the symmetries of affine space are affine transforms. One of these symmetries is translational invariance. Mankind learned about this long ago, at least as regards horizontal translations. With Galileo and Newton, we realized that space was also invariant along the third dimension. From this point of view affine space does qualify. However, one may object, affine space

is too symmetrical for the purpose, for one cannot pretend that physics is invariant with respect to scaling and shearing. They are many physical events in which the symmetry of affine space is broken : for example, we can translate or rotate all rigid bodies, but not stretch or deform all of them without altering their inner structure. Mathematically, what is required for that is a metric structure. Metric is conferred onto a vector space V_n by endowing it with a **dot product**. There are a lot of dot products on V_n. A way to get them all is to select some frame $\{e_1, ..., e_n\}$ and to set $v \cdot w = \sum_{i,j} g_{i,j} v^i w^j$, where the metric coefficients g_{ij} are the entries of a square strictly positive definite symmetric matrix. As soon as we have adopted a dot product, notions of orthogonality and angles begin to make sense. We also know what distance means, speaking of two points x and y of the associated affine space A_n : it is the number $d(x,y) =\mid x - y \mid= \sqrt{(x-y)\cdot(x-y)}$, of which we immediately sees it satisfies all properties required of a distance ($d(x,y) = d(y,x) > 0$, unless $x = y$, and the triangular inequality). This turns A_n into a **metric space** with a bonus : the metric is compatible with the affine structure, which means that it is invariant by translations ($d(x+v, y+v) = d(x,y)$). Translations are thus **isometries** i.e. transforms that preserve distance. It can be shown that isometries in A_n must be affine transforms, but the converse is not true. Those affine transforms that do preserve distances are called **displacements** and they form a group smaller than GA_n. Among them, those at fix point are called **orthogonal transforms** and include rotations and mirror reflections (transforms $v \longmapsto v - 2u \cdot vu$, where u is a unit vector). Orthogonal transforms which fix a given point form what crystallographers call a **point group** : this group is isomorphic to the group of orthogonal matrices of order n. A **space group**, in contrast to point group, is a subgroup of displacements which contains translations in all three directions. Such notions are fundamental for the modelling of photonic crystals, but should we commit ourselves to a metric when only electromagnetism is involved ? The simple example of a light-ray falling on a mirror suggests that there are optical experiments which cannot be described in exclusively affine terms : equality of angles in light-ray reflection (thanks to the Snell-Descartes laws) is not an affine notion. What is very exciting, however, is that all aspects of Maxwell's theory are not alike in this respect. Some are affine invariant, some require a metric. The metric structure of spaces intervenes in the constitution laws thanks to the so-called $\star$ **Hodge operator** which links physical entities represented by really different mathematical entities, that is converts intensities in flux density (and conversely) : $\mathbf{D} = \varepsilon \star \mathbf{E}$ (dielectric law), $\mathbf{B} = \mu \star \mathbf{H}$ (magnetic law), $\mathbf{J} = \sigma \star \mathbf{E}$ (conductive law). In vector analysis, the Hodge operator is completely hidden by having represented $\mathbf{D}$, $\mathbf{B}$, $\mathbf{E}$, $\mathbf{H}$ and $\mathbf{J}$ as vector fields.

Still, a last element of structure is lacking, which one allows to make difference between $\mathbf{E}$ and $\mathbf{H}$: the orientation of space. Orientation, like metric, is an element of structure that one may lay over a vector space. These are independent structures. So here, we assume a given vector space V_n of dimension n, but no dot product. Consider two frames in V_n, $\{e_i\ ,\ i = 1, ..., n\}$ and $\{f_j\ ,\ j = 1, ..., n\}$. One mays express the e_is as linear combinations of the f_js, hence a **transition matrix** T such that $e_i = \sum_j T_i^j f_j$. As T is regular, its determinent has a definite sign. We say that $\{e_i\}$ and $\{f_j\}$ have the same orientation if the sign is positive, opposite orientations if the sign is negative. This defines two classes of frames, two of them belonging to the same class if they have the same orientation.

An **oriented vector space** is a composite mathematical object, a pair, which consists of a finite dimensional vector space and one of its two orientation classes. So for each vector space, there are two oriented vector spaces, with opposite orientations, which can be associated with it. To orient V_n consists in making a choice between these two possibilites, that is, designating a distinguished class of frames. It is convenient to name this class Or, and the other one $-Or$. The two possible oriented space are thus $V_n^+ = \{V_n, Or\}$ and $V_n^- = \{V_n, -Or\}$. It is worth noting that a vector remains a vector when the vector space is oriented : the so-called **axial** and **polar** vectors will come later. An affine space A_n is oriented by orienting its associate vector space V_n : a **bound frame** at x in A_n is direct or skew if the n independent vectors form a direct or a skew frame in V_n. They induce two new structures A_n^+ and A_n^-. Vector subspaces of a given vector space (of affine subspaces of an affine space) can have their own orientation. For this, consider two subspaces U and W complementary in V i.e. such that $V = U \oplus W$. We say that U has an **external** or **outer** orientation if an orientation is provided for one of its complements, W say. On the contrary, we shall call **inner** orientation what was simply orientation up to this point. These notions pass to affine subspaces of an affine space the obvious way. It is clear that if the encompassing space V itself is oriented, then an outer orientation of U gives it an inner orientation : to know the orientation class of a frame in U, append to it a direct frame of W, thus obtaining a frame in V, and look to which class the latter belongs. But two possible orientations for V make two ways to do that, so outer orientation and inner orientation are different, as are their intuitive meanings. For instance, inner orienting a line means distinguishing forward and backward directions along it. But outer orienting the line, that is to say, inner orienting a transverse plane, amounts to make choice between the two ways to turn around the line. If ambient space is oriented, the direct way to turn around a line implies a way to go forward along it. Similarly, outer orienting a plane means specifying a crossing direction through it. Curved lines also can be internally and externally oriented. The case of surfaces is a bit more complex. Orienting a surface means orienting all of its tangent planes at all points, in a consistent way. For neighboring points, tangent spaces are different, but close enough to have a common transversal. Orientations at these points are consistent if they give the same outer orientation to this transversal, which can always be achieved. But though this ensures consistent orientation locally, it may not be possible to maintain such consistency all over, as the Möbius band testifies. On the other hand, surfaces which enclose a volume can be oriented : going inside out defines a consistent crossing direction. This is outer orientation, from which inner orientation stems, if the ambient space is oriented.

We are now in possesion of a framework in which to model electromagnetic phenomena : oriented Euclidean three-dimensional affine space, that will be denoted E_3^+. It is A_3^+ coated with two layers of structure : a dot product and an orientation. Dimension 3 has this in particular that one can define a new operation, the cross product : given two vectors u and v, the cross product $u \times v$ is a vector orthogonal to both of them, of squared length $|\, u \,|^2 |\, v \,|^2 - (u \cdot v)^2$, and such that the frame $\{u,\ v,\ u \times v\}$ be direct. The very notion, therefore, does not make sense without a metric and an orientation. Its sensitivity to orientation is showed by the following fact : if T is an affine transform, $T(u \times v) = \pm Tu \times Tv$, the sign depending on the parity of T (it is $-$ for a mirror reflexion). This contrasts to

what happens with respect to vector addition, since we have $T(u+v) = Tu+Tv$. The cross product operation hence belongs to the structure of oriented 3-dimensional Euclidean space. This is true of other operations, notoriously the curl operator. Having adopted a direct orthonormal Cartesian system of basis vectors and axes, thanks to the Stokes theorem we get that $\mathrm{curl}(Mu) = -M(\mathrm{curl}\, u)$, if M is the mirror reflection with respect to a plane m. As for div, the metric structure is irrelevant in this case : the operator div belongs to the affine structure (think of v as the velocity field of some compressible fluid, then $\mathrm{div}\, v$ expresses the rate of change of the volume along the flow, which is an affine concept.). If we use the vector calculus notation $\mathrm{curl}\, v = \nabla \times v$, we therefore see that ∇ is immune to orientation diseases, contrary to curl (do not forget that such notations are dangerous since they lead for example to the false formula $\mathrm{curl}(u \times v) = \nabla \times (u \times v) = (\mathrm{div}\, v)\ u - (\mathrm{div}\, u)\ v$.). Let us now push on the scene new geometrical objects : covectors (instead of vectors) and differential forms (instead of vector fields).

A.2 Notion of differential form on a manifold

In the sequel, we give a brief survey on differential calculus. During the overall expose we will keep in mind the goal of our purpose : numerical implementation to solve spectral problems arising in electromagnetics.

Let $\mathbb{R}^{n+}$ denote the set of points $x = (x^1, ..., x^n)$ of $\mathbb{R}^n$ such that $x^1 \geq 0$. Unlike $\mathbb{R}^n$, $\mathbb{R}^{n+}$ has a boundary made of points x such that $x^1 = 0$. Let us thus introduce the notion of a n-dimensional manifold X as a set of points which have a neighbourhood in bijection with an open bounded set $I \subset \mathbb{R}^n$ or $I' \subset \mathbb{R}^{n+}$ (in the first case, the points belong to the interior of X, and in the second case they belong to the boundary of X). Roughly speaking, a n-dimensional manifold is thus a set which looks like $\mathbb{R}^n$ in the neighbourhood of its points. The bijection between $\mathbb{R}^n$ and X allows to express every point in a neighbourhood of a given point P of X in terms of its local coordinates $\{x^1(P), ..., x^n(P)\}$ thanks to the theorem of implicit functions. Thanks to the bijection, classical properties such as continuity and derivability in $\mathbb{R}^n$ are preserved in X. It is worth noting that there is in fact an infinity of such bijections (this family of maps is called atlas) and that they are not explicitely given. Therefore, the distances and angles on $\mathbb{R}^n$ do not induce distances and angles on X : the atlas preserves the topology but not the metric. More intuitively, when we represent the atlas of the World in a plane thanks to a stereographic projection, we see a distortion of many countries. There is another important property for a manifold called compatibitlity that can be simply visualised : when we look at two maps of the France, we can note that there is a kind of compatibility between them. Although of different scales, orientations and shapes, the two maps represent the same country and must therefore satisfy some constraints. The same holds true for manifolds : they are in fact locally defined by maps which intersect two by two. If two maps recovering the same area have opposite properties, the resulting atlas has no sense. What could we say about this tesselation ? It seems obvious that the very different natures of these shapes (of smooth boundary, with corners and with a chaotic boundary) could led to paradoxical properties for the atlas ! One may require for example a continuous map to exist which transforms

a shape in another (which is obviously not the case !). More precisely, let us consider two maps φ_1 and φ_2 with domains $dom(\varphi_1)$ and $dom(\varphi_2)$ sharing a common part. We then define two maps φ_{12} and φ_{21} such that :

$$\varphi_{12} = \varphi_{1|dom(\varphi_2)} \text{ and } \varphi_{21} = \varphi_{2|dom(\varphi_1)} \tag{A.1}$$

that is, two maps restricted to the domain of each other. Since φ_{12} is a bijection, it admits a reciprocal application and one can therefore introduce the notion of **transition function** :

$$\psi = \varphi_{21} o \varphi_{12}^{-1} \tag{A.2}$$

which maps $\mathbb{R}^n$ in $\mathbb{R}^n$. We can thus clearly define notions of continuity and derivability for this application (which is not the case for φ_1 and φ_2). In fact, ψ defines the common local properties shared by two maps. If we want to assign global properties to the manifold, we thus have to consider a family of applications ψ_i (locally defined) sharing the same properties. Generally, the assumptions are made on the derivability of such maps : if the maps are differentiables and their kth derivative too, one speaks of a C^k-manifold (if $k = 0$, the manifold is a topological one). If the bijections ψ_i map X in $\mathbb{R}^{n+}$, one can define the regularity of the boundary of the manifold.

Remark :

All these notions are closely related to the numerical tesselation of a manifold : in numerical analysis, the finite element spaces are usually attached to some finite subspaces (the so-called **Galerkin** spaces) which closely approximate the Hilbert spaces, home of the electromagnetic field. The counterpart of these Galerkin spaces in differential geometry is a set of discrete differential forms (Whitney complex) whose properties depend upon the tesselation of the manifold : we will see that some compatibility conditions between the tiles of the mesh (e.g. tetrahedra) are needed (no more than a facet in common, same orientation...) which induces common properties for some applications mapping these tiles into a reference square triangle.

A.3 Tangent space to a manifold

Let us consider a trajectory (curve) on a manifold X that is a smooth function mapping $\mathbb{R}$ in X, whose domain is a segment. A scalar field is defined as a regular function mapping X in $\mathbb{R}$. The manifold X being connected, its image is a segment in $\mathbb{R}$. A point x belongs to a trajectory g if $0 \in dom(g)$ and $g(0) = x$. A scalar field f is null in x if $f(x) = 0$. If x belongs to two trajectories g and g', then they are said to be tangent in x if, for a given map ψ in x :

$$\frac{\mid \psi(g(t)) - \psi(g'(t)) \mid}{t} = o(t) \tag{A.3}$$

such a definition defines an equivalence class between trajectories. It is to be noticed that one require the map ψ to be C^1. These definition is in fact independent of the map provided that we take a manifold of class C^1. Two scalar fields f and f' null in x are said to be tangent in x if, for every $y \in dom(\psi)$:

$$f(y) - f'(y) = o(\mid \psi(y) - \psi(x) \mid) \tag{A.4}$$

We then call a tangent vector in x (resp. covector in x) an equivalence class of trajectories g satisfying A.3 (resp. scalar functions satisfying A.4).

We now can introduce the notion of tangent space T_x in a given point x of a manifold X. If u is a smooth application mapping X in another manifold Y, for a given trajectory g in $x \in X$ we then have a trajectory $u \circ g$ in $y \in Y$. $u \circ g$ defines a tangent vector since $u \circ g$ and $u \circ g'$ are equivalent if g and g' are equivalent (in the sense of A.4). We note this application uog as $u_*(x) : T_xX \longmapsto T_yY$. Analogously, if f is a scalar field on Y (null in y), $f \circ u$ is a scalar field on u (null in x), the corresponding covector is denoted by u^*f^*. It clearly defines an application $u^* : T_y^*Y \longmapsto T_x^*X$. We thus have the following associative rules when u and v denote two applications $u : X \longmapsto Y$ and $v : Y \longmapsto Z$:

$$(v \circ u)_* = v_*\, u_* \text{ and } (v \circ u)^* = u^*\, v^* \tag{A.5}$$

(note the inversion of u and v in the second equality). Let us now consider that X and Y are affine spaces $X = V_m$ and $Y = V_n$. Let us choose an arbitrary origin in the affine space $X = V_m$ (resp. $Y = V_n$). We can therefore associate to every point x (resp. y) of the affine space V_m (resp. V_n) a vector in the vectorial space V_m (resp. V_n). We can thus choose a canonic basis $\{e_J\}$, $J = 1, ..., m$ in V_m and $\{e_i\}$, $i = 1, ..., n$ in V_n. We now express the point $u(x)$ (in the linear space V_n) as a linear combination of the components u^i of the its associated vector $u(x)$ (in the vectorial space V_n) :

$$x = \sum_{J=1,...,m} x^J e_J \text{ and } u(x) = \sum_{i=1,...,n} y^i e_i \tag{A.6}$$

with $y^i = u^i(x^1, ..., x^m)$ and u^i a function such that $u^i : \mathbb{R}^m \longmapsto \mathbb{R}$. Let us now consider the trajectory $t \longmapsto x + t\, e_J$. We thus see that the vertice in x, whose definition is obvious, is nothing else than e_J. We therefore denote e_J the vector of the tangent space T_xX in x of the trajectory. The image of this trajectory in x by the map u is a trajectory in $u(x)$, $t \longmapsto u(x + t\ e_J)$, whose vertice for $t = 0$ is by definition $u_*(x)e_J$. If we derive $t \longmapsto u(x + t\, e_J)$ we have :

$$u_*(x)e_J = \sum_{i=1,...,n} \frac{\partial u^i}{\partial x^J}(x) e_i \tag{A.7}$$

$u_*(x)$ is therefore a rectangular matrix representing the Jacobian of the u^is.

Analogously, we denote by $\{e^J\}$, $J = 1, ..., m$, the covectors of the canonical basis of V_m. They are linear functions $x \longmapsto x^J$ such that $e^I e_J = \delta_{IJ}$ (i.e. 1 if $I = J$ and 0 otherwise). Let $\{e^i\}$, $i = 1, ..., n$ denote the canonical basis of V_n. A covector in point $y = u(x)$ is the class of the affine function $y' \longmapsto e^i(y' - u(x))$, still denoted by e^i. We then define $u^*(y)e^i$ as the class of the function $x' \longmapsto u^i(x') - u^i(x)$. We thus have :

$$u_*(x)e^i = \sum_{J=1,...,m} \frac{\partial u^i}{\partial x^J}(x) e^J \tag{A.8}$$

We therefore see that if $X = V_m$ and $Y = V_n$, the application u_* (taken in the point x) is the Jacobian $\dfrac{\partial u^i}{\partial x^J}$ and u^* (taken in the point $u(x)$) is its transpose. We now want

to see that in the general case of two manifolds X and Y, u^* is still the transpose of the linear operator u_*. For this, we must verify that T_xX and T_yY are two vectorial spaces. Let thus X be a n-dimensional manifold, g_* a vector in x and ψ a map in x. Then $\psi_* g_*$ is a vector in $\psi(x)$. The application ψ_* is injective, because if $\psi \circ g$ and $\psi \circ g'$ are two tangent trajectories so are g and g'. We thus transport the vectorial structure of V_n on T_xX. If g_* and h_* are two tangent vectors, we indeed see that $\psi_*^{-1}(\psi_* g_* + \psi_* h_*)$ is a tangent vector too. T_xX is thus a vectorial space whose basis is given by the trajectories

$$g^i = \psi^{-1} \circ \gamma^i \tag{A.9}$$

with $\gamma^i : t \longmapsto \psi(x) + t\ e_i$, e_i being the ith vector of the canonical basis of V_n. By a one to one correspondence between the n components of $\psi(y)$ and the n components of $\psi_*(x)g_*(x)$ (which is a vector in $\psi(y)$), we thus obtain a map for the manifold of the tangent vectors $\{y, g_*(y)\}$. One has to be carefull to the sense given to this couple : it locally looks like the cartesian product of two manifolds but it is not a cartesian product. Let us for instance consider the famous Möbius strip which cannot be identified with the cartesian product of the segment $[0;1]$ with the unit circle (a cylinder). To clarify this difference, we introduce the notion of fiber bundle TX to a manifold X as following :

$$TX = \bigcup_{x \in X} T_xX \tag{A.10}$$

This is a $2n$-dimensional manifold. The tangent vectors $\{y, g_*(y)\}$ therefore belong to TX. More precisely, this fiber bundle is a manifold built thanks to the identification of the couples $\{y, g_*(y)\} \in \mathbb{R}^n \times V_n$ with the following rule : $\{y_1, g_{*1}(y_1)\}$ and $\{y_2, g_{*2}(y_2)\}$ are equivalents if

i) $\psi_1^{-1}(y_1) = \psi_2^{-1}(y_2)$ i.e. y_1 and y_2 are the image of the same point $x \in X$

ii) Let G be a family of diffeomorphisms on X, that is a family of bijective differentiable applications, with differentiable reciprocal applications. Then the transition function ψ_{12} (A.2) which maps X in G satisfies :

$$g_{*1}(y_1) = \psi_{12}(x) g_{*2}(y_2) \tag{A.11}$$

The assertion i) says how to stuck the images of the domains of ψ_1 and ψ_2 such that we get a tesselation of X. The assertion ii) says how to put the fibers together. Let us digress for a while about the connection between the notion of manifold and the one of group. The capital G refers in fact to a group structure which is determined by the very structure of TX. First of all, one sees that $\psi_{12} \circ \psi_{21}$ is the identity, thanks to (A.12). Similarly, if x belongs to the domains of three distinct maps, we get $\psi_{12} \circ \psi_{23} = \psi_{13}$. We therefore see that the values $\psi_{12}(x)$ have a group structure : we thus choose G as a group of diffeomorphisms of the fiber. furthermore, if v is a point in V_n, that is class of equivalence of $\{y, g_*(y)\}$, the functions $v \longmapsto \{y, g_*(y)\}$ are maps in v, which must be compatible that is there associated transition function ψ are continuous. The correspondence between $\{y_1, g_{*1}(y_1)\}$ and $\{y_2, g_{*2}(y_2)\}$ thus induces that the function

$$\{y, g_*(y)\} \longmapsto \{\psi_2 \circ \psi_1^{-1}(y), \psi_{21}(\psi_1(y)) g_*(y)\} \tag{A.12}$$

must be differentiable. The transition functions ψ_{12} are therefore differentiables, and the group G must have a structure of differentiable manifold. Such groups are called Lie groups and depend continuously on several parameters. For instance, the group of rotations in $\mathbb{R}^2$

$$SO(2,\mathbb{R}) = \left\{ A(\theta) = \begin{pmatrix} \cos\theta & \sin\theta \\ -\sin\theta & \cos\theta \end{pmatrix},\ \theta \in [0;2\pi] \right\}$$

is a Lie group since it satisfies the following properties :

i) $A(\theta_1)A(\theta_2) = A(f(\theta_1,\theta_2))$ with $f \in C^\infty$.

ii) $A(0) = Id$ where 0 is the origin for the paramaters of the group.

iii) $A(\theta)^{-1}$ exists and is defined by $A(g(\theta))$ with $g \in C^\infty$.

One can see that $f(x,y) = x+y$ and $g(x) = -x$ satisfy the assertions. Such a continuous group has an associative law since

$$\begin{aligned} A(\theta_1)\Big(A(\theta_2)\ A(\theta_3)\Big) &= A(\theta_1)A(\theta_2+\theta_3) = A(\theta_1+\theta_2+\theta_3) \\ &= A(\theta_1+\theta_2)A(\theta_3) = \Big(A(\theta_1)\ A(\theta_2)\Big)A(\theta_3) \end{aligned} \tag{A.13}$$

But this is a non-commutative group, a property shared by a lot of manifolds. In the general case, the group G can be finite : a finite set can be seen as a manifold with a discrete topology. The finite groups therefore belong to Lie groups (so do the groups $\mathbb{Z}$, $\mathbb{Z}^n$...). It is worth noting that for a manifold X with a vectorial structure, one has to take an adequate group G to keep the vectorial structure for the fiber bundle (we thus say that we have a vector bundle). For example, one must take the group GL_n of isomorphisms (linear inversible applications on X) on a n-dimensional vectorial space X : the representation of the elements of GL_n by matrices in a basis is a map which gives to the group a structure of manifold. Let us consider for instance a sphere S_2 of $\mathbb{R}^3$ and the vectors tangents to its points. We thus have a 4-dimensional manifold, which is not $S_2 \times \mathbb{R}^2$, denoted by TS_2. With the structure of the group GL_2, TS_2 is a vector bundle. Thanks to the very definition of an equivalence class $\{y, g_*(y)\}$ in TX, we know that it corresponds to this class a point x in the manifold X given by $\psi(x) = y$ for all the maps ψ in x. We call it the projection of $\{y, g_*(y)\}$ on the manifold X (X is said to be the basis of the fiber) and denote it by $x = p(\{y, g_*(y)\})$. The images of the inverse of the projection p

$$r(x) = p^{-1}(x) \tag{A.14}$$

are isomorphic tangent spaces called fiber over x and denoted T_xX. We are now ready to introduce the important notion of the section of a fiber bundle. We denote by the section of a fiber bundle TX of basis X every function $s \in X \longmapsto TX$ such that

$$p(s(x)) = x\ \forall x \in dom(s) \tag{A.15}$$

The sections of fibers are the adequate mathematical objects to represent the physical fields. In the sequel, we will call vector fields on X, the sections of TX.

Let us now introduce the notion of cotangent space that is the space of covectors. Let thus f^* be a covector in x. If ψ is a map in x, $(\psi^{-1}) * f^*$ is a covector in $\psi(x)$ and T_x^*X

can therefore be identified to a n-dimensional vector space V_n. The covectors of the basis are the classes of functions

$$f_i = y \longmapsto \psi_i(y) - \psi_i(x) \tag{A.16}$$

that is $f_i = \varphi_i \circ \psi$, where $\varphi_i : \eta \in \mathbb{R}^n \longmapsto \eta^i - \psi^i(x)\mathbb{R}$, and ψ^i is the i-th component of the map ψ. To the n components of $\psi(y)$ corresponds the n components of $(\psi)^{-1} * (x)\ f(y)$ which is a covector in $\psi(y)$. We thus obtain a map for the manifold of couples $\{y, f^*(y)\}$, that is for the $2n$-dimensional manifold of covectors denoted by T^*X. Analogously to TX, T^*X is a vector bundle with the same group of structure. The sections of T^*X, the fields of covectors, are called differential forms of degree 1 or 1-forms.

If X and Y are two manifolds and $u : X \longmapsto Y$ is a differentiable application, we now can explain what is the derivative of u. If g is a trajectory in x, it is an application between two fibers denoted u_* and defined as follows :

$$u_* : \{x, g_*\} \in TX \longmapsto \{u(x), u_*(x)\ g_*\} \in TY \tag{A.17}$$

It is called tangent application and it is defined on the domain of differentiability of u. We can see that u induces the existence of u_* and that u_* induces the existence of an application $u^* : T^*Y \longmapsto T^*X$.

A.4 Vectors and covectors

Let us now discuss about the duality between vectors and covectors. If $g : \mathbb{R} \longmapsto X$ is a trajectory in x, and $f : X \longmapsto R$ is a null function in x, which are both smooth, $f \circ g : \mathbb{R} \longmapsto \mathbb{R}$ admits a derivative in 0

$$< g_*, f^* >= \frac{d}{dt}(f \circ g)\mid_{t=0} \tag{A.18}$$

This is a number that only depends upon the classes of f and g thanks to (A.3) and (A.4). We thus obtain a bilinear application on $T_xX \times T_x^*X$. This map is not degenerated i.e. it is null for all f^* only if $g_* = 0$ and *vice versa*. We thus have a duality between T_xX and T_x^*X. Let us now consider the map $u : X \longmapsto Y$, g a trajectory in x, f a function in $y = u(x)$ and the following diagram :

$$\mathbb{R} \xrightarrow{g} X \xrightarrow{u} Y \xrightarrow{f} \mathbb{R} \tag{A.19}$$

Thanks to (A.18), we therefore have that

$$\frac{d}{dt}(f \circ u \circ g)_{t=0} = < u_*(x)\ g_*\ ,\ f^* >_{T_yY, T_y^*Y} = < g_*\ ,\ u^*(y)\ f^* >_{T_xX, T_x^*X} \tag{A.20}$$

which proves that the linear map $u_*(x)$ is the transpose of $u^*(y)$, and conversely. We say that these maps are in duality, as it was seen for the particular case $X = V_m$ and $Y = V_n$.

The application of vectors on covectors and *vice versa* is said to be a **contraction** or **interior product**. We will see in the sequel that it is a derivation. The value of the gradient of a scalar function taken in a point is for example a covector.

By analogy to (A.18), we want to write

$$< g_*, f^* >= \frac{\partial f}{\partial x}\frac{dg}{dt} \mid_{t=0} \tag{A.21}$$

Mathematically speaking, this is an incorrect equation, since its right member has no sense. But it suggests that the action of a covector f^* on the vector g_* can be seen as the derivative of f in the direction of the vector g_* (this interpretation would be correct if X were V_n and $\frac{\partial f}{\partial x}$ would therefore be the gradient of f in x). We thus call gradient of f in x the covector f^* (recall that g_* is the vector vertice in x on the trajectory g).

In (A.21), we see that a vector field (that is to say a section of TX) is a differential operator $\partial f \ : \ x \longmapsto < v_x, f^* >$. In other words, the vector fields are the differential operators of first order on the manifolds. We hence note ∂_v the vector field v. We denote v^i the components of v in the basis of vectors $\frac{\partial}{\partial_i}$ and thus write

$$v = \partial_v = \sum_{i=1,...,n} v^i \partial_i \tag{A.22}$$

If $v = g_*$, we can thus rewrite (A.21) as follows :

$$\partial_v f = \sum_{i=1,...,n} v^i \partial_i f \tag{A.23}$$

Let us now consider two manifolds X and Y of dimensions n and m, a map $u \ : \ X \longmapsto Y$ and a function $f \ : \ Y \longmapsto \mathbb{R}$. Let v be a vector field on V and $w = u_* \ v$. In the bases $\{\partial_J \ : \ J = 1, ..., m\}$ of $T_x X$ and $\{\partial_i \ : \ i = 1, ..., n\}$ of $T_y Y$ $(y = u(x))$, we write

$$\partial_v = \sum_{J=1,...,m} v^J \partial_J \text{ and } \partial_w = \sum_{i=1,...,n} w^i \partial_i \tag{A.24}$$

Thanks to the definition of u_*, we know that $\partial_w f = \partial_v (f \circ u)$. We thus want to write

$$\partial_v (f \circ u) = \sum_{J=1,...,m} v^J \partial_J (f \circ u) = \sum_{J=1,...,m} v^J \sum_{i=1,...,n} \partial_i f \partial_J u^i \tag{A.25}$$

which is equivalent to say

$$\partial_w = \sum_{J=1,...,m} v^J \sum_{i=1,...,n} \partial_J u^i \partial_i \tag{A.26}$$

It is worth noting that this expression has no rigorous mathematical meaning since $\partial_J u^i$ is not defined. But we know that $\partial_w = u_* \partial_v$, then (A.24) induces that

$$\partial_w = \sum_{J=1,...,m} v^J u_* \partial_J \tag{A.27}$$

Furthermore, $u_* \ \partial_J$ is a vector which can be written in the basis $\{\partial_i\}$ as

$$u_* \partial_J = \sum_{i=1,...,n} \partial_J u^i \partial_i \tag{A.28}$$

If we then decide to denote its components by $\partial_J\ u^i$, we therefore get (A.26). The $\partial_J\ u^i$ in (A.26) are therefore defined as the components of the vector $u_*\ \partial_J$. It is worth noting that this expression is equivalent to (A.7)). We can thus extend to the manifolds the usual derivation laws of the differential calculus on vectorial spaces.

Concerning the covectors, we denote by $\{dx^i\}$ or d^i their basis, which linearly map a $v \in T_xX$ in its components v^i. We thus have

$$d^i v = v^i \tag{A.29}$$

We therefore can express the duality between a vector v and its covector f^* as follows

$$< v, f^* > \ = \sum_{i=1,\ldots,n} \partial_i f\ v^i = (\sum_{i=1,\ldots,n} \partial_i f d^i)v = \partial_v f := v(f) \tag{A.30}$$

(A.30) suggests that we should denote df the fields of covectors spaned by f and we should write

$$df = \sum_{i=1,\ldots,n} \partial_i f\ d^i = \sum_{i=1,\ldots,n} \frac{\partial f}{\partial x_i} dx^i \tag{A.31}$$

its expression in the basis of covectors. d is called **exterior derivative** and we can now write

$$df(v) = \partial_v f = v(f) \tag{A.32}$$

which is equivalent to (A.21) for $g_* = v$. We call df the gradient of f : this is a covector field, that is a 1-form, associated to f. When applied to a given vector field v, df gives the derivative of f in every points in the direction of v. df is thus the differential of the function f which gives its variation (of the first order) in a neighbourhood of a point x. The variation is a function of the vector of displacement v and is denoted $df(v)$. But for a given vector of displacement v, we can also say that this variation is a function of f, which consists in deriving f with respect to v. We thus denote it by $\partial_v f$ (or $v(f)$). Differentiation and derivation are therefore dual point of views.

Let us summarize the previous paragraph. Let us consider two manifolds X and Y and a map $u\ :\ X \longmapsto Y$. We have seen that the vectors on X are transformed in vectors on Y thanks to a map u_*, which is therefore called a **push-forward**. The covectors on Y are transformed in covectors on X thanks to u^*, which is therefore called a **pull-back**. The vectors and covectors can be written as linear combinations of vector and covector bases. The vector bases are identified to derivatives over lines of coordinates and the covector bases map a vector in its coordinates. When applied to a covector, a vector gives a real number which does not depend upon the maps of the atlas. We thus obtain a bilinear application which is a non-degenerated one. There is therefore a duality between vectors (operators of derivation) and covectors (differentials of functions).

We are now ready to introduce new objects living on a manifold, the so-called tensors.

A.5 Tensors and p-forms

We already know two covectors in electromagnetism : the first one is the electric field $\mathbf{E}$, and the second one is the magnetic field $\mathbf{H}$. But what could we say about the electric and

magnetic flux **D** and **B** ? For instance, the flux of **B** across an element of surface is defined by two vectors, say v_1 and v_2, which are tangents to the surface in a given point. This flux is obviously a linear function of v_1 and v_2. Furthermore, the sign of the flux depends upon the order of the vectors v_1 and v_2 on the orientation of the element of surface (spaned by $\{v_1, v_2\}$ or $\{v_2, v_1\}$). This notion is related to that of 2-**covector** in x which is a bilinear antisymmetric application $\omega \ : \ T_xX \times T_xX \longmapsto \mathbb{R}$ i.e.

$$\omega(v_1, v_2) = -\omega(v_2, v_1) \ , \ \forall v_1, \ v_2 \in T_xX \tag{A.33}$$

$\mathbf{B}(x)$ is such a 2-covector in x and the magnetic field **B** is a section of the fiber of 2-covectors. It is the so-called 2-**form B**. We generalize this notion to p-forms thanks to p-covectors in x, which are sesquilinear alternate applications on T_xX i.e. their signs depend upon a cyclic permutation of the p variables. If $p = 0$, we just have a regular function on X. We now have a new family of fiber bundles on X. What is the dimension of such fibers ? For $p = 2$, let us consider a 2-covector ω_x in x and $\{\partial_i \ : \ i = 1, ..., m\}$ a basis of T_xX. If we denote $v_j = \sum i = 1, ..., m v_j^i \partial_i$ the two components of v $(j = 1, 2)$, we have

$$\omega_x(v_1, v_2) = \omega_x(\sum_i v_1^i \partial_i \ , \ \sum_j v_2^j \partial_j) = \sum_{i,j} \omega_x(\partial_i \ , \ \partial_j) v_1^i \ v_2^j \tag{A.34}$$

Thanks to its antisymmetric properties, it sufficies to know the $\dfrac{n(n-1)}{2}$ numbers $\omega_x(\partial_i \ , \ \partial_j)$ for $i < j$ to calculate ω. The dimension of the fiber bundle is thus $\dfrac{n(n-1)}{2}$. We can thus write

$$\omega_x(v_1, v_2) = \sum_{1 \leq i < j \leq n} \omega_x(\partial_i \ , \ \partial_j)(v_1^i v_2^j - v_2^i v_1^j) \tag{A.35}$$

There are two kinds of factors in (A.35) : the factors $\omega_x(\partial_i \ , \ \partial_j)$ that can be denoted by $\omega_{ij}(x)$ characterize ω_x ; the factors $(v_1^i v_2^j - v_2^i v_1^j)$ are the result of a 2-covector acting on (v_1, v_2) and are denoted by $d^i \wedge d^j$ or $dx^i \wedge dx^j$. We thus have

$$(dx^i \wedge dx^j)(v_1, v_2) = (d^i \wedge d^j)(v_1, v_2) = v_1^i v_2^j - v_2^i v_1^j \tag{A.36}$$

The $d^i \wedge d^j$ are the vector basis in the fiber bundle of 2-covectors in x. When ω is a 2-form, we can write in the neighbourhood of a point x

$$\omega \ : \ x \longmapsto \sum_{i<j} \omega_{ij}(x) dx^i \wedge dx^j \tag{A.37}$$

When ω is a p-form $(p > 2)$, analogously to (A.37) we have in the neighbourhood of a point x

$$\omega \ : \ x \longmapsto \sum_{\sigma \in C(n,p)} \omega_\sigma(x) d^{\sigma(1)} \wedge ... \wedge d^{\sigma(p)} \tag{A.38}$$

where $C(n, p)$ denotes the set of increasing injections from $\{1, ..., p\}$ to $\{1, ..., n\}$. The dimension of the fiber bundle therefore is $\dfrac{n!}{(n-p)!p!}$. One can see that there are no non-trivial p-covectors for $p > n$, since p vectors are never independent if $p > n$ on a vector space of dimension n. Concerning the case $p = n$, one can see that a n-covector is nothing

else than a determinent of n vectors times a scalar : the determinent is a well-known n-covector on a vector space V_n, and is given by a change of basis of the given n-covector that induces the scalar factor. The fiber bundle of n-covectors is thus of dimension 1. We say that a field of n-covectors is a **volume** if it is never null on X and a local volume if it is never null in a neighbourhood of x. There is a strong analogy with the geometrical aspect of a determinent which is the volume spaned by n vectors. The sign of the determinent gives the **orientation** of the n vectors. It is worth noting that we call p-vector an element of the dual space of p-covectors, although it is not a collection of p-vectors !

To end this paragraph, let us say a few words about the tensors. They are fields of sesquilinear applications which are not necessarily alternate ones. They do not act exclusively on vectors of the tangent space (contrary to p-covectors), neither do they exclusively on covectors (contrary to p-vectors). They actually act on both of them. More precisely, let us consider some linear maps $v, ..., w \ : \ T_x^*X \longmapsto \mathbb{R}$ (the vectors) and $\omega, ..., \sigma \ : \ T_xX \longmapsto \mathbb{R}$ (the covectors). A tensor of type $\begin{pmatrix} q \\ p \end{pmatrix}$ (p-covariant and q-contravariant) is a multilinear map

$$T \ : \ \underbrace{T_xX \times ... \times T_xX}_{p \text{ terms}} \times \underbrace{T_x^*X \times ... \times T_x^*X}_{q \text{ terms}} \longmapsto \mathbb{R} \tag{A.39}$$

with p vectors and q covectors denoted by $T(v, ..., w; \omega, ..., \sigma)$. A covector is thus a tensor of type $\begin{pmatrix} 0 \\ 1 \end{pmatrix}$ and a vector is a tensor of type $\begin{pmatrix} 1 \\ 0 \end{pmatrix}$. The tensor product $\otimes$ of two tensors of type $\begin{pmatrix} 0 \\ 1 \end{pmatrix}$, ω and σ, is defined as follows :

$$(\omega \otimes \sigma)(v, w) = \omega(v)\sigma(w) \tag{A.40}$$

One can easily generalize this definition to tensors of any types. It is worth noting that the tensor product is not commutative. In the bases $\{dx^i\}$ of vectors and $\{\frac{\partial}{\partial x^j}\}$ of covectors, every tensor of type $\begin{pmatrix} q \\ p \end{pmatrix}$ can be written as follows

$$\begin{array}{ll} T & = T^{k...l}_{i...j} dx^i \otimes ... \otimes dx^j \otimes \dfrac{\partial}{\partial x^k} \times ... \times \dfrac{\partial}{\partial x^l} \\ T(v, ..., w; \omega, ..., \sigma) & = T^{k...l}_{i...j} v^i ... w^j \omega_k ... \sigma_l \end{array} \tag{A.41}$$

We can also make contractions only on selected vectors and covectors

$$T(..., v, ...; ..., \omega, ...) = T^{k..n..l}_{i..m..j} v^m \omega_n \tag{A.42}$$

The set of tensors of type $\begin{pmatrix} q \\ p \end{pmatrix}$ defined in a point x of the manifold X is a vector space denoted by $\otimes^p T_xX \otimes^q T_x^*X$. The set of tensor fields of type $\begin{pmatrix} q \\ p \end{pmatrix}$ defined on the manifold X is denoted by T^q_pX. What is the link between tensors and p-forms ? To adress this question, let us first introduce the notion of a completely symmetric tensor T^s of order

$\begin{pmatrix} 0 \\ p \end{pmatrix}$ or $\begin{pmatrix} p \\ 0 \end{pmatrix}$, that is a tensor invariant by any permutation of its variables. On the contrary, a completely antisymmetric tensor T^a changes of sign by any permutation of its variables. We thus have that :

$$\begin{array}{ll} T^s(...,v,...,w,...) & = T^s(...,w,...,v,...) \\ T^a(...,v,...,w,...) & = -T^a(...,w,...,v,...) \end{array} \tag{A.43}$$

whatever the v and w are. The components of tensors of type $\begin{pmatrix} 0 \\ 2 \end{pmatrix}$ verify for example

$$\begin{array}{lll} T^s_{ij} & = \dfrac{(T^s_{ij} + T^s_{ji})}{2!} & = T^s_{ji} \\ T^a_{ij} & = \dfrac{(T^a_{ij} - T^a_{ji})}{2!} & = -T^a_{ji} \end{array} \tag{A.44}$$

A p-form is actually a completely antisymmetric tensor of type $\begin{pmatrix} 0 \\ p \end{pmatrix}$. It is to be noticed that the antisymmetry does not appear for 0-forms and 1-forms, since there are less than two variables for their associated tensors.

A.6 The exterior product

Between the differentials of a p-form a and a q-form b is an implied exterior product, denoted by a wedge $\wedge$, which satisfies :

$$a \wedge b = (-1)^{pq} b \wedge a \tag{A.45}$$

More generally, the exterior product between n forms $d_1 \wedge d_2 \wedge ... \wedge d_n$ is the determinant of n vectors. As a consequence of A.50, any differential form with a repeated differential vanishes : $a \wedge a = 0$ provided that p is odd. In a three-dimensional space, each term of a p-form will always contain a repeated differential if $p > 3$, so there are no nonzero p-forms for $p > 3$. Furthermore, the exterior product of 1-forms is anticommutative, so that $dx \wedge dy = -dy \wedge dx$. The exterior product of two 1-forms is analogous to the vector cross product $\times$. The exterior product of a 1-form and a 2-form corresponds to the dot product $\cdot$. The coefficient of the resulting 3-form is equal to the dot product of the vector fields dual to the 1-form and 2-form in the euclidean metric. Using (A.50), one can easily manipulate arbitrary products of forms. For example, the identities :

$$a \cdot (b \times c) = c \cdot (a \times b) = b \cdot (c \times a) \tag{A.46}$$

are special cases of :

$$a \wedge b \wedge c = c \wedge a \wedge b = b \wedge c \wedge a \tag{A.47}$$

where a, b and c are 1-forms (the exterior product is an associative law, unlike the cross product). Thanks to the very properties of the exterior product, one can consider the p-covectors defined in $x \in \mathbb{R}^n$ as elements of the so-called Grassmann algebra. The exterior product is closely related to the notion of exterior derivative of a p-form. If we

consider a 0-form $f(x, y, z)$ and differentiate with respect to each of the coordinates, we obtain :

$$df = \frac{\partial f}{\partial x}dx + \frac{\partial f}{\partial y}dy + \frac{\partial f}{\partial z}dz \tag{A.48}$$

which is a 1-form, the exterior derivative of f. The differentials dx, dy and dz are the exterior derivatives of the coordinate functions x, y, z. The 1-form df is dual to the gradient of f. The exterior derivative of a 1-form is analogous to the vector curl operation. Indeed, if we consider the electric 1-form $\mathbf{E} = E_1dx + E_2dy + E_3dz$, using the antisymmetry of the exterior product, we get :

$$d\mathbf{E} = (\frac{\partial E_3}{\partial y} - \frac{\partial E_2}{\partial z})dy \wedge dz + (\frac{\partial E_1}{\partial z} - \frac{\partial E_3}{\partial x})dz \wedge dx + (\frac{\partial E_2}{\partial x} - \frac{\partial E_1}{\partial y})dx \wedge dy \tag{A.49}$$

which is a 2-form dual to the curl of the vector field $\mathbf{E} = E_1e_x + E_2e_y + E_3e_z$. Analogously, one can see that the exterior derivative of a 2-form $\mathbf{B}$ is a 3-form dual to the divergence of the vector field $\mathbf{B}$.

The exterior derivative of a p-form a and a q-form b obeys the product rule :

$$d(a \wedge b) = da \wedge b + (-1)^{p+q}a \wedge b \tag{A.50}$$

A special case of (A.50) is the Poynting identity :

$$div(E \times H) = H \cdot \operatorname{curl} E - E \cdot \operatorname{curl} H \tag{A.51}$$

where E is a 1-form and H a 1-twisted form.

A.7 Integration of differential forms

The notion of *twisted* form is closely related to that of integrability on a manifold. If X is a n-dimensional connex manifold without any orientation, one can define in an analogous manner to the Riemann integration theory, the integration of a n-twisted form, or density. It is worth noting that unlike the integration of real functions, we do not have to use the notion of measure. In the sequel, we will see that this point of view is very fruitfull in finite element theory and particularly in electromagnetic computations. To adress the question of integrability of differential forms on a manifold, we first have to mesh the manifold (thanks to triangles in $\mathbb{R}^2$ or tetrahedra for example in $\mathbb{R}^3$). For this, we define a p-simplex as the following closed subset of $\mathbb{R}^p$:

$$S^p = \{x \in \mathbb{R}^p : x_i \geq 0 \ \forall i, \sum_i x_i \leq 1\} \subset X \tag{A.52}$$

The subsets of S^p obtained by considering $x \in \mathbb{R}^p$ such that $x_i = 0$ and/or $\sum_i x_i = 1$ are the nodes, edges and facets of S^p. For the sake of simplicity, we say that a map $S^p \longmapsto S^q$ is simplicial is it is affine, injective and transforms the nodes, edges and facets of S^p in nodes, edges and facets of S^q. We then define a simplicial tesselation as the family $\mathcal{S}$ of applications $s \in \mathbb{R}^n \longmapsto X$ such that $dom(s) = S^n$, still denoted by n-simplices, with the following properties :

i) If s_1 and s_2 are two simplices of $\mathcal{S}$, then $s_1 o s_2^{-1}$ is simplicial too.
ii) If $s_1 \neq s_2$ then $s_1(S^n) \neq s_2(S^n)$.
iii) $\bigcup_{s\in\mathcal{S}} s(S^n) = X$.
iv) Every compact subset of X can be recovered by a finite union of $s(S^n)$.

We will see in the sequel that this definition is exactly the one of a mesh used in finite element theory : from a numerical point of view, we can consider a mesh of a physical body of interest (e.g. waveguide) as the tesselation of a manifold. This point of view allows us to make use of curved elements adapted to the shape of the body. It is to be noticed that one can refine the tesselation of a manifold by subdividing a simplicial mesh. The convergence of a finite element scheme depends upon the smoothness of the manifold representing the body of interest, that is to the capability of a simplicial mesh to imitate the manifold for a given refinement.

For a given n-form a on the n-dimensional manifold X, we now want to assign to each n-simplex s a complex number $< a, s >$ and then define the finite sum :

$$I_s(a) = \sum_{s\in\mathcal{S}} < a, s > \tag{A.53}$$

We then could say that a is integrable if I_s tends to a finite limit when we indefinitely refine the tesselation $\mathcal{S}$. The existence of the limit and its independence upon the initial pavage, is a question a not adressed here.

Remark :

Any p-form a for which $da = 0$ is called closed and represent a conservative field. Any p-form a for which there exists a $(p-1)$-form b such that $b = da$ is called exact. Since $d^2 = 0$, every exact form is closed. Analogously, we say that a manifold X is closed if $\partial X = 0$ and a boundary if there exists a manifold Y such that $X = \partial Y$. Conversely, when a closed form (resp. manifold) defines an exact form (resp. a boundary) ? Such questions are related to the notions of homology and cohomology, which belong to algebraic topology. Roughly speaking, it depends upon the connexity of the manifold.

Annexe B

Quasi-periodic structures

'Il faut n'appeler Science que l'ensemble des recettes qui réussissent toujours.'
'Tel quel' Paul Valery

B.1 Cristallographie des quasi-cristaux

Les méthodes de construction systématiques de réseaux quasi-cristallins que nous proposons dans cette section s'appuient sur les approches cristallographiques exposées dans les thèses de Nicolas Menguy (1993, [153]) et de Marc De Boissieu (1989, [59]). Les estimations des séries qui interviennent dans le chapitre 5 ont été données par Philippe Tchamitchian.

B.1.1 Introduction à la quasi-cristallographie

L'objet de cet annexe est d'illustrer les propriétés des quasi-cristaux que nous avons rencontrées lors du chapitre 5. On adopte résolument le point de vue du cristallographe afin de mettre en lumière des caractéristiques remarquables de ces structures qui sous-tendent toute l'étude mathématique qui a été menée.

En premier lieu, on notera qu'un quasi-cristal $Q \subset \mathbb{R}^n$ (issu d'une coupe-projection) est un **système de Delauney** c'est à dire que la distance entre deux points de Q est toujours supérieure à un nombre $R > 0$ et par ailleurs,

$$\exists R > 0 \ , \ \forall x \in \mathbb{R}^n, B(x, R) \cap Q \neq \emptyset \ .$$

Il faut noter qu'un cristal est lui-même un système de Delaunay. De plus, à chaque système de Delaunay on associe sa **partition de Voronoï** qui le divise en cellules de Dirichlet ou de Wigner-Seitz. Un réseau périodique n'a qu'un seul domaine de Voronoï, alors qu'un quasi-cristal en a un nombre fini. En particulier, le pavage de Penrose a 8 domaines de Voronoï et le pavage icosaédrique en a 24.

En deuxième lieu, on notera qu'un quasi-cristal est non périodique, mais possède un **ordre translationnel quasi-périodique** à longue distance avec m vecteurs linéairement indépendants (m est égal à la dimension de l'espace de périodicité) sur les entiers (notion de $\mathbb{Z}$-module) :

$$\exists F \subset \mathbb{R}^n \ , \quad F \text{ ensemble fini } \ , \ 1 - Q \subset Q + F \ .$$

En d'autres termes, le rapport des quasi-périodes est incommensurable. Si Q est un réseau de $\mathbb{R}^n$, alors $F = \emptyset$: la notion de quasi-cristal généralise bien celle de réseau.

En troisième lieu, on notera que les pavages de Penrose et leur équivalent tridimensionnel, le pavage icosaédrique, sont autosimilaires : chaque partie finie de tels pavages se retrouve à une échelle plus grande avec un certain facteur d'inflation donné par un irrationnel algébrique. Plus généralement, un théorème dû à Yves Meyer nous assure que si il existe un réel $\theta > 1$ et un quasi-cristal Q dans $\mathbb{R}^n$ tels que $\theta Q \subset Q$, alors Q est nécessairement un irrationnel algébrique dont tous les conjugués sont majorés par 1. Par exemple, dans le cas d'un multi-couche du type "suite de Fibonacci" (équivalent unidimensionnel du pavage de Penrose, cf. section 1) ce facteur d'échelle est donné par τ. On note que les racines conjuguées τ et $\frac{1}{\tau}$ de l'équation algébrique $x^2 - x - 1$ rentrent bien dans le cadre du théorème.

En dernier lieu, on notera que chaque partie finie d'un pavage quasi-périodique s'y retrouve une infinité de fois. Cette propriété pour le moins surprenante est à rapprocher de celle d'isomorphisme local : il existe une infinité de pavages quasi-périodiques différents ayant la même symétrie globale, que l'on regroupe par classes d'isomorphisme local. Deux quasi-réseaux appartiennent à une même classe si toute partie finie de l'un, se retrouve dans l'autre. En pratique, le cristallographe classe les clichés de diffraction identiques dans une même classe d'isomorphisme local : la position des pics de diffraction reste invariante quelque soit la classe d'équivalence, mais les intensités changent d'une classe à l'autre. En effet, le physicien a accès en pratique à la transformée de Fourier du quasi-cristal qui est une mesure atomique dont les masses de Dirac donnent la position des pics de diffraction. Il s'avère que ces positions sont données par des combinaisons linéaires entières d'un nombre fini de vecteurs ou $\mathbf{Z}$-module obtenus par rotation du repère attaché au quasi-réseau dans l'espace de périodicité. Il y a donc une indétermination provenant du groupe des rotations dans l'espace périodique : les structures générées par une rotation de ces vecteurs sont indiscernables et appartiennent donc à une même classe. En outre, la position des pics de diffraction étant entièrement déterminée par le $\mathbf{Z}$-module, elle reste inchangée sous une rotation des vecteurs générant le $\mathbf{Z}$-module : seuls les poids affectés à chaque masse de Dirac changent (i.e. l'intensité des pics de diffraction). Par ailleurs, le cristallographe a accès à la dimension de périodicité sur un cliché de diffraction dès lors qu'il a déterminé le nombre de vecteurs générant le $\mathbf{Z}$-module.

B.1.2 Construction des pavages de Penrose

Un deuxième type de phase quasi-cristalline du système $AlMn$ est la phase décagonale (AL_4Mn), découverte en 1985 par Bendersky. Cette phase présente la particularité d'avoir une direction périodique dans son diagramme de diffraction, les deux autres directions étant quant à elles quasi-périodiques. Cette structure peut être vue comme un empilement de pavages de Penrose bidimensionnels suivant l'axe de périodicité. Le diagramme de diffraction peut être indexé avec quatre vecteurs pointant suivant les axes d'un pentagone dans le plan perpendiculaire à l'axe périodique et un vecteur parallèle à l'axe périodique. On remarque en effet que quatre vecteurs suffisent pour décrire un pentagone : le cinquième vecteur est redondant et il n'y a alors pas de correspondance univoque entre un vecteur de

l'espace parallèle et un vecteur de l'espace périodique (de dimension cinq). De ce fait, le calcul de la transformée de Fourier d'une telle structure n'est plus aussi simple que dans le cas icosaédrique. En pratique, la transformée de Fourier inverse du réseau dont on fait la coupe-projection dans l'espace de périodicité (dans l'espace réciproque), nous donne un réseau (dans l'espace direct) dont les vecteurs ne sont pas orthogonaux. Il y a alors une étape supplémentaire dite d'orthogonalisation par rapport au calcul de la matrice M_τ.

Pour décrire le protocole expérimental qui conduit à la détermination de la matrice $M_{penrose}$, on décompose tout d'abord l'espace réciproque E^* en somme directe de deux sous-espaces orthogonaux de dimension 3 et 2, $E^*_\parallel$ et $E^*_\perp$. L'espace $E^*_\parallel$ est lui-même somme directe d'un espace de quasi-périodicité de dimension 2, encore noté $E^*_\parallel$, et d'un espace de périodicité de dimension 1 : il s'avère que la description du pavage de Penrose bidimensionnel par coupe projection dans $\mathbb{R}^4$ est strictement équivalente à celle réalisée à partir d'un réseau cubique de dimension 5 (la direction de périodicité de l'empilement des pavages ne joue en quelque sorte aucun rôle). En pratique, l'expérimentateur indexe les cinq vecteurs donnant les directions des sommets du dodécagone sur les clichés de diffraction dans $E^*_\parallel$ et $E^*_\perp$. Il faut alors noter que seules les projections orthogonales des quatre vecteurs e^*_1 , e^*_2 , e^*_3 , e^*_4 sur le sous-espace $E^*_\perp$ de l'espace E^* sont non nulles (les quatre premiers vecteurs se projètent sur $E^*_\parallel$ suivant des vecteurs pointant vers les sommets d'un pentagone et le cinquième vecteur est colinéaire à la direction de périodicité). L'expérimentateur sélectionne alors ces quatre vecteurs et il obtient la matrice (non orthogonale) suivante :

$$M_{penrose} = \frac{1}{2}\begin{pmatrix} \cos\frac{2\pi}{5} & \cos\frac{4\pi}{5} & \cos\frac{4\pi}{5} & \cos\frac{2\pi}{5} \\ \sin\frac{2\pi}{5} & \sin\frac{4\pi}{5} & -\sin\frac{4\pi}{5} & -\sin\frac{2\pi}{5} \\ -\cos\frac{4\pi}{5} & \cos\frac{2\pi}{5} & \cos\frac{2\pi}{5} & -\cos\frac{4\pi}{5} \\ \sin\frac{4\pi}{5} & -\sin\frac{2\pi}{5} & \sin\frac{2\pi}{5} & -\sin\frac{4\pi}{5} \end{pmatrix}$$

où les coefficients de la matrice sont donnés par les cosinus directeurs des quatre vecteurs e^*_i [1] sur les bases orthonormées de $E^*_\parallel$ et $E^*_\perp$ (noter que la composante de ces quatres vecteurs suivant la direction de périodicité est nulle). Par ailleurs, leurs projections sur $E^*_\parallel$ et $E^*_\perp$ n'ont pas toutes la même norme. On définit alors deux constantes d'orthonormalisation n_1 et n_2 par :

$$n_1 = \sqrt{2}\sqrt{\cos^2(\frac{2\pi}{5}) + \cos^2(\frac{4\pi}{5})} \quad \text{et} \quad n_2 = \sqrt{2}\sqrt{\sin^2(\frac{2\pi}{5}) + \sin^2(\frac{4\pi}{5})}$$

Finalement, la matrice $M'_{penrose}$ suivante jouit des mêmes propriétés que la matrice M_τ :

$$M'_{penrose} = \frac{1}{2}\begin{pmatrix} \frac{1}{n_1}\cos\frac{2\pi}{5} & \frac{1}{n_1}\cos\frac{4\pi}{5} & \frac{1}{n_1}\cos\frac{4\pi}{5} & \frac{1}{n_1}\cos\frac{2\pi}{5} \\ \frac{1}{n_2}\sin\frac{2\pi}{5} & \frac{1}{n_2}\sin\frac{4\pi}{5} & \frac{-1}{n_2}\sin\frac{4\pi}{5} & \frac{-1}{n_2}\sin\frac{2\pi}{5} \\ \frac{-1}{n_1}\cos\frac{4\pi}{5} & \frac{1}{n_1}\cos\frac{2\pi}{5} & \frac{1}{n_1}\cos\frac{2\pi}{5} & \frac{-1}{n_1}\cos\frac{4\pi}{5} \\ \frac{1}{n_2}\sin\frac{4\pi}{5} & \frac{-1}{n_2}\sin\frac{2\pi}{5} & \frac{1}{n_2}\sin\frac{2\pi}{5} & \frac{-1}{n_2}\sin\frac{4\pi}{5} \end{pmatrix}$$

On vérifie en effet sans peine que la matrice $M'_{penrose}$ est bien orthogonale, un de ses pseudo-inverses à droite étant donné par sa transposée. Il est alors utile d'exprimer les

1. Plus généralement, les vecteurs e^*_i ont des cosinus directeurs en $\left\{\frac{2\pi}{m}, \frac{4\pi}{m}, ..., \frac{(m-1)\pi}{m}\right\}$ pour une symétrie d'ordre m (dimension de l'espace de périodicité), si m est impair.

cosinus directeurs en fonction du nombre d'or :

$$\cos(\frac{2\pi}{5}) = \frac{\tau - 1}{2} \ , \ \cos(\frac{4\pi}{5}) = \frac{-\tau}{2} \ , \ \sin(\frac{2\pi}{5}) = \frac{\sqrt{2+\tau}}{2} \ , \ \text{ et } \ \sin(\frac{4\pi}{5}) = \frac{\sqrt{3-\tau}}{2}$$

En notant que $\tau^2 = \tau + 1$, on calcule alors aisément la valeur des coefficients de normalisation n_1 et n_2 :

$$\begin{aligned} n_1 &= \sqrt{2}\sqrt{\frac{(\tau-1)^2}{4} + \frac{\tau^2}{4}} = \frac{\sqrt{2}}{2}\sqrt{\tau^2 - 2\tau + 1 + \tau^2} = \frac{\sqrt{3}}{\sqrt{2}} \\ n_2 &= \sqrt{2}\sqrt{\frac{\tau+2}{4} + \frac{3-\tau}{4}} = \frac{\sqrt{5}}{\sqrt{2}} \end{aligned}$$

La matrice de Penrose orthogonalisée s'exprime alors comme suit :

$$M'_{penrose} = \frac{1}{\sqrt{2}} \begin{pmatrix} \frac{\tau-1}{\sqrt{3}} & \frac{-\tau}{\sqrt{3}} & \frac{-\tau}{\sqrt{3}} & \frac{\tau-1}{\sqrt{3}} \\ \frac{\sqrt{\tau+2}}{\sqrt{5}} & \frac{\sqrt{3-\tau}}{\sqrt{5}} & \frac{-\sqrt{3-\tau}}{\sqrt{5}} & \frac{-\sqrt{\tau+2}}{\sqrt{5}} \\ \frac{\tau}{\sqrt{3}} & \frac{\tau-1}{\sqrt{3}} & \frac{\tau-1}{\sqrt{3}} & \frac{\tau}{\sqrt{3}} \\ \frac{\sqrt{3-\tau}}{\sqrt{5}} & \frac{-\sqrt{\tau+2}}{\sqrt{5}} & \frac{\sqrt{\tau+2}}{\sqrt{5}} & \frac{-\sqrt{3-\tau}}{\sqrt{5}} \end{pmatrix}$$

Par ailleurs, la phase icosaédrique est donnée en pratique par la projection des points de $\mathbb{Z}^4$ dans $E_{\parallel} = \mathbb{R}^3$ associée à la matrice P_τ suivante :

$$P_{penrose} = \frac{1}{\sqrt{2}} \begin{pmatrix} \frac{\tau-1}{\sqrt{3}} & \frac{-\tau}{\sqrt{3}} & \frac{-\tau}{\sqrt{3}} & \frac{\tau-1}{\sqrt{3}} \\ \frac{\sqrt{\tau+2}}{\sqrt{5}} & \frac{\sqrt{3-\tau}}{\sqrt{5}} & \frac{-\sqrt{3-\tau}}{\sqrt{5}} & \frac{-\sqrt{\tau+2}}{\sqrt{5}} \end{pmatrix}$$

La matrice $R_{penrose}$ ci-dessous est l'un des pseudo-inverses à droite de $P_{penrose}$:

$$R_{penrose} = \frac{1}{\sqrt{2}} \begin{pmatrix} \frac{\tau-1}{\sqrt{3}} & \frac{\sqrt{\tau+2}}{\sqrt{5}} \\ \frac{-\tau}{\sqrt{3}} & \frac{\sqrt{3-\tau}}{\sqrt{5}} \\ \frac{-\tau}{\sqrt{3}} & \frac{-\sqrt{3-\tau}}{\sqrt{5}} \\ \frac{\tau-1}{\sqrt{3}} & \frac{-\sqrt{\tau+2}}{\sqrt{5}} \end{pmatrix}$$

B.2 Construction de pavages apériodiques

En électromagnétisme, il est assez courant d'utiliser une "assemblée" d'objets identiques appelés diffuseurs, ces objets étant caractérisés par leur indice optique et leur forme. Il se pose alors la question de savoir si l'on peut "générer" une assemblée d'objets identiques répartis quasi-périodiquement au sens de la coupe-projection généralisée. Autrement dit, il s'agit de trouver une fonction périodique $f_\sharp(X_1, ..., X_n)$ et une matrice de relèvement R telle que

$$f_R(x_1, x_2, x_3) = f_\sharp(R(X))$$

où f_R représente la fonction constante par morceaux décrivant un motif répété non périodiquement. La réponse à cette question est positive et nous donnons un algorithme permettant de générer *ad libitum* de telles structures.

On peut donner un procédé de construction de matrices M de projection orthogonale pour générer des pavages apériodiques par projection de $\mathbb{R}^m$ sur un sous-espace $\mathbb{R}^n$. En

effet, notant $X = (X_1, ..., X_m)$ un point de $\mathbb{R}^m$ dans le repère $(O, E_1, .., E_k, .., E_m)$ attaché à $\mathbb{Z}^m$ et $x_\parallel = (x_1, ..., x_n)$ sa projection orthogonale sur l'hyperplan $E_\parallel = \mathbb{R}^n$, on a :

$$x_\parallel = \sum_{i=1}^{n} x_i e_i = \sum_{i=1}^{n} (X \mid e_i) e_i$$

où $\{e_i\}_{i=1,..,n}$ est une base de $E_\parallel$. Notant que $e_i = \sum_{k=1}^{m} b_{i,k} E_k$, on obtient :

$$\begin{aligned} x_\parallel &= \sum_{i=1}^{n} (\sum_{j=1}^{m} X_j E_j \mid \sum_{k=1}^{m} b_{i,k} E_k) e_i = \sum_{i=1}^{n} \sum_{j=1}^{m} \sum_{k=1}^{m} X_j b_{i,k} (E_j \mid E_k) e_i \\ &= \sum_{i=1}^{n} \sum_{j=1}^{m} X_j b_{i,j} e_i = \sum_{i=1}^{n} \sum_{j=1}^{m} X_j b_{i,j} \sum_{k=1}^{m} b_{i,k} E_k \end{aligned}$$

On a donc

$$x_\parallel = \sum_{k=1}^{m} \sum_{j=1}^{m} M_{k,j} X_j E_k = \sum_{k=1}^{m} X_k^\parallel E_k$$

avec $X_k^\parallel = \sum_{j=1}^{m} M_{k,j} X_j$, et M la matrice de projection orthogonale donnée par :

$$M_{k,j} = \sum_{i=1}^{n} b_{i,j} b_{i,k} = (B^T B)_{k,j}$$

Pour fixer les idées, on choisit une coupe-projection de $\mathbb{R}^4$ dans $\mathbb{R}^2$. Ainsi, pour générer un pavage apériodique de $\mathbb{R}^2$, on prend par exemple deux vecteurs orthonormés de $\mathbb{R}^4$, e_1 et e_2 tels que :

$$e_1 = \frac{1}{\sqrt{2(2+\tau)}} \begin{pmatrix} 1 \\ \tau \\ -1 \\ 0 \end{pmatrix} \; ; \; e_2 = \frac{1}{\sqrt{2(2+\tau)}} \begin{pmatrix} 0 \\ 1 \\ \tau \\ 0 \end{pmatrix}$$

La matrice B^T est alors donnée par :

$$B^T = \frac{1}{\sqrt{2(2+\tau)}} \begin{pmatrix} 1 & 0 \\ \tau & 1 \\ -1 & \tau \\ 0 & 0 \end{pmatrix}$$

On en déduit que la matrice de projection orthogonale M s'écrit :

$$M = B^T B = \frac{1}{2(2+\tau)} \begin{pmatrix} 2+\tau & 2\tau & \tau & 0 \\ 2\tau & 2+\tau & 0 & -\tau \\ \tau & 0 & 2+\tau & 2\tau \\ 0 & -\tau & 2\tau & 2+\tau \end{pmatrix}$$

Contrairement à la matrice M_τ, la matrice M est symétrique (par construction), R se déduit donc immédiatement de M :

$$R = \frac{1}{2(2+\tau)} \begin{pmatrix} 2+\tau & 2\tau \\ 2\tau & 2+\tau \\ \tau & 0 \\ 0 & -\tau \end{pmatrix}$$

Il faut noter que le choix de R est arbitraire et qu'il existe une infinité de tels relèvements. Par ailleurs, la matrice R vérifie bien la condition d'admissibilité pour la convergence deux-échelles, savoir $R^t k \neq 0$, $\forall k \in \mathbb{Z}^4 \setminus \{0,0,0,0\}$.

On définit alors la fonction χ issue d'une coupe-projection de la manière suivante :

$$\chi(x_1, x_2) = \chi_\sharp(X) = \tilde{\chi}(X - E(X)) = \tilde{\chi}((X))$$

$E(X)$ notant la partie entière de $X = (X_1, X_2, X_3, X_4)$ (E est une fonction Y^4-périodique) et $\tilde{\chi}$ étant définie par :

$$\tilde{\chi}(X_1, X_2, X_3, X_4) = \begin{cases} 1 & \text{, si } X_1^2 + X_2^2 \leq r^2 \text{ et } \mid X_k \mid \leq d,\ \forall k \in \{3,4\} \\ 0 & \text{, sinon} \end{cases}$$

Notant ε_0 la permittivité de l'air et ε_1 celle de la sphère, on construit alors ε de la manière suivante :

$$\varepsilon(x_1, x_2) = \varepsilon_0 + (\varepsilon_1 - \varepsilon_0)\chi(x_1, x_2)$$

Cette dernière fonction décrit bien la permittivité d'un milieu constitué de diffuseurs, disques de rayon r ($r \leq \frac{1}{2}$), placés aux noeuds d'un pavage quasi-périodique. Si l'on souhaite réaliser d'autres pavages apériodiques de $\mathbb{R}^2$ avec des disques de rayon $r \leq \frac{1}{2}$, on pourra prendre une coupe projection par des cylindres de $\mathbb{R}^m$ avec $m > 2$, en s'assurant toutefois que le rapport $\frac{d}{r}$ soit suffisamment grand pour que les disques du pavage apériodique de $\mathbb{R}^2$ ne s'intersectent pas.

Puisque nous savons qu'ainsi, on génère un ensemble d'objets identiques, il suffit de connaître le centre de gravité de chacun de ces dits objets pour décrire la structure étudiée. Posant $r = 0$, la fonction caractéristique du lieu de ces centres est alors donnée par :

$$\chi_\sharp(X_1, X_2, X_3, X_4) = \begin{cases} 1 & \text{, si } (X_k) = 0,\ \forall k \in \{1,2\} \text{ et } \mid (X_k) \mid \leq d,\ \forall k \in \{3,4\} \\ 0 & \text{, sinon} \end{cases}$$

Pour déterminer la position des centres des disques placés aux noeuds du réseau quasi-périodique donné par R on doit alors résoudre le système suivant :

$$\begin{cases} \dfrac{(2+\tau)x_1 + 2\tau x_2}{2(2+\tau)} = i_1 \\ \dfrac{2\tau x_1 + (2+\tau)x_2}{2(2+\tau)} = i_2 \\ \mid \dfrac{\tau x_1}{2(2+\tau)} - E(\dfrac{\tau x_1}{2(2+\tau)}) \mid \leq d \\ \mid \dfrac{-\tau x_2}{2(2+\tau)} - E(\dfrac{-\tau x_2}{2(2+\tau)}) \mid \leq d \end{cases}$$

où $i_j = E(X_j)$, $\forall j \in \{1,2\}$. L'algorithme qui permet de calculer numériquement la position des centres des disques est alors le suivant : on fixe une variable réelle d et un entier N (troncature de $\mathbb{Z}$). Pour 2 entiers i_1 et i_2 allant de $-N$ à N, on cherche les réels x_1, et x_2 qui satisfont :

$$\begin{cases} x_1 = \dfrac{2(2+\tau)}{\tau+1}\Big((2+\tau)i_1 - \tau i_2\Big) \\ x_2 = \dfrac{2(2+\tau)}{\tau+1}\Big((2+\tau)i_2 - \tau i_1\Big) \\ \mid \dfrac{\tau x_1}{2(2+\tau)} - E(\dfrac{\tau x_1}{2(2+\tau)}) \mid \leq d \\ \mid \dfrac{-\tau x_2}{2(2+\tau)} - E(\dfrac{-\tau x_2}{2(2+\tau)}) \mid \leq d \end{cases}$$

On remarque que cet algorithme permet de paver quasi-périodiquement une partie de $\mathbb{R}^2$ en ne faisant appel qu'à l'ensemble discret $\mathbb{Z}^2 \cap [-N;N]^2$.

On définit maintenant la fonction caractéristique d'un ensemble de sphères de rayon r ($r \leq \dfrac{1}{2}$) placées aux sommets d'un icosaèdre (alliage $Al_{63.5}Fe_{12.5}Cu_{24}$) par :

$$\chi(x_1,x_2,x_3) = \chi_\sharp(X) = \tilde{\chi}(X - E(X)) = \tilde{\chi}((X))$$

$E(X)$ notant la partie entière de X (E est une fonction Y^6-périodique) et $\tilde{\chi}$ étant définie par :

$$\tilde{\chi}(X_1,X_2,X_3,X_4,X_5,X_6) = \begin{cases} 1 & \text{, si } X_1^2+X_2^2+X_3^2 \leq r^2 \text{ et } \mid X_k \mid \leq d,\ \forall k \in \{4,..,6\} \\ 0 & \text{, sinon} \end{cases}$$

Notant ε_0 la permittivité de l'air et ε_1 celle de la sphère, on construit alors ε de la manière suivante :

$$\varepsilon(x_1,x_2,x_3) = \varepsilon_0 + (\varepsilon_1 - \varepsilon_0)\chi(x_1,x_2,x_3)$$

Si l'on souhaite réaliser d'autres pavages apériodiques de $\mathbb{R}^3$ avec des sphères de rayon $r \leq \dfrac{1}{2}$, on pourra prendre une coupe projection par des cylindres de $\mathbb{R}^m$ avec $m > 3$, en s'assurant toutefois que le rapport $\dfrac{d}{r}$ soit suffisamment grand pour que les sphères du pavage apériodique de $\mathbb{R}^3$ ne s'intersectent pas.

Si l'on veut déterminer la position des centres des sphères placés aux sommets de l'icosaèdre donné par R_τ on doit résoudre le système suivant :

$$\begin{cases} \dfrac{x_1+\tau x_2}{\sqrt{2(2+\tau)}} = i_1 \\ \dfrac{\tau x_1 + x_3}{\sqrt{2(2+\tau)}} = i_2 \\ \dfrac{x_2+\tau x_3}{\sqrt{2(2+\tau)}} = i_3 \\ \mid \dfrac{-x_1+\tau x_2}{\sqrt{2(2+\tau)}} - E(\dfrac{-x_1+\tau x_2}{\sqrt{2(2+\tau)}}) \mid \leq d \\ \mid \dfrac{\tau x_1 - x_3}{\sqrt{2(2+\tau)}} - E(\dfrac{\tau x_1 - x_3}{\sqrt{2(2+\tau)}}) \mid \leq d \\ \mid \dfrac{-x_2+\tau x_3}{\sqrt{2(2+\tau)}} - E(\dfrac{-x_2+\tau x_3}{\sqrt{2(2+\tau)}}) \mid \leq d \end{cases}$$

où $i_j = E(X_j)$, $\forall j \in \{1, ..., 3\}$. L'algorithme qui permet de calculer numériquement la position des centres des sphères est alors le suivant : On fixe une variable réelle d et un entier N (troncature de $\mathbb{Z}$). Pour 3 entiers i_1, i_2 et i_3 allant de $-N$ à N, on cherche les réels x_1, x_2 et x_3 qui satisfont :

$$\begin{cases} x_1 = \dfrac{\sqrt{2(2+\tau)}}{2\tau+2}\Big(i_1 + (\tau+1)i_2 - \tau i_3\Big) \\ x_2 = \dfrac{\sqrt{2(2+\tau)}}{2\tau+2}\Big((\tau+1)i_1 - \tau i_2 + i_3\Big) \\ x_3 = \dfrac{\sqrt{2(2+\tau)}}{2\tau+2}\Big(-\tau i_1 + i_2 + (\tau+1)i_3\Big) \\ \mid \dfrac{-x_1+\tau x_2}{\sqrt{2(2+\tau)}} - E(\dfrac{-x_1+\tau x_2}{\sqrt{2(2+\tau)}}) \mid \leq d \\ \mid \dfrac{\tau x_1 - x_3}{\sqrt{2(2+\tau)}} - E(\dfrac{\tau x_1 - x_3}{\sqrt{2(2+\tau)}}) \mid \leq d \\ \mid \dfrac{-x_2+\tau x_3}{\sqrt{2(2+\tau)}} - E(\dfrac{-x_2+\tau x_3}{\sqrt{2(2+\tau)}}) \mid \leq d \end{cases}$$

On remarque que cet algorithme permet de paver quasi-périodiquement une partie de $\mathbb{R}^3$ en ne faisant appel qu'à l'ensemble discret $\mathbb{Z}^3 \cap [-N; N]^3$.

B.3 Un exemple de fonction quasi-périodique continue

Il y a plusieurs définitions équivalentes des fonctions quasi-périodiques, dont la suivante qui est due à Harald Bohr [26] :

Définition :

Une fonction continue $f : \mathbb{R} \longmapsto \mathbb{R}$ est dite quasi-périodique si

$$\forall \varepsilon > 0,\ \exists l_\varepsilon > 0 \quad \text{tel que tout intervalle de longueur } l_\varepsilon \text{ contient un réel } a \text{ vérifiant } \sup_{x \in \mathbb{R}} \mid f(x) - f(x+a) \mid \leq \varepsilon \qquad (1)$$

Les nombres a sont appelés **quasi-périodes** de f, attachées à ε et l_ε **longueur d'inclusion**. Il faut noter que toute fonction périodique vérifie trivialement cette condition, ses quasi-périodes étant données par les multiples de sa période fondamentale.

Montrons que la fonction $f(x) = \sin(2\pi x) + \sin(2\pi\tau x)$ $\Big($où τ est le nombre d'or $\tau = \dfrac{1+\sqrt{5}}{2} = 1 + \cos\dfrac{2\pi}{5}\Big)$ est quasi-périodique sur $\mathbb{R}$.

En premier lieu, on note que f ne peut-être périodique, car sinon il existerait un réel T tel que pour tout $x \in \mathbb{R}$:

$$\sin(2\pi(x+T)) + \sin(2\pi\tau(x+T)) = \sin(2\pi x) + \sin(2\pi\tau x)$$

ce qui entrainerait que T vérifie :

$$\cos(2\pi T) = 1\ ,\ \cos(2\pi\tau T) = 1\ ,\ \sin(2\pi T) = 0\ ,\ \sin(2\pi\tau T) = 0$$

ce qui est impossible pour un irrationnel τ.

Cherchons pour $\varepsilon \geq 0$ fixé des quasipériodes a telles que $a \in \mathbb{N}$. Pour a entier, on remarque que :

$$\begin{aligned} \mid f(x) - f(x+a) \mid &= \mid \sin(2\pi\tau(x+a)) - \sin(2\pi\tau x) \mid \\ &= \mid \sin(2\pi\tau x)\cos(2\pi\tau a - 1) + \cos(2\pi\tau x)\sin(2\pi\tau a) \mid \\ &\leq 1 - \cos(2\pi\tau a) + \mid \sin(2\pi\tau a) \mid \\ &= 2 \mid \sin(\pi\tau a) \mid \Big[\mid \sin(\pi\tau a) \mid + \mid \cos(\pi\tau a) \mid \Big] \\ &\leq 4 \mid \sin(\pi\tau a) \mid \end{aligned}$$

d'où

$$\sup_{x \in \mathbb{R}} \mid f(x) - f(x+a) \mid \leq \varepsilon$$

dès que :

$$K(a) := \inf_{k \in \mathbb{N}} \Big\{ k \ / \mid \tau a - k \mid < \frac{\varepsilon}{4} \Big\}$$

Première étape :

Montrons que pour tout $\varepsilon > 0$, il existe un couple $(a, k) \in \mathbb{N}^2$ (en fait, une infinité, comme nous allons le voir par la suite) qui vérifie

$$0 \leq \tau a - k < \frac{\varepsilon}{4} \tag{2}$$

Pour réaliser la condition (2), on utilise alors l'approximation de τ à l'aide de la suite de Fibonacci[2] (0 , 1 , 1 , 2 , 3 ,; 5 , 8 , 13 , 21;, 34 , 55 ...)[3] induite par la relation de récurrence $u_n = u_{n-1} + u_{n-2}$. La suite (u_n) tend vers l'infini et $\dfrac{u_{n+1}}{u_n} = 1 + \dfrac{u_{n-1}}{u_n}$ converge vers le point fixe τ de $g(x) = 1 + \dfrac{1}{x}$ à une vitesse que l'on peut estimer à l'aide de l'inégalité suivante [110] :

$$\mid \tau - \frac{u_{n+1}}{u_n} \mid \leq \frac{1}{u_n^2} \tag{3}$$

(noter que $\mid \dfrac{u_{10}}{u_9} - \tau \mid \sim \mid 1,6176 - 1,6180 \mid \leq 10^{-2}$), de sorte que :

$$\mid \tau u_n - u_{n+1} \mid \leq \frac{1}{u_n} \ ,$$

qui converge vers 0 quand n tend vers l'infini. La condition (2) est donc réalisée pour $a = u_n$ dès que $\dfrac{1}{u_n} < \dfrac{\varepsilon}{4}$, donc pour le terme général de la suite de Fibonacci à partir d'un certain rang n_0 ((u_n) prend des valeurs entières et tend vers l'infini).

Deuxième étape :

2. Cette suite fut découverte vers 1202 par Léonard de Pise, fils de Bonaccio, où "Filius Bonacci", ou "Fibonacci".

3. Ces approximants ont été utilisés dans la construction d'instruments de musique comme le violon et la guitare. Ils interviennent aussi dans l'architecture spiralée des boutons de marguerite et de tournesol.

Parmis tous les entiers u_n qui satisfont (2), il faut selectionner ceux qui seront des quasi-périodes de f.[4]

Soit (u_{n_0}, k_0) une solution de (2). Posons,

$$\tau u_{n_0} - k_0 = \varphi(u_{n_0}) \ , \quad \text{avec } 0 < \varphi(u_{n_0}) < \frac{\varepsilon}{4}$$

Si l'on prend la suite des multiples entiers de $\varphi(u_{n_0})$, on note que pour un entier j donné, l'entier $p_{j-1} := E(\frac{j}{\varphi(u_{n_0})})$ est tel que :

$$p_{j-1}\varphi(u_{n_0}) < j < p_j\varphi(u_{n_0})$$

De plus, nous sommes assurés que :

$$j < p_j\varphi(u_{n_0}) < j + \frac{\varepsilon}{4}$$

A chaque entier p_j correspond un entier $u_{n_j} = u_{n_0}p_j$ tel que :

$$j < \tau u_{n_j} - kp_j < j + \frac{\varepsilon}{4}$$

Par ailleurs, on a :

$$u_{n_j} = \tau\Big[1 + E(\frac{j}{\varphi(u_{n_0})})\Big] \ , \quad \text{et } u_{n_{j+1}} = \tau\Big[1 + E(\frac{j+1}{\varphi(u_{n_0})})\Big]$$

On peut donc conclure que :

$$u_{n_{j+1}} - u_{n_j} = \tau E(\frac{j+1}{\varphi(u_{n_0})}) - \tau E(\frac{j}{\varphi(u_{n_0})}) < \tau\frac{j+1}{\varphi(u_{n_0})} - \tau\frac{j-1}{\varphi(u_{n_0})} = \frac{2\tau}{\varphi(u_{n_0})}$$

La différence de deux entiers consécutifs de la suite u_{n_j} est inférieure à un nombre fixe (dépendant de ε par le choix de $\varphi(u_{n_0})$). Puisque dans tout intervalle $]x \ , \ x + \frac{2\tau}{\varphi(u_{n_0})}[$, il y a au moins un entier u_{n_j} (sinon $u_{n_{j+1}} - u_{n_j}$ serait toujours supérieur à $\frac{2\tau}{\varphi(u_{n_0})}$), le nombre $l_\eta = \frac{2\tau}{\varphi(u_{n_0})}$ est une longueur d'inclusion pour la fonction quasi-périodique f.

4. Le couple d'entiers (u_{n+1}, u_n) est un candidat (il en existe bien entendu d'autres). En effet, notant $\sigma = \frac{1-\sqrt{5}}{2}$ la solution négative de l'équation algébrique $\sigma^2 = \sigma + 1$, on en déduit que $u_n = \frac{1}{\sqrt{5}}(\tau^{n+1} - \sigma^{n+1})$. Puisque $\mid \sigma \mid < 1$, le comportement asymptotique de u_n est donné par $u_n \sim \frac{\tau^{n+1}}{\sqrt{5}}$ pour les grandes valeurs de n. À partir du rang $n_0 = E\Big(-\frac{4\sqrt{5}\log(\varepsilon)}{\log(\tau)}\Big) + 1$, nous sommes donc assurés que $\frac{1}{u_{n_0}} \sim \frac{\sqrt{5}}{\tau^{n_0+1}} < \frac{\varepsilon}{4}$.

B.4 Estimation de séries pour le chapitre 5

B.4.1 Majoration de la série pour les nombres algébriques

Nous allons établir des résultats de majoration pour les séries

$$\sum_{(m,n)\in B_\eta} \mid C_{n,m} \mid^2 \quad \text{et} \quad \sum_{(m,n)\in B_\eta^\delta} \left| C_{m,n}\, sinc(\frac{\pi(m+\alpha n)}{\eta}) \right| ,$$

quand α est un nombre algébrique.

Lemme 1

Soit α un irrationnel algébrique d'ordre ξ. On considère $\varepsilon_\sharp$, la permittivité du réseau de $\mathbb{R}^2$ dont on prend la coupe-projection suivant la droite de pente α. Alors,

i) Si le réseau est constitué de rectangles répartis périodiquement, $\sum_{(m,n)\in B_\eta} \mid C_{n,m} \mid^2 = o(\eta^{\frac{3}{\xi-1}})$.

ii) Si le réseau est constitué de disques répartis périodiquement, $\sum_{(m,n)\in B_\eta} \mid C_{n,m} \mid^2 = o(\eta^{\frac{2}{\xi-1}})$.

Preuve :

i) Si le réseau de $\mathbb{R}^2$ est formé de motifs rectangulaires de côtés a et b, le comportement asymptotique des coefficients de Fourier $C_{m,n}$ de $\varepsilon_\sharp$ est donné par :

$$C_{m,n} = sinc(m\pi a)\; sinc(n\pi b) = O(\frac{1}{m}\,\frac{1}{n})$$

où la fonction sinus cardinal est définie par $sinc(x) = \dfrac{\sin(x)}{x}$ sur $\mathbb{R}_*$ et prolongée par continuité à 1 à l'origine. Par ailleurs, le théorème de Liouville nous assure que pour un irrationnel algébrique d'ordre ξ et pour des entiers m et n dans B_η, il existe une constante $M > 0$ telle que :

$$\frac{M}{\mid m \mid^\xi} < \mid \frac{n}{m} + \alpha \mid \leq \frac{\eta}{\mid m \mid}$$

Si l'on se restreint aux irrationnels α positifs (ce qui n'enlève rien au caractèregénéral de la démonstration), on en déduit qu'il existe une constante $C_1 > \alpha$ telle que :

$$\mid m \mid > (\frac{M}{\eta})^{\frac{1}{\xi-1}} \quad \text{et} \quad \mid n \mid > C_1(\frac{M}{\eta})^{\frac{1}{\xi-1}}$$

On en déduit qu'il existe des constantes C_2, C_3 et C_4 strictement positives telles que :

$$\sum_{(m,n)\in B_\eta} \mid C_{n,m} \mid^2 \leq C_2 \sum_{|n|>C_1(\frac{M}{\eta})^{\frac{1}{\xi-1}}} \sum_{|m|>(\frac{M}{\eta})^{\frac{1}{\xi-1}}} (\frac{1}{\mid mn \mid})^2 \leq C_3 \sum_{|m|>\min(C_1,1)(\frac{M}{\eta})^{\frac{1}{\xi-1}}} (\frac{1}{m})^4 \leq C_4(\frac{\eta}{M})^{\frac{3}{\xi-1}}$$

ii) En revanche, si le réseau de $\mathbb{R}^2$ est formé de motifs circulaires, le comportement asymptotique des coefficients de Fourier $C_{m,n}$ de$\varepsilon_\sharp$ est donné par :

$$C_{m,n} = \frac{J_1(\sqrt{n^2+m^2})}{\sqrt{n^2+m^2}} = O(\frac{1}{(n^2+m^2)^{\frac{3}{4}}})$$

puisqu'il existe une constante $A > 1$ telle que pour tout $x \geq A$, $J_1(x) = \sqrt{\frac{2}{\pi x}} \cos(x - \frac{3\pi}{4}) + O(\frac{1}{x^{\frac{3}{2}}})$ [1].

Par ailleurs, pour tout couple (m, n) dans B_η, on a :

$$-\eta \leq m + \alpha n \leq \eta$$

Sans perte de généralité, on peut se restreindre à $\alpha > 0$, $m > 0$ et $n < 0$ (*a fortiori* $\alpha n < 0$). On a alors :

$$-\alpha n - \eta \leq m \leq -\alpha n + \eta$$

Dorénavant, on prend $\eta < \frac{1}{2}$. On déduit alors de l'inégalité précédente que pour un entier n donné, et pour tout $\eta < \frac{1}{2}$, il existe au plus un entier m tel que :

$$m = E(\eta - \alpha n)$$

Par ailleurs, d'après i), on sait qu'il existe des constantes $M > 0$ et $C_1 > \alpha$ telles que :

$$\mid n \mid > C_1 (\frac{M}{\eta})^{\frac{1}{\xi - 1}}$$

On en déduit qu'il existe une constante C_5 strictement positive telle que :

$$\sum_{(m,n) \in B_\eta} \mid C_{n,m} \mid^2 = 2 \sum_{|n|>0} \frac{1}{(n^2 + E(\eta - \alpha n)^2)^{\frac{3}{2}}} \leq 2\, C_5 \sum_{|n| > C_1 (\frac{M}{\eta})^{\frac{1}{\xi-1}}} \frac{1}{(n^2 + E(\eta - \alpha n)^2)^{\frac{3}{2}}}$$

Par ailleurs, η et $-\alpha n$ étant des réels positifs, nous sommes assurés que :

$$E(\eta - \alpha n) \geq -\alpha n - 1$$

On en déduit qu'il existe une constante $C_6 > 0$ telle que :

$$\sum_{(m,n) \in B_\eta} \mid C_{n,m} \mid^2 \leq 2\, C_5 \sum_{|n| > C_1 (\frac{M}{\eta})^{\frac{1}{\xi-1}}} \frac{1}{\left(n^2 + (\alpha n + 1)^2\right)^{\frac{3}{2}}} \leq \frac{2C_5}{\alpha^2} \sum_{|n| > C_1 (\frac{M}{\eta})^{\frac{1}{\xi-1}}} \left(\frac{1}{\mid n \mid}\right)^3 \leq C_6 (\frac{\eta}{M})^{\frac{2}{\xi-1}}$$

Remarque :
Le lemme annonce que pour un irrationnel quadratique ($\xi = 2$), on a :

$$\sum_{(m,n) \in B_\eta} \mid C_{m,n} \mid^2 = o(\eta^3)$$

dans le cas de motifs rectangulaires, et

$$\sum_{(m,n) \in B_\eta} \mid C_{m,n} \mid^2 = o(\eta^2)$$

dans le cas de motifs circulaires.

Lemme 2

Soit α un irrationnel algébrique d'ordre ξ. On considère $\varepsilon_\sharp$, la permittivité du réseau de $\mathbb{R}^2$ dont on prend la coupe-projection suivant la droite de pente α. Alors,

i) Si le réseau est constitué de rectangles répartis périodiquement,

$$\sum_{(m,n)\in B_\eta} \mid C_{n,m} \mid\mid sinc\frac{\pi(m+\alpha n)}{\eta}\mid = o(\eta^{\frac{2}{\xi-1}}) \ .$$

ii) Si le réseau est constitué de disques répartis périodiquement,

$$\sum_{(m,n)\in B_\eta} \mid C_{n,m} \mid^2 = o(\eta^{\frac{3}{2(\xi-1)}}) \ .$$

Preuve :

i) Si le réseau de $\mathbb{R}^2$ est formé de motifs rectangulaires de côtés a et b, le comportement asymptotique des coefficients de Fourier $C_{m,n}$ de $\varepsilon_\sharp$ est donné par :

$$C_{m,n} = sinc(m\pi a)\ sinc(n\pi b) = O(\frac{1}{m}\ \frac{1}{n}) \tag{26}$$

Par ailleurs, le théorème de Liouville nous assure que pour un irrationnel algébrique d'ordre ξ et pour des entiers m et n dans B_η, il existe une constante $M > 0$ telle que :

$$\frac{M}{\mid m \mid^\xi} < \mid \frac{n}{m} + \alpha \mid \leq \frac{\eta}{\mid m \mid} \tag{27}$$

Si l'on se restreint aux irrationnels α positifs (ce qui n'enlève rien au caractère général de la démonstration), on en déduit qu'il existe une constante $C_1 > \alpha$ telle que :

$$\mid m \mid > (\frac{M}{\eta})^{\frac{1}{\xi-1}} \quad \text{et} \quad \mid n \mid > C_1(\frac{M}{\eta})^{\frac{1}{\xi-1}} \tag{28}$$

On en déduit qu'il existe des constantes C_2, C_3 et C_4 strictement positives telles que :

$$\begin{aligned}
\sum_{(m,n)\in B_\eta} \mid C_{n,m} \mid\mid sinc\frac{\pi(m+\alpha n)}{\eta}\mid \ &\leq C_2 \sum_{|n|>C_1(\frac{M}{\eta})^{\frac{1}{\xi-1}}} \ \sum_{|m|>(\frac{M}{\eta})^{\frac{1}{\xi-1}}} \frac{1}{\mid mn \mid}\frac{\eta}{\mid m+\alpha n \mid} \\
&\leq C_3\eta \sum_{|m|>\min(C_1,1)(\frac{M}{\eta})^{\frac{1}{\xi-1}}} \Big(\frac{1}{\mid m \mid}\Big)^2 \mid m \mid^{\xi-1} \\
&\leq C_3\eta \sum_{|m|>\min(C_1,1)(\frac{M}{\eta})^{\frac{1}{\xi-1}}} \Big(\frac{1}{\mid m \mid}\Big)^{3-\xi} \\
&\leq \eta C_4\Big(\frac{\eta}{M}\Big)^{\frac{3-\xi}{\xi-1}} = C_4\Big(\frac{\eta}{M}\Big)^{\frac{2}{\xi-1}}
\end{aligned}$$

où on a utilisé (26) et (28) dans la première inégalité et (27) dans la deuxième inégalité. Cette estimation nous assure que pour un irrationnel de degré $\xi = 2$,

$$\sum_{(m,n)\in B_\eta} \mid C_{n,m} \mid\mid sinc\frac{\pi(m+\alpha n)}{\eta}\mid = o(\eta^2) \ .$$

ii) En revanche, si le réseau de $\mathbb{R}^2$ est formé de motifs circulaires, le comportement asymptotique des coefficients de Fourier $C_{m,n}$ de $\varepsilon_\sharp$ est donné par :

$$C_{m,n} = \frac{J_1(\sqrt{n^2+m^2})}{\sqrt{n^2+m^2}} = O(\frac{1}{(n^2+m^2)^{\frac{3}{4}}})$$

On en déduit qu'il existe des constantes C_2, C_3 et C_4 strictement positives telles que :

$$\begin{aligned}
\sum_{(m,n)\in B_\eta} \mid C_{n,m} \mid\mid sinc\frac{\pi(m+\alpha n)}{\eta}\mid &\leq C_2 \sum_{|n|>C_1(\frac{M}{\eta})^{\frac{1}{\xi-1}}} \sum_{|m|>(\frac{M}{\eta})^{\frac{1}{\xi-1}}} \frac{1}{(m^2+n^2)^{\frac{3}{4}}} \frac{\eta}{\mid m+\alpha n \mid} \\
&\leq C_3\eta \sum_{|m|>\min(C_1,1)\left(\frac{M}{\eta}\right)^{\frac{1}{\xi-1}}} \Big(\frac{1}{\mid m \mid}\Big)^{\frac{3}{2}} \mid m \mid^{\xi-1} \\
&\leq C_3\eta \sum_{|m|>\min(C_1,1)\left(\frac{M}{\eta}\right)^{\frac{1}{\xi-1}}} \Big(\frac{1}{\mid m \mid}\Big)^{\frac{5-2\xi}{2}} \\
&\leq \eta C_4\Big(\frac{\eta}{M}\Big)^{\frac{5-2\xi}{2(\xi-1)}} = C_4\Big(\frac{\eta}{M}\Big)^{\frac{3}{2(\xi-1)}}
\end{aligned}$$

où on a utilisé (26) et (28) dans la première inégalité et (27) dans la deuxième inégalité. Cette estimation nous assure que pour un irrationnel de degré $\xi = 2$,

$$\sum_{(m,n)\in B_\eta} \mid C_{n,m} \mid\mid sinc\frac{\pi(m+\alpha n)}{\eta}\mid = o(\eta^{\frac{3}{2}}) \ .$$

Les résultats de majorations établis dans cette annexe ne sont optimaux. L'annexe suivante nous donne une estimation beaucoup plus précise dans le cas où α est le nombre d'or.

B.4.2 Estimation précise de la série pour le nombre d'or

Lemme

Soit $\varepsilon \in H_\sharp^{\frac{1}{2}-r}(Y^2)$, $\forall r > 0$, *alors :*

$$\sum_{(m,n)\in B_\eta} \mid C_{n,m} \mid^2 = \sum_{\substack{n\in\mathbf{Z}_* \\ |[\tau n]|\leq\eta}} \mid C_{n,-E(\tau n)} \mid^2$$

Démonstration :

Soit (m,n) un couple d'entiers de $\mathbb{Z}^2 \setminus \{0,0\}$ dans B_η, alors :

$$\mid m+\tau n \mid = \mid m + E(\tau n) + [\tau n] \mid \leq \eta$$

Soit $\eta < \frac{1}{2}$, si m était un entier différent de $-E(\tau n)$, alors $\mid m+\tau n \mid$ serait supérieur à 1r". On a alors nécessairement $m = -E(\tau n)$ et $[\tau n] \leq \eta$.

(QED)

À ce stade, on suppose que ε est une fonction périodique constante par morceaux à support sur des rectangles. Ses coefficients de Fourier sont donc donnés par :

$$C_{m,n} = sinc(m\nu)sinc(n\nu) = O(\frac{1}{mn})$$

Par ailleurs, $-E(\tau n) \geq -\tau n - 1$, on en déduit qu'il existe une constante $C_1 > 0$ telle que :

$$\begin{aligned}\sum_{(m,n)\in B_\eta} |\, C_{n,m}\,|^2 &\leq C_1 \sum_{(m,n)\in B_\eta} |\, \frac{1}{mn}\,|^2 = C_1 \sum_{\substack{n\in\mathbf{Z}_* \\ [\tau n]\leq\eta}} \frac{1}{(-E(\tau n))^2\, n^2} \\ &\leq C_1 \sum_{\substack{n\in\mathbf{Z}_* \\ [\tau n]\leq\eta}} \frac{1}{(\tau n+1)^2\, n^2} \leq \frac{C_1}{\tau^2} \sum_{\substack{n\in\mathbf{Z}_* \\ [\tau n]\leq\eta}} \frac{1}{n^4}\end{aligned}$$

De même, si l'on considère une permittivité ε à support sur des disques, on a vu que le comportement asymptotique des coefficients de Fourier $C_{m,n}$ est donné par :

$$C_{m,n} = \frac{J_1(\sqrt{n^2+m^2})}{\sqrt{n^2+m^2}} = O(\frac{1}{(n^2+m^2)^{\frac{3}{4}}})$$

On en déduit qu'il existe une constante $C_2 > 0$ telle que :

$$\begin{aligned}\sum_{(m,n)\in B_\eta} |\, C_{n,m}\,|^2 &\leq C_2 \sum_{(m,n)\in B_\eta} \frac{1}{(n^2+m^2)^{\frac{3}{2}}} = C_2 \sum_{\substack{n\in\mathbf{Z}_* \\ [\tau n]\leq\eta}} \frac{1}{((-E(\tau n))^2+n^2)^{\frac{3}{2}}} \\ &\leq C_2 \sum_{\substack{n\in\mathbf{Z}_* \\ [\tau n]\leq\eta}} \frac{1}{((\tau n+1)^2+n^2)^{\frac{3}{2}}} \leq \frac{C_2}{\tau^3} \sum_{\substack{n\in\mathbf{Z}_* \\ [\tau n]\leq\eta}} \frac{1}{|\, n\,|^3}\end{aligned}$$

Considérons alors la fonction définie pour $s > 1$ par :

$$f(\eta) = \sum_{[q\tau]\leq\eta} \frac{1}{q^s}$$

où $[q\tau] = q\tau - E(q\tau) = q\tau - p$, et où τ est la racine positive de l'équation algébrique du second degré :

$$\tau^2 - \tau = 1$$

Proposition 2

Pour tout $s > 1$, si τ désigne le nombre d'or $\tau = \frac{1+\sqrt{5}}{2}$, on a :

$$f(\eta) = \sum_{[q\tau]\leq\eta} \frac{1}{q^s} = O(\eta^s)$$

Démonstration :

Une façon d'approcher l'irrationnel τ est de le développer en fraction continuée. On génère ainsi une suite de rationnels $\frac{p_n}{q_n}$ qui vérifie :

$$(1)\begin{cases} q_n &= p_{n-1} \\ p_n &= q_{n-1} + p_{n-1} \\ p_0 &= q_0 = 1 \end{cases}$$

Il est connu que (cf. [110]) :

$$(2)\begin{cases} p_n &= \frac{1}{\sqrt{5}}\Big(\tau^{n+2} - (\frac{-1}{\tau})^{n+2}\Big) \\ p_n - \tau q_n &= \frac{(-1)^{n+1}}{\sqrt{5}}\frac{1}{q_n} + O(\tau^{-2n}) \end{cases}$$

La suite de rationnels $\frac{p_n}{q_n}$ est le convergent qui donne la meilleure approximation de τ. Nous sommes alors assurés que pour tout entier $q$tel que $q_{n-1} < q \leq q_n$ et $(q\tau) \leq \eta$:

$$q|\ \frac{p_n}{q_n} - \tau\ | \leq q|\ \frac{p}{q} - \tau\ | \leq \eta\ .$$

De (2) on déduit que :

$$|\ \frac{p_n}{q_n} - \tau\ | = \frac{1}{\sqrt{5}}\frac{1}{q_n^2} + O(\tau^{-n-1}) \leq \frac{\eta}{q}\ .$$

Puisque $q_{n-1} < q$, on obtient que :

$$q_{n-1}\frac{1}{\sqrt{5}}\frac{1}{q_n^2} \leq \eta\ . \tag{3}$$

De (1) et (2), on tire par ailleurs que :

$$q_n - \tau q_{n-1} = p_{n-1} - \tau q_{n-1} = \frac{(-1)^n}{\sqrt{5}}\frac{1}{q_{n-1}} + O(\tau^{-2n+2})\ .$$

Or d'après (1) et (2), $q_n = p_{n-1} = \frac{1}{\sqrt{5}}\Big(\tau^{n+1} - (\frac{-1}{\tau})^{n+1}\Big)$. On obtient donc que :

$$-1 + \tau\frac{q_{n-1}}{q_n} = \frac{(-1)^{n+1}}{\sqrt{5}}\frac{1}{q_{n-1}q_n} + O(\tau^{-n+4})\ ,$$

soit encore :

$$\frac{q_{n-1}}{q_n} = \frac{1}{\tau}\Big(1 + \frac{(-1)^{n+1}}{\sqrt{5}}\frac{1}{q_{n-1}q_n} + O(\tau^{-n+4})\Big)\ . \tag{4}$$

De plus, de (1) et (2) on tire que :

$$\begin{aligned} q_{n-1}q_n &= \frac{1}{5}\Big(\tau^{n+1} - (-\frac{1}{\tau})^{n+1}\Big)\Big(\tau^n - (-\frac{1}{\tau})^n\Big) \\ &= \frac{1}{5}\Big(\tau^{2n+1} - \tau^n(-\frac{1}{\tau})^{n+1} - \tau^{n+1}(-\frac{1}{\tau})^n + (-\frac{1}{\tau})^{2n+1}\Big) \\ &= \frac{1}{5}\Big(\tau^{2n+1} + \tau + \frac{1}{\tau} + (-\frac{1}{\tau})^{2n+1}\Big) \end{aligned} \tag{5}$$

D'après (4) et (5) nous sommes assurés que :

$$\frac{q_{n-1}}{q_n} = \frac{1}{\tau}\Big(1 + O(\tau^{-n+4})\Big)\ . \tag{6}$$

De (3) et (6) on déduit qu'il existe un entier n_0 tel que pour tout $n \geq n_0$, on a :

$$\frac{1}{\tau\sqrt{5}}\frac{1}{\eta} \leq q_n \ . \tag{7}$$

La suite de Fibonacci $(q_n)_n$ étant croissante, nous considérons maintenant un entier Ntel que :

$$q_{N-1} < \frac{1}{\tau\sqrt{5}}\frac{1}{\eta} \leq q_N \ .$$

Supposons que N soit pair. Alors (1) et (2) nous assurent que $q_N = p_{N-1} = \frac{1}{\sqrt{5}}\Big(\tau^{N+1} - (\frac{-1}{\tau})^{N+1}\Big)$ et on déduit de l'encadrement précédent que N doit nécessairement vérifier :

$$\frac{\tau^N}{\sqrt{5}} < \frac{1}{\eta\tau\sqrt{5}} < \frac{\tau^{N+1}}{\sqrt{5}} \ ,$$

soit encore :

$$\tau^{-N-2} < \eta < \tau^{-N-1} \ . \tag{8}$$

Il suffit pour cela de choisir N tel que :

$$-N-2 < \frac{\log\eta}{\log\tau} < -N-1 \ .$$

L'entier N est alors donné par :

$$N = -E(\frac{\log\eta}{\log\tau}) - 2 \ .$$

On peut alors réécrire la fonction f comme suit :

$$f(\eta) = \sum_{n\geq N} \sum_{\substack{(q\tau)\leq\eta \\ q_{n-1}<q\leq q_n}} \frac{1}{q^s} \ . \tag{9}$$

Un majorant de f est donc donné par :

$$f(\eta) \leq \sum_{n\geq N} \text{ Card } \{q \in]q_{n-1}; q_n]; (q\tau) \leq \eta\} \frac{1}{q_{n-1}^s} \ . \tag{10}$$

À ce stade de la démonstration, nous devons démontrer un lemme basé sur l'équirépartition des q_n. Cette dernière nous permet d'estimer que le cardinal de $\{q \in]q_{n-1}; q_n]; (q\tau) \leq \eta\}$est de l'ordre de $\eta(q_n - q_{n-1})$, donc de l'ordre de ηq_n.

Lemme

Il existe une constante $C > 0$ telle que :

$$\text{Card } \{q \in]q_{n-1}; q_n]; (q\tau) \leq \eta\} \leq C\ \eta\ q_n \ .$$

Démonstration :

Il existe un unique entier $p = q\tau - (q\tau)$ tel que :

$$| p - q\,\tau | \leq \eta\ .$$

On en déduit que :

$$| p\ q_n - q\ q_n\ \tau | \leq \eta\ q_n\ . \tag{11}$$

Par ailleurs, (2) nous assure que :

$$| p_n - q_n\ \tau | \leq \frac{1}{\sqrt{5} q_n}\ .$$

On a donc la majoration suivante :

$$| q\ p_n - q\ q_n\ \tau | \leq \frac{q}{\sqrt{5} q_n}\ .$$

De l'inégalité (7), on en déduit que :

$$| q\ p_n - q\ q_n\ \tau | \leq \eta\tau q \leq \eta\tau q_n\ . \tag{12}$$

L'inégalité triangulaire appliquée à (11) et (12) nous assure alorsde l'existence d'une constante $C = (\tau + 1)$ telle que :

$$| p\ q_n - q\ p_n | \leq \eta\ C\ q_n\ .$$

Considérons alors l'application suivante :

$$\begin{array}{ll} \varphi : \{q \in]q_{n-1}; q_n]; (q\tau) \leq \eta\} & \to \mathbb{Z} \\ q & \longmapsto p\ q_n - q\ p_n\ . \end{array}$$

Si l'on montre que φ est bijective, on pourra en déduire que

$$\text{Card Im } (\varphi) = \text{Card } \{q \in]q_{n-1}; q_n]; (q\tau) \leq \eta\} \subset [-C\ \eta\ q_n; C\ \eta\ q_n]\ .$$

Soient p, p', q et q' des entierstels que :

$$p\ q_n - q\ p_n = p'\ q_n - q'\ p_n\ ,$$

soit encore tels que :

$$(p - p')\ q_n = (q - q')\ p_n\ . \tag{13}$$

Notant que pour $n > 2$, p_n et q_n sont des entiers premiers entre eux (propriétéde la suite de Fibonacci, voir $[Hardy - Wright]$), on en déduit que q_n divise $q - q'$. Par hypothèse, $q_{n-1} < q < q_n$ et $q_{n-1} < q' < q_n$, ce qui implique que :

$$| q - q' | \leq q_n - q_{n-1} < q_n\ . \tag{14}$$

On déduit de (13) et (14) que $q = q'$. Le même raisonnement s'appliquant pour p et p', on a donc montré que φ est bijective.

(QED)

Le lemme appliqué à (10), nous assure qu'il existe une constante $C > 0$ telle que :

$$f(\eta) \leq C\ \eta \sum_{n \geq N} \frac{1}{q_n^{s-1}}$$

De (1) et (2) on tire par ailleurs que $q_n \leq \frac{1}{\sqrt{5}} \tau^{n+1}$. On en déduit qu'il existe une constante $C' > 0$ telle que :

$$f(\eta) \leq C'\ \eta \sum_{n \geq N} (\tau)^{-(n+1)(s-1)} \leq C'\ \eta\ (\tau)^{-(N+2)(s-1)}$$

Or (8) nous assure que $\tau^{-N-2} < \eta$. On en conclut qu'il existe une constante $C'' > 0$ telle que :

$$f(\eta) \leq C''\ \eta\ \eta^{s-1} = C''\ \eta^s$$

(QED)

Remarque :

Il faut noter que si l'on remplace p_0 par 3 dans (1), on obtient une suite totalement différente, appelée suite de Lucas :

$$1,\ 3,\ 4,\ 7,\ 11,\ 18,\ 29,\ 47,\ 76,\ 123...$$

Cette suite est étudiée dans [110] en connexion avec les nombres de Mersenne :

$$u_n = x^n + y^n$$

Pour définir des suites **récursives** telles que celles de Fibonacci et Lucas, il faut bien préciser à la fois les valeurs de départ p_0 et q_0 (la base) et la récursion $p_n = p_{n-1} + p_{n-2}$. Cette sensibilité aux conditions initiales est une caractéristique des suites récursives. Si l'on conserve maintenant la base de la suite de Fibonacci et que l'on transforme quelque peu la définition de récursion :

$$F(n) = F(n - F(n-1)) + F(n - F(n-2))\ ,\ \forall n > 2$$

on aboutit à la suite d'entiers suivante :

$$1,\ 1,\ 2,\ 3,\ 3,\ 4,\ 5,\ 5,\ 6,\ 6,\ 6,\ 8,\ 8,\ 8,\ 10,\ 9,\ 10,\ 11...$$

Cette fois ci, chaque nouvelle valeur de la suite n'est pas la somme des deux termes précédents : les deux valeurs qui précèdent indiquent de combien de nombres il faut reculer pour trouver les valeurs, qui additionnées, donnent la nouvelle valeur de la suite : par exemple, $F(18) = F(18-9) + F(18-10) = 5 + 6 = 11$. Plus on avance dans la suite, plus elle paraît incensée. Le **chaos** est ici produit de manière très ordonnée i.e. déterministe.

Bibliographie

[1] M. ABRAMOWITZ and I.E. STEGUN. *Handbook of mathematical functions*, volume 55. National Bureau of Standards Applied Mathematics series, 1972.

[2] G. ALLAIRE. Homogenization and two-scale convergence. *SIAM J. Math. Anal.*, 23 :1482–1518, 1992.

[3] G. ALLAIRE and M. BRIANE. Multiscale convergence and reiterated homogenization. *Proc. Roy. Soc. Edimburgh*, 126.

[4] G. ALLAIRE and C. CONCA. Analyse asymptotique spectrale de l'équation des ondes. Complétude du spectre de Bloch. *C. R. Acad. Sci. Paris Série I Math.*, 321 :557–562, 1995.

[5] G. ALLAIRE and C. CONCA. Analyse asymptotique spectrale de l'équation des ondes. Homogénéisation par ondes de Bloch. *C. R. Acad. Sci. Paris Série I Math.*, 321 :293–298, 1995.

[6] G. ALLAIRE and C. CONCA. Bloch wave homogenization for a spectral problem in fluid-solid structures. *Arch. Rational. Mech. Anal*, 135 :117–257, 1996.

[7] G. ALLAIRE and C. CONCA. Bloch wave homogenization and spectral asymptotic analysis. *J. Math. Pures Appl.*, 77 :153–208, 1998.

[8] G. ALLAIRE and C. CONCA. Boundary layers in the homogenization of a spectral problem in fluid-solid structures. *SIAM J. Math. Anal.*, 1999.

[9] H. AMMARI and T. ABBOUD. Diffraction par un réseau courbe : le cas TM, homogénéisation. *C.R.A.S., Paris, Série I, Mathématiques 319*, 4 :371–376, 1994.

[10] H. AMMARI and T. ABBOUD. Diffraction par un réseau courbe : approximation par un plan infini. *C.R.A.S., Paris, Série I, Mathématiques 320*, 1 :113–118, 1995.

[11] H. AMMARI and T. ABBOUD. Diffraction par un réseau courbe bi-périodique : homogénéisation. *C.R.A.S., Paris, Série I, Mathématiques 320*, 3 :301–306, 1995.

[12] H. AMMARI and T. ABBOUD. Diffraction at a curved grating : TM and TE cases, homogenization. *Jour. math. anal. and appl. 202*, 3 :995–1026, 1996.

[13] H. AMMARI and S. HE. Homogenization and scattering for gratings. *Jour. of Elec. Waves and Appl. 11*, 12 :1669–1683, 1997.

[14] H. ATTOUCH. *Variational convergence for functions and operators.* Applicable mathematics series, Pitman Publishing, 1984.

[15] I. BABUSKA. Homogenization and its application. Mathematical and computational problems. *Numerical solution of Partial differential Equations, III, Proc. Third Sympos. Synspade, Univ. Maryland, college Park, Md.*, 1975.

[16] I. BABUSKA. . Academic Press, New York (pp. 89-116), 1976.

[17] J. BASS. *Cours de mathématiques*, volume 3. Masson, Paris, 1971.

[18] A. BENSOUSSAN, J. L. LIONS, and G. PAPANICOLAOU. *Asymptotic analysis for periodic structures.* North-Holland, Amsterdam, 1978.

[19] Y. BENVENISTE. Correspondence relations among equivalent classes of heterogeneous piezoelectric solids under anti-plane mechanical and in-plane electrical fields. *Jour. Mech. Phys. Solids*, 43 :553–571, 1995.

[20] V. L. BERDICHEVSKI. *Variational principles in mechanics of continuum media.* Nauka, Moscow, 1983.

[21] G. BERGER and B. GOSTIAUX. *géométrie différentielle : variétés, courbes et surfaces.* Presses Universitaires de France, 1992.

[22] D. J. BERGMAN and D. STROUD. Physical properties of macroscopically inhomogeneous media. *Solid State Phys.*, 46 :147–269, 1992.

[23] A. BESICOVITCH. *Almost Periodic Functions.* Cambridge, 1932.

[24] T. A. BIRKS, J. C. KNIGHT, and P. ST. J. RUSSELL. Endlessly single-mode photonic crystal fiber. *OPTICS LETTERS*, 22 :961–963, 1997.

[25] F. BLOCH. Über die quantenmechanik der electronen in kristallgittern. *Z. Phys.*, 52 :555–600, 1928.

[26] H. BOHR. Zur theorie der fast periodischen funktionen. *Acta Math. 45*, pages 29–127, 1925.

[27] H. BOHR. Zur theorie der fast periodischen funktionen. *Acta Math. 46*, pages 101–214, 1925.

[28] A.S. BONNET. *Analyse mathématique de la propagation de modes guidés dans les fibres optiques.* PhD thesis, Université PARIS VI, 1988.

[29] A. BOSSAVIT. A rationale for edge-elements in 3-D fields computations. *IEEE Transactions on Magnetics, no 1*, 24 :74–79, 1988.

[30] A. BOSSAVIT. Solving Maxwell equations in a closed cavity, and the question of spurious modes. *IEEE Transactions on Magnetics*, 26 :702–705, 1990.

[31] A. BOSSAVIT. Electromagnétisme en vue de la modélisation, Mathématiques et applications. *Springer Verlag*, 14, 1993.

[32] A. BOSSAVIT. On the geometry of electromagnetism. *Jour. Japan Soc. Appl. Elect. and Mech.*, 6 :17–28, 1998.

[33] G. BOUCHITTÉ and D. FELBACQ. Low frequency scattering by a set of parallel metallic rods. *Mathematical and numerical aspects of wave propagation (Santiago de Compostela), SIAM, Philadelphia, PA*, pages 226–230, 2000.

[34] G. BOUCHITTE, S. GUENNEAU, and F. ZOLLA. Homogenization of quasicrystals. *in preparation.*

[35] G. BOUCHITTÉ, S. GUENNEAU, and F. ZOLLA. Spectral asymptotic analysis of heterogeneous cavities. *in preparation.*

[36] G. BOUCHITTE, S. GUENNEAU, F. ZOLLA, and P. TCHAMITCHIAN. Estimate between the almost-periodic and the homogenized solution of one-dimensional second-order operator. *in preparation.*

[37] G. BOUCHITTÉ and R. PETIT. Homogenization techniques as applied in the electromagnetic theory of gratings. *Electromagnetics*, 5 :17–36, 1985.

[38] G. BOUCHITTÉ and R. PETIT. On the concepts of a perfectly conducting metal and that of a perfectly thin screen. *Radio-Science, no 24*, 1 :13–26, 1989.

[39] A. BOURGEAT and A. PIANITSKI. Estimate in probability of the residual between the random and the homogenized solutions of one-dimensional second-order operator. *Asymptot. Anal. no 3-4*, 21 :303–315, 1999.

[40] A. BRAIDES. Almost Periodic Methods in the Theory of Homogenization. *Preprint SISSA 188M, Trieste.*

[41] A. BRAIDES. Homogenization of Some Almost Periodic Functionals. *Rend. Acad. Naz. Sci. XL*, 103 :313–322, 1985.

[42] L. BRAUQUIER. *Aux armes de Cardiff.* Editions de la Table Ronde, Paris, 2000.

[43] H. BREZIS. *Analyse fonctionnelle. Theorie et applications.* Masson, Paris, 1983.

[44] J. BROENG, D. MOGILEVSTEV, S. E. BARKOU, and A. B. BJARKLEV. Photonic crystal fibers : a new class of optical waveguides. *Optical fiber technology.*

[45] D. A. G. BRUGGEMAN. . *Ann. Physik (Leipz.), No 24, Vol. 665 (1935), No 25, Vol. 645 (1936), No 29, Vol. 160 (1937), Phys. Z., No 37*, 906, 1936.

[46] A. C. CLARKE. *2001, a space odyssey.* Edition ROC, 1968.

[47] M. CADILHAC and R. PETIT. *On the diffraction problem in electromagnetic theory : a discussion based on concepts of functional analysis including an example of practical application.* Huygens' Principle 1690-1990 : Theory and Applications, 1992.

[48] Z. CASTRO and E. ZUAZUA. Une remarque sur l'analyse asymptotique spectrale en homogénéisation. *C. R. Acad. Sci. Paris Série I Math.*, 322 :1043–1047, 1996.

[49] E. CENTENO. *Contribution à l'étude de la diffraction des ondes électromagnétiques par les cristaux photoniques bidimensionnels.* PhD thesis, Université de Clermont-Ferrand, 2000.

[50] E. CENTENO and D. FELBACQ. Guiding waves with photonic crystals. *Opt. Com.*, 160 :57–60, 1999.

[51] M. CESSENAT. *Mathematical methods in electromagnetism*, volume 41. World Scientific, 1996.

[52] J. CHANDEZON. *Les équations de Maxwell sous forme covariante : application à l'étude de la propagation dans les guides périodiques et à la diffraction par les réseaux.* PhD thesis, Université de Clermont-Ferrand 2, 1979.

[53] S. K. CHIN, N. A. NICOROVICI, and R. C. MC PHEDRAN. Green's Function and Lattice Sums for Electromagnetic Scattering by a Square Array of Perfectly Conducting Cylinders. *Physical Review E*, 49 :4590–4602, 1994.

[54] P. G. CIARLET. *The finite element method for elliptic problems.* North-Holland, Amsterdam, 1978.

[55] J. M. COMBES. Spectral problems in the theory of photonic crystals. *Preprint Centre Physique Théorique.*

[56] C. CONCA, J. PLANCHARD, and M. VANNINATHAN. *Fluids and periodic structures.*, volume 38. RMA, J. Wiley and Masson, Paris, 1995.

[57] S. DATTA, C.T. CHAN, K.M. HO, and SOUKOULIS C.M. Effective dielectric constant of periodic composite structures. *Phys. Rev. B*, 48 :14936–14943, 1993.

[58] R. DAUTRAY and J. L. LIONS. *Analyse mathématique et calcul numérique pour les sciences et les techniques.* Masson, 1987.

[59] M. DE BOISSIEU. *Structure atomique des alliages quasi cristallins AlMnSi et AlLiCu.* PhD thesis, Université de Loraine, 1989.

[60] N. G. DE BRUIJN. . *Nederl. Akad. Wetensch. Proc. Ser. A*, 43 :39–66, 1981.

[61] R.C. DE LA RUE and T.F. KRAUS. Strategies for the fabrication of photonic microstructures in semiconductors. *in Microcavities and photonic bandgaps Kluwer Acad. Pub., Netherlands*, pages 175–192, 1996.

[62] G.H. DERRICK, R.C. MCPHEDRAN, D. MAYSTRE, and M. NEVIERE. Crossed gratings : a theory and its applications. *Appl. Phys.*, 18 :39–52, 1979.

[63] J. DODZIUK. Finite-difference approach to the Hodge theory of harmonic forms. *Amer. J. Math.*, 98 :79–104, 1976.

[64] P. DULAR, C. GEUZAINE, . HENROTTE, and W. LEGROS. A general environment for the treatment of discrete problems and its application to the finite element method. *IEEE Transactions on Magnetics, no 5*, 34 :3395–3398, 1998.

[65] P. DULAR, C. GEUZAINE, F. HENROTTE, and W. LEGROS. A general environment for the treatment of discrete problems and its application to the finite element method. *IEEE Transactions on Magnetics, 5*, 34 :3395–3398, 1998.

[66] M. DUNEAU and A. KATZ. . *Phys. Rev. Lett.*, 54 :2688–, 1985.

[67] M. DUNEAU and A. KATZ. 'Quasiperiodic structures obtained by the projection method'. *Jour. Phys. Paris C3*, 47 :103–113, 1986.

[68] A.M. DYKHNE. Conductivity of a two-dimensional two-phase system. *Soviet Physics JETP*, 32 :63–65, 1970.

[69] I. EKELAND and R. TEMAM. *Analyse convexe et problèmes variationnels.* Dunod et Gauthier-Villars, Paris, 1973.

[70] K. J. FALCONER. *The geometry of fractal sets.* Cambridge Univ. Press, 1985.

[71] D. FELBACQ. *Etude théorique et numérique de la diffraction de la lumière par des ensembles de tiges parallèles.* PhD thesis, Université Aix-Marseille III, 1994.

[72] D. FELBACQ and G. BOUCHITTÉ. Homogenization of a set of parallel fibers. *J. of Waves in Random Media*, 7 :245–256, 1997.

[73] D. FELBACQ, B. GUIZAL, and F. ZOLLA. Limit analysis of the diffraction of a plane wave by a stratified periodic medium. *J. Math. Phys.*, 39 :4604–4607, 1998.

[74] D. FELBACQ, B. GUIZAL, and F. ZOLLA. Wave propagation in one-dimensional photonic crystals. *Optics Commun.*, 152 :119–126, 1998.

[75] D. FELBACQ, G. TAYEB, and D. MAYSTRE. Scattering by a random set of parallel cylinders. *J. Opt. Soc. Am. A*, 11 :2526–2538, 1994.

[76] A. FIGOTIN and V. GOUNTSVEIG. Localized electromagnetic waves in a layered periodic dielectric medium with a defect. *Phys. Rev. B, No 1*, 58, 1998.

[77] A. FIGOTIN and A. KLEIN. Localization of Classical Waves II. Electromagnetic Waves. *Comm. Math. Phys.*, 184 :411–441, 1997.

[78] A. FIGOTIN and P. KUCHMENT. Spectral properties of classical waves in high contrast periodic media. *SIAM J. Appl. Math.*

[79] A. FIGOTIN and P. KUCHMENT. Band-Gap Structure of the Spectrum of Periodic Dielectric and Acoustic Media. I. Scalar model. *SIAM J. Appl. Math.*, 56 :68–88, 1996.

[80] A. FIGOTIN and P. KUCHMENT. Band-Gap Structure of the Spectrum of Periodic Dielectric and Acoustic Media. II. 2D Photonic Crystals. *SIAM J. Appl. Math.*, 56 :561–620, 1996.

[81] G. FLOQUET. Sur les équations différentielles linéaires à coefficients périodiques. *Ann. École Norm. Sér.*, 122 :47–89, 1883.

[82] G. FRANCFORT. Homogenization of a class of fourth order equations with application to incompressible elasticity. *Proc. Roy. Soc. Edin. A*, 120 :25–46, 1992.

[83] GALILEO GALILEI. *Il saggiatore.* Acc. Linceo Nobile Fiorentino, 1623.

[84] J. GARNIER. *Ondes en milieu aléatoire.* PhD thesis, Ecole Polytechnique, Paris, 1996.

[85] F. W. GAYLE. Free-surface solidification habit and point group symmetry of a faceted icosahedral Al-Li-Cu phase. *J. Mater. Sci.*, 2 :1–4, 1987.

[86] M. GERADIN and D. RIXEN. *Mechanical vibrations : theory and applications to structural dynamics.* John Wiley and Son, 2nd edition, 1997.

[87] P. GÉRARD. Mesures semi-classiques et ondes de Bloch. *Sém. Équations aux Dérivées Partielles, École Polytechnique, Palaiseau*, 16, 1991.

[88] C. GEUZAINE. *High order hybrid finite element schemes for Maxwell's equations taking thim structures and global quantities into account.* PhD thesis, Université de liège, 2001.

[89] R. GHOSH, A. KUMAR, and J. P. MEUNIER. Waveguiding properties of holey fibres and the effective-V model. *Electron. Lett.*, 34 :1347–1348, 1999.

[90] K. GODEL. Über formal unentscheidbare Sätze der Principia Mathematica und verwandter Systeme I. *Monatshefte für Mathematik und Physik*, 38 :173–198, 1931.

[91] K. GOLDEN and G. PAPANICOLAOU. Bounds for the effective parameters of heterogeneous media by analytic continuation. *Comm. Math. Phys.*, 90 :473–491, 1983.

[92] Y. GRABOVSKY, G. W. MILTON, and D. S. SAGE. Exact relations for effective tensors of composites : necessary conditions and sufficient conditions. *Comm. Pure. Appl. Math.*, pages 300–353, 2000.

[93] B. Gralak. *Etude théorique et numérique des propriétés des structures à bandes interdites photoniques.* PhD thesis, Université Aix-Marseille III, 2001.

[94] B. GRALAK, S. ENOCH, and G. TAYEB. Anomalous refractive properties of photonic crystals. *J. Opt. Soc. Am. A*, 17 :1012–1020, 2000.

[95] S. GUENNEAU, S. LASQUELLEC, A. NICOLET, and F. ZOLLA. Design of photonic band gap optical fibers using finite elements. *accepted in COMPUMAG2001 (France, July), submitted in COMPEL*, 2001.

[96] S. GUENNEAU, S. LASQUELLEC, A. NICOLET, and F. ZOLLA. Fibres Optiques à Cristaux Photoniques : détermination des modes par une méthode d'éléments finis. *Groupe de Recherche du CNRS Cristaux Photoniques, École Centrale Lyon, Décembre*, 2001.

[97] S. GUENNEAU, S. LASQUELLEC, A. NICOLET, F. ZOLLA, C. GEUZAINE, and P. DULAR. Numerical and theoretical study of leaky modes in photonic crystal fibers. *in preparation.*

[98] S. GUENNEAU, A. NICOLET, and F. ZOLLA. Theoretical and numerical study of photonic crystal fibers. *PIERS 2000 (USA, July), invited talk in the session on Photonic Band Gaps*, 2000.

[99] S. GUENNEAU, A. NICOLET, F. ZOLLA, C. GEUZAINE, and B. MEYS. Numerical study of coupling between optical waveguides. *EMF2000 (Belgium, May)*, 2000.

[100] S. GUENNEAU, A. NICOLET, F. ZOLLA, C. GEUZAINE, and B. MEYS. A finite element formulation for spectral problems in optical fibers. *Journal for Computation and Mathematics in Electrical and Electronic Engineering, No 1*, 20 :120–131, 2001.

[101] S. GUENNEAU, A. NICOLET, F. ZOLLA, and S. LASQUELLEC. Theoretical and numerical study of photonic crystal fibers. *PIER, special volume on Photonic Band Gaps, selected papers of PIERS 2000 (submitted).*

[102] S. GUENNEAU, A. NICOLET, F. ZOLLA, and S. LASQUELLEC. Modeling of photonic crystal optical fibers with finite elements. *accepted in COMPUMAG2001 (France, July) and submitted in IEEE Transactions on Magnetics*, 2001.

[103] S. GUENNEAU, A. NICOLET, F. ZOLLA, S. LASQUELLEC, C. GEUZAINE, and P. DULAR. Electric field edge element modelling for twisted open waveguides. *in preparation.*

[104] S. GUENNEAU and F. ZOLLA. Homogenization of finite photonic crystals with heterogeneous permittivity and permeability. *in preparation.*

[105] S. GUENNEAU and F. ZOLLA. Homogenization of three-dimensional finite photonic crystals. *Journal of Electromagnetic Waves and Applications, Vol. 14, pp. 529-530 and full article in Progress In Electromagnetics Research vol. 27 pp. 91-127, (2000).*

[106] S. GUENNEAU, F. ZOLLA, and NICOLET. Theoretical and numerical study of photonic crystal waveguides in the low frequency limit. *in preparation.*

[107] C. A. GUERIN and M. HOLSCHNEIDER. On equivalent definitions of the correlation dimension for a probability measure. *Jour. Stat. Phys., 3/4*, 86 :707–720, 1997.

[108] P. HALEVI, A.A. KROKHIN, and J. ARRIAGA. Photonic crystal optics and homogenization of 2D periodic composites. *Phys. Rev. Lett.*, 82 :719–722, 1999.

[109] R.W. HAMMING. *Numerical Methods for scientists and engineers.* Dover Publications, Inc., New York, 1962.

[110] G. H. HARDY and E. M. WRIGHT. *An Introduction to the Theory of Numbers.* Oxford Science Publications, 5th edition.

[111] Z. HASHIN and S. SHTRIKMAN. A variational approach to the theory of effective magnetic permeability of multiphase materials. *J. Applied Phys.*, 33 :3125–3131, 1962.

[112] J. HESLING, G. W. MILTON, and A. B. MOVCHAN. Duality relations, correspondences, and numerical results for planar elastic composites. *J. Mech. Phys. Solids*, 45 :565–590, 1997.

[113] D. HOFSTADTER. *Gödel, Escher, Bach : an eternal Golden Braid.* Basic Books, 1979.

[114] L. HORMANDER. *Linear partial differential operators.* Springer-Verlag, 1976.

[115] V. JIKOV, S. KOZLOV, and O. OLEINIK. *Homogenization of Differential Operators.* Springer-Verlag, Berlin, 1995.

[116] J. JOANNOPOULOS, R. MEADE, and J. WINN. *Photonic Crystals.* Princeton Press, Princeton, NJ, 1995.

[117] J. B. KELLER. A theorem on the conductivity of a composite medium. *Jour. Math. Phys.*, 5 :548–549, 1964.

[118] C. KITTEL. *Physique de l'état solide.* Dunod, 1983.

[119] J. C. KNIGHT, T. A. BIRKS, R. F. CREGAN, P. ST. J. RUSSELL, and J. P. DE SANDRO. Large mode area photonic crystal fibre. *ELECTRONICS LETTERS, 13*, 34 :1347–1348, 1998.

[120] J. C. KNIGHT, T. A. BIRKS, P. ST. J. RUSSELL, and J. P. DE SANDRO. Properties of photonic crystal fiber and the effective index model. *JOSA A*, 15 :748, 1998.

[121] J. C. KNIGHT, J. BROENG, T. A. BIRKS, and P. ST. J. RUSSELL. Photonic band gap guidance in optical fibers. *SCIENCE*, 282 :1476–1478, 1998.

[122] S. M. KOZLOV. Averaging differential operators with almost-periodic rapidly oscillating coefficients. *Math. USSR-Sb*, 35 :481–498, 1979.

[123] S. M. KOZLOV. On duality of a class of variational problems. *Funkt. Anal. Prilozh.*, 2 :101–126, 1984.

[124] S. M. KOZLOV. Reducibility of quasiperiodic differential operators and averaging. *Trans. Moscow Math. Soc.*, 2 :101–126, 1984.

[125] J. LAMINIE and S. M. MEFIRE. Three-dimensional computation of a magnetic field by mixed finite elements and boundary elements. *Appl. Num. Math.*, 35 :221–244, 2000.

[126] R. LANDAUER. . *Comments Solid State Phys., No 4*, 139, 1972.

[127] S. LASQUELLEC. *Elaboration d'un modèle de machine synchrone saturée compatible avec la simulation de l'ensemble "Convertisseur Machine Commande"*. PhD thesis, Université de Nantes, 1998.

[128] S. LASQUELLEC, S. GUENNEAU, A. NICOLET, and F. ZOLLA. Symmetries in finite element computation of propagating modes in waveguides. *in preparation.*

[129] J. M. LEVY LEBLOND. *La pierre de touche. La science a l'epreuve...* Folio Essai, 1997.

[130] J. LOBRY. *Symétries et éléments de Whitney en magnétodynamique tridimensionnelle.* PhD thesis, Faculté Polytechnique de Mons, 1993.

[131] H. A. LORENTZ. The Theory of electrons. *B. G. Teubner, Leipzig, 1909, Reprint Dover, N.Y.*, 1952.

[132] L. LORENZ. . *Wiedemannsche Annalen, No 11*, 70, 1880.

[133] D. A. LOWTHER, E. FREEMAN, and B. FORGHANI. A sparse matrix open boundary method for finite element analysis. *IEEE transactions on magnetics, No 4*, 25 :2810–2812, 2000.

[134] A. L. MACKAY. No title. *Physica (Amsterdam)*, 114 :66–613, February 1982.

[135] J.C. MAXWELL. *A Treatise on Electricity and Magnetism.* Clarendon Press, 3rd ed. (Dover edition, New York, 1954), 1891.

[136] J. C. MAXWELL GARNETT. . *Philos. Trans. R. Soc. Lond., No 203*, 385, 1904.

[137] D. MAYSTRE. Electromagnetic study of photonic band gaps. *Pure Appl. Opt.*, 3 :975–993, 1994.

[138] D. MAYSTRE, G. TAYEB, and D. FELBACQ. Theoretical study of photonic band gap structures. *in Optics for Science and New Technology, ED. J. Chang, J. Lee, S. Lee and C. Nam*, 2778 :740–743, 1996.

[139] V. G. MAZ'JA. *Sobolev Spaces.* Springer Verlag, Berlin Heidelberg, 1985.

[140] P. R. MC ISAAC. Symmetry-Induced Modal Characteristics of Uniform Waveguides. *IEEE Trans. on Micro. The. and Tech., No 5*, 23 :421–433, 1975.

[141] D. R. MC KENZIE and R. C. MC PHEDRAN. Optical constants of cermet materials including proximity effects. *Conference on the Electrical Transport and Optical Properties of Inhomogeneous Media (Columbus, Ohio, 1977), A.I.P. Conference Proceedings 40*, pages 283–287, 1978.

[142] D. R. MC KENZIE, R. C. MC PHEDRAN, and G. H. DERRICK. The conductivity of lattices of spheres. II. The body-centred cubic lattice. *Proceedings of the Royal Society of London A 362*, pages 211–232, 1978.

[143] R. C. MC PHEDRAN. Transport properties of cylinder pairs and of the square array of cylinders. *Proceedings of the Royal Society of London A 408*, pages 31–43, 1986.

[144] R. C. MC PHEDRAN and D. H. DAWES. Lattice sums for an electromagnetic scattering problem. *Journal of Electromagnetic Waves and Applications*, 6 :1327–1340, 1992.

[145] R. C. MC PHEDRAN and D. R. MC KENZIE. Exact solutions for transport properties of arrays of spheres. *Conference on the Electrical Transport and Optical Properties of Inhomogeneous Media (Columbus, Ohio, 1977), A.I.P. Conference Proceedings 40*, pages 294–299, 1978.

[146] R. C. MC PHEDRAN and G. W. MILTON. Transport properties of touching cylinder pairs and of the square array of touching cylinders. *Proceedings of the Royal Society of London A 411*, pages 313–326, 1987.

[147] R. C. MC PHEDRAN and A. B. MOVCHAN. The Rayleigh Multipole Method for Linear Elasticity. *Journal of the Mechanics and Physics of Solids*, 42 :711–727, 1994.

[148] R. C. MC PHEDRAN, L. POLADIAN, and G. W. MILTON. Asymptotic studies of closely spaced, highly conducting cylinders. *Proceedings of the Royal Society of London A 415*, pages 185–196, 1988.

[149] R.C. MC PHEDRAN, L.C. BOTTEN, M.S. CRAIG, M. NEVIERE, and D. MAYSTRE. Lossy lamellar gratings in the quasistatic limit. *Optica Acta*, 29 :289–312, 1982.

[150] R. MC WEENY. *Symmetry, an introduction to group theory and its applications.* New-York : Macmillan, 1963.

[151] R. C. MCPHEDRAN, C. G. POULTON, N. A. NICOROVICI, and A. B. MOVCHAN. Low frequency corrections to the static effective dielectric constant of a two-dimensional composite material. *Proc. Royal Soc. Lon. A*, 452 :2231–2245, 1996.

[152] R.C. MCPHEDRAN, G.H. DERRICK, and L.C. BOTTEN. *Theory of crossed gratings.* in Electromagnetic theory of gratings. Springer-Verlag, Berlin, edited by R. Petit, 1980.

[153] N. MENGUY. *Transition de phase réversible icosaédrique- rhomboédrique d'un alliage Al63.5Fe12.5Cu24.* PhD thesis, INP Grenoble, 1993.

[154] B. MEYS. *Modélisation des champs électromagnétiques aux hyperfréquences par la méthode des éléments finis. Application au problème du chauffage diélectrique.* PhD thesis, Université de liège, 1999.

[155] G. W. MILTON and A. B. MOVCHAN. A correspondence between plane elasticity and the two-dimensional real and complex dielectric equations in anisotropic media. *Proc. Roy. Soc. Lond. A, 450, pp. 293-317, 1995*, 450 :293–317, 1995.

[156] G. W. MILTON and N. PHAN-THIEN. New bounds on effective elastic moduli of two-component materials. *Proc. Roy. Soc. Lond.*, pages 305–331, 1982.

[157] A. MOROZ and C. SOMMERS. Photonic band gaps of three-dimensional face-centered cubic lattices. *Phys. Lett. A.*

[158] O. F. MOSSOTTI. . *Memorie di Matematica e di Fisica della Societa Italiana delle Scienze Residente in Modena, pt 2*, 24 :49–74, 1850.

[159] A. B. MOVCHAN, N. A. NICOROVICI, and R. C. MC PHEDRAN. Green's Tensors and Lattice Sums for Elastostatics and Elastodynamics. *Proceedings of the Royal Society, A*, 453 :643–662, 1997.

[160] J. C. NEDELEC. Mixed finite element in R3. *Numer. Math.*, 35 :315–341, 1980.

[161] J. C. NEDELEC. Éléments finis mixtes incompressibles pour l'équation de Stokes dans $\mathbb{R}^3$. *Numer. Math.*, 39 :97–112, 1982.

[162] J. C. NEDELEC. *Notions sur les techniques d'éléments finis.* Ellipses, 1991.

[163] S. NEMAT-NASSER and L. NI. A duality principle and correspondence relations in elasticity. *Int. Jour. Solids Structures*, 32 :467–472, 1995.

[164] G. NGUETSENG. A general convergence result for a functional related to the theory of homogenization. *SIAM J. Math. Anal.*, 20 :608–623, 1989.

[165] A. NICOLET. *Modélisation du champ magnétique dans les systèmes comprenant des milieux non linéaires.* PhD thesis, Université de Liège, 1991.

[166] A. NICOLET, J. F. REMACLE, B. MEYS, A. GENON, and W. LEGROS. Transformation methods in computational electromagnetism. *J. Appl. Phys.*, 75 :10, 1994.

[167] N. A. NICOROVICI, R. C. Mc. PHEDRAN, and L. C. BOTTEN. Photonic Band Gaps : Non-Commuting Limits and the "Acoustic Band". *submitted to Phys. Rev. Lett.*

[168] N. A. NICOROVICI, R. C. MC PHEDRAN, and BAO KE-DA. Propagation of Electromagnetic Waves in Periodic Lattices of Spheres : Green's Functions and Lattice Sums. *Physical Review E*, 51 :690–702, 1995.

[169] O. A. OLEINIK and V. V. ZHIKOV. On the homogenization of elliptic operators with almost-periodic coefficients. *Rend. Sem. Mat. Fis. Milano*, 52 :149–166, 1982.

[170] G. PAPANICOLAOU and S. R. S. VARADHAN. Diffusion in regions with many small holes. *Stochastic differential systems, proc. IFIP-WG 7/1 Working Conf., Vilnius*, pages 190–206, 1978.

[171] G. PAPANICOLAOU and S. R. S. VARADHAN. *Lectures Notes in Control and Information Sci., 25.* Springer, Berlin-New-York, 1980.

[172] J. B. PENDRY. . *Phys. Rev. Lett.*, 85 :3966, 2000.

[173] J. B. PENDRY, A. J. HOLDEN, D. J. ROBBINS, and W. J. STEWART. Magnetism from Conductors and Enhanced Nonlinear Phenomena. *IEEE Trans. Micro. Wav. Theo. Tech., no 11*, 47 :2075–2084, 1999.

[174] R. PENROSE. *The emperor's new mind. Concerning computers, minds, and the laws of physics.* Oxford University Press, New-York, 1989.

[175] W. T. PERRINS, D. R. MC KENZIE, and R. C. MC PHEDRAN. Transport properties of regular arrays of cylinders. *Proceedings of the Royal Society of London A 369*, pages 207–225, 1979.

[176] R. PETIT. *Ondes électromagnétiques en radioélectricité et en optique.* Masson, 1993.

[177] R. PETIT and G. BOUCHITTÉ. Replacement of a very fine grating by a stratified layer : homogenisation techniques and the multiple-scale method. *SPIE Proceedings, Application and Theory of Periodic Structures, Diffraction Gratings, and Moiré Phenomena 431*, 815, 1987.

[178] R. PETIT and F. ZOLLA. The method of fictitious sources as applied to the conical diffraction by a homogeneous rod. *J. of Electromagnetic Waves and Applications*, 8 :1–18, 1994.

[179] L. POLADIAN and R. C. MC PHEDRAN. Effective transport properties of periodic composite materials. *Proceedings of the Royal Society of London A 408*, pages 45–59, 1986.

[180] C. G. POULTON. *Asymptotics and Wave Propagation in Cylindrical Geometries.* PhD thesis, University of Sydney, 1999.

[181] C.G. POULTON, L.C. BOTTEN, R.C. McPHEDRAN, N.A. NICOROVICI, and A.B. MOVCHAN. Non-Commuting limits in electromagnetic scattering : asymptotic analysis for an array of highly conducting inclusions. *SIAM Jour. of Appl. Math. (to appear).*

[182] J. K. RANKA, R. S. WINDELER, and A. J. STENTZ. Optical properties of high-delta air-silica microstructure optical fibers. *Optics Letters*, 25 :796–797, 2000.

[183] M. REED and S. SIMON. *Methods of modern mathematical physics.* Academic Press, New York, 1978.

[184] F. RELLICH. Uber das asymptotische verhalten der losungen von $\Delta u + \lambda u = 0$ in unendlichen gebieten. *Uber. Deutsch. Math. Verein*, 53 :57–65, 1943.

[185] Z. REN, F. BOUILLAULT, A. RAZEK, A. BOSSAVIT, and J. C. VÉRITÉ. A new hybrid model using electric field formulation for 3-D eddy current problems. *IEEE Transactions on Magnetics, no 2*, 26 :470–473, 1990.

[186] A.J. REUBEN, J.G. YARDLEY, and R.C. McPHEDRAN. Laplace transform methods and the Rayleigh identity for an array of elliptical cylinders. *Proceedings IUTAM99, Kluwer*, 4, 2001.

[187] Y. SAAD. Numerical methods for large eigenvalue problems. *Manchester Univ. Press, Ser. in alg. arch. for adv. sci. comp.*, 1991.

[188] E. SANCHEZ-PALENCIA. équations aux dérivées partielles dans un type de milieux hétérogènes. *C. R. Acad. Sci. Paris, Sér. A-B*, 272 :395–398, 1972.

[189] M. SCHECHTER. *Operator methods in quantum mechanics.* North Holland, 1981.

[190] D. SCHECHTMAN, I. BLECH, D. GRATIAS, and J. W. CAHN. . *Phys. Rev. Lett.*, 53 :1951–, 1984.

[191] A. W. SNYDER and J. D. LOVE. *Optical waveguide theory.* Chapman and Hall, New York, 1983.

[192] S. SPAGNOLO. Sulla convergenza di soluzioni di equazioni paraboliche ed ellitiche. *Ann. Scuola Norm. Sup. Pisa (3)*, 22 :571–597, 1968.

[193] R. S. STRICHARTZ. Besicovitch meets Wiener-Fourier expansions and fractal measures. *Bull. A.M.S. no 1*, 20, 1989.

[194] J.W. STRUTT. On the influence of obstacles arranged in rectangular order upon the properties of a medium. *Phil. Mag.*, 34 :481–502, 1892.

[195] L. TARTAR. Problèmes de contrôle des coefficients dans des équations aux dérivées partielles. *Lectures Notes in Econom. and Math. Systems, Springer, Berlin , No 107, 1975 Internat. sympos., IRIA LABORIA, Roquencourt, 1974*, pages 420–426, 1974.

[196] L. TARTAR. Estimations fines des coefficients homogénéisés. *Ennio De Giorgi colloquium (Paris, 1983), pp. 168-187, Res. Notes in Math, 125, Pitman, Boston, MA-London, 1985*, 1985.

[197] G. TAYEB and D. MAYSTRE. Rigorous theoretical study of finite size two-dimensional photonic crystals doped by microcavities. *J. Opt. Soc. Am. A*, 14 :3323–3332, 1997.

[198] A. TIP, A. MOROZ, and J. M. COMBES. Bloch decomposition and band structure for absorptive photonic crystals.

[199] A. M. TURING. 'Systems of logic based on ordinals. *Proc. Lond. Math. Soc.*, 45 :161–228, 1939.

[200] C. VASSALO. *Théorie des guides d'ondes en électromagnétisme.* CNET, Eyrolles editions, 1985.

[201] P. VINCENT. *Contribution à l'étude théorique et numérique de la propagation des ondes électromagnétiques en présence d'un objet cylindrique : tiges et réseaux.* PhD thesis, Université Aix-Marseille III, 1978.

[202] P. VINCENT. Singularity expansions for cylinders of finite conductivity. *Appl. Phys.*, 17 :239–248, 1978.

[203] H. WANG. *Popular lectures on mathematical logic.* Dover, New-York, reprint of Van Nostrand, New-York, 1981, 1993.

[204] X. WENG CHO CHEW. *Waves and fields in inhomogeneous media.* Van Nostrand Reinhold, 1990.

[205] T. WHITE. Microstructured Optical Fibres : a Multipole formulation. *Research Project Report of University of Sidney*, 2000.

[206] H. WHITNEY. *Geometric integration theory.* Princeton University Press, 1957.

[207] O. WIENER. Abhandlungen der Mathematish-Physischen Klasse der Koenigl. *Saechsischen Gesellschaft der Wissenschaften, No 32*, 509, 1912.

[208] A. WILES. Modular elliptic curves and Fermat's Last Theorem. *Annals of Mathematics*, 142 :443–551, 1995.

[209] E. YABLONOVITCH. Inhibited spontaneous emission in solid-state physics and electronics. *Phys. Rev. Lett.*, 58 :2059–2062, 1987.

[210] J.G. YARDLEY, R.C. McPHEDRAN, N.A. NICOROVICI, and L.C. BOTTEN. Addition formulas and the Rayleigh identity for arrays of elliptical cylinders. *Phys. Rev. E*, 60 :6068–6080, 1999.

[211] J.G. YARDLEY, A.J. REUBEN, and R.C. McPHEDRAN. Transport properties of layers of elliptical cylinders. *Proc. Roy. Soc. Lon. (to appear).*

[212] F. ZOLLA. *Contribution à l'étude de la diffraction et de l'absorption des ondes électromagnétiques : structures bipériodiques minces, structures cylindriques par la Méthode des Sources Fictives.* PhD thesis, ONERA/Université Aix-Marseille III, 1993.

[213] F. ZOLLA, D. FELBACQ, and B. GUIZAL. A remarkable diffractive property of photonic quasi-crystals. *Optics Commun.*, 148 :6–10, 1998.

[214] F. ZOLLA and S. GUENNEAU. Homogénéisation de cristaux photoniques 3D de taille finie. *Groupe De Recherche du CNRS Cristaux Photoniques, Marseille, Décembre 1999.*

[215] F. ZOLLA, R. PETIT, and M. CADILHAC. Electromagnetic theory of diffraction by a system of parallel rods : the method of fictitious sources. *J. Opt. Soc. Am. A*, 11 :1087–1096, 1994.